

Mechatronic Modeling and Simulation Using Bond Graphs

Shuvra Das



CRC Press
Taylor & Francis Group

Mechatronic Modeling and Simulation Using Bond Graphs

This page intentionally left blank

Mechatronic Modeling and Simulation Using Bond Graphs

Shuvra Das



CRC Press

Taylor & Francis Group

Boca Raton London New York

CRC Press is an imprint of the
Taylor & Francis Group, an **informa** business

CRC Press
Taylor & Francis Group
6000 Broken Sound Parkway NW, Suite 300
Boca Raton, FL 33487-2742

© 2009 by Taylor & Francis Group, LLC
CRC Press is an imprint of Taylor & Francis Group, an Informa business

No claim to original U.S. Government works
Printed in the United States of America on acid-free paper
10 9 8 7 6 5 4 3 2 1

International Standard Book Number-13: 978-1-4200-7314-0 (Hardcover)

This book contains information obtained from authentic and highly regarded sources. Reasonable efforts have been made to publish reliable data and information, but the author and publisher cannot assume responsibility for the validity of all materials or the consequences of their use. The authors and publishers have attempted to trace the copyright holders of all material reproduced in this publication and apologize to copyright holders if permission to publish in this form has not been obtained. If any copyright material has not been acknowledged please write and let us know so we may rectify in any future reprint.

Except as permitted under U.S. Copyright Law, no part of this book may be reprinted, reproduced, transmitted, or utilized in any form by any electronic, mechanical, or other means, now known or hereafter invented, including photocopying, microfilming, and recording, or in any information storage or retrieval system, without written permission from the publishers.

For permission to photocopy or use material electronically from this work, please access www.copyright.com (<http://www.copyright.com/>) or contact the Copyright Clearance Center, Inc. (CCC), 222 Rosewood Drive, Danvers, MA 01923, 978-750-8400. CCC is a not-for-profit organization that provides licenses and registration for a variety of users. For organizations that have been granted a photocopy license by the CCC, a separate system of payment has been arranged.

Trademark Notice: Product or corporate names may be trademarks or registered trademarks, and are used only for identification and explanation without intent to infringe.

Library of Congress Cataloging-in-Publication Data

Das, Shuvra.
Mechatronic modeling and simulation using bond graphs / Shuvra Das.
p. cm.
Includes bibliographical references and index.
ISBN 978-1-4200-7314-0 (alk. paper)
1. Mechatronics. 2. Bond graphs. 3. Engineering models. I. Title.

TJ163.12.D37 2009
621--dc22

2008037629

Visit the Taylor & Francis Web site at
<http://www.taylorandfrancis.com>

and the CRC Press Web site at
<http://www.crcpress.com>

*This book is dedicated
to the memory of my
two grandmothers,
Kamala and Sarama. They
recognized very early
in their lives that
education is the sure
path to success in life and
ensured that their children
and grandchildren got the
best education possible.*

This page intentionally left blank

Contents

Preface	xiii
Acknowledgments	xvii
Author	xix

Chapter 1 Introduction to Mechatronics and

System Modeling	1
1.1 What Is Mechatronics?	1
1.2 What Is a System and Why Model Systems?	4
1.3 Mathematical Modeling Techniques Used in Practice	7
1.4 Software	10
Problems	11

Chapter 2 Bond Graphs: What Are They? 13

2.1 Engineering Systems	14
2.2 Ports	16
2.3 Generalized Variables	20
2.3.1 Power Variables	20
2.3.2 Energy Variables	20
2.3.3 Tetrahedron of State	21
2.4 Bond Graphs	23
2.4.1 Word Bond Graphs	23
2.5 Basic Components in Systems	26
2.5.1 1-Port Components	26
2.5.1.1 1-Port Resistor: Energy Dissipating Device	27
2.5.1.2 1-Port Capacitor: 1-Port Energy Storage Device	28
2.5.1.3 1-Port Inductor/Inertia: 1-Port Energy Storage Device	30
2.5.1.4 Other 1-Port Elements	33
2.5.2 2-Port Components	35
2.5.2.1 Transformer Element	35
2.5.2.2 Gyrator Element	39
2.5.3 3-Port (or Higher-Port) Components	41
2.5.3.1 Flow Junction, Parallel Junction, 0 Junction, and Common Effort Junction	42
2.5.3.2 Effort Junction, Series Junction, 1 Junction, and Common Flow Junction	43
2.5.4 Modulated Components: Transformers, Gyrators, Resistances, and More	46

2.6	A Brief Note about Bond Graph Power Directions	46
2.7	Summary of Bond Direction Rules	47
	Problems	48

Chapter 3 Drawing Bond Graphs for Simple Systems:

	Electrical and Mechanical.....	55
3.1	Simplification Rules for Junction Structure	56
3.2	Drawing Bond Graphs for Electrical Systems	62
	3.2.1 Formal Method of Drawing Bond Graphs for Electrical Systems	65
3.3	Drawing Bond Graphs for Mechanical Systems	69
	3.3.1 Formal Method of Drawing Bond Graphs for Mechanical Systems in Translation and Rotation.....	72
	3.3.2 A Note about Gravitational Forces on Objects	73
	3.3.3 Examples of Systems in Rotational Motion.....	79
3.4	Causality	83
	3.4.1 Transformer	85
	3.4.2 Gyrator.....	86
	3.4.3 Junctions.....	86
	3.4.4 Storage Elements: I , C	87
	3.4.4.1 I , for Mass Elements or Inductances.....	88
	3.4.4.2 C , for Capacitive or Spring Elements.....	89
	3.4.5 R , for Resistive Elements.....	91
	3.4.6 Algorithm for Assigning Causality in a Bond Graph Model.....	92
	3.4.7 Integral Causality versus Differential Causality for Storage Elements	100
	3.4.8 Final Discussion of Integral and Differential Causality	105
	3.4.9 Causality Summary.....	106
	Problems	107

Chapter 4 Drawing Bond Graphs for Hydraulic and Electronic

	Components and Systems.....	113
4.1	Some Basic Properties and Concepts for Fluids	114
	4.1.1 Mass Density	114
	4.1.2 Force, Pressure, and Head	115
	4.1.3 Bulk Modulus.....	115
	4.1.4 Mass Conservation for Steady, Irrotational, Nonviscous Flows.....	115
	4.1.5 Energy Conservation for Steady, Irrotational, Nonviscous Flows.....	116
4.2	Bond Graph Model of Hydraulic Systems.....	117
	4.2.1 Fluid Compliance, C Element.....	117
	4.2.2 Fluid Inertia, I Element	118
	4.2.3 Fluid Resistances, R Element.....	119

4.2.4	Sources (Effort and Flow)	121
4.2.5	Transformer Elements	121
4.2.6	Gyrator Elements	122
4.2.7	Bond Graph Models of Hydraulic Systems	122
4.3	Electronic Systems	127
4.3.1	Operational Amplifiers	128
4.3.2	Diodes	133
	Problems	136

Chapter 5 Deriving System Equations from Bond Graphs..... 145

5.1	System Variables	145
5.2	Deriving System Equations	146
5.2.1	Review	147
5.2.2	Junction Power Direction and Its Interpretation.....	147
5.3	Tackling Differential Causality.....	159
5.4	Algebraic Loops	162
	Problems	166

Chapter 6 Solution of Model Equations and Their Interpretation.... 173

6.1	Zeroth Order Systems	174
6.2	First Order Systems	176
6.2.1	Solution of the First-Order Differential Equation	178
6.3	Second Order System	180
6.3.1	System Response for Step Input	189
6.3.2	System Response to Sinusoidal Inputs	191
6.3.3	System Response Study Using State–Space Representation.....	194
6.4	Transfer Functions and Frequency Responses.....	197
6.4.1	System Response in the Frequency Domain	199
6.5	Summary.....	206
	Problems	206

Chapter 7 Numerical Solution Fundamentals 211

7.1	Techniques for Solving Ordinary Differential Equations	211
7.2	Euler's Method	212
7.3	Implicit Euler and Trapezoidal Method	215
7.4	Runge–Kutta Method	217
7.5	Adaptive Methods	219
7.6	Summary.....	223
	Problems	224

Chapter 8 Transducers: Sensor Models..... 227

8.1	Resistive Sensors	228
8.2	Capacitive Sensors	233
8.2.1	Multipoint Storage Fields: C-Field	235

8.3	Magnetic Sensors	242
8.3.1	Magnetic Circuits and Fields	242
8.3.1.1	Faraday's Law of Electromagnetic Induction.....	243
8.3.1.2	Ampere's Law	243
8.3.1.3	Gauss's Law for Magnetism	243
8.3.2	Simple Magnetic Circuit	245
8.3.2.1	Magnetic Circuit with Air Gap	247
8.3.2.2	Magnetic Bond Graph Elements	249
8.3.2.3	Inside C-Field	257
8.4	Hall Effect Sensors.....	266
8.5	Piezo-Electric Sensors	271
8.6	MEMS Devices	277
8.6.1	MEMS Examples.....	279
8.6.1.1	Microcantilever-Based Capacitive Sensors	279
8.6.1.2	Comb Drives	281
8.6.1.3	MEMS Gyroscopic Sensors.....	281
8.7	Sensor Design for Desired Performance—Mechanical Transducers.....	287
8.8	Signal Conditioning	295
8.9	Summary.....	297
	Problems	297
Chapter 9 Modeling Transducers: Actuators		303
9.1	Electromagnetic Actuators	303
9.1.1	Linear.....	303
9.1.2	Rotational Actuators: Motors	314
9.1.2.1	Permanent Magnet DC Motor.....	316
9.1.2.2	Motor Load.....	322
9.1.2.3	Parallel Wound Motor (Shunt)	323
9.1.2.4	Series Wound Motor	327
9.1.2.5	Separately Excited DC Motors	332
9.1.3	Example of a Motor That Is Driving a Load	332
9.2	Hydraulic Actuators	336
9.2.1	Hydraulic Cylinders	336
9.2.2	Pumps.....	337
9.2.3	Hydraulic Valves.....	338
9.3	Summary.....	345
	Problems	345
Chapter 10 Modeling Vehicle Systems.....		351
10.1	Vehicle Systems	352
10.2	Vehicle Dynamics	358
10.2.1	Ride: Heave and Pitch Motion	358
10.2.1.1	Transformer Parameter Calculation	362
10.2.1.2	Active Dampers	369
10.2.2	Handling: Bicycle Model	371

10.3	Vehicle Systems	374
10.3.1	Electric Braking	374
10.3.2	Power Steering Model	377
10.3.3	Steer-by-Wire System (SBW).....	380
10.4	Energy Regeneration in Vehicles	386
10.4.1	First Square Wave Generator.....	388
10.4.2	Second Square Wave Generator.....	390
10.5	Planar Rigid Body Motion.....	390
10.6	Simple Engine Model: A Different Approach	399
10.7	Summary.....	402
	Problems	403
Chapter 11 Control System Modeling		405
11.1	PID Control	407
11.1.1	Proportional Control	407
11.1.2	Proportional Integral Control	411
11.1.3	Proportional Derivative Control.....	413
11.1.4	Proportional Integral Derivative Control.....	416
11.1.5	Ziegler–Nichols Closed Loop Method.....	422
11.2	Control Examples.....	422
11.3	Nonlinear Control Examples	427
11.3.1	Inverted Pendulum.....	428
11.3.2	Motor	432
11.3.3	Controller	433
11.4	Summary.....	441
	Problems	441
Chapter 12 Other Applications		443
12.1	Case Study 1: Modeling CNC Feed-Drive System	444
12.1.1	Bond Graph Modeling of an Open and Closed Loop System	446
12.1.2	Backlash, Stick–Slip, and Cutting Force.....	451
12.1.2.1	Backlash.....	451
12.1.2.2	Stick–Slip Friction	453
12.1.2.3	Cutting Force Model.....	454
12.2	Case Study 2: Developing a System Model for a MEMS Electrothermal Actuator	458
12.2.1	FEA Analysis	460
12.2.1.1	Steps Involved in the FEA Analysis	460
12.2.2	Simulation of ETM Actuator Using 20Sim.....	462
References		469
Bibliography.....		475
Index.....		477

This page intentionally left blank

Preface

Many years ago when I was an undergraduate student of mechanical engineering at Indian Institute of Technology, Kharagpur, India, Professor Amalendu Mukherjee was our teacher for a course on systems and controls. Probably a year or two before this, he had come across an intriguing technique for systems modeling called bond graphs. He was very excited about it and was quickly becoming an expert in this area. The great teacher that he was, he got equally excited about teaching this technique to as many of his students as possible. Our class was, therefore, one of the first in the institute to learn about bond graphs and the joy of bond graphing. I cannot say that bond graphing was a joy to everyone in the class. There were probably three broad opinions in the class about bond graphs. Some did not care; to them this was just another one in a list of courses that they had to take. A second group just did not get it! But by far the largest group was the one that felt an increased level of excitement as they learned something that was logical, easy once you got the basics, and powerful. In retrospect, probably the excitement was more because of a great teacher's ability to convey the material than the material itself. Nevertheless, many of us were bitten by the bond graphing bug.

In pursuing advanced studies, I was taken away from the systems modeling world because of other academic interests. But many years later, I had the opportunity to develop and teach courses in the area of mechatronics. Even when I first learned about bond graphs, the unifying nature of the topic appealed to me a lot. That was when I first realized that mechanics, circuits, and hydraulics are not so far apart from each other as they have been thought to be. If one starts looking at the forest rather than the trees, a very unifying theme emerges.

Naturally, for the multidisciplinary area of mechatronics, I felt that bond graph-based modeling would be an ideal fit. Once I reviewed what had happened in bond graphing since I had first been excited by it, I found that I was not the only one making the connection between bond graphs and mechatronics. Many established researchers in the field had already connected those dots. Karnopp, Rosenberg, and Margolis (2006) modified their text and its title to reflect this connection. Others, such as Hrovat et al. (2000), Margolis and Shim (2001), DeSilva (2005), Brown (2001), have been making significant contributions to mechatronics research and were using bond graphs as the modeling tool.

When we first learned about bond graphs in our course on systems and controls, we came away with the idea that the technique was rather exciting, but we were unsure about its practical use. Most of us thought that perhaps only about a handful of excited researchers, such as Professor

Mukherjee, were going to use it. In the many years that have passed since my undergraduate days, several software tools have come to the market. 20Sim, CAMP-G, AMESIM, and Professor Mukherjee's very own SYMBOLS 2000 are now all commercial tools, which means people are using them to solve real problems.

Why are bond graphs well suited for mechatronic systems? Engineering system modeling has always been multidisciplinary in nature. A review of any of the classical texts in system modeling, such as Ogata (2003), reveals this fact. In the mechatronic systems world, it is more so the case. In traditional approaches to modeling multidisciplinary systems, the governing equations are derived from a combination of Newton's laws, Kirchoff's laws, Bernaulli's equations, and other fundamental governing equations in different domains of knowledge. I have always seen that students have a difficult time dealing with the application of these laws in the derivation of system equations, especially since they almost always have some level of mastery in their own discipline but lack confidence in disciplines that are not theirs. While students struggle with deriving the governing equations for a variety of systems, texts using this traditional approach quickly move to solutions of these equations in time and frequency domains, their meanings, different ways the solutions can be plotted, the information these plots convey, etc. This leads to a situation where even at the end of a course, many students are not confident of developing the equations to model a new system that they encounter.

Bond graphing has three advantages in comparison to the traditional approach. First, it utilizes the similarities that exist between all disciplines so that students learn to see the engineering system as a whole and not in terms of its separate pieces. This is the characteristic we try to teach in a systems course. Second, basic components from different disciplines and their behaviors are categorized under a few generalized elements. So, for example, students are not thinking of capacitances and springs as two different entities, but as the same generalized entity. Third, the bond graph is a visual representation of the system from which derivation of the governing equations is algorithmic. Therefore, it can be automated. As a result of this, students are not struggling with and losing confidence at the early stage of the learning process; they are able to more easily transition to a stage where they can learn about behavior of systems, interpretation of data, etc.

While users of the bond graph methodology claim that it is the "greatest thing since sliced bread," people who have not used it before find it confusing and formidable. Bond graph users sometimes lament about why more people don't "see it their way." I believe it should be the job of bond graph enthusiasts to educate others and introduce them to this technique. Through this text I have attempted to do exactly that. My motivation in writing this book is to help students, especially the first-time users, get familiar with the technique and develop confidence in using it. If an introductory

mechatronics course is a first course in a mechatronics sequence, this text is intended to be for a second course in that sequence. It is assumed that students have some idea about mechatronics systems, its different components, and have had some hands-on experience with some of them prior to learning how to model mechatronic systems. The structure of this book and the handling of different topics have been done with this goal in mind. I have purposely stayed away from elaborate mathematical derivations and proofs. There are many texts that address that information. I have tried to deal with the method from the perspective of a modeler who is seeking results. Key concepts are uncovered slowly with a lot of rudimentary examples at the early stage so that readers can develop some confidence in their ability to use the method. In the second half of the book, when readers have potentially learned how to develop bond graph models, I have included simulation results for most of the examples that are part of the text. This ensures that readers can model, simulate, and practice as they progress through the chapters. Although the models can be simulated using any software tool that can handle bond graphs, 20Sim has been used for all the simulation work in this text. A free version of 20Sim can be downloaded from the software Web site. I would strongly encourage readers to model the examples in this text for themselves. There is no better way to learn than to try things out for oneself.

This book is not a result of many years of research on this topic. Rather, it is a result of several years of teaching this topic. Hence, I have tried to focus on the student who is learning this topic for the first time. If students benefit from this work it will be the biggest reward for me. Also, I consider this text as a “work in progress.” Already I feel that other topics could have been added to make the book more comprehensive. But I will be realistic about goals and deadlines and hold those back for some future publication.

This page intentionally left blank

Acknowledgments

Although only one person's name is listed as the author, there are always a few other individuals whose contributions are vital in any successful production. First and foremost I would like to thank my friend and colleague Dr. N. Mohankrishnan, professor of electrical engineering at University of Detroit Mercy. Our initial discussions over coffee led to many years of interdisciplinary curriculum development, teaching, and research. I would also like to thank my good friend and colleague Dr. Sandra Yost, the other member of our three-person mechatronics team. Our initial effort in designing and offering courses in mechatronics was supported by the National Science Foundation through two very generous grants (National Science Foundation Award IDs 9950862 and 0309719). This support enabled us to develop three very successful courses: Introduction to Mechatronics; Sensors, Actuators and Emerging Systems; and Modeling and Simulation of Mechatronic Systems. All three of these courses are regularly offered at University of Detroit Mercy. This book was born out of the material used to teach the third class in this list. The author is indebted to all of his current and former students who have directly or indirectly contributed to this text. Some of the examples used in the text were developed from the end-of-term projects carried out by individuals in this course. Within this group, I would like to especially mention Reta Elias, Divesh Mittal, Tony Copp, Vishnu Vijaykumar, Srinivas Chandrasekharan, and Pariksha Tomar.

I would especially like to mention Professor Amalendu Mukherjee of the Indian Institute of Technology in Kharagpur, India, for introducing me to bond graphs when I was a senior undergraduate. He is an inspiring teacher and left a lasting impression on me with his teaching style. Special thanks to the CRC team who made this book possible: Jonathan Plant, senior editor, who took special interest in this project and guided me through the whole process of publishing; Marsha Pronin, who coordinated the whole project; Arlene Kopeloff, who made sure that I was able to meet all the deadlines and requirements that were needed to keep this project moving along on schedule; and the editorial team at CRC and the production team at diacriTech.

And finally, this book would not have been possible without the support, sacrifice, and encouragement of my friends and family, especially my parents, Sunil and Chameli Das, my in-laws, Nirmal B. and Jharna Chakrabarti, my wife Mitali Chakrabarti, and my daughter Madhurima.

This page intentionally left blank

Author

Shuvra Das is a professor of mechanical engineering at University of Detroit Mercy. He received his undergraduate degree from the Indian Institute of Technology in Kharagpur, India in 1985. Both his master's and doctoral degrees in engineering mechanics are from Iowa State University.

Dr. Das's research and teaching interests include engineering mechanics, computational mechanics using finite and boundary element methods, modeling and simulation, inverse problems, mechatronics, condition-based health monitoring of engineering systems, etc. He has written over 50 conference and journal publications and has received several awards including the best teacher award from the North Central section of ASEE in 2002 and the Junior Achievement Award at University of Detroit Mercy.

This page intentionally left blank

1

Introduction to Mechatronics and System Modeling

1.1 What Is Mechatronics?

The word mechatronics was coined by Japanese engineers sometime in the mid-1960s and is derived from the words mechanical and electronics. Mechatronics has now become synonymous with multidisciplinary engineering systems that comprise mechanical, electrical, hydraulic, magnetic, and so forth, components working together in a synergistic manner. One vital ingredient in a mechatronic system that is not part of the term itself is a computer or brain (or decision maker). A Mechatronic system, therefore, contains multidisciplinary components integrated through a computer or decision maker.

The most commonly used definition for a mechatronic system is: a synergistic combination of precision mechanical engineering, electronic control, and intelligent software in a systems framework, used in the design of products and manufacturing processes.

It is hard to pinpoint the origin of this definition since it is found in so many different sources, including the 1997 article in *Mechanical Engineering* by Steven Ashley (1997). Giorgio Rizzoni, professor at Ohio State University, defined it as “the confluence of traditional design methods with sensors and instrumentation technology, drive and actuator technology, embedded real-time microprocessor systems, and real-time software” (Rizzoni 2004). Other similar definitions are

- The design and manufacture of products and systems possessing both a mechanical functionality and an integrated algorithmic control
- The interdisciplinary field of engineering dealing with the design of products whose function relies on the integration of mechanical and electronic components coordinated by a control architecture
- Putting intelligence onto physical systems
- Designing intelligent machines

These are all similar sounding statements and convey the same kind of information about mechatronics. Figure 1.1 shows a schematic that represents this field. It is obvious from all these definitions and the schematic that mechatronics refers to a multidisciplinary field. What is not obvious is that the concept of “synergy” is a vital part of mechatronics. Synergy implies a new way of designing these systems. In the past, electromechanical devices were designed in a sequential manner; that is, the mechanical device was designed first by mechanical engineers who then handed the design over to the electrical engineers to add on the electrical components. The electrical engineers then handed the design over to the control engineers who had to come up with a control strategy. Synergy in mechatronics implies that engineers from different disciplines are involved in the product design together and right from the beginning. This ensures that the process is concurrent in nature and the product uses the best technology and is the most efficient.

Figure 1.2 shows the flow of information within a mechatronic system. At the core of the system is a mechanical system, for example, an autonomous vehicle such as the one shown in Figure 1.3. The state of the system is determined by sensors. For this particular autonomous vehicle, sensors such as proximity switches, sonar, and so forth, were used. Information gathered by the sensors is passed to an onboard microcomputer. Since sensor data is analog and computers only work with digital information, analog to digital conversion is necessary prior to sending the data to the computer. Once sensor information is received by the computer, it decides a course of action as per the programmed algorithm. In the vehicle shown in Figure 1.3, a PIC based microprocessor called Basic Stamp II was used for

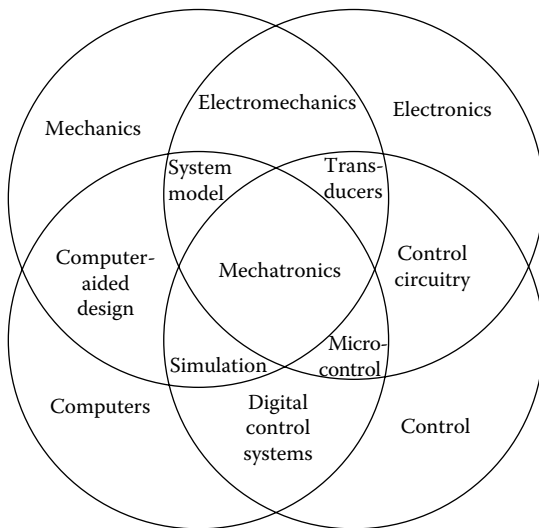
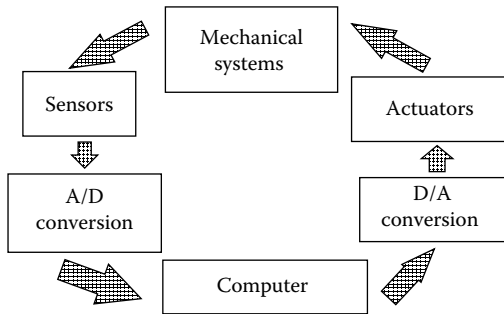
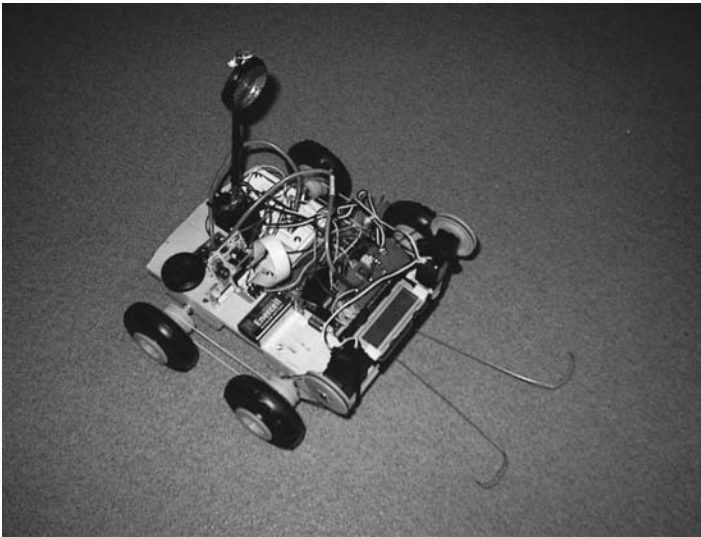


FIGURE 1.1
Schematic showing the field of mechatronics.

**FIGURE 1.2**

Flowchart showing the flow of information in mechatronic devices.

**FIGURE 1.3**

Mechatronic system: An autonomous vehicle.

this purpose. A signal is sent to the actuators, which takes some action on the mechanical system. The actuators used in this autonomous vehicle were two servo motors attached to the wheels of the vehicle. Just as the sensor–computer interaction requires analog to digital conversion, computer–actuator interaction will require digital to analog conversion of data as well. In a way, the behavior of mechatronic devices mirrors the way human bodies work. At the core is a mechanical system, the human body. The sensors—eyes, ears, and so forth—gather information about the surroundings and the information is sent as signals to the brain, the computer. The brain makes decisions that are then transmitted to the muscles (the actuators); the muscles move the system in the manner desired.

Concepts of mechatronics are particularly vital in today's engineering world because boundaries between traditional engineering disciplines are breaking down in new products. If we consider a reasonably complex machine, such as the automobile, we realize that with the passage of time the automobile has changed drastically. The basic functionality of an automobile, that is, using power derived from an internal combustion engine to drive the vehicle along a path as per the desire of the vehicle's controller or the driver, has not changed. However, the way this function is achieved in an optimal manner has changed significantly. Over time and with technological advancement, less efficient systems have been replaced by more efficient ones. In recent times, this has resulted in many purely mechanical devices and subsystems being replaced by mechatronic or electronic ones. Fuel injectors are nothing new in modern automobiles; they replaced less efficient carburetors quite sometime ago. Antilock brakes are important safety devices and are becoming part of the basic package for all automobiles. Similarly "by-wire" subsystems such as drive by-wire, brake by-wire, steer by-wire, and smart suspensions are systems that are slowly becoming adapted for automobiles. In all of these cases, the more efficient mechatronic systems are replacing the less efficient, purely mechanical ones. It seems that we have reached the efficiency limits of purely mechanical devices. To get any further improvements in efficiency, multidisciplinary or mechatronic devices are necessary. *Mechanical Engineering* magazine published an article a few years ago titled "The end of ME?" (Huber and Mills, 2005). It raised the question as to whether the discipline of mechanical engineering as we know it is coming to an end.

It is quite clear that mechatronics is a buzzword that has become very popular due to a practical necessity derived from technological progress. Today's engineers can no longer confine themselves to the safe haven of their own familiar disciplines. The technological world will force them to venture into multidisciplinary territory. The sooner they can adapt to this the better suited will they be for success.

During the last few years, many textbooks have been published on the topic of mechatronics. Some of them are by authors such as Cetinkunt (2007); Alciatore (2005); De Silva (2005); Bolton (2004); Shetty and Kolk (1997); Karnopp, Margolis, and Rosenberg (2006); and Brown (2001) (see References). All except the last two are introductory texts on the topic of Mechatronics and they all do a good job of introducing the topic.

1.2 What Is a System and Why Model Systems?

We have discussed that at the core of the mechatronic world is a mechanical system. We have all come across terms such as engineering systems, transmission system, transportation system, digestive system, financial system,

system engineering, and so on. These are terms used in different domains with the common theme being the concept of a “system.” A system may be defined as an entity that is separable from the rest of the universe (the environment) through physical and/or conceptual boundaries. The system boundary is a logical separation between what is inside the boundary and what lies in the outside world. Although a system is separable from the surroundings, it can interact with the surroundings (Karnopp, Margolis, and Rosenberg, 2006). Systems can receive information and energy from the outside world and also send out information and/or energy (Figure 1.4). Systems may be made of interacting parts such as subsystems, and subsystems are made of components. For example, an automobile can be considered an engineering system that interacts with the surroundings. It receives input from the surroundings such as input from the driver, friction from the road, and wind drag; it releases exhaust and heat, makes noise, and so forth. The automobile is made of many subsystems such as the drive train, transmission, brakes, and more. These subsystems are in turn made of components such as pistons, gears, bearings, and pumps, for example. While systems are made of components (or subsystems), a system is much more than just the sum of all its parts. Even though the parts that make up a system can be well designed and work well independently, it does not necessarily mean that the system will function well when these components are all put together. Ensuring that the system functions well after assembly is not a trivial task and has to be done well. For a successful final product, a “systems viewpoint” is therefore very important.

Systems are dynamic as nature; that is, with the passing of time their behavior changes in response to varying external inputs. So understanding any system’s dynamic behavior is much more important than knowing its static behavior. An understanding of system behavior is a core requirement of taking a “system viewpoint.” Models of systems are very useful tools for understanding dynamic behavior of systems. System models may be

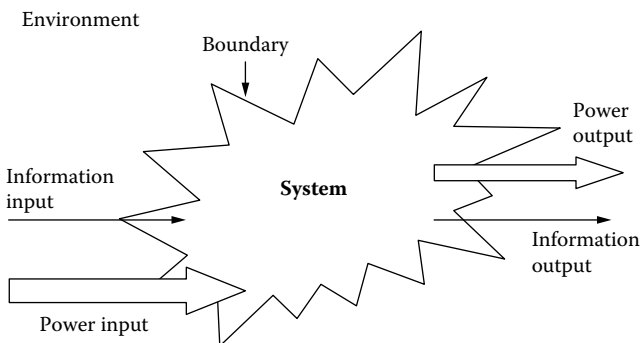


FIGURE 1.4

Schematic showing system, system boundary, and inputs and outputs.

scaled physical models or mathematical models. Scaled physical models may be physical prototypes and provide a hands-on understanding of system behavior. For many real-life systems, building physical models may often be cost prohibitive or not possible for other reasons. At the conceptual design stage, building a physical model is not possible either. Mathematical models are much cheaper to construct and are extremely powerful if they are constructed properly. Building useful mathematical models requires a good understanding of system behavior at the component level, and the model builder needs to make realistic assumptions. Just as the name suggests, a model is a representation of a system, but it is not necessarily the whole system. Models always involve some simplifications that are a result of assumptions made by the developer. The actual assumptions may vary from one situation to another, but some of common approximations that are typically used for system modeling are

- Neglect small effects: Include the dominant effects but neglect effects that have relatively small influence.
- Independent environment: The environment is not affected by what happens in the system.
- Lumped characteristics: Physical properties for system components are assumed to be lumped even though they are, in reality, distributed across the geometry.
- Linear relationships: Constitutive relationships are assumed to be linear over the range of operation of the system even though, in reality, they may not be exactly linear.
- Constant parameters: Parameters defining component properties are assumed to be constant.
- Neglect uncertainty and noise: Any uncertainty or noise in the data are neglected.

As a result of making these assumptions, the governing equations in the system model turn out to be a set of linear ordinary differential equations with constant parameters. The solutions of these ordinary differential equations are relatively easier to obtain, and they describe the dynamic behavior of the system. If these simplifying assumptions are not made, the equations would be a set of nonlinear partial differential equations with time and space varying parameters. This later set of equations would perhaps yield a more accurate mathematical model of the system, but would not be very useful because these types of equations are much harder to solve. Without good and efficient solution techniques, the model would not yield results that would be useful for engineers. The advantages gained by making the simplifications far outweigh the bits of information that get lost due to these assumptions.

Mathematical system models and their solutions become powerful tools in the hands of system designers. They can be used for answering different questions such as:

- Analysis: For given input and known system (and state variables), what would be the output?
- Identification: For given input history, the output history is known; What would the model and its state variables be?
- Synthesis: For given input and a desired output, can a system be designed (along with its state variables) such that the system performs the way desired?

Learning how to develop useful system models takes time and experience. We therefore go about the three listed activities in the order that they are stated. Beginning system modelers spend a lot of time learning to “analyze” systems. Only after a good bit of experience do they venture into system “identification.” And “synthesis” requires the maximum amount of experience in the field.

Because a model is somewhat a simplification of reality, there is a great deal of art in the construction of models. An overly complex and detailed model may contain parameters virtually impossible to estimate and introduce irrelevant details that may not be necessary. Any system designer should have a way to find models of varying complexity so as to find the simplest model capable of answering the questions about the system under study. A system could be broken into many parts depending on the level of complexity one needs. System analysis, through a breakdown into its fundamental components, is an art in itself and requires expertise and experience.

In this book we will go through a systematic methodology of developing models of engineering systems so that their dynamic behavior may be studied. Unless otherwise specified, we will always make the assumptions that we have discussed here. Model development and its use will be focused mainly towards the process of analyzing system behavior. We hope that with some practice in the area of system analysis, students would be ready to start tasks in system identification and design.

1.3 Mathematical Modeling Techniques Used in Practice

Many different approaches have been used in the development of system models. One of the most common methods is deriving the state-space equations from first principles, specifically Newton’s laws for mechanics, Kirchoff’s voltage and current laws for electrical circuits, and so forth. These

bonds that connect different blocks in the model transmit information about a single variable. In bond graphs the bonds transmit information of two variables, the product of which is power. Figure 1.6 shows the bond graph representation of the same motor whose signal flow model is shown in Figure 1.5.

In our presentation here we have chosen the bond graph approach to model systems. The most important reason for this is that within the bond graph method, basic components that make up systems in different disciplines may be represented using a few generalized components. The similarities that already exist among the different disciplines are used very efficiently by this method. Thus, this method is very well suited for modeling mechatronic systems. Bond graph method is based on the flow of power. Power is a product of two quantities, force and velocity or voltage and current (these are called effort and flow as generalized quantities). Every component in a mechatronic system has to deal with these two quantities that make up power. Drawing of the bond graph representations is algorithmic and, as a result, the user can become productive quite quickly. The derivation of equations from the bond graph representation of a system is algorithmic as well, so a computer program can easily do it. Even if the user has to derive the mathematical equations, the algorithmic approach is a lot more robust and confidence generating for the user than any other method. All these advantages make the bond graph method a very powerful tool for modeling mechatronic systems.

Figure 1.7 shows a schematic of how the bond graph method works. A bond graph model showing power flow among different system components is drawn. The bonds are assigned causal information to the bonds. This leads to the process of deriving the governing equations for the system. The equations, also called the state-space equations, are a set of coupled ordinary differential equations. These equations are solved numerically (usually). And the solution provides information about system response.

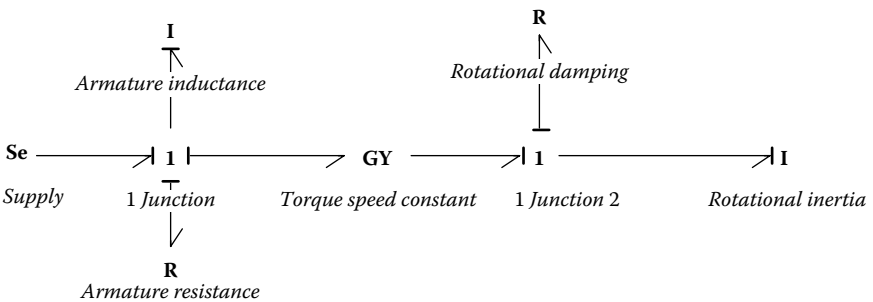
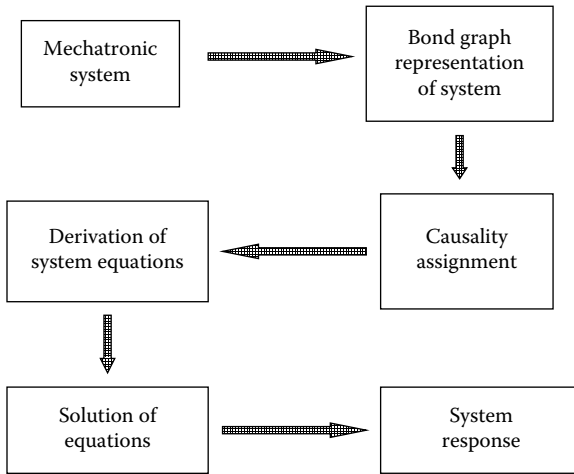


FIGURE 1.6

A bond graph representation of a permanent magnet DC motor.

**FIGURE 1.7**

Flowchart showing the bond graph based modeling process.

1.4 Software

Several commercial software tools use bond graphs to model systems. 20Sim, Symbols2000, AMESIM, and CAMP-G are four such tools. Using the editing features of these tools the user may build up the bond graph model and then perform necessary simulation studies. Most of these tools have an object-oriented modeling feature as well. This means, for example, that if the user wants to use a motor in a model, an object icon for a motor already exists in the software database and the user just needs to add it to the model. This feature makes modeling even easier for people who do not want to deal with the details of what happens within these objects but want to focus entirely on putting together a system model. Underneath the object icon, though, the model is still bond graph based in these tools.

In this text we have used 20Sim for all the simulation models and analyses results that have been reported. This is only because the author is most familiar with this particular tool and has had a very pleasant experience working with it. 20Sim has a very user-friendly editing capabilities that the user can build a bond graph model with quite quickly. The solution algorithms are robust as well as fast. The user can quickly visualize the result of their work. Users can easily revise the constitutive relationships for all the basic components in order to model advanced behavior. One of the things I have tried to do throughout the text is perform simulations

and demonstrate how the simulation results look for almost every example model that has been developed. I feel this is necessary for students learning this technique for the first time. In the example simulations included in the book, I have not put great effort in using exact representative data. In a few cases when such data was readily available, I have made use of it. But in many others, I have made it up using engineering judgment. Also, in some example simulations, I have specified units for parameters and in others I have not. In cases where units are not specified, parameters used are still in consistent units; throughout this text I have used SI units only.

Problems

- 1.1. Choose a mechatronic system or subsystem. Some possible examples are steer-by-wire, autofocus camera, disk drive, scanner, and microwave. Study the physical system (if available) and or information about the system carefully to understand the system boundaries, what type of input the system receives, and what output it provides. If you designed such a system, what would possible design specifications be? What are some of the design constraints? What sensors and actuators would be used in this system?
- 1.2. One of the mechatronic systems that has been in the news a lot is the Mars Rover. The Mars Rover has been very successful in a harsh environment and at a remote location. Research the Mars Rover, and identify the different components that make this a mechatronic system. Also research how the designers achieved the solution to tough design problems associated with the Mars Rover and its mission.
- 1.3. Many of the systems in today's automobile have transitioned from purely mechanical to mechatronic systems. Pick one such system, and identify how the task this system did was done in the old design versus how it is done in the newer version. What components are replaced and with what have they been replaced?

This page intentionally left blank

2

Bond Graphs: What Are They?

System modeling has evolved along different paths within different disciplines. For mechanical systems, traditional training teaches us to rely on Newton's equations of motion to model system behavior, while for electrical circuits, Kirchoff's laws determine the basic system behavior. For hydraulic systems sometimes the electric circuit analogy is used as well. The different disciplines that we mention here, such as mechanical, electrical, hydraulic, and so forth, are artificial divisions we have used for many ages to study system behavior. These artificial divisions were formed a long time ago to handle information as well as for the purposes of keeping education and training manageable. Real-world systems often contain components from many different domains interacting with each other. Although the analysis techniques developed by experts in various disciplines have been different, the inherent behavior of systems is essentially the same. The underlying governing law is the same, that is, conservation of energy (or power). Leibnitz alluded to this concept (Mukherjee and Karmakar, 2000) when he stated, "The forces are of two kinds, namely dead and live. The dead force depends on position and/or configuration, and the live force is proportional to the square of velocity. The sum of the two forces in the universe remains constant." If the word force is replaced by the word energy, Leibnitz was actually stating the conservation of energy principle. Even though the immediate successors of Leibnitz and Newton found that the problems of mechanics are more easily solved using the energy approach, the Newtonian approach of using actions and reactions became more popular. Part of the reason may be because the concept proposed by Leibnitz and its usefulness was unclear as many other areas of the physical sciences (such as electricity and magnetism) were not yet developed at that time.

In the study of engineering systems, the diverse methodologies that exist within different disciplines, their unique terminology, and names for components pose a problem for students and experts whose training is in one but not all disciplines. The need for a more unifying approach was felt a long time ago. Bond graphs is one method that provides a very logical and succinct way of dealing with the variety from different disciplines.

In the 1960s Professor H. M. Paynter of MIT proposed a method of system modeling that was both unifying and algorithmic. He called the technique bond graphs, and it is based on power flow diagrams (as opposed to signal flow) and is independent of physical domain. The approach is simple yet very powerful, especially when one is working in areas that

are multidisciplinary. Although earlier applications of bond graphs were confined to mechanical and electrical systems, future developers such as Karnopp, Rosenberg, Thoma, Brown, and others, have successfully applied the bond graph technique to systems such as hydraulic, thermodynamic, magnetic, and even in many social science applications.

When it was developed (in the mid-1960s), only a small group of individuals realized its importance. Now, when artificial barriers between different disciplines are breaking down and new interdisciplinary areas such as mechatronics, biomechanics, MEMS, and NEMS are becoming so important, the need for a modeling technique such as bond graph is paramount. In the rest of this chapter, we will discuss more about bond graphs—how they are developed, what they represent, and more. Therefore, the overall objectives of this chapter will be to

- Introduce students to bond graphs, its basic concepts and usefulness.
- Discuss the concepts of energy exchange and relate it to flow and effort exchanges.
- Introduce the generalized variables of power and energy.
- Discuss all the basic elements that could occur in a bond graph model.
- Highlight many of the conventions used and their meanings.

2.1 Engineering Systems

Real engineering systems are multidisciplinary. Consider any of the many engineering systems that we use in our daily lives. For example, the automatic car window system is a basic feature of most modern automobiles. The purpose of this system is to move the glass window up or down as per instructions received from the user in the form of a button push. The power needed to move this reasonably heavy piece of glass is provided by an electric motor. There is a logic circuit that has to determine the action based on the intention of the user, such as holding the window at a desired height, moving it all the way up or down, and so forth. Although it is not yet available in automatic window systems, a form of safety device using sensors is being developed as well. The safety system would stop the window if a child's (or an adult's) hand got caught between the moving window and the door frame. We see, therefore, the system consists of components from at least two disciplines. The window (and its inertia) is mechanical, the motor is an electrical device, and there is a control system, some possible sensor use, and safety features. To model the behavior of this system, one needs to consider the behavior of all its components, which happen to be from different disciplines of engineering.

In the car window system, at least two domains are involved. In any mechatronic system many other domains may be involved as well. Examples of physical phenomena (or domains) involved in real engineering systems are

1. Mechanical translation
2. Mechanical rotation
3. Hydraulic
4. Electrical (static and current) and electronics
5. Magnetic
6. Thermal

In a sense all these domains are artificial divisions that have been used for ease of operation. In the bond graph and other energy-based approaches in system modeling, it will be apparent that many components in different domains are quite similar in behavior. In the bond graph technique we will use this similarity to our advantage.

Systems are divided into subsystems, which can be subdivided into components. For example, an automobile can be considered a system that consists of many subsystems such as: drive train, steering, braking, exhaust, and so on. Subsystems are in turn made of components that behave in a predictable manner. Component behavior is determined by its constitutive relationship, that is, every component's behavior follows some basic law of physics. For example, the behavior of a spring (an elastic element) is governed by the simple linear spring equation where the displacement and the force are linearly related to each other through the spring constant:

$$\text{Force} = \text{spring constant} * \text{displacement} = kx$$

Or the voltage drop across an electrical resistance in a circuit is equal to the product of the resistance value and the current that is passing through it:

$$\text{Voltage} = \text{Resistance} * \text{Current} = RI$$

In these examples the spring or the electrical resistance are components. These may be part of subsystems that make up more complex systems; and the spring equation and the Ohm's law are constitutive equations for these components respectively. Although the examples used here are both linear, constitutive equations can be nonlinear as well, such as the drag force exerted by the wind on a car driving down the highway is proportional to the square of the velocity of the car. We will discuss the constitutive relationships a little later.

2.2 Ports

As was mentioned earlier, different parts (or subsystems) of an engineering system exchange power. Places at which subsystems can be interconnected are places at which power can flow between the subsystems. Such places (or points on the subsystem) are called ports and actual subsystems with one or more ports are called multiports. Figure 2.1 shows a schematic with two ports. Power enters through one of the ports and leaves through the other. Sometimes the power may be exchanged along one path, which will mean that the subsystem/component has only one port.

A system (or component) with a single port is called a 1-port system (or component). A system (or component) with two ports is called a 2-port system (or component).

Figure 2.2 shows a variety of multiport systems. A motor with electrical input at one port and rotational mechanical output at a second port is a 2-port system. Similarly, a pump can be considered a 2-port system with mechanical torque and rotation coming in at one port and the pressure difference and fluid flow rate exiting at the other port. A slider crank mechanism that converts rotary motion into linear motion (or vice versa) is a 2-port system with rotational power associated with one port and linear power associated with the other.

A separately excited DC motor with two electrical ports and a mechanical port has three ports with power for the magnetic field coming in at one port, power for the armature coming at a second port, and rotational output at the third.

In this context it should be understood that the examples mentioned here are relatively simple. In a real system the level of complexity may be significantly higher. One of the fundamental skills necessary in analyzing/modeling/designing systems is the ability to break down a system into subsystems and components in a way that is useful or understandable for us. This is a skill that has to be acquired through experience, careful observation, and practice in attempting to breakdown real systems into simpler parts. We will offer an example here to illustrate the process.

Figure 2.3 shows a schematic of a system consisting of a motor that is receiving electrical power. The motor rotates a shaft supported on bearings. The shaft is connected to a drum that rotates along with the shaft and raises or lowers a mass that is attached by a cable to the drum. If we

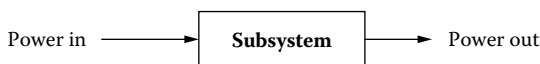


FIGURE 2.1

Schematic showing power flowing in and out of a subsystem.

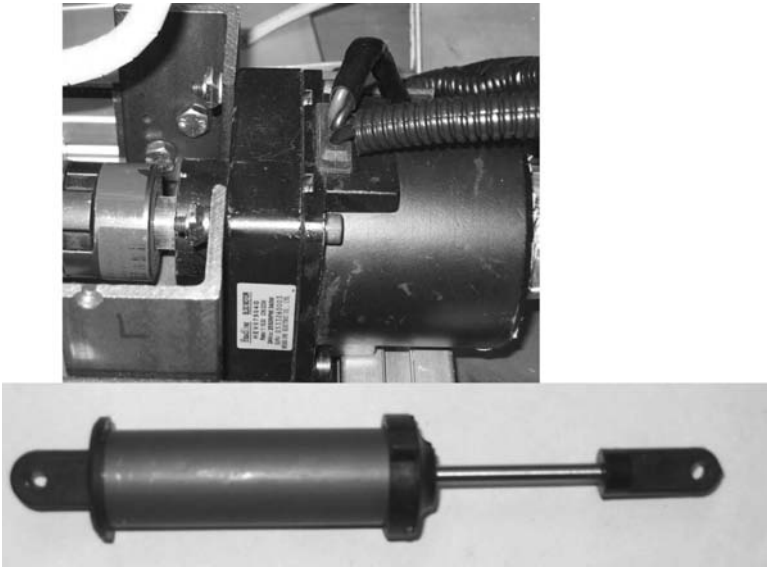
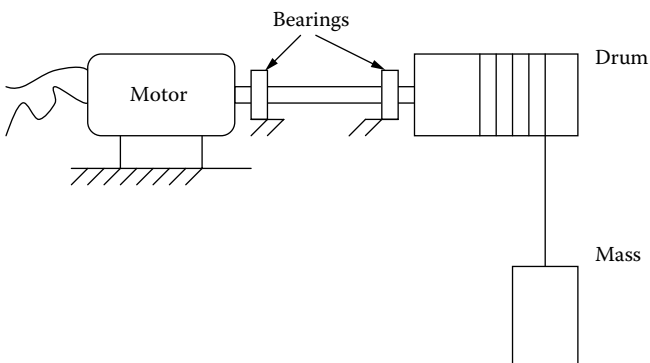
observe closely we can see that the system can be subdivided into several subsystems. One may list them as:

1. Motor
2. Output shaft and bearings
3. Drum, cable, and mass



FIGURE 2.2

Examples of subsystems that have one or more ports (compressors, motors, dampers, speakers, etc.).

**FIGURE 2.2***(Continued)***FIGURE 2.3**

Schematic of a motor driven system.

In coming up with this division we consider the system to be made of three things: the power source (motor), the power transmission (shaft), and the power user (mass hoisting device). Further examinations of these sub-systems indicate that these can be divided into individual components. For example, a DC motor can be modeled as a circuit with an electrical source, an armature resistance, and an armature inductance. The shaft may be treated as a torsional spring, the bearings treated as power dissipative

devices or rotational resistances, the drum is an inertia element, and the cable could be treated as rigid or elastic. If it is assumed to be elastic, then it is a linear spring. The mass that is being hoisted is an inertia element as well. The list of all the separate elements that are in the system will be

1. Armature resistance
2. Armature inductance
3. Electrical power source
4. Rotational spring (shaft)
5. Rotational damping (bearing resistance)
6. Drum inertia
7. Cable, linear spring
8. Hoisted mass
9. Gravity effects on the mass

Apart from these components we also need to recognize that there are two locations in the system where power is being transferred from one domain to another. In the motor, power goes from the electrical domain to rotational domain (via the magnetic domain) and at the drum, power is being transferred from rotational motion to linear translation. Figure 2.4 shows the same system with some more details of the system included.

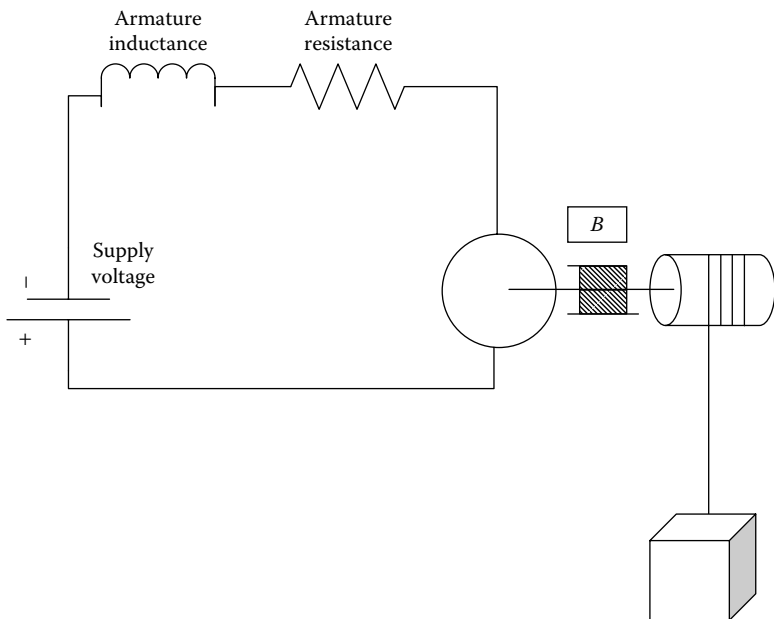


FIGURE 2.4
Schematic of the motor driven system with more details of individual subsystems.

This example illustrates the process of how one can go about dissecting a system to identify all the important subsystems as well as components. While doing this, one has to also identify locations where power conversion from one domain to another happens. This is a critical step in system analysis and modeling and needs to be practiced by students.

2.3 Generalized Variables

Before we start modeling systems and components, we will define a few generalized quantities that will be useful in our discussion. The method that we will use throughout the text is based on power and energy flow. To introduce this concept we will first define four generalized variables. These variables are of two types:

1. Power variables
2. Energy variables

2.3.1 Power Variables

When power travels through a port, the two variables that are actually passing through are called power variables. And the product of these two is equal to power. These variables are also the same two variables that flow from one port to another when two multiports are connected. All power variables are either an effort or a flow. At every port, therefore, there are two power variables:

1. **Effort**, variable denoted as $e(t)$
2. **Flow**, variable denoted as $f(t)$

such that,

$$\text{Power} = e(t) * f(t)$$

2.3.2 Energy Variables

Related to the two power variables are two energy variables. They are

1. **Momentum**, variable denoted as $p(t)$
2. **Displacement**, variable denoted as $q(t)$

Relationship between the variables are

$p(t) = \int e(t) \cdot dt$, is the generalized momentum variable; it can also be thought of as accumulation of effort over time.

$q(t) = \int f(t) \cdot dt$, is the generalized displacement variable; it can also be thought of as accumulation of velocity over time.

The energy variables may be used to represent the energy in two possible ways.

Since power is the rate of change of energy, we can write:

$$E = \int (\text{Power}) dt = \int e(t) \cdot f(t) dt = \int e(q) \cdot dq(t) = \int f(p) \cdot dp(t) \quad (2.1)$$

This means energy can be written either as a function of displacement variables or as a function of momentum variables, as follows:

$$E(q) = \int e(q) \cdot dq \quad (2.2)$$

or

$$E(p) = \int f(p) dp \quad (2.3)$$

For example, kinetic energy associated with a mass moving at a velocity may be written as K.E. = $\frac{1}{2} (mv^2) = \frac{1}{2} m (mv)^2 = \frac{1}{2} m (p)^2$, a function of momentum.

And potential energy associated with a mass held at a certain height may be written as P.E. = $mgh = mg(q)$, a function of displacement.

2.3.3 Tetrahedron of State

A graphical representation of the relationships between the four generalized variables just defined is through the tetrahedron of state. As Figure 2.5 shows, the four vertices of the tetrahedron are associated with four different generalized variables: e, f, p, q .

The four generalized variables that make up the tetrahedron of state have specific meanings within different engineering domains. We will consider some of them here. In the domain of mechanical translation, the effort variable is the force, and the flow variable is the velocity of motion. The momentum variable is the linear momentum (mass \times velocity), and the displacement variable is the distance moved. In the electrical domain, the effort variable is the voltage drop or potential difference and the flow variable is the current (flow of charges). The displacement variable is the accumulation of current, that is, charge. The momentum variable in the electrical domain is a lesser-known quantity called flux linkage. Table 2.1 lists all the variables and their units within four

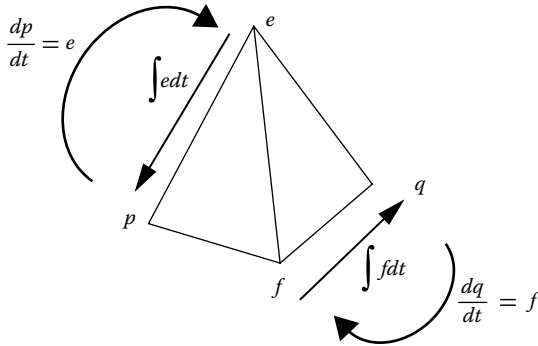


FIGURE 2.5
Tetrahedron of state.

TABLE 2.1
Generalized Variables in Different Domains

Generalized Variables	Mechanical Translation	Mechanical Rotation	Electrical	Hydraulic
e (effort)	Force, F (N)	Torque, T (N-m)	Electric potential, V (Volt)	Pressure, P (N/m ²)
f (flow)	Velocity, v (m/s)	Angular velocity, ω (rad/s)	Current, i ($A = C/s$)	Volume flow rate, Q (m ³ /s)
p (momentum)	Linear momentum, p (N-s)	Angular momentum pT (N-m-s)	Flux linkage variable, λ , (Vs)	Pressure momentum P_p (N-s/m ²)
q (displacement)	Displacement, d (m)	Angle, θ (rad)	Charge, Q , (Coulomb = As)	Volume, V (m ³)
Power	$F * v$ (watts)	$T * \omega$ (watts)	$V * i$ (watts)	$P * Q$ (watts)
Energy	$\int Fdx, \int VdP$	$\int Td\theta, \int \omega dp_r$	$\int edq, \int id\lambda$	$\int PdV, \int Qdp_p$

engineering domains mechanical translation, mechanical rotation, electrical, and hydraulic.

As is clear from the table: even though the effort and flow variables are known by different names in different domains, the product of these two variables is always power. In any system, therefore, when power is transmitted from one part of the system to another, there are actually two of these generalized variables that are involved, that is, the effort and the flow variables. Power can be viewed as the common currency that is exchanged between different parts of any system such that it is always the product of flow and effort.

2.4 Bond Graphs

A bond graph is a mechanism for studying dynamic systems. Bond graphs are used to map the flow of power from one part of a system to another. In the simplest form, a bond graph consists of subsystems linked together by lines representing power bonds.

Let us consider a generic system shown as a schematic in Figure 2.6. A motor is connected to a pump. The motor receives electrical power, and the output from the pump is pressurized fluid at a certain volume flow rate.

This block diagram representation shows the flow of power from one part of the system to another. In a sense this is the starting point of a bond graph representation. This is sometimes called a word bond graph and will be discussed in the next section.

Bond graphs are not the only graphical means of system representation. There are other graphical ways of representing systems. Block diagrams and signal flow graphs are two such well-known techniques. Although they are similar to bond graphs, they are not quite the same. In both block diagrams and signal flow graphs, the links (arrows) used to link parts of a system carry only one type of information. In bond graphs (as discussed a little later) the half-arrows, or power bonds, carry power information that is made of two variables, effort and flow.

2.4.1 Word Bond Graphs

When modeling a complex system, one has to start with a word bond graph. In word bond graphs different parts of the system are represented by their names rather than as specific components. For example, the system just discussed in Figure 2.6 can be represented as a word bond graph in a way shown in Figure 2.7. Two types of arrows are used in bond graphs.

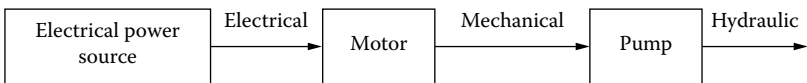


FIGURE 2.6
Schematic showing power path for a multidomain system.

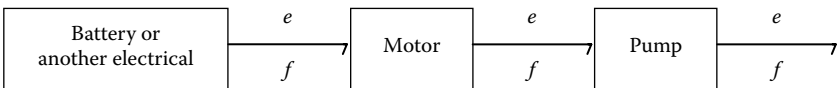




FIGURE 2.7
Word bond graph of the schematic in Figure 2.6.

The half-arrow  is used to represent power bonds; power bonds carry information about two variables and the direction of power bonds indicate the flow of power when it is positive. The full arrow  indicates flow of information with little or negligible power involved. A full arrow will carry information about only one variable and is called a signal bond. An example of the use of signal bond is when a switch is turned on or a signal is used to control a process.

In Figure 2.7 the reader should note that the e and f symbols written above and below the half-arrows represent the flow of effort and flow variables. This is a convention used in bond graphs to reiterate that power bonds are made of flow and effort. A note of caution regarding this convention: while the power bond shows the direction of positive power flow, the half-arrow does not show the direction of either effort or flow. As of now, we do not know their directions. In the next chapter we will be discussing their directions in Section 3.4.

While word bond graphs are good initial steps in representing a system for better understanding, we need to go a few steps beyond them by including individual components in the representation. This is necessary in order to develop a fundamental understanding of system behavior. System behavior is dependent on the behavior of individual components in a system, and we need to incorporate them in the model representation. Consider for example an RLC circuit. Figure 2.8 shows such a circuit. In this circuit, there are four elements: a source of effort (battery), a resistor, an inductor, and a capacitor. They are all connected in series, which means that the current through all of these elements will be the same at any point in time. Also, the power supplied by the battery is divided amongst the other three elements. The shaded arrows in the circuit indicate the flow of power (coming from the battery and being distributed amongst all the other components). The bond graph representation of this system is shown in the figure as well. At this point we are not explaining all parts of the bond graph model, but one can see that the power flow is coming into the system from a source (Se) and is being distributed among three elements (I, C, and R).

Similarly, Figure 2.9 shows a simple mechanical system. It is a spring mass damper system that is being driven by an external force. The shaded arrows show how the power is flowing through the system. The power coming into the system is divided into three parts, one each for the mass, the spring, and the damper which are all attached at one point and this point moves with one velocity. Thus, just as the RLC series circuit has one current flowing through all the elements, the velocity of all the elements at this point is the same. As per this logic, the elements in this mechanical system will also be connected to each other in "series." The bond graph representation, which is directly derived from the power flow in this system, is also shown in the figure and is identical to the bond graph model for the RLC circuit. These examples are presented here to introduce

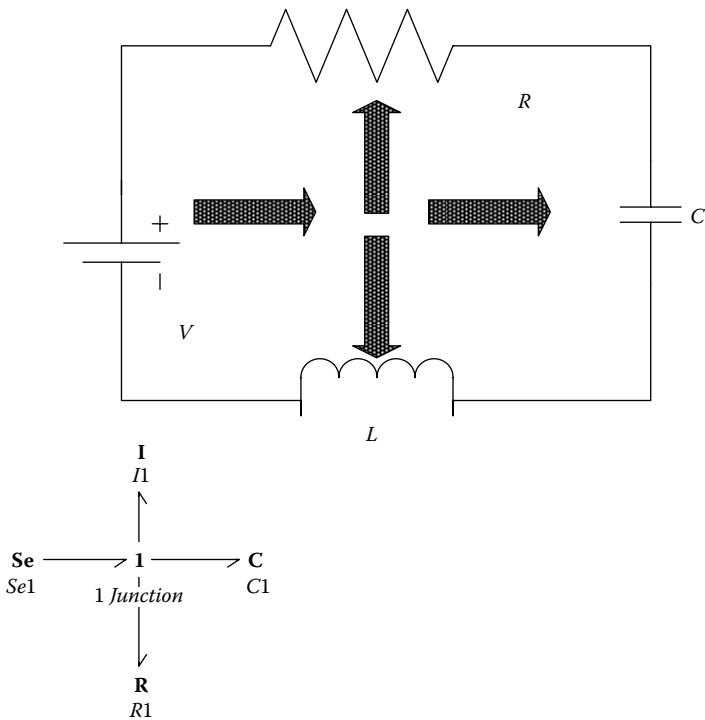


FIGURE 2.8
An RLC circuit and the corresponding bond graph representation.

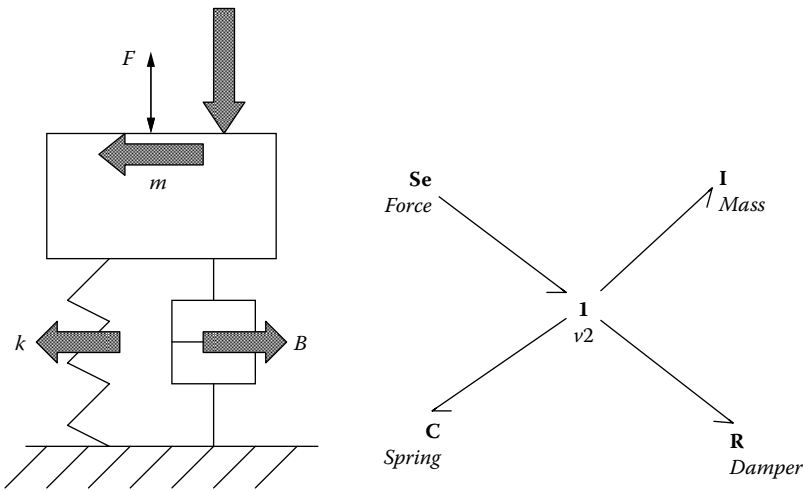


FIGURE 2.9
A spring-mass-damper system and the corresponding bond graph.

the concept of bond graphs and how they could be drawn. These will be discussed in more detail and in a more formal manner in the next chapter. But before we get there, it is necessary to learn about representing a system in terms of all its basic components, because the behavior of all the basic components will determine the system behavior. In the next few sections we will discuss some of the basic components that we would come across in all systems.

2.5 Basic Components in Systems

In our study of the basic components in engineering systems, we will divide them into subcategories as 1-port components, 2-port components, and 3- or higher-port components.

2.5.1 1-Port Components

There are three main 1-port components. These are categorized by the nature of their behavior. One way to understand the differences between these is to consider what type of energy/power is handled by each of these 1-port components. If we consider energy flow as a result of work done on a mechanical system, we have three possible options, as shown in Equation 2.4:

$$\begin{aligned}\Delta W &= F \int v dt = F \int dx = \Delta E_{\text{potential}} \\ \Delta W &= v \int F dt = v \int dp = \Delta E_{\text{kinetic}} \\ \Delta W &= \int (Fv) dt = \Delta E_{\text{dissipative}}\end{aligned}\tag{2.4}$$

Similarly, for an electrical system, the energy flow as a result of energy input to the system has three possible options, as shown in Equation 2.5:

$$\begin{aligned}\Delta W &= V \int i dt = V \int dq = \Delta E_{\text{electrical}} \\ \Delta W &= i \int V dt = i \int d\lambda = \Delta E_{\text{magnetic}} \\ \Delta W &= \int (Vi) dt = \Delta E_{\text{dissipative}}\end{aligned}\tag{2.5}$$

A pattern emerges from the nature of the energy distribution among different types of elements. The potential energy in the mechanical domain is similar in nature to “electrical” energy in the electrical domain. The kinetic energy is similar to the magnetic, and the dissipative energy is similar in the two domains. These similarities are more apparent once one

starts considering the basic variables that constitute these energy expressions. A close look will reveal that they are all made of some of the four generalized variables, and the energy types that are being identified as similar are made of the same generalized variables within the respective domains (e.g., the potential and electrical energies are made of displacement and effort variables, etc.). Similarities such as these exist among these two and other domains, such as hydraulic, thermal, and so forth. Using these energy domains as guidelines, there are three types of basic 1-port elements (that receive energy) and the energy input to a system gets distributed among these elements if they are present. These basic element types are discussed in detail in the next few sections.

2.5.1.1 1-Port Resistor: Energy Dissipating Device

The 1-port resistive element is a power dissipating device, that is, the power that this element receives is lost from the system in the form of heat (most commonly) or in some other form of energy. These elements cannot store energy. Figure 2.10 shows some examples of these types of devices in different domains. There are three common resistance elements: an electrical resistor, a mechanical damper, and hydraulic flow through a tube where there is pressure loss due to wall roughness.

All these resistance elements from different domains behave the same way. These can be represented by a 1-port general resistance element. In the bond graph representation, it is shown as:

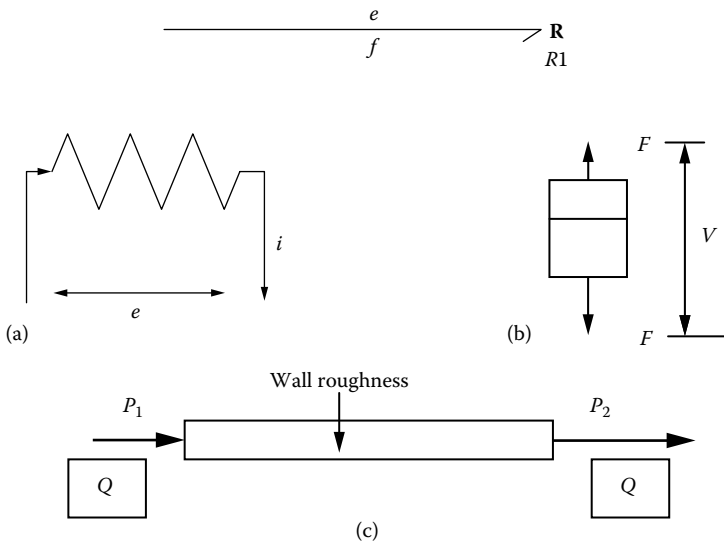


FIGURE 2.10

1-port resistive elements: (a) electrical resistance, (b) mechanical damper, and (c) flow through a tube.

The general constitutive relationship for the resistance element is

$$e = Rf \quad (2.6)$$

For the electrical resistance this relationship is

$$\text{Voltage} = R * (\text{current}),$$

where R is the electrical resistance.

For linear mechanical damping this relationship is

$$\text{Force} = B * (\text{velocity}),$$

where B is the damping coefficient.

For rotational mechanical damping the relationship is

$$\text{Torque} = B * (\text{angular velocity}),$$

where B is the rotational damping coefficient.

For the hydraulic resistance the equation is

$$P = R * (\text{volume flow rate}),$$

where R is hydraulic resistance.

In terms of the generalized variables, the rate of energy dissipated is the product of e and f , the effort and flow variables. Thus, the power dissipated may be written as:

$$\text{Power}(t) = e(t)f(t) \quad (2.7)$$

For the specific domain of electrical systems, the power dissipated may be written as:

$$\text{Power}(t) = \text{Volts}(t)\text{Current}(t)$$

Specific relationships for other domains are listed in Table 2.2.

Although the examples shown here are all linear relationships, the resistance relationship does not necessarily have to be linear. There are many practical situations where the resistance elements could have nonlinear relationships. Some of them will be discussed in this text in due course.

2.5.1.2 1-Port Capacitor: 1-Port Energy Storage Device

The 1-port capacitor is a power storage device that stores and releases energy but does not dissipate it. The constitutive relationship for the

TABLE 2.2

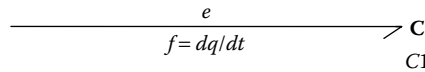
Examples of *R*-Elements

	Domain Specific Relationship	Units for the Resistance Parameter	Power Dissipated
Generalized variables	$e = Rf; f = e/R$		$ef = e^2/R = f^2R$
Mechanical translation	$F = B v; v = F/B$	$B = \text{N-s/m}$	$Fv = F^2/B = v^2B$
Mechanical rotation	$T = B\omega; \omega = T/B$	$B = \text{N-m-s}$	$T\omega = T^2/B = \omega^2B$
Electrical	$V = RI; I = V/R$	$R = V/A = \text{Ohms } (\Omega)$	$VI = V^2/R = I^2R$
Hydraulic	$P = RQ; Q = P/R$	$R = \text{N-s/m}^5$	$PQ = P^2/R = Q^2R$

1-port capacitor relates the displacement variable with the effort variable and can be written as:

$$e = q/C \quad (2.8)$$

The bond graph representation of the 1-port capacitor is



While writing the effort and flow variables above and below the bond, the flow is written as a derivative of the displacement (unlike in the case of the resistance element). This is because the constitutive equation for a capacitive element relates effort and displacement, while the resistive element in the constitutive relationship relates the effort and flow directly.

Figure 2.11 shows some examples of capacitive elements in different domains. The electrical capacitor and the mechanical spring are both capacitive elements. In the hydraulic domain, the potential energy stored

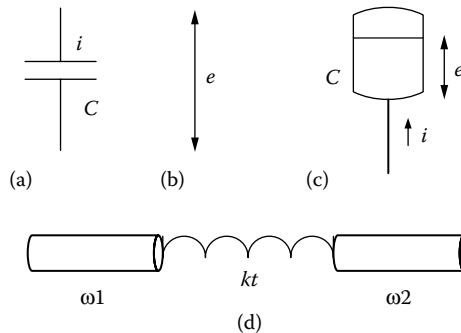


FIGURE 2.11

1-port capacitive elements: (a) linear electric capacitor, (b) mechanical spring, (c) fluid stored at some height or accumulator, and (d) torsional spring.

in a fluid that is stored in a tank at a height serves as a capacitive element. So does an accumulator in a hydraulic circuit. The specific relationships in each domain can be represented as:

For the electrical domain the relationship is

$$V = \frac{Q}{C}; \text{ i.e., voltage} = \text{charge/capacitance}$$

For the translational mechanical domain the relationship is

$$F = k * x; \text{ force} = \text{spring constant (displacement)}$$

For the rotational mechanical domain the relationship is

$$T = k_t * \theta; \text{ Torque} = \text{rotational spring constant (angular displacement)}$$

For the hydraulic domain the relationship is

$$P = V/C; \text{ pressure} = \text{volume/capacitance}$$

Energy stored in these types of devices may be written as an integral of instantaneous power. And instantaneous power is equal to the product of instantaneous flow and effort variables. The derivation below is written for the electrical specific quantities but is applicable for all domains.

$$\begin{aligned} \text{Energy}(t) &= \int \text{Power}(t)dt = \int e(t)f(t)dt = \int V(t)I(t)dt = \int V(t)\frac{dQ(t)}{dt}dt \\ &= \int V(t)C\frac{dV(t)}{dt}dt = \frac{1}{2}CV^2 = \frac{1}{2C}q^2 \end{aligned} \quad (2.9)$$

In terms of generalized variables, the energy stored in a capacitive element can therefore be expressed as:

$$E = \frac{1}{2} \frac{q^2}{C} \quad (2.10)$$

Table 2.3 summarizes pertinent information about capacitive elements in different domains.

2.5.1.3 1-Port Inductor/Inertia: 1-Port Energy Storage Device

The 1-port inductor is a second type of single-port energy storage device. Although, like the capacitor element the inductor is an energy storage device, we need to consider the inductor separately because the constitutive relationship (i.e., the nature of its behavior) is different from the capacitor elements. For the capacitor elements, the constitutive relationship is a relationship between the effort and the displacement variables. For the

TABLE 2.3

Examples of C-Elements

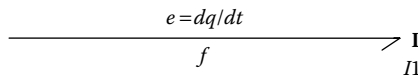
	Domain Specific Relationship	Units for the Capacitance Parameter	Energy Stored
Generalized variables	$E = q/C; q = eC$		$E = \frac{1}{2} \frac{q^2}{C} = \frac{1}{2} Ce^2$
Mechanical translation	$F = k x; x = F/k$	$k = N/m$	$E = \frac{1}{2} kx^2 = \frac{1}{2} \frac{F^2}{k}$
Mechanical rotation	$T = k_t \theta; \theta = T/k_t$	$k_t = N \cdot m / rad$	$E = \frac{1}{2} k_t \theta^2 = \frac{1}{2} \frac{T^2}{k_t}$
Electrical	$V = q/C; q = VC$	$C = A \cdot s / V = Farad (F)$	$E = \frac{1}{2} \frac{q^2}{C} = \frac{1}{2} CV^2$
Hydraulic	$P = V/C; V = PC$	$C = m^5 / N$	$E = \frac{1}{2} \frac{V^2}{C} = \frac{1}{2} CP^2$

inductor elements, the constitutive relationship is between the momentum and the flow variables. The general form of the constitutive relationship is

$$p = If \quad (2.11)$$

where p is the momentum variable, f is the flow variable and I is inertia (or inductor) parameter for the component.

The bond graph representation for the inductor element is represented as:



While writing the effort and flow variables above and below the bond, the effort is written as a derivative of the momentum (unlike the case of the resistance element or the capacitive element). This is because the constitutive equation for an inductive element relates momentum and flow, while for the resistive element, the constitutive relationship relates the effort and flow directly. The specific constitutive relationships in different domain are:

For the electrical domain:

$$\lambda = Li; \text{Flux linkage} = (\text{Inductance}) (\text{current})$$

For the translational mechanical domain:

$$p = mv; \text{momentum} = (\text{mass}) (\text{velocity})$$

For the rotational mechanical domain:

$p = J\omega$; angular momentum = (Polar momentum of inertia) (angular velocity)

For the hydraulic domain:

$P_p = IQ$; pressure momentum = (Hydraulic inertia) (volume flow rate)

Some actual components that behave the same as these types of elements are mass or inertia in the mechanical domain, electrical inductance of a coiled wire that carries a current, and the inertia of a mass of fluid that flows through a conduit. Figure 2.12 shows schematics that represent these types of elements in the different domains.

The energy stored in these devices may be written as an integral of instantaneous power. And instantaneous power is equal to the product of instantaneous flow and effort variables. The derivation below is written for the electrical specific quantities but is applicable for all domains.

$$\begin{aligned} \text{Energy}(t) &= \int \text{Power}(t)dt = \int e(t)f(t)dt = \int V(t)I(t)dt = \int \frac{d\lambda(t)}{dt} I(t)dt \\ &= \int \frac{1}{L} \lambda(t) \frac{d\lambda(t)}{dt} dt = \frac{1}{2L} \lambda^2 = \frac{1}{2} LI^2 \end{aligned} \quad (2.12)$$

In terms of generalized variables, the energy stored in an inductive element can be thus expressed as:

$$E = \frac{1}{2L} p^2 \quad (2.13)$$

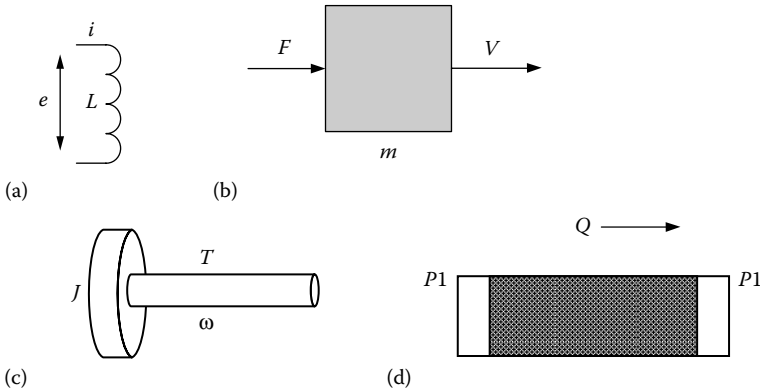


FIGURE 2.12

1-port inductive elements: (a) electrical inductor, (b) mechanical mass, (c) rotational inertia, and (d) fluid inertia.

Table 2.4 summarizes the inductor variables in different domains, as well as the constitutive relationships.

Figure 2.13 shows the tetrahedron of state along with the variables that form the constitutive relationship between them for each type of the three elements discussed so far.

TABLE 2.4
Examples of *I*-Elements

	Domain Specific Relationship	Units for the Inductance Parameter	Energy
Generalized variables	$p = If; f = p/I$		$E = \frac{1}{2} If^2 = \frac{1}{2} \frac{p^2}{L}$
Mechanical translation	$p = mv; v = p/m$	$m = kg = N \cdot s^2/m$	$E = \frac{1}{2} mv^2 = \frac{1}{2} \frac{p^2}{m}$
Mechanical rotation	$p_t = J\omega; \omega = p_t/J$	$J = N \cdot m \cdot s^2$	$E = \frac{1}{2} J\omega^2 = \frac{1}{2} \frac{p_t^2}{J}$
Electrical	$\lambda = Li; i = \lambda/L$	$L = V \cdot s/A = \text{Henry's (H)}$	$E = \frac{1}{2} Li^2 = \frac{1}{2} \frac{\lambda^2}{L}$
Hydraulic	$p_p = IQ; Q = p_p/I$	$I = N \cdot s^2/m^5$	$E = \frac{1}{2} IQ^2 = \frac{1}{2} \frac{P_p^2}{I}$

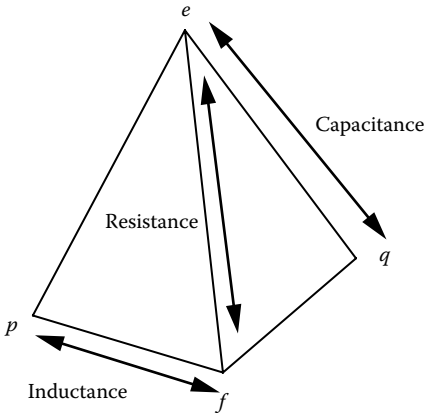


FIGURE 2.13
The tetrahedron of state showing the generalized variables that are in the constitutive relationship for different 1-port elements.

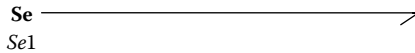
2.5.1.4 Other 1-Port Elements

Apart from the three 1-port elements for energy storage and dissipation, there are two other 1-port elements. These two elements have to do with

sources that supply either effort or flow to any system. Thus, when the power flow is positive, it always flows out of these sources. These two elements are, therefore, represented with the half-arrow pointing away from the element.

Source of effort: These elements supply power to the system such that the effort component of the power is constant and the flow is determined by the load in the system. Some examples of these types of elements are batteries or voltage sources, gravitational force, fluid head, or any known external effort that is acting on a system.

The source of effort is represented in bond graph models as **Se**.



Source of flow: These elements supply power to the system such that the flow component of the power is constant and the effort is determined by the load in the system. Some examples of these types of elements are constant current sources, fluid pumps, constant speed of rotation, and shaker providing a known motion.

The source of flow is represented in bond graph models as **Sf**.



Figure 2.14 shows the nature of variation of effort and flow for *Se* and *Sf* elements respectively. In a source of effort, the effort remains constant irrespective of the flow values. For a source of flow element, the flow remains constant, irrespective of the effort. These are definitions of the two ideal sources. Most real sources are not ideal and do not remain constant over time. These sources can be modeled as modulated sources of effort and flow. Modulated devices will be discussed a little later in this chapter.

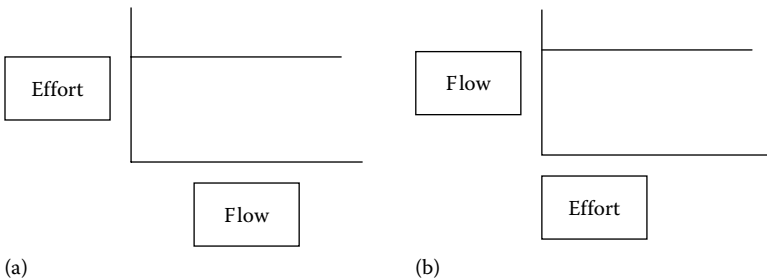


FIGURE 2.14

Schematic showing the variation of effort and flow for (a) constant effort and (b) constant flow sources.

Notice that unlike the first three 1-port elements (resistor, capacitor, inductor), for the sources of effort and flow, the half-arrow points away from the element. In the case of the R , C , and I elements, the half-arrow was pointing towards them.

One should also realize that even though the power bonds point in one direction, the actual power flow is not necessarily happening in that direction at all times. Power flow is a time dependent quantity. Hence, it can occur in the direction shown by the power bond direction or opposite to that. Having the arrow in the given direction means that when the power is positive, it flows in the direction of the arrow.

2.5.2 2-Port Components

2-port elements in a system are components that receive power from part of the system through one of its ports and supply (or transfer) power to another part of the system through the other port. These transfers of power through 2-port elements may follow one of two procedures. Hence, there are two main 2-port elements. They are referred to as the transformer and the gyrator.

2.5.2.1 Transformer Element

A transformer element is such that the input effort and the output effort are related to each other by a factor and the inlet flow and the outlet flow are also related to each other by the same factor. These relationships also satisfy the requirement that the total input power is the same as the total output power. Figure 2.15 shows a schematic for a transformer element with a transformer factor N .

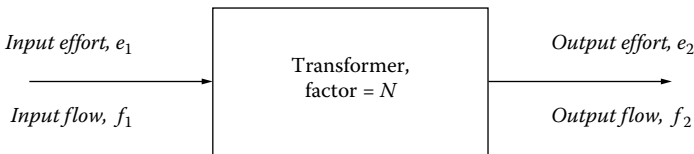
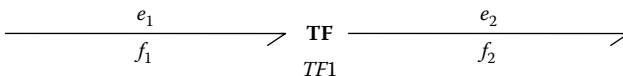


FIGURE 2.15

A schematic for the transformer element.

A bond graph element to represent a transformer can be shown as:



The constitutive relationship for a transformer and the power relationship may be written as follows:

$$\begin{aligned} e_2(t) &= N e_1(t) \\ f_1(t) &= N f_2(t) \end{aligned} \quad (2.14)$$

Since the input power is equal to the output power, the relationships may be written as:

$$e_1 f_1 = \left(\frac{e_2}{N}\right)(N f_2) = e_2 f_2 \quad (2.15)$$

Some examples of transformer elements are: electrical transformer, lever, gear trains, hydraulic plunger-cylinder, rack and pinion, and so forth. Figure 2.16 shows schematics of some of the transformer elements. In each

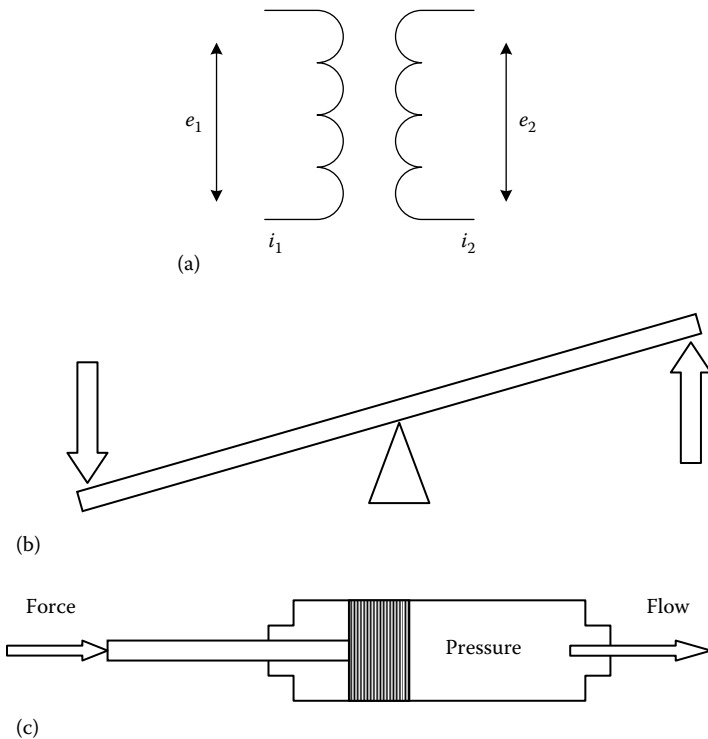


FIGURE 2.16

Schematics showing transformer elements within different domains: (a) electrical transformer, (b) mechanical transformer (lever), and (c) hydraulic transformer (plunger).

case the transformer factor may be obtained from one's basic understanding of the system behavior. For example, in the electrical transformer, the factor would be the ratio of the number of coils in both the windings. The transformer factor for a lever would be the ratio of the lengths of the lever arms. For a gear train it could be the ratio of the gear teeth, for a hydraulic ram it would be the area of the plunger (since the pressure multiplied by area is equal to the force).

Figure 2.17 shows pictures of some actual transformers from different domains.

If multiple transformers are used in series, the net result is equivalent to one transformer with an effective transformer factor that is equal to the product of all the transformer factors. Thus, the first representation shown below is equivalent to the second one.



Electrical transformer



Hydraulic jack

FIGURE 2.17

Transformer devices from different domains.

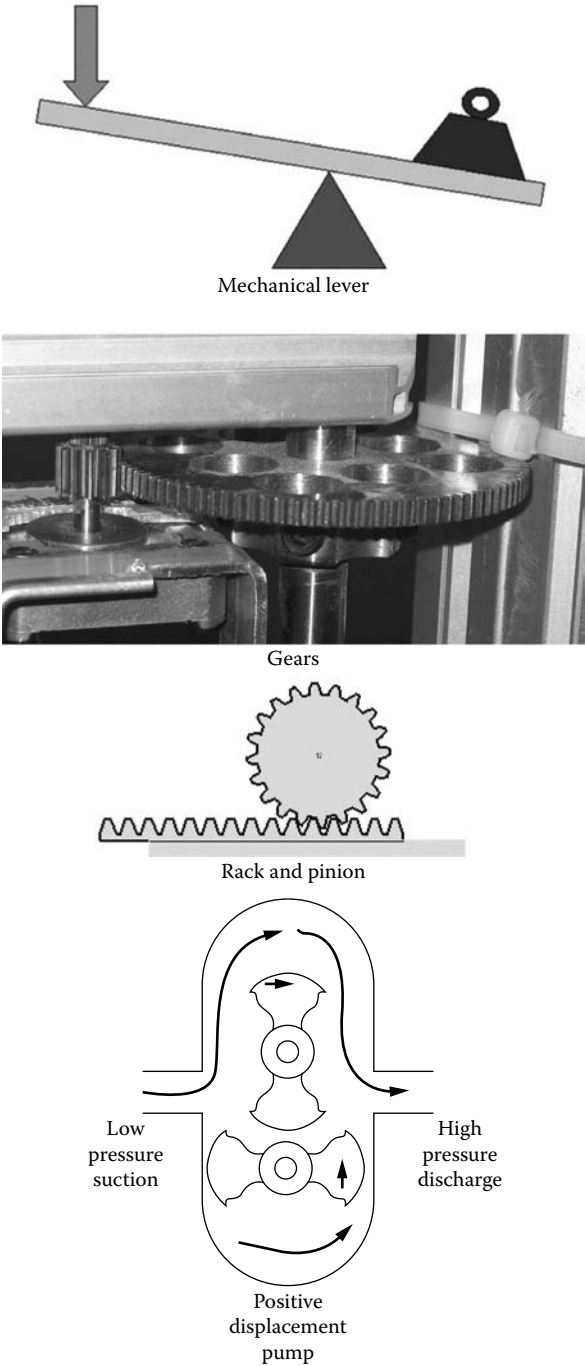
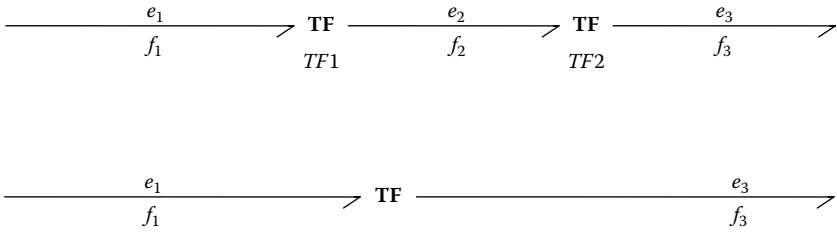


FIGURE 2.17
(Continued)



$$\begin{aligned}
 e_1 &= N_1 e_2; e_2 = N_2 e_3 \\
 \Rightarrow e_1 &= N_1 N_2 e_3 \\
 N_1 f_1 &= f_2; N_2 f_2 = f_3 \\
 \Rightarrow N_1 N_2 f_1 &= f_3
 \end{aligned} \tag{2.16}$$

2.5.2.2 Gyrator Element

A gyrator element is such that the input effort and the output flow are related to each other by a factor, and the inlet flow and the outlet effort are also related to each other by the same factor. These relationships also satisfy the requirement that the total input power is the same as the total output power. Figure 2.18 shows a schematic for a gyrator element, with a gyrator factor M .

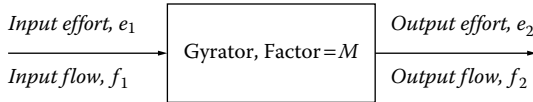
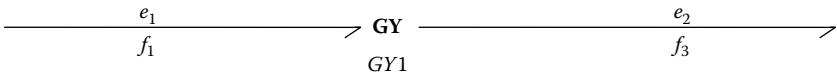


FIGURE 2.18

Schematic of a gyrator element.

The bond graph representation of a gyrator element is written as:



The constitutive relationship for a gyrator may be expressed as:

$$\begin{aligned}
 e_2(t) &= M f_1(t) \\
 e_1(t) &= M f_2(t)
 \end{aligned} \tag{2.17}$$

Since the input power is equal to the output power, the relationships may be written as:

$$e_1 f_1 = (M f_2) \left(\frac{e_2}{M} \right) = e_2 f_2 \quad (2.18)$$

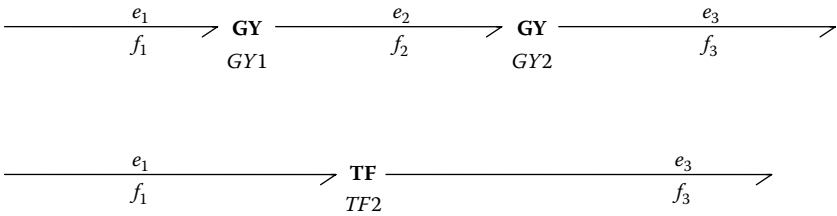
Some examples of gyrator elements are: centrifugal pumps and turbines. One of the most common type of gyrator is the DC motor. The output torque (effort) of a DC motor is a linear function of the current (flow) in the motor armature and the back *emf* (effort) induced in the motor circuit is a function of the rotation in the shaft. Thus,

$$\begin{aligned} T &= MI \\ E &= M\omega. \end{aligned} \quad (2.19)$$

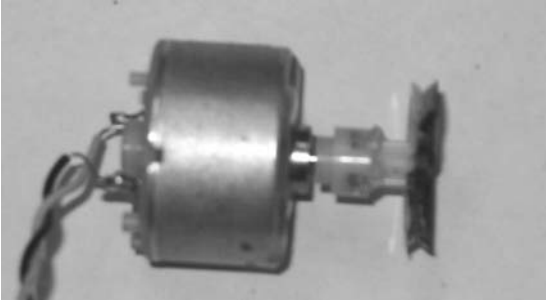
The most well-known gyrator element is the gyroscope.

Figure 2.19 shows schematics and pictures of actual gyrator elements. In each case the gyrator factor may be obtained from one's basic understanding of the system behavior. For example, in the DC motor the factor would be torque constant for the motor that is dependent on several factors including the magnetic flux density and motor geometry. In a similar manner the gyrator factor may be computed in other cases using fundamental physical laws. More will be discussed about these in later chapters.

If multiple gyrators are used in series, the net result is equivalent to one transformer for every two gyrators with an effective transformer factor that is equal to the ratio of the two gyrator factors. Thus, the first representation shown below is equivalent to the second one.



$$\begin{aligned} e_1 &= M_1 f_2; e_3 = M_2 f_2 \\ \Rightarrow e_1 &= \frac{M_1}{M_2} e_3 \\ M_1 f_1 &= e_2; e_2 = M_2 f_3 \\ \Rightarrow \frac{M_1}{M_2} f_1 &= f_3 \end{aligned} \quad (2.20)$$



Electrical gyrator: DC motor

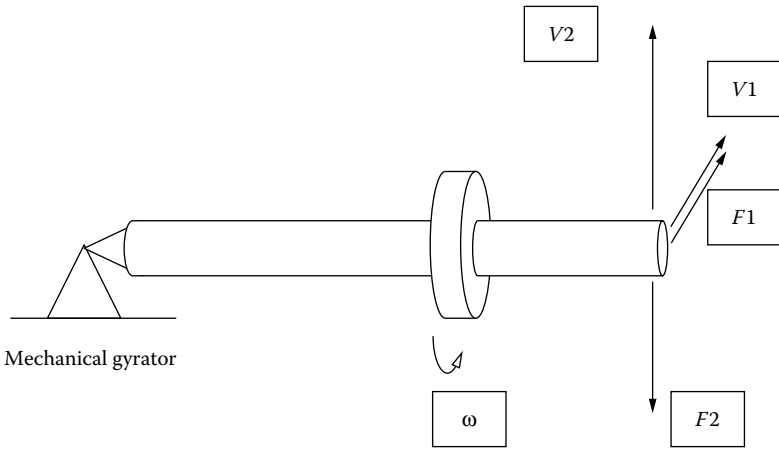


FIGURE 2.19
Examples of gyrator elements.

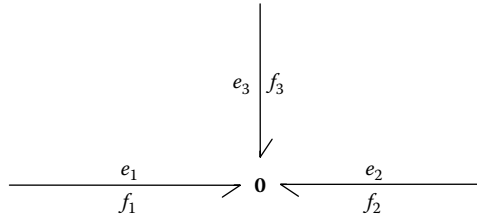
2.5.3 3-Port (or Higher-Port) Components

These ports are used to denote locations where multiple elements are joined to each other. There are two main types of joints or junctions. They are sometimes called common flow junction and common effort junction. These are similar to parallel and series connections as seen in electrical or hydraulic circuits. For the generalized nature of bond graphs, they are also referred to as effort (summing) junction and flow (summing) junction.

In bond graph nomenclature, parallel and series junctions are sometimes represented as P and S. More commonly these junctions are referred to as 1 and 0 junctions. These two types of junction elements are discussed below.

2.5.3.1 Flow Junction, Parallel Junction, 0 Junction, and Common Effort Junction

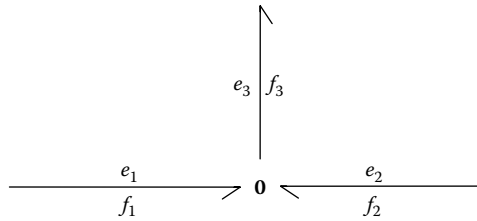
These are junctions where the effort is the same in all arms, but the flow is different. These behave in a manner similar to parallel paths in electrical circuits where the currents through each path are different, but the voltage across all the parallel paths is the same. These junctions are represented in bond graphs as 0 junctions (zero junction). Efforts are the same in all arms, but the flow is related through an algebraic sum, that is, sum of all flows is 0.



$$e_1(t) = e_2(t) = e_3(t)$$

$$f_1(t) + f_2(t) + f_3(t) = 0 \quad (2.21)$$

It is worth mentioning here that the direction of power bonds (half-arrows) for the junction elements is less well-defined than the previously discussed elements. So the 0 junction with the three bonds shown above may be drawn as:



While it is equally correct to draw the arrow directions in the second representation as in the first, the form of the equations changes to accommodate the new arrow direction. The effort still remains the same in all the branches, but the flow relationship alters, as shown in Equation 2.22:

$$e_1(t) = e_2(t) = e_3(t)$$

$$f_1(t) + f_2(t) = f_3(t) \quad (2.22)$$

Examples of situations that will lead to 0 junctions are shown in Figure 2.20. These are parallel electrical circuit, a hydraulic line that has three flows in three paths, and a mechanical system of two masses and a spring and damper where the forces on both masses are the same but their velocities are different.

2.5.3.2 Effort Junction, Series Junction, 1 Junction, and Common Flow Junction

These are junctions where the flow is the same in all arms, but the effort is different. These behave in a manner similar to series circuits in electrical

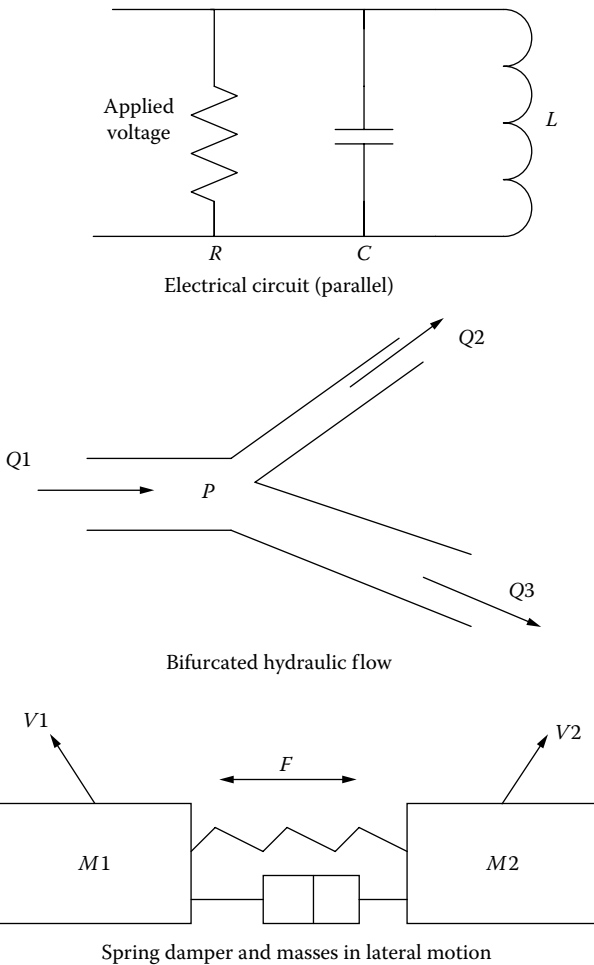
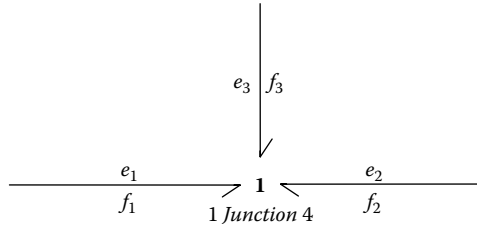


FIGURE 2.20

Examples of situations that result in a 0 junction.

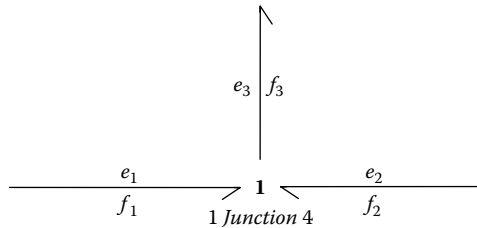
circuits where the current through each component is the same but the voltage drop across these components is different. These junctions are represented in bond graphs as 1 junctions (one junction). Flows are the same in all arms, but the effort is related through an algebraic sum, that is, sum of all efforts is 0.

The bond graph representation of this junction is



$$\begin{aligned} f_1(t) &= f_2(t) = f_3(t) \\ e_1(t) + e_2(t) + e_3(t) &= 0 \end{aligned} \quad (2.23)$$

It is worth repeating here that the direction of power bonds (half-arrows) for the junction elements are less well-defined than the previously discussed elements. So the one junction with the three bonds shown above may very well be drawn as:



While it is equally correct to draw the arrow directions in the second representation as in the first, the form of the equations change to accommodate the new arrow direction. The effort still remains same in all the branches, but the flow relationship alters as shown in Equation 2.24:

$$\begin{aligned} f_1(t) &= f_2(t) = f_3(t) \\ e_1(t) + e_2(t) &= e_3(t) \end{aligned} \quad (2.24)$$

Examples: Figure 2.21 shows some typical systems where the 1 junction is used to model the system behavior. A series circuit, a spring mass damper system, and a series hydraulic line are common examples.

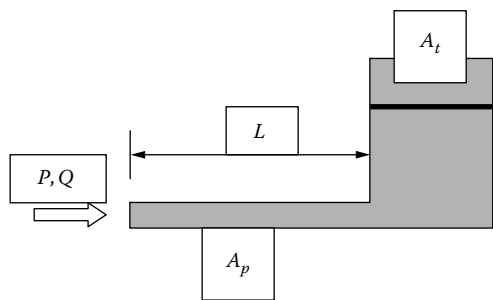
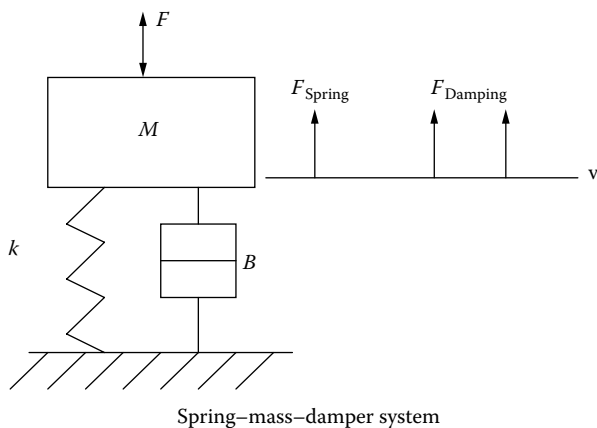
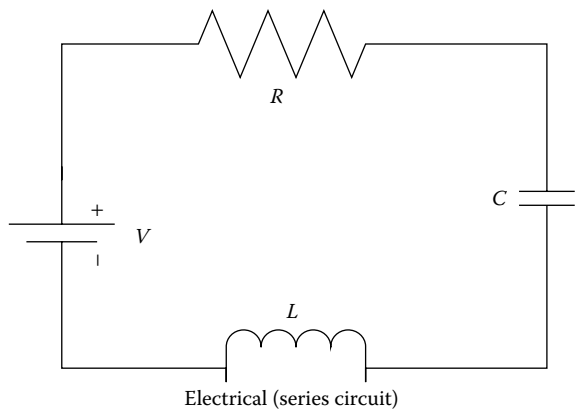
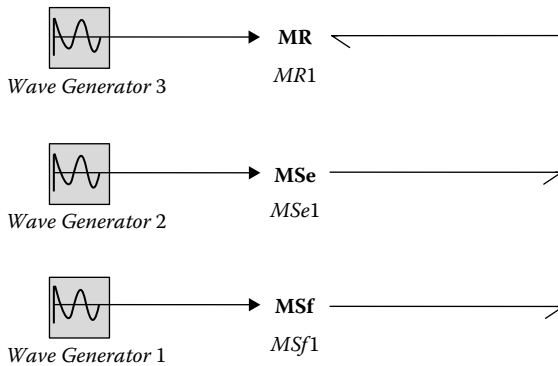


FIGURE 2.21
Examples of situations that result in a 1 junction.

2.5.4 Modulated Components: Transformers, Gytrators, Resistances, and More

So far we have talked about components in system whose properties remain unchanged with time, for example, the resistance value of a resistive element, the effort value of a source of effort, and so forth. In many practical situations, this condition may not be true at all times. For example, the supply voltage from a battery drops over a time period, or capacitances may vary during the operational time period of the system, or the force acting on a body may be varying with time. In order to capture these variable properties modulated components are used. These are components whose property varies during the time period under consideration. These are separately denoted in the bond graphing world as a *MR* or a *MSe* or a *MTF* element where the letter *M* stands for modulated. These components in a modeling environment are designed to receive a signal input along with the necessary power bond(s). The signal bond is denoted by a full arrow. Following are some examples of how these components are represented. In the representation the terms “wave generator” are used to represent a known time varying signal that is being used in each case. The exact form of that signal is unimportant for this discussion.



In each of the examples shown, a time varying waveform is used to send a signal to the modulated element. This signal determines how this element behavior varies with time.

2.6 A Brief Note about Bond Graph Power Directions

In this chapter we have introduced some of the very basic concepts of bond graphs. We are yet to learn how to construct bond graphs, how and when to use them, the particular advantages, and so forth. In the next few

chapters we will be discussing those concepts. As we get into these details, we would like to remind the readers/students that the half-arrows used in the drawing of bond graphs are used to represent the flow of power. In this chapter we discussed some of the basic elements, and in each case, the half-arrow pointed in particular directions (either towards or away from the component). By definition, power is positive in the direction of the power bond. Power flows in the direction of the half-arrow if it is positive (i.e., the product of effort and flow is positive) and the other way if it is negative. This does not mean that power will always flow in the direction of the arrow. Sometimes it may flow opposite to the arrow direction (when power is negative). As long as the convention is not violated, the user will not be in trouble, but it is important that the user be aware of the reasons for doing certain things in a certain way. Also, power directions indicate directions of positive power but they convey no information about the direction of the components of power, namely flow and effort. Often students make the mistake of confusing power direction with the direction for force and velocity.

In the next chapter we will learn several techniques for drawing bond graphs. Some of the basic elements will be joined by bonds to 1 and 0 junctions and to each other. Sometimes we will have to choose bond directions in an arbitrary direction. While at times these choices may be arbitrary, their impact on the final outcome is not. Since governing state space equations will be derived from the bond graphs, the bond directions will have an impact on the exact form of these equations. We will refer to this discussion again at a later point in the text when the need arises.

2.7 Summary of Bond Direction Rules

1. R , C , and I elements have an incoming power direction (this results in positive parameters when modeling real-life components).
2. For source elements Se and Sf , the standard is outgoing as sources mostly deliver power to the rest of the system.
3. For TF and GY elements, one bond is incoming, another is outgoing.
4. For 1 and 0 junctions, some bonds could be incoming and others outgoing. The modeler has some freedom in choosing bond direction. More often than not bond directions are determined by the components that are attached to the junctions. The form of the resulting equations will change based on directions of bonds chosen.

Problems

- 2.1. Figure P2.1 shows a system to pump water. List all the important components in this system, identify locations where power is changing from one domain to another, and indicate what these transformations are.

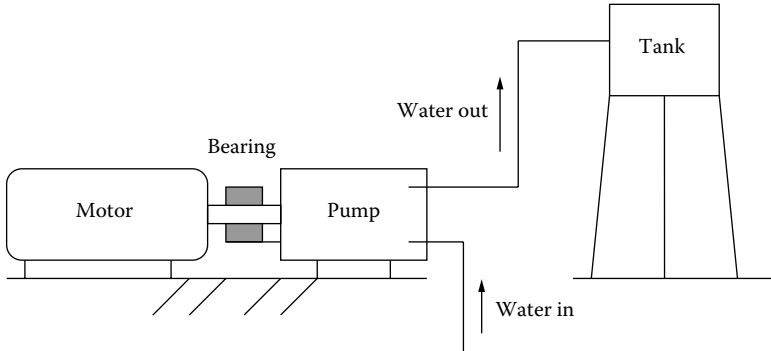


FIGURE P2.1

Figure for Problem 2.1, motor driven pump used to fill an overhead tank.

- 2.2. Figure P2.2 shows a loudspeaker. The circuit that supplies a current through the coil is not shown in the figure but is a part of the system. Coil resistance and inductances are part of that circuit. List all the important components in this system, identify

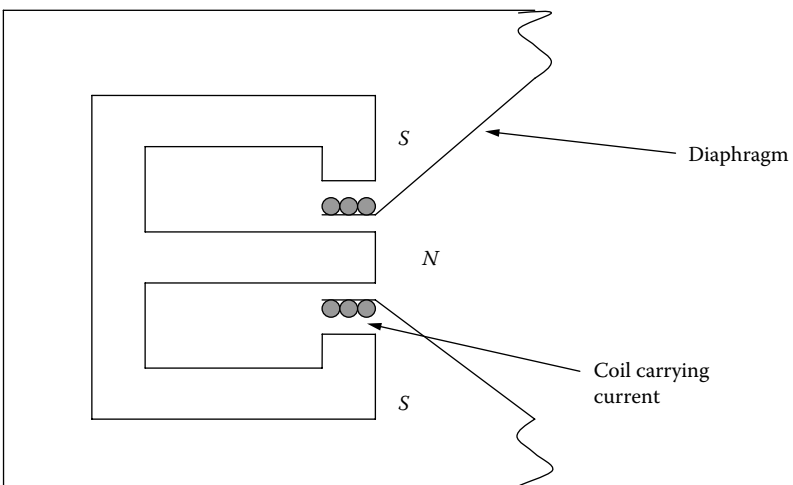


FIGURE P2.2

Figure for Problem 2.2, loudspeaker.

locations where power is changing from one domain to another, and indicate what these transformations are.

- 2.3. Consider two mechanical springs (capacitive elements). The first spring is linear, so the constitutive equation is $F = k_1 x$ and the second is quadratic so the constitutive relationship is $F = k_2 x^2$.

A test was run to determine the spring constants, and it was observed that for a 50 N force both the springs had a displacement of 2 cm. Determine:

The spring constants of the two springs

The displacement in each spring if the force is doubled

The energy stored in each spring during the initial extension

- 2.4. A cantilever (Figure P2.3) is a very common feature used in many MEMS device (the schematic shows one). This device is used both as a sensor and as an actuator in microdevices. If this microscale device is to be modeled, what are the different basic components that need to be included in the model?

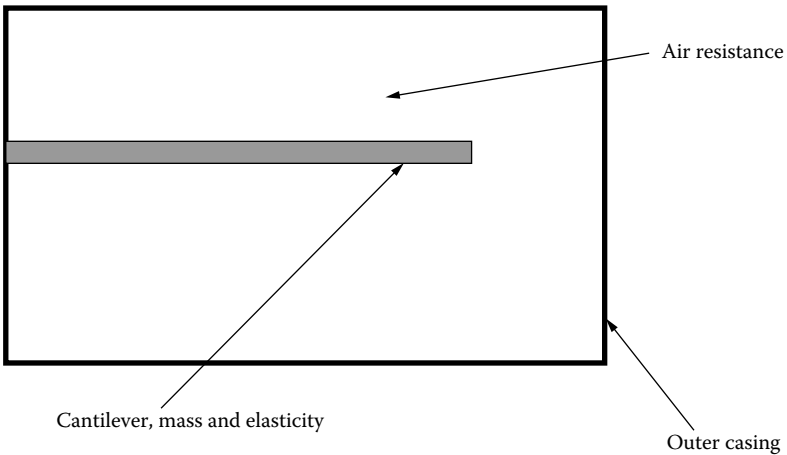


FIGURE P2.3

Figure for Problem 2.4, schematic of a MEMS device involving a cantilever in a casing.

- 2.5. Consider two electrical conductors of the same material and length. One is 0.5 mm in diameter, and the other one is 1 mm. For the same potential difference applied across both these conductors, which will allow higher current?

- 2.6. Figure P2.4 is a broad overview of an automobile with some of the main items identified. If a model were to be developed to study the dynamic behavior of the vehicle, determine the different subsystems, and, within each subsystem, the different components and their behaviors for which accounting is needed.

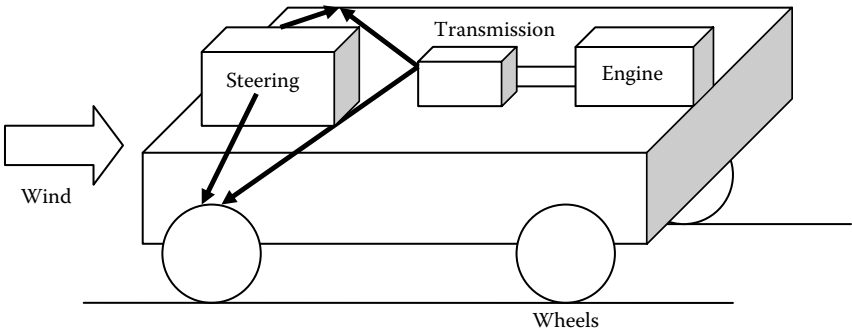


FIGURE P2.4

Figure for Problem 2.6, schematic of a moving vehicle.

- 2.7. The velocity function of a moving body is given by $v(t) = 5t + 7$. Compute the distance traveled over a time of 3 seconds starting from a 0 initial position. Plot both the velocity and the distance traveled as a function of time for this time period. What is the acceleration for this time period?
- 2.8. Figure P2.5 shows a simple system with a motor driving a fan. Identify all the basic elements that are part of this system so that a system model can be developed.

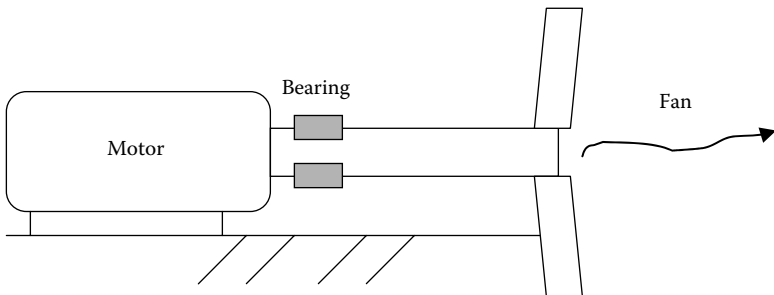


FIGURE P2.5

Figure for Problem 2.8, schematic of a motor driven fan.

- 2.9. An electric heater is rated at 1500 W and is connected to a 110 V supply. What is the resistance of the heating coil? How much current is flowing through the coil? If the supply is not a constant DC source but is a 60 Hz AC source, how does the current change with time?
- 2.10. In an electric car, regenerative braking is used to recharge batteries. The principle of regenerative braking involves converting the kinetic energy of the vehicle into energy stored in a battery. If a car is traveling at a speed of 30 km/h and is stopped completely by braking, what would be the energy stored in the battery if the mass of the car is 1000 kg and the energy conversion efficiency is assumed to be 100%? If this braking happens at a constant rate for 5 seconds, what is the average rate of power transfer?
- 2.11. For mechanical translation, rotation, hydraulic, and electric domains draw a tetrahedron of state. For each case write the relevant variables for each domain at the four corners and write down the relationships between these variables.
- 2.12. Figure P2.6 shows a platform that supports a rotating machine with a mass imbalance in the rotor. The platform is supported by springs and dampers. The mass imbalance is a source of force that is periodic due to the rotor angular speed. For this system identify all the important components necessary to develop a system model.

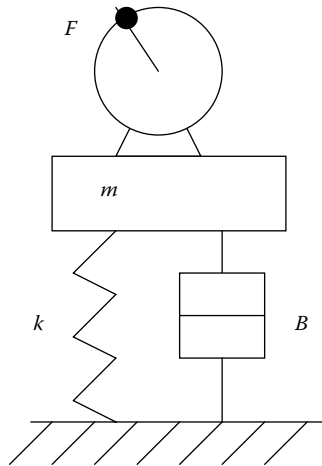
**FIGURE P2.6**

Figure for Problem 2.12, a motor mounted on suspensions with an unbalanced rotor.

- 2.13. The inductance of a coil is computed from:

$$L = \frac{N^2 \mu A}{l}$$

where L is the inductance in Henrys, N is the number of windings, A is the cross-section area of the core, and μ is the permeability of the medium. An inductor of 2 cm core diameter and 200 turns in the coil is 6 cm long. If the current flowing through the conductor is 0.5 A and the permeability of the medium is $1.257\text{E-}6$ N/m, compute the energy stored in the coil.

- 2.14. The inductor energy in the previous problem is now used to charge a parallel plate capacitor for a terminal voltage of 10 V. The capacitor plates have 1 sq cm plate overlap area and the distance between the plates is 1 cm. The permittivity of the medium is $0.885\text{E-}11$ F/m. Compute the charge developed across the plates.

(The capacitance of a parallel plate capacitor is given by $C = \frac{\epsilon A}{d}$)

- 2.15. The velocity in a system is expressed in the following relationship:

$$v = 2t^2 \text{ m/s}, 0 \leq t \leq 5$$

$$v = 50t \text{ m/s}, 5 < t \leq 20$$

If the damping coefficient $B = 10$ Ns/m, plot the power dissipated through this damper as a function of time. How much is the total energy dissipated over the time period of 20 seconds?

- 2.16. The plot in Figure P2.7 shows the voltage across an inductor of 0.5 mH. Use the data from the plot to determine the current in the inductor at $t = 15\mu\text{s}$.
- 2.17. The time dependent voltage across a capacitor of 50 μF is shown in Figure P2.8. Determine the current through the capacitor as a function of time using this data.

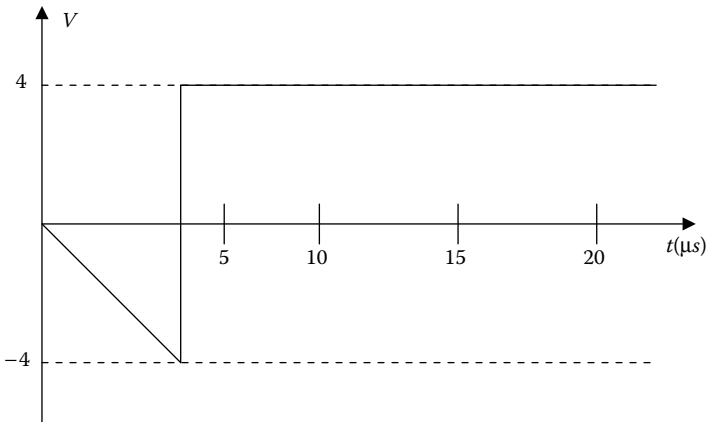


FIGURE P2.7

Figure for Problem 2.16, voltage versus time data for Problem 2.16.

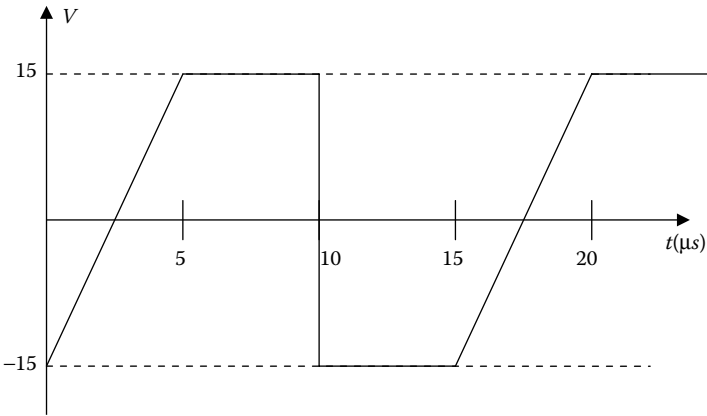


FIGURE P2.8

Figure for Problem 2.17, voltage versus time data for Problem 2.17.

This page intentionally left blank

3

Drawing Bond Graphs for Simple Systems: Electrical and Mechanical

In the previous chapter we discussed the basic components that frequently occur in a bond graph based system model. In this chapter we will discuss the methods and techniques used to construct bond graph models for a variety of engineering systems. For a start, we will keep our discussion confined to mechanical and electrical systems, only because it is important that students understand the techniques and master the process to gain confidence in building bond graph models. Other systems (and their models), such as hydraulic, magnetic, and so forth, will be handled in later chapters. Bond graph construction techniques remain quite similar within other domains. It is hoped that new users of this technique will gain confidence through repeated use of the methodologies presented in this chapter.

The overall objectives of this chapter are to

- Introduce students to algorithms for drawing bond graph models of mechanical and electrical systems.
- Introduce students to the basic rules of bond graph simplification and their applications.
- Introduce the concept of causality and highlight its importance.
- Increase the confidence of students in the area of bond graph modeling so that they are comfortable in modeling a variety of basic engineering systems.

Before we start going through the techniques of developing bond graph representations of different systems, we need to be aware of some of the commonly used rules of simplification that help us in drawing simplified bond graph representations of systems. In the next section we discuss the commonly used six rules of simplification.

3.1 Simplification Rules for Junction Structure

The rules of simplification can be used on the basic bond graph structure to make it more crisp and compact. While the need for simplification is not absolute (i.e., the system equations derived from an unsimplified model will be the same as a simplified model), simplification makes the model more elegant and, sometimes, compact. There are six commonly used rules of simplification. They are described below. The first four are easy to understand and use. The last two are a little less intuitive. Hence, a proof of one of them is included.

Figure 3.1 shows two bond graph representations. These two are equivalent, so the first may be replaced by the second. If a zero junction connects only two bonds all the effort coming in from the left of the 0 junction is the same effort leaving the junction from the right. Similarly, all the flow that is coming in from the left is the same flow leaving from the right. Thus, the first representation may be simplified as the second one. (Note: This simplification does not work if a third element is connected to the 0 junction through another bond.)

Figure 3.2 shows two bond graph representations. These two are equivalent so the first may be replaced by the second. If a one junction connects only two bonds all the effort coming in from the left side of the 1 junction is the same effort leaving the junction from the right. Similarly, all the flow that is coming in from the left is the same flow leaving from the right. Thus, the first representation may be simplified as the second one. (Note: This simplification does not work if third element is connected to the 1 junction through a bond.)

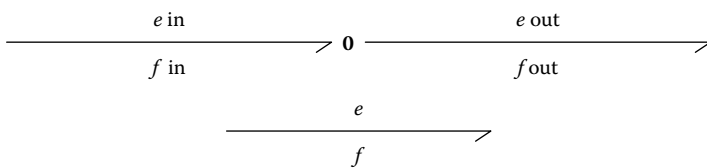


FIGURE 3.1
Simplification rule.

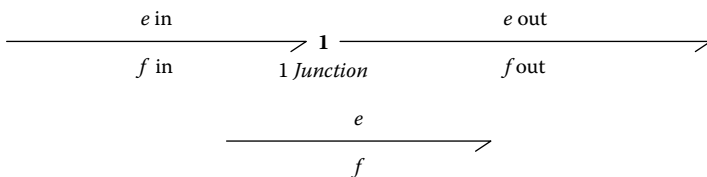


FIGURE 3.2
Simplification rule.

Figure 3.3 shows two bond graph representations. These two are equivalent, so the first may be replaced by the second. A 0 junction is a “same effort” junction. Hence, $e_1 = e_2 = e_3 = e_4 = e_5$ (in the first representation). The flow, on the other hand, gets separated at 0 junctions. Therefore, in the first picture, $f_1 = f_2 + f_3$ and $f_3 = f_4 + f_5$. Therefore, $f_1 = f_2 + f_4 + f_5$, from the first picture. Now considering the second picture, the same two relationships for effort and flow are valid, that is, $e_1 = e_2 = e_4 = e_5$ and $f_1 = f_2 + f_4 + f_5$. So the first bond graph may be replaced by the simplified second version.

Figure 3.4 shows two bond graph representations. The two are equivalent, so the first may be replaced by the second. A 1 junction is a “same flow” junction. Hence, $f_1 = f_2 = f_3 = f_4 = f_5$ in the first representation. The flow, on the other hand, gets separated at 0 junctions. Therefore, in the first picture, $e_1 = e_2 + e_3$ and $e_3 = e_4 + e_5$. Therefore, $e_1 = e_2 + e_4 + e_5$, from the first picture. Now considering the second picture, the same two relationships for effort and flow are valid, that is, $f_1 = f_2 = f_4 = f_5$ and $e_1 = e_2 + e_4 + e_5$. So the first bond graph may be replaced by the simplified second version.

Figure 3.5 shows two bond graph representations. These two bond graph models are equivalent, so the first may be replaced by the second. The equivalence of these two bond graph representations is nontrivial. Hence, it needs to be demonstrated.

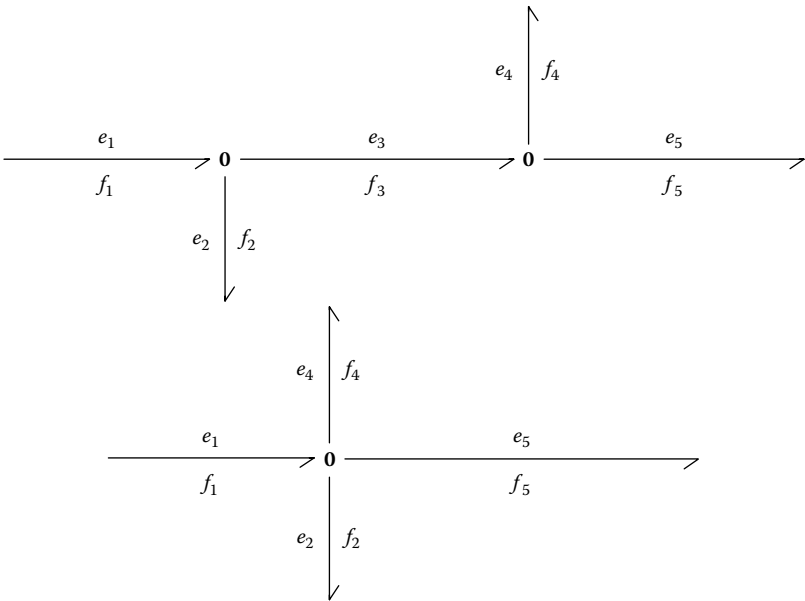


FIGURE 3.3
Simplification rule.

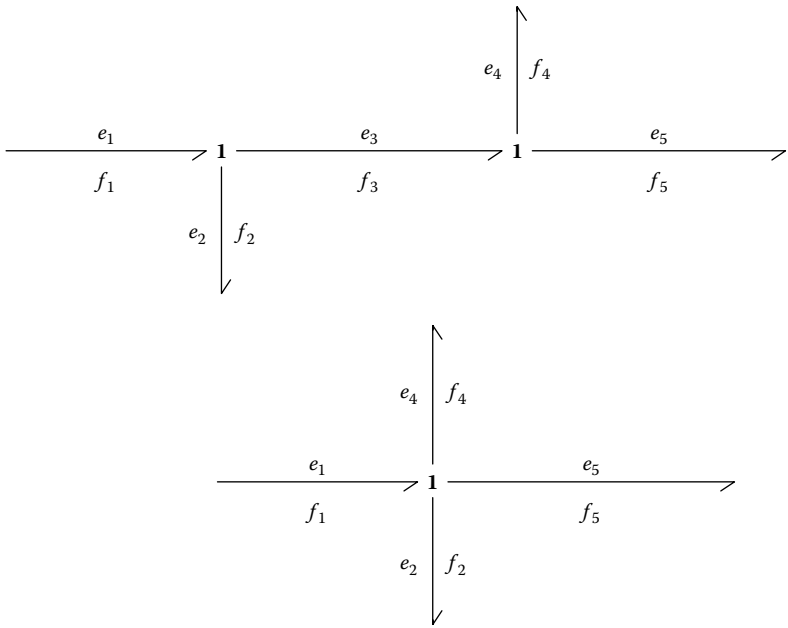


FIGURE 3.4
Simplification rule.

Proof

To show that the two bond graphs in Figure 3.5 are equivalent.

First Bond Graph

Consider the first bond graph. There are four junctions shown in Figure 3.5. We will refer to them as junctions 1, 2, 3, and 4, as marked.

At junction 1

$$e_1 = ea = eb \quad (3.1)$$

$$f_1 = fa + fb \quad (3.2)$$

At junction 2

$$ea = e_2 + ec \quad (3.3)$$

$$fa = f_2 = fc \quad (3.4)$$

At junction 3

$$eb = e_3 + ed \quad (3.5)$$

$$fb = f_3 = fd \quad (3.6)$$

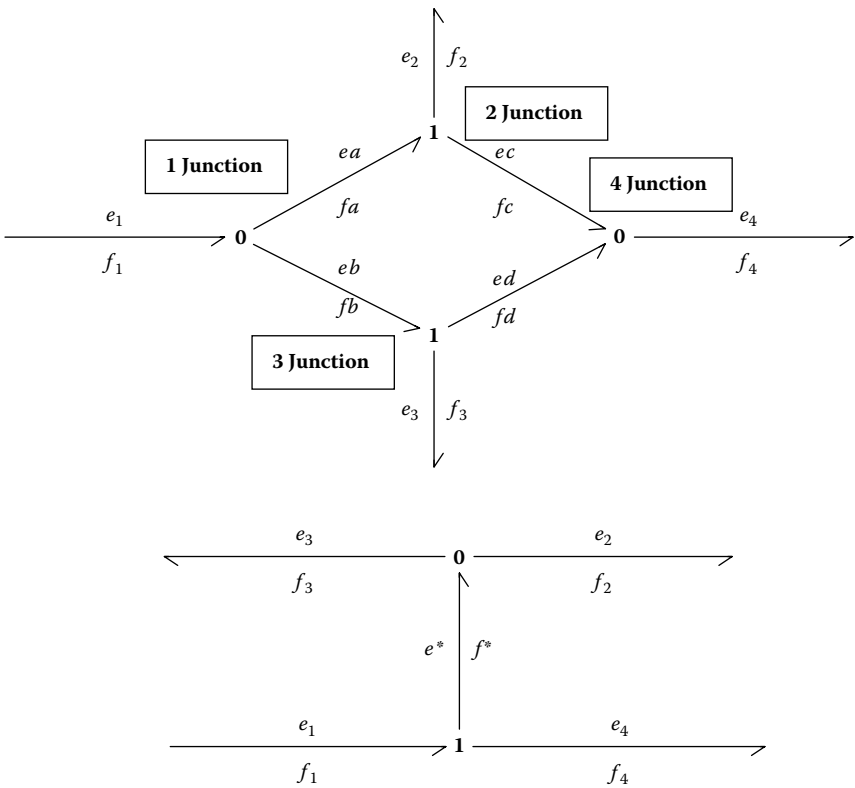


FIGURE 3.5
Simplification rule.

At junction 4

$$ec = e_4 = ed \quad (3.7)$$

$$fc + fd = f_4 \quad (3.8)$$

Combining the flow equations for junctions 1 and 2 (i.e., Equations 3.2 and 3.4), we get:

$$f_1 = f_2 + fb \quad (3.9)$$

But, $fb = f_3$ from the flow Equation 3.6 of junction 3. Therefore:

$$f_1 = f_2 + f_3 \quad (3.10)$$

Consider the flow Equation 3.8 at junction 4. Since $fc = f_2$ and $fd = f_3$ we can write:

$$f_2 + f_3 = f_4 \quad (3.11)$$

Combining the two flow Equations 3.10 and 3.11, we can write:

$$f_1 = f_2 + f_3 = f_4 \quad (3.12)$$

Combining the effort Equations 3.1 and 3.3 from junctions 1 and 2, we get:

$$e_1 = e_2 + ec \quad (3.13)$$

But, $ec = e_4$ from junction 4, Equation 3.7. Hence:

$$e_1 = e_2 + e_4 \quad (3.14)$$

Combining the effort Equations 3.1 and 3.5 from junctions 1 and 3, we get:

$$e_1 = e_3 + ed \quad (3.15)$$

But, $ed = e_4$ from the junction 4, Equation 3.7. Hence:

$$e_1 = e_3 + e_4 \quad (3.16)$$

Therefore, combining the two relationships for e_1 (Equations 3.14 and 3.16), we can write:

$$e_1 = e_2 + e_4 = e_3 + e_4 \quad (3.17)$$

Second Bond Graph

Now, let's consider the second representation.

At junction 1

$$e_1 = e^* + e_4 \quad (3.18)$$

$$f_1 = f_4 = f^* \quad (3.19)$$

At junction 0

$$e^* = e_2 = e_3 \quad (3.20)$$

$$f^* = f_2 + f_3 \quad (3.21)$$

Combining the two sets of effort and flow equations for the two junctions we get:

$$e_1 = e_2 + e_4 = e_3 + e_4 \quad (3.22)$$

$$f_1 = f_2 + f_3 = f_4 \quad (3.23)$$

Thus, it has been demonstrated that first and the second representations are indeed equivalent since both the effort and the flow relationships for both the representations are equivalent (i.e., Equation 3.12 is the same as Equation 3.23, and Equation 3.17 is the same as Equation 3.22).

Figure 3.6 shows two bond graph models that are equivalent, so the first may be replaced by the second. The proof for this rule can be obtained along the same lines as the previous one.

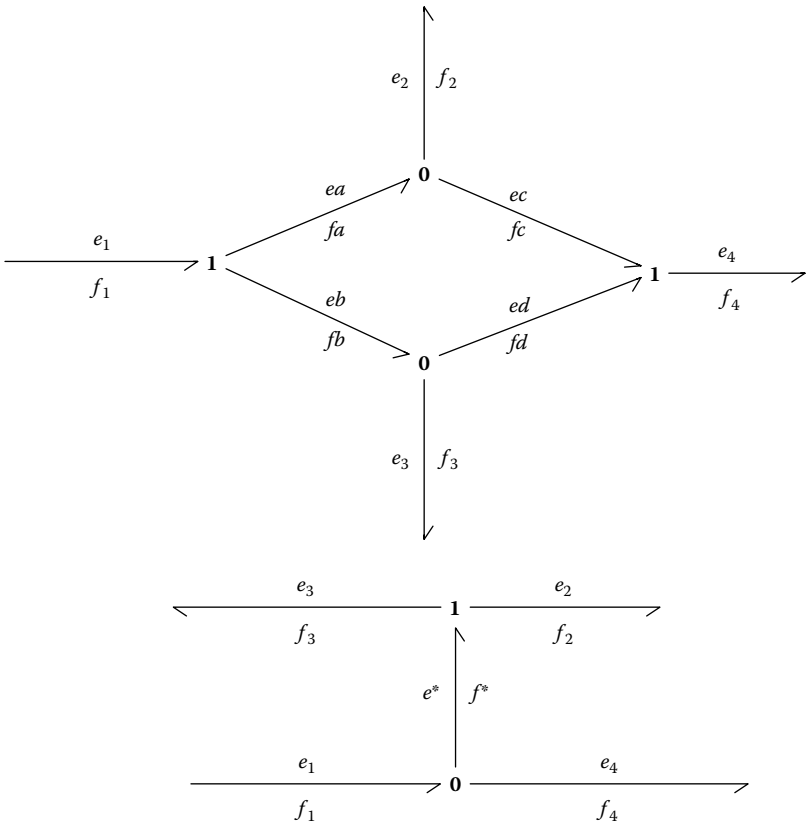


FIGURE 3.6
Simplification of rule.

Now that we have discussed the different rules of simplification, we will go through the process of developing bond graph representations for electrical and mechanical systems. There are several techniques for doing this. The simplest one is the method of inspection. It works well for electrical systems because series and parallel connections can be directly represented as 1 and 0 junctions, respectively. Students familiar with series and parallel circuit analysis can find the method of inspection quite intuitive. The method is somewhat less intuitive for mechanical systems. In practice, inspection works well for experienced users, but not as well for beginners. In this book we have used the method of inspection initially to demonstrate bond graph models for simple electrical systems. However, a conscious decision was made to not teach the method of inspection in great detail but, instead, to teach a method that is more algorithmic and, therefore, can develop more confidence for beginning users. Using this algorithmic approach, we will first discuss the development of bond graph models for electrical systems and then for mechanical systems.

3.2 Drawing Bond Graphs for Electrical Systems

EXAMPLE 3.1

Figure 3.7 shows one of the simplest possible electrical circuits: the RLC circuit with R , C , and L elements connected in a series along with a voltage source (battery). We know that the current or flow in this circuit is the same through all elements, whereas the voltage drop across each element is different. The sum of all voltage drops across the loop is equal to 0 (Kirchoff's law). The bond graph representation of this system is, therefore, a simple one and can be obtained by inspection: all four elements are connected through a series, or a 1 junction, and are shown in Figure 3.8. (In 1 junctions, the flow is the same in all the bonds, but the effort is different in each, such that the sum of all efforts is equal to 0.)

In the bond graph model shown in Figure 3.8, the battery voltage is Se (source of effort), R is the resistance, C the capacitance, and I the inductance.

EXAMPLE 3.2

A second simple example is shown in Figure 3.9 by an ideal current source that is connected in parallel to the same three common electrical elements. In this case the voltage drop across each is the same (because they are connected in parallel). The current in each element is different, but their sum is equal to the total current supplied by the current source. The bond graph

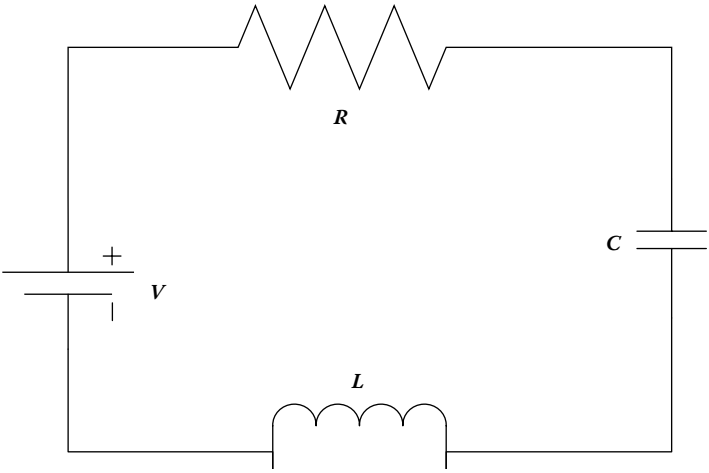


FIGURE 3.7
An RLC circuit.

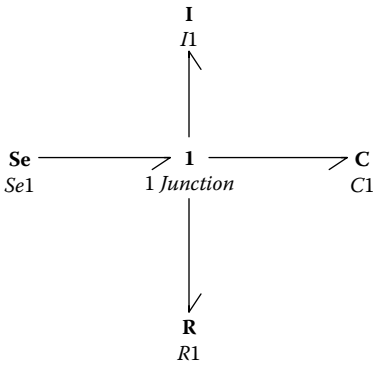


FIGURE 3.8
Bond graph model of a RLC series circuit.

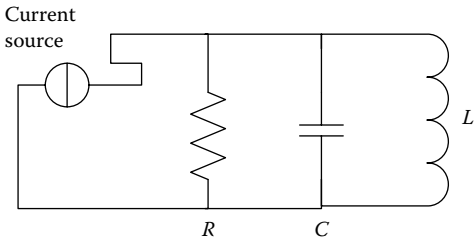


FIGURE 3.9
A parallel RLC circuit.

representation (obtained by inspection) is shown in Figure 3.10 where the resistance, capacitance, and the inductance are joined by a 0, or a parallel, junction with each other and a source of flow.

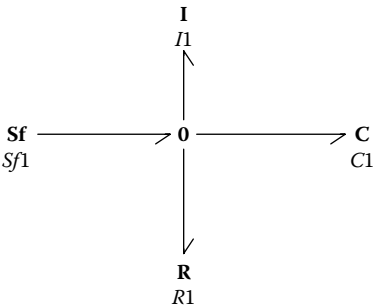


FIGURE 3.10
Bond graph model of the parallel RLC circuit.

Examples 3.1 and 3.2 are relatively simple ones where, by using experiences, we could determine that the circuit was connected in series or in parallel. However, if we encounter cases that are a little more complex, we can run into difficulties with the method of inspection. Some examples are shown in Figure 3.11.

There is a second method of drawing bond graphs for electrical circuit elements that is more useful for both simple and complex circuits because it is more algorithmic than the method of inspection.

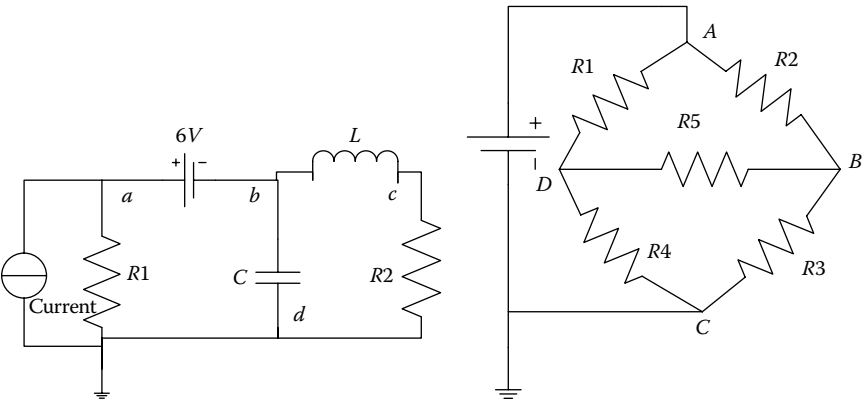


FIGURE 3.11
Examples of electrical circuits.

3.2.1 Formal Method of Drawing Bond Graphs for Electrical Systems

1. For each location in the circuit with a distinct potential, assign a 0 junction.
2. Insert each “single port” circuit element by connecting it to a 1 junction with a power bond and inserting it between relevant 0 junctions.
3. Assign power direction to all bonds in the model.
4. If the ground potential locations are known, then delete that 0 junction and all bonds connected with it. (If no explicit ground exists, then choose a suitable 0 junction and delete it along with all the bonds connected to it.)
5. Simplify the bond graphs by using all rules of simplification (discussed earlier).

EXAMPLE 3.3

Figure 3.12 shows a circuit with letters a, b, c, and d indicating four unique potential locations. To develop the bond graph representation of the system, the algorithmic steps are executed one at a time. After the first three steps, we arrive at the diagram shown in Figure 3.13. In this diagram junction d represents the ground potential, and it has to be removed (as per Step 4). Once junction d is removed, the bond graph looks simpler, as shown in Figure 3.14. Further simplification is possible by removing some redundant junctions that are connected only to a single element (i.e., by applying relevant simplification rules described before). Once these are applied, the bond graph looks even simpler, as shown in Figure 3.15. The vertical lines shown at the end of each bond are called a causal stroke. More discussion about causality and causal strokes is coming is included later in this chapter.

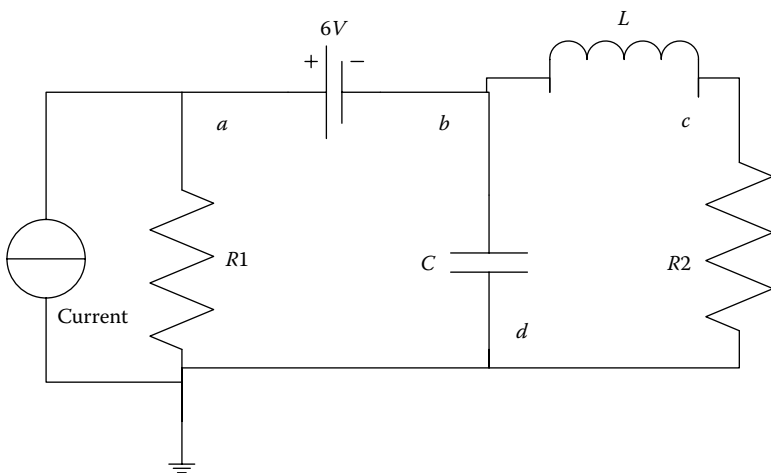


FIGURE 3.12

Circuit for Example 3.3.

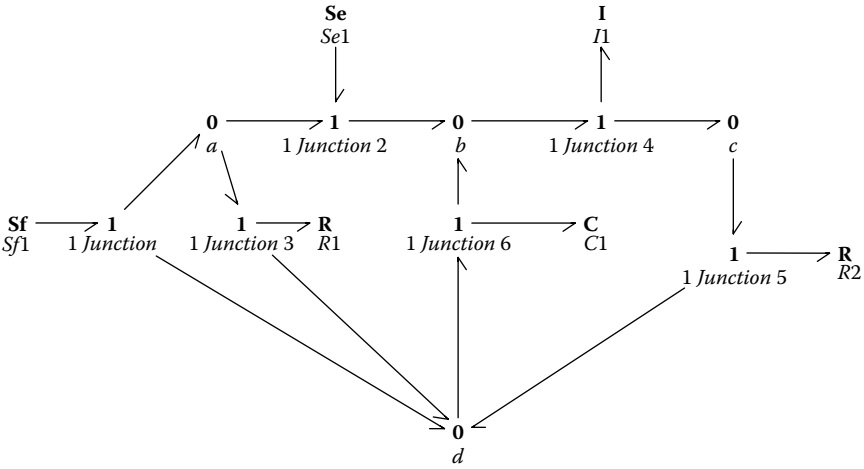


FIGURE 3.13
Initial bond graph for Example 3.3.

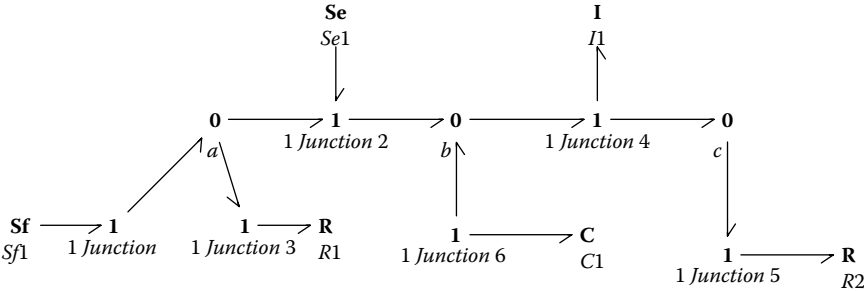


FIGURE 3.14
Simplified model for Example 3.3.

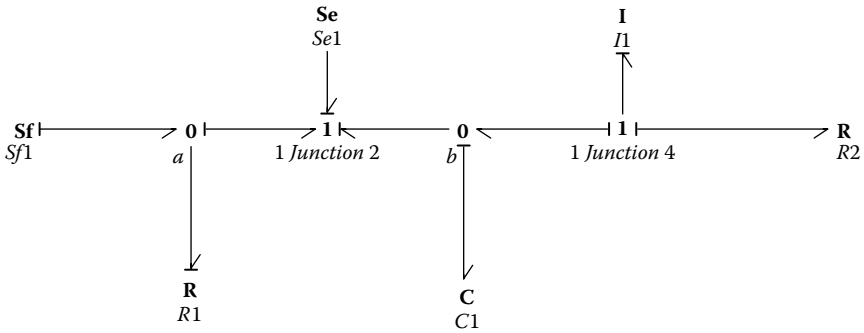
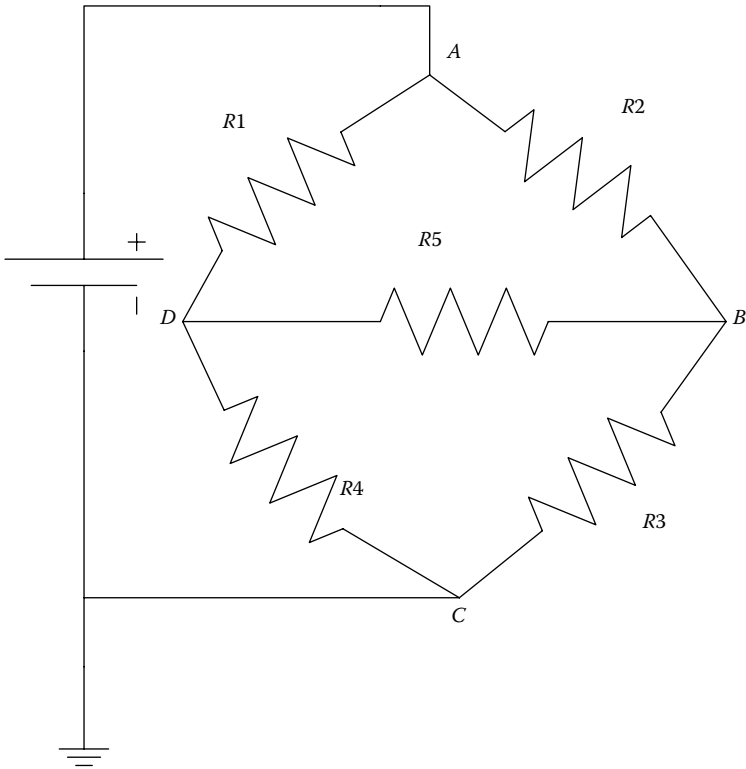


FIGURE 3.15
Final bond graph for Example 3.3.

EXAMPLE 3.4

Let us consider the wheatstone bridge circuit shown in Figure 3.16. The different resistors are marked as R_1 , R_2 , R_3 , R_4 , and R_5 , and the four different potential points are shown as A, B, C, and D.

**FIGURE 3.16**

Wheatstone bridge, Example 3.4.

As in the Example 3.3, the steps are executed one at a time, and after the first three steps, we get the model in Figure 3.17. As per rule number 4, the bonds associated with the ground potential need to be removed. Once this rule is executed, the bond graph representation looks like the one shown in Figure 3.18.

Upon simplification, this bond graph representation looks like the one shown in Figure 3.19.

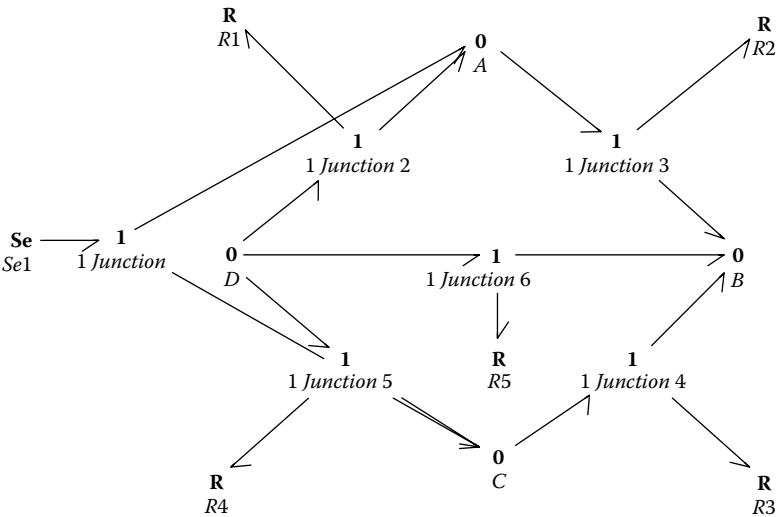


FIGURE 3.17
Initial bond graph for Example 3.4.

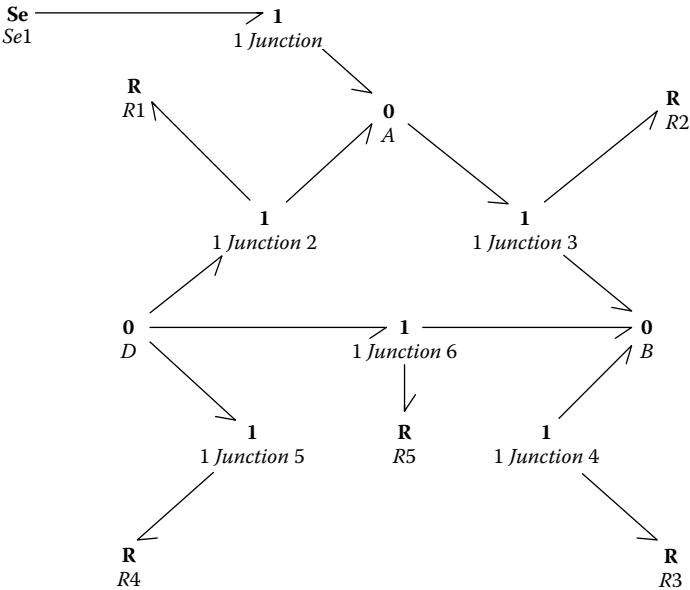


FIGURE 3.18
Simplified model for Example 3.4.

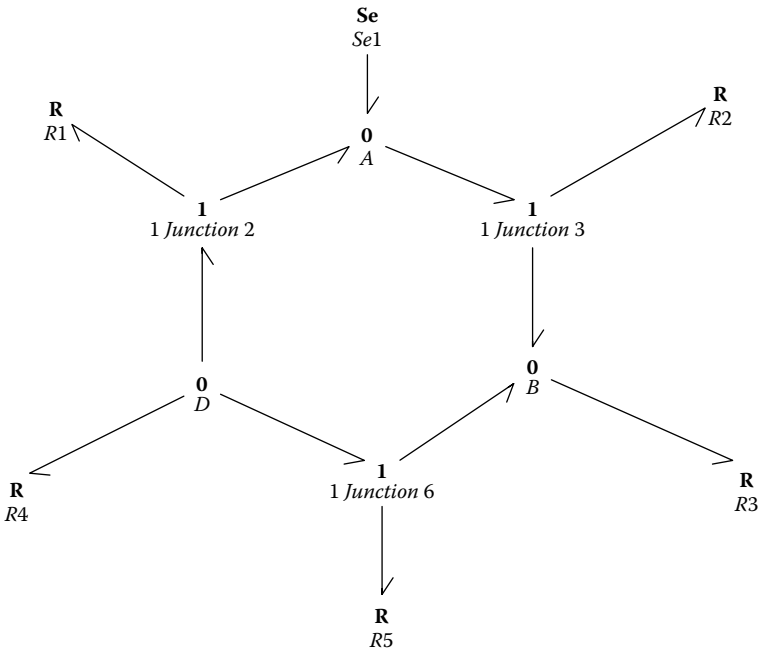


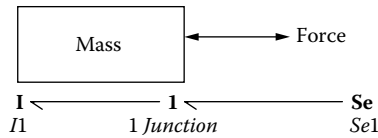
FIGURE 3.19
Final bond graph model for Example 3.4.

3.3 Drawing Bond Graphs for Mechanical Systems

The 1 and 0 junctions in an electrical system are quite intuitive because the concepts of series and parallel junctions are well established for electrical systems. The same concepts could be somewhat tricky for mechanical systems. So, before we start drawing bond graph representations for mechanical systems, the use and meaning of the 1 and 0 junctions are discussed a little more.

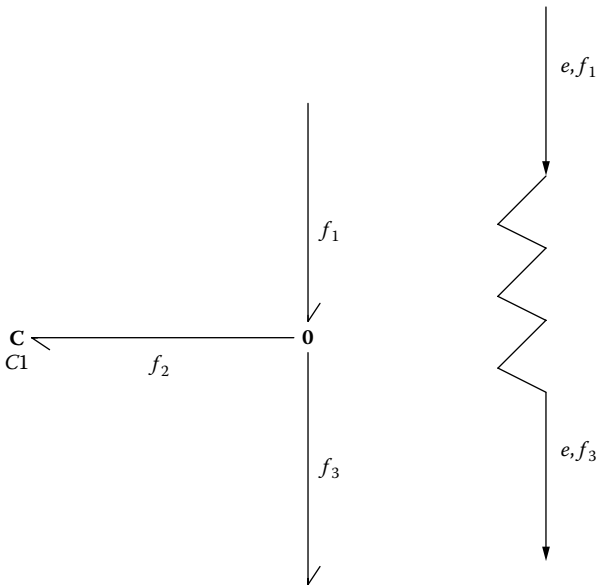
Consider the 1 junction. The basic governing relationship in one junction is that flow is the same in all bonds connected to a 1 junction. Consider a mass that is being forced by an external force and is moving as a result. The velocity of any point on the mass and the point where the force is acting are one and the same; that is, the mass, being a rigid body, is moving with a single velocity. Therefore, to represent something like this, the 1 junction can be used to join the mass with the source of effort. The bond graph representation is shown in Figure 3.20.

Now consider the 0 junction. To understand the behavior of the 0 junction, remember the basic constitutive relationships for 0 junctions. The effort remains the same in all the bonds connected to a 0 junction, but

**FIGURE 3.20**

Mass and force and their bond graph.

the flows are additive. Now consider a spring (or a damper) element. The velocities (flows) at the two ends of this component are different because the two ends are connected to different objects. The force, however, is one value throughout the component. The effort in the spring shown in Figure 3.21 is the same throughout. The flows at the two ends are f_1 and f_3 , respectively. Therefore, the flow in the spring (rate of compression/extension) is $f_1 - f_3 = f_2$. The accompanying bond graph shows exactly the same thing through the use of the 0 junction.

**FIGURE 3.21**

A spring and the corresponding bond graph.

EXAMPLE 3.5

Using this basic concept, the bond graph representation of the system shown in Figure 3.22 may be obtained through inspection. The velocity v_1 is obviously 0, and v_2 is the velocity of the mass M as well as the velocity of the upper ends of both the spring and the damper. So a 1 junction connects the mass to the source of effort and to the R and C elements through the 0 junctions. Using

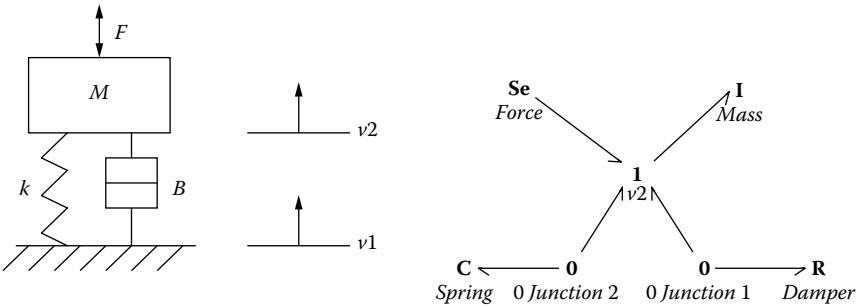


FIGURE 3.22
Schematic and bond graph for Example 3.5.

one of the rules of simplification, the 0 junctions can be collapsed to yield a bond graph of all the four elements connected through a 1 junction (just as in the series RLC circuit).

EXAMPLE 3.6

Consider the example shown in Figure 3.23. The bond graph representation is obtained by the method of inspection and is shown right next to the system

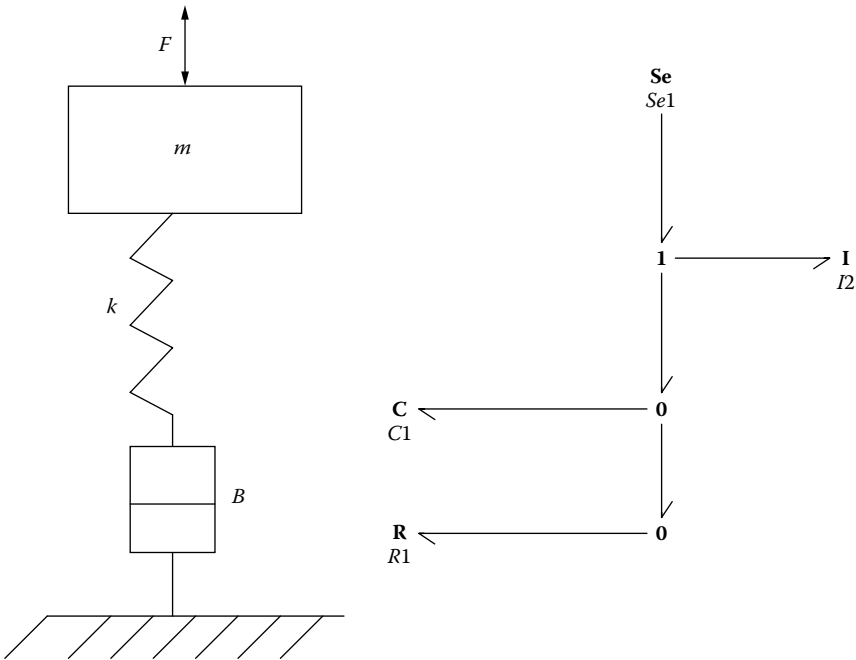


FIGURE 3.23
Schematic and bond graph for Example 3.6.

itself. The velocity of the mass and the upper end of the spring are the same. And the force in the damper is the same as the force in the spring. Upon simplification, the two 0 junctions collapse into one, and we get the bond graph representation shown in Figure 3.24.

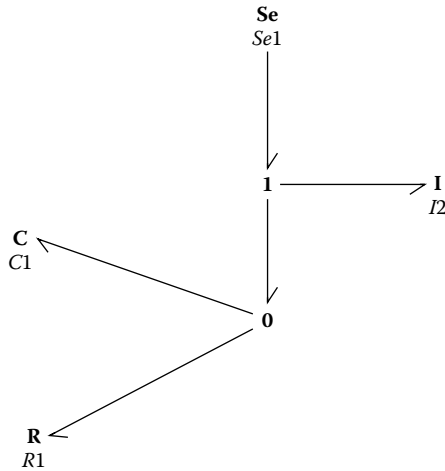


FIGURE 3.24

Final bond graph representation for Example 3.6.

In Examples 3.5 and 3.6 the bond graph representation is obtained by inspection. However, it is rather difficult for a lot of users of bond graphs (especially new ones) to develop complex models using this approach of inspection. A more formal algorithmic approach is necessary.

3.3.1 Formal Method of Drawing Bond Graphs for Mechanical Systems in Translation and Rotation

1. For each distinct velocity (angular velocity for rotation), establish a 1 junction. Some 1 junctions will represent absolute velocities, and some will represent relative velocities.
2. Insert the 1-port force (torque for rotation) generating elements between pairs of 1 junctions using 0 junctions. Attach capacitive and resistive elements to power bonds and connect them between two 1 junctions using a 0 junction. Also add inertia elements to the respective 1 junctions.
3. Assign power direction to all bonds.

4. Eliminate any 0 velocity 1 junctions (grounds) and all the bonds connected to these.
5. Simplify using the rules of simplification.

3.3.2 A Note about Gravitational Forces on Objects

In the examples that will be used to discuss the method of model development for mechanical systems, gravity (or gravitational force) has not been specifically considered. This is not because it does not play a part. It actually does for systems where there is any linear motion involved in the vertical direction. The focus here is to teach students how to draw bond graph representations, and gravity effect is just another source of force on any mass. So once students master the concepts of drawing bond graph models, the effect of gravity can be easily added to the model as a constant source of effort to every mass that is moving in the vertical direction.

EXAMPLE 3.7 (3.5 REVISITED)

Consider Example 3.5 again. The components are a spring, a mass, and a damper. A force is acting on the system as shown in Figure 3.25. We will try to draw the bond graph representation of this system again. Define v_1 and v_2 as two velocities (one of them is 0). And use 1 junctions for the two velocities. Then follow the steps as described before. For the velocity v_1 , a source of flow is added to the system. The initial bond graph is also shown in Figure 3.25.

Simplifying the model by removing the 0 junctions, we get Figure 3.26, and, upon further simplification, it becomes the one shown in Figure 3.27.

EXAMPLE 3.8

Consider a spring mass damper system with two masses, springs, and dampers, as shown in Figure 3.28. Using the algorithmic approach, the bond graph representation can be drawn as shown in Figure 3.29. The three distinct velocities shown in the schematic as v_1 , v_2 , and v_3 are represented on the bond graph by three 1 junctions. The corresponding masses (inertia) are attached to the respective 1 junction. The plate at the bottom is assumed to be massless. In between the 1 junctions, the pairs of springs and dampers are included using 0 junctions, and the sources of effort and force are added at the respective locations. This bond graph representation can be simplified a little more (using the fifth and sixth rules of simplification), but we have not done that here.

EXAMPLE 3.9

Please see Figure 3.30 for the schematic for this example. In this representation, members B_1 and B_2 represent power loss from frictional resistance from

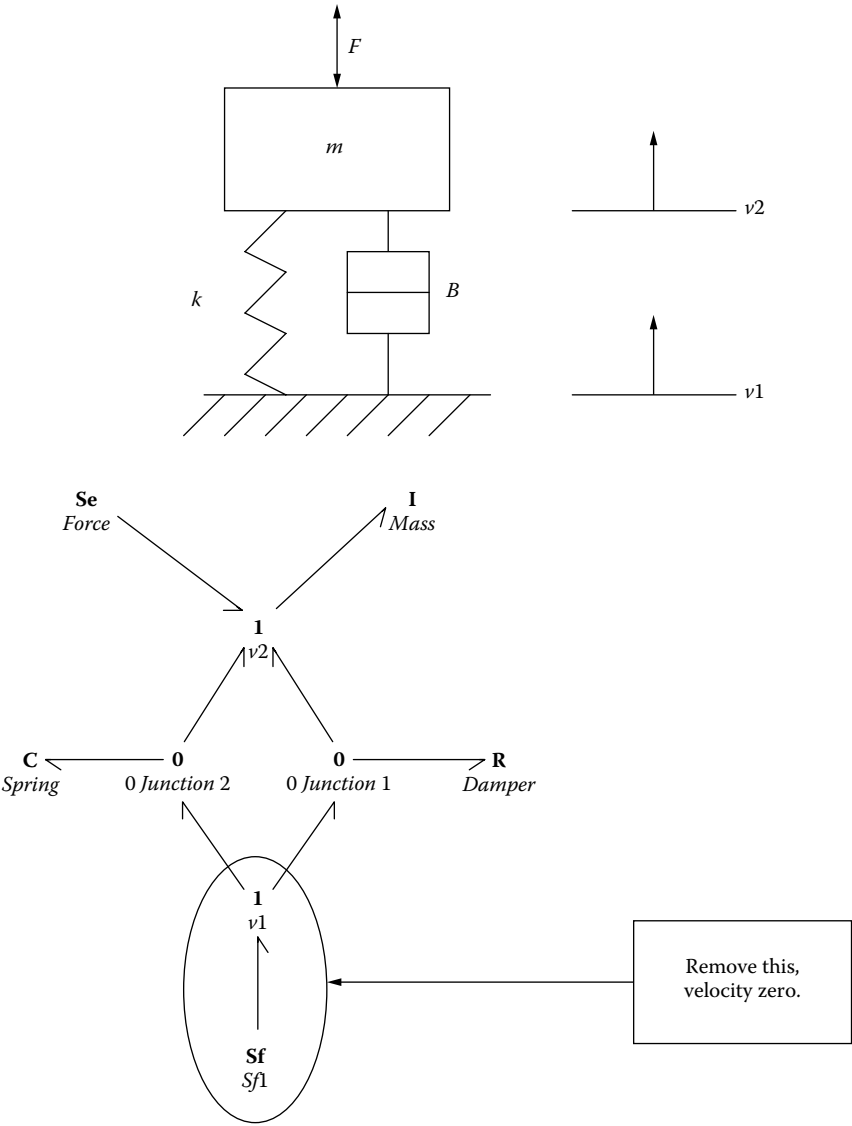


FIGURE 3.25
Initial bond graph representation.

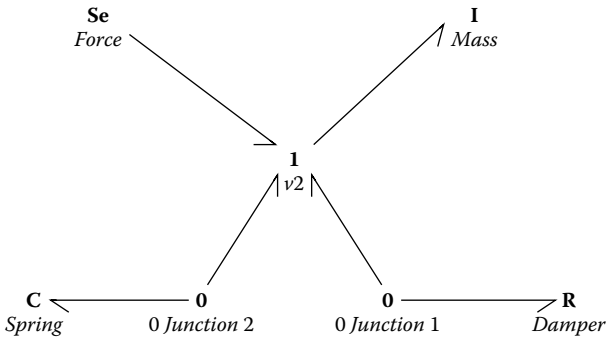


FIGURE 3.26

Bond graph representation of Example 3.7 after some simplification.

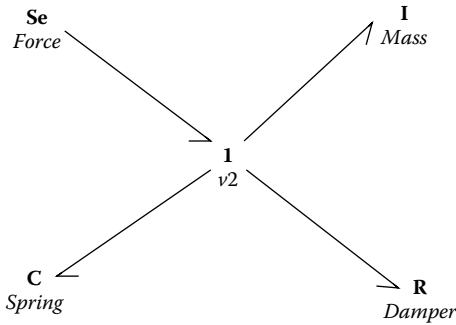


FIGURE 3.27

Final form of the bond graph representation.

friction with the ground. There are three distinct velocity points here, the two velocities of the two masses and the 0 ground velocity.

Using the algorithm described before, the initial bond graph representation is shown in Figure 3.31.

Now throwing away the 1 junction associated with the ground and the bonds associated with it and simplifying, we get the bond graph shown in Figure 3.32. This is simplified as much as possible.

EXAMPLE 3.10

Figure 3.33 shows another mechanical system whose bond graph representation is needed. There are several distinct velocity points. They are shown in the picture as V_1 , V_2 , V_3 , V_4 , and V_5 . The flexibility in the cable that is used with the pulley is represented as a lumped spring K_1 . The lever is a transformer element and is considered to be massless, and the pulley is massless and frictionless. Since the spring on the other end and the damper are not attached to the same point, there are two transformers needed, as shown in Figure 3.34. After simplification, we get the bond graph shown in Figure 3.35.

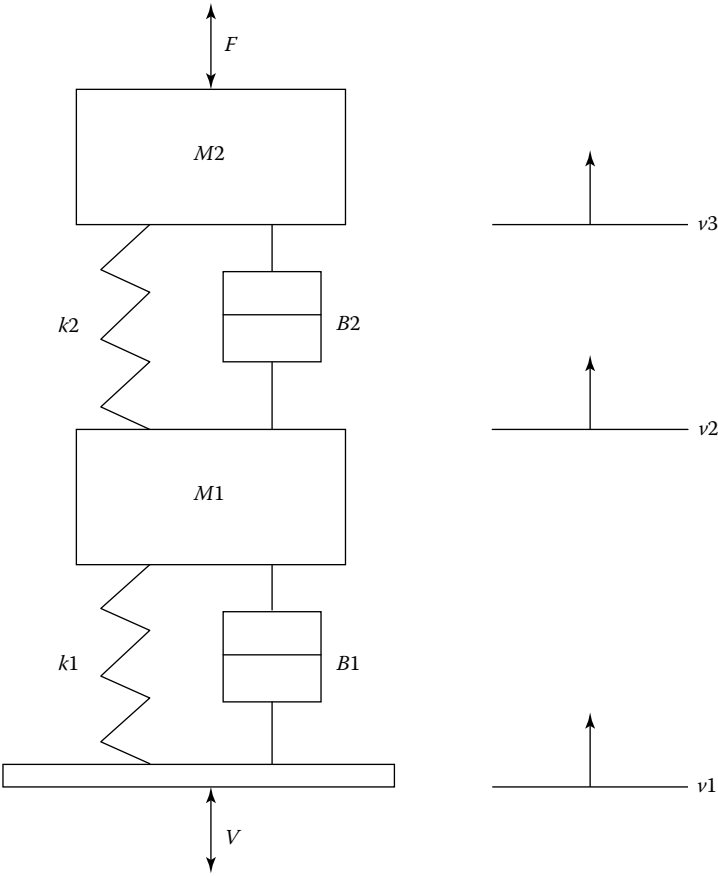


FIGURE 3.28
Schematic for Example 3.8.

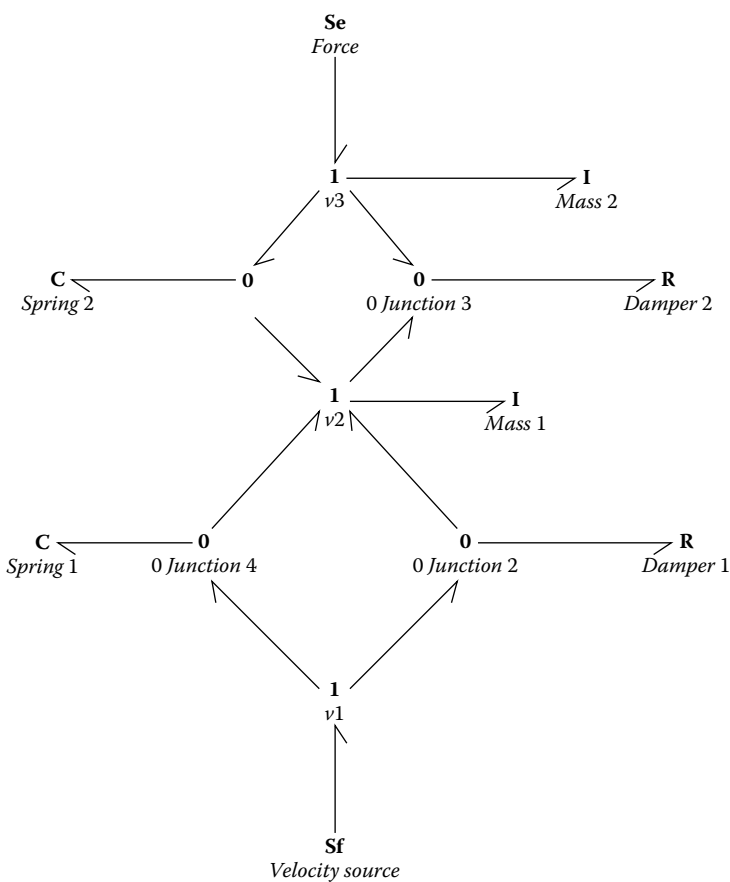


FIGURE 3.29
Bond graph representation for Example 3.8.

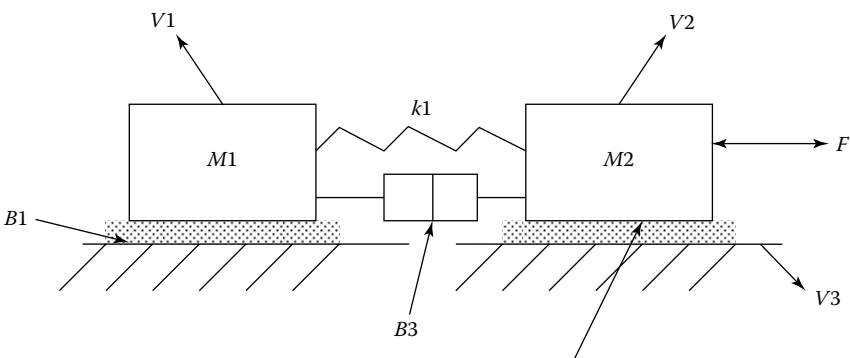


FIGURE 3.30
Schematic for Example 3.9.

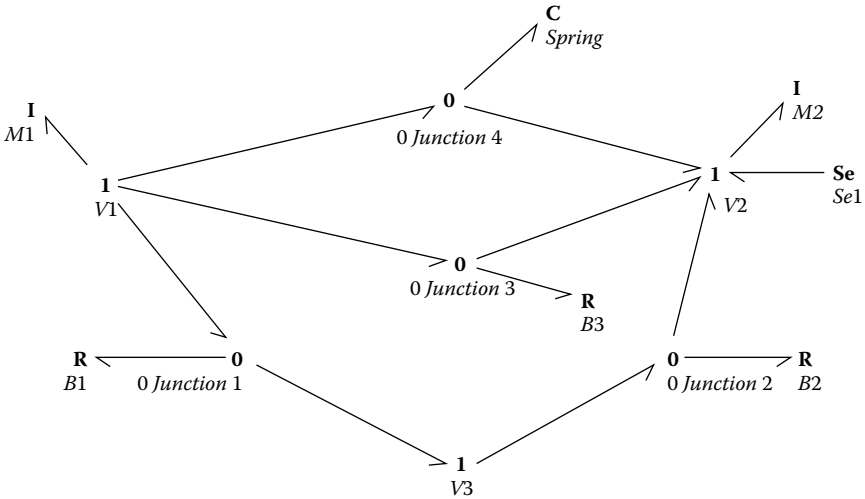


FIGURE 3.31
Initial bond graph representation for Example 3.9.

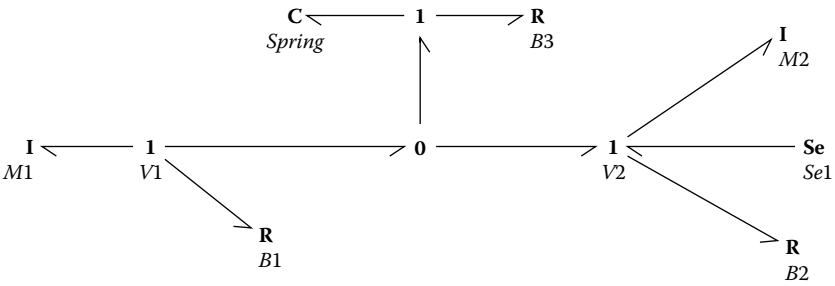


FIGURE 3.32
Final simplified bond graph for Example 3.9.

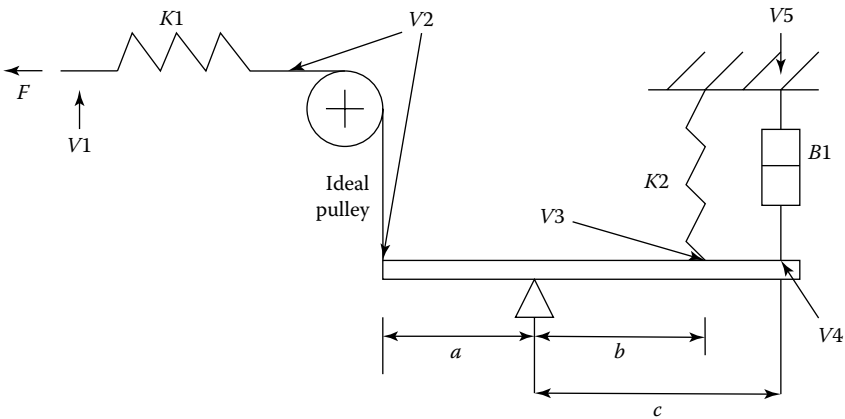


FIGURE 3.33
Schematic for Example 3.10.

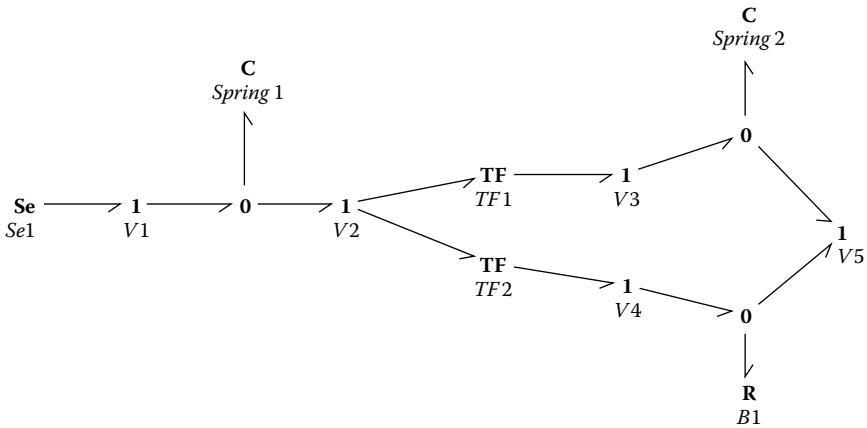


FIGURE 3.34
Initial bond graph model for Example 3.10.

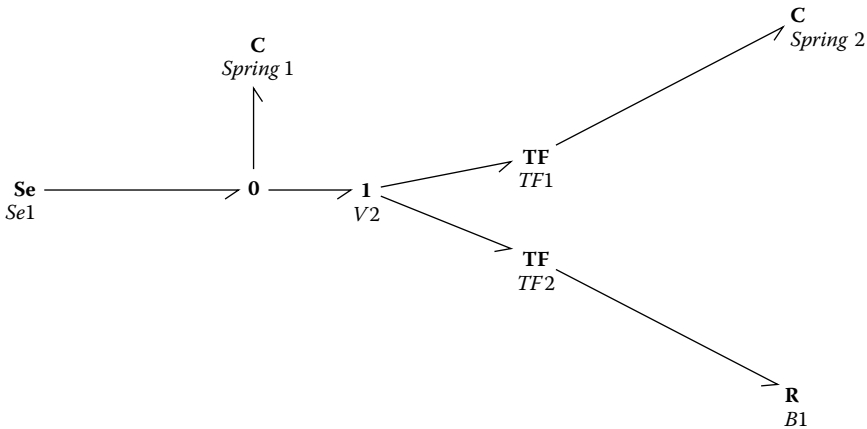


FIGURE 3.35
Final simplified model for Example 3.10.

3.3.3 Examples of Systems in Rotational Motion

For rotational mechanical systems, the process will be similar to that of translational systems. The algorithmic steps are identical with the linear velocity points being replaced by angular velocity points. We have considered a few systems to illustrate the process.

EXAMPLE 3.11

The schematic shown in Figure 3.36 is a simple example of a rotational system. It has three inertia elements (J_1 , J_2 , and J_3) and a torque source, and the two shafts can be treated as torsional springs. The shafts are mounted on bearings, and the bearing damping factors are shown as B_1 , B_2 , and B_3 .

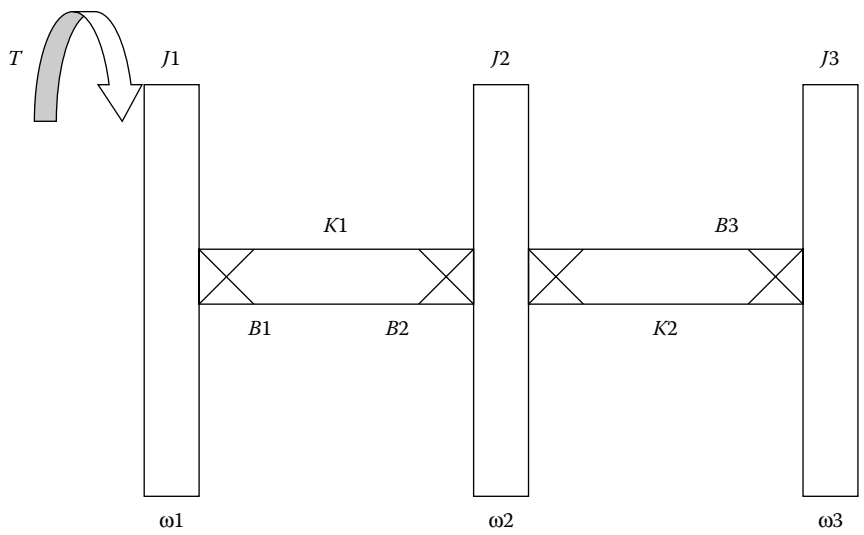


FIGURE 3.36
Schematic for Example 3.11.

Using the ground as the fourth velocity point, the initial bond graph model can be developed as shown in Figure 3.37. Note that since the bearing would be attached to the static housing on which such a system would be mounted, the bearing elements are initially drawn between the shaft and the ground.

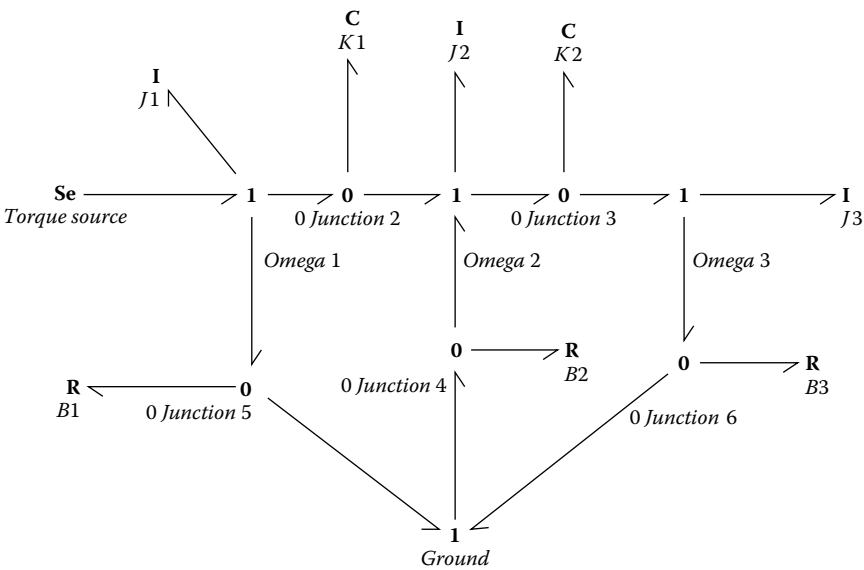


FIGURE 3.37
Initial bond graph model for Example 3.11.

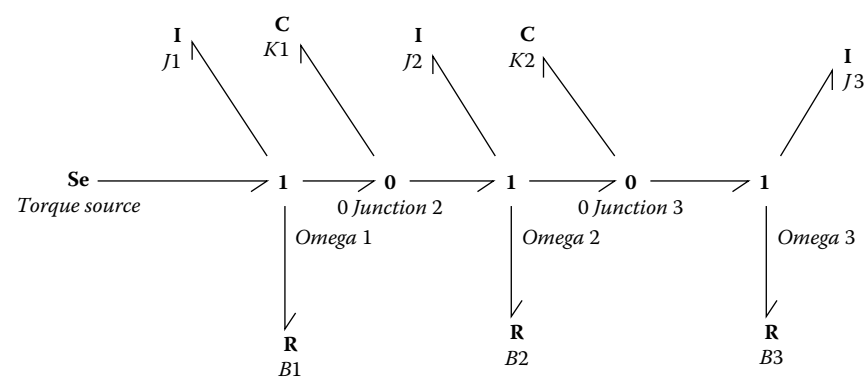


FIGURE 3.38
Bond graph model after simplification.

Removing the ground and then simplifying, we get the version shown in Figure 3.38.

EXAMPLE 3.12

The schematic for Example 3.12 is shown in Figure 3.39. There are four inertia elements $J1$, $J2$, $J3$, and $J4$. $J1$ and $J3$ are two gears that are meshing. The gears are also transformer elements. The four inertia elements are four velocity points as well. Along with this, we have a ground velocity point. $B1$, $B2$, $B3$, and $B4$ are four damping coefficients representing the damping resistance effects of the four bearings.

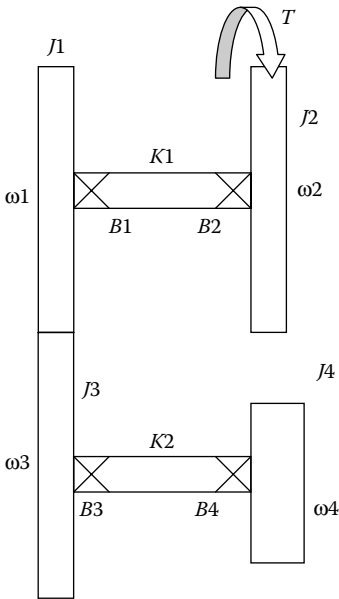


FIGURE 3.39
Schematic for Example 3.12.

Once again, using the algorithmic approach that we have been using so far, the initial bond graph representation looks like the one shown in Figure 3.40.

Once the 1 junction for the ground velocity is removed and the rest of the model is simplified, the bond graph looks like the one shown in Figure 3.41.

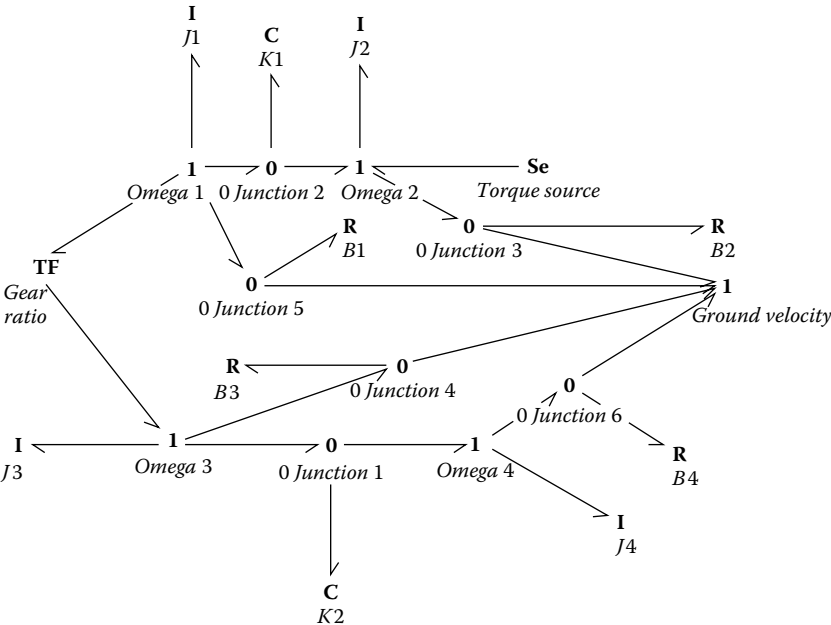


FIGURE 3.40
Initial bond graph for Example 3.12.

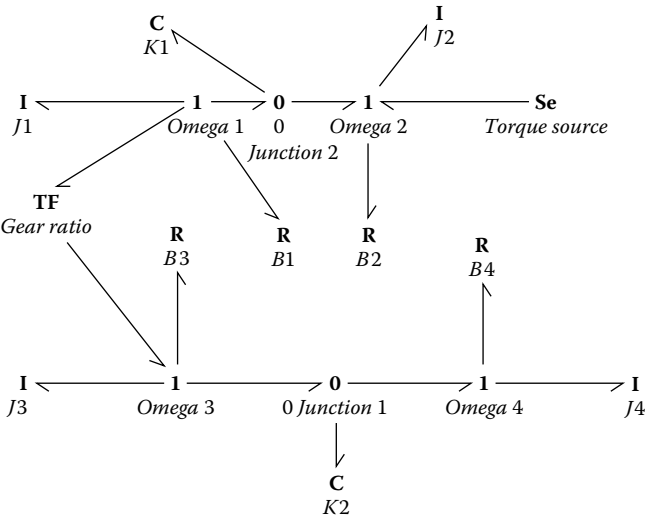


FIGURE 3.41
Simplified bond graph for Example 3.12.

So far in this chapter we have described the bond graph model development process and illustrated it through several examples from the fields of linear and rotational mechanical systems, as well as electrical systems. New users of this methodology should take some time and practice developing their own bond graph models for some typical engineering systems. This practice will provide the much needed understanding and confidence in independently working out bond graph representations.

We will now move onto a very important topic of bond graphing based model development. The topic is causality. A good understanding of the concepts of causality is necessary for a complete understanding of bond graph methodology.

3.4 Causality

The term causality is used to describe the concepts of cause and effect. This is an important conceptual step that one needs to take to develop the mathematical model of a system from its bond graph representation. To understand the concept of causality and how it works in bond graph representation, it is important for the reader to remember a few concepts discussed earlier. They are

- The half-arrow is used to denote the flow of power.
- When power flow is positive, it flows in the direction of the half-arrow.
- Although power is a product of effort and the flow, the half-arrow does not denote the direction of either the effort or the flow (but it actually denotes the direction of its product).

To develop the model equation, we need to find out a little more about flow and effort variables. As per convention, the flow and the effort associated with each bond are denoted with the symbols e and f placed above and below the bond, as shown in Figure 3.42. Causality is related to determining the direction of flow and effort variables.

For an example, consider a force applied on a mass. To represent this, a source of effort is connected to the left end of the bond, and the right end is connected to the rest of a system (the mass in this case). Then the effort information comes from the effort source to the rest of the system,

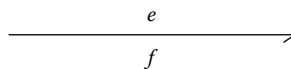


FIGURE 3.42

Effort and flow associated with a bond.

but the system determines what the flow will be and sends the flow information back to the source of effort. The force (i.e., an effort source) acts on the mass to make it move with some velocity (flow). The effort information travels to the mass. The source of effort controls the effort but does not control the flow directly. The velocity (flow) is determined by what the force does to the mass. Hence, it is actually determined by how the rest of the system (i.e., the mass in this case) reacts to the force. This situation may be interpreted to mean that the force information travels from the source of effort to the mass (system), and the flow information travels back from the mass (system) to the source of effort. This is shown on Figure 3.43 with directional arrows added to the effort and flow quantities. The effort travels from the left to the right, and the flow travels from the right to the left.

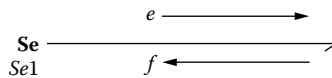


FIGURE 3.43

Effort and flow direction for an effort source.

If the bond is considered to be a 2-port element (one on the left and one on the right), we just showed that each port brings in the information about one of the quantities, effort or flow. Thus, if the effort information travels from the left to the right, the flow information will travel from the right to the left. This is true in real systems at all times because no basic component in a system can control both the effort and the flow. It can control only one of the two.

Similarly, for a source of flow, the flow information is provided to the system from the source, and other components in the system determine what the effort will be. The effort information comes back to the source, as shown in Figure 3.44.

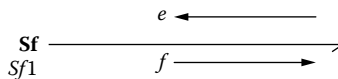


FIGURE 3.44

Effort and flow direction for a flow source.

For example, if a current source is attached to a couple of electrical components, the current source determines the flow that is going into the system. The voltage difference, or effort, is determined by the rest of the system, that is, the other components in the system. This information is passed back to the source of flow.

So, in a sense, for source of effort, it is the effort that comes first and causes the flow. And for the source of flow, the flow happens first and generates the effort.

A special symbol is used with the bond graph representation to convey this information of cause and effect or causality. A vertical line at the end of a bond indicates the port (or end) towards which the effort is flowing. This vertical line is called the causal stroke. The direction of flow is always opposite to the effort. Hence, there is no need to show its direction separately. Figure 3.45 shows these vertical lines for the sources of effort and flow.

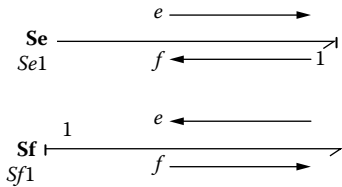


FIGURE 3.45
Causal strokes for effort and flow sources.

What we just discussed may be summarized as two laws of information exchange in bond graph theory.

1. One energy port (or end of bond) can impart information of only one of the factors of power to the interfacing element or junction.
2. The two ends (energy ports) at the 2-end of a bond cannot impart information of the same factor of power to their corresponding interfacing element or junction.

We have defined the causal structure of the 2-source types. Let us now look at the other common elements in a bond graph model.

3.4.1 Transformer

A transformer neither stores nor dissipates power, but transmits it from one side to the other. And the flow on one side is related to the flow on the other side. Similarly, the effort on one side is related to the effort on the other side. So the two possible causal structure of a transformer are shown in Figure 3.46. For the first case, flow information comes into the

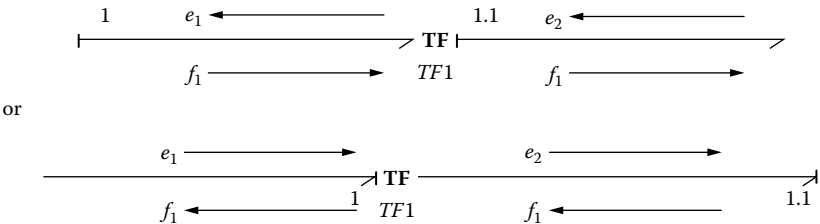


FIGURE 3.46
Causal structure of transformer element.

transformer from the left, and flow information goes out from the right (and effort comes from the right and goes towards the left). In the second case, the exact opposite happens.

3.4.2 Gyrator

Like a transformer, a gyrator neither stores nor dissipates power, but transmits it from one side to the other. In the gyrator element, the effort on one side determines the flow on the other, and the flow on one side determines the effort on the other. Hence, the causal structure for a gyrator could be one of the two forms shown, in Figure 3.47.

In the first case, the effort coming from the left determines the flow going out from the right through the gyrator factor (and, therefore, the effort coming from the right determines the flow leaving the left side). In the second case, the flow coming from the left determines the effort going out from the right (and the flow coming from the right determines the effort leaving the left side). Thus, the causal structure of a gyrator will be one of the two possible forms shown in Figure 3.47.

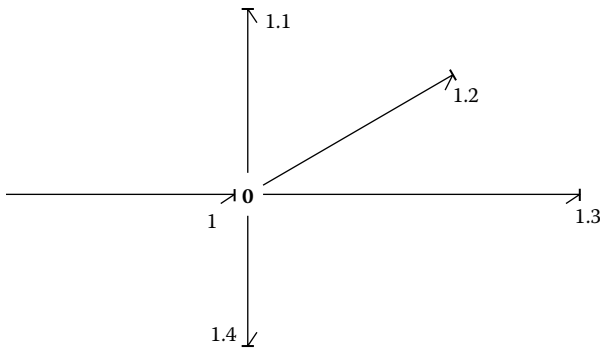


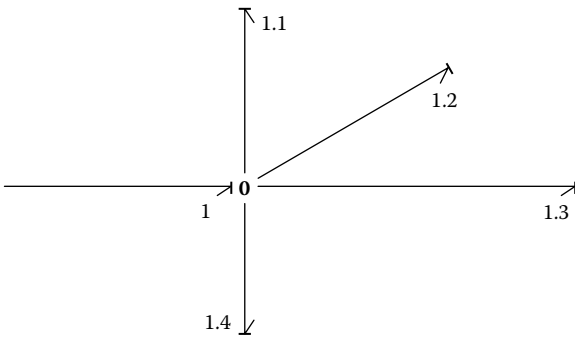
FIGURE 3.47

Two possible causal arrangements for gyrator elements.

3.4.3 Junctions

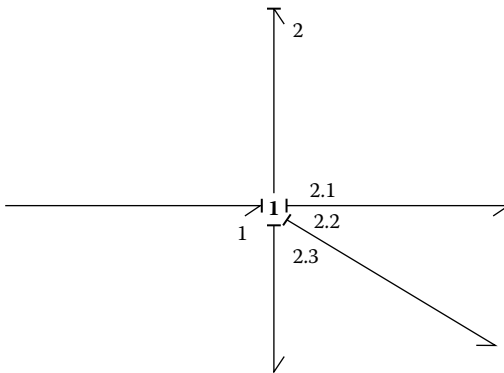
A 0 junction equates efforts, that is, effort is same in all bonds while flow is different. At the 0 junction, the effort information is brought by one of the bonds, and every other bond takes away the same effort information. That is why only one bond attached to the 0 junction will have the causal stroke close to the junction. All the other bonds will have the causal stroke away from the junction. The bond that brings in the effort information is also called the strong bond. Figure 3.48 indicates this.

A 1 junction equates flows, that is, flow is same in all bonds while effort is different. Hence, at the 1 junction, the flow information is brought by

**FIGURE 3.48**

Causal structure for a 0 junction.

one of bonds and every other bond takes away the same flow information. That is why only one bond attached to the 1 junction will have the causal stroke away from the junction. All the other bonds will have the causal stroke close to the junction. The bond that brings in the flow information is also called the strong bond. Figure 3.49 shows this causal structure.

**FIGURE 3.49**

Causal structure for a 1 junction.

3.4.4 Storage Elements: I , C

Storage elements receive energy from the system, store it, and release energy back into the system. Ideal storage elements do not dissipate energy. The causal structure discussion of storage elements is not as straightforward as the discussion for other elements that we have considered so far.

There are two terms that we will need to understand in this context. They are integral causality and differential causality. In simple terms,

integral causality means that past “causes” are integrated or accumulated to arrive at the “effect” at present. Differential causality means that differentiation of the “cause” at present will determine the “effect” of the future. Since the future is not usually known as well as the past, differential causality, which makes the system dependent on the future, is less acceptable. The preferred causal structure for storage elements is integral causality. However, integral causality is not always achievable, and at times, differential causality has to be accepted. Following is a discussion of these two types of causality, what they mean, and when and how they occur for the two types of storage elements.

To understand this in slightly more concrete terms, we need to consider the constitutive equations of the storage elements. We start first with the *I* element.

3.4.4.1 *I*, for Mass Elements or Inductances

The constitutive equation for the *I* element may be written as Momentum = inertia * velocity ($p = m * v$, $\lambda = L * i$, etc.) In terms of generalized variables this may be written as:

$$p = m * v \quad (3.24)$$

But p , momentum, can be written as:

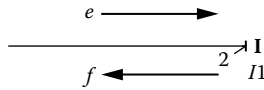
$$\int_{-\infty}^t e \cdot dt = p. \quad (3.25)$$

Therefore, after minor manipulation:

$$\frac{1}{m} \int_{-\infty}^t e \cdot dt = f \quad (3.26)$$

If one looks at this representation carefully, it relates flow to the integral of effort (i.e., accumulation of effort). This should be interpreted as accumulated effort over time causes flow. This is the meaning of integral causality for the *I* element.

The preferred causal structure for the *I* element should be Integral causality: receiving effort information and sending out flow information. This is represented by the vertical causal stroke at the end of the bond that is close to the *I* element, as shown in Figure 3.50. The effort information is received by the element and the “accumulation” of effort information generates flow information, which is sent back to the system.


FIGURE 3.50

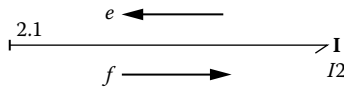
 Integral causality for I element.

The same constitutive equation for the I element may be rewritten in the following form:

$$e = \frac{dp}{dt} = m \cdot \frac{dv}{dt} = m \cdot \frac{df}{dt} \quad (3.27)$$

This means that the effort is related to the derivative of the flow. The derivative of the flow at the current time determines the future effort. This is the derivative form of the constitutive equation for the I element, and this representation is called the differential causality.

Sometimes, as we will see a little later, integral causality assignment will not be possible, and differential causality will be the only possibility, that is, receiving flow info and giving out effort info. In that case, the representation will be as shown in Figure 3.51. The causal stroke will have to be put on the bond end opposite to where the I element is.


FIGURE 3.51

 Differential causality for I element.

3.4.4.2 C , for Capacitive or Spring Elements

The constitutive equation for the I element may be written as effort = capacitive constant * displacement ($F = k * x$, $V = 1/C * Q$, etc.). In terms of generalized variables, this is written as:

$$e = q/C \quad (3.28)$$

But q , the displacement, can be written as:

$$\int_{-\infty}^t f \cdot dt = q, \quad (3.29)$$

Therefore,

$$\frac{1}{C} \int_{-\infty}^t f \cdot dt = e \quad (3.30)$$

If one looks at this representation carefully, it relates effort to the integral of flow (i.e., accumulation of flow). This should mean accumulated flow over time causes effort. This is integral causality for the C element.

The preferred causal structure for the C element should be integral causality: receiving flow information from the rest of the system and sending out effort information to the rest of the system. This is represented by the vertical line at the end of the bond that is away from the C element, as shown in the Figure 3.52.



FIGURE 3.52

Integral causality for the C element.

The same constitutive equation for the C element may be written in the following form:

$$f = \frac{dq}{dt} = C \cdot \frac{de}{dt} \quad (3.31)$$

This means that the flow is related to the derivative of the effort. The derivative of the current effort determines the future flow. This is the derivative form of the constitutive equation for the C element, and this representation is called the differential causality.

Sometimes differential causality will be the only possibility, that is, receiving effort information and sending out flow information. In that case, the causal representation will be as shown in Figure 3.53. The causal stroke will be put at the end of the bond that is closest to the C element.

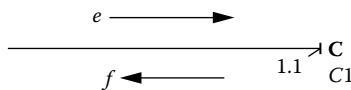


FIGURE 3.53

Differential causality for the C element.

3.4.5 R , for Resistive Elements

The resistance element is not an energy storage device, it dissipates energy. The constitutive relationship between effort and flow is algebraic.

$$e = Rf \quad (3.32)$$

Hence, R elements have neither integral nor differential forms, and the causal structure could be either type, that is, the causal stroke for an R element could be either of the two shown in Figure 3.54. Both are equally acceptable. This means that if flow information comes in from the system, the R element can easily determine the effort information by algebraic manipulation. It is just as easy to do the opposite. The causality of R elements is actually determined by what is happening in the rest of the model.

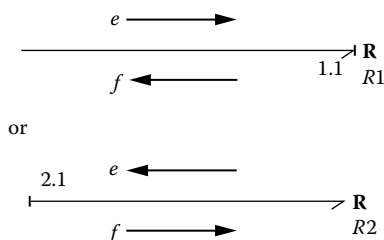


FIGURE 3.54

Causal structure for an R element.

Now that we have discussed the causal structure of all the basic elements, it is necessary to have a discussion of how the causal strokes are assigned to different bonds in an actual model. While these assignments are carried out, sometimes we will encounter difficulties with seemingly conflicting requirements, and the modeler needs to know how these can be resolved. We will outline the process through a series of algorithmic steps. But before we do, it is important to remind the readers of a few things. They are

- The causal strokes for the sources of effort and flow **will have to be the way they have been** described earlier.
- The causal strokes for the 0 and 1 junctions **will have to be the way they have been** described earlier.
- The transformer and gyrator causality can be **one of two types**.
- For the storage elements, **integral causality is preferred but differential is acceptable**.
- For the dissipative elements, there are **no preferred causal directions**.

These items are listed here to re-emphasize that the first two are very stringent requirements while the last three have varying degrees of flexibility.

Keeping this in mind, one can come up with an algorithm for assigning causality in a bond graph model.

3.4.6 Algorithm for Assigning Causality in a Bond Graph Model

1. Choose any source and assign its required causal stroke. Extend the causal implications through the bond graphs as far as possible using 0, 1, TF, GY, and so forth.
2. Repeat this for all sources.
3. Choose the storage element (I or C) and assign its preferred causality (integral causality). As in (1), extend the implications through the rest of the bond graphs.
4. Repeat step (3) for all storage elements.
5. Choose any unassigned R element, assign a causality to it (arbitrary), and extend the implications throughout the bond graph. (Many R elements would be assigned causal strokes by this time.)
6. Repeat (5) for all unassigned R s.
7. Choose any unassigned bond and assign arbitrarily and extend through the rest of the bond graph.
8. Repeat step (7) until you are done.

In most models, the first four steps will result in complete causal structure determination for the model. In relatively complex models, one needs to include steps 6, 7, and 8. While executing these steps, the user should keep in mind that every step should try to extend the causal implications onto as many bonds as can possibly be done. We will now demonstrate the process through Examples 3.13–3.18.

EXAMPLE 3.13

The bond graph of a simple spring-mass-damper system, or an RLC circuit, (Figure 3.55), is shown again in Figure 3.56.

Following the steps given above, the causality structure for the bond graph model for either of these systems is shown in Figure 3.56 as well.

This structure satisfies the integral causality requirements for I and C elements, the requirement for Se element, and the requirement for the 1 junction. The causal stroke for the R element is applied last to fit all these requirements because there is no particular constraint for the R element.

Let's consider a few more examples.

EXAMPLE 3.14

Figure 3.57 shows another simple circuit and its corresponding bond graph. Following the algorithm, the bond graph representation, after the causal strokes are applied, is shown in Figure 3.58.

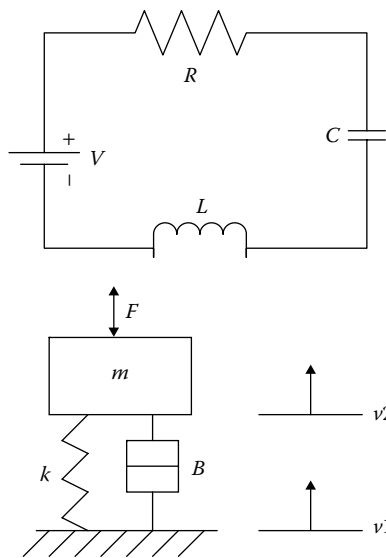


FIGURE 3.55
An RLC circuit and a spring-mass-damper system.

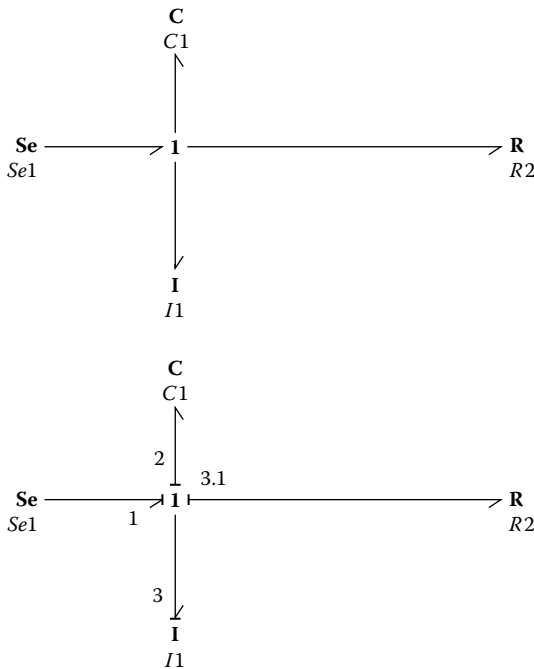


FIGURE 3.56
Basic bond graph and causal bond graph for the systems in Figure 3.55.

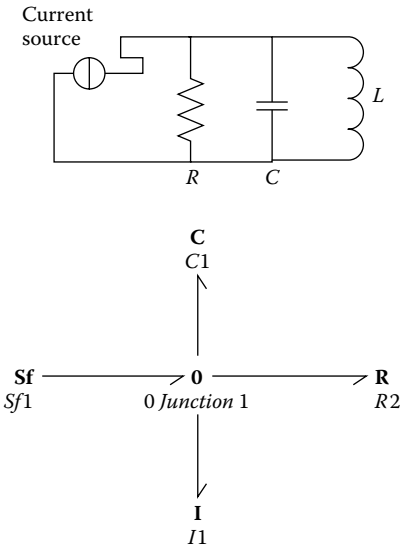


FIGURE 3.57
A parallel RLC circuit with its corresponding bond graph.

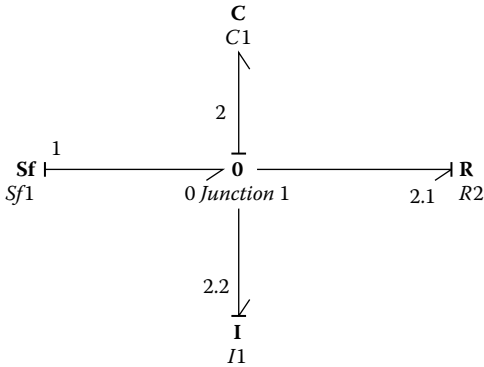


FIGURE 3.58
Causalled bond graph for the system in Figure 3.57.

Once again, it is seen that the structure satisfies the integral causality requirements for I and C elements, the requirement for the Sf element, and the requirement for the 0 junction. The causal stroke for the R element is applied last to fit all these requirements because there is no particular constraint for the R element. Compared with the previous example, one can see that the R element has a different causal stroke to satisfy all the requirements.

EXAMPLE 3.15

Figure 3.59 shows a mechanical system that we encountered earlier and its bond graph.

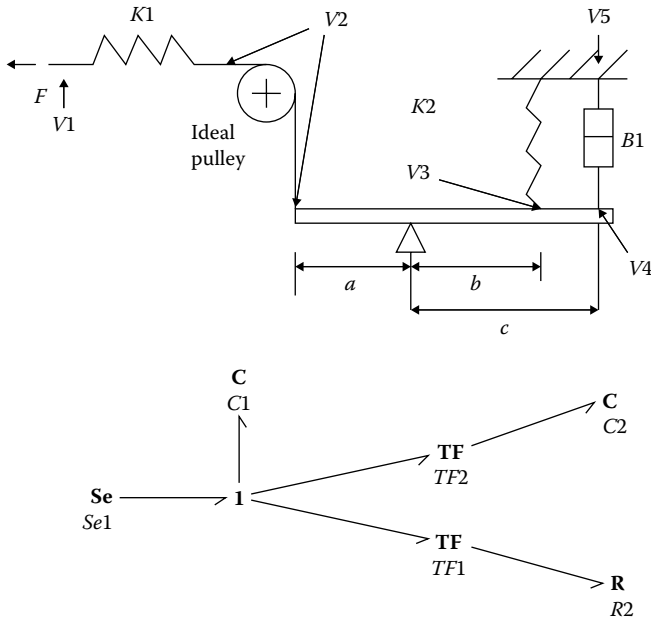


FIGURE 3.59

A mechanical system and the corresponding bond graph.

Using the algorithm given above, the causal structure for this system may be shown as in Figure 3.60. One starts with the source of effort and applies the causal stroke for it. We cannot proceed any more beyond the 1 junction.

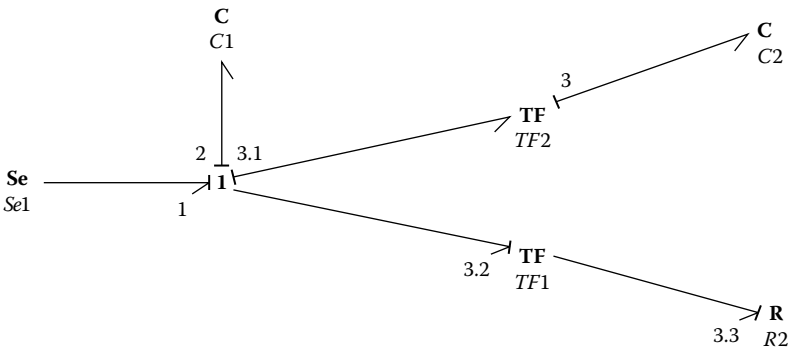


FIGURE 3.60

Causalled bond graph for the system shown in Figure 3.59.

The C1 element is then assigned an integral causality, but we still cannot proceed beyond the 1 junction. C2 is now assigned integral causality, and we can work backwards through the transformer TF2 back to the 1 junction. Now, all the bond ends at the 1 junction have causal strokes except the one bond connected to the transformer element TF1. This bond will have a noncausal end adjacent to the

EXAMPLE 3.17

Figure 3.63 shows an electrical circuit along with its bond graph representation. From the bond graph, its final form with the causal structure can be obtained using the algorithm described before as shown in Figure 3.64.

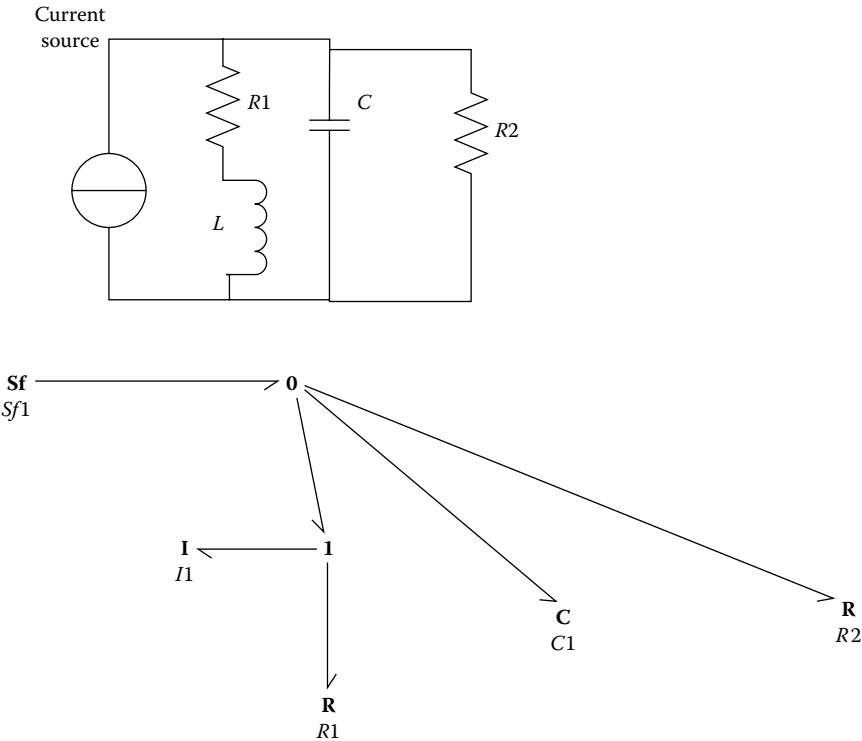


FIGURE 3.63
An electrical system and its bond graph representation.

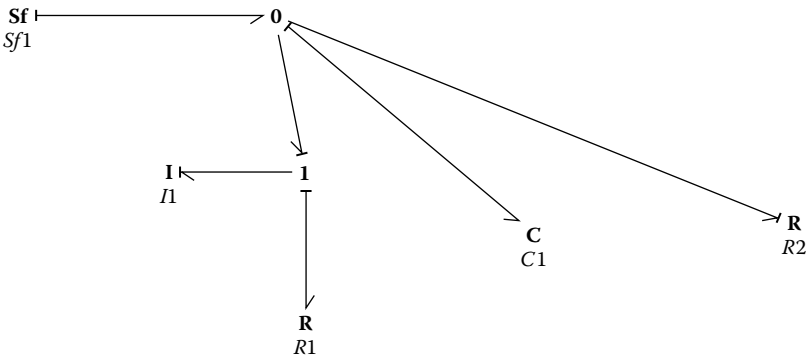
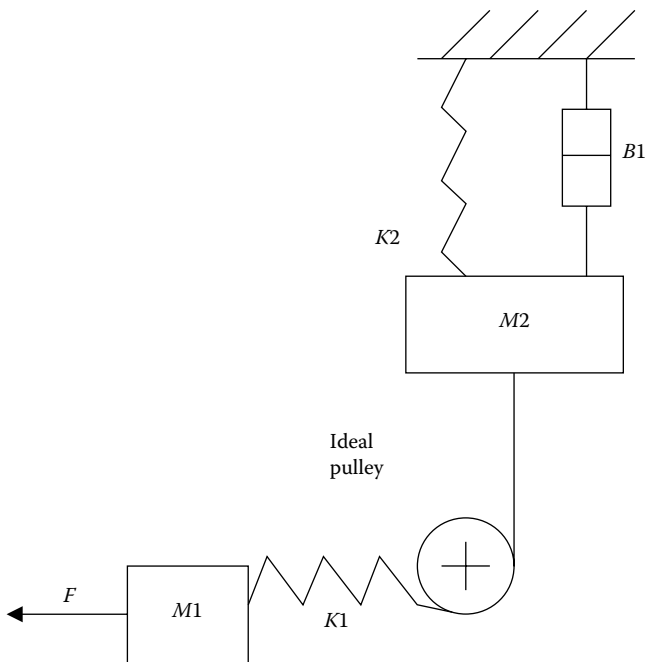


FIGURE 3.64
Causalled bond graph for the system shown in Figure 3.63.

EXAMPLE 3.18

This example consists of a mechanical system, and its corresponding bond graphs are shown in Figure 3.65. Analyzing the causality of this system using the approach described before, we get the causalled bond graph as shown in Figure 3.66.

In all the above cases we obtained integral causality for the energy storage elements I and C . With so many examples shown, one may think that integral causality can be taken for granted all of the time. This is not true, and, in many cases, one would encounter situations where integral causalities will not be possible. In the next section, some of those possibilities are discussed along with what the suitable course of action should be.

**FIGURE 3.65**

A mechanical system and its basic and final simplified bond graph.

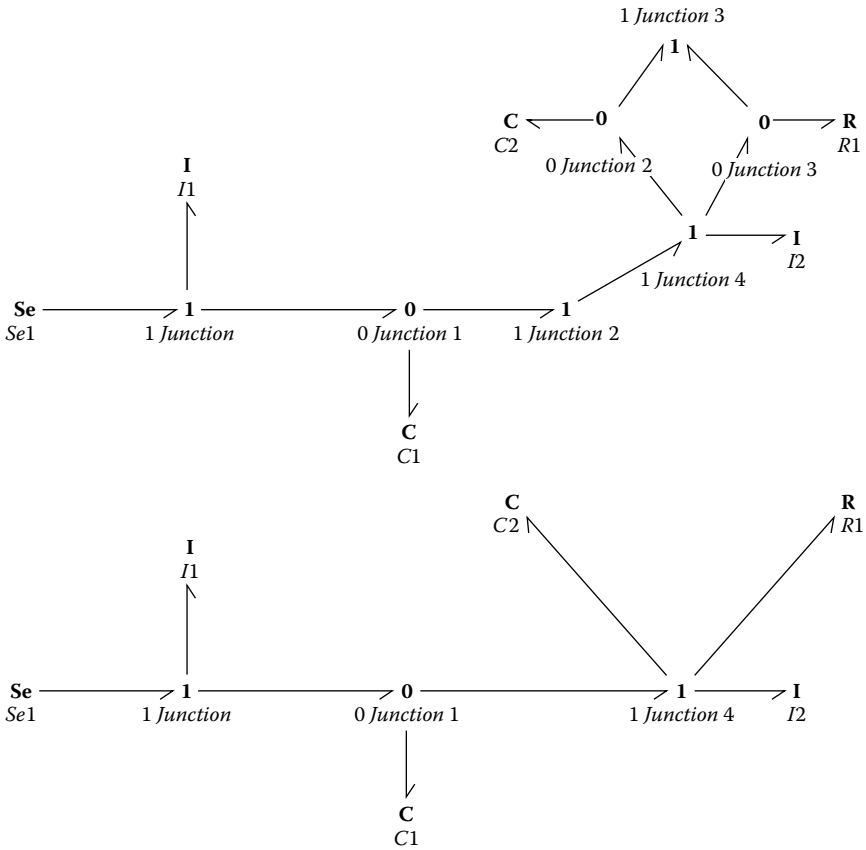


FIGURE 3.65
(Continued)

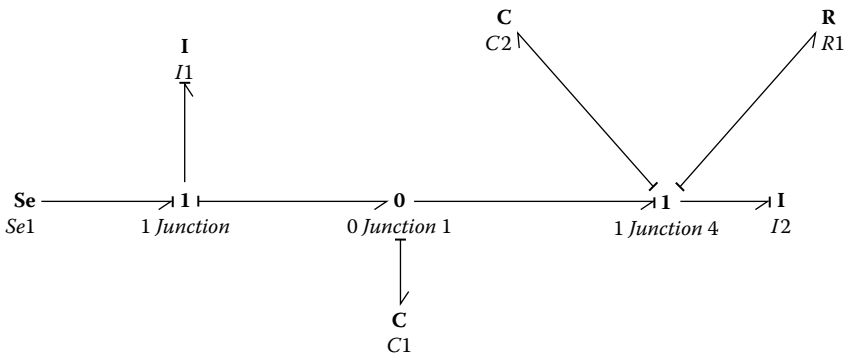


FIGURE 3.66
The causalled bond graph for the system in Figure 3.65.

3.4.7 Integral Causality versus Differential Causality for Storage Elements

Examples 3.13–3.18 had storage elements with integral causality. Although this is the desirable outcome, this is not always achievable. Sometimes, the causal structure of the system is such that one or more of the energy storing devices end up having differential causality. Before we look at some of these examples, it is important to understand the different implications (in terms of the final model) of an integral and differential causality.

For an energetic system, the state variables must at least uniquely define the energy stored in the system. The minimum number of state variables required is determined by the number of independent energy storage elements in the system model. Energy storage devices that have been integrally causalled are independent.

An energy storage element that has derivative causality is not independent. Its stored energy is determined by the variables associated with the element from which the causal propagation began. Derivative causality on an energy storage element is not an error, but it can have undesirable consequences. It leads to implicit ordinary differential equations rather than explicit ordinary differential equations. Since explicit differential equations are more easily solved, the implicit equations may lead to extensive algebra in deriving state equations and may also lead to numerical difficulties when simulating system behavior on a computer. If one or more energy storage elements in a model have derivative causality, the model developer may want to modify the model to eliminate the differential causalities. Although this is neither essential nor is it always possible, an attempt to change the causality is always recommended.

Examples 3.19–3.21 describe where derivative causality may occur.

EXAMPLE 3.19

The first example is that of a circuit with a voltage source and a capacitor (Figure 3.67). The correctly causalled bond graph for this system is shown in Figure 3.68. The causal requirement for the 1 junction and the Se element are not violated, but the C element attains a derivative causality. If one tries to explore the origin/reason for this, it will eventually be clear that this circuit is not possible to construct. It is presumed that the circuit is being made to charge a capacitor. And charging a capacitor happens if a current starts flowing through this circuit. However, without any resistance in the circuit, the current drawn could be infinite. Thus, the circuit has to have some resistance in it, however small. If we add a resistance in the circuit, it looks like Figure 3.69 and its bond graph representation can be seen in Figure 3.70. Addition of the R element makes the actual circuit realistic and its model accurate. As a result, the causal description of the C element becomes integral as well.

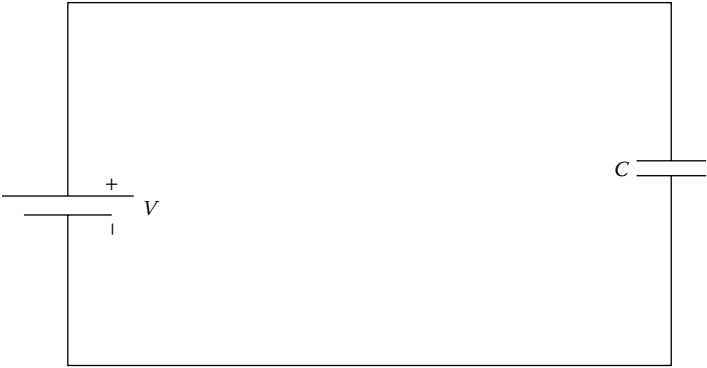


FIGURE 3.67
A circuit with a voltage source and a capacitor.

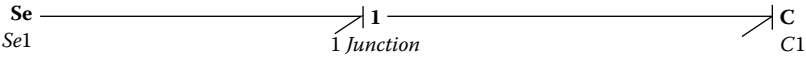


FIGURE 3.68
The causalled bond graph for the circuit in Figure 3.67.

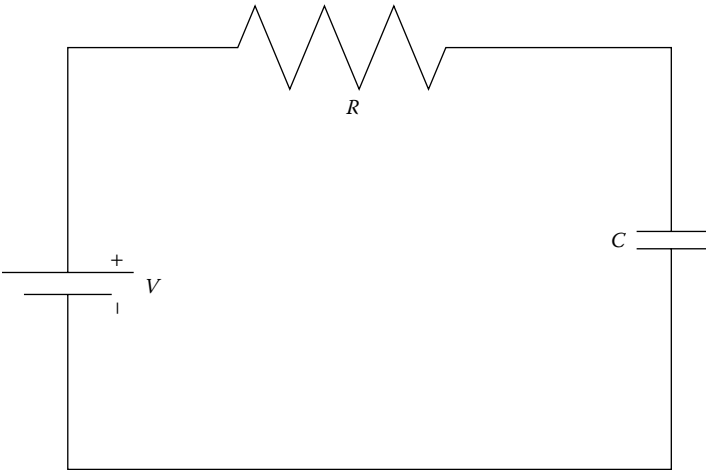


FIGURE 3.69
Capacitor circuit modified with resistance.

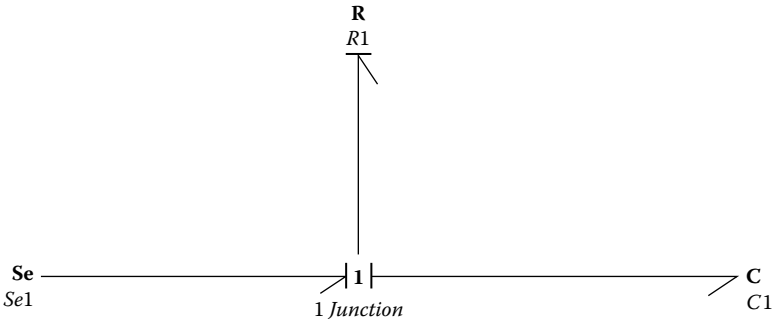


FIGURE 3.70
Bond graph for Figure 3.69.

EXAMPLE 3.20

Let us look at another example. Here is a circuit with two inductors in series and a voltage source. The circuit and the causalised bond graph are shown in Figure 3.71.

Note that when we built the bond graph representation of the two *Is*, one will have a differential causality and another will have an integral causality. This is because both the storage elements cannot have behavior that is

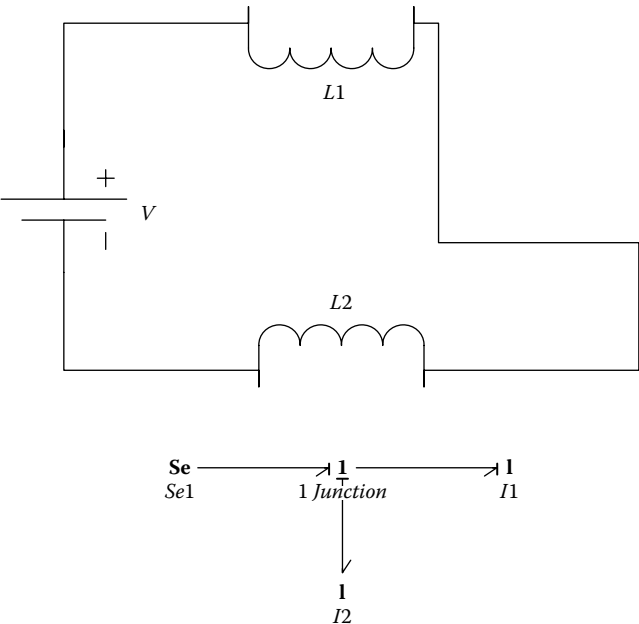


FIGURE 3.71
Circuit with two inductances and its corresponding bond graph.

independent of each other. What happens in one will influence the other. Hence, one is an integral causality and the other is a differential causality. If we modify this circuit by a single I equivalent (instead of using two I elements) as it is taught in EE circuits classes, the problem of differential causality will disappear and we will have a bond graph representation that will look as shown in Figure 3.72.

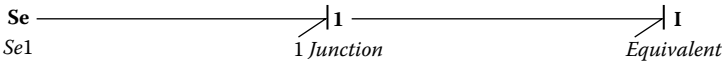


FIGURE 3.72
Modified bond graph for system in Figure 3.71.

EXAMPLE 3.21

Consider the mechanical system and its initial bond graph shown in Figure 3.73. After removing the ground velocity, the 1 junction labeled fixed end, and

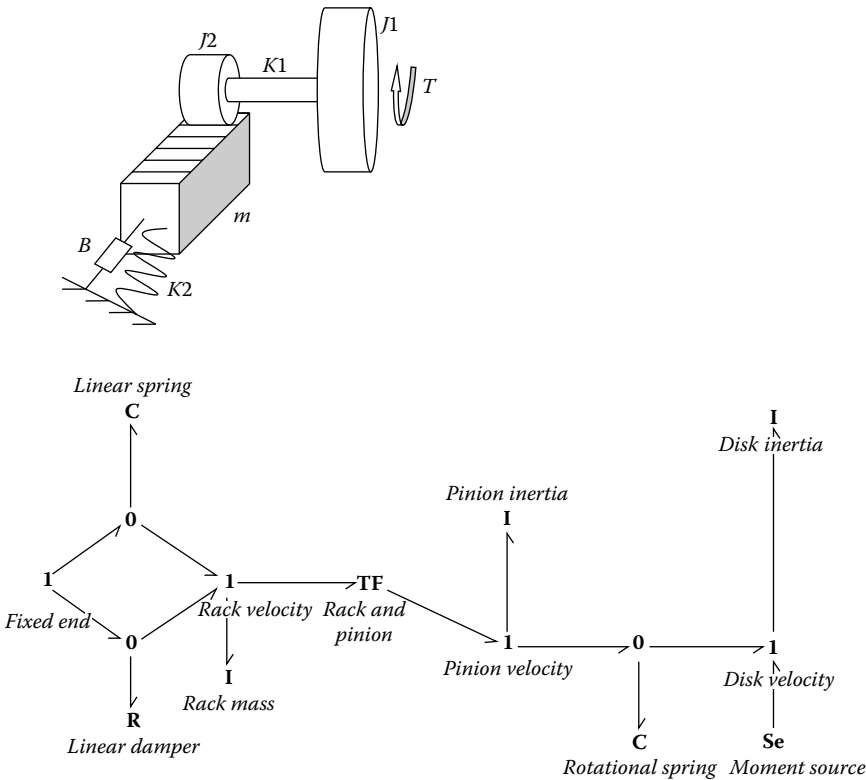


FIGURE 3.73
A mechanical system and its corresponding initial bond graph.

simplifying, the bond graph representation looks like the first one shown in Figure 3.74.

Note that after all the causal structure was determined one of the elements (the I element called pinion inertia) has a differential causality. Once again, this is a result of a modeling assumption that was made. Consider the transformer element, the rack and pinion. We are assuming that it is an ideal transformer, that is, there is no energy used to do anything other than to rotate the pinion. This is possible if the teeth of the rack and pinion are ideally rigid. However, they are not and some of the energy is used to bend the teeth elastically. To modify the model, this elasticity needs to be accounted for using another C element after the transformer (or before), as shown in Figure 3.75. After adding this new C element, known as transformer compliance, all the storage elements now have integral causality.

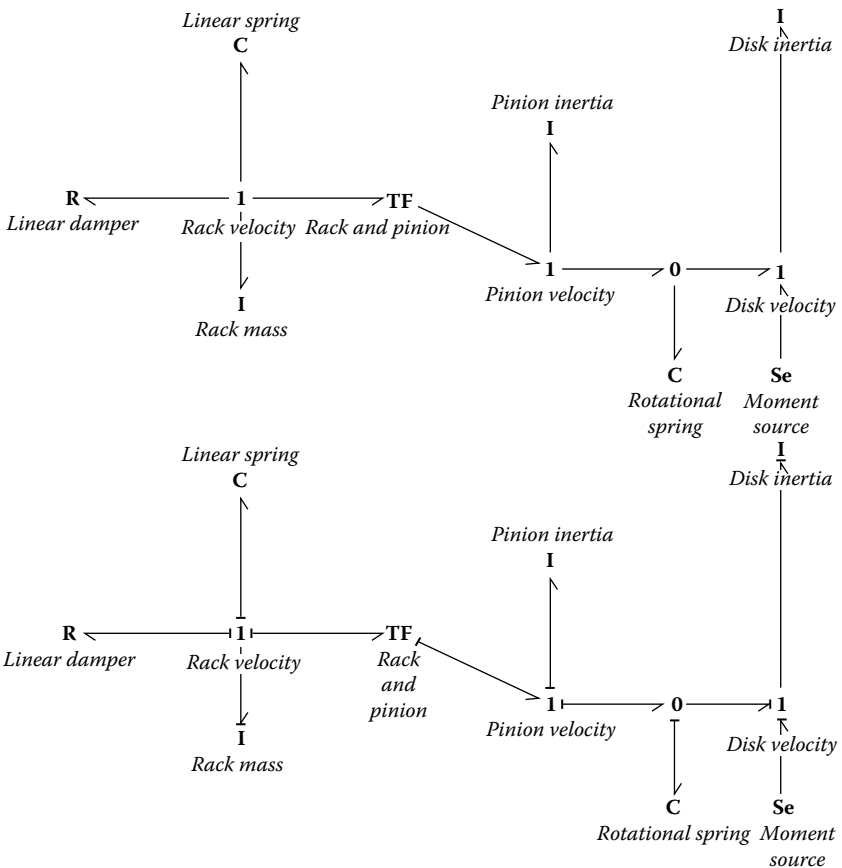


FIGURE 3.74

Modified bond graph and after the causal strokes are added.

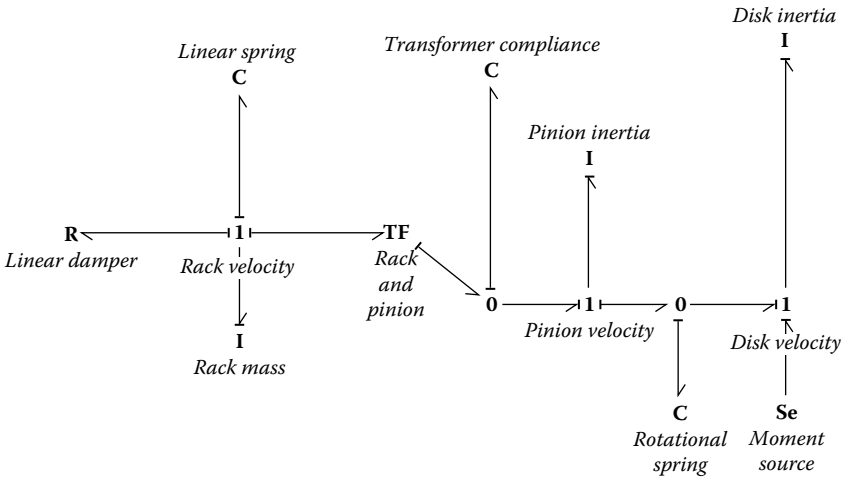


FIGURE 3.75
Causal structure after the C element is added.

Through Examples 3.19–3.21 we have demonstrated several ways to modify bond graph models to not only reflect reality more closely but also to achieve integral causality for the storage elements in the model. In a very informative paper, Jose Granda (1984) offers a very insightful discussion on this same topic. He summarized the different techniques that may be used to avoid differential causality. They are

1. Combine storage element into an equivalent storage element
2. Add an energy storage element
3. Add a resistive element
4. Remove some storage elements

Although these are general rules, these cannot be used without any relevance to the actual system. One must have some understanding of the system and the system model to determine which technique, if any, could be used in a given situation.

3.4.8 Final Discussion of Integral and Differential Causality

Once the causal structure of a bond graph model is determined and no rules of causality are violated, the number of energy storage elements with integral causality indicates the order of the system. This means that the number of integrally causalled storage elements will be the same as the number of independent state variables in the set of differential equations that will govern this system. If there is an energy storage element that has

differential causality, it means that the state variable for this element is not an independent variable, but its behavior is dependent on other energy storage elements. As has been demonstrated in the previous section, differential causality could be caused by a modeling error or simplifying assumption. Many times it can be fixed (as just shown), but sometimes it cannot be fixed.

3.4.9 Causality Summary

1. One energy port (end of a bond) can provide only one type of “information” (either f or e) to the adjoining bond.
2. The two ends of the bond cannot provide the same information to the adjoining bonds.
3. Power half-arrows are unrelated to the causal strokes.
4. In a bond graph representation one should always attempt to provide integral causality to all storage elements (I, C).
5. Differential causalities are possible at times.
6. The number of independent integrally causalled storage elements (I, C), determine the order of the system (= number of independent ODEs).
7. If the system model has only integral causality, the differential equations look like:

$$\begin{aligned}\dot{x} &= f(x, y, t) \\ \dot{y} &= f(x, y, t)\end{aligned}$$

and can be solved by explicit methods.

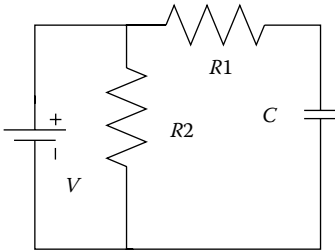
If the system has 1 differentially causalled element, the equations look like:

$$\begin{aligned}\dot{x} &= f(\dot{x}, x, y, t) \\ \dot{y} &= f(\dot{y}, x, y, t)\end{aligned}$$

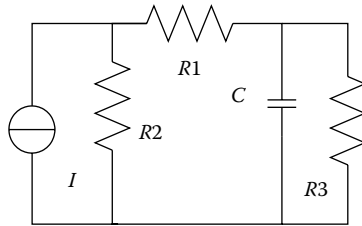
and will have to be solved by implicit methods. Modifying a bond graph that has differential causality to obtain integral causality ensures that the differential equations for the model changes from implicit to explicit. This item was not specifically discussed here, but will be discussed in the chapter on equation derivation.

Problems

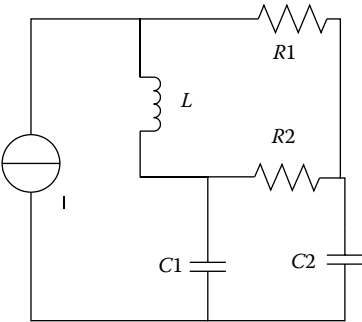
- 3.1. In Section 3.1, six simplification rules were discussed. A proof was shown for the fifth rule. Using the same approach, show that the sixth rule of simplification is also valid.
- 3.2. For the electrical and mechanical systems shown in the Figure P3.1 a–m, develop a bond graph representation for the system, simplify the bond graphs using the rules of simplification, and then add the causal strokes using the process discussed in this chapter.



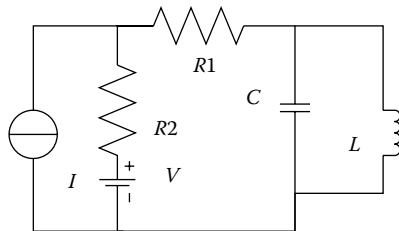
(a)



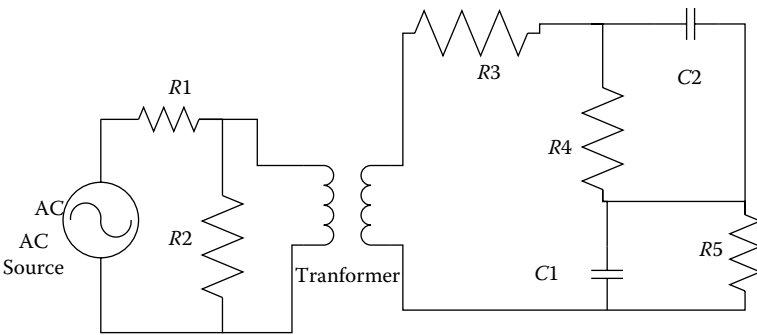
(b)



(c)



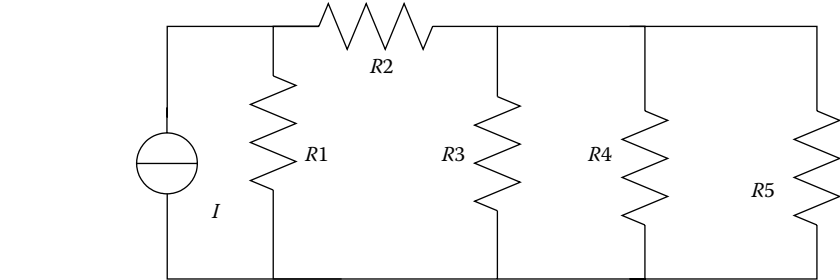
(d)



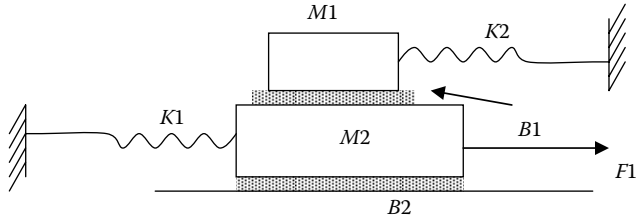
(e)

FIGURE P3.1(a–m)

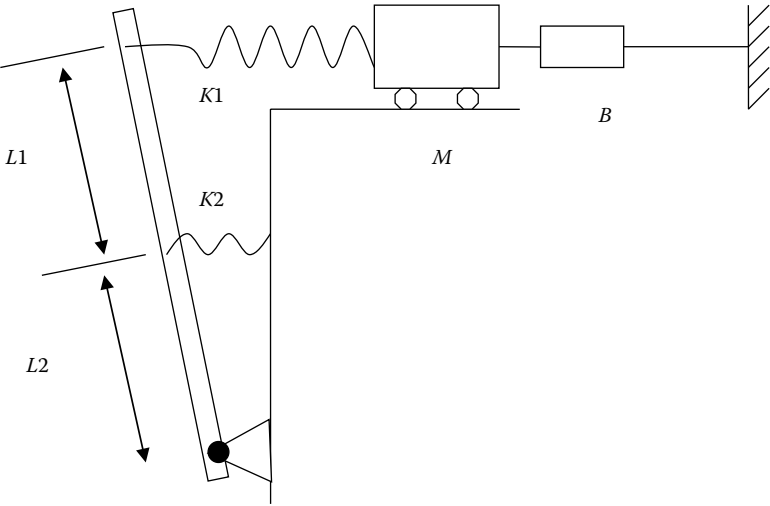
Figures for Problem 3.2, electrical and mechanical systems whose causalled bond graphs need to be developed.



(f)



(g)



(h)

FIGURE P3.1(a–m)
(Continued)

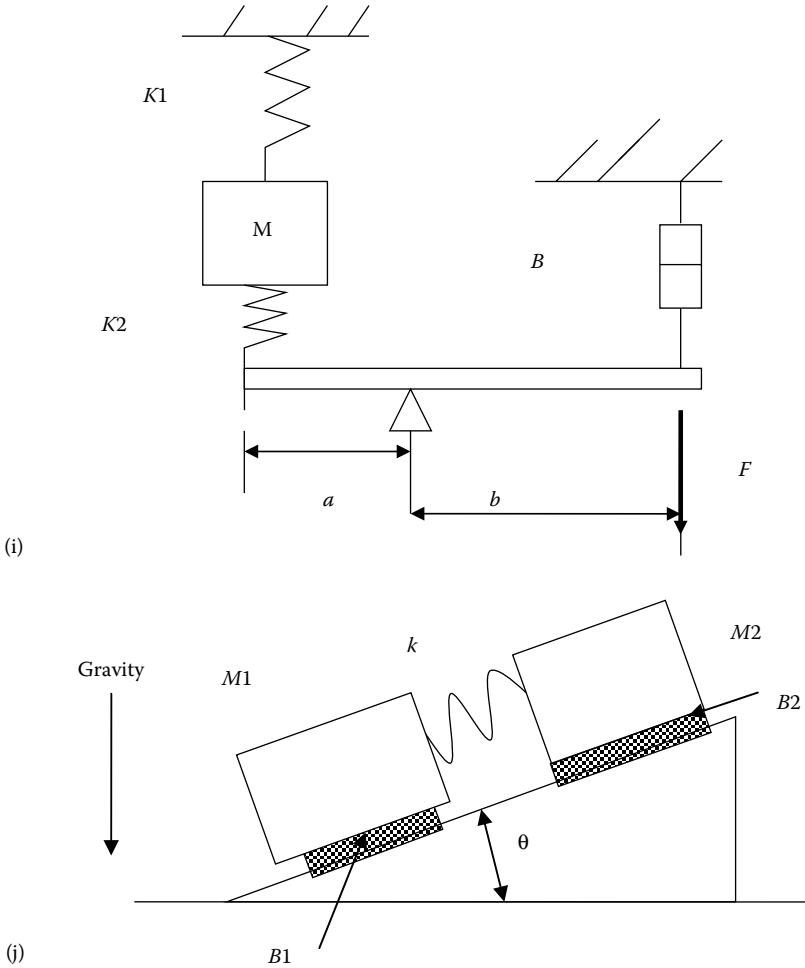
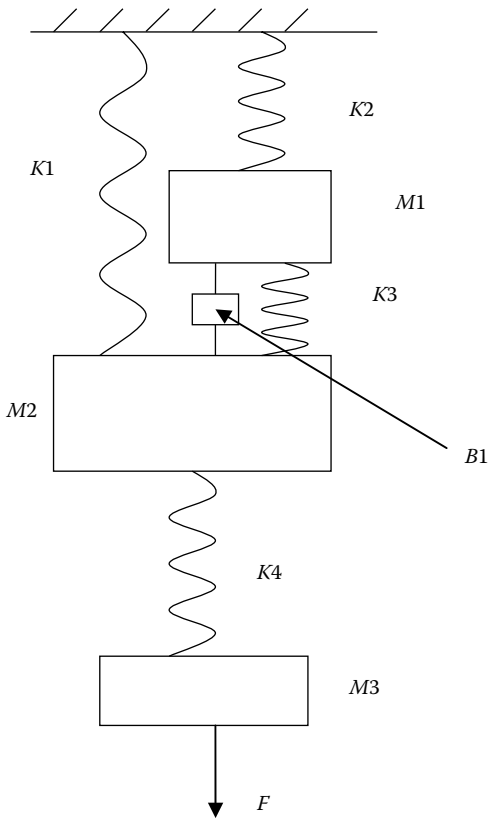


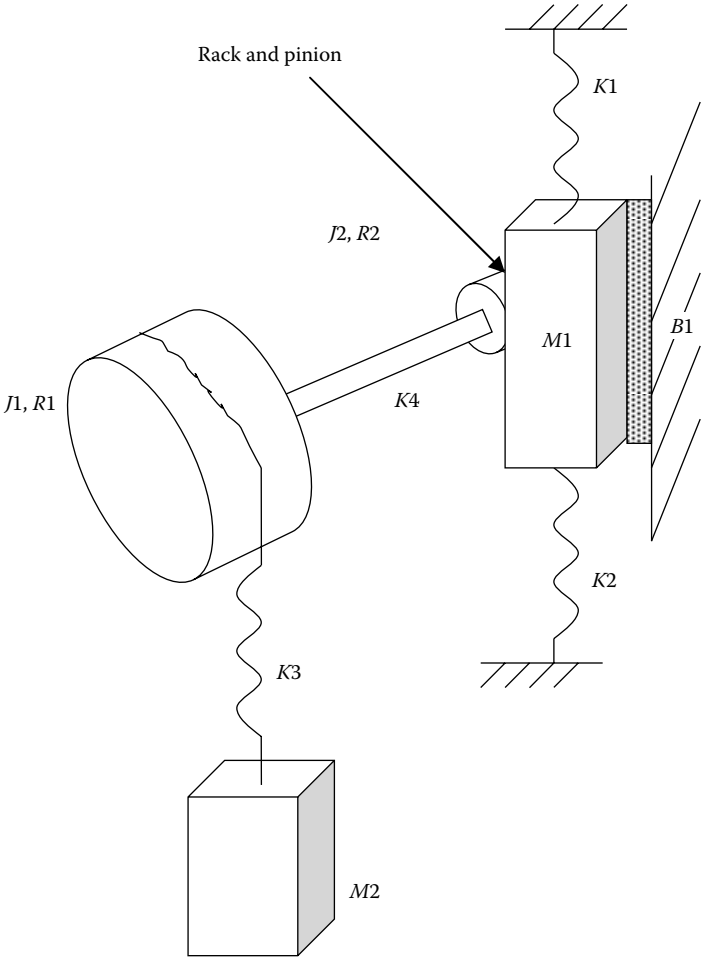
FIGURE P3.1(a-m)
(Continued)



(k)

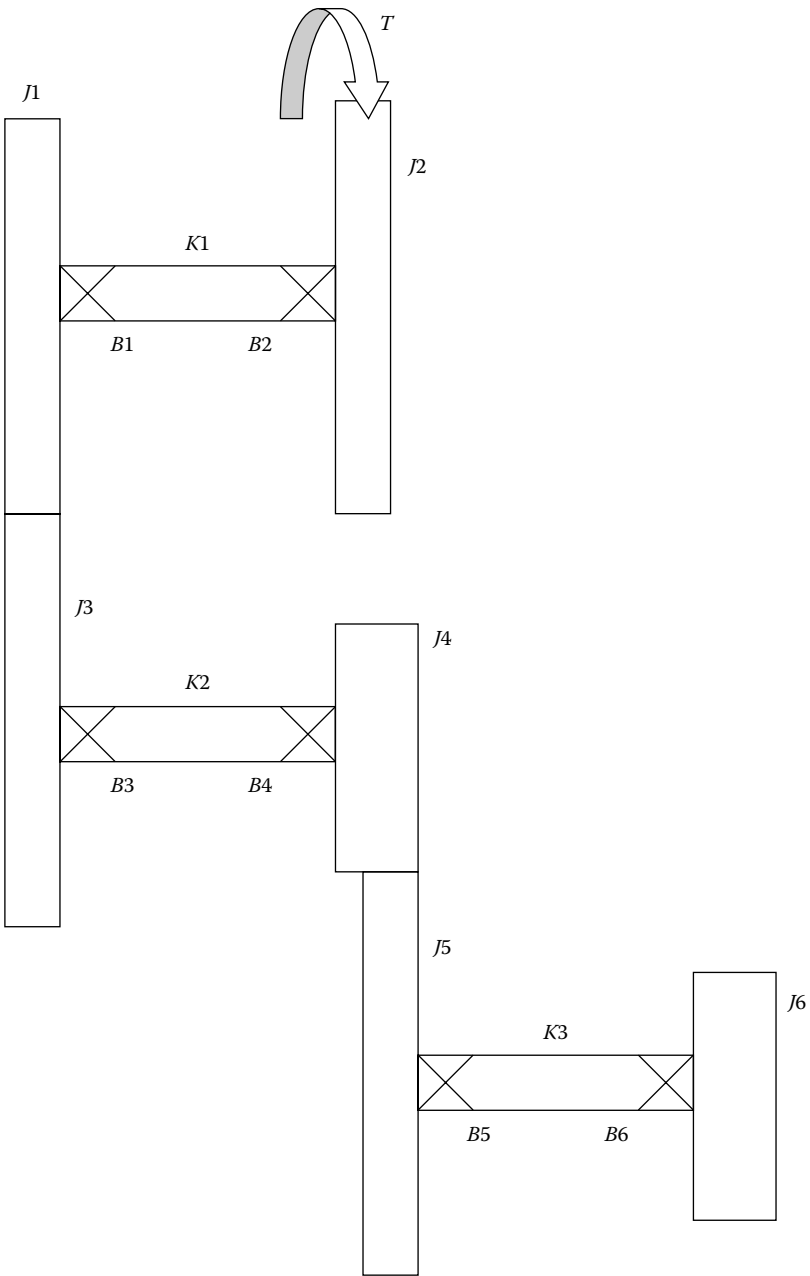
FIGURE P3.1(a–m)

(Continued)



(l)

FIGURE P3.1(a-m)
(Continued)



(m)

FIGURE P3.1(a-m)
(Continued)

4

Drawing Bond Graphs for Hydraulic and Electronic Components and Systems

In Chapter 2 we discussed some of the basic components that constitute systems in different domains. We had the chance to relate the behavior of similar components from different domains. The domains we considered were mechanical translation, mechanical rotation, electrical, and hydraulic. Building on the basic concepts discussed in Chapter 2, we explored different ways of developing bond graph models for mechanical and electrical systems in Chapter 3. In Chapter 4 we will consider two other domains, specifically, hydraulic and electronic, and try to develop bond graph models for systems within these domains. We expect that the expertise we developed in Chapter 3 will be helpful in making quick progress in these other domains. Similar discussions on hydraulic components can be found in other texts on bond graphs, such as in the works of Brown (2001), Gawthrop and Smith (1996), and Mukherjee and Karmakar (2000).

In mechanical and electrical domains, behavior of basic components, such as springs, resistances, and so forth, remain linear over most behavioral range. This is not true for fluids. Fluid behavior can quite easily change from laminar to turbulent; resistances in fluid paths are nonlinear whenever there is a valve or an orifice. Because of these reasons, this domain has been separated for study. Also, before we start talking about the process of building models for hydraulic systems, we will devote attention to some of the physical laws within this domain, the behavior of basic components and their constitutive equations, and the limitation of the approach that we are following: that is, treating elements of the fluid flow world as lumped components.

Electronic components behave somewhat differently from electrical components, primarily because of the properties of semiconductors. Hence, electronic devices have been separated from electrical components for consideration. Within the section about electronic components, we will focus primarily on some of the basic components, such as the operational amplifiers and diodes, because these components are “workhorses” within the electronic world. In this chapter we will find out how to build bond graph models of these systems. In a later chapter on sensors, we will devote a section on signal conditioning where electronic components play an important part as devices, including amplifiers, filters, and so forth.

The overall objectives of this chapter are to

- Build on the basic understanding of the bond graph method by extending its application in two other areas: hydraulics and electronics.
- Develop an understanding of how to use the techniques learned so far to build bond graph models of simple hydraulic and electronic systems.
- Be able to relate the generalized elements to specific ones in the hydraulic and electronic domains.

4.1 Some Basic Properties and Concepts for Fluids

Fluids are substances that flow. Both gases and liquids fall under this category. Fluids can be compressible (i.e., its volume can be significantly altered through the application of pressure) or practically incompressible (i.e., application of pressure causes little or no change in the fluid volume). Modeling fluid flow can be attempted from a variety of perspectives and can be inherently quite complex. Fluid flow is governed by a set of partial differential equations (Navier-Stokes') and demonstrates various behaviors in different flow regimes and as a result of the different fluid property values such as viscosity, density, temperature, and so forth. For the purpose of system modeling, we will not attempt to model from these fundamental principles. We will, however, attempt to model fluid systems as hydraulic systems. There are many inherent assumptions in doing this. They are

- Hydraulic systems are typically high-pressure, low-velocity flows.
- Flows are steady, uniform, laminar, isothermal (constant temperature), adiabatic (without heat loss).
- Components of hydraulic circuits, such as pumps, pistons, plungers, pipes, tanks, accumulators, restrictions, hydraulic motors, and so forth, can be modeled as lumped parameters.

4.1.1 Mass Density

Mass density is an inherent property of a fluid and is defined as:

$$\rho \left(\frac{\text{kg}}{\text{m}^3} \right) = \frac{\text{Mass}}{\text{unit volume}} \quad (4.1)$$

Mass density varies with temperature and (most of the time) with pressure.

4.1.2 Force, Pressure, and Head

A force applied to a fluid generates pressure on the fluid. Pressure is the intensity of force, that is, pressure is force per unit area. If force is applied on a closed volume of fluid, pressure is generated in it. Force can be applied in either of two ways on a fluid:

1. Through the application of an external force (F)
2. From the weight of the overhead fluid, also called the head (H)

Thus, mathematically, the relationships can be expressed as:

$$p \left(\frac{N}{m^2} \right) = \frac{F}{A} = \frac{\rho g H A}{A} = \rho g H \quad (4.2)$$

4.1.3 Bulk Modulus

The bulk modulus of elasticity is a measure of the compressibility/stiffness of the fluid. It is defined as the ratio of pressure change to volume change for a given volume of fluid.

$$\beta \left(\frac{N}{m^2} \right) = \frac{\Delta P}{\frac{\Delta V}{V}} \left(\frac{\frac{N}{m^2}}{\frac{m^3}{m^3}} \right) \quad (4.3)$$

4.1.4 Mass Conservation for Steady, Irrotational, Nonviscous Flows

If a control volume of fluid (such as in Figure 4.1) is considered, the total fluid flowing into the control volume is the same that is flowing out of the volume. The mass flow rate at the inlet is a product of the density, velocity, and cross-sectional area. The same is true for the outlet. So for mass conservation, one can write the continuity equation as:

$$\rho_1 A_1 v_1 = \rho_2 A_2 v_2 \quad (4.4)$$

or

$$\rho A v = C \quad (4.5)$$

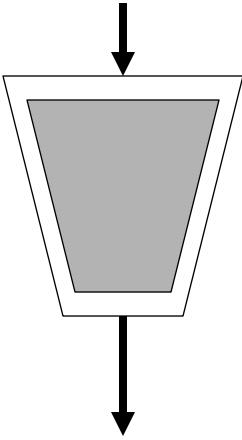


FIGURE 4.1
Fluid control volume.

For incompressible fluids, the density at the inlet and outlet remains unchanged, and, therefore, the continuity (or conservation of mass) equation can be simplified as:

$$A_1 v_1 = A_2 v_2 \quad (4.6)$$

When dealing with incompressible fluid, we essentially deal with volume flow rate rather than the mass flow rate (by literally taking density out of the equation).

Since this is similar to the flow of current, the continuity equation (or conservation equation) is similar to Kirchoff's current law: that is, it is a conservation of flow.

4.1.5 Energy Conservation for Steady, Irrotational, Nonviscous Flows

The energy difference between two points in the flow is equal to the energy that is added to (or lost from) the system. The mathematical representation of this statement is called Bernoulli's equation. For two locations in a fluid, Bernoulli's equation may be stated as:

$$\frac{P_1}{\rho_1 g} + \frac{v_1^2}{2g} + H_1 + E_{\text{net}} = \frac{P_2}{\rho_2 g} + \frac{v_2^2}{2g} + H_2 \quad (4.7)$$

where P represents the pressure, v the velocity, and H represents the height of the point under consideration with reference to some datum. The total energy added minus the energy subtracted is also included as E_{net} . Leaving E_{net} out, the other terms that appear in Bernoulli's equation can be categorized as dynamic pressure and static pressure. The term that includes the square of the velocity is referred to as dynamic pressure, and the height effect and the pressure term together is called static pressure, that is

$$P + H\rho g = P_{\text{static}} \quad (4.8)$$

$$\frac{\rho v^2}{2} = P_{\text{dynamic}} \quad (4.9)$$

The static pressure and the dynamic pressure together are called the stagnation pressure.

4.2 Bond Graph Model of Hydraulic Systems

When volume flow is conserved and the fluid is nearly incompressible, the hydraulic circuits can be modeled in a way similar to the electrical circuits. Under these conditions, the use of the bond graph based approach is particularly useful because the circuit can be assumed to be made of lumped components. These components can be represented as one of the several generalized elements used in bond graph representations.

Before we consider some of the basic components in a hydraulic circuit, it will be worthwhile to review the particular meaning of the generalized variables within this domain. For this purpose, Table 2.1 is included here again as Table 4.1. Here we can see one more time the contextual meaning of the effort, flow, momentum, and displacement variables in the hydraulic domain.

TABLE 4.1

Generalized Variables in Different Domains

Generalized Variables	Mechanical Translation	Mechanical Rotation	Electrical	Hydraulic
E (effort)	Force, F (N)	Torque, T (N-m)	Electric potential, V (Volt)	Pressure, P (N/m ²)
f (flow)	Velocity, v (m/s)	Angular velocity, ω (rad/s)	Current, i ($A = C/s$)	Volume flow rate, Q (m ³ /s)
P (momentum)	Linear momentum (N-s), p	Angular momentum (N-m-s), p_T	Flux linkage variable, λ , (Vs)	Pressure momentum P_p (N-s/m ²)
Q (displacement)	Displacement, d (m)	Angle, θ (rad)	Charge, Q , (Columb = As)	Volume, V (m ³)
Power	F^*v (watts)	$T^*\omega$ (watts)	V^*i (watts)	P^*Q (watts)
Energy	$\int Fdx, \int VdP$	$\int Td\theta, \int \omega dp_T$	$\int edq, \int id\lambda$	$\int PdV, \int Qdp_p$

4.2.1 Fluid Compliance, C Element

Fluid compliance is similar to the mechanical spring and the electrical capacitor. The constitutive relation of the fluid compliance element needs to be similar to the mechanical and electrical element; that is, the pressure (the generalized effort) should be proportional to the fluid displacement (integral of generalized flow). The most common form of this in fluid circuits is a storage tank of constant cross-sectional area. When fluid enters the tank and fills it, potential energy is stored. The height of the fluid in

the tank is given by $H = V/A$, and the pressure in the tank at any level is given by $H\rho g$. Therefore, the constitutive equation can be written as:

$$C = \frac{q}{e} = \frac{V}{P} = \frac{V}{H\rho g} = \frac{V}{\frac{V}{A}\rho g} = \frac{A}{\rho g} \quad (4.10)$$

This particular compliance definition can be called fluid compliance due to gravity. A second type of fluid compliance is also to be considered in fluid circuits, especially when fluids are somewhat compressible. This is particularly useful when an accumulator is part of a fluid circuit. The compressibility of fluids is captured through the bulk modulus of the fluid.

$$\beta = \frac{\Delta P}{\frac{\Delta V}{V}} \quad (4.11)$$

This representation may be rewritten as:

$$\frac{1}{C} = \frac{\beta}{V} = \frac{\Delta P}{\Delta V} \quad (4.12)$$

Another type of compliance can be considered, the one that arises from using flexible tubing through which the fluid flows. This is not being discussed here.

4.2.2 Fluid Inertia, I Element

To determine the fluid inertia, we must keep in mind that the inertance is the second type of energy storage element. The compliance element stores generalized potential energy derived from displacement. The inertance stores energy of motion, that is, generalized kinetic energy. To determine the inertance of a fluid element, consider a tube of length L , through which some fluid is flowing. The pressures at the two ends of the pipe are P_1 and P_2 . Consider that the tube contains a plug of fluid moving with one velocity (Figure 4.2). Using P as the generalized effort and Q as the generalized flow rate, from Newton's law:

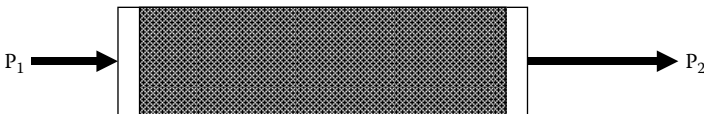


FIGURE 4.2
A plug of fluid in a tube.

$$F = ma;$$

$$(P_2 - P_1)A = \rho LA \left(\frac{Q}{A} \right);$$

$$(P_2 - P_1) = \left(\frac{\rho L}{A} \right) Q; \quad (4.13)$$

$$I = \frac{\rho L}{A}$$

For tubes with discrete changes in area, the total inertance can be calculated as the sum of the inertances of individual sections ($I = I_1 + I_2$). If, however, the area of cross-section of the tube varies continuously with length, then the inertance can be written as:

$$I = \rho \int_0^L \frac{1}{A(S)} dS \quad (4.14)$$

4.2.3 Fluid Resistances, R Element

A common linear fluid resistance results from the assumption of viscous laminar fully developed flow through a circular tube. The resistance value is described in fluid mechanics texts as:

$$R = \frac{8\mu L}{\pi a^4} \quad (4.15)$$

where μ is the absolute viscosity of the fluid, L is the length of the tube, and a is the inner radius of the tube. The resistance can be assumed to be linear (above relation) when the Reynold's number is low such that the viscous forces are larger than the inertial forces.

The more practical contribution in the resistance estimation in hydraulic applications is the fluid resistance associated with the change in area of flow (also called Bernoulli resistance, see Figure 4.3). If Bernoulli's equation is used

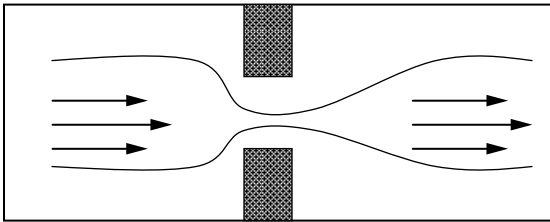


FIGURE 4.3

Schematic for a change in area of flow due to the presence of an orifice in the flow path.

to model the flow between an upstream state with 0 velocity and the point in the throat where it achieves maximum velocity, the dissipation of the kinetic energy happens downstream, and the relationship is expressed as:

$$\Delta P = \frac{1}{2} \rho v^2 = \frac{1}{2} \rho \left(\frac{Q}{C_d A_0} \right)^2 = \left[\frac{\rho}{2 C_d^2 A_0^2} \right] Q^2 \quad (4.16)$$

In a slightly different formulation, this same equation is written as:

$$\Delta P = \frac{1}{2} \rho v^2 = \frac{1}{2} \rho \left(\frac{Q}{C_d A_0} \right)^2 = \left[\frac{\rho}{2 C_d^2 A_0^2} \right] Q |Q| \quad (4.17)$$

This second formulation ensures that even if the flow rate is negative, the pressure differential attains the right sign when it is calculated as a function of the flow rate. Here C_d is a flow coefficient that represents the fact that the flow separates from the walls of the orifice to form a narrower vena contracta, or effective orifice, area of $C_d A_0$ (C_d is about 0.611 for sharp edged orifices). The above relation for resistance means that the pressure–volume flow rate (i.e., effort–flow) relationship is nonlinear in nature when the Bernoulli resistance term becomes dominant. This type of a resistance is quite common in hydraulic applications whenever there is a valve, nozzle, orifice, or any other variation of area.

Since the causality of the resistance element could be one of two possibilities, it means that depending on the causality, sometimes the pressure drop will be calculated from the flow rate using the above form of the equation, and at other times, the flow rate will be calculated from the pressure drop. For that purpose, the above equation can be rewritten as:

$$Q = C_d A_0 \sqrt{\frac{2}{\rho}} \operatorname{sgn}(\Delta P) \sqrt{\Delta P} \quad (4.18)$$

If, instead of the situation described above, we have a nozzle where the flow velocity is two non-zero quantities in the upstream and the downstream regions (as shown in Figure 4.4), the pressure difference can be derived from the Bernoulli's equation as:

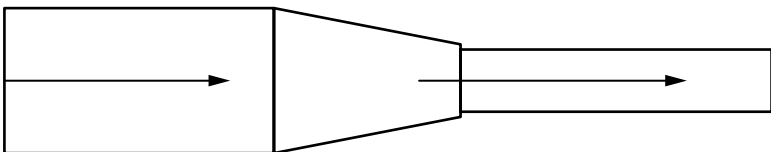


FIGURE 4.4

Flow through a tube with a nozzle.

$$\Delta P = -\frac{1}{2} \rho Q^2 \left[\frac{1}{A_u^2} - \frac{1}{A_d^2} \right] \quad (4.19)$$

where A_u stands for the area of the upstream part of the tube and A_d stands for the area of the downstream section of the tube. This is another version of the Bernoulli's resistance term.

4.2.4 Sources (Effort and Flow)

Various types of positive displacement pumps (Figure 4.5), such as gear pumps, vane pumps, axial flow pumps, and so forth, can be represented as sources of flow. These sources provide hydraulic fluid to the circuit at a rate that can be determined from the speed of rotation and its design parameters. Sources of effort need to deliver a steady pressure input. A huge source of fluid, such as a tank with constant level that is connected to a hydraulic circuit, can be assumed to be a source of effort.

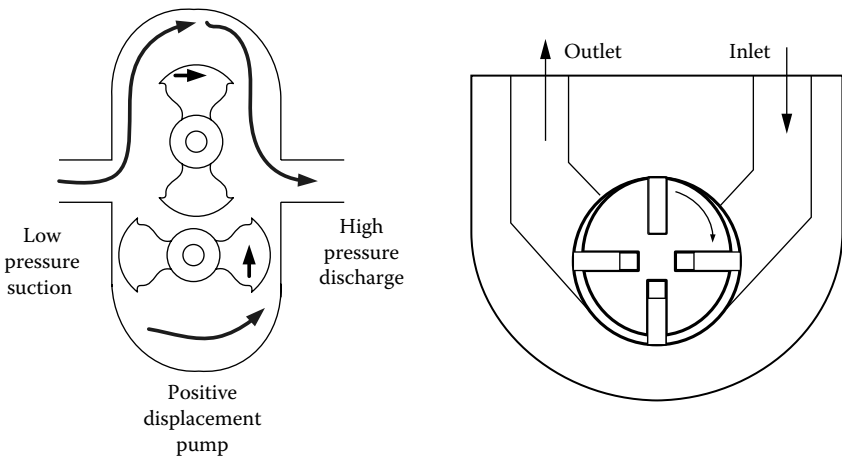


FIGURE 4.5
Examples of positive displacement pumps.

4.2.5 Transformer Elements

One may encounter many transformer elements in a hydraulic circuit. The most common one is a piston/plunger (Figure 4.6). In ideal situations (i.e., neglecting leakage and resistive losses), the transformer relationships can be expressed as:

$$\begin{aligned} Q &= Av; \\ P &= \frac{F}{A}; \end{aligned} \quad (4.20)$$

**FIGURE 4.6**

Schematic of a hydraulic piston.

where F and v are the force and velocity, respectively, on the plunger side, and P and Q are the pressure and volume flow rate of fluid on the other side. Obviously A , the area of the plunger, is the transformer factor.

If the energy required to drive pumps is included in the model, the positive displacement pumps can be treated as transformer elements as well where the amount of fluid flowing is directly proportional to the speed of rotation of the pump. Pump capacity (or transformer factor) is expressed as volume of fluid displaced per unit rotation (radian) of the pump rotor. So the transformer relationships will be

$$\begin{aligned} Q &= V_p \omega; \\ T &= V_p P; \end{aligned} \quad (4.21)$$

where V_p is the volume of fluid displaced per unit radian of rotation.

4.2.6 Gyration Elements

Gyrator elements are not very common in hydraulic circuits except for a few special cases such as centrifugal pumps and reaction turbines.

4.2.7 Bond Graph Models of Hydraulic Systems

For flows that are almost incompressible, the hydraulic circuits can be treated in a manner similar to the electric circuit if volume flow is conserved. The bond graph representation may be achieved algorithmically in a way quite similar to mechanical and electrical systems. The steps to be followed are

1. For each distinct pressure, establish a 0-junction.
2. Insert the component models between appropriate 0-junction pairs using 1-junctions; add pressure and volume flow sources.
3. Assign power directions.
4. Define all pressures relative to reference (usually atmospheric) pressure, and eliminate the reference 0-junction (atmospheric pressure) and its bonds.
5. Simplify the bond graph (using the standard rules of simplification that were previously discussed).

Examples 4.1–4.5 discuss bond graph based models of hydraulic systems.

EXAMPLE 4.1

This example shows a simple system where fluid is traveling through a pipe and filling a tank. The fluid input is treated as a constant effort source. The inertia of the fluid in the pipe, the viscous losses, and the capacitance of the tank all play a role. Points a, b, and c show locations with different pressures. We start drawing the bond graph by assigning 0 junction to represent each of these three points. The other elements are connected to 1 junctions, which are connected to two adjacent 0 junctions (as per the algorithm). The bond graph representation can, therefore, be written first as shown in Figure 4.7, and the simplified bond graph, obtained by removing the 0 junction representing the atmospheric pressure (point c), is shown in Figure 4.8. The I and R elements are connected using the same 1 junction since the flow rate through the tube between points a and b is the same. The inertia of the fluid in this region experiences the resistance from the wall.

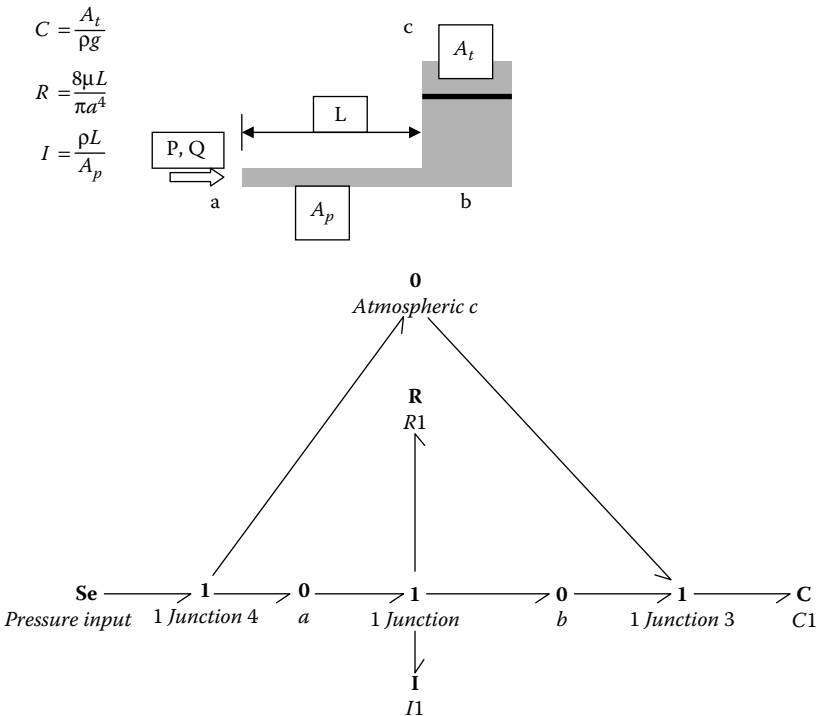


FIGURE 4.7
Schematic for Example 4.1 and its initial bond graph.

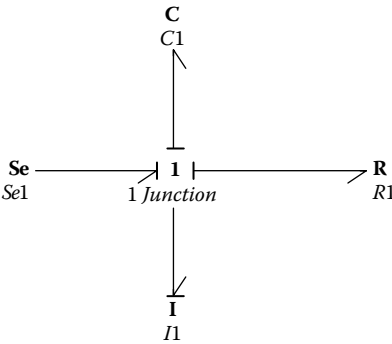


FIGURE 4.8
Final simplified bond graph for Example 4.1.

EXAMPLE 4.2

This example shows fluid flowing through a pipe that is used to store fluid in two different tanks (Figure 4.9). The pressure and flow rate at the entry point

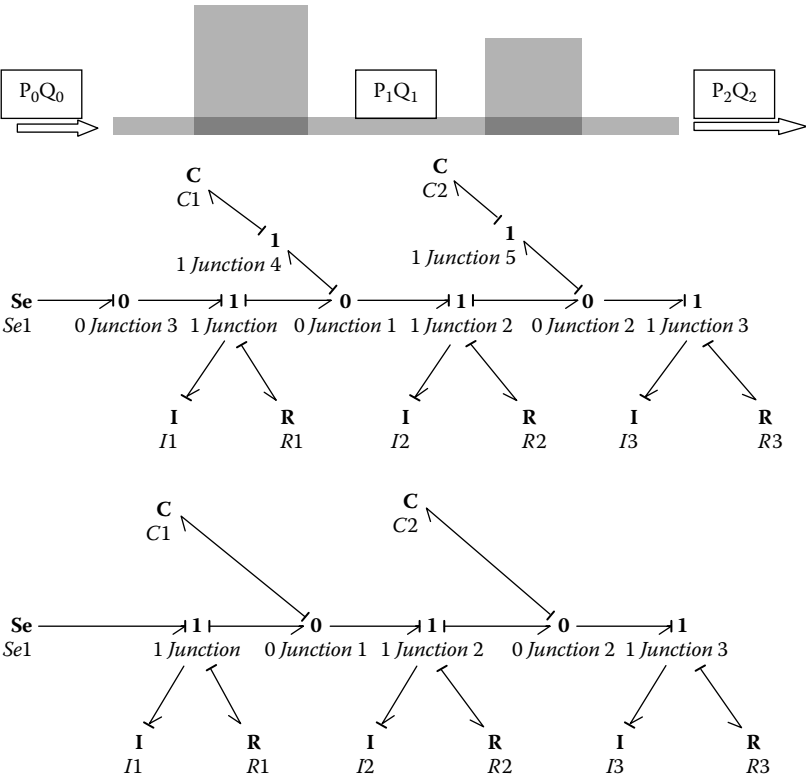


FIGURE 4.9
Schematic for Example 4.2 and its initial and final bond graph representation.

and exit are shown in the picture. The schematic is followed by the initial model that was drawn up using the list of rules listed before and then the final simplified model. The inertia elements represent the inertia of the fluid in the three pipe sections. These can be eventually ignored in many situations, e.g. if the pipes are short. The R elements represent the pipe resistance for the three sections, and the C elements are used to capture the energy stored in the tanks. The source of effort represents the pressure at the inlet.

EXAMPLE 4.3

Figure 4.10 shows a source of steady flow that is supplying two tanks. There is a pipe that connects the two tanks, and there is a leaky drain through which the fluid is flowing out of the second tank. The bond graph for the model is shown right below. The I and the $R1$ element represents the inertia of the fluid in the tube and tube resistance respectively. The resistance for the drain is represented by the $R2$ element in the model. The two C s represent the capacitances of the two tanks, and the source of flow represents the fluid input as a flow source.

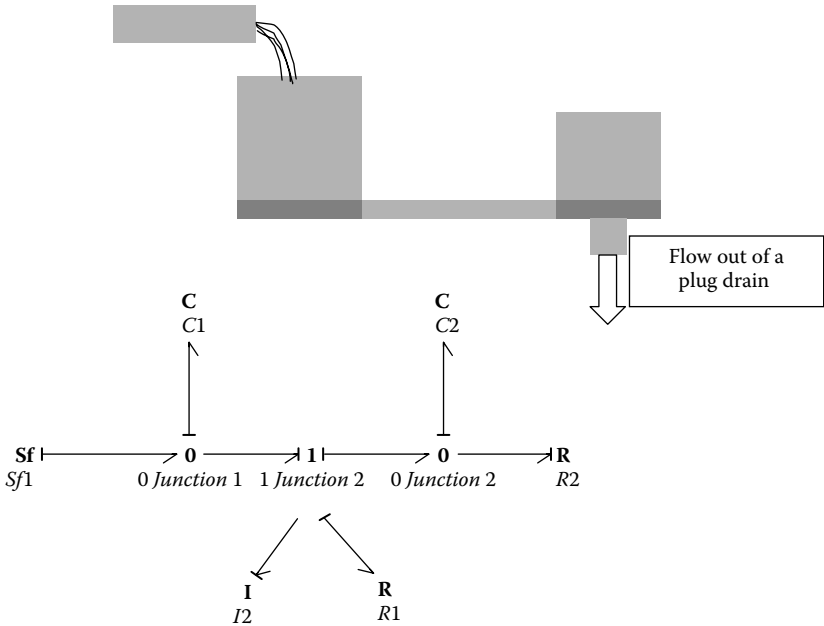


FIGURE 4.10
Schematic for Example 4.3 and its bond graph representation.

EXAMPLE 4.4

Figure 4.11 shows a schematic for a needle and a plunger that is used to push the fluid through the needle at a constant rate. The many different pressure points in the system are shown. The plunger itself works as a transformer transforming

force and velocity of motion to pressure and volume flow rate. The different elements in the model are the wall resistance for the section 1–2, the inertia of the section 1–2, the resistance and inertia of the section 3–4, and the Bernoulli resistance for dimension change in region 2–3. The final simplified bond graph is shown in Figure 4.12.

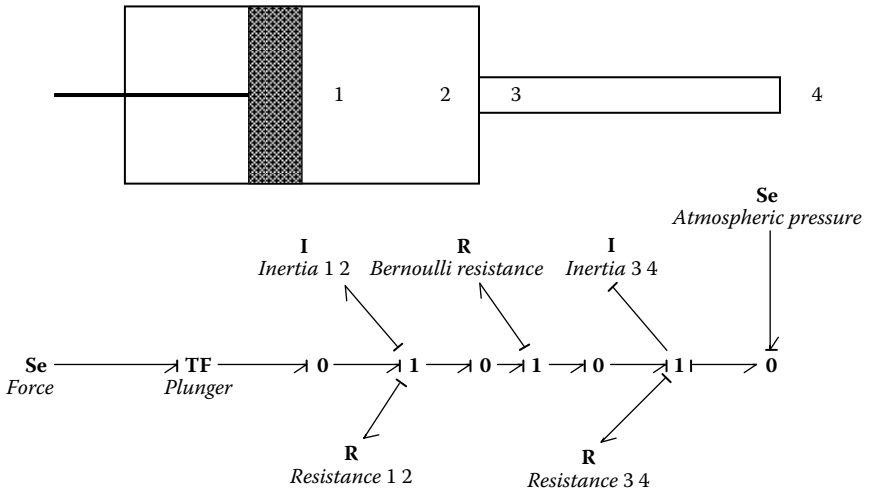


FIGURE 4.11
Schematic for Example 4.4 and its initial bond graph.

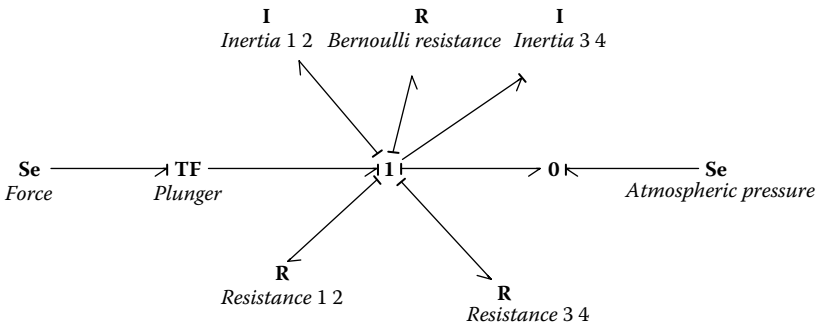


FIGURE 4.12
Simplified bond graph of Example 4.4.

EXAMPLE 4.5

Figure 4.13 shows a generic hydraulic system that has most of the basic components in the system. The bond graph representation that accompanies the system is a generic bond graph showing how different aspects of the system can be accounted for in a bond graph representation. It accounts for two types of resistances, the wall resistance for the flow-through tubes and Bernoulli

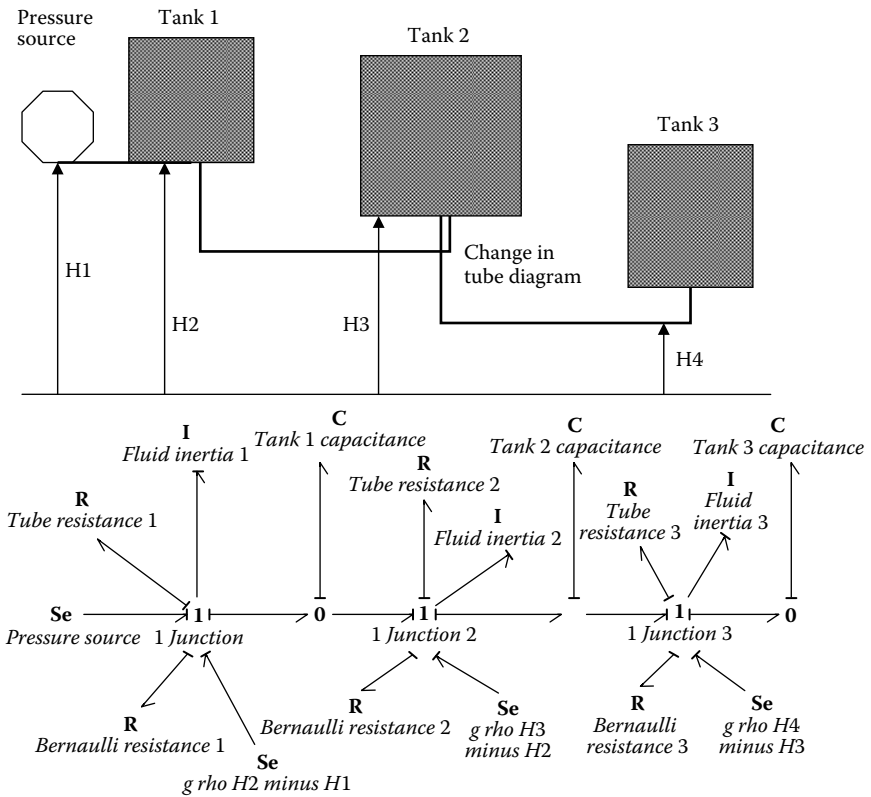


FIGURE 4.13
A generic hydraulic circuit and its corresponding bond graph.

resistance due to change in flow path cross-section, use of valves, bends, and so on in the line. The inertias of different fluid sections are also accounted for. The storage tanks are treated as capacitive elements, and the effect of gravity due to height differences is taken into account through the effort bonds. This generic bond graph representation will be useful in developing bond graph representation of specific hydraulic circuits because it shows how all the common features can be accounted for.

Several other examples of components in hydraulic systems will be discussed in the context of our discussion on hydraulic actuators in a later chapter.

4.3 Electronic Systems

In the previous chapter, we discussed the basic concepts of bond graphs as applied to modeling mechanical and electrical systems. Similarly,

hydraulic systems were discussed in the previous sections of this chapter. We will now deal with modeling some of the basic components used in electronic circuits that are particularly useful in mechatronic applications. Electronic components are often integrated in circuits that behave in a certain characteristic fashion, and it makes sense to model them as a whole rather than as a composite of numerous circuit elements. Also, many electronic components (semiconductors) demonstrate nonlinear behavior, and the nonlinearity needs to be accounted for in the component models. We are, therefore, devoting a separate section to electronic components and circuits. We will not, however, try to model every possible electronic component. Instead we will focus on one or two main ones that are typically used in mechatronic applications, particularly in the area of signal conditioning. In the chapter on sensors, some of the common signal conditioning applications and their models are discussed as well. Those models use the concepts discussed here.

4.3.1 Operational Amplifiers

Operational amplifiers are sometimes called the “work horse” of electronic applications. Operational amplifiers (op-amps) form the core of many signal conditioning applications, such as amplifiers, filters, integrators, differentiators, and so forth. Using the same basic op-amp and with proper combination of resistors, capacitors, and feedback loops, a large number of applications of op-amps can be implemented.

The op-amp is an integrated circuit (IC) that consists of many electronic components. Overall behavior of op-amps is characterized by a very high input resistance and a very low output resistance. In the open circuit mode (although op-amps are never used in this mode), they can provide voltage amplification in the order of millions. By using proper external circuit elements (resistors and/or capacitors), the user can control this amplification factor to almost any desired value.

The operational amplifier is an IC that is rectangular with eight pins used for specific connections. Figure 4.14 shows a schematic of it. A triangular symbol is used to represent the op-amp in an electronic circuit. Figure 4.15 shows a schematic of what an op-amp actually looks like. The specific purpose of each pin is shown in the figure as well. As was mentioned before, the internal circuit of an op-amp is rather complex and there is no need to go into the circuit details. Figure 4.16 shows a schematic that will capture its basic overall behavior. There are two input voltage sources shown in the figure as V^+ and V^- . The resistance on the input side is connected to these two source pins, such that the voltage across the input resistance is $(V^+ - V^-)$. This is represented as V_{in} in the figure. On the output side of the op-amp is another voltage source connected to the output resistance. The voltage source on the output side is given as kV_{in} , where “ k ” is the open circuit amplification factor of the

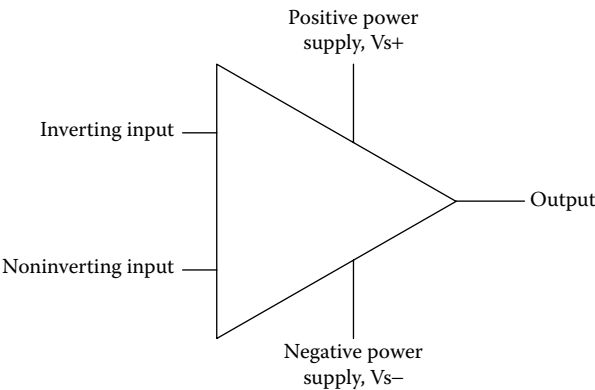


FIGURE 4.14
Schematic of an op-amp as used in circuits.

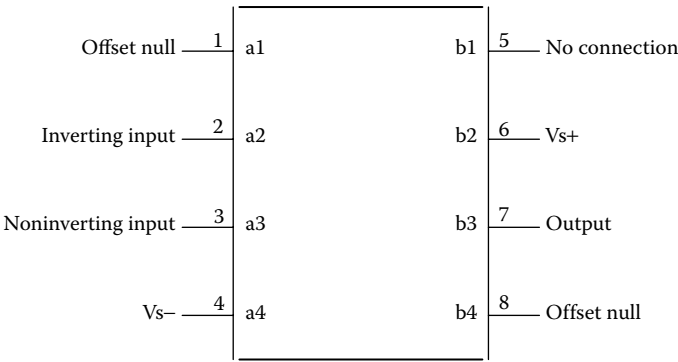


FIGURE 4.15
Schematic of an op-amp as it looks.

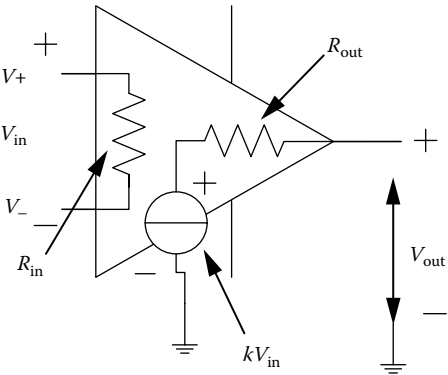


FIGURE 4.16
Schematic showing how an op-amp is modeled.

op-amp. The output voltage (with respect to the ground) is measured at the output pin.

The equivalent bond graph model for the basic op-amp is shown in Figure 4.17. The left-hand side of the figure until the *MSe* represents the input to the op-amp. The right-hand side represents the output side.

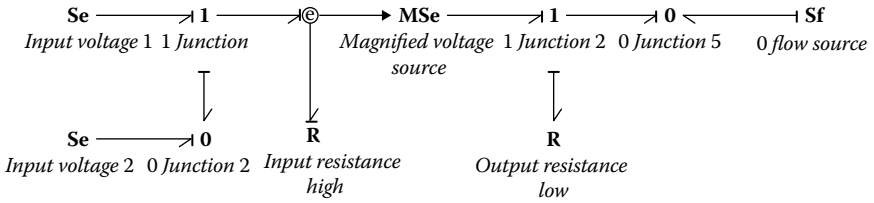


FIGURE 4.17

Bond graph model of an op-amp.

The two *Se* elements represent the two voltage sources. The bond directions are chosen so that the voltage across the resistance on the input side is a difference of the two voltage values. The effort sensor shown in the model as the *e* inside a circle uses the effort signal in the bond as a signal source to the *MSe* element. *MSe* is a modulated source of effort. Within *Mse*, the input effort signal is multiplied with the open circuit gain value to compute the output voltage, which is applied across the output resistance. A zero flow source is used at the output pin so that the effort value at that pin can be easily obtained in the model. The *MSe* model is expressed through the following statements:

Parameters

```
real open_circuit_amp; //open_circuit_amp is the open
circuit amplification factor, k.
```

Variables

```
real flow;
```

Equations

```
p.e = effort * open_circuit_amp; //effort information is
brought in from the effort sensor in the model
flow = p.f;
```

where `open _ circuit _ amp` is the op-amp magnification factor in the open circuit mode (designated as *k* in our earlier discussion). Simulation

voltages are shown in Figure 4.20. The plot clearly shows that the input voltage is amplified by a factor of -5 . A particular advantage of this type of circuit is that the actual value of the op-amp application factor does not affect the final circuit amplification factor, which can be controlled through the ratio of the supply and the feedback resistances.

Parameters Initial Values Constants			
Name	Value	Quantity	Unit
Magnified_voltage_source\Open_circuit_amp	1000000000		
Input_voltage_2\effort	0 {V}	Electric Potential	volt
Input_resistance_high\r	1 {Mohm}	Electric Resistance	ohm
Zero_flow_source\flow	0		
Output_resistance_low\r	1 {ohm}	Electric Resistance	ohm
Feedback_resistance\r	10 {ohm}	Electric Resistance	ohm
Supply_resistance\r	2 {ohm}	Electric Resistance	ohm
WaveGenerator1\amplitude	1	Magnitude	none
WaveGenerator1\omega	1 {rad/s}	Angular Velocity	radian per

FIGURE 4.19
Parameter values used for simulating the inverting amplifier.

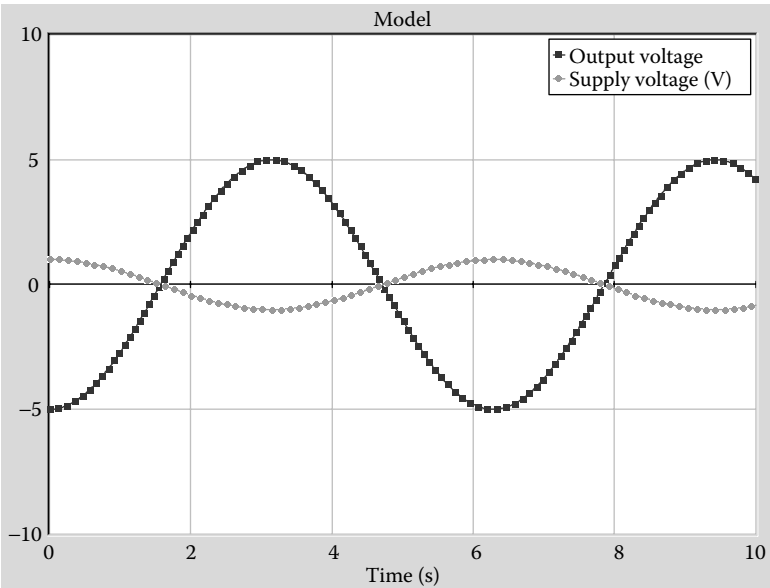


FIGURE 4.20
Simulation results from the inverting amplifier model.

4.3.2 Diodes

Diodes are another vital component in many electronic circuits. Diodes are semiconductor devices typically used to control the flow of current much the same way that one way valves are used to control fluid flow in a hydraulic system. Under normal operating conditions, diodes can allow large currents when the potential across them is one way (forward bias) and little or no current when the potential difference is in the opposite direction (reverse bias). Diodes are constructed using a junction of p-type and n-type semiconductors in a manner shown in Figure 4.21. The figure also shows the symbol of a diode that is used in any circuit diagram, with the tip or vertex of the triangular symbol pointing toward the forward bias direction. For a full explanation of p-n junction behavior and how it applies to diode characteristics, one may refer to more fundamental texts on electrical circuits and/or electronics such as Rizzoni's *Principles and Applications of Electrical Engineering*. For these junctions, the current flowing through the diode is somewhat like the one shown in Figure 4.22. A mathematical representation of this is

$$I = I_0(e^{\frac{qV}{kT}} - 1) \quad (4.22)$$

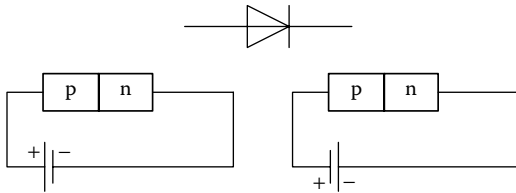


FIGURE 4.21

PN junctions with forward and reverse bias and the symbol of a diode.

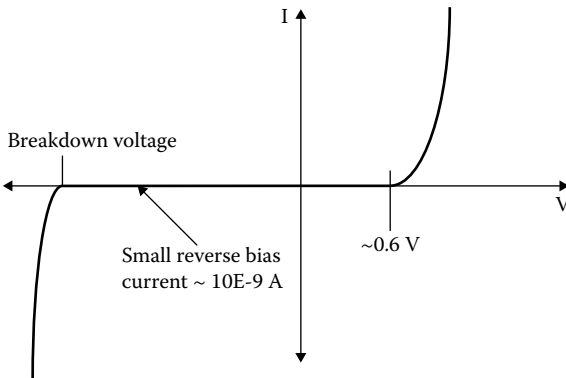


FIGURE 4.22

Current profile in a diode.

where q is the charge of a single electron, $1.6\text{E-}19\text{C}$, k is the Boltzmann's constant, $1.381\text{E-}23\text{ J/K}$, V is the applied voltage and T the absolute temperature ($= 298\text{K}$ for normal ambient conditions), and I_0 is the reverse bias leakage current of the order of $1\text{E-}9 - 1\text{E-}15\text{ A}$. The current grows exponentially after a forward bias voltage of about 0.6V is exceeded under forward bias condition. The current is small or negligible ($1\text{E-}9 - 1\text{E-}15\text{ A}$) in reverse bias until a breakdown voltage is reached when the current is infinite. In many modeling applications, diodes are treated as ideal devices with infinite current under positive bias and 0 current under negative bias (i.e., short circuit under positive bias and open circuit for negative bias) conditions. This is one possible way of modeling the device in the bond graph method as well. A more realistic way, perhaps, is to model the device as an actual diode using the diode current equation to model it as a resistive element with the current equation as the constitutive model. This approach could pose a problem with convergence because the current value shoots up to a very high value and may cause difficulties with convergence when this model has to interact with other standard circuit elements. So the model recommended here is based on the concept of the diode's behavior as an open circuit/short circuit resistive device. A standard resistance model is modified as:

Variables

real r1; //r1 controls the resistance magnitude

Equations

```

if (p.e>0.6) then //i.e. the forward bias voltage is greater
                    than 0.6 V
  r1 = 0.000000001; //the r1 value is such that the diode
                    works as a short circuit
else
  r1 = 10000000000; //the r1 value is such that the diode
                    works as a open circuit
end;
p.f = p.e/r1; // the current is determined from the voltage
                    difference and the diode resistance

```

One of the most common applications of a diode is in a rectifier circuit, where an AC source may be rectified into a DC voltage across a load resistor. The simple rectifier circuit is shown in Figure 4.23. The bond graph representation of this circuit is shown in Figure 4.23 as well, where the resistance marked Diode is the diode model. Figure 4.24 shows simulation results from this model where the output across the load resistance is a value that is greater than or equal to 0 when a sinusoidal input is applied to the circuit. For negative applied voltage the output across the load resistance is zero since there is no current through the diode. For positive applied voltage the output across the load resistance matches the general profile of the input voltage very closely.

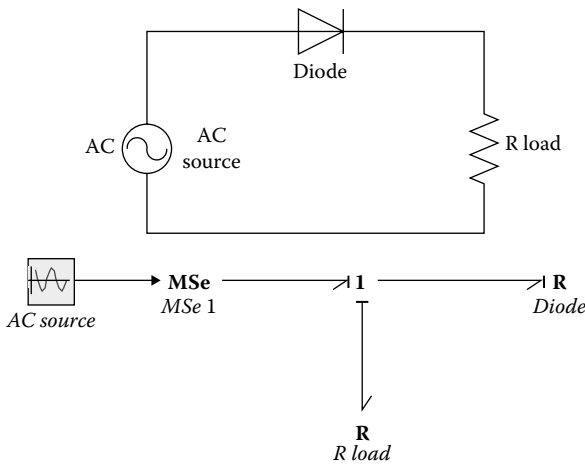


FIGURE 4.23
A simple rectifier circuit and its corresponding bond graph.

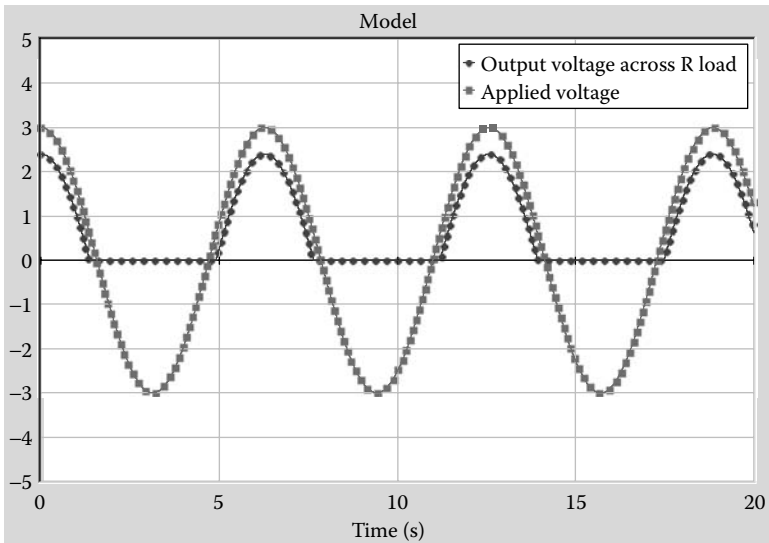


FIGURE 4.24
Simulation results from the rectifier circuit.

In this chapter we have discussed how the various concepts of bond graph modeling may be applied to model the dynamic behavior of systems/components that are common in hydraulic applications as well as electronic applications.

Problems

- 4.1. Develop a bond graph model for the hydraulic circuit shown in Figure P4.1.

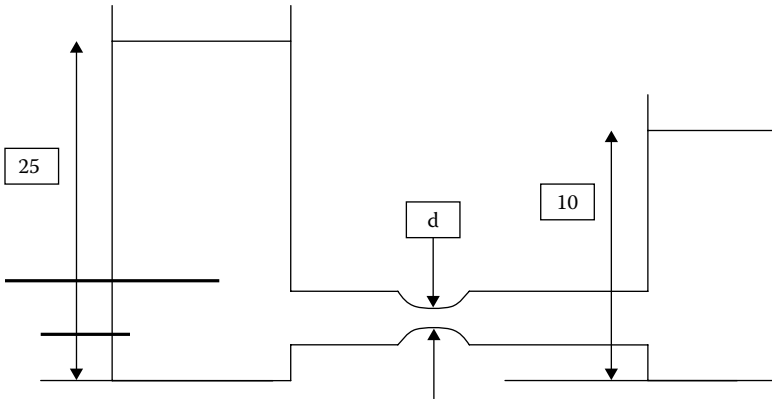


FIGURE P4.1

Figure for Problem 4.1, hydraulic circuit.

- 4.2. Develop a bond graph model of this or the hydraulic circuit shown in Figure P4.2.

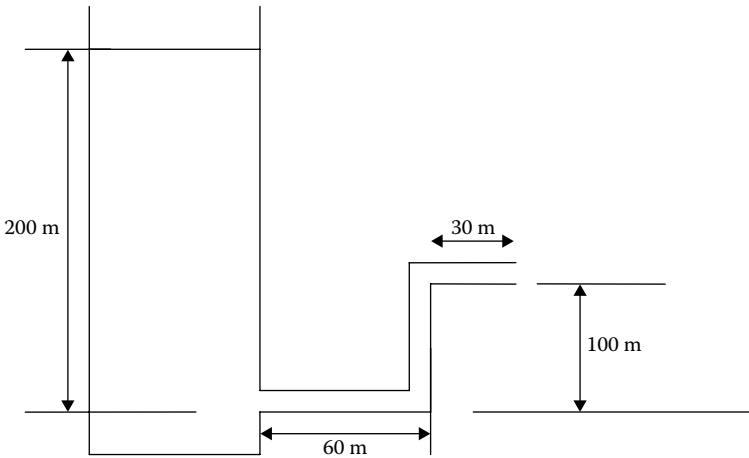


FIGURE P4.2

Figure for Problem 4.2, hydraulic circuit.

- 4.3. Figure P4.3 is a circuit for a noninverting amplifier. Develop a bond graph model for this integrator and then simulate the model. Use a periodic signal to demonstrate that the amplification factor is $(1+R_{\text{feedback}}/R_{\text{source}})$.

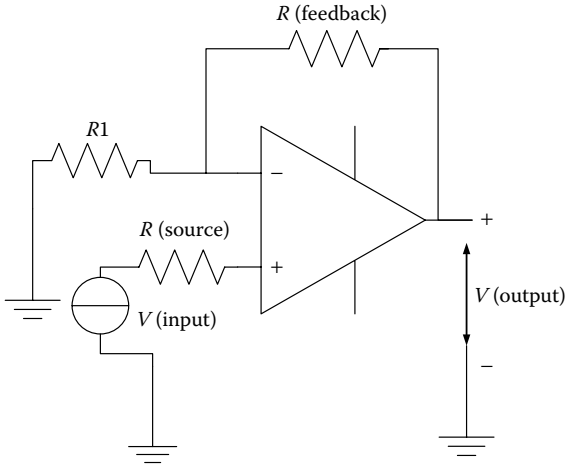


FIGURE P4.3

Figure for Problem 4.3, a noninverting amplifier.

- 4.4. Figure P4.4 is a circuit for an integrator. Develop a bond graph model for this integrator and then simulate the model. Use a square wave input to find out what the output of this model is.

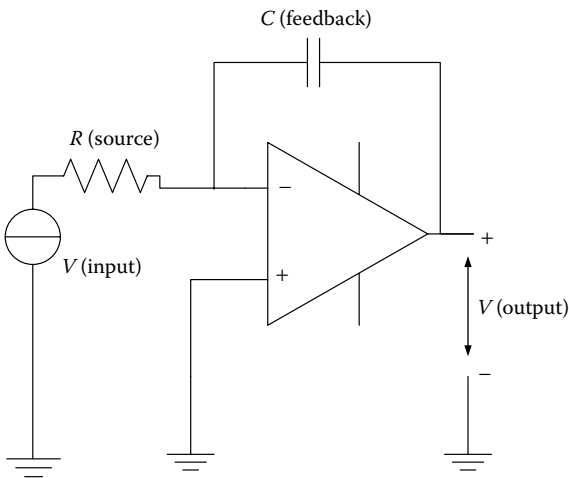


FIGURE P4.4

Figure for Problem 4.4, an integrator.

- 4.5. Figure P4.5 shows the circuit for a low-pass filter. Using the bond graph model for this circuit, simulate its behavior. Typical values that may be used for the different components are: R (source) = 220 Ohms, R (feedback) = 68 kOhm, R (load) = 1 kOhm, C (feedback) = 0.47 nF.

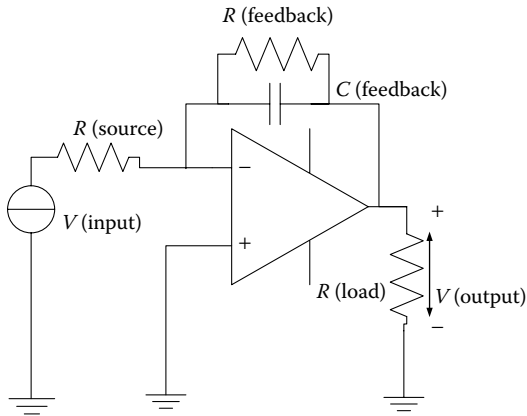


FIGURE P4.5

Figure for Problem 4.5, a low-pass filter.

- 4.6. Figure P4.6 shows a circuit for a band pass filter. Using the bond graph model for this circuit, simulate its behavior. Typical values that may be used for the different components are: R (source) = 2.2 kOhms, R (feedback) = 100 kOhm, R (load) = 1 kOhm, C (feedback) = 1nF, $C1$ = 2.2 microF.

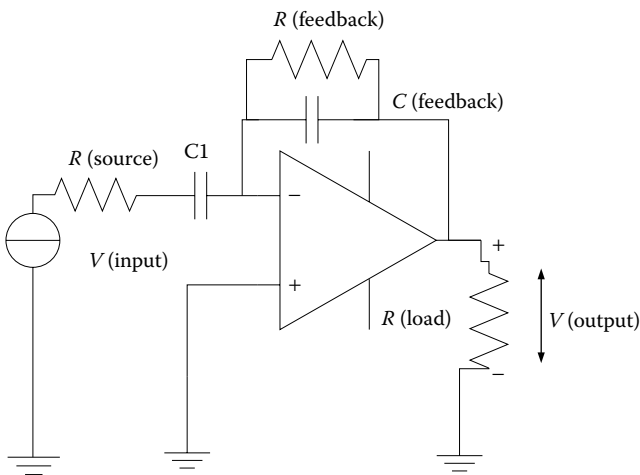


FIGURE P4.6

Figure for Problem 4.6, a band-pass filter.

4.7. Figure P4.7 shows a circuit for a filter. Using the bond graph model for this circuit, simulate its behavior. From the results, can you decipher whether this is a low-pass or a high-pass filter? Typical values that may be used for the different components are: R (source) = 9.1 kOhms, R (feedback) = 22 kOhm, R (load) = 2.2 kOhm, C (feedback) = 0.47microF.

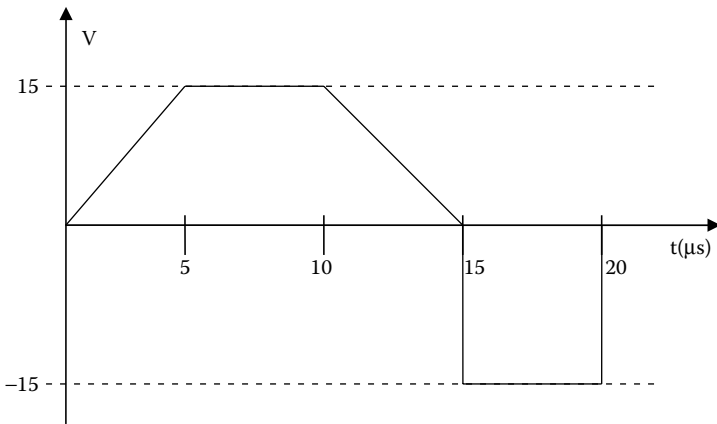
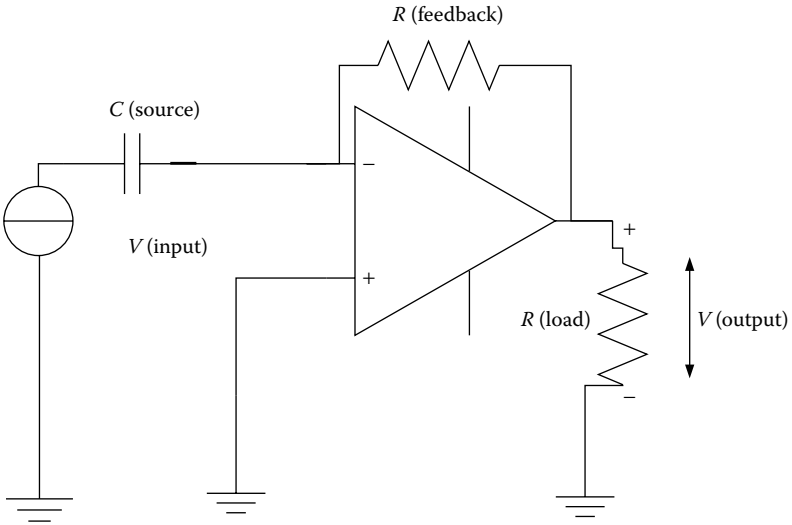


FIGURE P4.7

Figure for Problem 4.7, circuit for a filter.

4.8. Figure P4.8 shows a circuit involving an op-amp. Using the bond graph model for this circuit, simulate its behavior. From the results, can you decipher whether this is a differentiator or an integrator? Typical values that may be used for the different components are: $C1 = 1$ microF, R (feedback) = 10 kOhm, R (load) = 1 kOhm. Using the profile shown in the accompanying plot, determine what the output of this circuit is.

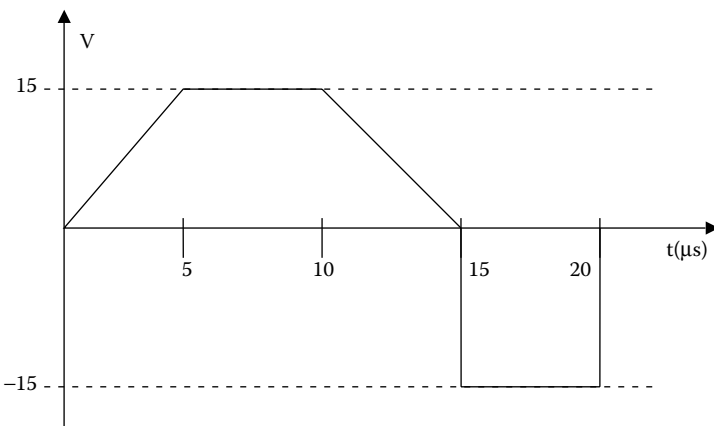
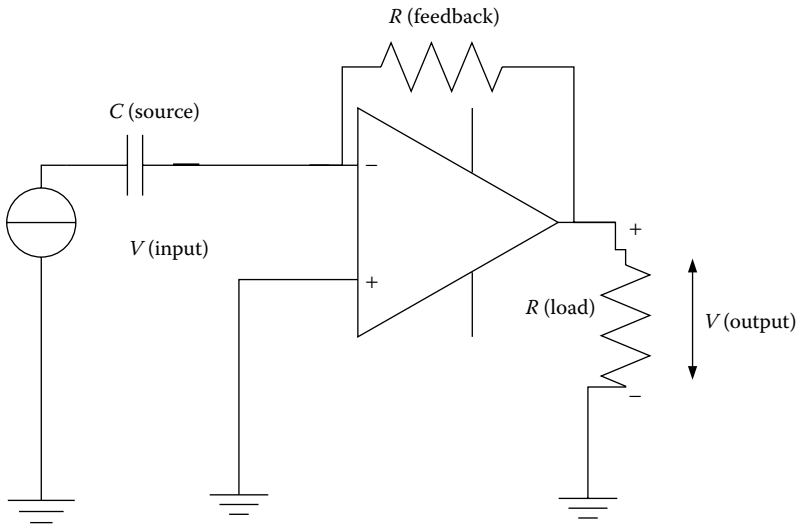


FIGURE P4.8

Figure for Problem 4.8, circuit involving an op-amp.

- 4.9. Figure P4.9 shows a rectifier circuit where four diodes are in a circuit in the form of a wheatstone bridge. Develop a bond graph model for this circuit and for a sinusoidal voltage input determine the output across the load resistance shown in the figure.

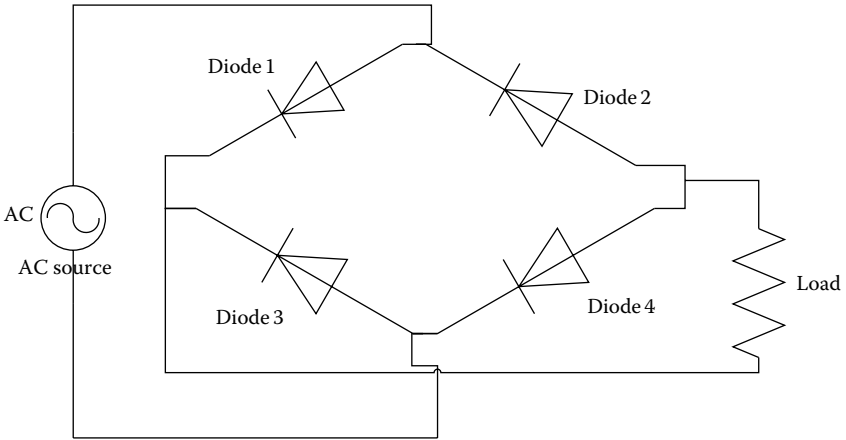


FIGURE P4.9

Figure for Problem 4.9, rectifier circuit.

- 4.10. Develop a bond graph model for the cramping circuit shown in the Figure P4.10. Use a sinusoidal input for the source and develop the output results from the simulation.

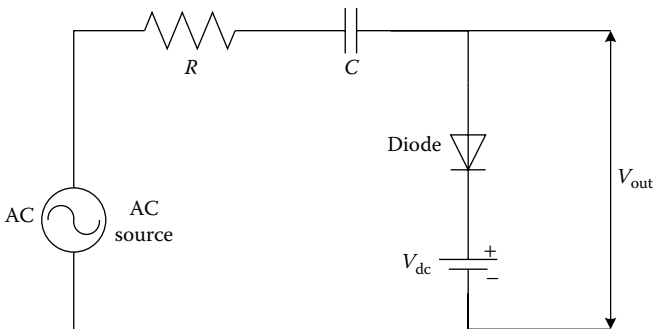


FIGURE P4.10

Figure for Problem 4.10, cramping circuit.

- 4.11. In the diode circuit shown in Figure P4.11, the supply voltage is a saw-toothed wave as shown in the accompanying plot. Model this circuit using the bond graph method and simulate the model to determine the output of this circuit.

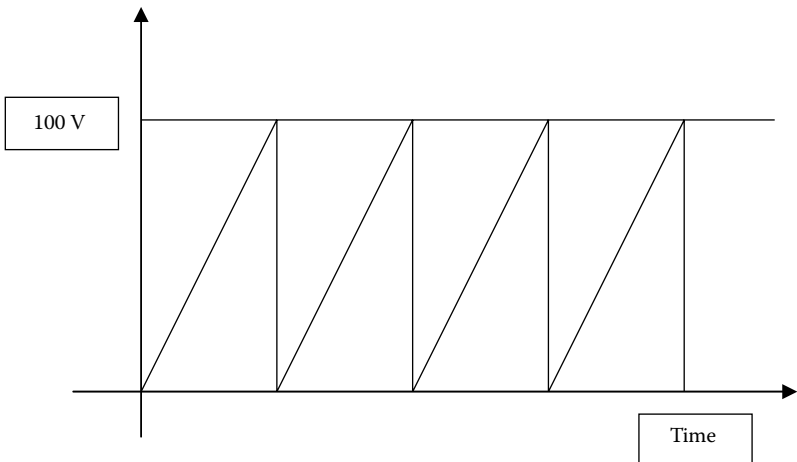
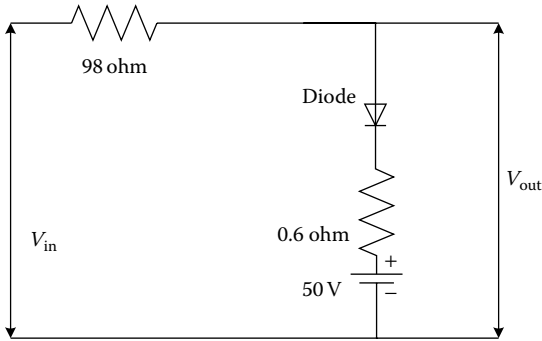


FIGURE P4.11

Figure for Problem 4.11, circuit and waveform.

4.12. Develop a bond graph model for the hydraulic circuit shown in the Figure P4.12.

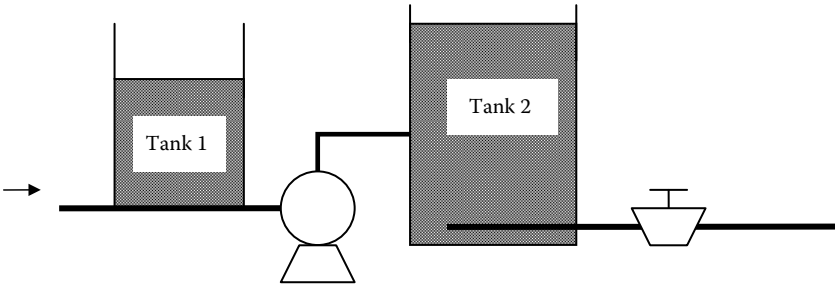


FIGURE P4.12

Figure for Problem 4.12, hydraulic circuit.

4.13. Develop a bond graph model for the hydraulic circuit shown in the Figure P4.13.

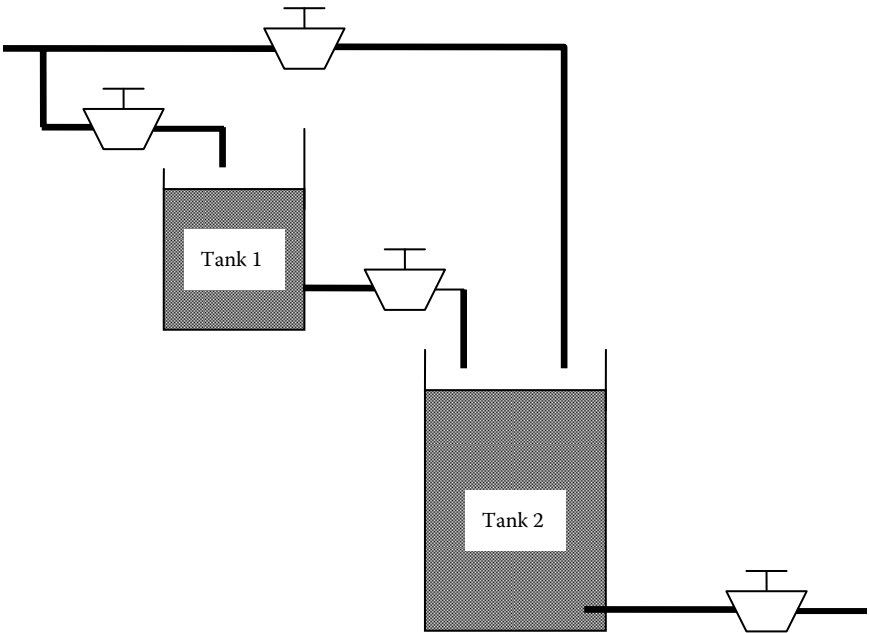


FIGURE P4.13

Figure for Problem 4.13, hydraulic circuit.

This page intentionally left blank

5

Deriving System Equations from Bond Graphs

Once the bond graph representation of a system is complete with the causal structure well defined, it is ready for use. The governing equations for this model may be derived from the bond graph representation. The development of the equations is quite algorithmic and can be easily automated (software tools have actually done it). No decision needs to be made about directions of force, action, reaction, positive direction or negative direction, and so forth. This makes it very easy for the user. In this chapter we will formalize the process of deriving the governing equations for systems from the bond graph model. We will also discuss the effect of causal structure in the bond graphs (such as differential versus integral) on the specific form that the differential equation takes. So the primary objectives of this chapter are to

- Develop an understanding of how the governing system equations may be derived from a bond graph model.
- Derive the governing equations for some typical systems from the system bond graphs.
- Develop an understanding of the effect of differentially causal storage elements on the forms of the system equations.
- Develop an understanding of algebraic loops and how to tackle them.

5.1 System Variables

The reader may recall that there are four system variables: the two generalized power variables, effort and flow, and the two generalized energy variables, momentum and displacement. Relationships between these variables are

Effort, $e = \dot{p}$, p is momentum.

Flow, $f = \dot{q}$, q is displacement.

p and q are also known as the state variables, and the governing differential equations for the model are derived in terms of the state variables.

The system variables in which the equations are derived are the absorbed causes in storage elements with integral causality. Spring/capacitive elements receive flows, which accumulate into displacement/charges.

$$q = \int_{-\infty}^t f dt \quad (5.1)$$

Inertia/inductance receives effort, which accumulates into momentum (generalized).

$$p = \int_{-\infty}^t e dt \quad (5.2)$$

Therefore, the system variable for bond graph based analysis is

$$\text{system variable} = \int_{-\infty}^t (\text{cause}) dt \quad (5.3)$$

where cause is the information going into the storage elements with integral causality.

5.2 Deriving System Equations

One of the critical steps in completing the development of a bond graph model is the derivation of the system equations. These equations are a set of ordinary differential equations in terms of the system's energy variables. In all the text books on bond graphs, extensive discussions of this particular step can be found. They are all quite elaborate and exhaustive. The one used here is not the most fundamental one, but is very effective from a practical standpoint. This approach is modeled after the one taken by Mukherjee and Karmakar (2000). One may recall that each bond in any bond graph model carries information about two quantities, effort and flow, and the directions of flow of this information is always opposite to each other. So in this derivation approach, the process is started by answering two simple questions. They are

Question 1: What do *all the elements* give to the system?

Question 2: What does the system give back to *the storage elements*?

are written as Equation 5.7. Figure 5.2b shows a junction configuration whose flow and effort equations are written as Equation 5.8. Similarly, Figure 5.2c–f shows different junction configurations whose equations are written as Equations 5.9 through 5.12, respectively.

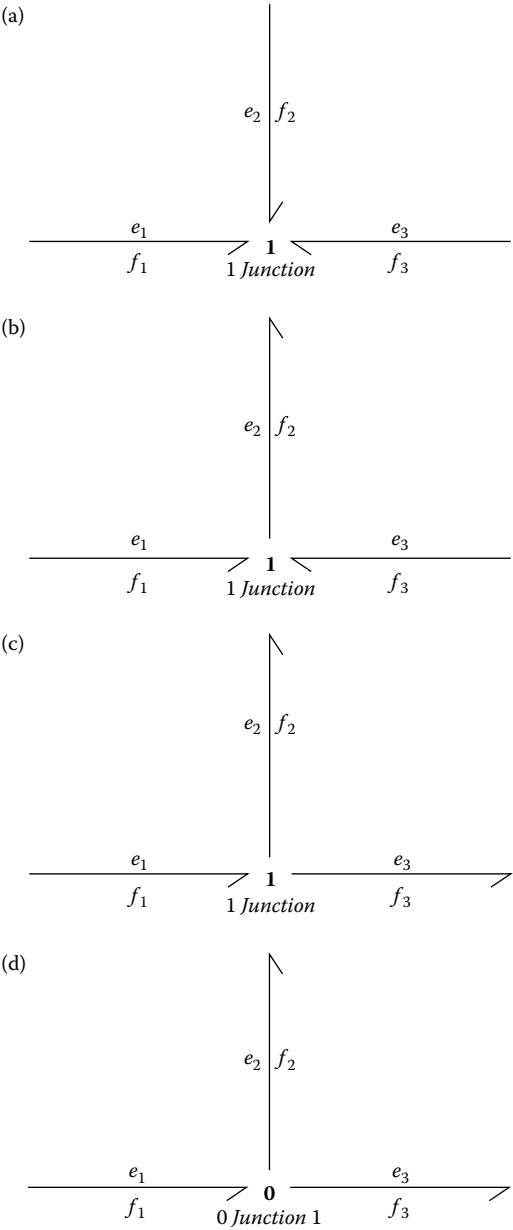


FIGURE 5.2
Some of the different possible joint configurations.

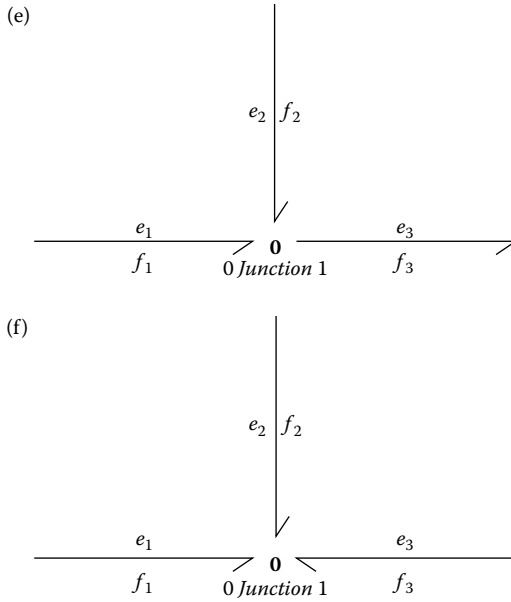


FIGURE 5.2
(Continued)

$$\begin{aligned} f_1 &= f_2 = f_3 \\ e_1 + e_2 + e_3 &= 0 \end{aligned} \quad (5.7)$$

$$\begin{aligned} f_1 &= f_2 = f_3 \\ e_1 + e_3 &= e_2 \end{aligned} \quad (5.8)$$

$$\begin{aligned} f_1 &= f_2 = f_3 \\ e_1 &= e_2 + e_3 \end{aligned} \quad (5.9)$$

$$\begin{aligned} f_1 &= f_2 + f_3 \\ e_1 &= e_2 = e_3 \end{aligned} \quad (5.10)$$

$$\begin{aligned} f_1 + f_2 &= f_3 \\ e_1 &= e_2 = e_3 \end{aligned} \quad (5.11)$$

$$\begin{aligned} f_1 + f_2 + f_3 &= 0 \\ e_1 = e_2 = e_3 \end{aligned} \quad (5.12)$$

We will now discuss the process of deriving the governing equations from a fully causalled bond graph representation. For the first example (Example 5.1), we have chosen the well-known RLC circuit from the electrical domain (which is equivalent to the spring-mass-damper system in the mechanical domain).

EXAMPLE 5.1: RLC CIRCUIT

Figure 5.3 shows an RLC circuit along with its bond graph representation. The effort and flow associated with each bond are marked up in the figure.

Answers to Q1 (written in terms of the constitutive equations).

Q1. What do *all the elements* give to the system?

Answers: The answers are written for each bond.

Bonds:

$$1. \quad e_1 = V(t) \quad (5.13)$$

Bond 1 gives back effort to the system.

$$2. \quad e_2 = R \cdot f_2 \quad (\text{resistor}) \quad (5.14)$$

Bond 2 gives back effort to the system.

$$3. \quad f_3 = \frac{P_3}{L} \quad (\text{inductor}) \quad (5.15)$$

Bond 3 gives back flow to the system.

$$4. \quad e_4 = \frac{1}{C} q_4 \quad (\text{capacitor}) \quad (5.16)$$

Bond 4 gives back effort to the system.

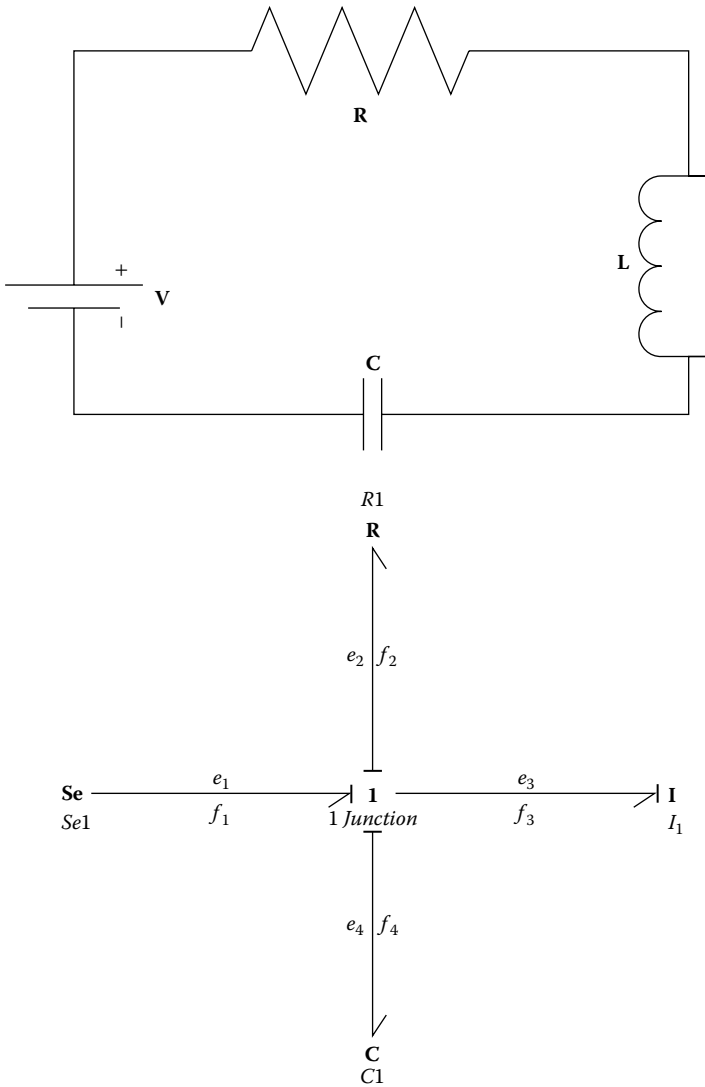


FIGURE 5.3
An RLC circuit and its corresponding bond graph.

Answers to Q2: In writing the answers to this question, we need to use the answers from Q1 and the joint equations for effort and flow.

Q2. What does the system give back to *the storage elements*?

Bond 4 (for storage element C1)

$$\dot{q}_4 = f_4 = f_1 = f_2 = f_3 = \frac{p_3}{L} \quad (5.17)$$

Flows are equal in 1 junction and f_3 brings the flow information to the junction.

Bond 3

$$\begin{aligned}\dot{p}_3 &= e_3 = e_1 - e_2 - e_4 \\ \dot{p}_3 &= V(t) - Rf_2 - \frac{q_4}{C} \\ \dot{p}_3 &= V(t) - R\frac{p_3}{L} - \frac{q_4}{C}\end{aligned}\tag{5.18}$$

Summing of efforts at the 1 junction.

Final form is (by rewriting Equations 5.17 and 5.18):

$$\begin{aligned}\dot{p}_3 &= V(t) - R\frac{p_3}{L} - \frac{q_4}{C} \\ \dot{q}_4 &= \frac{p_3}{L}\end{aligned}\tag{5.19}$$

Note a few important things in the final form of these equations. These are important issues to keep in mind when the reader wants to develop the governing equations:

- There are two first order equations, one each for the two storage elements with integral causality.
- The two equations are coupled, that is, they have to be solved simultaneously. The two state variables that appear in the equations are the p and q associated with the storage elements that is, p_3 and q_4 (and their first derivatives).
- The final forms of the equations are written in terms of the input to the system, system parameters, and state variables only and no other terms.
- Although intermediate variables, such as effort and flow of individual bonds, are used in the intermediate steps, they vanish from the final equations.
- This is a second order system because there are two equations state space equations.

We are more familiar with the second order ordinary differential equation representing a second order system. It can be shown that the above two equations may be combined to give a second order ODE for the system.

$$\begin{aligned}\dot{p}_3 &= V(t) - R \frac{p_3}{L} - \frac{q_4}{C} \\ \dot{q}_4 &= \frac{p_3}{L} \Rightarrow \dot{p}_3 = \ddot{q}_4 L\end{aligned}\quad (5.19)$$

Converting it into second order function by taking derivatives of Equation 5.19 and combining them, we get:

$$\begin{aligned}L \cdot \ddot{q}_4 &= V(t) - R \cdot \frac{p_3}{L} - \frac{q_4}{C} \\ L \cdot \ddot{q}_4 &= V(t) - R \cdot L \cdot \frac{\dot{q}_4}{L} - \frac{q_4}{C}\end{aligned}\quad (5.20) \text{ or}$$

$$V(t) = L \cdot \ddot{q}_4 + R \dot{q}_4 + \frac{q_4}{C} \quad (5.20)$$

Equation 5.20 is the standard form that many are familiar with for an RLC circuit. A similar equation written for a mechanical system will be the well-known spring-mass-damper equation for a vibrating mass:

$$F(t) = m\ddot{x} + B\dot{x} + kx \quad (5.21)$$

where x is the displacement, F is the external force applied, B is the damping coefficient, and m is the mass.

It is thus shown that a set of two state-space equations is equivalent to a single second order differential equation, and the two can be used to describe the same second order system. To reiterate, the system has two energy storage elements. Hence, it is a second order system.

EXAMPLE 5.2

Figure 5.4 shows the system and the corresponding bond graph. This is a mechanical system containing the basic components that make up typical mechanical systems. Based on what we learned in the previous example, the equations will be for the state variables associated with the energy storage elements, that is, q_4 , p_1 , q_8 , and p_{10} .

This example has a transformer element. Before we start deriving the equations, we need to obtain the transformer parameter.

Figure 5.5 shows how the transformer element could move. This means that f_6 and f_7 are proportional to each other in the following way:

$$\frac{f_6}{l_1} = -\frac{f_7}{l_2} \Rightarrow f_7 = -\frac{l_2}{l_1} f_6 \quad (5.22)$$

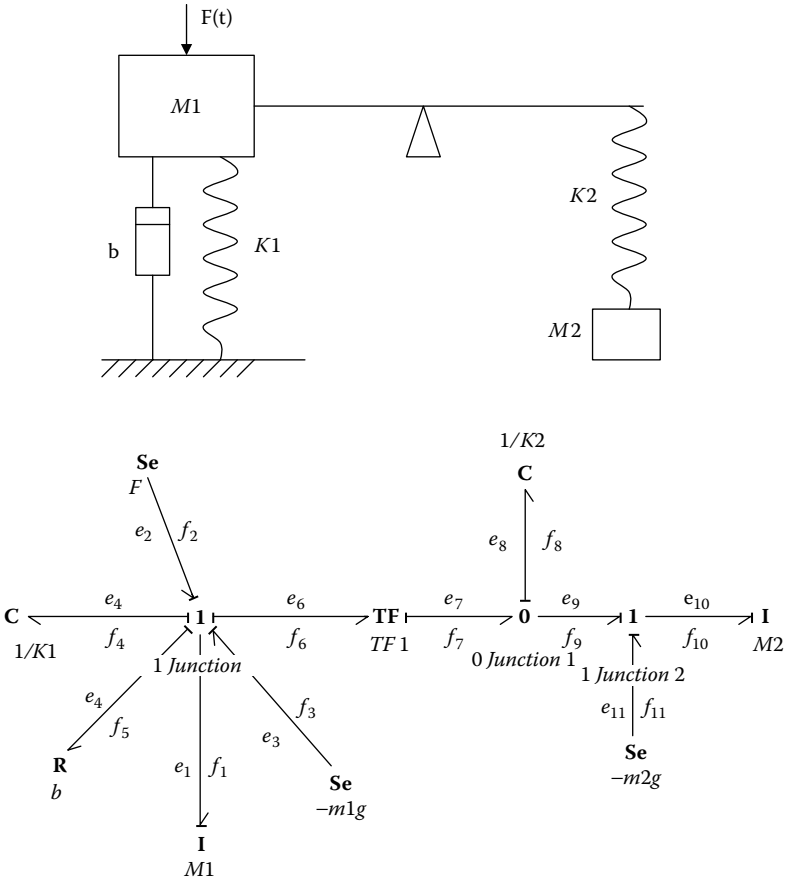


FIGURE 5.4
A generic mechanical system and its corresponding bond graph.

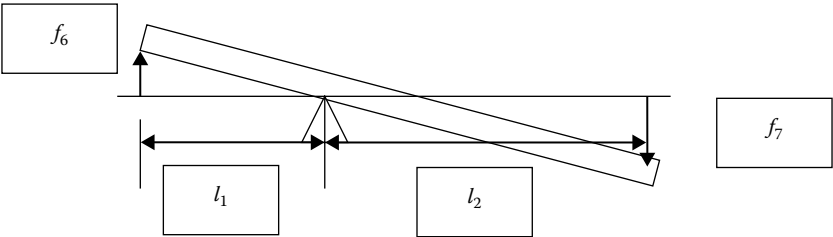


FIGURE 5.5
A schematic of the lever as a transformer.

The negative sign in the above relationship means that the two flow directions are opposite to one another. Since the transformer conserves power (i.e., $e_7 f_7 = e_6 f_6$) a similar relationship will exist between e_6 and e_7 .

$$e_6 I_1 = -e_7 I_2 \Rightarrow e_6 = -\frac{I_2}{I_1} e_7 \quad (5.23)$$

So the transformer factor is

$$TF = -\frac{I_2}{I_1}.$$

Now we will attempt to derive the governing equations.

Answers to Q1 (written in terms of the constitutive equations).

Q1. What do *all the elements* give to the system?

Answers:

Bonds

$$1. \quad f_1 = \frac{p_1}{m_1} \quad (5.24)$$

$$2. \quad e_2 = F(t) \quad (5.25)$$

$$3. \quad e_3 = -m_1 g \quad (5.26)$$

$$4. \quad e_4 = k_1 q_4 \quad (5.27)$$

$$5. \quad e_5 = b f_5 \quad (5.28)$$

$$8. \quad e_8 = k_2 q_8 \quad (5.29)$$

$$10. \quad f_{10} = \frac{p_{10}}{m_2} \quad (5.30)$$

$$11. \quad e_{11} = -m_2 g \quad (5.31)$$

Answers to Q2: Use the answers from Q1 and the joint equations.

Q2. What does the system give back to *the storage elements*?

Bond 1

$$\begin{aligned}
 \dot{p}_1 &= e_1 = e_2 + e_3 - e_4 - e_5 - e_6 \\
 \dot{p}_1 &= F(t) - m_1 g - k_1 q_4 - b f_5 - \left(-\frac{l_2}{l_1} \right) e_7 \\
 \dot{p}_1 &= F(t) - m_1 g - k_1 q_4 - b \frac{p_1}{m_1} + \frac{l_2}{l_1} (k_2 q_8)
 \end{aligned}
 \quad
 \begin{bmatrix}
 \because f_1 = f_2 = f_3 = f_4 = f_5 \\
 f_1 = f_5 = \frac{p_1}{m_1} \\
 \because e_7 = e_8 = e_9 \\
 e_6 = (TF)e_7, TF = -\frac{l_2}{l_1}
 \end{bmatrix}
 \quad (5.32)$$

Bond 4

$$\dot{q}_4 = f_4 = f_1 = \frac{p_1}{m_1} \quad (5.33)$$

Bond 8

$$\begin{bmatrix}
 \because f_6 = f_1 \\
 f_7 = (TF)f_6 \\
 f_9 = f_{10}
 \end{bmatrix}$$

$$\begin{aligned}
 \dot{q}_8 &= f_8 = f_7 - f_9 = -\frac{l_2}{l_1} (f_1) - f_{10} \\
 \dot{q}_8 &= -\frac{l_2}{l_1} \left(\frac{p_1}{m_1} \right) - \frac{p_{10}}{m_2}
 \end{aligned}
 \quad (5.34)$$

Bond 10

$$\begin{aligned}
 [\because e_9 = e_8] \\
 \dot{p}_{10} &= e_{10} = e_9 + e_{11} \\
 \dot{p}_{10} &= k_2 q_8 - m_2 g
 \end{aligned}
 \quad (5.35)$$

All four equations may be represented together as:

$$\begin{bmatrix} \dot{p}_1 \\ \dot{q}_4 \\ \dot{q}_8 \\ \dot{p}_{10} \end{bmatrix} = \begin{bmatrix} -\frac{b}{m_1} & -k_1 & \frac{l_2 k_2}{l_1} & 0 \\ \frac{1}{m_1} & 0 & 0 & 0 \\ -\frac{l_2}{l_1} \frac{1}{m_1} & 0 & 0 & -\frac{1}{m_2} \\ 0 & 0 & k_2 & 0 \end{bmatrix} \begin{bmatrix} p_1 \\ q_4 \\ q_8 \\ p_{10} \end{bmatrix} + \begin{bmatrix} F(t) - m_1 g \\ 0 \\ 0 \\ -m_2 g \end{bmatrix} \quad (5.36)$$

Four first order equations are describing the behavior of this system. Each equation represents one of the energy storage devices. The state-space variables representing the energy storage devices are displacement or momentum—the energy variables. This set of coupled ordinary differential equations

(5.36) can be solved simultaneously to obtain the system behavior. In order to solve these equations, four initial conditions will also be required.

EXAMPLE 5.3: AN ELECTROMECHANICAL SYSTEM, A PERMANENT MAGNET DC MOTOR

The bond graph shown in Figure 5.6 is that of a permanent magnet DC motor. We will discuss the detailed derivation of this bond graph from the actual physical system in a later chapter. For now we will try to use the method that we just learned to develop the governing equations for this model.

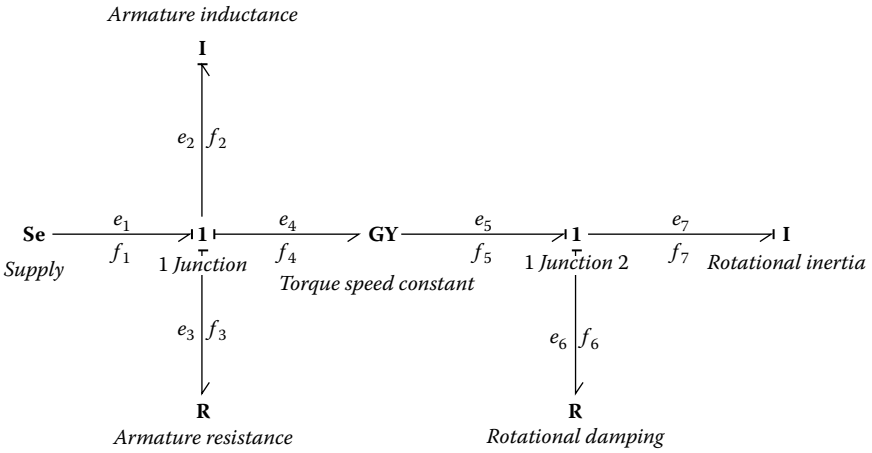


FIGURE 5.6
Bond graph representation of a permanent magnet DC motor.

Before we start deriving the equations, let's make sure the gyrator factor is determined. Let us assume the gyrator factor be m . Therefore, from the bond graph representation of the system, it is clear that:

$$\begin{aligned} e_5 &= mf_4 \\ e_4 &= mf_5 \end{aligned} \quad (5.37)$$

Now we will attempt to derive the governing equations.

Answers to Q1 (written in terms of the constitutive equations).

Q1. What do *all the elements* give to the system?

Answers

Bonds

$$1. \quad e_1 = V(t) \quad (5.38)$$

$$2. \quad f_2 = \frac{p_2}{L} \quad (5.39)$$

$$3. \quad e_3 = Rf_3 \quad (5.40)$$

$$6. \quad e_6 = bf_6 \quad (5.41)$$

$$7. \quad f_7 = \frac{p_7}{J} \quad (5.42)$$

Answers to Q2: Use the answers from Q1 and the joint equations.

Q2. What does the system give back to the storage elements?

Bond 2

$$\begin{aligned} \dot{p}_2 &= e_2 = e_1 - e_3 - e_4 \\ \dot{p}_2 &= V(t) - Rf_3 - mf_5 \\ \dot{p}_2 &= V(t) - R\frac{p_2}{L} - m\frac{p_7}{J} \end{aligned} \quad \left[\begin{array}{l} \because f_1 = f_2 = f_3 = f_4 \\ f_1 = f_2 = \frac{p_2}{L} \\ \because f_5 = f_6 = f_7 = \frac{p_7}{J} \end{array} \right] \quad (5.43)$$

Bond 7

$$\left[\begin{array}{l} \because f_1 = f_2 = f_3 = f_4 \\ f_4 = \frac{p_2}{L} \\ \because f_5 = f_6 = f_7 = \frac{p_7}{J} \end{array} \right] \quad \begin{array}{l} \dot{p}_7 = e_7 = e_5 - e_6 \\ \dot{p}_7 = mf_4 - bf_6 \\ \dot{p}_7 = m\frac{p_2}{L} - b\frac{p_7}{J} \end{array} \quad (5.44)$$

The two equations may be represented together as:

$$\begin{bmatrix} \dot{p}_2 \\ \dot{p}_7 \end{bmatrix} = \begin{bmatrix} \frac{-R}{L} & \frac{-m}{J} \\ \frac{m}{L} & \frac{-b}{J} \end{bmatrix} \begin{bmatrix} p_2 \\ p_7 \end{bmatrix} + \begin{bmatrix} V(t) \\ 0 \end{bmatrix} \quad (5.45)$$

In Examples 5.1–5.3, the energy storage devices ended up with integral causality. We have, in a previous chapter, talked about both integral and differential causality. We also said that although integral causality is desired, it is not always possible to have integral causality, and, instead, a differential causality may result. Example 5.4 in Section 5.3 discusses the governing equation derivation process in the presence of a differential causality.

$$4. \quad e_4 = k_1 q_4 \quad (5.49)$$

$$6. \quad f_6 = \frac{p_6}{J_2} \quad (5.50)$$

$$9. \quad e_9 = k q_9 \quad (5.51)$$

$$10. \quad e_{10} = M \dot{f}_{10} \quad (5.52)$$

$$11. \quad e_{11} = R f_{11} \quad (5.53)$$

Since the I element associated with bond 10 is the element with differential causality, the form of this equation is, therefore, somewhat unnatural and written in terms of rate of change of flow, for an inertia storage element.

Answers to Q2: Use the answers from Q1 and the joint equations.

Q2. What does the system give back to the storage elements?

Bond 2

$$\begin{aligned} \dot{p}_2 &= e_2 = e_1 - e_3 \\ \dot{p}_2 &= F(t) - k_1 q_4 \end{aligned} \quad (5.54)$$

Bond 4

$$\begin{aligned} \dot{q}_4 &= f_4 = f_3 - f_5 \\ \dot{q}_4 &= \frac{p_2}{J_1} - \frac{p_6}{J_2} \end{aligned} \quad (5.55)$$

Bond 6

$$\begin{aligned} \dot{p}_6 &= e_6 = e_5 + e_7 \\ \dot{p}_6 &= k_1 q_4 + \frac{e_8}{m} \\ \dot{p}_6 &= k_1 q_4 - \frac{1}{m} (k q_9 + M \dot{f}_{10} + R f_{11}) \\ \dot{p}_6 &= k_1 q_4 - \frac{1}{m} \left(k q_9 + M \dot{f}_{10} + R \frac{p_6}{m J_2} \right) \end{aligned} \quad \left[\begin{array}{l} \because e_5 = e_4 \\ e_8 = -(e_9 + e_{10} + e_{11}) \\ f_{11} = f_8 = \frac{f_7}{m} = \frac{f_6}{m} \end{array} \right] \quad (5.56)$$

Bond 9

$$\begin{aligned}\dot{q}_9 &= f_9 = f_8 = \frac{f_7}{m} = \frac{f_6}{m} \\ \dot{q}_9 &= \frac{f_7}{m} = \frac{f_6}{m} \\ \dot{q}_9 &= \frac{p_6}{mj_2}\end{aligned}\tag{5.57}$$

Bond 10

$$\begin{aligned}f_{10} &= f_8 = \frac{p_6}{mj_2} \\ \dot{f}_{10} &= \frac{\dot{p}_6}{mj_2}\end{aligned}\tag{5.58}$$

Substitute the \dot{f}_{10} obtained in Equation 5.58 into Equation 5.56. We get:

$$\dot{p}_6 = k_t q_4 - \frac{1}{m} \left(k q_9 + M \frac{\dot{p}_6}{mj_2} + R \frac{p_6}{mj_2} \right)\tag{5.59}$$

This can be manipulated by taking \dot{p}_6 to the left-hand side. The simplified equation becomes:

$$\dot{p}_6 = \frac{1}{\left(1 + \frac{M}{m^2 j_2}\right)} \left[k_t q_4 - \frac{1}{m} \left(k q_9 + R \frac{p_6}{mj_2} \right) \right]\tag{5.60}$$

The four equations that are coupled (for the four independent energy storage devices) are

$$\begin{aligned}\dot{p}_2 &= F(t) - k_t q_4 \\ \dot{q}_4 &= \frac{p_2}{j_1} - \frac{p_6}{j_2} \\ \dot{p}_6 &= \frac{1}{\left(1 + \frac{M}{m^2 j_2}\right)} \left[k_t q_4 - \frac{1}{m} \left(k q_9 + R \frac{p_6}{mj_2} \right) \right] \\ \dot{q}_9 &= \frac{p_6}{mj_2}\end{aligned}\tag{5.61}$$

The four equations in Equation 5.61 have to be solved simultaneously. After the solution of the four equations, the equation for Bond 10 may be solved using:

$$\dot{f}_{10} = \frac{\dot{p}_6}{mJ_2} \quad (5.62)$$

In the matrix form, the first four equations can be written as:

$$\begin{bmatrix} \dot{p}_2 \\ \dot{q}_4 \\ \dot{p}_6 \\ \dot{q}_9 \end{bmatrix} = \begin{bmatrix} 0 & -k_2 & 0 & 0 \\ \frac{1}{J_1} & 0 & -\frac{1}{J_2} & 0 \\ 0 & \frac{k_t}{\left(1 + \frac{M}{m^2 J_2}\right)} & \frac{R}{m^2 J_2 \left(1 + \frac{M}{m^2 J_2}\right)} & -\frac{k}{m \left(1 + \frac{M}{m^2 J_2}\right)} \\ 0 & 0 & \frac{1}{mJ_2} & 0 \end{bmatrix} \cdot \begin{bmatrix} p_2 \\ q_4 \\ p_6 \\ q_9 \end{bmatrix} + \begin{bmatrix} F(t) \\ 0 \\ 0 \\ 0 \end{bmatrix} \quad (5.63)$$

The behavior of the four independent energy storage devices is governed by the above four equations. The fifth energy storage device (the one that is differentially caussed and, as a result, not independent) is related to the behavior of the others and can be represented through the relationship:

$$\dot{f}_{10} = \frac{\dot{p}_6}{mJ_2} \quad (5.64)$$

From the standpoint of system behavior and its solution, this means that the set of differential equations (Equation 5.63) will first have to be solved simultaneously and then its solution can be used to solve Equation 5.64. This is the mathematical implication of the differential causality and the dependent behavior of the device with differential causality.

5.4 Algebraic Loops

When deriving the governing equations for a system, one may encounter another problem, which is referred to as algebraic loops. Algebraic loops and derivative causality received a lot of attention from researchers during the early days of bond graph research. For more detailed discussion of this topic, refer to the works of Granda (1984), Felez and Vera (2000), Karnopp (1983), and others. Figure 5.8 shows an example and a bond graph that illustrates a situation when an algebraic loop is encountered and how it could be handled. In Example 5.5, we will attempt to derive the governing equations in a manner similar to earlier examples.

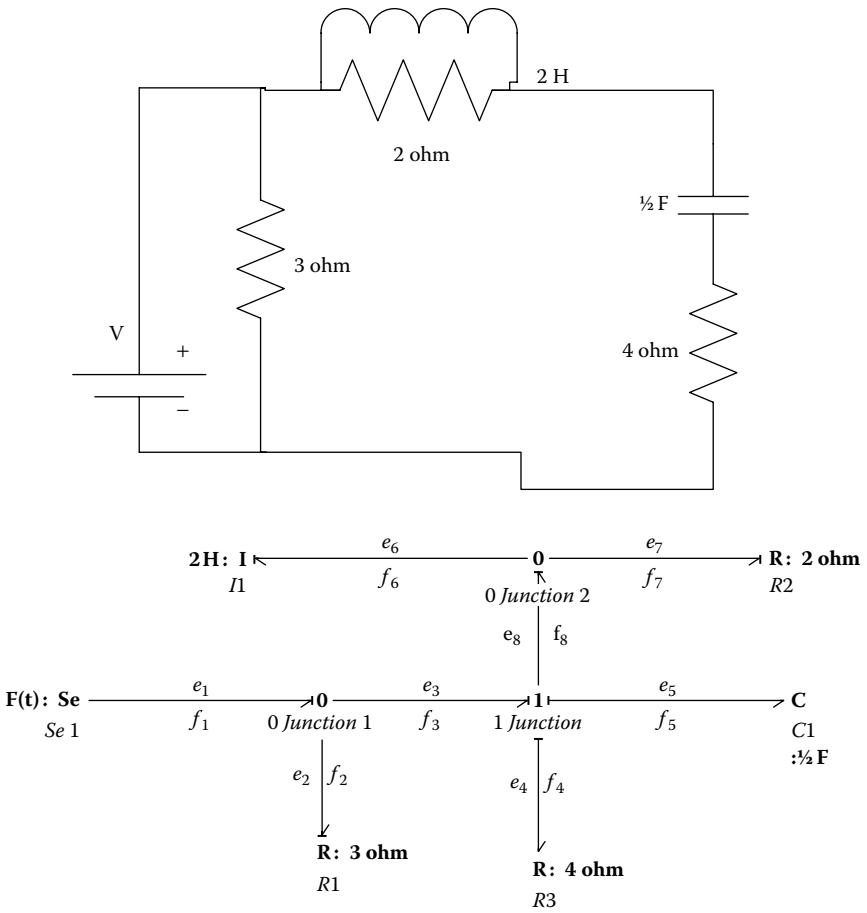


FIGURE 5.8
A circuit and its bond graph representation.

EXAMPLE 5.5

Answers to Q1 (written in terms of the constitutive equations).

Q1. What do all the elements give to the system?

Answers

Bonds

$$1. \quad e_1 = F(t) \quad (5.65)$$

$$2. \quad f_2 = \frac{e_2}{R_1} = \frac{e_2}{3} \quad (5.66)$$

$$4. \quad e_4 = R_3 f_4 = 4f_4 \quad (5.67)$$

$$5. \quad e_5 = \frac{q_5}{C} = 2q_5 \quad (5.68)$$

$$6. \quad f_6 = \frac{p_6}{I} = \frac{p_6}{2} \quad (5.69)$$

$$7. \quad f_7 = \frac{e_7}{R_2} = \frac{e_7}{2} \quad (5.70)$$

Answers to Q2: Use the answers from Q1 and the joint equations.

Q2. What does the system give back to the storage elements?

Bond 6

$$\begin{aligned}
 \dot{p}_6 &= e_6 = e_8 = e_3 - e_5 - e_4 \\
 \dot{p}_6 &= e_3 - 2q_5 - 4f_4 \\
 \dot{p}_6 &= F(t) - 2q_5 - 4f_8 \\
 \dot{p}_6 &= F(t) - 2q_5 - 4\left(\frac{p_6}{2} + \frac{e_7}{2}\right) \\
 \dot{p}_6 &= F(t) - 2q_5 - 2p_6 - 2e_8 \\
 \dot{p}_6 &= F(t) - 2q_5 - 2p_6 - 2\dot{p}_6 \\
 3\dot{p}_6 &= F(t) - 2q_5 - 2p_6 \\
 \dot{p}_6 &= \frac{1}{3}(F(t) - 2q_5 - 2p_6)
 \end{aligned}
 \quad \left[\begin{array}{l} \because f_8 = f_6 + f_7 \\ e_8 = \dot{p}_6 \end{array} \right] \quad (5.71)$$

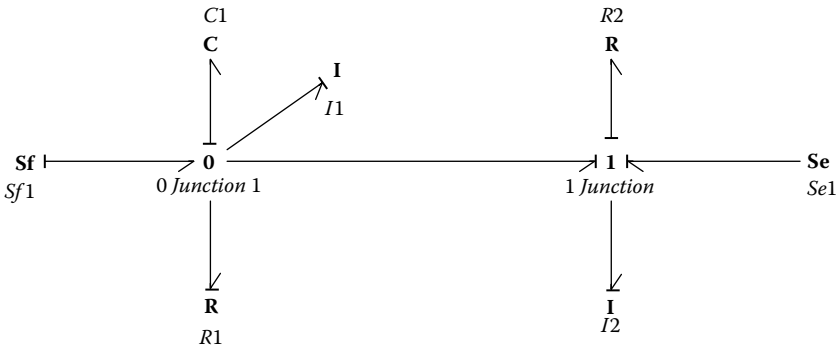
We substituted \dot{p}_6 in place of e_8 and simplified the equation further to get it in terms of p , q and $F(t)$.

Bond 5

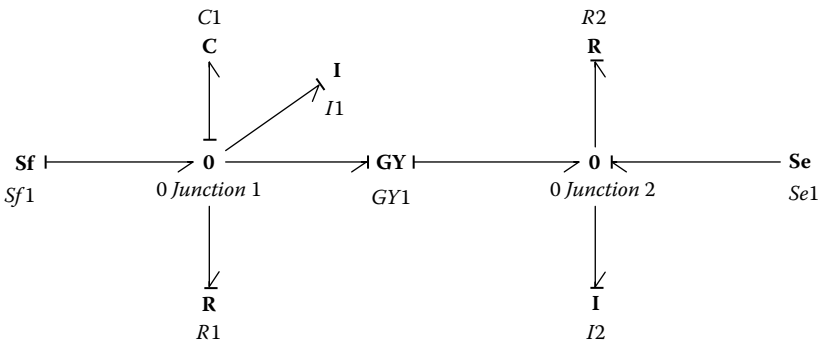
$$\begin{aligned}
 \dot{q}_5 &= f_5 = f_8 = f_6 + f_7 \\
 \dot{q}_5 &= \frac{p_6}{2} + \frac{e_7}{2} \\
 \dot{q}_5 &= \frac{p_6}{2} + \frac{e_8}{2} = \frac{p_6}{2} + \frac{\dot{p}_6}{2} \\
 \dot{q}_5 &= \frac{p_6}{2} + \frac{1}{(3)} \frac{1}{(2)} (F(t) - 2q_5 - 2p_6) \\
 \dot{q}_5 &= \frac{p_6}{2} + \frac{F(t)}{6} - \frac{q_5}{3} - \frac{p_6}{3} \\
 \dot{q}_5 &= \frac{1}{6}[p_6 + F(t) - 2q_5]
 \end{aligned}
 \quad \left[\begin{array}{l} \because f_8 = f_6 + f_7 \\ e_8 = \dot{p}_6 \end{array} \right] \quad (5.72)$$

Problems

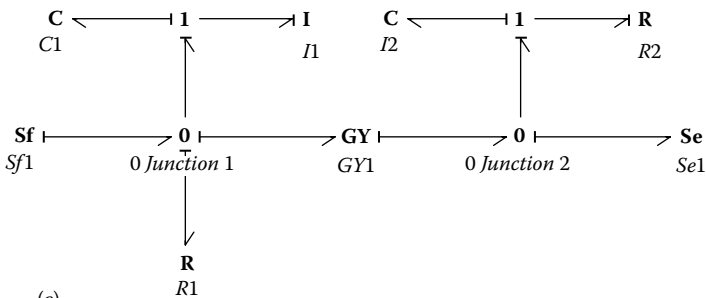
- 5.1. For all the problems in Figure P3.2a–m (for figure see the Problems section of Chapter 3) draw the bond graphs, assign causal strokes, and derive the governing equations for the systems.
- 5.2. Derive the governing equations for the bond graph models shown in Figure P5.1a–e. Use appropriate bond numbers and symbols for the elements in the bond graph.



(a)



(b)



(c)

FIGURE P5.1

Figure for Problem 5.2, bond graph models.

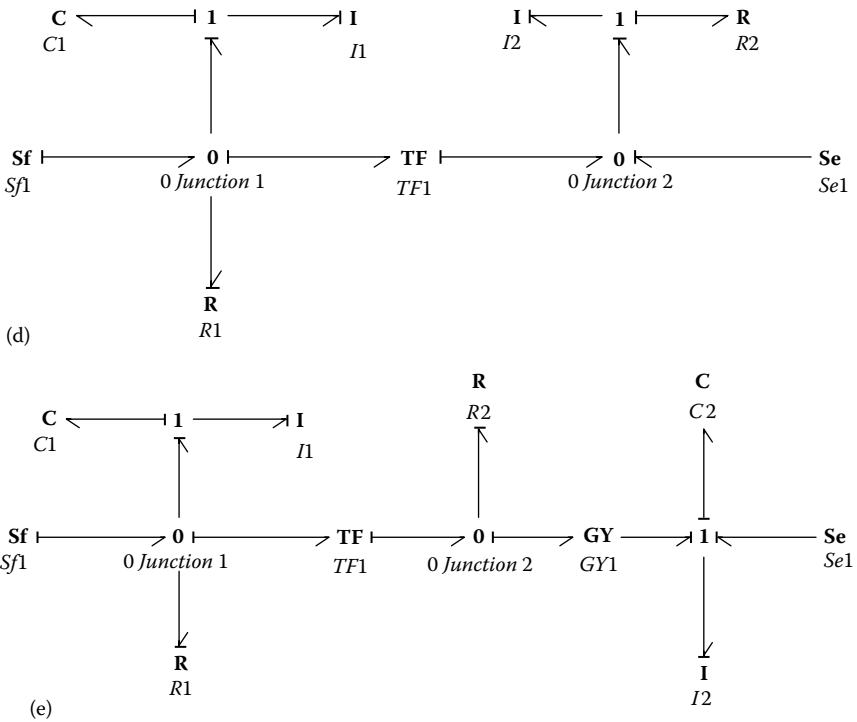


FIGURE P5.1
(Continued)

5.3. Consider the problem shown in Figure P3.1g and j (for the figures see the Problems section of Chapter 3). The constitutive behavior of the resistances B1 and B2 are different from the constitutive behavior of the standard R elements. All these resistances are due to friction force and the constitutive relationship of the friction force is

$$F_{\text{friction}} = F_0 \text{Sgn}(V) = F_0 \frac{V}{|V|}$$

Using this constitutive behavior model for the resistances, derive the set of governing differential equations for the behavior of these two systems.

5.4. Figure P5.2 shows a system. Derive its governing equations from the bond graph model.

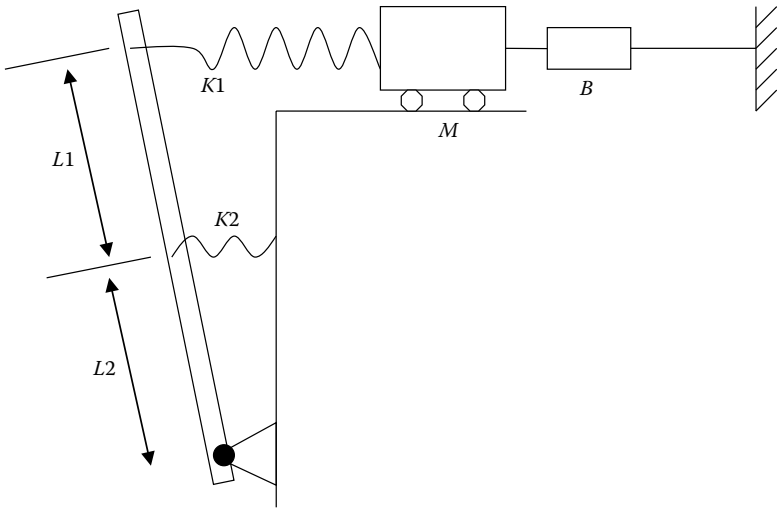


FIGURE P5.2

Figure for Problem 5.4, mechanical system.

5.5. Figure P5.3 shows a mechanical system. Derive its governing equations from the bond graph model.

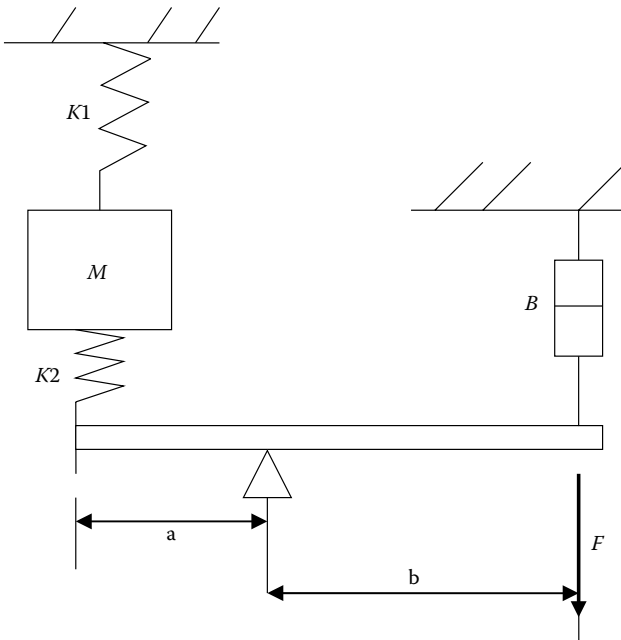


FIGURE P5.3

Figure for Problem 5.5, mechanical system.

5.6. Figure P5.4 shows a bond graph model. Will this have an algebraic loop? Develop the governing equations for this system.

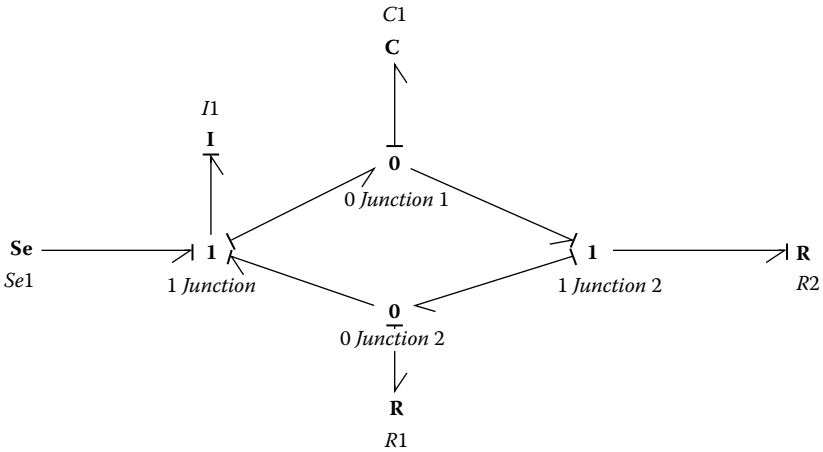


FIGURE P5.4

Figure for Problem 5.6, bond graph model.

5.7. For the system shown in Figure P5.5, develop the bond graph model of the system and then derive the system governing equation(s), first with a velocity input from the right. Do the same if the input is not a velocity but a force input.

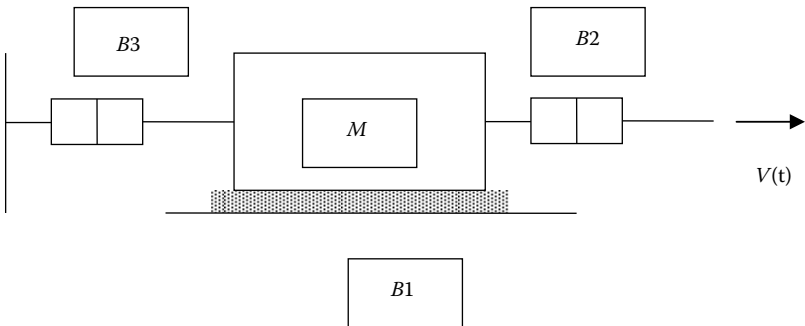


FIGURE P5.5

Figure for Problem 5.7, mechanical system.

5.8. For the system shown in Figure P5.6, develop the bond graph model of the system and then derive the system governing equation.

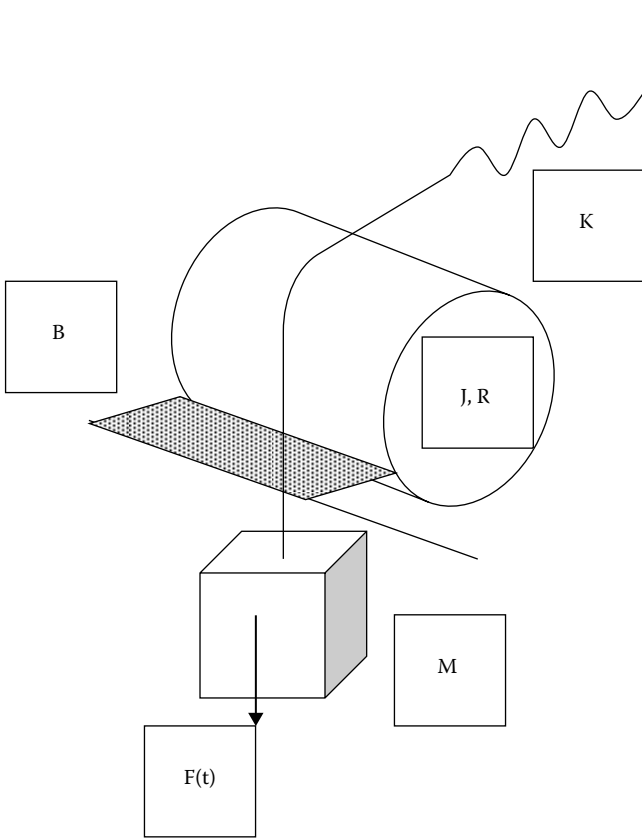


FIGURE P5.6

Figure for Problem 5.8, mechanical system.

5.9. Consider the electrical system shown in Figure P5.7. Derive its governing equations from the bond graph model.

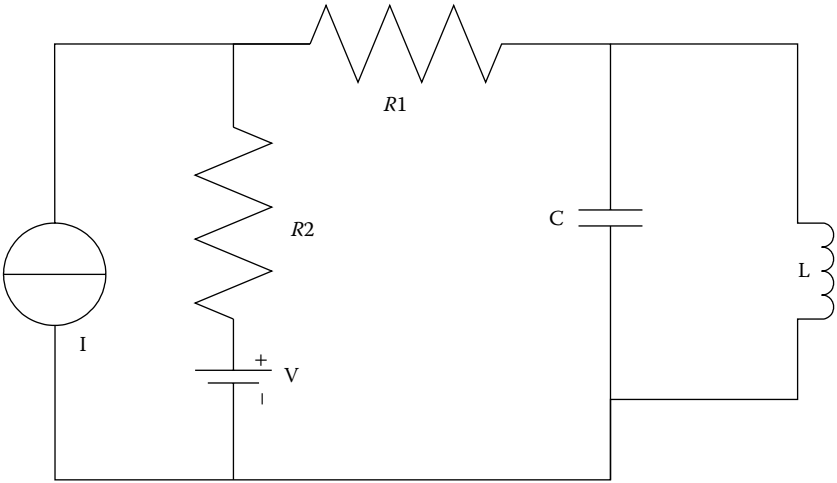


FIGURE P5.7

Figure for Problem 5.9, electrical system.

- 5.10. Consider the electrical system shown in Figure P5.8. Derive its governing equation from the bond graph model.

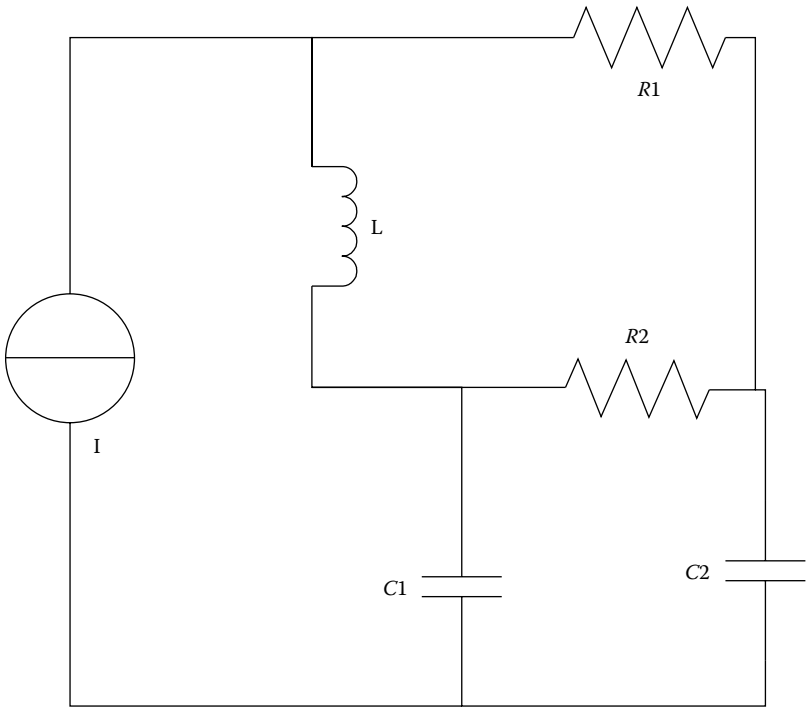


FIGURE P5.8

Figure for Problem 5.10, electrical system.

- 5.11. Put together two bond graph models that could have two possible causal structures without violating any rules of causal assignments. Then derive the governing equations to demonstrate whether algebraic loops are encountered.

6

Solution of Model Equations and Their Interpretation

Solution of dynamic system equations tells us a lot about system behavior. The solution of these equations provides information about the stability of the system, the kind of external force that will excite the system and could take it out of control, how the system will respond to these external disturbances, and so forth. These solutions also enable us to design or modify systems so that we can get a desired behavior from the system. System behavior is not random, and this means that system parameters will determine how the system behaves under different conditions. This makes the study of the system behavior a manageable exercise. To understand system behavior, it is necessary to separate systems by their order. Systems can be ordered as zeroth, first, second, third, and so forth. System order is determined by the number of independent energy storage components that are present in the system. So a very simple system can be a zeroth order system, while a very complex system can be of the tenth order. Although system behavior varies significantly when it changes from zeroth order to first order and from first order to second order, beyond the second order, the system behavior can be easily understood if one understands the behavior of the three lower order systems. Therefore, in most texts, only the first and second order systems are discussed in detail, and the higher order system behavior can be interpreted by understanding the behavior of lower order systems.

The objectives of this chapter are to

- Understand the behavior of a typical zeroth order system.
- Understand the behavior of a typical first order system.
- Understand the behavior of a typical second order system.
- Understand the behavior of system under the effect of different types of forcing functions and interpret simulation results.
- Understand and use time domain and frequency domain solutions.

6.1 Zeroth Order Systems

Systems that do not have any energy storage element are categorized as a zeroth order system. Figure 6.1 shows some examples of zeroth order systems. Careful review of these systems reveals that they have generalized elements, such as transformers, resistors, and sources, but no energy storage devices. Since there are no energy storage elements in zeroth order systems, the order of the differential equation that is derived for these systems is zero; that is, algebraic equations are sufficient to describe the behavior of these systems.

To understand the behavior of a simple zeroth order system, let us consider a resistive circuit with a single voltage source. A schematic of the system and its bond graph representation are shown in Figure 6.2. The governing equations for this system may be derived using the approach outlined in Chapter 5:

By answering Question 1 from Section 5.2: What do all the elements give to the system?

$$1. e_1 = V \quad (6.1)$$

$$2. f_2 = \frac{e_2}{R} \quad (6.2)$$

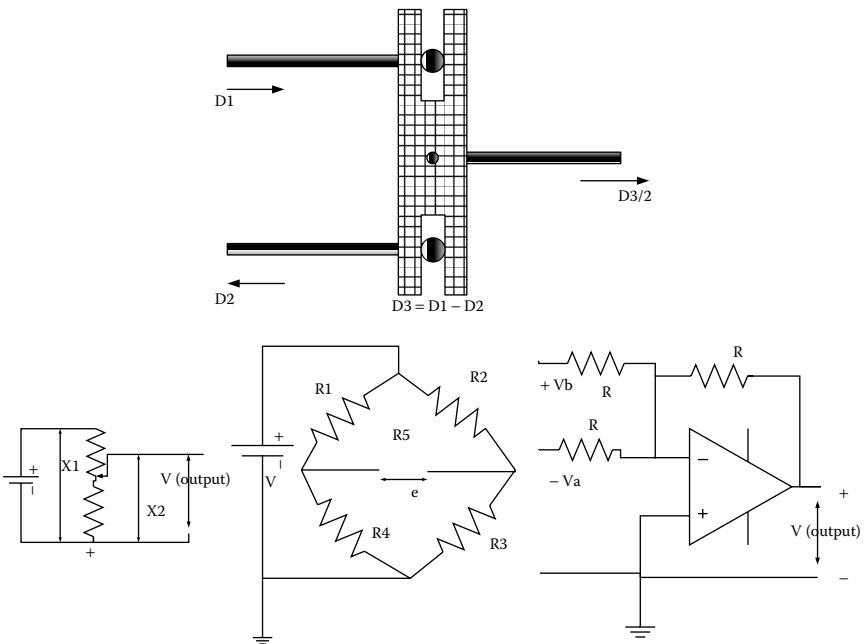


FIGURE 6.1

Examples of zeroth order systems.

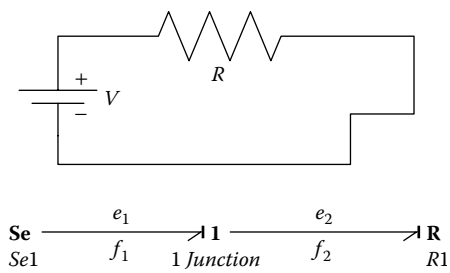


FIGURE 6.2
A zeroth order system with its bond graph.

The derivation continues now by answering Question 2 from Section 5.2: What does the system give back to the storage elements?

$$1. e_1 = e_2 \tag{6.3}$$

$$2. f_1 = f_2 \tag{6.4}$$

Combining the results from Questions 1 and 2 we get:

$$f_1 = f_2 = f = \frac{e_2}{R} = \frac{e_1}{R} = \frac{V}{R} \tag{6.5}$$

Equation 6.5 is nothing new. It is just a confirmation of Ohm’s law. Note that the result is an algebraic equation (not a differential equation). To simulate the system, the following parameters were chosen: $V = 10$, $R = 2$. The simulation result shown by the graph in Figure 6.3 shows a flow of five units through the resistor.

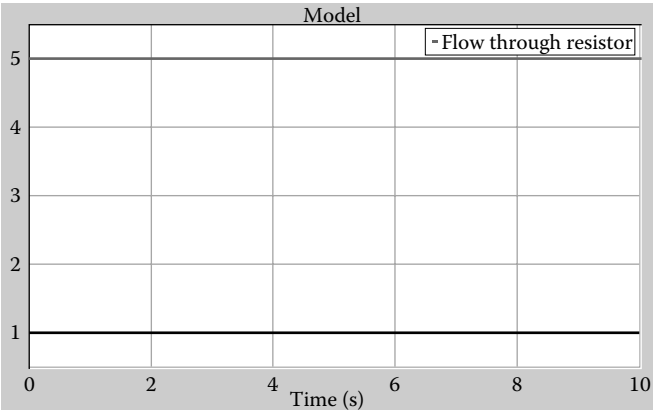


FIGURE 6.3
Zeroth order system response.

Since the governing equations are algebraic, the simulation results are not time variant when the source input is constant. If the source input is time variant, the system behavior will vary with time in exactly the same manner as the source.

6.2 First Order Systems

Figure 6.4 shows some examples of first order systems. First order systems have a single energy storage element. As the figure demonstrates, either a C or I element occurs in all of these systems along with other types of basic elements. In order to understand the behavior of the first order system, let us consider a simple first order system. Figure 6.5 is a circuit with a single C element (capacitor, energy storage device) and a resistor along with a voltage source. The bond graph representation of this system is also shown in the figure. The governing equations for this system are derived using the approach outlined in Chapter 5 as follows:

By answering Question 1 from Section 5.2: What do all the elements give to the system?

$$1. e_1 = V \quad (6.6)$$

$$2. f_2 = \frac{e_2}{R} \quad (6.7)$$

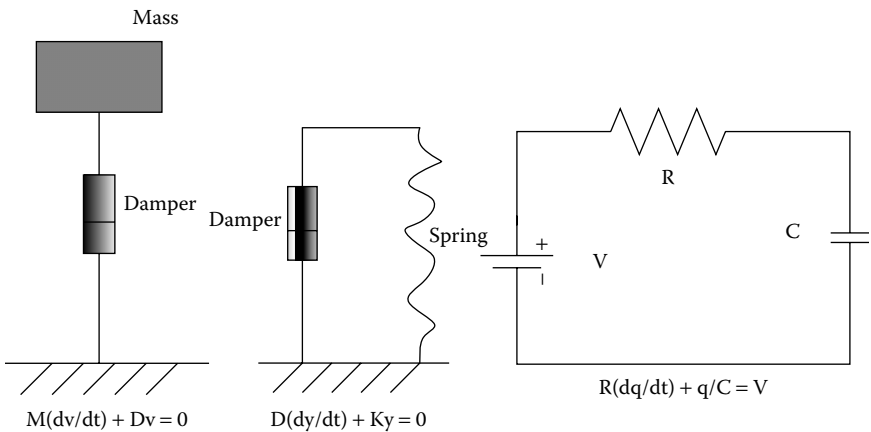
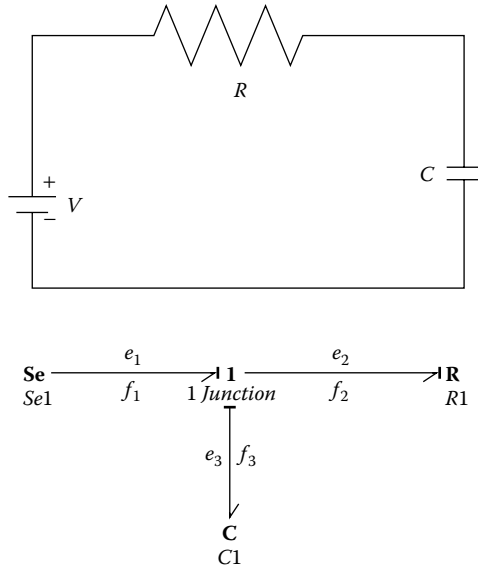


FIGURE 6.4
Examples of first order systems.

**FIGURE 6.5**

A sample first order system and corresponding bond graph.

$$3. e_3 = \frac{q_3}{C} \quad (6.8)$$

The derivation continues by answering Question 2 from Section 5.2: What does the system give back to the storage elements? (Following approach in previous chapter):

$$1. f_3 = \dot{q}_3 = f_1 = f_2 = \frac{e_2}{R} \quad (6.9)$$

$$2. e_2 = e_1 - e_3 = \left\{ V - \frac{q_3}{C} \right\} \quad (6.10)$$

$$3. \dot{q}_3 = f_3 = \frac{e_2}{R} = \frac{1}{R} \left\{ V - \frac{q_3}{C} \right\} = \frac{V}{R} - \frac{q_3}{RC} \quad (6.11)$$

So the governing equation for this system is a single first order differential Equation 6.11 that describes the flow into the energy storage device, the capacitor.

6.2.1 Solution of the First-Order Differential Equation

Equation 6.11 can be rearranged as:

$$\dot{q}_3 = -q_3 \frac{1}{RC} + \frac{V}{R} \quad (6.12)$$

If we substitute a dummy variable $q = q_3 \frac{1}{RC} - \frac{V}{R}$, then $\dot{q} = \dot{q}_3 \frac{1}{RC}$ and Equation 6.12 may be rewritten as:

$$RC\dot{q} = -q \text{ or } \frac{dq}{q} = -\frac{1}{RC} dt \quad (6.13)$$

Integrating we get:

$$\int_0^q \frac{dq}{q} = -\int_0^t \frac{1}{RC} dt \Rightarrow [\ln q]_0^q = -\left[\frac{t}{RC}\right]_0^t \quad (6.14)$$

$$\begin{aligned} \left[\ln \left(\frac{q_3}{RC} - \frac{V}{R} \right) \right]_0^{q_3} &= -\frac{t}{RC} \\ \Rightarrow \left[\ln \left(\frac{q_3}{RC} - \frac{V}{R} \right) - \ln \left(-\frac{V}{R} \right) \right] &= -\frac{t}{RC} \\ \Rightarrow \ln \frac{\left(\frac{q_3}{RC} - \frac{V}{R} \right)}{-\frac{V}{R}} &= -\frac{t}{RC} \end{aligned} \quad (6.15)$$

Therefore, the final form of the solution (using original variables) becomes:

$$\frac{q_3}{RC} = \frac{V}{R} \left(1 - e^{\frac{-t}{RC}} \right) \quad (6.16)$$

This is an exponential function. The initial condition was that when time $t = 0$ and the charge in the capacitor was $q_3 = 0$.

The solution of this differential equation describes the behavior of this first order system. The system model is now simulated to observe its behavior and for the initial simulation, the following variables were chosen:

$$V = 10$$

$$R = 1$$

$$C = 1$$

Figure 6.6 shows the charging of the capacitor versus time and the current versus time in the circuit. By changing the R value from 1 to 0.1, the charging of the capacitor is re-plotted along with the earlier result for charging, and this is shown in Figure 6.7. The capacitor now charges faster.

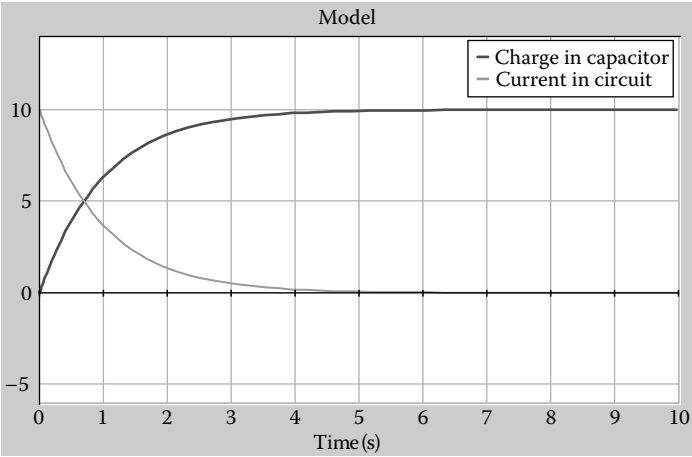


FIGURE 6.6
Response of the first order system.

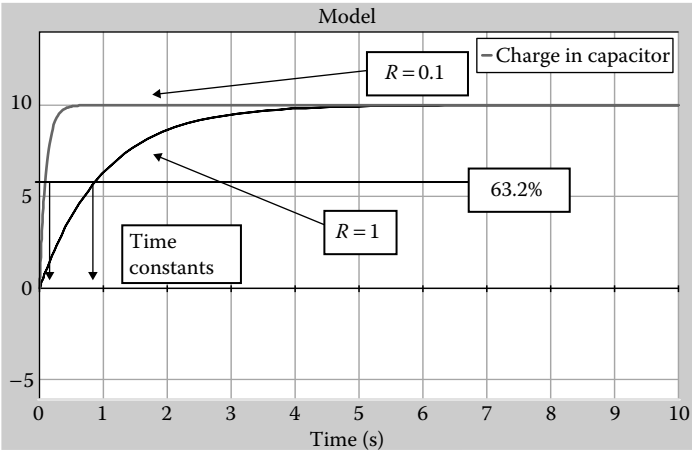


FIGURE 6.7
Response of first order system for two different values of R .

All first order system responses have a few common characteristics. The system response approaches the steady state value exponentially. The system does not overshoot the steady state value, but it approaches asymptotically from one side (either from below or from above). The speed at which the response approaches the steady state is controlled by the time constant of the system.

The concept of time constant is the most important one for the first order system response. Consider the solution in Equation 6.16 again. The time constant is the denominator of the fraction that appears as the power of the exponential function. In this case, the time constant is RC . Its unit is the same as time.

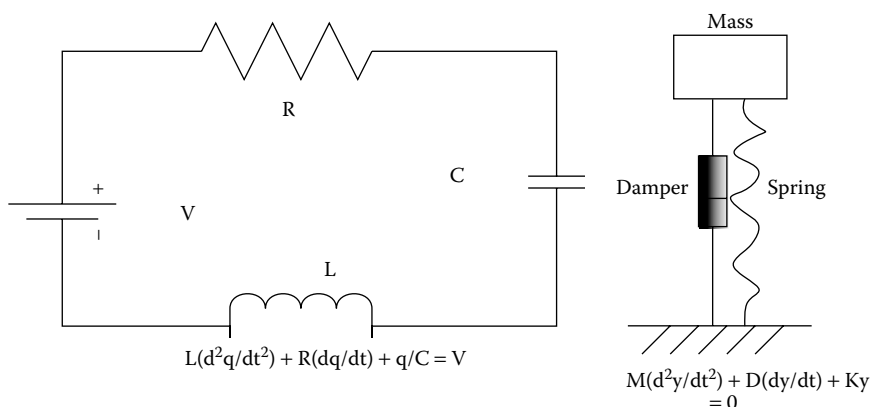
$$\frac{q_3}{RC} = \frac{V}{R} \left(1 - e^{\frac{-t}{RC}} \right) \quad (6.17)$$

The time constant can be calculated in two different ways. One is to find the magnitude of RC (or the inverse of the quantity that multiplies time in the power of the exponential function) in a given system. If the time constant is to be determined from graphical data, it is the time required to achieve 63.2% of the total rise/drop that the system will eventually achieve. Figure 6.7 shows the response at two different values of R and also shows a horizontal line for 63.2% of the total rise. It is quite clear from the figure that at $R = 1$ the time required to get to the 63.2% mark is much higher than that at the R value of 0.1. In other words, the time constant for the first case is higher than in the second case. Thus time constant is a measure of how quickly or slowly a system responds to external disturbance.

For first order systems, time constant is the primary indicator of system behavior.

6.3 Second Order System

Understanding the behavior of the second order system is critical in understanding the behavior of all systems. On one hand, the second order system behavior is significantly different from that of the first order system. On the other hand, all systems that are of orders higher than the second order behave in ways that are similar to the second order systems. Hence, understanding the second order system well will ensure a good understanding of higher order systems. Figure 6.8 shows several examples of second order systems. Second order systems have two energy storage devices, most commonly a C and an I element.

**FIGURE 6.8**

Examples of second order systems.

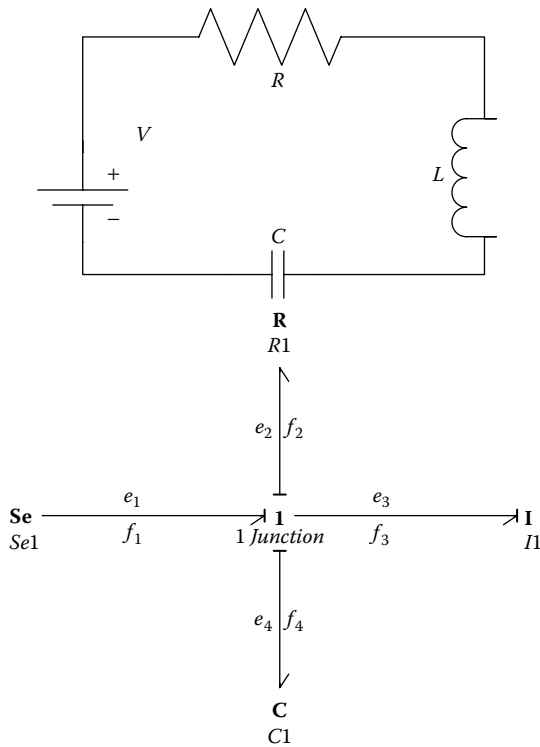
In order to study the behavior of second order systems, we will consider some of the equations derived in the previous chapter for an RLC circuit. As we saw then, the second order system may be described using two first order ordinary differential equations known as the state-space equations. The primary variables in these equations are the states in the energy storage devices, namely the displacement/charge in the capacitive element and the momentum/flux linkage in the Inductive element. The equations that we had derived for the RLC series circuit (circuit and bond graph model shown in Figure 6.9) are

$$\begin{aligned}\dot{p}_3 &= V(t) - R \frac{p_3}{L} - \frac{q_4}{C} \\ \dot{q}_4 &= \frac{p_3}{L}\end{aligned}\tag{6.18}$$

The other way of expressing these equations is to put them together and write as a single second order differential equation with the state of one of the storage devices as the primary variable (the other one can be computed when the solution of the second order equation is obtained). Two forms of this second order equation are given below for an electrical system and a mechanical system, respectively.

$$V(t) = L \cdot \ddot{q}_4 + R\dot{q}_4 + \frac{q_4}{C}\tag{6.19}$$

$$F(t) = m\ddot{x} + B\dot{x} + kx\tag{6.20}$$

**FIGURE 6.9**

Second order system and its bond graph model.

We will now discuss the response of second order systems using both the two state-space equations and the one second order equation.

Let's consider the second order equations shown in Equations 6.19 and 6.20 first. These are two forms of the equation (for the two domains). The left sides of these equations are known as forcing functions. The forcing functions may be 0 or non-0 (any arbitrary function). When the forcing function of the equation is 0, the equation is called homogenous.

$$L \cdot \ddot{q}_4 + R \dot{q}_4 + \frac{q_4}{C} = 0 \quad (6.21)$$

To solve this differential equation, the first step is to assume the solution to be a function of the following form:

$$q_4 = A e^{st} \quad (6.22)$$

where, A and s are unknown quantities.

Substituting this general form in Equation 6.22 gives:

$$\left(L \cdot s^2 + Rs + \frac{1}{C}\right) A e^{st} = 0 \quad (6.23)$$

For the product of the three functions in Equation 6.23 to be 0, either $A = 0$, or $e^{st} = 0$, or $\left(L \cdot s^2 + Rs + \frac{1}{C}\right) = 0$. The first two options result in a trivial solution. Hence, the third option $\left(L \cdot s^2 + Rs + \frac{1}{C}\right) = 0$, is the best acceptable choice. This quadratic equation is known as the characteristic equation, and the roots of this equation give us the insight into the behavior of second order systems.

The roots of this equation can be written as:

$$\begin{aligned} s_1 &= \frac{-R + \sqrt{R^2 - 4L \frac{1}{C}}}{2L} = -\frac{R}{2L} + \sqrt{\frac{R^2}{4L^2} - \frac{1}{LC}} = -\frac{R\sqrt{C}}{2\sqrt{L}} \frac{1}{\sqrt{LC}} + \sqrt{\frac{R^2 C}{4L} \frac{1}{LC} - \frac{1}{LC}} \\ s_2 &= \frac{-R - \sqrt{R^2 - 4L \frac{1}{C}}}{2L} = -\frac{R}{2L} - \sqrt{\frac{R^2}{4L^2} - \frac{1}{LC}} = -\frac{R\sqrt{C}}{2\sqrt{L}} \frac{1}{\sqrt{LC}} - \sqrt{\frac{R^2 C}{4L} \frac{1}{LC} - \frac{1}{LC}} \\ s_1 &= -\zeta \omega_n + \sqrt{\zeta^2 \omega_n^2 - \omega_n^2} = (-\zeta + \sqrt{\zeta^2 - 1}) \omega_n; \omega_n = \frac{1}{\sqrt{LC}}, \zeta = \frac{R}{2} \sqrt{\frac{C}{L}} \\ s_2 &= -\zeta \omega_n - \sqrt{\zeta^2 \omega_n^2 - \omega_n^2} = (-\zeta - \sqrt{\zeta^2 - 1}) \omega_n; \end{aligned} \quad (6.24)$$

Equation 6.24 shows the two roots s_1 and s_2 of the characteristic equation. They are written in terms of two system parameters: ω_n , the natural frequency, and ζ the damping coefficient. The final form of the two roots is written as:

$$\begin{aligned} s_1 &= (-\zeta + \sqrt{\zeta^2 - 1}) \omega_n \\ s_2 &= (-\zeta - \sqrt{\zeta^2 - 1}) \omega_n \end{aligned} \quad (6.25)$$

The behavior of the system is determined by specific values of s_1 and s_2 . There are four possibilities:

1. $R = 0, \zeta = 0$, the roots are imaginary and equal; the system has no damping (Case 6.1).
2. $\zeta < 1$, when the roots are unequal and imaginary; the system is underdamped (Case 6.2).

3. $\zeta = 1$, when the roots are real and equal; the system is critically damped (Case 6.3).
4. $\zeta > 1$, when the roots are real and unequal; the system is over-damped (Case 6.4).

CASE 6.1: $R = 0$

The system has no damping, and the roots are equal and imaginary. Hence, the solution for this system is $q_4 = A_1 e^{s_1 t} + A_2 e^{s_2 t}$. In this expression, s_1 and s_2 are equal and imaginary. So the final form of the total solution becomes a sinusoidal function,

$$q_4 = A_1 \sin \omega_n t + A_2 \cos \omega_n t \quad (6.26)$$

The behavior of this solution is pure sinusoidal with no reduction in amplitude. The constants A_1 and A_2 are determined from the initial conditions of the system. Figure 6.10 shows a graphical response of a system for this condition when damping is nonexistent. The system oscillation, once started, does not die out.

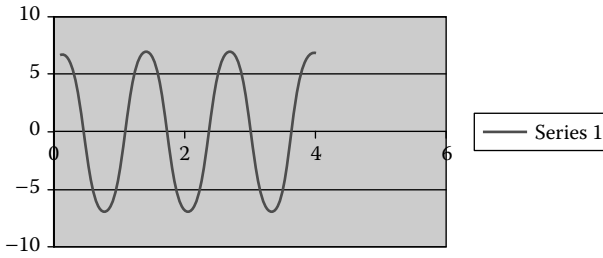


FIGURE 6.10

Response of a second order system with no damping.

CASE 6.2: $\zeta < 1$

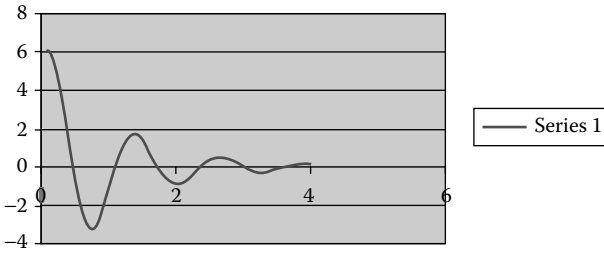
Since ζ is less than 1, the system is called an underdamped system. The roots s_1 and s_2 are unequal and imaginary. The final form of the solution eventually becomes:

$$q_4 = e^{-\zeta \omega_n t} (A_1 \sin \omega_d t + A_2 \cos \omega_d t) \quad (6.27)$$

where

$$\omega_d = (\sqrt{1 - \zeta^2}) \omega_n \quad (6.28)$$

ω_d is the damped natural frequency of this system. The solution is a product of two functions: a sinusoidal function and an exponentially decaying function. The behavior of this solution is thus an exponentially decaying sinusoidal with reduction in amplitude. Figure 6.11 shows this type of underdamped system response. The constants A_1 and A_2 are determined from the initial conditions of the system.

**FIGURE 6.11**

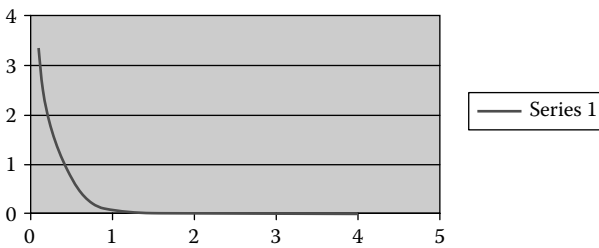
Response of an underdamped system.

CASE 6.3: $\zeta = 1$

When ζ is equal to 1, the system is called critically damped. The roots s_1 and s_2 are equal and real. The final form of the solution eventually becomes:

$$q_4 = (A_1 t + A_2) e^{-\omega_n t} \quad (6.29)$$

The solution is not sinusoidal anymore, but is an exponentially decaying function. The constants A_1 and A_2 are determined from the initial conditions of the system. The system behavior looks something like the one in Figure 6.12.

**FIGURE 6.12**

Response of a critically damped system.

CASE 6.4: $\zeta > 1$

When ζ is greater than 1, the system is called overdamped. The roots s_1 and s_2 are unequal and real. The final form of the solution eventually becomes:

$$q_4 = A_1 e^{-s_1 t} + A_2 e^{-s_2 t} \quad (6.30)$$

The solution is not sinusoidal anymore and is an exponentially decaying function. The constants A_1 and A_2 are determined from the initial conditions of the system. A graphical representation of system behavior is similar to that of a critically damped system (Figure 6.12).

To explore the natural response of a system, we consider the second order system shown in Figure 6.13. There is no forcing function, so the system has to be excited through the use of initial conditions. Figure 6.14 shows the different properties and initial conditions used. With a very low R value, the damping is nearly 0 and the system response is

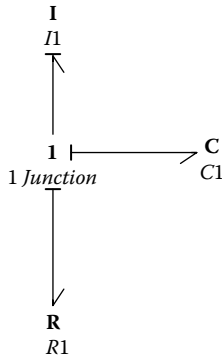


FIGURE 6.13

Generic homogenous second order system (with no forcing function).

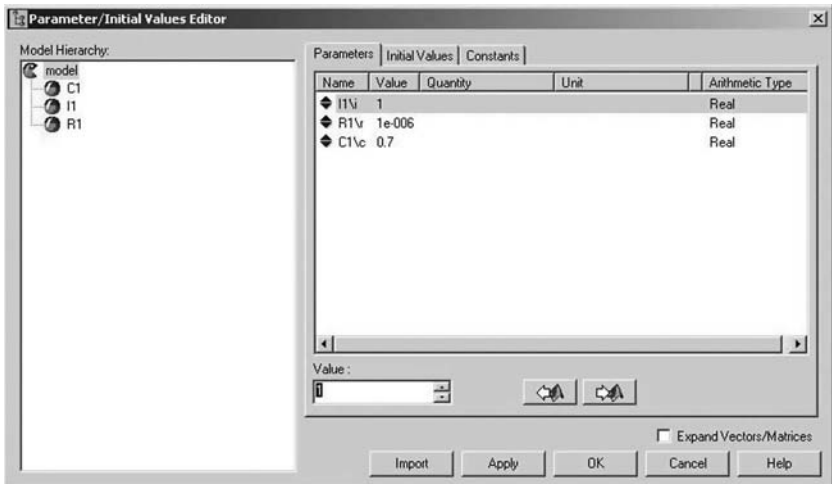


FIGURE 6.14

System parameters and initial conditions used (initial displacement and velocity are zero).

shown in Figure 6.15. The R value is increased to 1 and the system response changes to an underdamped system, as shown in Figure 6.16. When R is increased to 10, the system response changes to an overdamped condition;

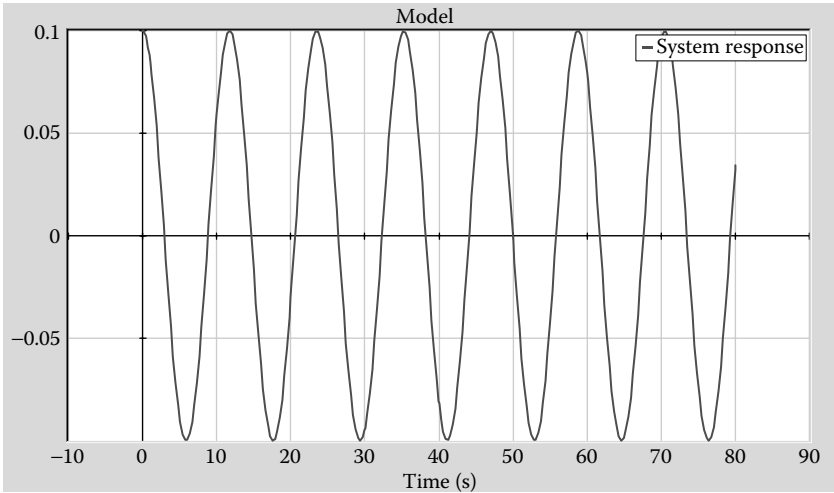


FIGURE 6.15
System response with very low (nearly 0) damping.

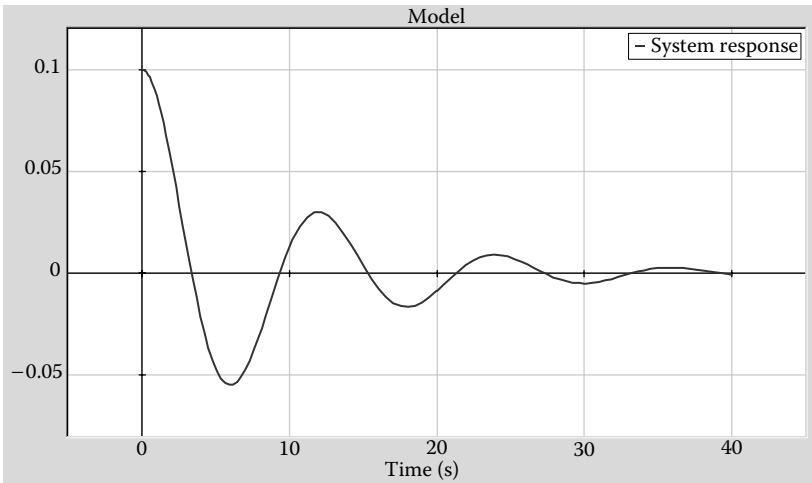


FIGURE 6.16
Underdamped system response.

the response is shown in Figure 6.17. When R is increased 10 times to 100, the overdamping in the system increases even more, and the response slows down significantly, as shown in Figure 6.18. The system response plots show a transition from an almost undamped oscillation, to underdamped, to overdamped, and finally to severely overdamped oscillation.

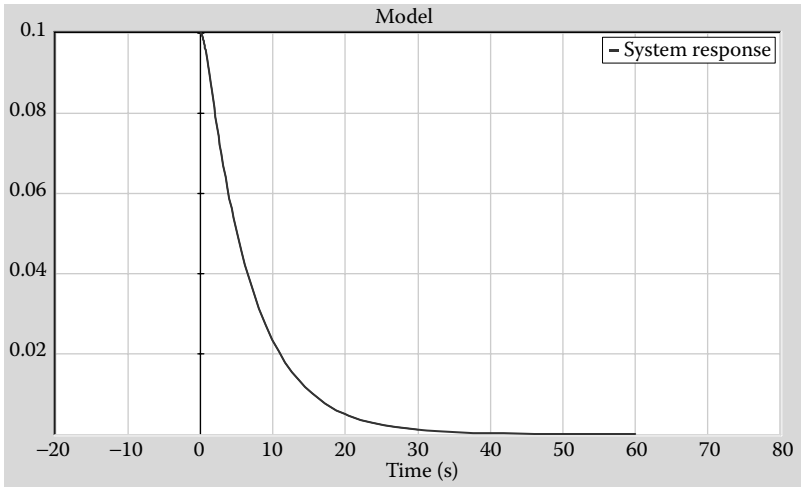


FIGURE 6.17
Overdamped system response.

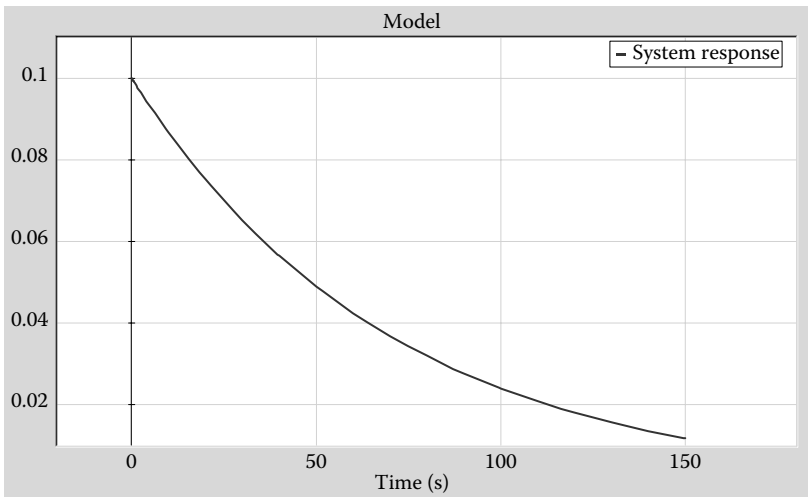


FIGURE 6.18
Severely overdamped system.

6.3.1 System Response for Step Input

The behavior of second order systems is often studied for a few standard forcing functions. The simplest one of these is the step input. Step input is a constant that is applied at a certain time and held steady for all future time. Thus, the complete equation is as shown in Equation 6.31 with F being a constant step function. The particular solution for this case will be the same form as the forcing function, and that would be a constant.

$$L \cdot \ddot{q}_4 + R \dot{q}_4 + \frac{q_4}{C} = F \quad (6.31)$$

So the particular solution for this equation that will satisfy the given forcing function will be a constant and in this particular case will be $q_4 = FC$. Substituting this in the equation satisfies differential equation, so the total solution for q_4 is

$$q_4 = \text{Homogenous_solution} + FC \quad (6.32)$$

The solution to the homogenous equation is called the complementary function, and the particular solution of FC is called the particular integral. We have already discussed the homogenous solution part that will be one of the four possible cases. Figure 6.19 shows a second order system with a step input. The initial parameters used in the simulation are shown in Figure 6.20. The system response for this condition is shown in Figure 6.21. The system shows oscillatory behavior because the transients don't go away with time. The R value is very low. When the R is increased to 1, the system response changes and the new response is shown in Figure 6.22.

Since the R value is significantly increased, the initial transients die down very quickly and the system response is constant (as expected) in

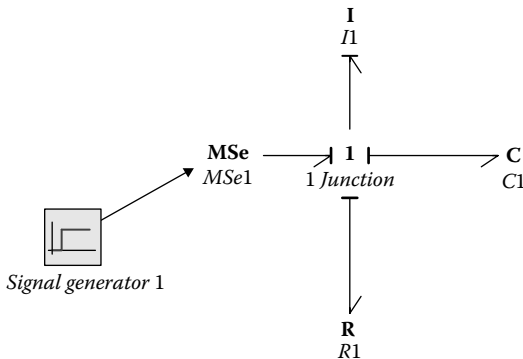


FIGURE 6.19

Bond graph of a second order system with step input.

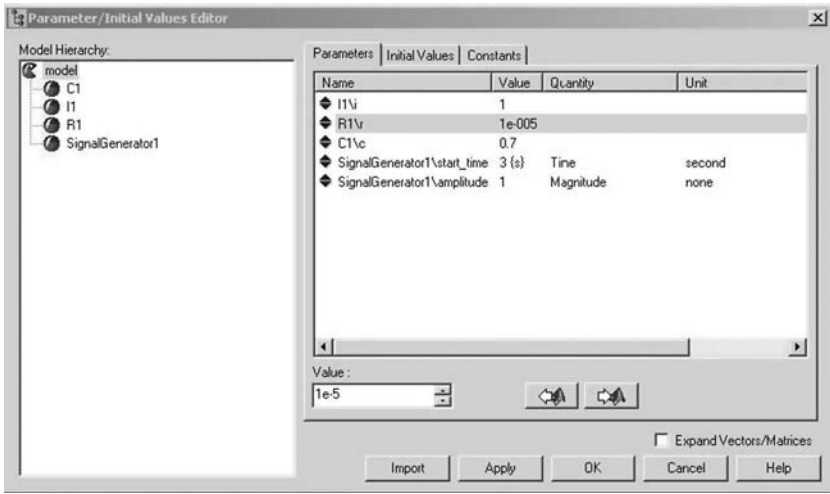


FIGURE 6.20
Initial parameters used for simulation.

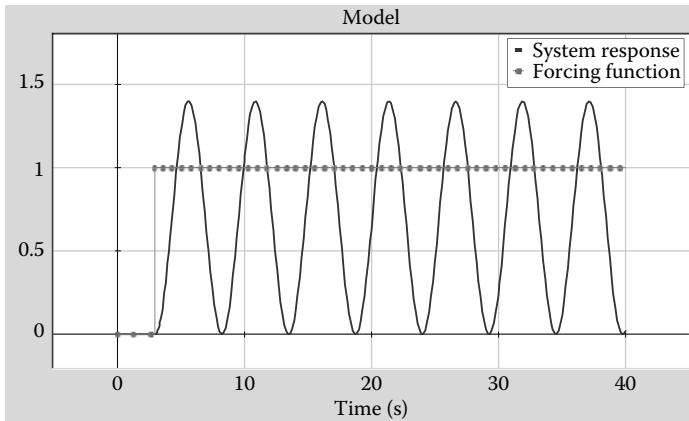


FIGURE 6.21
Response of the system and the step forcing function used.

the long run. If R is increased even more to 10, the response is shown in Figure 6.23. This value of R makes the system overdamped, and the response approaches exponentially the steady state value. When the R value is increased even more to 100, the system is severely overdamped and the response approaches very slowly to the final steady state value.

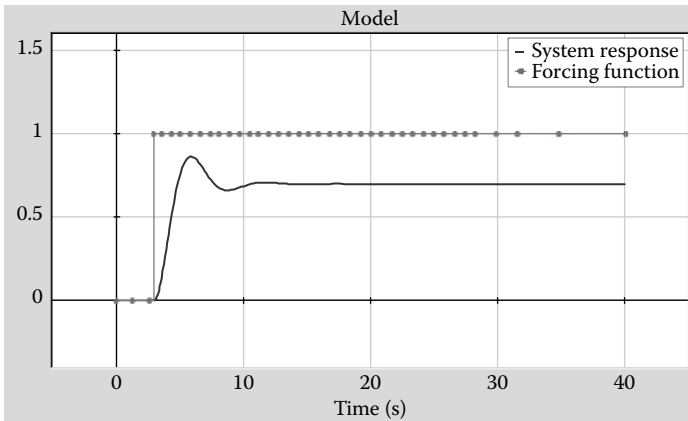


FIGURE 6.22

Response to step input with $R = 1$.

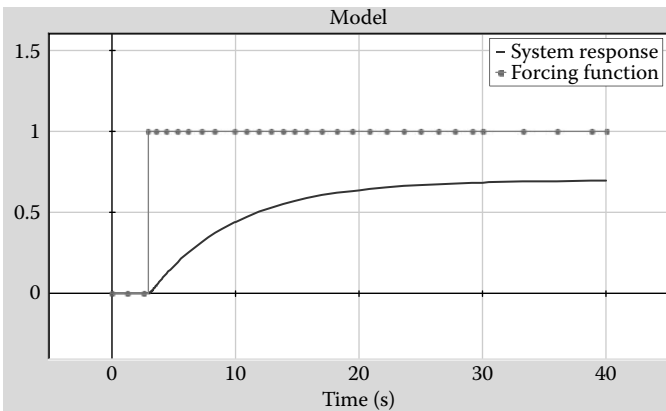


FIGURE 6.23

System response with even higher R .

6.3.2 System Response to Sinusoidal Inputs

This is the response of a system when the forcing function is varying sinusoidally with time. The governing equation is shown in Figure 6.33, with F being a sinusoidal function 9, as in Figure 6.34. These figures are in Example 6.2. The particular solution for this case will be the same form as the forcing function and that would be a sinusoidal function too.

$$L \cdot \ddot{q}_4 + R \dot{q}_4 + \frac{q_4}{C} = F \quad (6.33)$$

$$L \cdot \ddot{q}_4 + R\dot{q}_4 + \frac{q_4}{C} = F_0 \sin \omega t \quad (6.34)$$

So the solution for q_4 in this case will be $q_4 = X_0 \sin(\omega t + \phi)$. Substituting this in the equation satisfies differential equation. So the total solution for q_4 is

$$q_4 = \text{Homogenous_solution} + X_0 \sin(\omega t + \phi) \quad (6.35)$$

The solution to the homogenous equation is called the complementary function and the particular solution of $X_0 \sin(\omega t + \phi)$ is called the particular integral in this case. It can be shown that the amplitude of the response function and its phase will be

$$X_0 = \frac{F_0 C}{\left[\left(1 - \left(\frac{\omega}{\omega_n} \right)^2 \right)^2 + 4\zeta^2 \left(\frac{\omega}{\omega_n} \right)^2 \right]^{\frac{1}{2}}} \quad (6.36)$$

and

$$\phi = -\tan^{-1} \left[\frac{2\zeta \frac{\omega}{\omega_n}}{\left(1 - \left(\frac{\omega}{\omega_n} \right)^2 \right)} \right] \quad (6.37)$$

Consider the second order model shown in Figure 6.24. The magnitudes of different parameters used in the simulation are shown in Figure 6.25. The system response and the forcing function are shown in Figure 6.26.

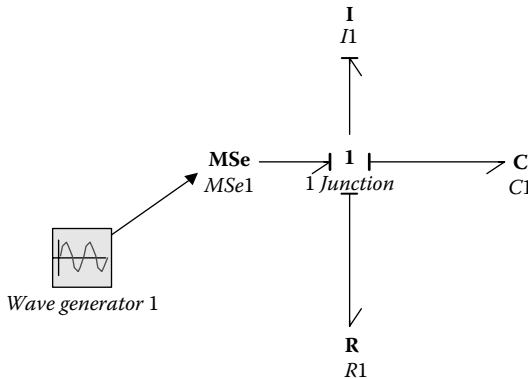


FIGURE 6.24

Second order system with sinusoidal forcing function.

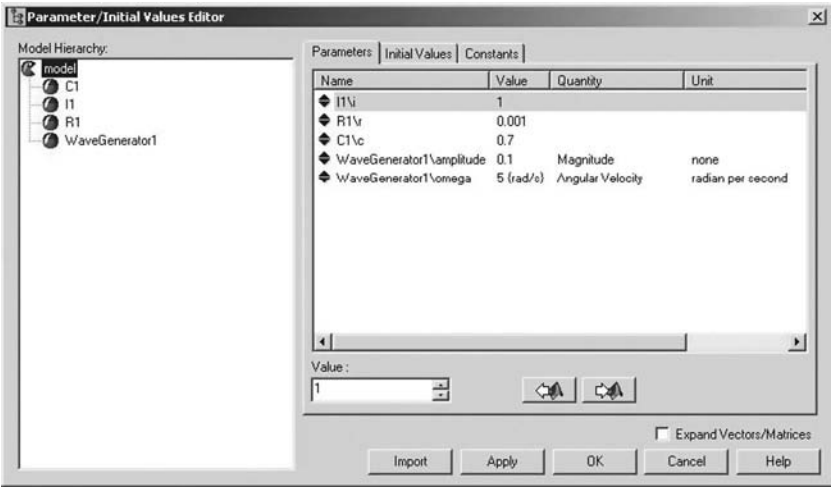


FIGURE 6.25
Parameters used in the simulation of the model from Figure 6.25.

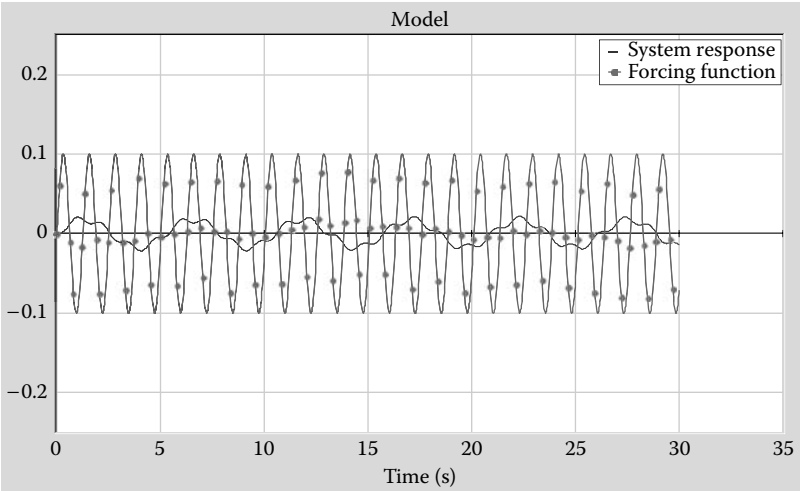
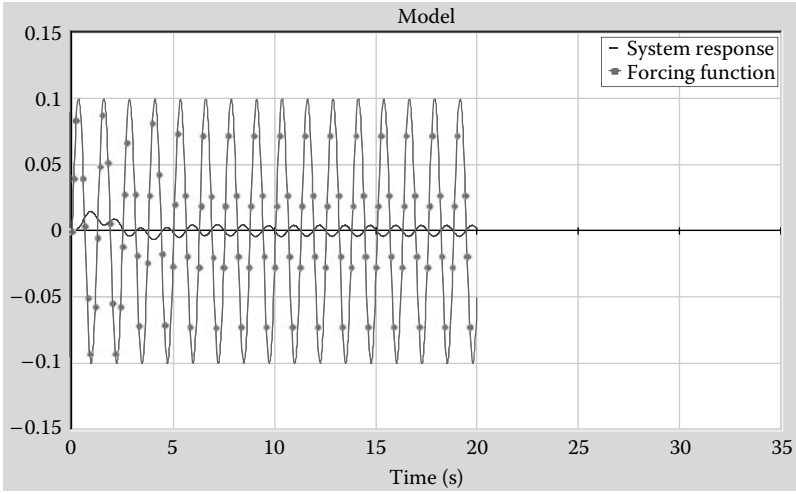


FIGURE 6.26
Sinusoidal forcing function and system response.

Although the forcing function is a sinusoidal with a single frequency, the output response has more than one frequency of oscillation. This is because the R value is very small and, as a result, this is an underdamped system and the response to the homogenous equation is not disappearing in the long run. If the R value is increased to 1, the response changes as is shown in Figure 6.27. Now that the R has increased, it is an overdamped

**FIGURE 6.27**

System response with higher R .

system. So, except for the very early stage, the system response has just one frequency of oscillation (the same one as the forcing function). The transients have died down very quickly.

6.3.3 System Response Study Using State–Space Representation

In the previous section, the system response was discussed using the second order ODE representing a typical second order system. Similar conclusions can be drawn by considering the system equations in the state–space form as a system of first order ODEs.

The system of first order ODEs representing a second order system would look like:

$$\begin{Bmatrix} \dot{p}_3 \\ \dot{q}_4 \end{Bmatrix} = \begin{bmatrix} \frac{-R}{L} & \frac{-1}{C} \\ \frac{1}{L} & 0 \end{bmatrix} \begin{Bmatrix} p_3 \\ q_4 \end{Bmatrix} + \begin{Bmatrix} V(t) \\ 0 \end{Bmatrix} \quad (6.38)$$

In order to find a solution for this system of equations, first we consider the homogenous form, that is, when $V(t)$ is 0. We can also assume that the general form of the solution for p_3 and q_4 should be $p_3 = Pe^{st}$ and $q_4 = Qe^{st}$ where s is a real or complex number and P and Q are the amplitudes

of the two variables p_3 and q_4 . If these are substituted in the state-space equation, the equation looks like:

$$\begin{Bmatrix} sP \\ sQ \end{Bmatrix} e^{st} = \begin{bmatrix} \frac{-R}{L} & \frac{-1}{C} \\ \frac{1}{L} & 0 \end{bmatrix} \begin{Bmatrix} P \\ Q \end{Bmatrix} \quad (6.39)$$

Combining both sides of the equation, we get:

$$\begin{bmatrix} s + \frac{R}{L} & \frac{1}{C} \\ -\frac{1}{L} & s \end{bmatrix} \begin{Bmatrix} P \\ Q \end{Bmatrix} e^{st} = 0 \quad (6.40)$$

In this set of equations (Equation 6.40), $P = Q = 0$ gives the trivial solution in which we are not interested. For the nontrivial solutions (i.e., the eigenvalues in this case), the determinant of the matrix has to be equal to 0. Therefore,

$$\begin{vmatrix} s + \frac{R}{L} & \frac{1}{C} \\ -\frac{1}{L} & s \end{vmatrix} = 0 \quad (6.41)$$

This results in:

$$\begin{aligned} s \left(s + \frac{R}{L} \right) + \frac{1}{LC} &= 0, \quad \text{or} \\ s^2 + \frac{R}{L}s + \frac{1}{LC} &= 0 \end{aligned} \quad (6.42)$$

This, of course, is the same characteristic equation as we saw before $\left(L \cdot s^2 + Rs + \frac{1}{C} = 0 \right)$ whose roots are s_1 and s_2 , as discussed before are

$$\begin{aligned}
s_1 &= \frac{-R + \sqrt{R^2 - 4L\frac{1}{C}}}{2L} = -\frac{R}{2L} + \sqrt{\frac{R^2}{4L^2} - \frac{1}{LC}} = -\frac{R\sqrt{C}}{2\sqrt{L}} \frac{1}{\sqrt{LC}} + \sqrt{\frac{R^2C}{4L} \frac{1}{LC} - \frac{1}{LC}} \\
s_2 &= \frac{-R - \sqrt{R^2 - 4L\frac{1}{C}}}{2L} = -\frac{R}{2L} - \sqrt{\frac{R^2}{4L^2} - \frac{1}{LC}} = -\frac{R\sqrt{C}}{2\sqrt{L}} \frac{1}{\sqrt{LC}} - \sqrt{\frac{R^2C}{4L} \frac{1}{LC} - \frac{1}{LC}} \\
s_1 &= -\zeta\omega_n + \sqrt{\zeta^2\omega_n^2 - \omega_n^2} = (-\zeta + \sqrt{\zeta^2 - 1})\omega_n; \omega_n = \frac{1}{\sqrt{LC}}, \zeta = \frac{R}{2}\sqrt{\frac{C}{L}} \\
s_2 &= -\zeta\omega_n - \sqrt{\zeta^2\omega_n^2 - \omega_n^2} = (-\zeta - \sqrt{\zeta^2 - 1})\omega_n;
\end{aligned} \tag{6.43}$$

For the two values of s_1 and s_2 , we have two sets of solutions for p_3 and q_4 , specifically:

$$p_{31} = Pe^{s_1t}, q_{41} = Qe^{s_1t} \tag{6.44}$$

and

$$p_{32} = Pe^{s_2t}, q_{42} = Qe^{s_2t} \tag{6.45}$$

Therefore, the total solution for p_3 and q_4 may be written as:

$$p_3 = P_1e^{s_1t} + P_2e^{s_2t} \tag{6.46}$$

and

$$q_4 = Q_1e^{s_1t} + Q_2e^{s_2t} \tag{6.47}$$

To obtain the values for P_1 , P_2 , Q_1 , and Q_2 , four equations are needed. Two of these equations are obtained from the initial conditions, and two more are obtained from the homogenous equations shown in Equation 6.40 by substituting P_1 and Q_1 , and P_2 and Q_2 for P and Q . The two equations obtained by substituting P_1 and Q_1 are equivalent, so only one is usable. Similarly, the two equations obtained by substituting P_2 and Q_2 are equivalent, so only one is usable. Therefore, the two usable equations are:

$$\begin{aligned}
\left(s_1 + \frac{R}{L}\right)P_1 + \frac{1}{C}Q_1 &= 0 \\
\left(s_2 + \frac{R}{L}\right)P_2 + \frac{1}{C}Q_2 &= 0
\end{aligned} \tag{6.48}$$

6.4 Transfer Functions and Frequency Responses

What we have discussed so far is the time domain response of systems. There is another way of exploring system behavior that is often more useful. This is known as the frequency response. In order to determine the response of the system in the frequency domain, usually the system equations are transformed from the time domain to the frequency domain. One such technique is called the transfer function. The transfer function is the ratio of output to the input.

To demonstrate the process let us consider a set of state–space equations:

$$\left\{ \frac{d\bar{x}}{dt} \right\} = [A]\{\bar{x}\} + [B]\{\bar{u}\} \quad (6.49)$$

where $[A]$ and $[B]$ are matrices/vectors that are made of system parameters such as R , C , and so forth.

\bar{u} is the input vector or the external input to the system. If we define s as the derivative operator, then s can be written as $s = \frac{d}{dt}$.

Therefore, the system equations may be re-written as:

$$\begin{aligned} s[I]\{\bar{x}\} &= [A]\{\bar{x}\} + [B]\{\bar{u}\} \\ \{\bar{x}\}\{s[I] - [A]\} &= [B]\{\bar{u}\} \\ \frac{\{\bar{x}\}}{\{\bar{u}\}} &= \{s[I] - [A]\}^{-1}[B] = G(s) \end{aligned} \quad (6.50)$$

where G is called the gain or transfer function. We will consider a typical example to make things clearer. Let the equations for an arbitrary system be

$$\begin{aligned} \frac{dp}{dt} &= -2p + 2q + 24u(t) \\ \frac{dq}{dt} &= 4p - 9q + 4\frac{du(t)}{dt} + 2u(t) \end{aligned} \quad (6.51)$$

Substituting the derivative operator, s :

$$sp = -2p + 2q + 24u(t) = (s + 2)p = 2q + 24u(t) \quad (6.52)$$

$$sp = 4p - 9q + 4\frac{du(t)}{dt} + 2u(t) = (s + 9)q = 4p + (4s + 2)u(t) \quad (6.53)$$

From Equation 6.52:

$$p = \frac{2q + 24u(t)}{(s + 2)} \quad (6.54)$$

Substituting Equation 6.54 in 6.53, we get:

$$\begin{aligned} (s + 9)q &= 4 \left(\frac{2q + 24u(t)}{(s + 2)} \right) + (4s + 2)u(t) \\ [(s + 9)(s + 2) - 8]q &= [96 + (4s + 2)(s + 2)]u \\ \frac{q}{u} &= \frac{4s^2 + 10s + 100}{s^2 + 11s + 10} = G(s) \end{aligned} \quad (6.55)$$

In Equation 6.55, $G(s)$ is called the transfer function for output q and input u . In a sense, it is a measure of how much and in what way the output q is influenced by the input u .

Going back to Equation 6.52 and substituting q :

$$\begin{aligned} p(s + 2) &= 2 \left[\left(\frac{4s^2 + 10s + 100}{s^2 + 11s + 10} \right) u \right] + 24u \\ \frac{p}{u} &= \frac{32s^2 + 284s + 440}{s^3 + 13s^2 + 32s + 20} = G^*(s) \end{aligned} \quad (6.56)$$

Equation 6.56 is for G^* the transfer function for output p with respect to input u .

This example shows how the transfer functions can be easily obtained from the state-space equations. Another way of obtaining these same transfer functions is by taking Laplace transform where s is the Laplace operator. We are not demonstrating it here, but one can find it in any standard book on control systems.

The transfer functions contain a lot of information about how the system will respond to different external inputs. The above discussion illustrates one of the many ways transfer functions can be developed. The process shown here is identical to assuming that the general forcing function is $u(t) = Ue^{st}$. The system response, as a result of this forcing function, would be $p(t) = Pe^{st}$ and $q(t) = Qe^{st}$. By substituting these in the above state-space equations, one can obtain the same expression as the one shown above for the transfer functions.

6.4.1 System Response in the Frequency Domain

From the transfer function, if we need to obtain the frequency response of the system, we can replace the s with $j\omega$ and write the transfer function as $G(j\omega)$. Then:

$$G(j\omega) = |G(j\omega)| e^{j\phi(\omega)} \quad (6.57)$$

where the function G is written as a product of its magnitude and phase. If the input to a stable system is a cosine function:

$$u(t) = U \cos(\omega t) = \operatorname{Re}(U e^{j\omega t}), \quad (6.58)$$

Then its steady state response is a sinusoidal function:

$$\begin{aligned} p(t) &= \operatorname{Re}(G * (j\omega) U e^{j\omega t}) \\ q(t) &= \operatorname{Re}(G(j\omega) U e^{j\omega t}) \end{aligned} \quad (6.59)$$

If we draw curves of $|G(j\omega)|$ and $\phi(\omega)$ versus ω we can see how the magnitude and phase angle of the steady-state response of the system changes with the frequency. This plot (or at least a version of it) is called the Bode plot, where a measure of the magnitude and phase of the system transfer function is plotted versus the input frequency. To be precise, the Bode plot actually plots $20\log G(s)$. By plotting it on the logarithmic scale, a vast range of frequency can be explored through this one plot. Also, as expressed above, the Bode plot unit is dB. If the forcing frequency is less than the natural frequency of the system, the phase angle is less than 90 degrees. At the natural frequency, the phase angle shifts to greater than 90 degrees. If the damping in the system is very low, this change over of the phase angle happens almost instantaneously. However, if the damping in the system is high, this changeover happens at a much slower rate.

The Bode plot provides a lot of information about the system response, as Example 6.1 will illustrate.

EXAMPLE 6.1

Consider a simple second order spring–mass–damper system (Figure 6.28). The parameters used in the analysis of the system are shown in Figure 6.29. In plotting the Bode Plot (Figure 6.30), the transfer function that is chosen is the ratio of the state of the C element and the effort from the source of effort, that is, the displacement of the spring divided by the forcing function is the transfer function that is plotted. The magnitude plot (by default) plots for a range of frequency from (nearly) 0 Hz close to 2 kHz. The magnitude plot is plotting $20\log(TF)$. There are three distinct regions in the magnitude plot. At low frequencies, the plot is essentially a straight line close to the 0 value. Then a sharp increase happens at around 0.085 Hz, and the magnitude reaches the value close to a positive 50. After that the magnitude steadily declines, and, at the 1 Hz mark, it is about -50 .

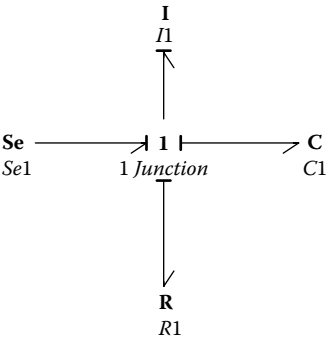


FIGURE 6.28
Bond graph for the Bode plot example.

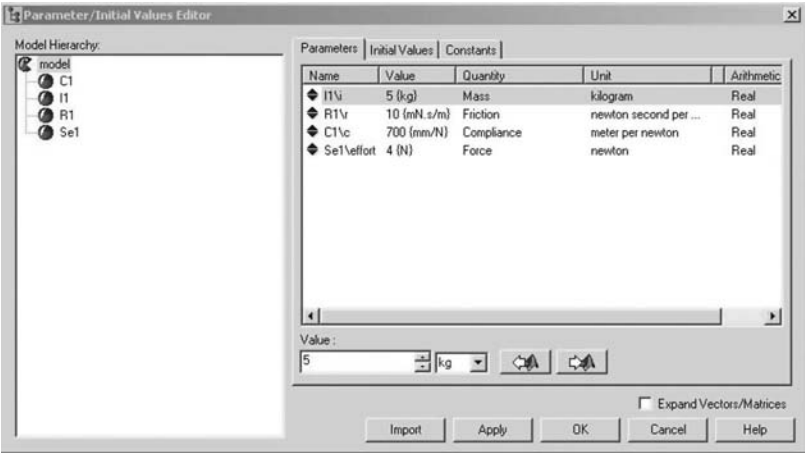
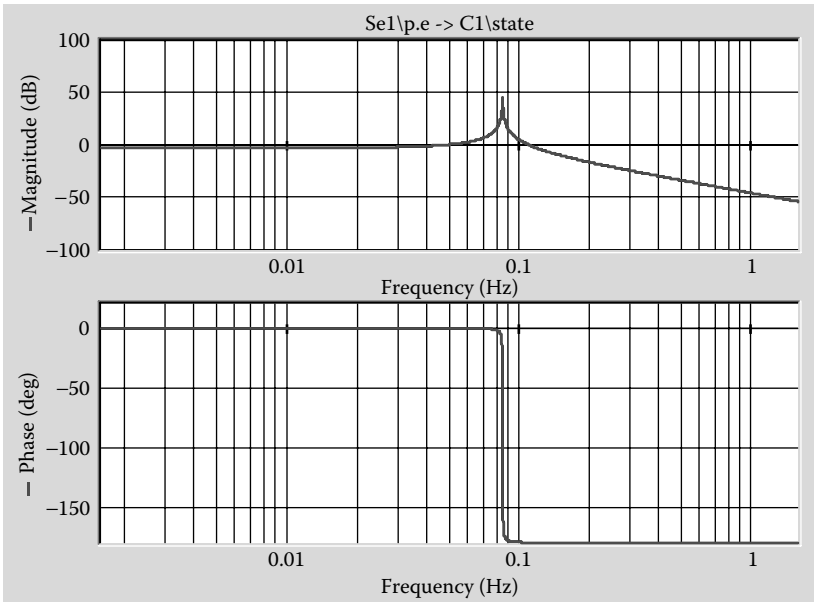


FIGURE 6.29
Parameters for the Bode plot.

To explain this behavior, let’s go back to the first region in the low frequency range. Since the logarithmic plot shows a value that is practically 0, it means that the TF is very close to 1. This means there is no magnification or attenuation in the system response as far as the spring displacement is concerned. The natural frequency of this system is

$$\sqrt{\frac{1}{5(0.7)}} = 0.5345 \text{ rad/s} = \frac{0.5345}{2\pi} = 0.085 \text{ Hz}$$

So at 0.085 Hz, the forcing frequency causes resonance in the system. As a result, the transfer function becomes very high. Working backwards from the dB value of about 50, we get $\frac{50}{20} = 2.5 \therefore TF = 10^{2.5} = 316.3$. This means that the system response is magnified by a huge number, and the displacement is

**FIGURE 6.30**

Bode plot with initial parameters.

very high at the resonance frequency. At higher frequencies, the magnitude goes down to -50 . The TF value at high frequencies is therefore

$$-\frac{50}{20} = -2.5 \therefore TF = 10^{-2.5} = 0.00316.$$

This indicates that the system gets severely attenuated at high frequencies and thus very little of the external disturbance gets transmitted to the system.

To see the effects of changes in the transfer function when some parameters are altered, we change I to 0.5 kg.

The simulation is re-done by changing the I value to 0.5 kg instead of 5 kg. The Bode plot (with the old plot superposed on the new one) is shown in Figure 6.31 indicates that the resonance frequency has changed from 0.85 Hz to approximately 0.275 Hz. Computation of the resonance frequency from the first principles give:

$$\sqrt{\frac{1}{0.5(0.7)}} = 1.69 \text{ rad/s} = \frac{1.69}{2\pi} \text{ Hz} = 0.269 \text{ Hz}$$

This matches very well with the results approximately determined from the plot.

Now, with the new value of I equal to 0.5 kg, the R value is increased first to 0.1 Ns/m and then to 1 Ns/m. The Bode plot is computed for both cases and is shown in Figure 6.32. This shows how the transfer function peak at the system natural frequency reduces as the R goes up, that is, as the damping increases.

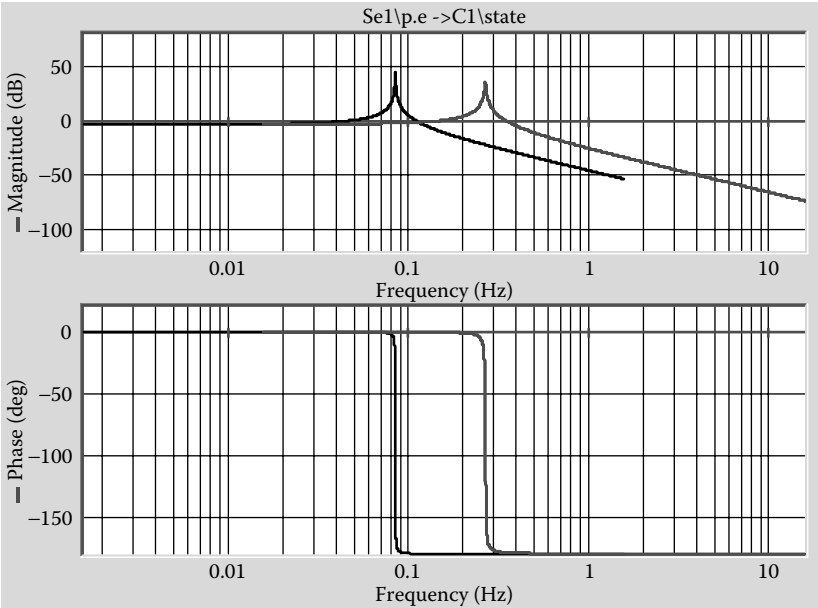


FIGURE 6.31
Bode plot with altered I .

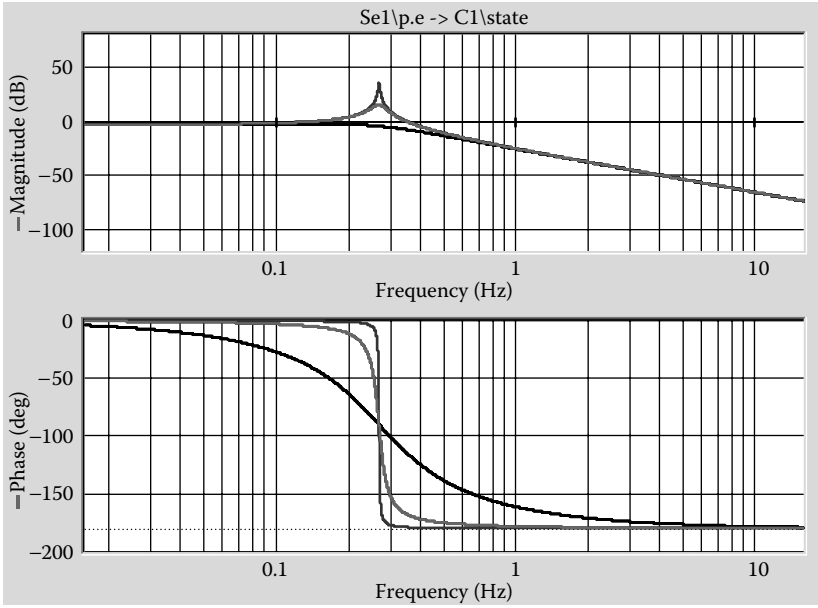


FIGURE 6.32
Bode plots obtained using different dampings.

With increased damping, thus, the amount of disturbance transferred to the system is drastically reduced.

EXAMPLE 6.2

Figure 6.33 shows a Bond graph representation of a permanent magnet DC motor that is rotating a drum that is raising a weight. The parameters used for the initial analysis are shown in Figure 6.34.

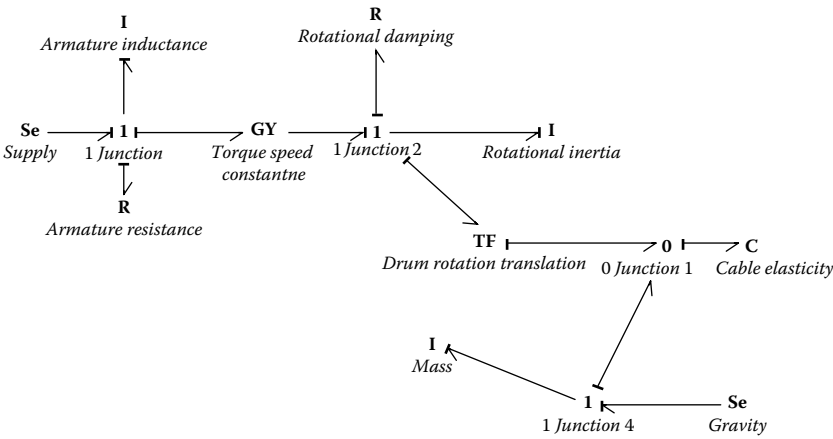


FIGURE 6.33
Bond graph model of a system.

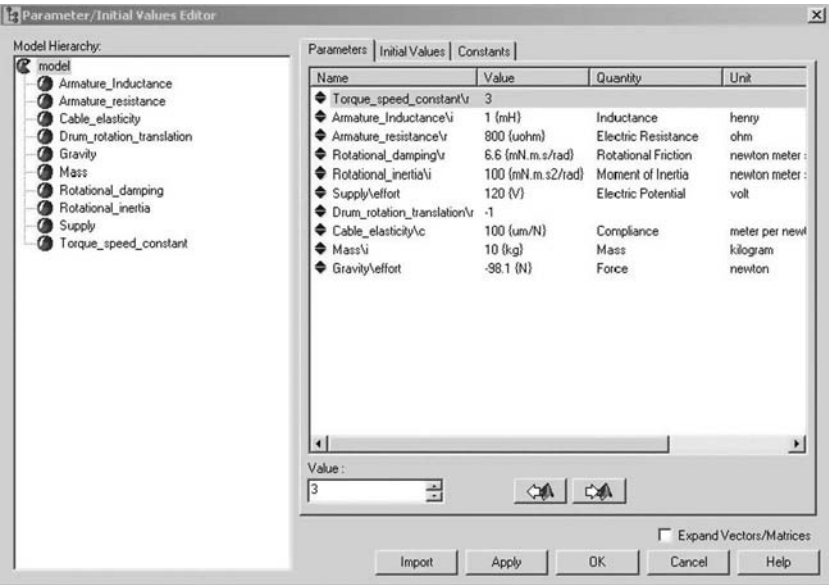


FIGURE 6.34
Parameters used in this model.

Take note that the two resistance values in the model (the electrical resistance as well as the rotational damping) are very low. So we can expect the transfer functions in the Bode plot to have sharp peaks. Figure 6.35 shows the Bode plot plotting the transfer function between the supply voltage and the force on the mass that is being lifted.

The two peaks occur at the two natural frequencies of the system, and at lower and higher frequencies the system attenuation is quite high. If the electrical resistance is increased by a factor of 1000 (i.e., if it changes from 800 micro ohms to 800 milli ohms), the Bode plot changes as shown in Figure 6.36. Notice that even though the peaks at the natural frequencies reduce quite a bit, the high and low frequency attenuations are no longer as good.

Now if the bearing resistance is altered to 66 Nms/rad and the Bode plot is recomputed, we observe in Figure 6.37 how both peaks are sufficiently removed.

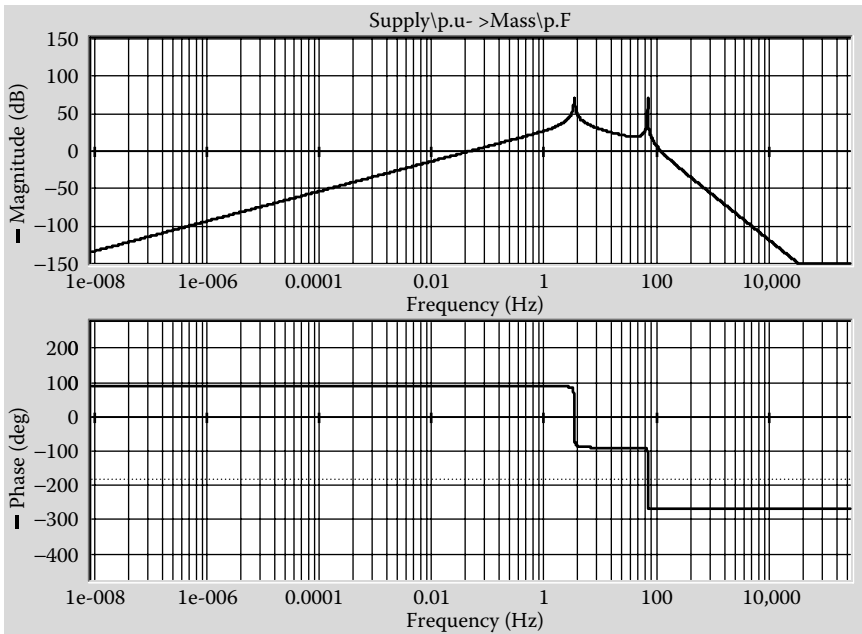


FIGURE 6.35
Bode plot of second example.

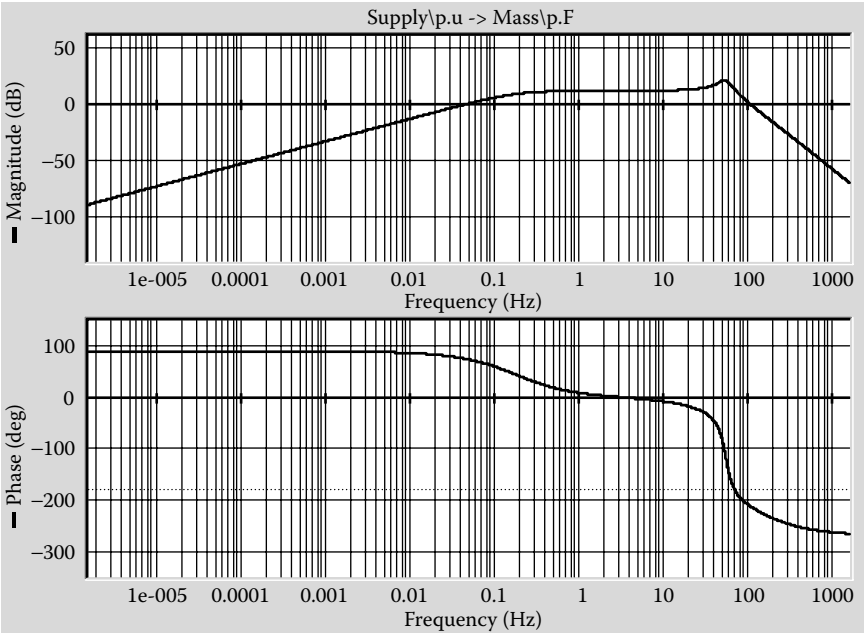


FIGURE 6.36
Altered Bode plot when electrical resistance is increased.

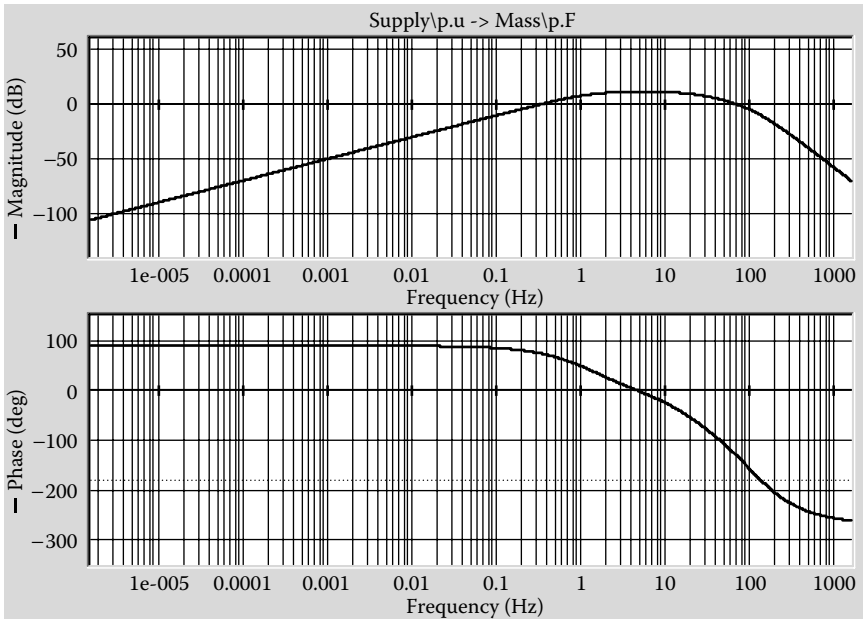


FIGURE 6.37
Bode plot with high electrical as well as mechanical resistances.

6.5 Summary

In this chapter we have tried to introduce the system solutions for zeroth, first, and second order systems. We have also discussed the interpretation of the solution of these systems both in the time as well as the frequency domains. System modelers need to understand both the time and frequency domain solutions because a lot of information about system behavior is conveyed through both these forms. We do not want to give the impression that our discussion on this topic is complete. Actually, we have just scratched the surface. If the focus of this book was more in the area of controlled systems, we would need to cover a lot of ground in the area of time and frequency domain analysis, such as Fourier and Laplace transfer, Nyquist plots, pole-0 analysis, and so forth. However, since our focus is on the modeling and simulation of mechatronics systems, we will not venture into a discussion of all these other important topics and instead focus on several other items that are more relevant to the focus of the book.

Problems

- 6.1. Consider a spring–mass–damper system with mass value of 6kg, spring constant of 50 N/m, and damping coefficient of 0.5 Ns/m. Is the system underdamped, overdamped, or critically damped? Simulate the system behavior and use a non-0 initial condition to simulate the system behavior. Does the observed behavior match with your prediction?
- 6.2. Consider the system shown Figure P6.1. What is the order of this system? From the bond graph model, derive the system equation. Find the solution of this differential equation, and write down the expression of the time constant. Simulate the system behavior using the following parameters: $L = 50$ mH, $R = 50$ Ohms. At zero

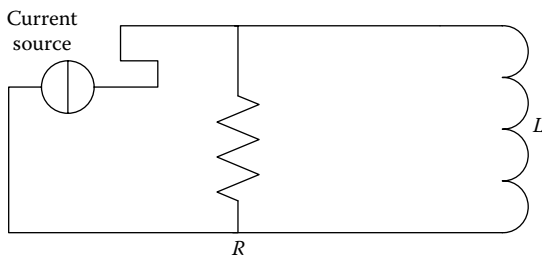


FIGURE P6.1

Figure for Problem 6.2, electrical system.

time, the current is 5A and is held constant. Determine the time constant from the plots as well as from the derived expression. How close are they? If the condition is somewhat different, that is, with a initial value of current 0 Amp and a ramp input of current, how does the system response change?

- 6.3. Consider the system shown in Figure P6.2. Assume the following values for the parameters: $M1 = 20$ kg, $M2 = 30$ kg, $M3 = 10$ kg, $K1 = 50$ N/m, $K2 = 35$ N/m, $K3 = 10$ N/m, $K4 = 5$ N/m, $B1 = 10$ Ns/m. The applied force is sinusoidal, and its value is $3\sin 15t$. What degree of freedom is this system? Simulate the behavior of this system, and plot the velocities of all the masses. Is this underdamped, overdamped, or critically damped? Plot the transfer functions of the effort on $M3$ with respect to force applied. What are the critical frequencies at which the gains are high? How do these match with the critical frequencies in the system?

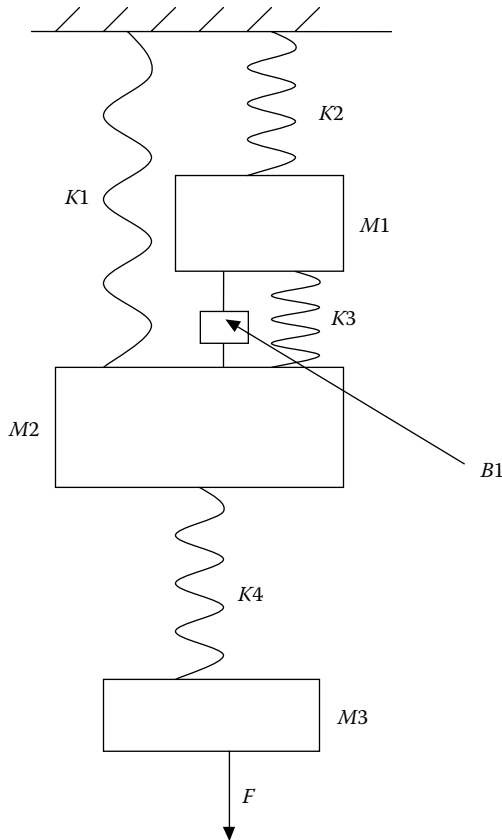


FIGURE P6.2

Figure for Problem 6.3, mechanical system.

- 6.4. Figure P6.3 shows the schematic for a vibration absorber. The mass $M1$ is a large mass and is excited at its own natural frequency due to some external disturbance from the floor. In order to reduce the vibration of the mass $M1$, a vibration absorber can be added to the mass (shown as spring $K2$ and small mass $M2$). These are designed in such a way that the natural frequencies of the whole system are moved away from the forcing frequency and the natural frequency of the main mass and spring system. Using the bond graph model of this system and the transfer function plots, develop the parameters for the vibration absorber. ($M1 = 50 \text{ kg}$, $K1 = 200 \text{ N/m}$, $B1 = 20 \text{ Ns/m}$, $V1 = 30 \sin 2t$).

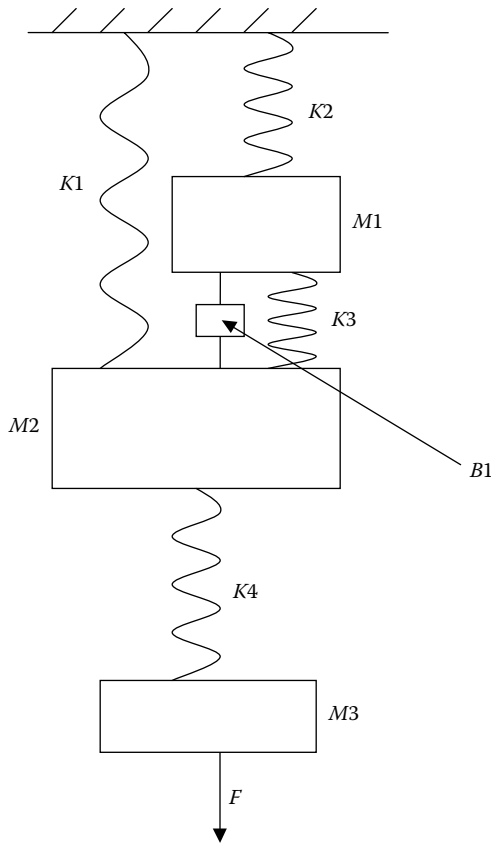


FIGURE P6.3

Figure for Problem 6.4, schematic for a vibration absorber.

- 6.5. Figure P6.4 shows an electrical circuit with several components. What is the order of this system? The system parameters are as follows: $R1 = 20 \text{ Ohm}$, $R2 = 100 \text{ Ohm}$, $C = 3 \text{ microF}$, and $L = 5 \text{ mH}$?

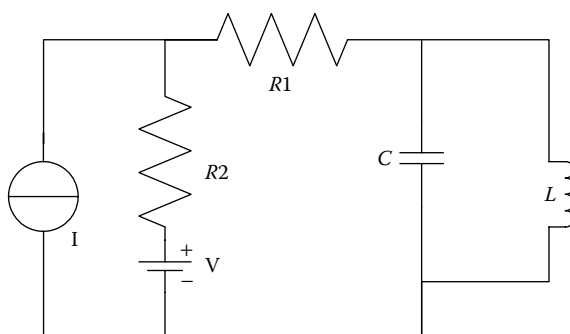
**FIGURE P6.4**

Figure for Problem 6.5, electrical circuit with several components.

Using the bond graph model of this system, derive its governing equations. Is this system underdamped, overdamped, or critically damped? Simulate the system for the following conditions, and confirm your predictions:

Current source, $I = 0$, Voltage = 12 V

Voltage $V = 0$, Current Source $I = 15$ A

Voltage $V = 0$, Current Source $I = 5 \sin 3t$

Voltage $V = 12$ V, Current Source $I = 5 \sin 3t$

- 6.6. Consider the spring-mass-damper system from Problem 6.1. This time, a forcing function of $20 \sin 3t$ is applied to this system. Simulate the behavior of this system. In the output, how many frequencies are involved. What are they? Explain what causes these frequencies. Can you suppress either of these frequencies? If so, which one and how?
- 6.7. For the following systems, derive the transfer functions of p and q with respect to the time dependent forcing functions in each case:

$$\dot{q} = 5q + 13p + Q(t)$$

$$\dot{p} = -3q + p$$

$$\dot{q} = Aq + Bp$$

$$\dot{p} = Cq + Dp + F(t)$$

$$\dot{q} = -13q + 2p$$

$$\dot{p} = -3q - 9p + V(t)$$

This page intentionally left blank

Numerical Solution Fundamentals

In Chapters 5 and 6 we discussed the derivation of equations and their solutions, respectively. During the discussion of solutions, we have used standard analytical solutions of generic first and second order systems and have talked about the interpretation of the solutions. We also talked about the conclusions one might draw about system behavior from the nature of the solution, both in the time domain and in the frequency domain. While that vital discussion provides us with a sound footing in interpreting the results, the actual simulation problem that we encounter every time will involve a new set of differential equations and, more often than not, a numerical technique will be necessary for its solution.

In this chapter we will discuss some of the well-known numerical techniques that are commonly used to solve these types of problems. The focus of this discussion is to introduce several well-known techniques and indicate their effectiveness with some examples. With the actual governing differential equations for the system, the techniques can be programmed using tools such as MATLAB® to generate solutions. Conversely, tools such as 20Sim generate the differential equations automatically in the background from user-defined bond graph models. 20Sim offers a choice for users as to which numerical technique is to be used. It will default to any one that is pre-set by the user. The user however, has to have some idea about the relative effectiveness of each of these techniques. In this chapter the focus is on the two aspects just described. It is expected that some readers will venture into developing one's own code, and many others will choose one of the existing solvers. In either case, the following discussion will be vital.

7.1 Techniques for Solving Ordinary Differential Equations

In this book we are dealing with system models where system parameters are assumed to be lumped. As a result, the mathematical representation of the model will always be a system of ordinary differential equations. Also, as was demonstrated in Chapter 6, each of the differential equations in the model will be of the first order. We will, therefore, confine our

discussion to the solution techniques that are used in solving a set of first order algebraic differential equations. If we consider a single equation, it may be written as:

$$\frac{dy}{dt} = f(y, t) \text{ with initial condition } y(t = 0) = y_0 \quad (7.1)$$

The general form of the solution for this equation may be written as:

$$y_{i+1} = y_i + (\text{slope})\Delta t \quad (7.2)$$

This means that the value of the function at a future time step is equal to the value at the current time step plus the slope of the function times an interval.

All the methods that have been developed use this general form of solution. The methods differ in how the quantity identified as “slope” in the equation is calculated.

7.2 Euler’s Method

Euler’s method is the simplest solution method for these types of equations. The slope is obtained by computing the derivative of y at the current time, such that:

$$(\text{slope}) = f(y_i, t_i) \quad (7.3)$$

and

$$y_{i+1} = y_i + f(y_i, t_i)\Delta t \quad (7.4)$$

where the slope necessary in the equation is computed at the current time and it is multiplied with the time step to obtain the y value at the new time. For any nonlinear problem, this method will clearly be problematic because the solution at a future time is extrapolated using the slope calculation at the current time. In order to demonstrate that, let us consider an example.

$$\frac{dy}{dt} = 6yt, \text{ and at } t = 0 \text{ } y = 3 \quad (7.5)$$

The analytical solution of this equation is

$$\ln y + C = 3t^2 \tag{7.6}$$

And after applying the boundary conditions, we obtain the complete solution as:

$$\begin{aligned} \ln y - \ln 3 &= 3t^2 \\ y &= 3e^{3t^2} \end{aligned} \tag{7.7}$$

Table 7.1 shows the comparison of the analytical results with Euler’s method results, along with the percentage error for a time step size of 0.1. It is clear from the results that the error increases quite significantly after a few time steps.

If the time step size is reduced to 0.01, the error is a lot less drastic. Table 7.2 shows a comparison of solutions for the same equation with a time step of 0.01. And Figure 7.1 shows a comparison of the results obtained for a time step size of 0.01 with analytical results.

An estimate of the error in the Euler’s method can be easily obtained by writing the Taylor’s series expansion of y about the starting point. This can be written as:

$$y_{i+1} = y_i + y_i' \Delta t + \frac{y_i''}{2!} (\Delta t)^2 + \frac{y_i'''}{3!} (\Delta t)^3 + \dots \tag{7.8}$$

In the Euler representation, the solution is approximated by choosing the first two terms on the right-hand side of the Taylor’s series expansion to represent the solution. Thus, the truncation error is equivalent to the

TABLE 7.1
Comparison of Analytical Results with Euler’s Method (Time Step, 0.1)

Time	Analytical Solution	Euler	Percent Error
0.0	3.0	3.0	0.0
0.1	3.091364	3.0	2.955447
0.2	3.382491	3.18	5.986434
0.3	3.929893	3.5616	9.371586
0.4	4.848223	4.202688	13.31488
0.5	6.351	5.211333	17.94468
0.6	8.834039	6.774733	23.31103
0.7	13.04771	9.213637	29.385
0.8	20.46288	13.08336	36.06292
0.9	34.07665	19.36338	43.17698
1.0	60.25661	29.8196	50.51231

TABLE 7.2
Comparison of Analytical Results with Euler’s Method (Time Step, 0.01)

Time	Analytical Solution	Euler	Percent Error
0.0	3.0	3.0	0.0
0.01	3.0009	3.0	0.029996
0.02	3.003602	3.0018	0.06
0.03	3.008111	3.005402	0.090049
0.04	3.014435	3.010812	0.120179
0.05	3.022585	3.018038	0.150426
0.06	3.032576	3.027092	0.180825
0.07	3.044426	3.037989	0.211411
0.08	3.058157	3.050749	0.242221
0.09	3.073793	3.065393	0.273289
0.10	3.091364	3.081946	0.30465
0.11	3.110901	3.100437	0.336341
0.12	3.13244	3.1209	0.368397
0.13	3.156022	3.143371	0.400851
0.14	3.181689	3.167889	0.433739
0.15	3.209491	3.194499	0.467097
0.16	3.239478	3.22325	0.500958
0.17	3.271708	3.254193	0.535357
0.18	3.306242	3.287386	0.57033
0.19	3.343146	3.32289	0.60591
0.20	3.382491	3.360771	0.642131

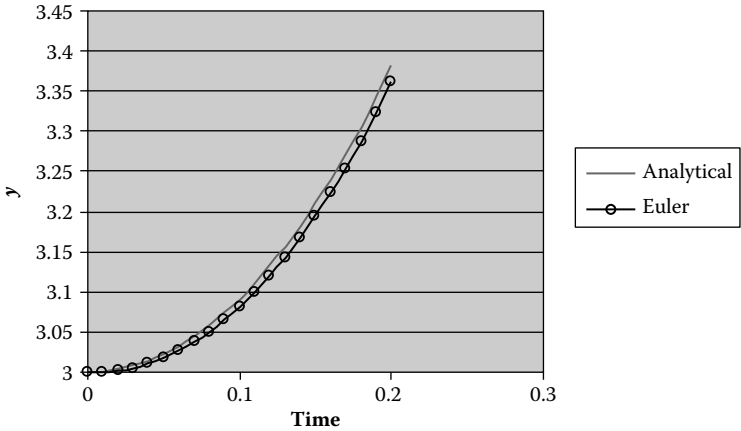


FIGURE 7.1
Comparison of analytical and Euler’s method (time step = 0.01).

terms that were not included. Neglecting the higher order terms, one can represent this as:

$$\text{Error} = \frac{y_i'''}{2!} (\Delta t)^2 \quad (7.9)$$

Or, the error may be represented as being of the order of the square of the time step. Hence, the smaller the time step is, the lesser is the error. This means that in order to use Euler's method, one has to keep the step size limited to small. There have been several methods developed to improve on this basic Euler's method. In the next few sections, we will talk about some of them.

7.3 Implicit Euler and Trapezoidal Method

Two methods that are improvements over the Euler's method are related to the basic Euler's method. They are similar and will be discussed together. The fundamental reason for the errors in the Euler's method is the fact that the slope is calculated at the current time to calculate the solution at a future time. The equation used in Euler's method is

$$y_{i+1} = y_i + f(y_i, t_i) \Delta t \quad (7.10)$$

The equation can be modified to replace the slope term $f(y_i, t_i)$ with a combination of terms where α is a factor such that $0 \leq \alpha \leq 1$.

$$y_{i+1} = y_i + [\alpha f(y_i, t_i) + (1 - \alpha) f(y_{i+1}, t_{i+1})] \Delta t \quad (7.11)$$

$\alpha = 1$ is the explicit Euler's method (discussed before)

$\alpha = 1/2$ is known as the trapezoidal method

$\alpha = 0$ is the backward or implicit Euler's method

An implementation of this general method can be demonstrated using the same example as the one we have used before.

$$\frac{dy}{dt} = f(y, t) = 6yt, \text{ and at } t = 0 \text{ } y = 3 \quad (7.12)$$

So the solution can be written as:

$$\begin{aligned} y_{i+1} &= y_i + [\alpha f(y_i, t_i) + (1 - \alpha) f(y_{i+1}, t_{i+1})] \Delta t \\ y_{i+1} &= y_i + [\alpha (6y_i t_i) + (1 - \alpha) (6y_{i+1} t_{i+1})] \Delta t \end{aligned} \quad (7.13)$$

Simplifying the terms, this can be written as:

$$\begin{aligned}
 y_{i+1} - (1 - \alpha)(6y_{i+1}t_{i+1})\Delta t &= y_i + \alpha(6y_it_i)\Delta t \\
 [1 - (1 - \alpha)6t_{i+1}\Delta t]y_{i+1} &= y_i + \alpha(6y_it_i)\Delta t \\
 y_{i+1} &= \frac{[y_i + \alpha(6y_it_i)\Delta t]}{[1 - (1 - \alpha)6t_{i+1}\Delta t]}
 \end{aligned}
 \tag{7.14}$$

If α is chosen to be $\frac{1}{2}$, the solution method is called trapezoidal. If α is chosen to be 0, then it is backward Euler. Table 7.3 provides the comparison of the solution obtained using all three methods, and Figure 7.2 shows a graphical comparison of the same results. It is clearly seen that the trapezoidal method matches the exact solution very well. In the other two methods, there are some errors.

TABLE 7.3
Comparison of Three Methods (Time Step = 0.01)

Time	Analytical Solution	Backward Euler	Trapezoidal	Euler
0.0	3.0	3.0	3.0	3.0
0.01	3.0009	3.001801	3.0009	3.0
0.02	3.003602	3.005408	3.003603	3.0018
0.03	3.008111	3.010827	3.008112	3.005402
0.04	3.014435	3.01807	3.014437	3.010812
0.05	3.022585	3.027152	3.022588	3.018038
0.06	3.032576	3.038089	3.032581	3.027092
0.07	3.044426	3.050903	3.044432	3.037989
0.08	3.058157	3.065618	3.058165	3.050749
0.09	3.073793	3.082262	3.073804	3.065393
0.10	3.091364	3.100867	3.091378	3.081946
0.11	3.110901	3.121469	3.110918	3.100437
0.12	3.13244	3.144106	3.132461	3.1209
0.13	3.156022	3.168823	3.156046	3.143371
0.14	3.181689	3.195667	3.181718	3.167889
0.15	3.209491	3.224689	3.209524	3.194499
0.16	3.239478	3.255946	3.239517	3.22325
0.17	3.271708	3.289499	3.271752	3.254193
0.18	3.306242	3.325414	3.306292	3.287386
0.19	3.343146	3.36376	3.343202	3.32289
0.20	3.382491	3.404616	3.382554	3.360771
0.21	3.424352	3.448061	3.424423	3.4011

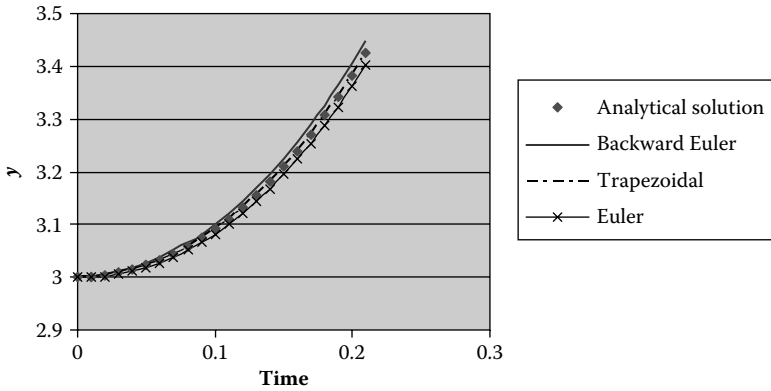


FIGURE 7.2
Comparison of Euler, backward Euler, trapezoidal, and analytical methods.

7.4 Runge–Kutta Method

There is a whole class of methods known as Runge–Kutta methods, which are very useful in the solution of ordinary differential equations. These R–K methods (for short) can achieve higher order accuracy (in the Taylor series sense discussed earlier) without having to compute higher order derivative terms. There are many variations that exist within the R–K method known as second order, third order, fourth order, eighth order, and so forth.

In the general sense, the solution for the R–K method is written as:

$$y_{i+1} = y_i + (\Phi)\Delta t \quad (7.15)$$

where the term Φ is called the increment function representing the slope of the variable over the interval that is being considered. In the most general form, Φ can be written as:

$$\Phi = a_1k_1 + a_2k_2 + a_3k_3 + \cdots + a_nk_n \quad (7.16)$$

where a s are constants and k s are written in the following way:

$$\begin{aligned} k_1 &= f(y_i, t_i) \\ k_2 &= f(y_i + q_{11}k_1\Delta t, t_i + p_1\Delta t) \\ k_2 &= f(y_i + q_{21}k_1\Delta t + q_{22}k_2\Delta t, t_i + p_2\Delta t) \\ &\vdots \\ &\vdots \end{aligned} \quad (7.17)$$

Thus, every k term is dependent on the previous k values. The p s and the q s are constants.

The second order R-K method:

$$y_{i+1} = y_i + (a_1 k_1 + a_2 k_2) \Delta t \quad (7.18)$$

where

$$\begin{aligned} k_1 &= f(y_i, t_i) \\ k_2 &= f(y_i + q_{11} k_1 \Delta t, t_i + p_1 \Delta t) \end{aligned} \quad (7.19)$$

The values of all the constants can be obtained by equating the expression to the Taylor's series expansion. If we do that, we would get:

$$\begin{aligned} a_1 &= 1 - a_2 \\ p_1 &= q_{11} = \frac{1}{2a_2} \end{aligned} \quad (7.20)$$

Since there are an infinite number of possibilities for choosing a_2 , there are an infinite number of second order R-K methods possible. They would all provide the same exact solution as long as the solution is of the quadratic order or less. For higher orders the errors may vary, and it is then perhaps better to choose a higher order R-K method for solution. For some of the more well-known second order R-K methods, $a_2 = 1/2$, 1, and $2/3$ have been used.

The best known R-K method is the fourth order R-K method, and the following representation is the most well-known used form:

$$y_{i+1} = y_i + \frac{1}{6} (k_1 + 2k_2 + 2k_3 + k_4) \Delta t \quad (7.21)$$

where

$$\begin{aligned} k_1 &= f(y_i, t_i) \\ k_2 &= f(y_i + \frac{1}{2} k_1 \Delta t, t_i + \frac{1}{2} \Delta t) \\ k_3 &= f(y_i + \frac{1}{2} k_2 \Delta t, t_i + \frac{1}{2} \Delta t) \\ k_4 &= f(y_i + k_3 \Delta t, t_i + \Delta t) \end{aligned} \quad (7.22)$$

Table 7.4 shows the calculation for the example discussed earlier using the fourth order R-K method. Comparison with analytical results show

TABLE 7.4
Comparison of 4th Order Runge–Kutta with Analytical Solution

Time	k1	k2	k3	k4	Fourth Order R–K	Analytical Solution
0.0	0.0	0.09	0.090014	0.180054	3.0	3.0
0.01	0.180054	0.270162	0.270203	0.360432	3.0009	3.0009
0.02	0.360432	0.450811	0.450878	0.54146	3.003602	3.003602
0.03	0.54146	0.632272	0.632367	0.723464	3.008111	3.008111
0.04	0.723464	0.814874	0.814997	0.906775	3.014435	3.014435
0.05	0.906775	0.998949	0.999101	1.091727	3.022585	3.022585
0.06	1.091727	1.184833	1.185015	1.278659	3.032576	3.032576
0.07	1.278659	1.372869	1.373081	1.467915	3.044426	3.044426
0.08	1.467915	1.563403	1.563647	1.659848	3.058157	3.058157
0.09	1.659848	1.756793	1.757069	1.854818	3.073793	3.073793
0.10	1.854818	1.953402	1.953712	2.053194	3.091364	3.091364
0.11	2.053194	2.153605	2.153951	2.255357	3.110901	3.110901
0.12	2.255357	2.357788	2.358172	2.461697	3.13244	3.13244
0.13	2.461697	2.566347	2.566771	2.672619	3.156022	3.156022
0.14	2.672619	2.779696	2.780161	2.888542	3.181689	3.181689
0.15	2.888542	2.998258	2.998768	3.109899	3.209491	3.209491
0.16	3.109899	3.222477	3.223035	3.337143	3.239478	3.239478
0.17	3.337143	3.452814	3.453421	3.570742	3.271708	3.271708
0.18	3.570742	3.689747	3.690407	3.811187	3.306242	3.306242
0.19	3.811186	3.933776	3.934493	4.058989	3.343146	3.343146
0.20	4.058989	4.185426	4.186204	4.314684	3.382491	3.382491
0.21	4.314684	4.445244	4.446086	4.578833	3.424352	3.424352

that there is absolute perfect match between the analytical solution and the solution obtained using the R–K method.

One can write the Taylor’s series expansion to demonstrate that the R–K methods of order n will have truncation error of the order of $O(\Delta t^{n+1})$. So a fourth order R–K method will have truncation error that is of the order of the fifth power of the step size.

7.5 Adaptive Methods

The techniques discussed so far all use constant time step sizes in the solution of differential equations. This works well when there is gradual or uniform variation of the solution over time. However, in many real

situations, sharp changes occur in system behavior as a result of impulse loading or sudden change in input variables and so forth. Figure 7.3 shows an example of such a behavior where, over a very short time period, the vehicle wheel velocity changes drastically due to braking. To capture the effect of these sudden changes, very small step sizes are necessary during the time when this change is happening. However, far away from this area of interest, the time step needs to be larger so that the simulation can be completed as quickly as possible. Any method that uses fixed step size will be problematic for this type of application. With a fixed step size method, the user will need to anticipate ahead of time the smallest time step that will work, and then keep the step size fixed at that same value for the whole time. This makes the solution process quite inefficient.

These inherent problems gave rise to a class of algorithms that are, together, known as adaptive methods. The word adaptive refers to the ability to change step sizes during the solution process based on some criteria. Many of the adaptive methods are R-K methods with variable step sizes and an algorithm to decide what step size to use.

The approaches used in these adaptive methods are broadly divided into two types. In the first type, the R-K method of the same order is used with two different step sizes to compute the new value of y . The error, which is the difference in these two calculated values, is used to decide whether the step size needs to change in some way or not. For example, in a well-known adaptive fourth order R-K method, each step is solved twice, once with the original step size and once with two steps each equivalent to half

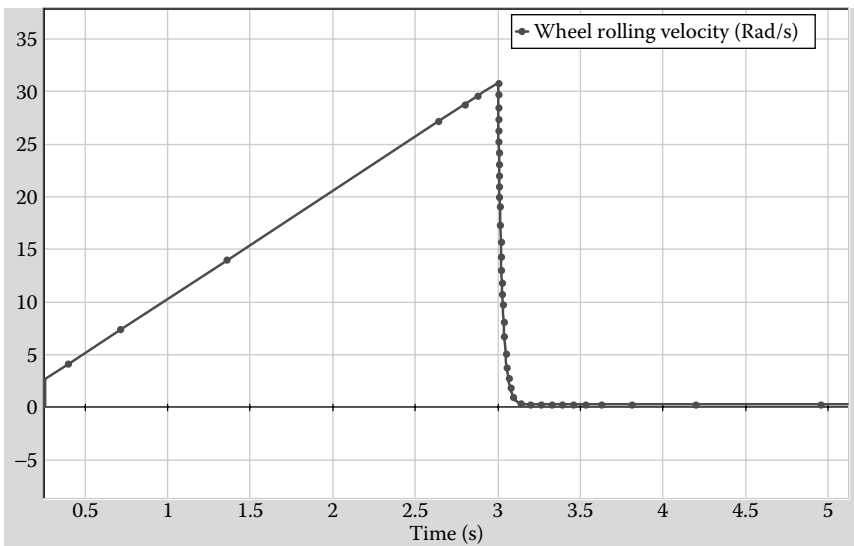


FIGURE 7.3

Example of a sharp change in system response.

the size of the original step. The difference between these two solutions provides a measure of the error. In the second approach, two different order R-K techniques are used with the same step size, and the error is estimated as the difference of these two values. In either case, the error is used to decide how to alter the step size.

There are several approaches in determining the step size adaptively. Press et al. have a discussion on this in the book *Numerical Recipes*. They have suggested that:

$$\Delta t_{\text{new}} = \Delta t_{\text{current}} \left| \frac{\Delta_{\text{new}}}{\Delta_{\text{present}}} \right|^{\alpha} \quad (7.23)$$

where Δt_{new} and $\Delta t_{\text{current}}$ are the new and current time steps. Δ_{present} is the computed error currently, and Δ_{new} is the new desired level of error. α is a constant power that is equal to 0.2 when the step size is increased and 0.25 when it is decreased. The most important parameter in this equation is Δ_{new} because it is to be used to specify the desired accuracy. This can be specified by the user as a relative error level. Δ_{new} may also be specified as:

$$\Delta_{\text{new}} = \epsilon y_{\text{scale}} \quad (7.24)$$

where ϵ is the overall tolerance level and y_{scale} determines how the error is scaled with respect to the range of solution values in a given problem. Some of the adaptive methods used in practice are Runge–Kutta–Fehlberg, Vode–Adams, and so forth. We are not going to discuss the details of these methods here, but will demonstrate the results from these methods and the impact of control parameters on the results.

Figure 7.3 shows the result from a simulation where the solution changes sharply over a very short time period. The results shown in that figure was obtained by fixing the relative error level to 1e-6. If that level is changed drastically to 1.0 and the simulation is repeated, we obtain the results shown in Figure 7.4.

Using a different adaptive method, Vode–Adams, and the relative error of 1.0, we obtain the results shown in Figure 7.5. Of course, by decreasing the relative error level to 1e-4 or 1e-6, we get the same solution as in Figure 7.3.

As a comparison, Figure 7.6 shows the results from a fixed step R-K fourth order method with a step size of 0.08. It is clear that this step size is giving a grossly inaccurate result, and the step size needs to be reduced. However, for someone who has never seen the actual solution before, it is rather hard to determine, looking at this result, that it is incorrect and the step size needs to be reduced. This is where the adaptive methods are so useful.

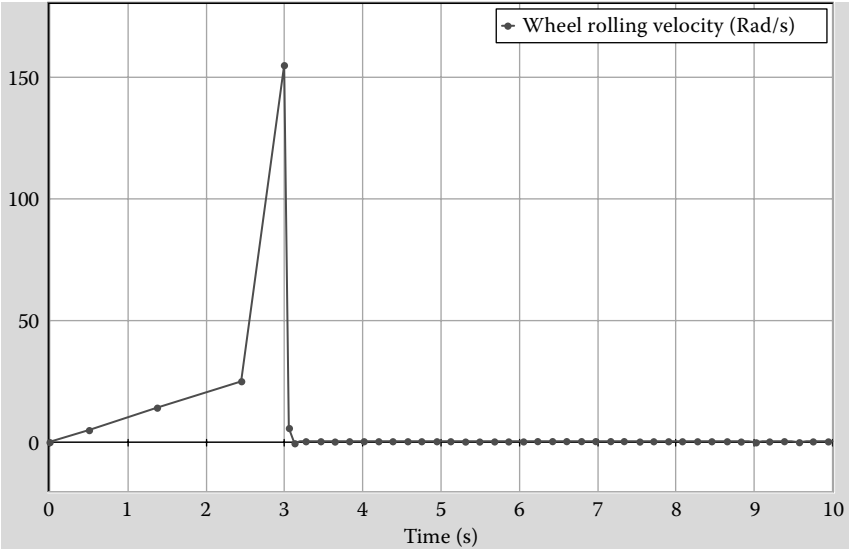


FIGURE 7.4
Runge-Kutta-Fehlberg results with relative error level fixed at 1.0.

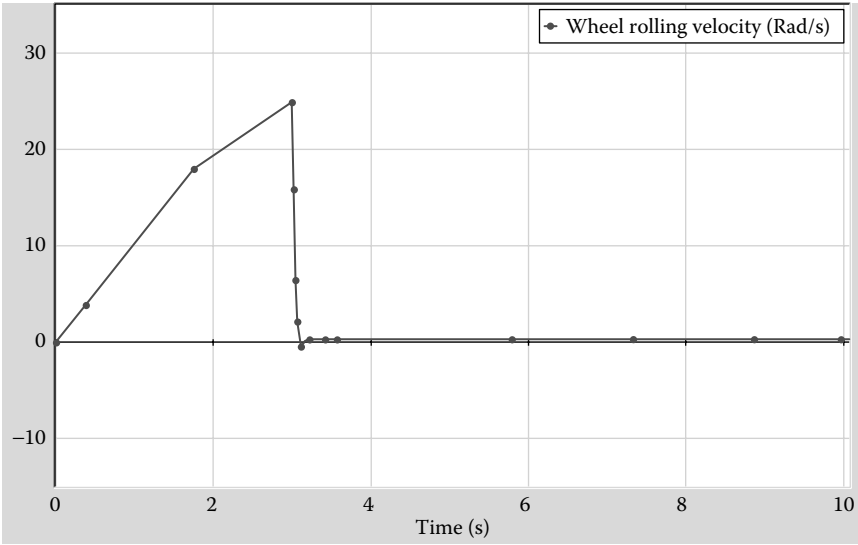


FIGURE 7.5
Vode-Adams result with relative error level fixed to 1.0.

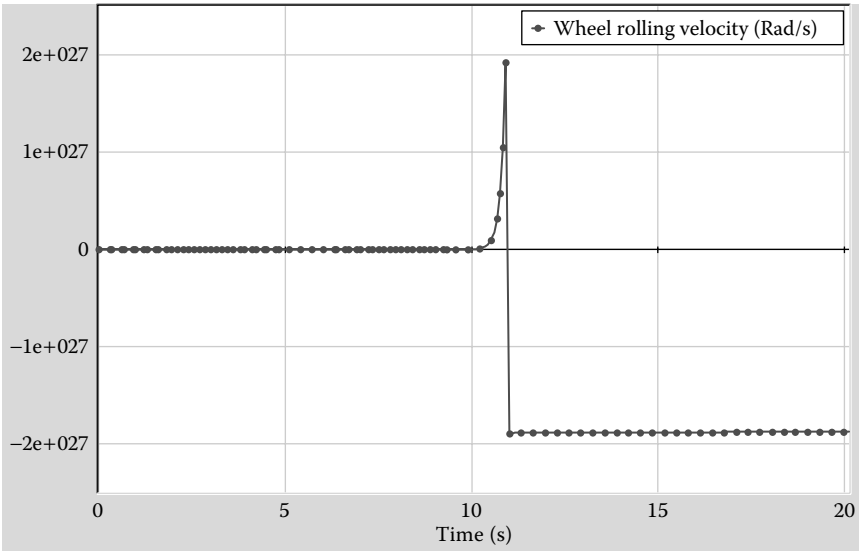


FIGURE 7.6
Runge–Kutta fourth order method with step size of 0.08.

7.6 Summary

To summarize the discussion of different solution methodologies, it should be said that in general it is best to choose adaptive methods where the step sizes are automatically adjusted as the simulation proceeds. Even while using a software tool such as 20Sim, the user will have some control over the level of accuracy one desires. In order to ensure that the accuracy is achieved and maintained, the user should be aware of how to adjust the control parameters. Simulation techniques have come a long way since the early days. Even as late as the early 1990s, simulation practitioners were writing their own codes and optimizing them and trying to use every known trick to get the maximum efficiency out of the computation tools. Most texts contain a lot of discussion on efficiency, error level, and accuracy. Things have changed quite drastically since those days. Today’s software tools are sleek, menu-driven, optimized, and modular. The computational speed and costs have changed so drastically that no one talks about small improvements in algorithms to increase speed or decrease memory use. All these positive developments, however, have a negative effect on the training of the people who use these tools. There is a tendency to use the software tools as “black boxes” without much effort to

understand why certain things are done in a certain way. This needs to be avoided by the user. Powerful tools are only as powerful as the expertise of the user. While the user may not need to understand simulation methods to write efficient codes anymore, she/he still needs to understand them to understand and use the power of the tool in their hand.

Problems

- 7.1. Consider the following equation, $\frac{dy}{dt} = 6yt^2 - 15y, y(0) = 2$. Solve this equation over the range of $t = 0.0$ to $t = 3.0$ using the following methods: analytical, Euler, backward Euler, and fourth order Runge–Kutta. Choose step sizes of 0.1 and 0.25, and compare your results for all the methods for the two different step sizes. Display your results graphically, and comment on the accuracy of each method.
- 7.2. Consider the following equation: $\frac{dy}{dt} = \text{Sint} + 2\text{Cos}t, y(0) = 1$. Solve this equation over the range of $t = 0.0$ to $t = 3.0$ using the following methods: analytical, Euler, backward Euler, fourth order Runge–Kutta. Choose step sizes of 0.025 and 0.1, and compare your results for all the methods for the two different step sizes. Display your results graphically, and comment on the accuracy of each method.
- 7.3. In Chapter 4 the model of a diode was discussed. The behavior of the diode involves sharp change in the output from 0 to a very high value over a short time period. Pick the example circuit of a diode given in Chapter 4, and simulate the bond graph model using the following methods: Euler, backward Euler, R–K 4, and one of the adaptive methods.
- 7.4. Figure P7.1 shows a bond graph. In this model replace the source of effort with a modulated source, and simulate the system behavior for an input of a sawtooth wave. Once again, use Euler, backward Euler, R–K 8, and one of the advanced adaptive methods to simulate the behavior of the system. Which method gives the best result?

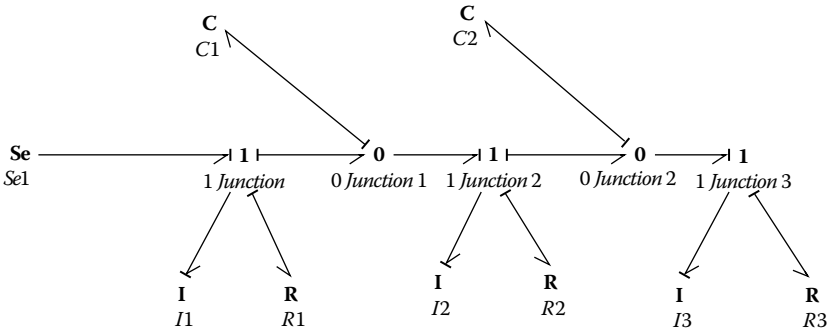


FIGURE P7.1
Figure for Problem 7.4, bond graph.

7.5. Figure P7.2 shows the model of an integrator. Develop the bond graph model of this circuit using the ideas discussed in Chapter 4, and simulate its behavior. Use a sawtooth wave input for the voltage. Use Euler, backward Euler, R-K 8, and one of the advanced adaptive methods to simulate the behavior. Adjust the time step of the Euler's method until the solution becomes unstable. Discuss the accuracy of each method.

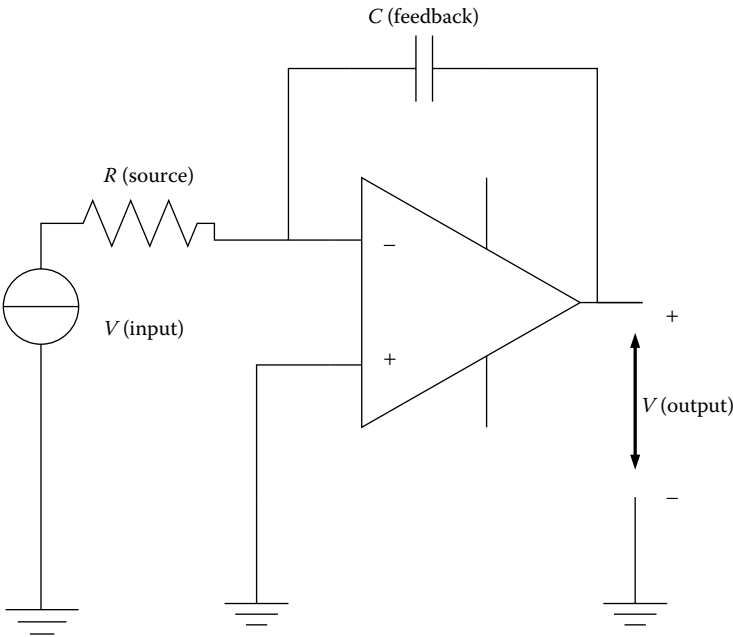


FIGURE P7.2
Figure for Problem 7.5, model of an integrator.

- 7.6. Consider the following equation: $\frac{dy}{dt} = y \cos 5t$, $y(0) = 1$. Solve this equation over the range of $t = 0.0$ to $t = 3.0$ using the following methods: analytical, Euler, backward Euler, fourth order Runge–Kutta. Choose step sizes of 0.025 and 0.1, and compare your results for all the methods for the two different step sizes. Display your results graphically, and comment on the accuracy of each method.

8

Transducers: Sensor Models

Transducers are key elements in any mechatronic system. They act as the eyes and ears of the system as well as the muscles. There are numerous transducers that are available on the market, and new ones are designed every day. To model and simulate the behavior of mechatronic systems, it is important to understand the behavior of transducers. Transducers have traditionally been divided into two broad categories: sensors and actuators. Sensors and actuators are similar in behavior because, in both cases, signals are converted from one physical form to another. Sensors are used to sense the status of the system, and sensor information is provided to the decision maker (usually an onboard computer). Computers use sensor data to take decisions as per the programmed logic. Computers then instruct the actuators to implement any action that needs to be taken within the system.

In this book, modeling of sensors and actuators has been divided into two chapters. This chapter deals primarily with sensors and the background necessary to model sensors; the next chapter deals with actuators. Sensors are typically designed such that they are minimally intrusive. This means that an ideal sensor will not affect system behavior in any way. In order to achieve this, sensors need to be physically small and draw a minimum amount of power. In real systems this cannot always be true. However small, a sensor that measures a system's response ends up affecting the system behavior as well. With a model of the sensor coupled with a system model, it is possible to quantify the level of this influence and account for it in the system behavior. Also, transducer designers designing macro as well as microelectromechanical (MEMS) devices find models to be powerful tools for design. Models are used to fine-tune MEMS designs so that the expected performance can be obtained. Finally, automatic control of mechatronic systems is an important aspect of any system design effort. Sensors and actuators are key components of this control loop. Hence, their models are very useful in developing control algorithms as well.

To study the behavior of sensors, they have been categorized in many different ways. For example, they can be categorized by application, that is, motion measurement, temperature measurement, humidity measurement, and so forth. This type of categorizing works well when one is looking for sensors for certain applications and has to choose the right one. A different way of categorizing them is by the physical phenomena that are used in the sensor design. For example, change in capacitance can be used to measure motion, forces, humidity, temperature, and so forth. While the

specific phenomenon used may be the same (i.e., change in capacitance), the application could be vastly different. This type of categorization helps with fundamental understanding of sensor workings. For our discussion here, we will separate sensors by the physical phenomena and not by application. This means that we will deal with the means of measurement, such as resistive, capacitive, magnetic, and so forth, rather than what we are measuring (such as acceleration, humidity, etc.). This helps to keep the discussion general and focused on the phenomenon being used in sensing, rather than going into the details of individual sensors. This approach also implies that once we have understood the modeling method of a capacitive sensor, we can model any capacitive sensor irrespective of its application. Using the above rationale, we will discuss different types of sensors in the next few sections of this chapter. Apart from the more traditional sensors, such as resistive, capacitive, and magnetic, we have devoted a small discussion on MEMS devices and another section on the use of the concepts of “activity” to design sensing devices in an optimal manner. In almost all texts on mechatronics, such as the ones by Cetinkunt (2007), Alciatore (2005), De Silva (2005), Bolton (2004), Shetty and Kolk (1997), Karnopp, Margolis, and Rosenberg (2006), and Brown (2001), there is some discussion on sensors and actuators. In many of these cases, the authors have tried to discuss sensors categorized by phenomena rather than by application. But Busch Vishniac (1999), in her book on sensors and actuators, has most consciously attempted this approach of categorization and the current author was most inspired by her.

To summarize, the overall objectives of this chapter are to

- Understand how different phenomena can be used to sense changes in a system.
- Learn how sensor models can be developed using generalized field elements.
- Model sensors such that causes and effects can be related to each other accurately through the model.
- Understand how transducers can be designed using system models.

8.1 Resistive Sensors

Resistive sensors constitute some of the oldest sensor types. These sensors depend on the variation of a resistance caused by some external disturbance, such as force, temperature, humidity, and so forth. This change is measured using some type of a measurement circuit, and the measurement is related

back to the phenomenon causing the change. The most well-known type of a resistive sensor is of the potentiometric type where there is a direct correlation between the electrical domain and the mechanical domain. A simple potentiometric sensor that consists of a voltage source applied across a constant total resistance circuit is shown in Figure 8.1. A measurement resistor is attached with a movable contact to the fixed total resistance. The slider is attached to the external disturbance source. As a result of this type of connection, the potential drop across the measurement resistor is directly proportional to the distance moved. The measured voltage can be shown to be equal to the ratio $\frac{R_2}{R_1 + R_2}$. If the resistance is uniformly varying across the length of the resistor, the ratio can be shown to be the same as the ratio $\frac{L}{L_0}$. By proper calibration of the circuit, the external source can be quite accurately sensed. The bond graph model of this simple device is shown in Figure 8.2. The two MRs are the modulated resistors. They are varied in a way such that the sum of their resistances is always a constant shown in the model by the $(R_1 + R_2)$, the potentiometer total

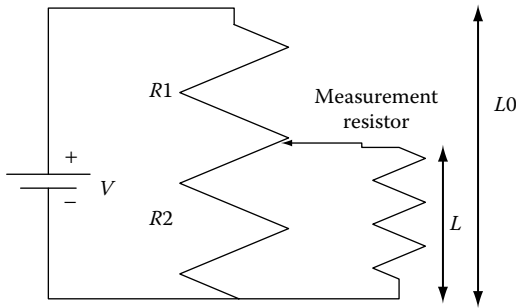


FIGURE 8.1
Schematic for a potentiometer.

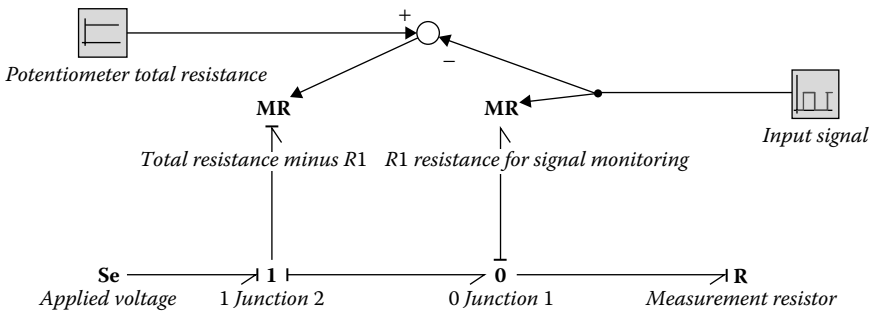
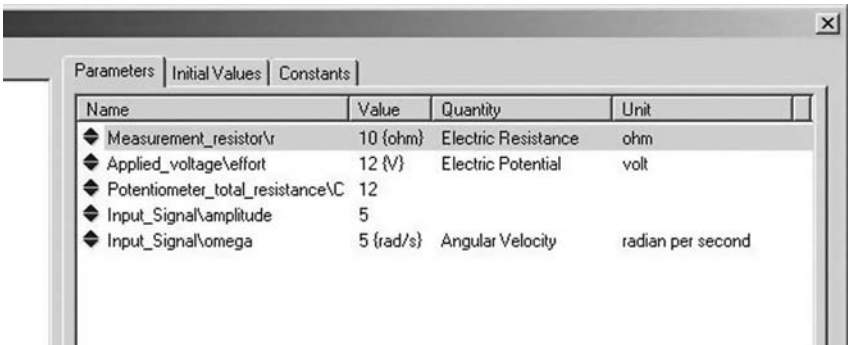


FIGURE 8.2
Bond graph representation of the potentiometer circuit.

resistance. The input signal moves the slider and hence controls the value of a portion of the total potentiometer resistance (shown in the model as R_2 , the resistance for signal monitoring). The voltage across the “measurement_resistor” is tracked as the sensor signal. Parameters used in the simulation are shown in Figure 8.3. Figure 8.4 shows a comparison of the input signal and the sensed signal on the same graph. Since the device does not contain any energy storage element (and only energy dissipative elements) the response pattern does not have any time lag. The one-to-one



Name	Value	Quantity	Unit
Measurement_resistor\i	10 {ohm}	Electric Resistance	ohm
Applied_voltage\effort	12 {V}	Electric Potential	volt
Potentiometer_total_resistance\C	12		
Input_Signal\amplitude	5		
Input_Signal\omega	5 {rad/s}	Angular Velocity	radian per second

FIGURE 8.3
Parameter values used to model the potentiometer circuit.

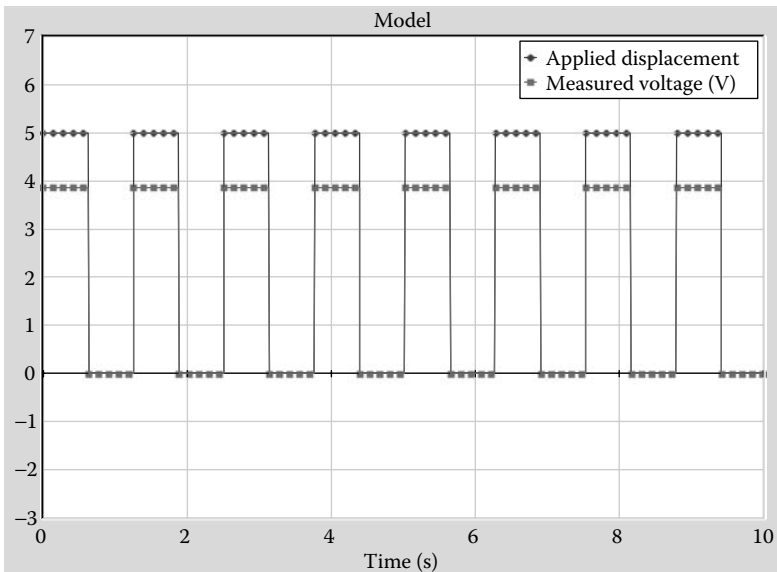


FIGURE 8.4
Comparison of the applied displacement and the sensed voltage to show one-to-one correspondence.

correspondence between the input signal and the measured output is a very useful feature for the sensor device.

The other type of well-known resistive sensor is a strain gauge. A strain gauge uses changes in electrical resistances to measure strains. These can be used to build load cells, torque sensors, pressure sensors, and so forth. The basic operation of a strain gauge sensor consists of a wheatstone bridge circuit (Figure 8.5), which is particularly useful in measuring small changes in resistance. The strain gauge (variable resistance) occupies one of the arms of a wheatstone bridge. Known constant resistances are used on the other arms. The system is balanced initially at its null position such that the voltage difference between points B and D is 0. Subsequent to this, when the strain gauge is strained and its resistance is changed, the potential difference between B and D is non-0, and its magnitude is directly proportional to the change in resistance of the strain gauge and hence to the strain itself. The bond graph model of the wheatstone bridge was developed earlier in Chapter 3. Here is a slightly modified version of the same model in Figure 8.6.

The variable resistance MR receives the external disturbance signal. The magnitudes of R_2 , R_3 , and R_4 are known constants. The source of effort is the voltage applied to the wheatstone bridge circuit. The source of flow added between the two 0 junctions representing points B and D is a 0 current source. This is added to the model for the purpose of simulation since the effort in the bond connected to the flow source is now automatically

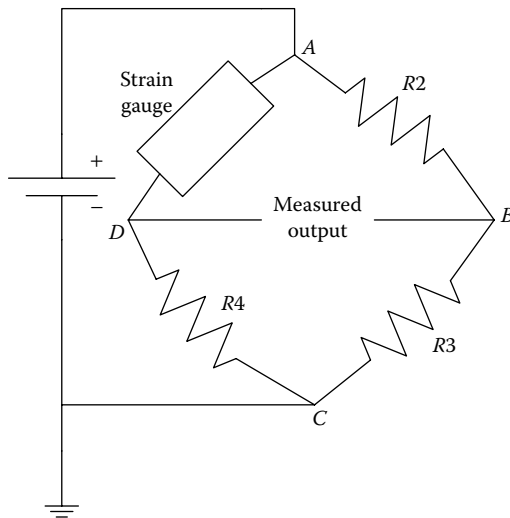


FIGURE 8.5

Schematic of a wheatstone bridge.

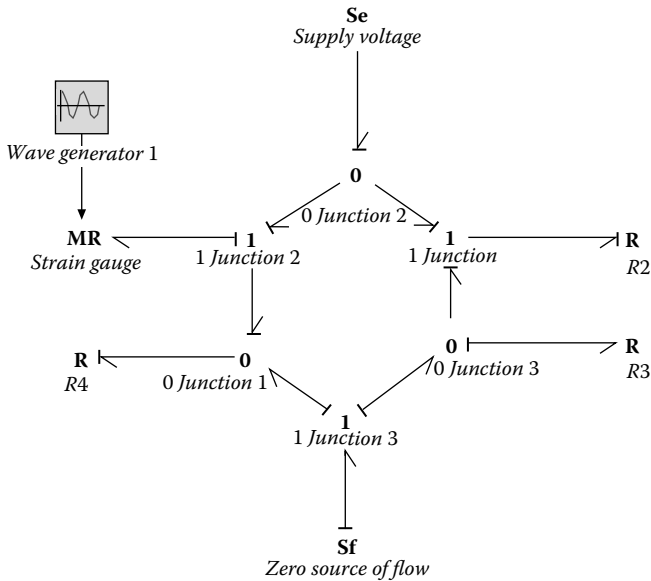


FIGURE 8.6
Bond graph model of the wheatstone bridge.

calculated as part of the simulation process. This calculated effort is the voltage difference between points B and D and is the sensed signal.

The parameters used in the model are shown in Figure 8.7, and the resulting simulation is shown in Figure 8.8.

The simulation result clearly shows that the measured voltage difference is directly proportional to the external signal that was used. This establishes that the strain gauge output can be easily related to the signal source through proper scaling.

Parameters					
Initial Values					
Constants					
Name	Value	Quantity	Unit		Att
R_2	120 (ohm)	Electric Resistance	ohm		Re
Supply_Voltage\effort	12 (V)	Electric Potential	volt		Re
Zero_source_of_flow\flow	0 (A)	Electric Current	ampere		Re
R_4	120 (ohm)	Electric Resistance	ohm		Re
R_3	120 (ohm)	Electric Resistance	ohm		Re
WaveGenerator1\amplitude	13	Magnitude	none		Re
WaveGenerator1\omega	1 (rad/s)	Angular Velocity	radian per second		Re

FIGURE 8.7
Parameters used for the strain gauge simulation.

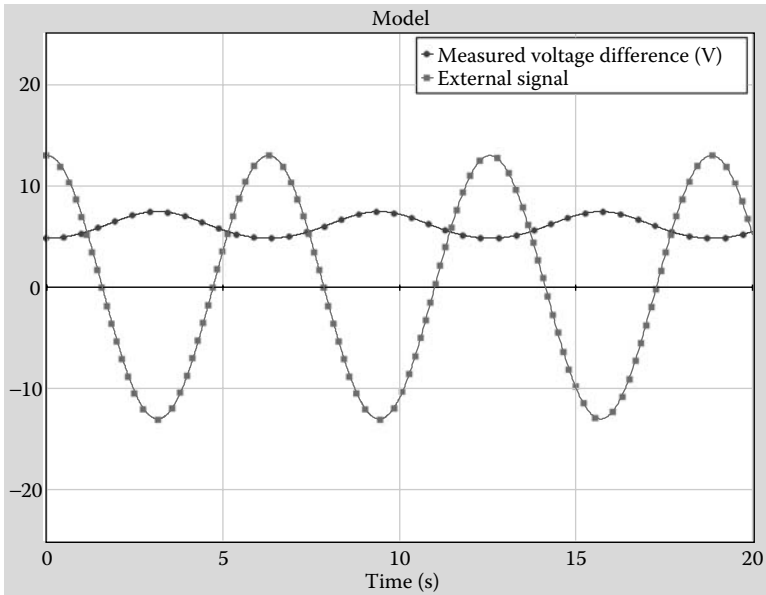


FIGURE 8.8
Simulation results from the wheatstone bridge simulation.

8.2 Capacitive Sensors

Capacitive sensors have been used in many different applications, such as mechanical movement (linear and rotational) measurement, humidity measurement, crash sensing, material composition, proximity, and so forth. Capacitive sensors are found in a soft-touch wall switch, a laptop sense pad, a washroom faucet hand sensor, a digital construction level, a digital caliper, an airbag accelerometer, or in a superaccurate laser positioner. Capacitive sensors are extremely rugged and simple to build. They are highly linear and immune to mechanical and electronic noise. However, because they rely on capacitance, they are sensitive to liquids. Any liquid that bridges the capacitive plates increases the capacitance. A drop of oil can increase the capacitance by a factor of 80!

The basic principle of operation is to monitor the change in capacitance of a parallel plate capacitor as a result of some external disturbance. The sensing of the disturbance is achieved through the measurement of the change in the capacitance via a simple circuit to measure the voltage across the capacitor. Some of the basic relationships that are useful here are given below. By definition capacitance is given as:

$$q = CV \quad (8.1)$$

where q is the charge, C is the capacitance, and V is the induced voltage across the capacitor. From the geometry of a parallel plate capacitor, the capacitance can be expressed as:

$$C = \frac{\epsilon A}{d} \quad (8.2)$$

where A is the overlap area of the plates, d is the distance between them, and ϵ is the permittivity of the material. Table 8.1 shows the permittivity of some common materials.

From the above two equations we get:

$$q = \frac{\epsilon A}{d} V \quad (8.3)$$

This equation applies to a specific geometry of a capacitor. However, in a capacitive sensor design, some of the parameters in the equation could change as a result of external disturbances. The change alters the value of capacitance, and, when attached to a circuit, the change in capacitance alters the voltage across it. This change in the electrical signal (voltage) provides a measure of the changed capacitance and thus the external disturbance.

While capacitors in typical electrical circuits could be modeled using the 1-port capacitor elements, capacitive sensor behavior is slightly different and needs to be modeled in a different manner. In a capacitive sensor, the capacitance will dynamically change due to an external disturbance. Hence, the capacitance is not fixed but is a function of the external disturbance along with other parameters.

To model this type of a behavior, we will introduce a new type of element here. These are called field elements. In this particular case, a capacitive field element is necessary. Before we explore the different configurations for capacitive sensors, we need to devote some attention to these capacitive field elements.

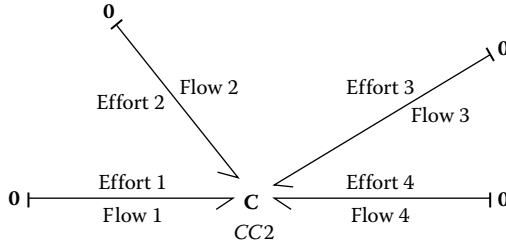
TABLE 8.1

Permittivity Values of Typical Materials Used in Capacitors

Material	$\epsilon (\times 10^{-12})$
Air	8.854
Beeswax	25.67
Nylon	30.98
Polyvinyl chloride	40.27
Salt	53.1
Water	694.72

8.2.1 Multiport Storage Fields: C-Field

Multiport field elements are elements that have more than one port associated with them. Thus, the bond graph representation of a 4-port C-field element may be represented as:



The constitutive relation of this C-field element is a function of the effort and displacement in all the ports and can be most generally expressed as:

$$C = f(e, q) \quad (8.4)$$

and the total energy stored in the energy storage field:

$$E = \int_{t_0}^t \sum_{i=1}^n (e_i f_i) dt \quad (8.5)$$

where n is the number of bonds/ports.

The causal structure for a C-field element is determined the same way as the 1-port C element. In 1-port C elements, the constitutive equation is expressed as:

$$e = F(q) \quad (8.6)$$

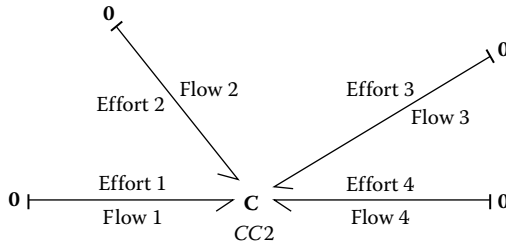
for integral causality, and

$$q = F^{-1}(e) \quad (8.7)$$

for differential causality.

Along similar lines, for C-field elements, when all the ports are integrally causalled the way it is shown in Figure 8.9, the constitutive equations become:

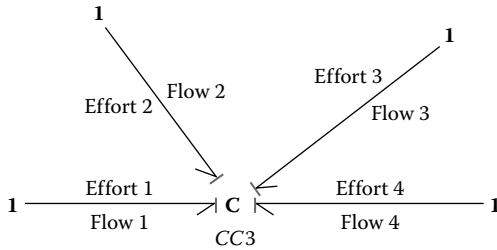
$$\begin{aligned} e_i &= f(q_i) \\ e_i &= f(q_1, q_2, q_3, q_4, \dots) \end{aligned} \quad \text{or} \quad (8.8)$$

**FIGURE 8.9**

C-field element with integral causality.

If all the bonds end up having differential causality and the bond graph representation looks like the one shown in Figure 8.10, the constitutive equation is

$$\begin{aligned} f_i &= \dot{q}_i = f^{-1}(e) & \text{or} \\ \dot{q}_i &= f^{-1}(e_1, e_2, e_3, e_4 \dots) \end{aligned} \quad (8.9)$$

**FIGURE 8.10**

C-field element with differential causality.

Instead of being purely integral or purely differentially causalled, the C-field could have mixed causal structure as shown in Figure 8.11. In that case, the constitutive relationship is in the mixed form as:

$$\begin{aligned} \dot{q}_i &= f^{-1}(e_i) \\ \dot{e}_i &= f(q_i) \end{aligned} \quad (8.10)$$

It is important for the reader to understand that while the exact form of the constitutive equation in a linear 1-port C element is standard, the constitutive equation for a C-field element is not standard. So for every application where this element is used, the modeler will need to derive the constitutive relationship for the C-field. In the next few examples of typical capacitive sensor models, this implementation of the C-field is discussed in detail.

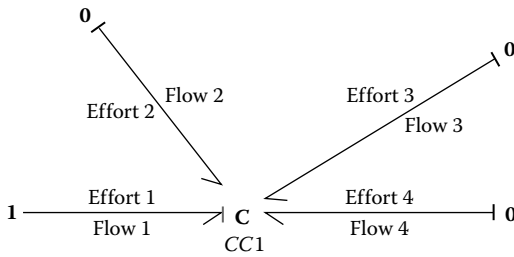


FIGURE 8.11
C-field element with mixed causality.

EXAMPLE 8.1

The simplest example is shown in Figure 8.12, where a parallel plate capacitor is used as the sensor with the initial distance between the plates d , and one of the plates will move away from the other as a result of some external disturbance. This will change the capacitance of the sensor, and this change in capacitance can be related to the movement of the plate.

The bond graph representation of such a component may be done through a C-field element. A C-field element may have multiple ports, and the flow and effort variables for the different ports are different but interrelated. Figure 8.13 shows a C-field element with two ports. The causality strokes as shown represent integral causality. This means that flow information is being received by the field element from both sides and this flow information is being used to calculate the effort information for both sides. The constitutive relationship of a C-field element is similar to a C element in the sense that the flow is integrated to generate the displacements, and the displacements are used to calculate the effort. On one side of the C-field is the electrical domain, and on the other side is the mechanical domain, and the constitutive relationship is a function of what happens in both these domains.

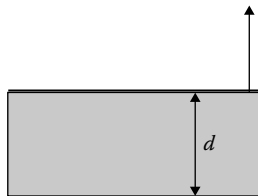


FIGURE 8.12
Schematic of capacitive sensor where one plate moves away from the other.

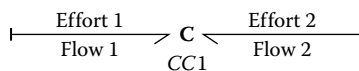


FIGURE 8.13
C-field element with two ports.

For the integrally causalled C-field, the general form of the constitutive equation will be

$$\begin{aligned}\text{effort1} &= f1(\text{displacement1}, \text{displacement2}) \\ \text{effort2} &= f2(\text{displacement1}, \text{displacement2})\end{aligned}\quad (8.11)$$

The constitutive relationship in the case of the parallel plate capacitor with a moving plate can be derived by considering the total energy stored in the capacitor:

$$\text{Energy} = \frac{q^2}{2C} \quad (8.12)$$

Replacing the basic definition for C (but with a moving plate, instead of fixed), the energy expression may be written as:

$$\text{Energy} = \frac{q^2(d+x)}{2A\epsilon} \quad (8.13)$$

where d is the initial fixed distance between the plates and x is the change in d . The time derivative of energy is power. Hence, using chain rule of differentiation we get:

$$\frac{d(\text{Energy})}{dt} = \text{Power} = \frac{\partial(\text{Energy})}{\partial q} \frac{dq}{dt} + \frac{\partial(\text{Energy})}{\partial x} \frac{dx}{dt} \quad (8.14)$$

Since dx/dt is the mechanical flow (velocity) and dq/dt is the electrical flow (current), the $\frac{\partial(\text{Energy})}{\partial q}$ must be the electrical effort (voltage) and $\frac{\partial(\text{Energy})}{\partial x}$ must be the mechanical effort (force). Therefore, the two constitutive equations may be written as:

$$V = \frac{q(d+x)}{A\epsilon} \quad (8.15)$$

V is the effort on the electrical side as a function of displacement on both the electrical and mechanical side.

$$F = \frac{q^2}{2A\epsilon} \quad (8.16)$$

F is the effort on the mechanical side as a function of the displacements.

Here is how it can be implemented in an actual system model. The circuit shown in Figure 8.14 is used to measure the change in the capacitance (in a capacitive sensor). One plate of the capacitive sensor is fixed, and another one moves as shown by the direction of motion.

As a result of this movement, there is a change in capacitance and the circuit current, voltage drop, and so forth change as well. These changes in the circuit are measurable and can be linked back to the disturbance measured by the sensor. The bond graph model of this system is shown in Figure 8.15.

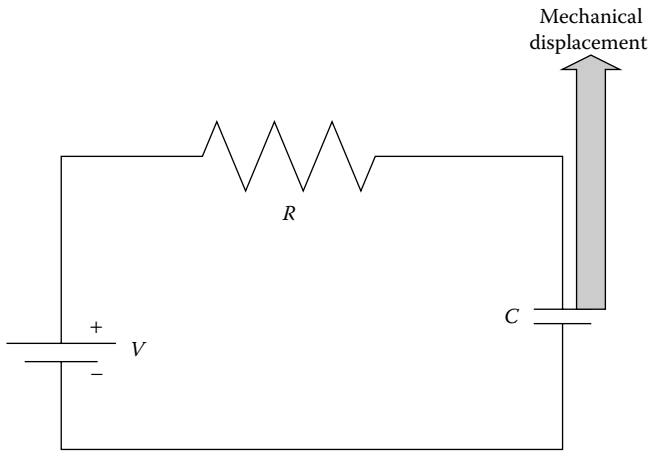


FIGURE 8.14

Circuit to measure the changing capacitance.

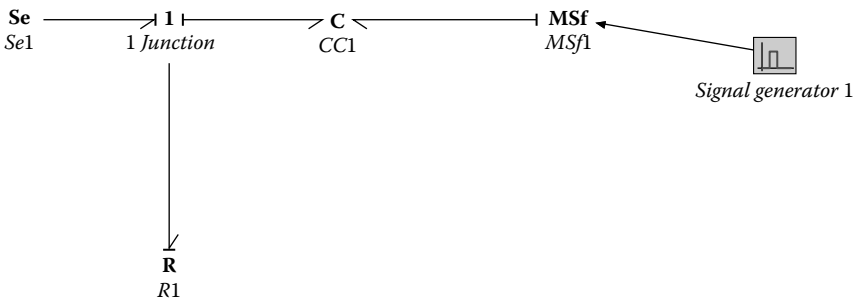


FIGURE 8.15

Bond graph for the sensor in Example 8.1.

The constitutive equations for the capacitor were derived earlier, and they are

$$V = \frac{q(d+x)}{A\epsilon} \quad (8.17)$$

$$F = \frac{q^2}{2A\epsilon} \quad (8.18)$$

The C-field constitutive equation needs to be modeled by modifying the C-field codes in the following fashion.

```
// this model represents a 2-port C element: p.e =
(1/C)*p.f written here as p.e = A*p.f
```


Parameters

```
real A = 1; // area of overlap between capacitor plates
real a21 = 0.0; // unused parameterreal al2 = 0.0;
// unused parameter
real eps = 1.0; // epsilon, permittivity
```

Equations

```
// You can change these equations into any (nonlinear)
version by adding your own functions. // Use f(x) button
at the left of the window to see all available functions.
state1 = int (p1.f); // integral of flow on the first arm,
// this is the charge in the capacitor
state2 = int (p2.f); // integral of flow in the second
// arm, this is the displacement of the
// movable plate
p1.e = state1*state2/(A*eps); // p1.e is the voltage induced
// on the first arm of the C-field
p2.e = state1*state1/(2*A*eps); // p2.e is the force on the
// second arm of the C-field
```

The parameters used in the simulation are shown in Figure 8.16.

It is important to also use proper initial conditions for the two states that are obtained through integration of flows. To decide about this, recall that state 1 is the charge in the capacitor and state 2 is the mechanical displacement. So the initial conditions represent the initial charge in the capacitor and the initial distance between the plates. Since the capacitor is already in a measurement circuit, at steady state (i.e., prior to the displacement disturbance) there will be a non-0 charge on the capacitor. Also, before any movement of the movable plate, there will be an initial separation between plates. The initial values used in this simulation are shown in Figure 8.17. It is worth noting that none of the parameters chosen in this simulation exercise are realistic. They have been arbitrarily chosen to demonstrate how the model can be set

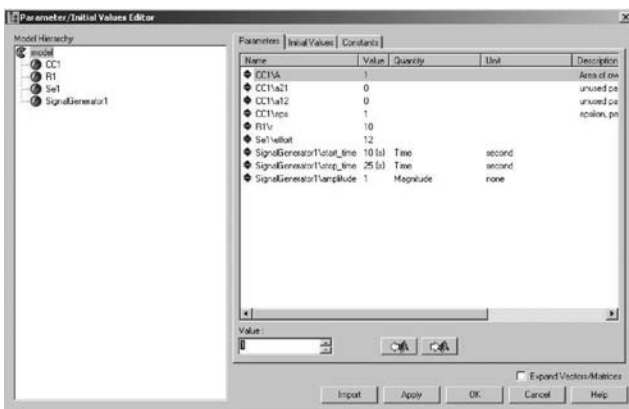


FIGURE 8.16
Parameters used in the simulation.

up and what the simulation results look like. Figure 8.18 shows the simulation results. The impulse input to the sensor is reflected in the change in the voltage induced on the capacitor. This can be measured and used to determine the nature of the input function. In reality the actual magnitude of the voltage induced may be much smaller, and an amplification circuit will be necessary to read these changes in the response.

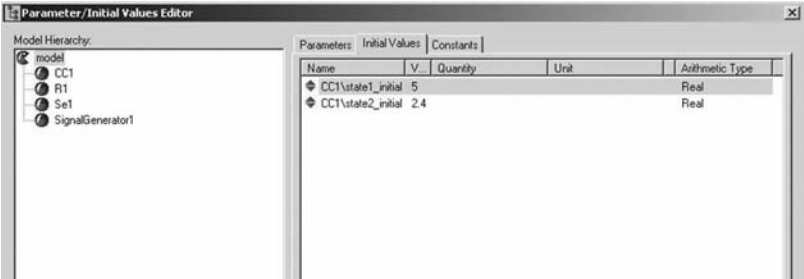


FIGURE 8.17
Initial conditions used.

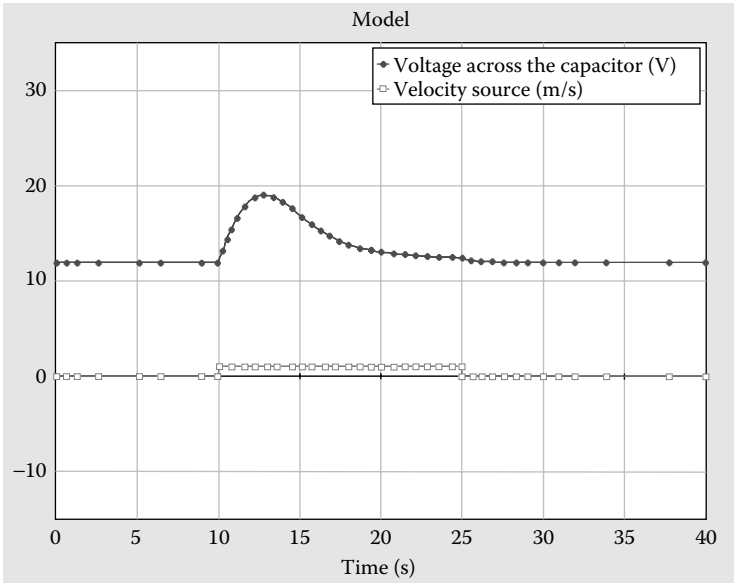
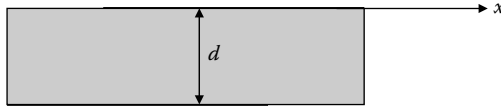


FIGURE 8.18
Simulation results.

EXAMPLE 8.2

Figure 8.19 shows another simple example where the distance between the plates is held constant, but one of the plates move horizontally in a fashion such that the overlap area between the plates changes.

**FIGURE 8.19**

Schematic for Example 8.2.

To derive the constitutive equations, we can write the equations:

$$\begin{aligned}
 A &= w(l - x) \\
 C &= \frac{\epsilon A}{d} = \frac{\epsilon w(l - x)}{d} \\
 E &= \frac{1}{2} CV = \frac{1}{2} \frac{q^2}{C} = \frac{1}{2} \left(\frac{q^2 d}{\epsilon w(l - x)} \right)
 \end{aligned} \tag{8.19}$$

where w is the width (depth) and l is the initial overlap length of the plate, and $(l - x)$ is the overlap length between the plates after one of the plates has moved by x . Hence, $w(l - x)$ is the overlap area between the plates. Following the same approach as outlined before:

$$\begin{aligned}
 \text{Effort on the electrical side} &= \frac{\partial}{\partial q} \left(\frac{q^2 d}{2\epsilon w(l - x)} \right) = \frac{2qd}{2\epsilon w(l - x)} \\
 &= \frac{qd}{\epsilon w(l - x)} = e_1
 \end{aligned} \tag{8.20}$$

$$\text{Effort in ME} = \frac{\partial}{\partial x} \left(\frac{q^2 d}{2\epsilon w(l - x)} \right) = \frac{(-1)(-1)q^2 d}{2\epsilon w(l - x)^2} = \frac{q^2 d}{2\epsilon w(l - x)^2} = e_2 \tag{8.21}$$

These are, therefore, the constitutive equations for the two sides of the C-field element. One can use these equations to easily modify the C-field model to simulate the behavior of this type of a sensor just like in the previous example.

8.3 Magnetic Sensors

8.3.1 Magnetic Circuits and Fields

Magnetic and electromagnetic phenomena are used extensively in a variety of sensor designs. These designs are all based primarily on the variation of the energy stored in magnetic fields. Before we start looking at the different phenomena that are typically used, we will go over some of the basic concepts of magnetic fields and the energy associated with them. There are several well-known laws of electricity and magnetism that need to be mentioned here.

8.3.1.1 Faraday's Law of Electromagnetic Induction

There are many ways of expressing Faraday's law. Here are some of the implications.

- Coils of wire and magnets interact to create electric and magnetic field.
- A force F is required to move a conductor of length L carrying a current i through a magnetic field of strength B ($F = BLi$).
- A magnet that moves in a coil causes a potential difference at the terminals of the coil.
- Current that flows through a coil creates a magnetic field.
- The time varying change in a magnetic field ϕ induces an electromotive force E .

8.3.1.2 Ampere's Law

The implication of Ampere's law can be listed as the following statements.

- An "electromotive force," such as created by current passing through a coil of wire, *forces* a magnetic field through a magnetic circuit.
- The product of the magnetic field intensity H and length in a circuit equals the magnetomotive force.

8.3.1.3 Gauss's Law for Magnetism

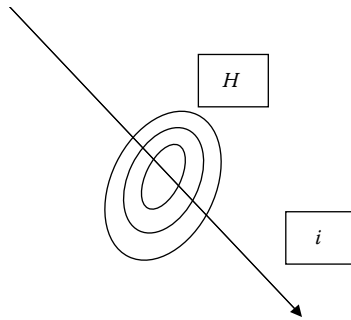
Gauss's law implies the following statements.

- Magnetic fields have north and south poles between which the field flows.
- The total magnetic flux ($\phi = B \cdot \text{area}$) across a closed boundary is 0 (there are no magnetic monopoles).

The basic concepts of electromagnetism can be summarized in mathematical forms using the basic laws mentioned above. In machines that do not use permanent magnets, the magnetic field is produced by a current that flows through a coil that is wound around a ferromagnetic material.

H is the symbol used for magnetic field intensity. Figure 8.20 is a schematic for the magnetic field around a current carrying conductor such that:

$$H = \frac{i}{2\pi r} \quad (8.22)$$

**FIGURE 8.20**

Magnetic field around a current carrying conductor.

for a straight wire. Its unit = $\frac{\text{ampere}}{m}$

Wherever there is a magnetic field, magnetic fluxes are produced. The symbol B is used to represent magnetic flux density. While B is dependent on the medium the magnetic field passes through, H is independent of the medium.

B = Magnetic flux density. Unit = $\frac{Wb}{m^2}$ or Tesla (Weber per square meter), and

$$B = \mu H \quad (8.23)$$

where, μ = Permeability of the medium. It can be expressed as:

$$\mu = \mu_r \mu_0 \quad (8.24)$$

where

... μ_0 is the permeability of the free space = $4\pi \times 10^{-7} \frac{Wb}{Amp-m}$

... μ_r is the relative permeability of the medium and is equal to 1 for free space. The relative permeability is ~2000–6000 for ferromagnetic materials such as iron, copper, nickel, and so forth. This means that for materials that have a higher relative permeability, a small current will produce a large flux density in the material.

In air or in vacuum, the B and H are linearly related, and the relationship may be expressed as:

$$B = \mu_0 H \quad (8.25)$$

In ferromagnetic material, the relationship is not exactly linear. Beyond a certain level of magnetization, saturation is reached. Also, there are

hysteresis effects associated with the B - H relationship. Standard B - H plots are available for most magnetic materials that accurately represent the actual nonlinear relationship between the two variables. As these plots show, however, for a certain range of the B - H relationship, a linear approximation is perfectly valid. For our discussion here, we will assume that we are operating in the linear range of the B - H relationship. Hence, $B = \mu H$ for ferromagnetic materials is an acceptable relationship.

8.3.2 Simple Magnetic Circuit

Consider a simple magnetic circuit where a current flows through the coil that is wound on a ferromagnetic core. When the current flows through the coil magnetic flux is mostly confined to the core.

If N = number of coils, it can be shown that:

$$Hl = Ni \Rightarrow H = \frac{Ni}{l} \quad (8.26)$$

where, l is the length of the medium or the magnetic path.

Since

$$B = \mu H, B = \mu \frac{Ni}{l} \Rightarrow BA = \left(\mu \frac{Ni}{l} \right) A \quad (8.27)$$

where A is the area of cross-section of the magnetic path or the area through which the flux is traveling. The product of BA gives us the total flux.

$$BA = \phi = \frac{Ni}{\frac{l}{\mu A}} \quad (8.28)$$

Using the analogy of electrical circuits, Equation 8.28 may be viewed as

Flux = (magnetomotive force)/reluctance.

Magnetomotive force = Ni is similar to electromotive force = e (voltage).

Flux = ϕ is similar to charge.

Reluctance = $\frac{l}{\mu A}$, and permeance = $1/(\text{reluctance})$; permeance may be considered similar to capacitance.

In traditional electromagnetic texts, reluctance is considered to be similar to resistance, flux is considered to be similar to current, and the magnetomotive force is considered similar to the electromotive force.

Although resistance is a power dissipative element, reluctance is not. Energy is stored in the magnetic circuit with reluctance in it. Also, current

is a flow rate of charge; however, magnetic flux is not a flow rate so magnetic flux should rather be treated as something similar to charge and not as something similar to current. Hence, a magnetic circuit, in reality, should be more like a capacitive circuit rather than a resistive circuit where $1/\text{reluctance} = \text{permeance} = \frac{\mu A}{l}$; and permeance is similar to electrical capacitance.

Also, $\lambda = N\phi$, is the flux linkage variable, and the rate of change of the flux linkage variable is equal to the voltage applied in the electrical circuit (effort), that is, $\dot{\lambda} = N\dot{\phi}$.

Thus, the electromagnetic circuits can be modeled in the following fashion. Figure 8.21 shows a schematic where an electrical coil on a core is energized using an applied emf e . The current flowing in the electrical circuit is i , and it determines the magnetomotive force induced on the magnetic side as Ni , i.e. the effort on the magnetic side is related to the flow on the electrical side. The flow on the magnetic side is flux flow rate and the back emf on the electrical side is the $\dot{\lambda} = N\dot{\phi}$, i.e. the effort induced on the electrical side is related to the flow on the magnetic side. Therefore, this device works as a gyrator, and the bond graph representation of this system may be shown as in Figure 8.22.

This gyrator element is an important building block in modeling magnetic circuits. The element links the electrical domain with the magnetic domain. The gyrator factor is the number of turns (windings) in the electrical coil, N .

There is another way of expressing this relationship in terms of the well-known electrical quantity called inductance. Since $\lambda = N\phi$ and $L = \lambda/i$; but the current i can be expressed as mmf/N and mmf is flux times reluctance. Therefore:

$$L = L = \lambda/i = N\phi/(\phi R)/N = (N*N)/R \quad (8.29)$$

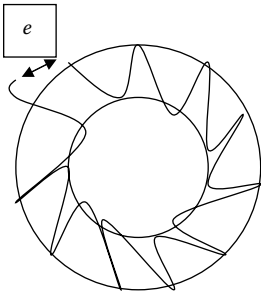


FIGURE 8.21
Current flowing through a conductor wound around a core.

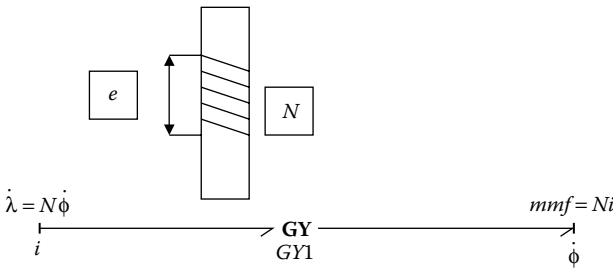


FIGURE 8.22
An electromagnet circuit and the corresponding bond graph representation.

Therefore,

$$L = (N^2 \mu A) / l \quad (8.30)$$

Table 8.2 summarizes all the variables we have used so far in this discussion and identifies the nature of these variables in the context of generalized quantities.

In the next few sections, some magnetic circuits are discussed in the context of representing them in the form of bond graph models. This leads to a discussion of sensors using magnetic effects in this chapter and actuators in the next chapter.

TABLE 8.2

Generalized Quantities and Their Magnetic Equivalents

Generalized Quantity	Magnetic Equivalent
Effort	Magnetomotive force, Ni
Flow	Flux rate, $d\phi/dt$
Disp	Flux, ϕ
Capacitance	Permeance, P
Stiffness parameter	Reluctance, R
	Magnetic flux density, B
	Magnetic field strength, H
Momentum	Flux linkage, $\lambda = N\phi$
Inertia	Inductance, $L = \text{Flux linkage}/i = N\phi/I = (N^2 \mu A)/l$

8.3.2.1 Magnetic Circuit with Air Gap

Consider the magnetic circuit in Figure 8.23 and its bond graph development.

Development of the bond graph for the magnetic circuit can be accomplished in the same way as an electrical circuit. The locations 1, 2, 3, and 4 represent different locations in the magnetic circuit that indicate different mmf points (just like potential points on an electrical circuit). Therefore, they can be represented on the magnetic circuit as 0 junctions and each 0 junction is connected with the next 0 junction with a 1 junction that is connecting a C element representing the permeance of that region. So the initial bond graph representation is shown in Figure 8.24. The items on the left side of the GY are items in the electrical circuit and the terms on the right of GY are the terms in the magnetic circuit. The I and the R represent the inductance and resistance of the electrical circuit respectively.

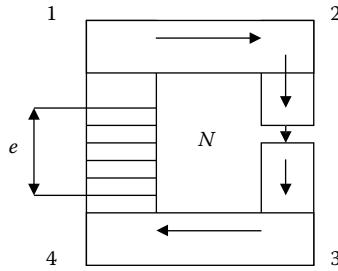


FIGURE 8.23

A generic magnetic circuit.

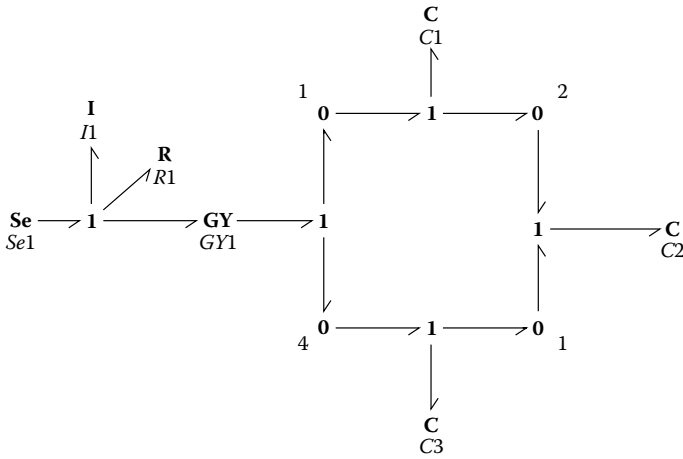


FIGURE 8.24

Initial bond graph representation of the magnetic circuit.

The 0 junction at point 4 can be treated as a reference and removed, and the circuit may be simplified as shown in Figure 8.25. Here I_1 and R_1 are the inductance and resistance of the electrical circuit, respectively. C_1 and C_3 represent the C s (permeance) of the iron and C_2 represents the C (permeance) for the air. The circuit equations for the magnetic circuit are written as:

$$\begin{aligned}\phi &= \frac{Ni}{R_{\text{Core}} + R_{\text{Gap}}} \\ \phi &= \frac{Ni}{\left(\frac{1}{p_1} + \frac{1}{p_3}\right) + \frac{1}{p_2}} \\ \phi &= \frac{Ni}{\frac{l_{\text{iron}}}{\mu A_{\text{iron}}} + \frac{l_{\text{air}}}{\mu_0 A_{\text{air}}}}\end{aligned}\tag{8.31}$$

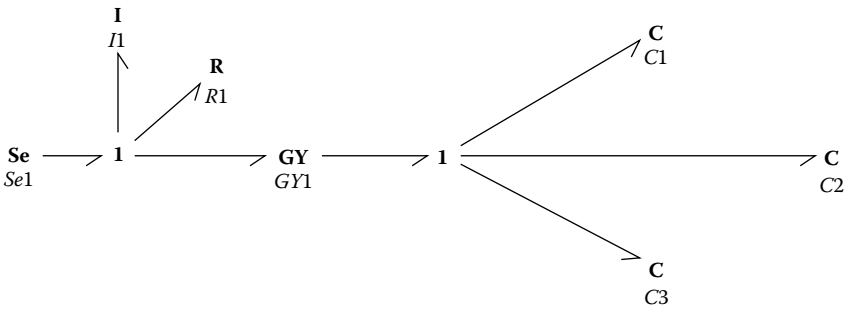


FIGURE 8.25
Final bond graph of the magnetic circuit.

8.3.2.2 Magnetic Bond Graph Elements

The Magnetic bond graph elements are

1. Effort, Ni = Ampere turns
2. Flow, $\dot{\phi}$ = Flux rate i.e., $\frac{wb}{s}$
3. Displacement, ϕ = Flux
4. Capacitance or Permeance, $P = \frac{\mu A}{l}$
5. Flux linkage, λ (momentum) = $N\phi$

Let's consider a slight variation of the above magnetic circuit and assume that instead of an electrical coil generating the magnetic C-field, there is a permanent magnet that is used to generate the magnetomotive force. Figure 8.26 shows such an arrangement. The shaded portion in the figure represents a permanent magnet with B as the magnetic flux density. We saw earlier that for the electrical coils generating a magnetomotive force.

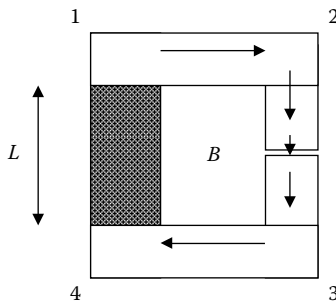


FIGURE 8.26
Schematic of a magnetic circuit with a permanent magnet providing the mmf.

$$B = \mu \frac{Ni}{l} \Rightarrow Ni = \frac{Bl}{\mu} = \frac{Bl}{\mu_0} \quad (\text{in air}) \quad (8.32)$$

Therefore, the magnetomotive force that is induced by a permanent magnet is given by $\frac{Bl}{\mu_0}$, where B is the magnetic strength, L is the length of the magnet. The bond graph model of this arrangement can be easily shown to be Figure 8.27 using the same approach as the previous example. The magnetic flux through this circuit may be computed in a manner similar to the previous example.

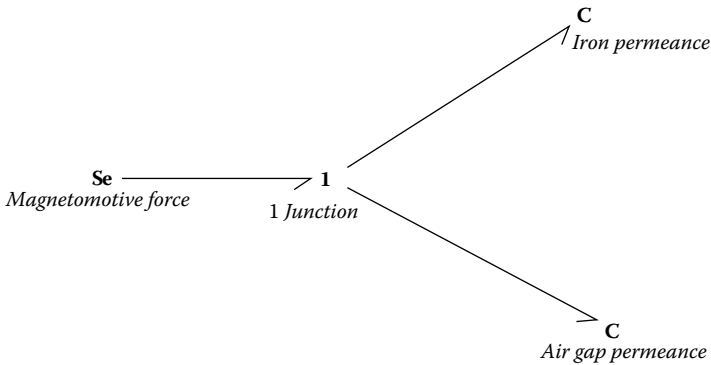


FIGURE 8.27

Bond graph representation of a magnetic circuit with a permanent magnet.

EXAMPLE 8.3: VARIABLE RELUCTANCE SENSOR

Figure 8.28 shows a variable reluctance sensor that may be used to measure displacement, velocity, or acceleration. This type of a sensor may be available in many configurations, and the figure shows the simplest possible configuration. The permanent magnet has an air gap, and a ferromagnetic piece is able to move in and out of the gap driven by some external source of flow. When the tab passes through the air gap, the reluctance/permeance of this set up changes. This induces an emf across the coil of wire wound around the magnet. The emf induced is proportional to the speed of movement. Also, the frequency with which this induced emf occurs is a measure of the speed.

A magnified view of the area of interest is shown in Figure 8.29 where the tab is partially in the slot representing the air gap. To develop the model, we can assume that when the magnetic tab is inside the slot, the reluctance is equivalent to that of twice the air gap (since the permeability of the tab and the magnetic material may be assumed to be very high in comparison to that of air) when the tab is in between the poles and the reluctance. When the tab is not in between the poles, the reluctance is very high (~infinite) because the air gap now is large. Permeance, the inverse of reluctance, varies accordingly. When

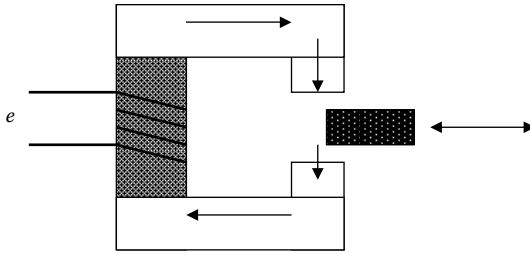


FIGURE 8.28
Schematic showing an arrangement for a variable reluctance sensor.

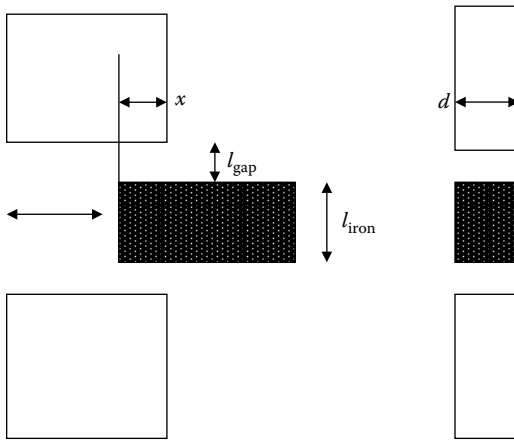
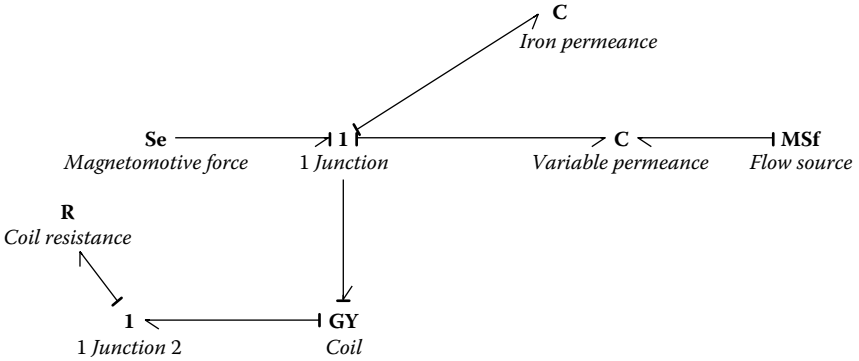


FIGURE 8.29
Magnified view of the area of interest.

the tab is partially in the air gap, the reluctance (permeance) may be computed based on the overlap area as shown in the figure. The variable reluctance (permeance) in the magnetic circuit needs to be modeled using a field element, specifically a C-field because the energy stored is dependent on both the magnetic displacement (flux) as well as the mechanical displacement. The bond graph model of the whole set up will look like Figure 8.30.

In the bond graph model, the source of effort is the mmf supplied by the permanent magnet. The C element in the model is used to model the permeance of the iron path in the circuit. The C-field element is used to model the variable permeance due to the tab that moves in and out of the gap between the two poles. The source of flow models the external velocity source that causes the movement (and this is what the sensor will be measuring). The GY element is used to model the magnetic to electric transformation in the electrical coil that is wound around the permanent magnet. As the tab moves in and out of the air gap in the poles, the reluctance in the circuit changes. This rate of change in the flux in the magnetic circuit induces a voltage across the winding. The GY element is used to capture this behavior. The GY factor here

**FIGURE 8.30**

Bond graph representing the variable reluctance sensor.

is the number of turns of the coil. The resistance element is the resistance in the electrical circuit. The voltage measured across this is the voltage output of this variable reluctance sensor.

The C-field equations need to be derived in the same fashion as we did for capacitive sensors:

One expression of energy stored in a magnetic C-field is $= \frac{\phi^2}{2}$. Reluctance Inside C-Field

$\dot{\phi}, \dot{x}$ are received information.

Integration of $\dot{\phi}$ to get ϕ , $\phi = \text{int}(\dot{\phi})$

Integration of \dot{x} to get x , $x = \text{int}(\dot{x})$

Differentiate energy w.r.t time

$$\frac{d}{dt}(\text{Energy}) = \text{Power} \quad (8.33)$$

$$\frac{d}{dt}(\text{Energy}) = \frac{\partial}{\partial \phi} \left(\frac{\phi^2 \cdot R}{2} \right) \cdot \frac{d\phi}{dt} + \frac{\partial}{\partial x} \left(\frac{\phi^2 \cdot R}{2} \right) \cdot \frac{dx}{dt} \quad (8.34)$$

Power on magnetic side

$$= \frac{\partial}{\partial \phi} \left(\frac{\phi^2 \cdot R}{2} \right) \cdot \frac{d\phi}{dt} = \text{effort} \cdot \text{flow} \quad (8.35)$$

Hence, effort on the magnetic side

$$\begin{aligned} &= \frac{\partial}{\partial \phi} \left(\frac{\phi^2 \cdot R}{2} \right) \\ &= \frac{2\phi R}{2} \\ &= \phi \cdot R \end{aligned} \quad (8.36)$$

Power on mechanical side

$$= \frac{\partial}{\partial x} \left(\frac{\phi^2 \cdot R}{2} \right) \cdot \frac{dx}{dt} \quad (8.37)$$

Effort on the magnetic side

$$\begin{aligned} &= \frac{\partial}{\partial x} \left(\frac{\phi^2 \cdot R}{2} \right) = \frac{\partial}{\partial x} \left(\frac{\phi^2}{2} \left[\frac{2l_{\text{gap}}}{\mu_0 A_{\text{overlap}}} + \frac{l_{\text{iron}}}{\mu A_{\text{overlap}}} \right] \right) = \frac{\partial}{\partial x} \left(\frac{\phi^2}{2xd} \left[\frac{2l_{\text{gap}}}{\mu_0} + \frac{l_{\text{iron}}}{\mu} \right] \right) \\ &= -\frac{\phi^2}{2dx^2} \left(\frac{2l_{\text{gap}}}{\mu_0} + \frac{l_{\text{iron}}}{\mu} \right) \end{aligned} \quad (8.38)$$

The constitutive equation for the C-field is

$$\text{Effort}_{\text{left}} = \phi \cdot R = \phi \left(\frac{2l_{\text{gap}}}{\mu_0 dx} + \frac{l_{\text{iron}}}{\mu dx} \right) \dots x \text{ is the movement of the tab} \quad (8.39)$$

$$\text{Effort}_{\text{right}} = -\frac{\phi^2 l_{\text{gap}}}{2dx^2} \left(\frac{2l_{\text{gap}}}{\mu_0} + \frac{l_{\text{iron}}}{\mu} \right) \quad (8.40)$$

These two expressions may be simplified by dropping the second term inside the parentheses because μ is a few thousand times larger than μ_0 . When the flow on the mechanical side is integrated, we get the displacement x of the mechanical side. We need to be careful that there is an initial position of x , that is, x_0 .

The constitutive equations for the C-field element as outlined above are programmed in a fashion as follows.

```
// This model represents a 2-port C-element: p.e = (1/C)*p.f
written here as p.e = A*p.f
```

Parameters

```
real lgap = 0.002; //gap length
real muo = 0.000001256; //permeability of air
real d = 0.1; //depth of the circuit
real a22 = 1.0; //unused variable
```

Equations

```
// You can change these equations into any (nonlinear)
version by adding your own functions.
// Use f(x) button at the left of the window to see all
available functions
state1 = int (p1.f);
state2 = int (p2.f);
p1.e = state1*(2*lgap/(muo*d*state2));
p2.e = -state1*state1*lgap*lgap/(d*state2*state2*muo);
```

Figure 8.31 shows the parameters used in the simulation. Along with these parameters the initial value of the displacement is assigned to a very small but non-0 value to avoid the division by 0 problem. The simulation results are shown in Figure 8.32. This example provides a very general idea of how the sensor behavior may be simulated. The actual values of the parameters were mostly chosen to be representative but arbitrary. While viewing the simulation results, the user should be aware of that.

Parameters				
Initial Values				
Constants				
Name	Value	Quantity	Unit	Ari
Iron_permeance\c	0.01			Re
Magnetomotive_Force\effort	1			Re
Variable_permeance\lgap	0.002			Re
Variable_permeance\muo	1.256e-006			Re
Variable_permeance\d	0.1			Re
Variable_permeance\alpha22	1			Re
Coil\r	1			Re
Coil_resistance\r	1			Re
WaveGenerator1\amplitude	1	Magnitude	none	Re
WaveGenerator1\omega	1 {rad/s}	Angular Velocity	radian per second	Re

FIGURE 8.31
The parameters used in the simulation.

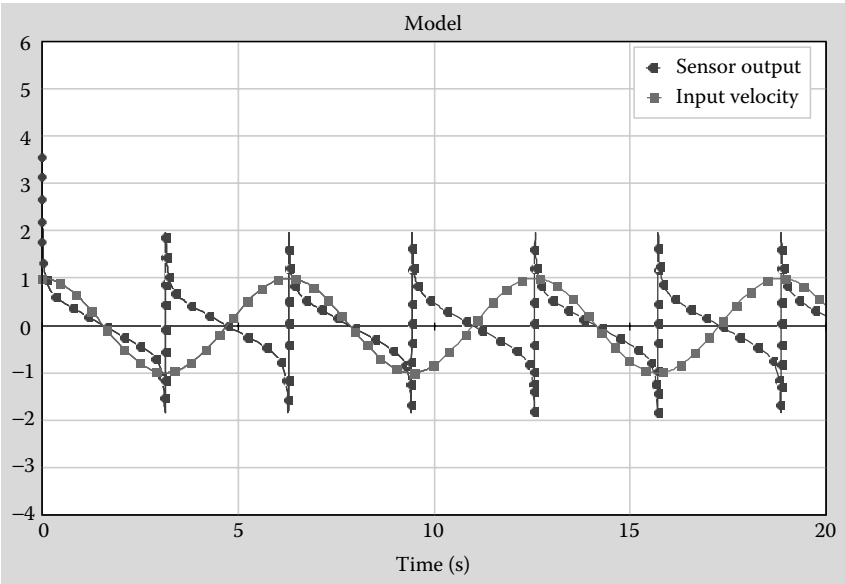


FIGURE 8.32
Simulation results from a variable reluctance sensor.

EXAMPLE 8.4: VARIABLE DIFFERENTIAL TRANSFORMERS

Linear variable differential transformers (LVDTs) and rotational variable differential transformers (RVDTs) are very commonly used sensors that measure displacements and rotations. These sensors are noncontact type sensors and, therefore, hold a distinct advantage over contact type sensors such as the potentiometer. These sensors are sometimes called variable-inductance sensors, mutual induction sensors, or a differential transformer.

Figure 8.33 shows two views of a schematic of the LVDT. This sensor consists of a primary coil that is energized by an AC source. There are two secondary coils that are connected to each other in a way such that the net output is the difference in the induced voltages in each (i.e., in series opposition). There is a movable iron core inside these coils providing the flux linkage between the coils. In the null position, the voltage induced in both the secondary coils are the same, and, thus, the difference would be 0. As the iron core is moved, the reluctance in the path of the magnetic fluxes change; for one of the secondary coils, it is a function of $+x$ while that of the other will be a function of $-x$. The voltage induced in each coil will correspondingly be functions of $+x$ and $-x$, and, therefore, the difference in the voltage will be additive. Because the input applied on the primary coil is sinusoidal, the outputs in the secondaries will be sinusoidal as well. But the amplitude of this output will be proportional to the displacement of the core. For transient displacements, the frequency of the reference source (i.e., the supply to the primary coil) should have a frequency that is at least 10 times as large as the largest significant frequency in the measured motion.

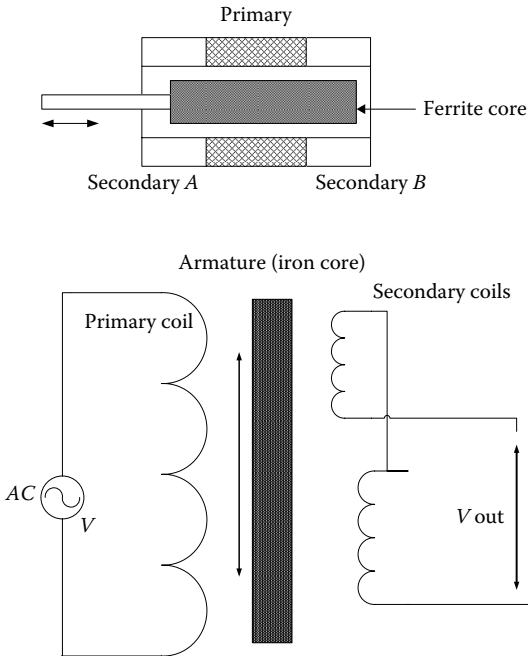


FIGURE 8.33
Schematic and circuit for LVDT.

In order to model this sensor, we need to remind ourselves of a few things we learned earlier. First, there are three locations where a domain transformation is happening; in the primary coil, there is a transformation from electrical to the magnetic domain, and in each of the secondary coils, there is a transformation from magnetic to electrical domain. This means that there need to be three gyrator elements to capture all of these. The movement of the iron core adds a different variation in the system. As in previous cases, the movement of the iron core changes the effective reluctance and is modeled using a C-field element. Thus, the model for the whole sensor looks like the one shown in Figure 8.34.

The bond graph model consists of three GY elements representing the three coils all attached to a C-field element that is used to model the variable reluctance due to the moving core. The external input to the C-field is a velocity of motion of the iron core. The gyrator factors are the number of turns in each coil. The output efforts from the two secondary gyrators are captured by means of the effort sensor and are subtracted so that the net output can be found. This last part of the bond graph is not modeling the actual series circuit on the secondary side because that circuit will have two inductances (outlet from GY elements) and will result in a differential causality in the model. To avoid that effort, signals are explicitly separated and subtracted to achieve the same result.

The exact model for the C-field element is derived below. Figure 8.35 shows a schematic that is used to derive the necessary relationships.

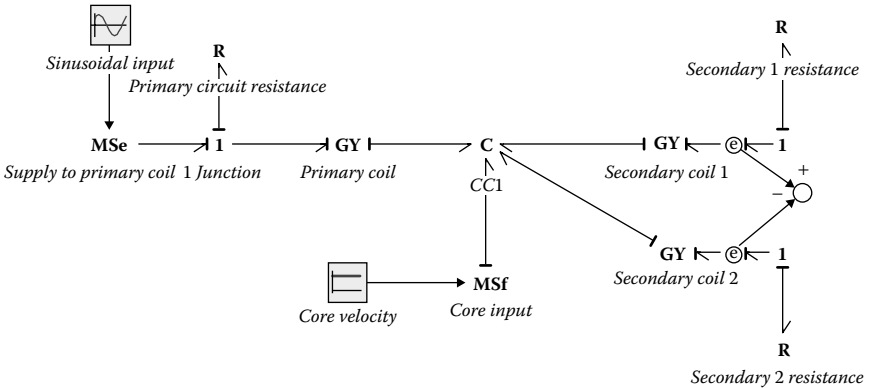


FIGURE 8.34
Bond graph model for the LVDT.

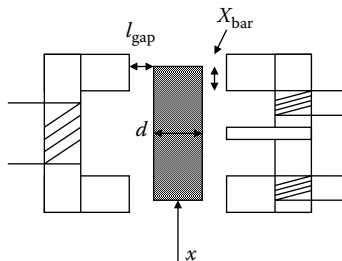


FIGURE 8.35
A schematic of LVDT used for deriving the C-field model.

8.3.2.3 Inside C-Field

We are making the assumption here that the magnetic effects are controlled primarily by the air gap and the reluctance of the air gap. The other reluctances of the magnetic materials are ignored here. $2 \cdot X_{\text{bar}}$ is the total length of the overlap of the core. At the null position this is equally distributed between the top and the bottom. We also assume that the magnetic flux induced is the same in all parts of the magnetic circuit.

Following the same approach as before:

$\dot{\phi}, \dot{x}$ are received information.

Integration of $\dot{\phi}$ to get ϕ , $\phi = \text{int}(\dot{\phi})$

Integration of \dot{x} to get x , $x = \text{int}(\dot{x})$

Differentiate energy w.r.t time:

$$\frac{d}{dt}(\text{Energy}) = \text{Power} \quad (8.41)$$

$$\frac{d}{dt}(\text{Energy}) = \frac{\partial}{\partial \phi} \left(\frac{\phi^2 \cdot R}{2} \right) \cdot \frac{d\phi}{dt} + \frac{\partial}{\partial x} \left(\frac{\phi^2 \cdot R}{2} \right) \cdot \frac{dx}{dt} \quad (8.42)$$

Power on magnetic side:

$$= \frac{\partial}{\partial \phi} \left(\frac{\phi^2 \cdot R}{2} \right) \cdot \frac{d\phi}{dt} = \text{effort} * \text{flow} \quad (8.43)$$

Hence, effort on the magnetic side:

$$\begin{aligned} &= \frac{\partial}{\partial \phi} \left(\frac{\phi^2 \cdot R}{2} \right) \\ &= \frac{2\phi R}{2} \\ &= \phi \cdot R \\ &= \phi \left(\frac{l_{\text{gap}}}{\mu_0 \pi d 2 X_{\text{bar}}} \right) \end{aligned} \quad (8.44)$$

For the two secondary coils, the mmf induced will be

$$= \phi \left(\frac{l_{\text{gap}}}{\mu_0 \pi d (X_{\text{bar}} - x)} \right) \text{ and } = \phi \left(\frac{l_{\text{gap}}}{\mu_0 \pi d (X_{\text{bar}} + x)} \right) \quad (8.45)$$

Power on mechanical side:

$$= \frac{\partial}{\partial x} \left(\frac{\phi^2 \cdot R}{2} \right) \cdot \frac{dx}{dt} \quad (8.46)$$

Effort on the magnetic side for one of the secondary coils:

$$\begin{aligned} &= \frac{\partial}{\partial x} \left(\frac{\phi^2 \cdot R}{2} \right) = \frac{\partial}{\partial x} \left(\frac{\phi^2}{2} \left[\frac{l_{\text{gap}}}{\mu_0 A_{\text{overlap}}} \right] \right) \\ &= - \frac{\phi^2}{2\pi d} \left(\frac{l_{\text{gap}}}{\mu_0 (X_{\text{bar}} + x)^2} \right) \end{aligned} \quad (8.47)$$

For the other secondary coil, the effort is

$$= \frac{\phi^2}{2\pi d} \left(\frac{l_{\text{gap}}}{\mu_0 (X_{\text{bar}} - x)^2} \right) \quad (8.48)$$

and the net effort is the sum of the two efforts.

This model is implemented in the software through the use of a C-field element.

Parameters

```
real d = 0.01;
real mu0 = 0.0000012566;
real lgap = 0.002;
real xbar = 0.01;
real pi = 3.14159;
```

Equations

```
// You can change these equations into any (nonlinear)
// version by adding your own functions.
// Use f(x) button at the left of the window to see all
// available functions.
state1 = int (p1.f); //magnetic flux associated with
                    // primary coil
state2 = int (p2.f); //mechanical displacement of the core
state3 = int (p3.f); //magnetic flux associated with the
                    // first secondary coil
state4 = int (p4.f); //magnetic flux associated with the
                    // second secondary coil
p1.e = (state1)*lgap/(mu0*pi*d*(2*xbar));
//mmf for the primary coil
p2.e = (state1*state1)*lgap/
(2*mu0*pi*d*(xbar-state2)^2)
- (state1*state1)*lgap/(2*mu0*pi*d*(xbar+state2)^2);
//force on the core insertp
```

```
3.e = (state1*lgap)/(pi*mu0*d*(xbar-state2));  
//mmf induced on the first secondary coil  
p4.e = (state1*lgap)/(pi*mu0*d*(xbar+state2));  
//mmf induced on the second secondary coil
```

For the purposes of simulation, the parameters used are shown in Figure 8.36. The results obtained from the simulation are shown in Figures 8.37 and 8.38.

Parameters					
Initial Values					
Constants					
Name	Value	Quantity	Unit		Ar
CC1\vd	0.01				Re
CC1\mu0	1.2566e-006				Re
CC1\lgap	0.002				Re
CC1\xbar	0.01				Re
CC1\pi	3.14159				Re
Primary_circuit_resistance\r	1				Re
Primary_coil\r	100				Re
Secondary_coil1\r	50				Re
Secondary_1_resistance\r	1				Re
Sinusoidal_input\amplitude	1				Re
Sinusoidal_irput\omega	50 (rad/s)	Angular Velocity	radian per second		Re
Sinusoidal_irput\phase	0 (rad)	Plane Angle	radian		Re
Secondary_coil2\r	50				Re
Secondary_2_resistance\r	1				Re
Core_velocity\c	8e-005				Re

FIGURE 8.36
Parameter values used in the simulation.

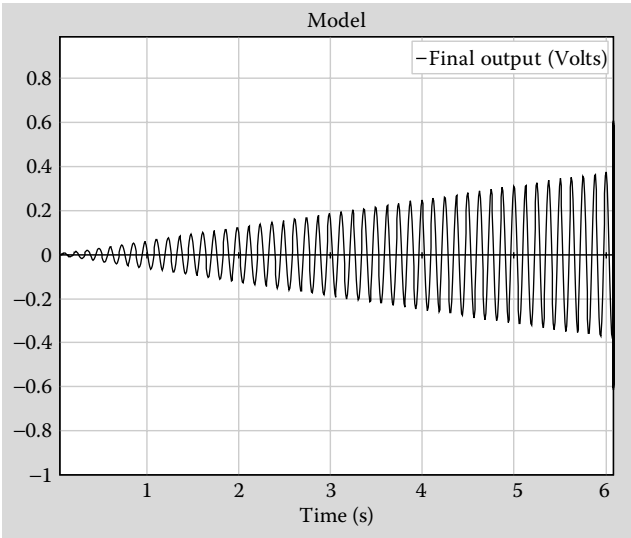


FIGURE 8.37
Output voltage obtained from simulation.

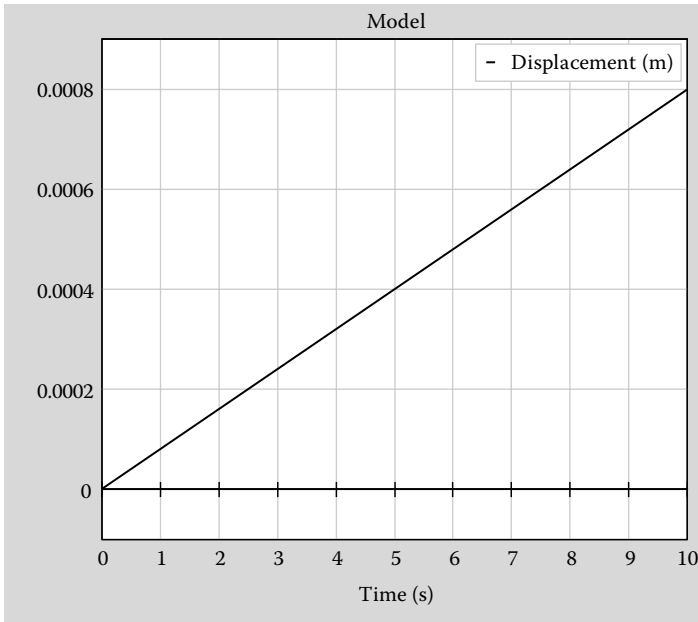


FIGURE 8.38

The displacement of the core used as input to the model.

The two plots shown here (Figures 8.37 and 8.38) indicate the raw voltage output as well as the actual displacement of the core. It is clear that the way the amplitude of the voltage increases is directly related to the actual displacement. The oscillation in the output is due to the oscillating input in the primary coil and will eventually be removed through proper signal conditioning. Thus, the output signal can be used to determine the distance moved.

EXAMPLE 8.5: A MAGNETIC SENSOR WITH A PERMANENT MAGNET

Figure 8.39 shows a seismic sensor that can be used to measure displacement, velocity, or acceleration of a body. The figure shows a permanent magnet of mass M that is supported by a spring, and there is some viscous damping between the magnet and the cover. The electric coil is fixed to the outer cover. The coil is assumed to have a length of l and a resistance of R_{coil} and inductance of L_{coil} , respectively; the permanent magnet exerts a field of B Tesla. The system is activated by the base motion, which results in the movement of the coil in the magnetic C-field, thus cutting the lines of force. This induces a voltage in the coil, and the voltage measured across the R_{out} (output resistance) works as the sensor output. The bond graph representation of this system is shown in Figure 8.40.

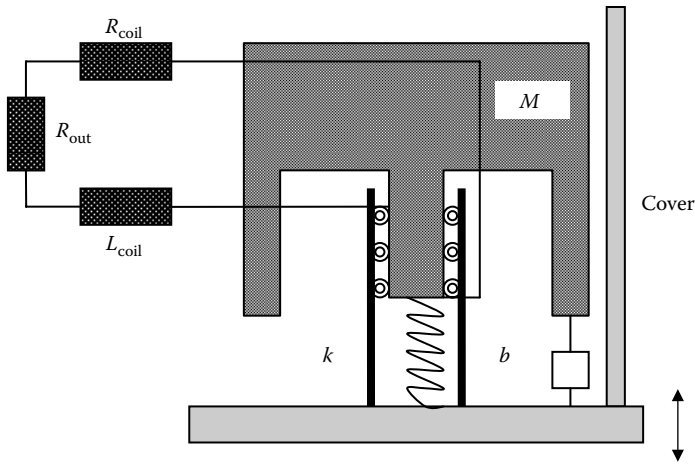


FIGURE 8.39
Schematic of the sensor.

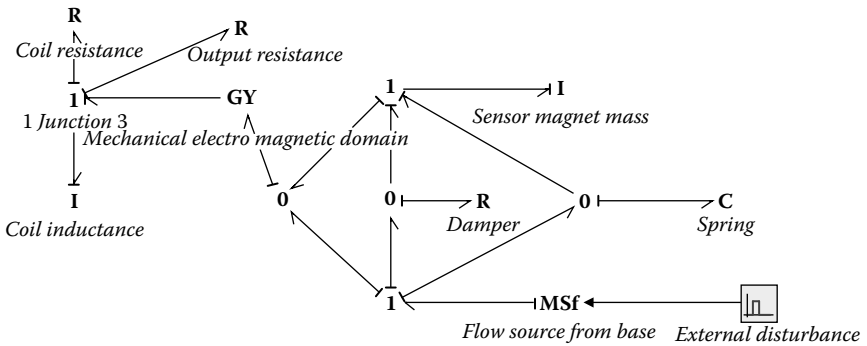


FIGURE 8.40
Bond graph model of the sensor.

Most of the components in this model are self explanatory. One item that needs some discussion is the gyrator factor. The GY member in the model represents the transformation from the mechanical domain to the electrical domain (via magnetics). In this particular case, there is a permanent magnet of strength B and the length of the coil in the magnetic C -field is l . The rate of change of displacement (velocity) on the mechanical side is directly responsible for the voltage induced on the electrical side in the coil; that is, electrical effort = $Bl(dx/dt)$, and the force induced on the mechanical side due to the movement of the coil in the magnetic C -field is directly proportional to the current in the coil; that is, mechanical effort = $Bl(i)$. Thus, the GY factor will have to be Bl .

The above system is simulated using the bond graph representation. For the purpose of this demonstration arbitrary values for the different parameters are assumed. The assumed values are shown in Figure 8.41.

The output results can be seen from the simulation plots shown in Figure 8.42. To simulate a more realistic seismic sensor, the input is modified by adding some random noise and the simulation is performed again. Graphs similar to the ones shown in Figure 8.42 are generated, and they are shown in Figure 8.43. This

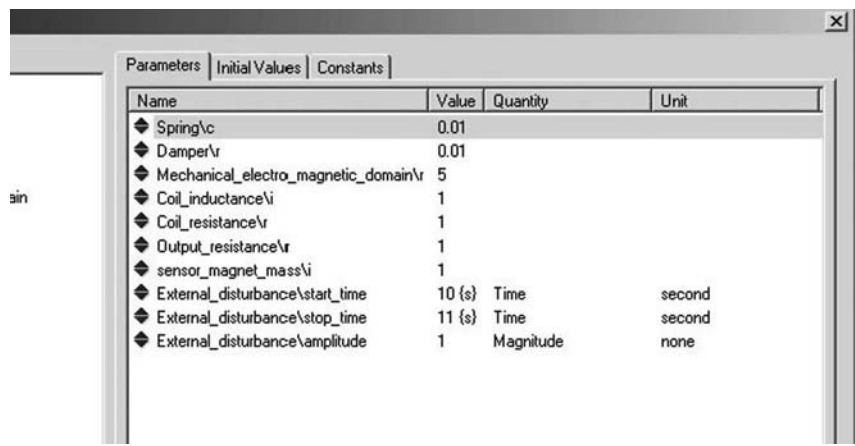


FIGURE 8.41
Parameters used to simulate system shown in Figure 8.41.

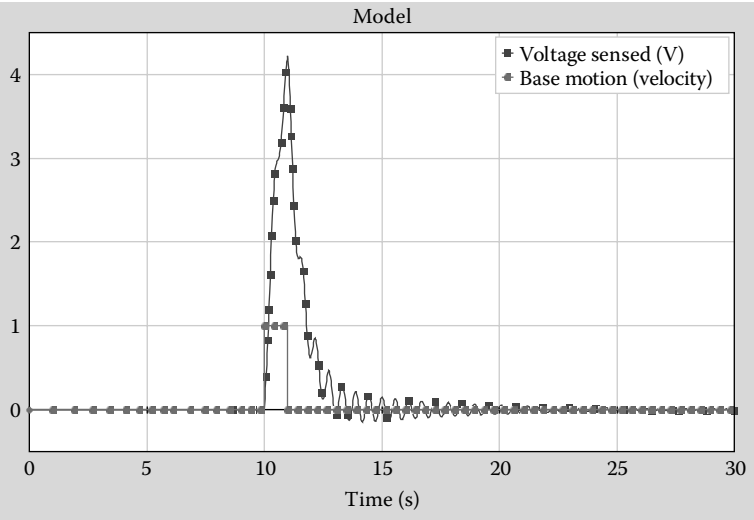


FIGURE 8.42
Base motion and induced voltage measured for the system in Figure 8.41.

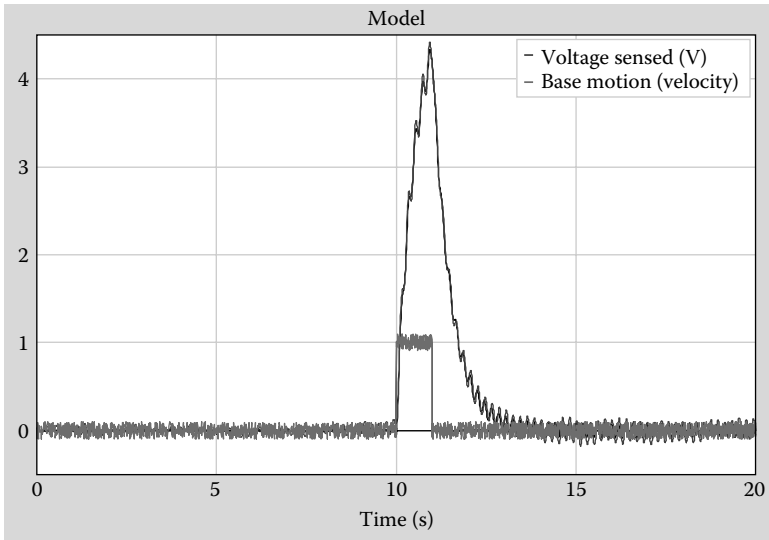


FIGURE 8.43
Simulation results with added noise in the input.

example demonstrates how this sensor would be working. In reality, when the sensor is designed, the sensor design parameters will be optimized so that the response function is cleaner. Signal conditioning circuits will also be used to clean out the noise in the signals, and so forth.

EXAMPLE 8.6: VARIABLE RELUCTANCE SENSOR—ROTATIONAL MOTION

Figure 8.44 shows two views of a variable reluctance sensor that may be used to measure displacement, velocity, or acceleration during rotational motion. This type of a sensor may be available in many configurations, and the figure shows only one possible configuration. An earlier example discussed a different configuration. The permanent magnet has an air gap, and a tabbed ring is able to rotate in a way such that the tab passes through the air gap. When the tab passes through the air gap, the reluctance/permeance of this set up changes. This induces an emf across the coil of wire wound around the magnet. The emf induced is proportional to the speed of rotation. Also, the frequency with which this induced emf occurs is a measure of the speed.

A different view of the schematic is shown in Figure 8.44, where the tab is about to approach the slot between the magnetic poles. To develop the governing equations, we can assume that the reluctance is equivalent to that of twice the air gap (because the permeability of the tab and the magnetic material may be assumed to be very high in comparison to that of air) when the tab is in between the poles and the reluctance. When the tab is not in between the poles, the reluctance is infinite. Permeance, the inverse of reluctance, varies accordingly. In the figure, some angular measures are shown to indicate when and how much of the tab lies in between the poles.

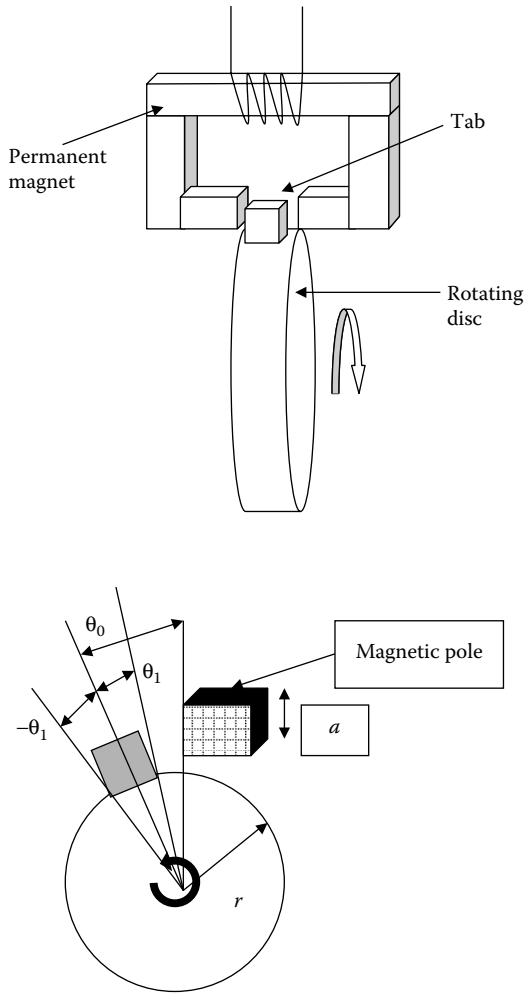


FIGURE 8.44

Two views of a variable reluctance sensor.

The reluctance for this situation may be calculated as:

$$R = \frac{2l_{\text{gap}}}{\mu_0 A} = \frac{2l_{\text{gap}}}{\mu_0 a r |(\theta_1 - \theta)|} \quad \text{for } -\theta_1 < \theta < \theta_1 \quad (8.49)$$

when θ is 0, the tab is perfectly aligned in the gap, and the reluctance is the minimum. As θ increases, the reluctance decreases until it shoots up to infinity when the angle moves beyond θ_1 . The absolute value is used to take

into account the situation when the tab is moving into the gap, as well as when it is leaving the gap.

Now, in order to develop a suitable bond graph model for this system, we consider the energy representation.

The energy in the magnetic C-field is $\frac{\phi^2}{2}$. Reluctance

Inside C-Field

$\dot{\phi}, \dot{x}$ are received

Integration of $\dot{\phi}$ to get ϕ , $\phi = \text{int}(\dot{\phi})$

Integration of \dot{x} to get x , $x = \text{int}(\dot{x})$

Differentiate energy w.r.t time:

$$\frac{d}{dt}(\text{Energy}) = \text{Power} \quad (8.50)$$

$$\frac{d}{dt}(\text{Energy}) = \frac{\partial}{\partial \phi} \left(\frac{\phi^2 \cdot R}{2} \right) \cdot \frac{d\phi}{dt} + \frac{\partial}{\partial x} \left(\frac{\phi^2 \cdot R}{2} \right) \cdot \frac{dx}{dt} \quad (8.51)$$

Power on magnetic side:

$$= \frac{\partial}{\partial \phi} \left(\frac{\phi^2 \cdot R}{2} \right) \cdot \frac{d\phi}{dt} = \text{effort} \cdot \text{flow} \quad (8.52)$$

Effort on the magnetic side:

$$\begin{aligned} &= \frac{\partial}{\partial \phi} \left(\frac{\phi^2 \cdot R}{2} \right) \\ &= \frac{2\phi R}{2} \\ &= \phi \cdot R \end{aligned} \quad (8.53)$$

$$= \phi R = \frac{\phi 2l_{\text{gap}}}{\mu_0 A} = \frac{\phi 2l_{\text{gap}}}{\mu_0 ar |(\theta_1 - \theta)|} \quad \text{for } -\theta_1 < \theta < \theta_1 \quad (8.54)$$

Outside the above range, the effort on the magnetic side will be infinite.

Power on mechanical side:

$$= \frac{\partial}{\partial \theta} \left(\frac{\phi^2 \cdot R}{2} \right) \cdot \frac{d\theta}{dt}$$

Effort on the magnetic side:

$$\begin{aligned}
 &= \frac{\partial}{\partial \theta} \left(\frac{\phi^2 \cdot R}{2} \right) \\
 &= \frac{\partial}{\partial \theta} \left(\frac{\phi^2 \cdot 2l_{\text{gap}}}{2\mu_0 ar |\theta_1 - \theta|} \right) \\
 &= - \frac{\phi^2 l_{\text{gap}}}{\mu_0 ar (\theta_1 - \theta)^2}
 \end{aligned} \tag{8.55}$$

In this particular set up, since it is a permanent magnet, ϕ can be considered to be nearly constant. So the mmf is essentially controlled by the variation of the reluctance. And for a coil wound around the permanent magnet, the mmf divided by the number of turns provides the current. The bond graph representation will be very similar to the bond graph of the linear variable reluctance sensor described earlier, and the development of the bond graph model and its simulation is left as an exercise for the reader.

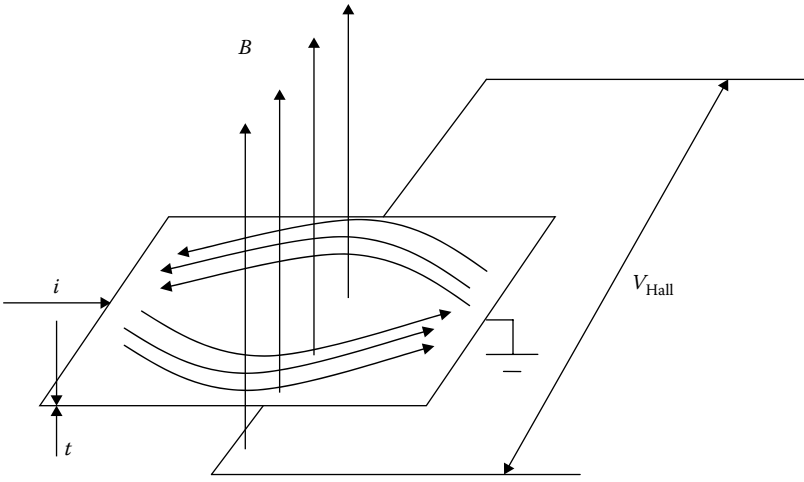
8.4 Hall Effect Sensors

Hall effect sensors are another class of sensors that uses the interaction of electric and magnetic field to monitor various different physical quantities such as force, motion, velocity, and so forth. The Hall effect sensors use two transduction mechanisms, electromechanical coupling based on the motion of charges in a magnetic field, and magnetoelectric coupling based on the Hall effect. This results in a coupling of voltage to the position of a magnet.

The Hall effect is named after Dr. Edwin Hall, who first noted this effect in 1879. When a magnetic field is applied in a direction perpendicular to a current carrying conductor (originally with uniform current density), not only is there a force on the conductor ($F = Bli$, Lorentz effect), it also tends to bend the current in a nonuniform way (Figure 8.45). Edwin Hall observed that this distortion in the current path tends to induce a voltage in a direction that is perpendicular to both the current path as well as the magnetic field. Measurement of this induced voltage can be used to link it to the effect that produced the distorted current path. One way to express this in a mathematical form is

$$e = \frac{R_H Bi}{t} \tag{8.56}$$

where i is the current, B is the magnetic flux density, t is the thickness of the conductor and R_H is the Hall coefficient of the material. Since Bli is

**FIGURE 8.45**

Schematic to demonstrate the Hall effect.

the force induced on the conductor the above relationship may also be expressed as:

$$e = \frac{R_H B l i}{l t} = \frac{R_H}{l t} F \quad (8.57)$$

This shows that there is a linear relationship between the voltage and the force. This could be represented in a bond graph model as a transformer element. This would also mean that an identical relationship exists between the flow parameters on both the sides of a transformer, that is, the velocity and the orthogonal current:

$$v = \frac{R_H}{l t} i \quad (8.58)$$

Although Hall effect sensors can be modeled as a transformer, it is not very practical to relate the force on a conductor with the voltage induced. These sensors are more practically used by varying the magnetic field by moving the magnet closer or farther away from the conductor. This way the magnetic flux density B becomes a function of x , the distance, and is not a constant anymore. Considering the original governing equation, we can modify it now as:

$$e = \frac{R_H B i}{t} = \frac{R_H B(x)}{t} i \quad (8.59)$$

Now the Hall effect relationship is expressed as a gyrator relationship where the current in the conductor is related to the Hall voltage induced. The gyrator coefficient is not a constant but a variable related to the variable B . Thus a more practical way of modeling a Hall effect sensor is through the use of a modulated gyrator.

Hall effect sensors are constructed in many different configurations depending on the particular application for which they are to be used. Most of these take advantage of the variation in the magnetic flux density by varying the distance between the sensor and the magnet. Figure 8.46 shows one configuration of the sensor application in velocity measurement. In this particular application, the gear ring is attached to the rotating device whose speed needs to be measured. The teeth pass in front of the sensor magnet (not shown in the figure) altering the magnetic field intensity. The Hall voltage varies proportional to the speed at which these teeth are passing in front of the sensor, and the output is measured to be a wave signal whose frequency determines the speed of rotation to be measured. The actual value of the voltage pulse may be irrelevant in this application since the frequency is what we need.

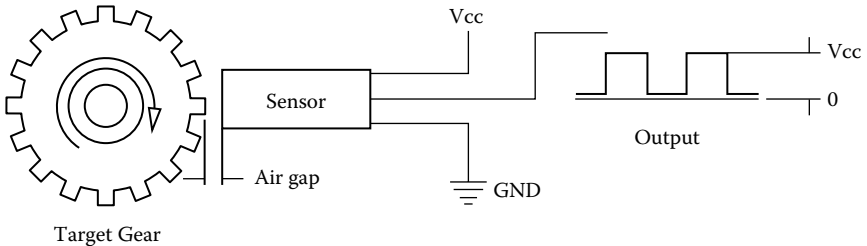


FIGURE 8.46

Hall effect sensor in a particular configuration.

The variation of magnetic flux density with distance is obtainable from magnet specification data sheet. Typically, this decay is somewhat similar to e^{-x^2} functions, where x is the distance from the magnetic pole (Figure 8.47).

A relatively straightforward bond graph representation of this sensor is shown in Figure 8.48. The gear ring is rotated at an input velocity represented by the source of flow “speed of rotation of ring,” and the damping resistance to rotation is represented by the resistive element attached to it. In more elaborate models, one can include the inertia term as well. The rotational speed is provided to the modulated gyrator as a signal. The input to the modulated gyrator is a current input to the Hall sensor. The output is supplied to an electrical resistor so that

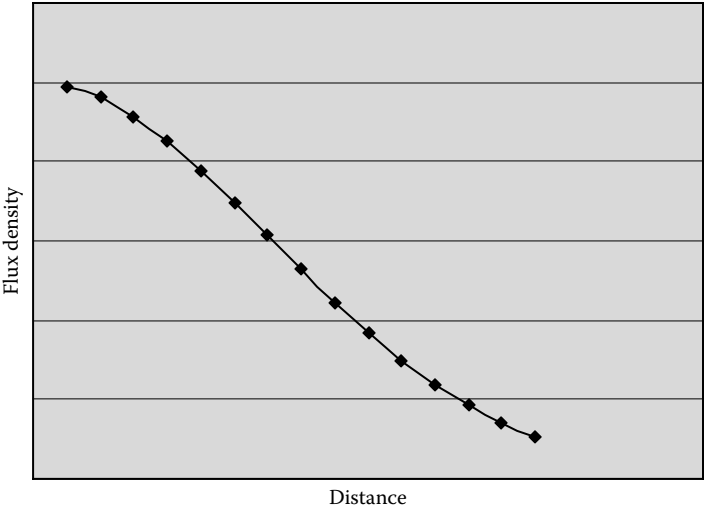


FIGURE 8.47
Variation of flux density with distance.

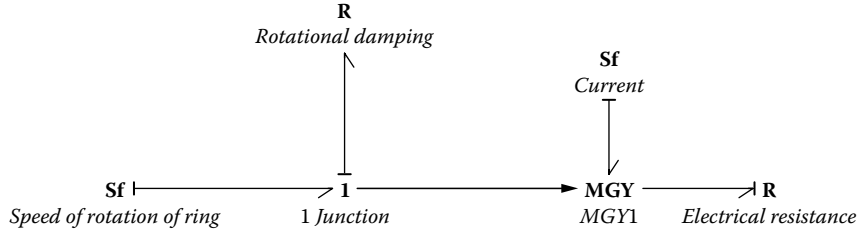


FIGURE 8.48
Bond graph representation of the configuration in Figure 8.47.

the voltage across that can be plotted. This approach is taken more for the modeling purpose than anything else so that the voltage output from the sensor can be easily tracked. For this model, the variation of B for the different distances have been taken as two discrete values, that is, when the tooth is nearest the sensor and when it is not. These two are called flux density when the distance is minimum and flux density when the distance is maximum, respectively. The other properties used in the simulation are shown in Figure 8.49, and the gyrator model is also shown below. The GY model essentially varies the GY factor similar to a square wave to model the passing of the gear teeth and root in front of the sensor.

Parameters Initial Values Constants			
Name	Value	Quantity	Description
◆ MGY1\RH	0.8		Hall coefficient
◆ MGY1\t	0.002		conductor thickness
◆ MGY1\Bzero	0.012		Flux density when the distance is minimum
◆ MGY1\B1	0.002		Flux density when the distance is maximum
◆ Rotational_damping\vr	1 {m.s/rad}	Rotational Friction C...	
◆ Speed_of_rotation_of_ring\flow	2 {rad/s}	Angular Velocity	
◆ Current\flow	48 {mA}	Electric Current	
◆ Electrical_Resistance\vr	1 {ohm}	Electric Resistance	

FIGURE 8.49

Parameters used for the simulation.

EXAMPLE 8.7: GY MODEL

Parameters

```
real RH = 0.8; //Hall coefficient
real t = 0.002; //conductor thickness
real Bzero = 0.012; // Flux density when the distance is
                    minimum
real B1 = 0.002; // Flux density when the distance is maximum
```

Variables

```
real B; //Flux density at any point in time during rotation
real fact; // Gyrator factor
real hidden s, half; // variables needed to generate the half
                    wave form
boolean hidden change; //variable needed to generate the half
                    wave form
```

Equations

```
"calculate at least 2 points per period
(just after the change in sign)"
half = pi / r;

change = frequencyevent (half, 1e-15);
"calculate the square wave"
s = sign (sin (r * time));
B = if( s == 0 ) then //computation of the B value
Bzero
else
```

```

((Bzero-B1) / 2) * (s + 1) + B1
end; // half wave form generation complete

fact = (B*RH)/t; //computation of gyrator factor
p1.e = fact* p2.f; //output calculation
p2.e = fact * p1.f; //output calculation

```

The voltage output of the sensor, as shown in Figure 8.50, is, thus, in the form of a square wave whose frequency is the same as the rotational speed of the rotating body.

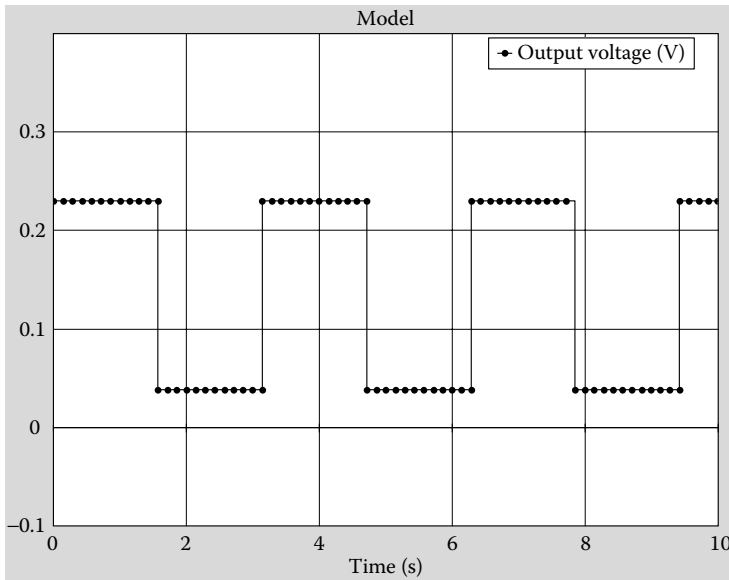


FIGURE 8.50

Output or measured voltage.

8.5 Piezo-Electric Sensors

Piezo-electric behavior, which is observable in some naturally occurring materials and some artificial materials, is a behavior where an electric potential may be induced in the material through the application of a force and vice versa. Examples of naturally occurring materials that exhibit this type of behavior are quartz crystals and Rochelle salt. There are many artificial piezo-electric materials such as polyvinylidene fluoride (PVDF), barium titanate (BaTiO_3), lithium sulphate (LS), and lead zirconium titanate (PZT).

The conversion of electrical pulses to mechanical movement and the conversion of mechanical movement back into electrical energy is the basis for piezo-electric crystals. The active element is the heart of the transducer as it converts the electrical energy to mechanical energy and vice versa. The active element is basically a piece of polarized material (i.e., some parts of the molecule are positively charged, while other parts of the molecule are negatively charged) with electrodes attached to two of its opposite faces. When an electric field is applied across the material, the polarized molecules will align themselves with the electric field, resulting in induced dipoles within the molecular or crystal structure of the material. This alignment of molecules cause the material to change dimensions. This phenomenon is known as electrostriction. In addition, a permanently polarized material, such as quartz (SiO_2) or barium titanate (BaTiO_3), will produce an electric field when the material changes dimensions as a result of an imposed mechanical force. This phenomenon is known as the piezo-electric effect.

In order to utilize this physical principle to make a sensor to measure force, we must be able to measure the surface charge on the crystal. A common method of using a piezo-electric crystal to make a sensor is to use two metal plates to sandwich the crystal, thus making a capacitor. As mentioned previously, an external force causes a deformation of the crystal and results in a charge that is a function of the applied force. In its operating region, a greater force will result in more surface charge. This charge results in a voltage $V = \frac{Q_f}{C}$, where Q_f is the charge resulting from a force f , and C is the capacitance of the device.

In the manner described above, piezo-electric crystals act as transducers that turn force or mechanical stress into electrical charge, which, in turn, can be converted into a voltage. Alternatively, if one were to apply a voltage to the plates of the system described above, the resultant electric field would cause the internal electric dipoles to realign, which would cause a deformation of the material. An example of this, piezo-electric transducers find use both as speakers (voltage to mechanical) and microphones (mechanical to electrical). Figure 8.51 shows two possible configurations in which the piezo-electric sensor can be operated. In the first case, the force axis and the voltage difference that is being measured are both longitudinal, whereas in the second case, they are transverse.

To model the piezo-electric sensors, one can take into account the following sets of relationships.

The charge induced in the crystal is directly proportional to the deformation in the crystal and the voltage induced is similarly proportional to the force applied. So the relationships can be written as $Q = n_{tr}\Delta x$ and $F = n_{tr}V$ where n_{tr} is the transformer modulus (or the proportionality

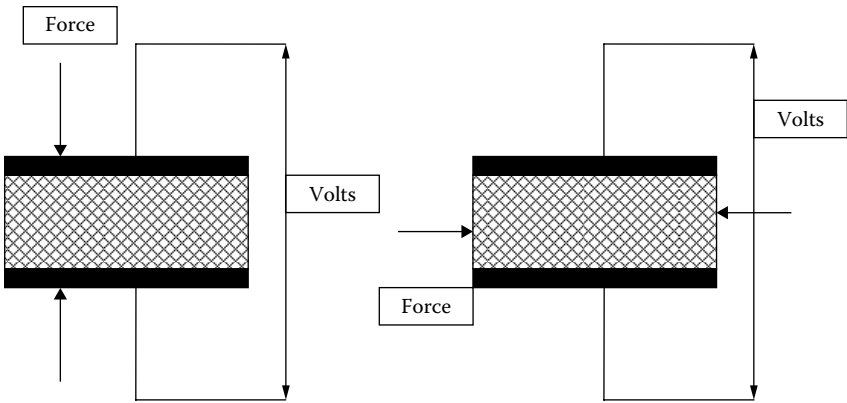


FIGURE 8.51
Two possible configurations of piezo crystals.

factor). Relating force to stress and subsequently to strain and displacement this same equation can be modified such that:

$$n_{tr} = \frac{d_{33}AE}{x} \quad (8.60)$$

where d_{33} is the piezo-electric charge constant, also known as piezo-electric coefficient, along the 3-3 direction or the longitudinal direction. If the force were perpendicular to the direction of voltage measurement, the constant would be different and we would represent it using the symbol d_{31} . Finally, on the electrical side, the voltage and the charge are related through the capacitance in the piezo crystal in a similar manner. If there are multiple layers of sensors, the transformer factor becomes:

$$n_{tr} = \frac{nd_{33}AE}{x} \quad (8.61)$$

where n is the number of layers.

Consider a situation where the piezo sensor is to be used to measure pressure inside a chamber. The schematic for the system is shown in Figure 8.52. This example is taken from the work of Cui et al. (2005)

Figure 8.52 shows a stack of “ n ” piezo crystals that have a mass of M , and the mount stiffness and damping coefficient is indicated in the figure. On the electrical side, the voltage generated from the piezo crystal is shown as a voltage source that is connected to the capacitance for the crystals and R represents leakage resistance across the piezo capacitance. The voltage is

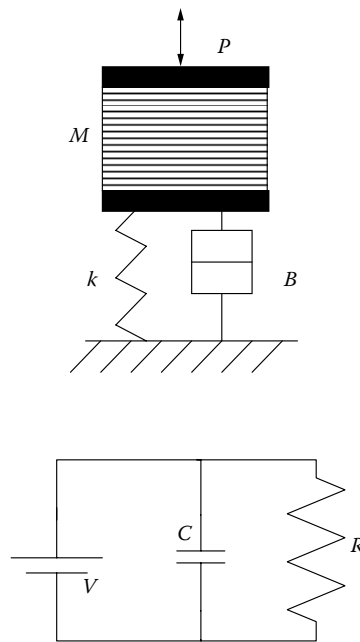


FIGURE 8.52
Schematic of the piezo sensor and the corresponding circuit.

measured across the capacitance. The bond graph model of this system is as shown in Figure 8.53.

The data used in simulating this system are as follows (Cui et al, 2005):

Parameters	Values
Piezo crystal mass	4.5E-3 kg
Mount stiffness	3E8 N/m
Mount damping	150 Ns/m
Outer diameter of ring	0.01 m
Inner diameter of ring	0.005 m
Piezo capacitance	9.12 pF
Leakage resistance	1000 Ohm (varied, see discussion)
Number of piezo rings	10
Young's Modulus	5.4E10 N/m ²
Piezo ring thickness	0.001 m
Area	5.853E-5 m ²
Charge constant	400E-12 m/V
Transformer mechanical to electrical	12.72

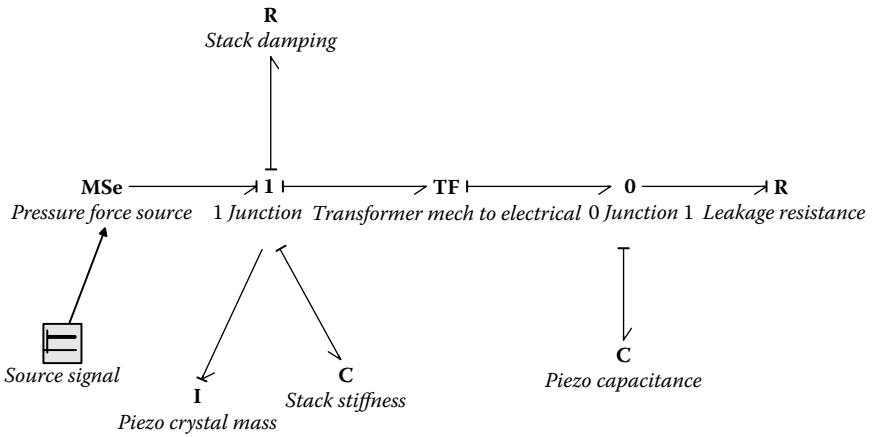


FIGURE 8.53
Bond graph model of the piezo sensor.

The transformer factor is calculated as:

$$n_{tr} = \frac{nd_{33}AE}{x} = \frac{10 * 400E - 12 * 5.4E10 * \frac{\pi}{4} (0.01^2 - 0.005^2)}{0.001} = 12.72 \quad (8.62)$$

The leakage resistance in the circuit plays an important role here. Once the charge develops across the piezo sensor, the leakage resistance and the resistance in the measuring device starts discharging the capacitor right away. The rate of this discharge is dependent on the time constant of this effective RC circuit (i.e., it is dependent on the value of RC). The charge developed at time zero directly correlates to the signal to be measured. Thus, in reality, signal conditioning circuits are needed to modify the output of this sensor so that accurate voltage may be measured. This can be achieved by a charge amplifier circuit, for example.

In the results shown, this effect is demonstrated by varying the leakage resistance value. Initially the leakage resistance is chosen to be an unrealistic value of 1000 ohms; the simulation results are shown in Figure 8.54. Then the leakage resistance value is increased to 1E9 ohms (once again, arbitrarily), and the result is shown in Figure 8.55. In both cases, we are plotting the voltage across the resistance (as the measurable output from the sensor for a 1000 N of applied force.)

Here, the solution is not only being affected by the very low value of leakage resistance, but it is also being affected by the simulation algorithm because it is not able to capture the proper peak because the step size needed is very small as a result of the discharge happening almost instantaneously.

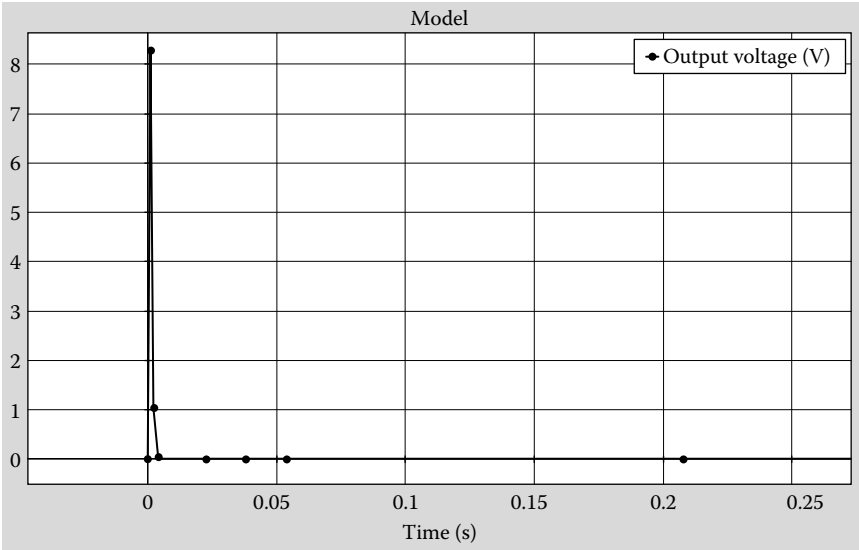


FIGURE 8.54
Measured voltage with 1000 ohm leakage resistance.

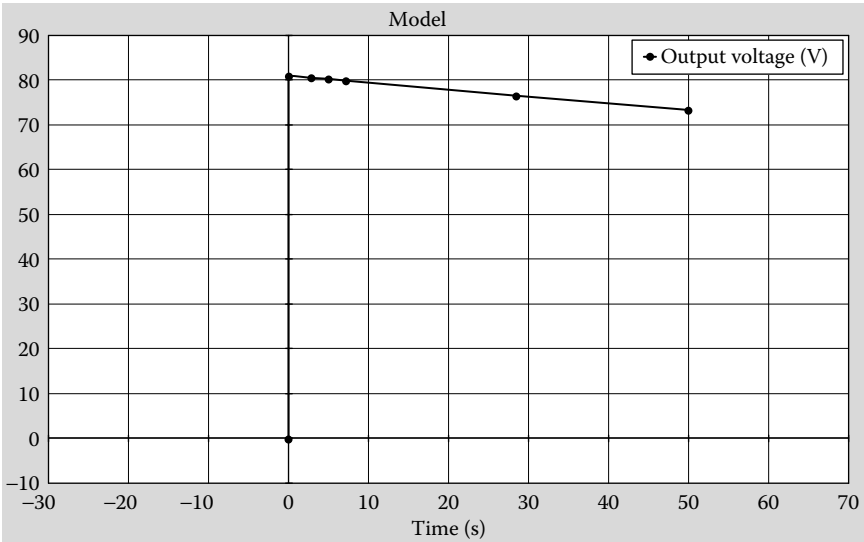


FIGURE 8.55
Measured voltage with 1 Gohm leakage resistance.

When the resistance is increased to 1 Gohms, the simulation shows the output voltage value of a little higher than 80 volts that is reached and is discharging very slowly because time constant is artificially increased

to a very high value by artificially increasing the leakage resistance. In reality, the leakage resistance is not easily controllable, but a signal conditioning circuit can be used to modify the output so that it can be easily discernable.

While the transformer based bond graph model is a commonly used approach for modeling a piezo sensor, the more consistent approach would be to use a C-field element. The rationale for this is that the piezo sensor stores energy that is made of multiple components, specifically, the energy due to the electric capacitive action, the energy from the elastic action, and the polarization energy. Thus, the total energy can be written as:

$$\text{Energy} = \frac{q^2(d+x)}{2\epsilon A} + Ep + \frac{kx^2}{2} \quad (8.63)$$

$$\frac{d}{dt}(\text{Energy}) = \frac{\partial}{\partial q} \left(\frac{q^2(d+x)}{2\epsilon A} \right) \frac{dq}{dt} + \frac{\partial}{\partial x} \left(\frac{q^2(d+x)}{2\epsilon A} + \frac{kx^2}{2} \right) \frac{dx}{dt} \quad (8.64)$$

$$\text{Electrical effort} = \frac{q(d+x)}{\epsilon A}; \text{Mechanical effort} = \frac{q^2}{2\epsilon A} + kx \quad (8.65)$$

So a C-field element may be used for modeling the piezo sensor as well with the above relationships as constitutive equations.

8.6 MEMS Devices

MEMS sensors and actuators have an important role in the modern engineering world. MEMS is an acronym for micro-electro-mechanical systems. Dimensions of MEMS devices are of the order of micrometers. Size is a particular advantage of these devices. Due to the advancement of miniaturization technology, sensors and actuators can be made that are light and occupy very little space. Yet they can perform the same types of tasks that are typically performed by macrosensors and actuators. Small sizes of MEMS devices also make it possible for users to implement sensors and actuators in applications that were hitherto impossible. Significant advancement in the field of integrated circuit manufacturing has been instrumental in the development of MEMS manufacturing as well. Several manufacturing techniques that have roots in IC manufacturing have turned out to be efficient techniques in making cost-effective and mass-produced MEMS devices. MEMS manufacturing techniques consist of lithography, chemical and optical etching, vapor deposition, and so forth.

MEMS sensors are now being used in a variety of different applications, such as in the measurement of pressure, force, vibration, angular rotation, temperature, tilt, and so forth. Behavior of microdevices is sometimes quite different from those of similar macrodevices because the relative importance of the different phenomena in the small scale is quite different from those in macrodevices. For example, in a macrosystem, gravitational force is a lot more important than surface forces such as surface tension. This is due to the difference in the orders of magnitude of the two. However, at microscale, this may not be true because the mass is significantly reduced, and the orders of magnitude of these two forces could be comparable.

MEMS sensors and actuators are a part of the emerging systems that are key components of the mechatronics world. There are many MEMS sensors and actuators that are currently used in engineering products, such as automobiles and aircraft as well as household appliances. Common transduction modes used in MEMS devices are: electrostatic, electromagnetic, thermal, piezo-electric, piezomagnetic, and so forth.

There are numerous books in the market on the subject of MEMS. A very comprehensive discussion of microtransduction may be found in the book by Lobontiu and Garcia (2005). *Modeling of MEMS and NEMS*, by Pelesko and Bernsstein (2003), is another text that addresses the modeling of MEMS devices. A good introductory text on MEMS and microsystems is by Hsu (2001). In this text, we are not going to attempt to model every possible MEMS device. Other texts have already done a very good job of it. We will, instead, provide a taste of how the bond graph methodology may be used in modeling MEMS devices.

MEMS devices can be modeled in much the same way as their macroscopic counterparts. The aspects that need some attention are identifying the relative importance of different phenomena in determining system behavior. Two of the very critical aspects of MEMS modeling are microsusensions and microactuation. Microsuspension deals with specific design and construction of different means to suspend/support the micromass or other parts of the device. From the modeling perspective, a closer understanding of microsuspensions helps the modeler determine the stiffness and damping characteristics of the device itself. Microactuation deals with energy conversion, for example, energy conversion of fluid flow to a voltage, pressure to displacement, magnetic to electric, and so forth.

In their book on the mechanics of microelectromechanical devices, Lobontiu and Garcia (2005) have devoted a long section on the discussion of the microsuspensions. They have discussed in detail how the suspension models for a variety of geometric configurations ranging from simple cantilevers to serpentine springs may be developed from first principles. In a bond graph model for such a device, all one has to do is incorporate the specific suspension model in the bond graph. Lobontiu and Garcia have also devoted a long section on microactuation where many of the basic actuation methods and their mathematical relationships are discussed.

8.6.1 MEMS Examples

8.6.1.1 Microcantilever-Based Capacitive Sensors

Microcantilevers are one of the most important components of many MEMS devices because they provide a simple mechanism where the elasticity of the structure can be effectively used to relate the source that causes the deflection and the measurement of that deflection using one of the many ways such as capacitive, resistive, or magnetic methods. Microcantilevers are used in accelerometers, pressure sensors, flow sensors, and in many other configurations. Figure 8.56 shows a schematic of a microcantilever that is deflected due to a external force acting at the end point of the cantilever.

The transduction mechanism for this sensor could be capacitive. A portion of the free end of the cantilever is part of a parallel plate capacitor. The capacitor response changes as a result of the bending of the cantilever and associated change in the distance between the plates, and this is measurable through the measurement of the voltage drop across the plates.

From basic mechanics of materials, it can be shown that the equation for a deflected beam due to an end load may be written as:

$$y = \frac{P}{6EI}(x^3 - 3Lx^2) \quad (8.66)$$

where E and I are the Young's modulus and the second moment of area of the beam cross-section respectively, x is the distance measured from the fixed end, and L is the length of the whole beam.

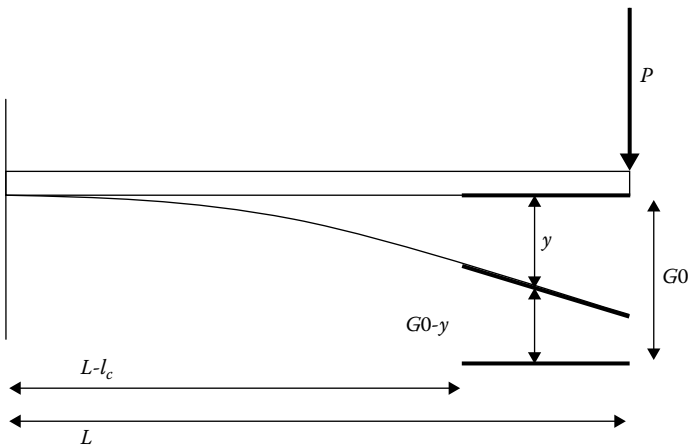


FIGURE 8.56
Schematic of a microcantilever.

As shown in the figure, the variable gap over the length $L-l_c$ through L can be expressed as G_0-y where G_0 is the gap between the undeformed cantilever and the fixed plate and y is the deflection at any point.

When the cantilever is undeformed, the capacitance of the parallel plate capacitor is given by:

$$C = \frac{\epsilon A}{G_0} = \frac{\epsilon l_c w}{G_0} \quad (8.67)$$

where the l_c is the length of the capacitor, and w is the depth. G_0 is the constant gap between the plates.

When the beam is deformed, the gap between the plates is not uniform. At this point, the capacitance for a small overlap length dx may be written as:

$$dC = \frac{\epsilon w dx}{\left(G_0 - \frac{P}{6EI} (x^3 - 3Lx^2) \right)} \quad (8.68)$$

An expression for the capacitance of the whole capacitor will be

$$C = \int_{L-l_c}^L \frac{\epsilon w}{\left(G_0 - \frac{P}{6EI} (x^3 - 3Lx^2) \right)} dx \quad (8.69)$$

The integration of this expression is nontrivial but could be performed either analytically or numerically.

The energy stored in the capacitor is given by:

$$\text{Energy} = \frac{q^2}{2C} \quad (8.70)$$

and the derivative of the energy with respect to q and x provides us with the voltage induced on the electrical side and the force on the mechanical side, respectively.

$$\frac{d(\text{Energy})}{dt} = \text{Power} = \frac{\partial(\text{Energy})}{\partial q} \frac{dq}{dt} + \frac{\partial(\text{Energy})}{\partial x} \frac{dx}{dt} \quad (8.71)$$

This approach has been discussed before for macrocapacitive sensors, and the same procedure may be applied to develop the model in this case

as well with a capacitive field element from the bond graph library much the same way as we have modeled other capacitive sensors.

8.6.1.2 Comb Drives

Figure 8.57 shows schematic of a comb drive. As is the microcantilever, the comb drive is also a very commonly used component in many MEMS devices. It can be used both as a sensor and as an actuator. The basic operational principle in this case is also through the alteration of the capacitance as there is relative motion between the two sides of this drive. The device can be designed to work with linear motion, angular motion, and so forth. The advantage of the comb drive over the more traditional parallel plate capacitor is that the capacitance obtained is N times that between a pair of plates where N is the total number of pairs of surfaces that are in use. This configuration enables the designer to get higher capacitance (and hence, better response) in a very small space. Bond graph modeling of this device follows the exact same process as the previous examples of capacitive sensors where the C-field element was used.

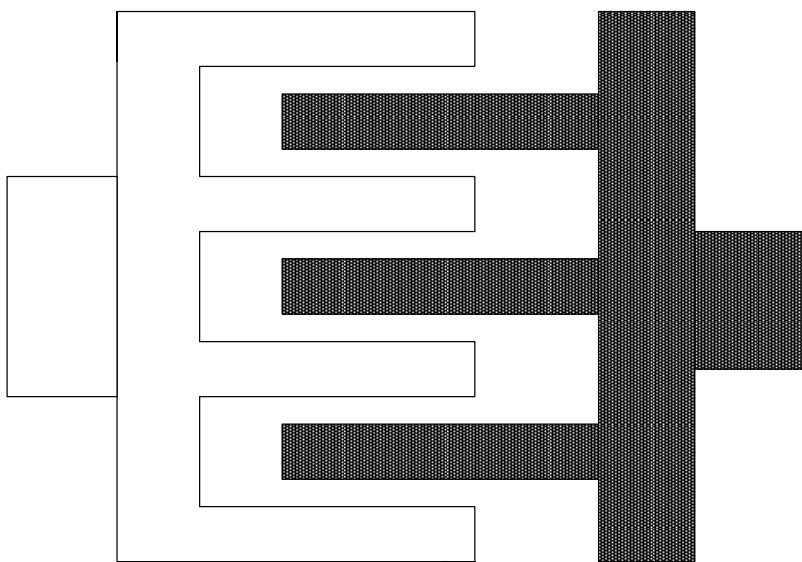


FIGURE 8.57

Schematic of a comb drive.

8.6.1.3 MEMS Gyroscopic Sensors

Gyroscope sensors are used to measure tilts or angular rotations in roll, yaw, or pitch directions. These sensors are key components in vehicle stability systems. Traditional gyroscopes are usually large and bulky. But

MEMS technology has enabled designers to design and fabricate micro-size gyro sensors. The schematic shown in the Figure 8.58 shows a view of the design used for these types of gyroscopes. The design consists of a mass that is mounted inside a casing and is free to vibrate in two mutually perpendicular directions, shown as X and Y directions in the figure. The casing in turn is mounted on a body that can tilt about the Z (axis perpendicular to the X and Y directions) and hence the casing tilts with the body as well. This angular rotation of the casing interacts with the velocities in the X and Y directions and produces an additional force on the mass in the X and Y directions. These forces are called Coriolis forces. Equation 8.72 shown are the equations of motion of the mass in the X and Y directions.

$$\begin{aligned} m\ddot{x} + B_1\dot{x} + k_1x &= F_1 + 2m\dot{\theta}\dot{y} \\ m\ddot{y} + B_2\dot{y} + k_2y &= F_2 - 2m\dot{\theta}\dot{x} \end{aligned} \quad (8.72)$$

In the two equations, not only are the elastic springs included but a term due to damping is included as well. Published work shows that designs of these types of gyros have been developed both with and without damping (Piyabongkarn and Rajamani [2002], Kim and Chun [2002]). The excitation force is applied in one of the two directions (usually X), and the motion of the mass is sensed in the other direction (usually Y). As Kim and Chun (2002) have described, in order to minimize damping, the system is usually operated in a vacuum. If we do not consider the damping

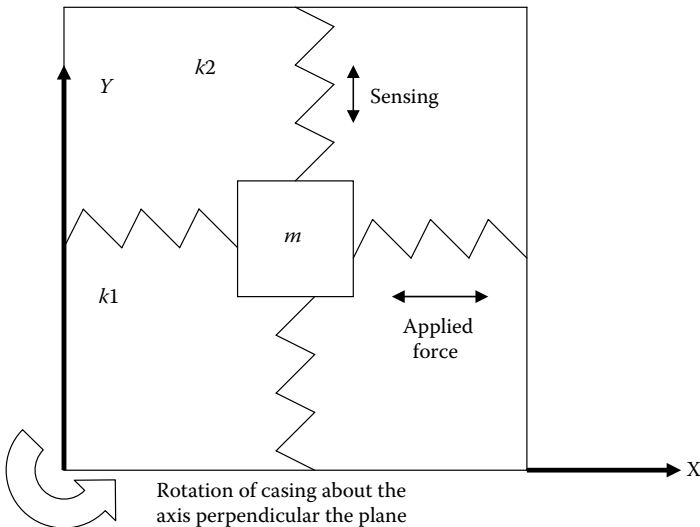


FIGURE 8.58
Schematic of the gyroscopic sensor.

and the external force acts only in one direction, the equations of motion will be slightly different (Equation 8.73)

$$\begin{aligned} m\ddot{x} + k_1x &= F_1 + 2m\dot{\theta}\dot{y} \\ m\ddot{y} + k_2y &= -2m\dot{\theta}\dot{x} \end{aligned} \quad (8.73)$$

In this model, the motion in the sensing direction can be shown to be

$$\Delta y = \frac{F_{\text{cor}} Q_y}{m\omega_y} \frac{1}{\sqrt{(\omega_x^2 - \omega_y^2)^2 + \frac{(\omega_x\omega_y)^2}{Q_y^2}}} \quad (8.74)$$

where Δy is the measurement in the y direction, ω_y and ω_x are the natural frequencies in the two directions respectively, m is the mass, and Q_y is the quality factor for the motion in the y direction. F_{cor} is the Coriolis force that is acting for the motion in the y direction and is equal to $2m\dot{\theta}\dot{x}$. Thus, from the displacement measurement in the y direction, the angular rate can be computed. The quality factor for the motion in the y direction can be written as:

$$Q_y = \frac{\sqrt{mk_y}}{B_2} \quad (8.75)$$

where B_2 is the damping coefficient.

Figure 8.59 shows the bond graph representation of this system. The bond graph representation models the spring–mass–damper system with a degree of freedom in both X and Y directions. The rotation about the Z axis is modeled through the modulated source of flow that in turn generates the Coriolis forces for both X and Y direction motion.

Initially the simulation was performed using parameter values shown in Figure 8.60. As discussed earlier, external excitation is provided in one direction (X in this case), and the motion of the mass is tracked in the second direction (Y in this case). This is why the forcing function on X is taken to be a non-0 value and that on Y is 0. There is an additional forcing function on both X and Y directions due to the Coriolis force, as described in the equations. The sensing is done in the Y direction, and from both the amplitude and the frequency measurements, one can determine the velocity of rotation in the Z direction. The y displacement obtained from the simulation is shown in Figure 8.61 (it is obtained by integrating the output velocity). This result combined with Equation 8.74 can be used to determine the angular rotation velocity.

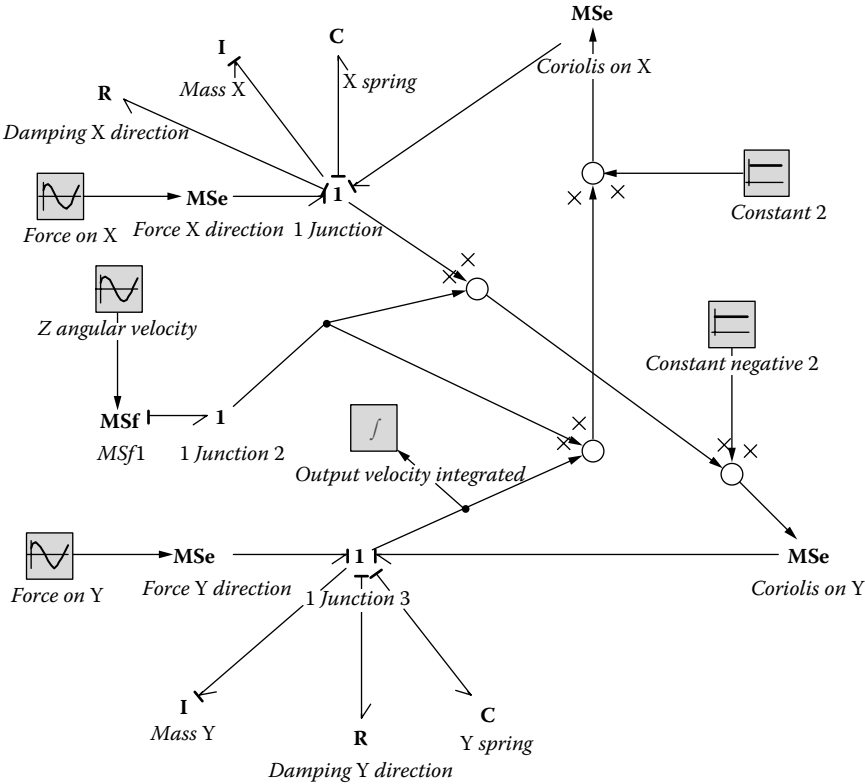


FIGURE 8.59
Bond graph model of the MEMS gyroscope.

Parameters					
Initial Values					
Constants					
Name	Value	Quantity	Unit	Arithmetic Type	
Damping_X_direction/r	0			Real	
Damping_Y_direction/r	3480			Real	
Mass_X/i	9.425e-010			Real	
Mass_Y/i	9.425e-010			Real	
Force_on_Y\amplitude	0			Real	
Force_on_Y\omega	0 (rad/s)	Angular Velocity	radian per second	Real	
Force_on_Y\phase	0 (rad)	Plane Angle	radian	Real	
Force_on_X\amplitude	1			Real	
Force_on_X\omega	515 (rad/s)	Angular Velocity	radian per second	Real	
Force_on_X\phase	0 (rad)	Plane Angle	radian	Real	
X_spring/c	0.00025			Real	
Y_spring/c	0.00025			Real	
Constant_2/C	2			Real	
Constant_negative_2/C	-2			Real	
Z angular_velocity\amplitude	1			Real	
Z angular_velocity\omega	20 (rad/s)	Angular Velocity	radian per second	Real	
Z angular_velocity\phase	0 (rad)	Plane Angle	radian	Real	

FIGURE 8.60
Parameters used for the gyro simulation.

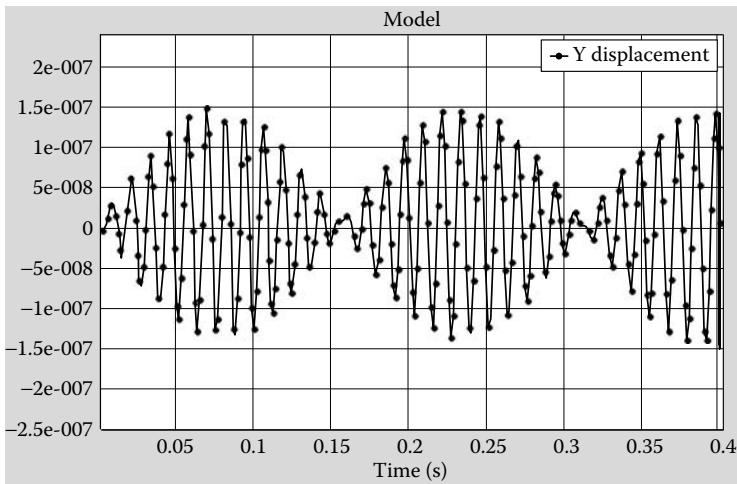


FIGURE 8.61
 y displacement of the mass.

The FFT analysis of the y displacement (Figure 8.62) shows that there are two dominant frequency contents in the output spectrum. They are 495 rad/sec and 535 rad/sec. These two frequency values are the sum and difference of the two forcing frequencies in the model, that is, 515 rad/sec and 20 rad/sec. If we look closely at the second equation in Equation 8.72, the forcing function is a product of velocity in y direction and velocity in

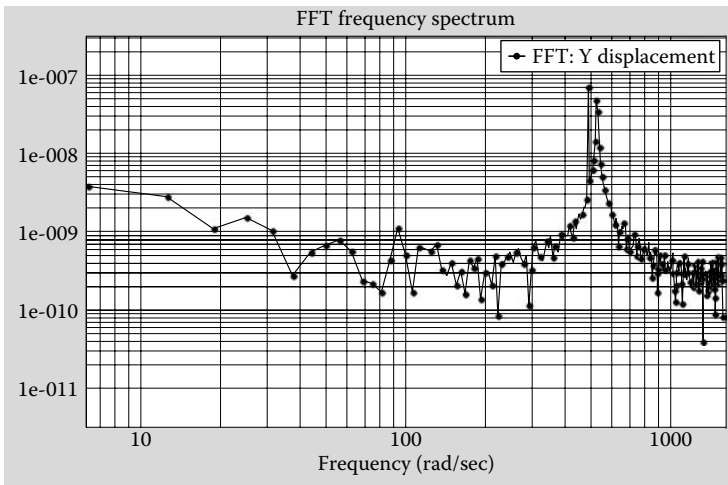


FIGURE 8.62
FFT of y displacement.

z direction, both of which are sinusoidal and these can be expressed as a sum of two sinusoidal functions whose frequencies are the sum and difference of the original forcing functions in the product.

The simulation was redone using a ramp input for angular displacement, and its slope as the angular velocity as shown by Figure 8.63. This replicates a constant velocity input. And the simulation was performed twice by keeping every other parameter the same except the slope of the angular displacement (i.e., angular velocity) about the Z axis. The slope was chosen a particular value first and then doubled for the second simulation. The two plots in Figure 8.64 show the Y response for the two cases, and it is clear that the amplitude of one response is twice that of the other. This confirms how the y displacement can be used to calculate the angular velocity about the z direction.

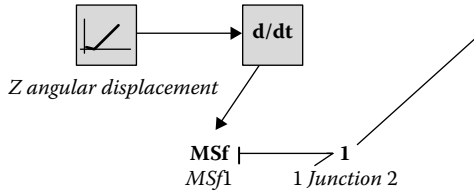


FIGURE 8.63

Alternate Input function (constant velocity).

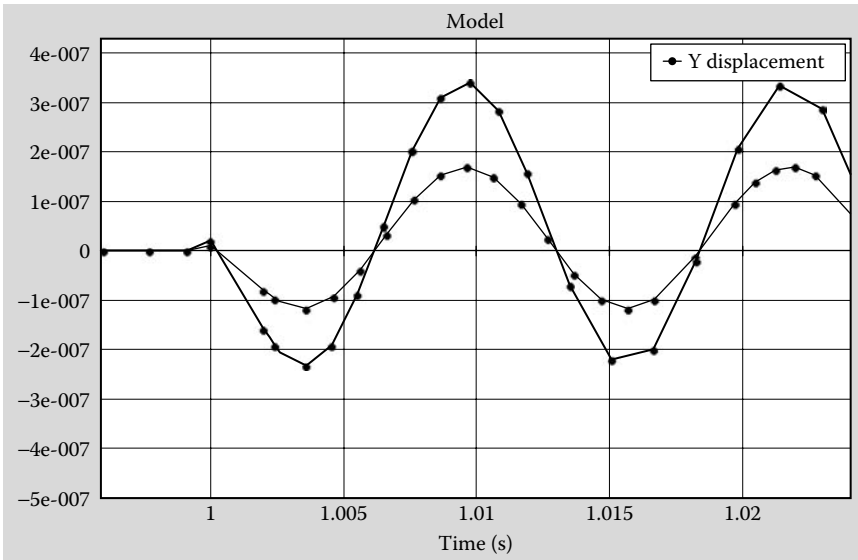


FIGURE 8.64

Y -displacement for the two different angular velocity inputs (one double the other).

8.7 Sensor Design for Desired Performance— Mechanical Transducers

As we have seen, different basic physical phenomena may be used to sense a whole variety of things, including physical movement, forces and torques, humidity, temperature, and so forth. Although the physical phenomena used may be the same, sensor design for different applications needs to be done in a way such that the sensor is able to provide high level of sensitivity for the physical quantity being measured. In order for this to happen, the components that make up a sensor need to be properly designed. Sensitivity analysis has been used in traditional design techniques to determine suitable design parameters for these types of applications. The bond graph technique offers a different and perhaps more powerful approach towards achieving the same goal. Since the bond graph methodology automatically tracks the power (and therefore, the energy) that is being stored/dissipated in each component, the relative power “use” in each component can be used to design the components for desired behavior. Due to the specific formulation of the bond graph method, no additional simulation/calculation needs to be done in order to use this approach. This makes the bond graph technique a very powerful design tool as well. In this section, such a design problem is discussed in some detail to illustrate how bond graphs may be used for the stated purpose.

For our discussion, we will consider sensors that use motion of a mechanical device, for example, a spring–mass–damper arrangement to sense the signal that needs to be tracked (Figure 8.65). Some very common examples of sensors that fall in this category are accelerometers, seismometers, geophone, and so forth. These and other sensors may use motion to measure quantities such as force, velocity, displacement, pressure, flow rate, temperature, and so forth. The basic construction of these sensors is simple; it consists of a spring–mass–damper system as shown in the figure. The corresponding bond graph is also shown.

The base motion is the disturbance that has to be measured. But by modifying the relative importance of the mass, spring, and the damper in this system, the sensor can be used to measure the various quantities such as displacement, acceleration, and velocity.

For a system such as this, the well-known equation of motion can be written as:

$$m\ddot{r} + C\dot{r} + kr = -m\ddot{u} \quad (8.76)$$

where m is the mass, C is the damping coefficient, k is the spring constant, \ddot{u} is the input displacement from external source (i.e., the signal to be measured), and r is the relative displacement between the base and the mass itself.

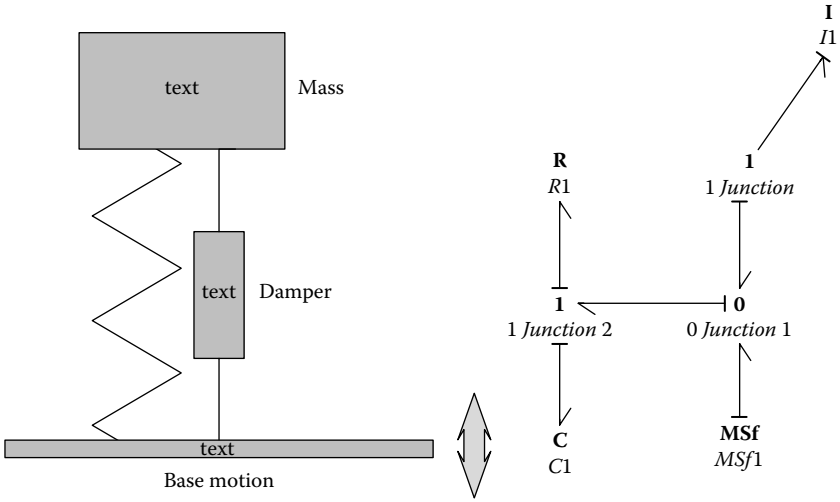


FIGURE 8.65
Schematic for the sensor.

By altering the relative magnitude of the three quantities, mass, spring constant, and the damping coefficient, the system can be used for a displacement measuring device, acceleration measuring device, or a velocity measuring device. The concept works in the following fashion:

In the above equation, if:

$$|m\ddot{r}| \gg |C\dot{r} + kr| \quad \text{then} \quad m\ddot{r} \approx -m\ddot{u} \Rightarrow r \approx -u \quad (8.77)$$

and this arrangement then works as a displacement sensor because the measured relative displacement is directly equivalent to the applied displacement. The seismometer is one such sensor.

As an alternate situation, if:

$$|kr| \gg |m\ddot{r} + C\dot{r}| \quad \text{then} \quad kr \approx -m\ddot{u} \Rightarrow r \approx -\frac{m}{k}\ddot{u} \quad (8.78)$$

Since r is the quantity being measured, in this case, it is directly related to the acceleration of the external source and therefore it works as an accelerometer.

The third possibility is if:

$$|C\dot{r}| \gg |m\ddot{r} + kr| \quad \text{then} \quad C\dot{r} \approx -m\ddot{u} \Rightarrow r \approx -\frac{m}{C}\dot{u} \quad (8.79)$$

Once again, because r will be measured, it is relatable directly to the velocity of the input disturbance and, therefore, for this special condition, the sensor works as a velocity measuring sensor.

In designing these types of sensors, one has to decide what kind of parameter values need to be used in order to achieve one of the above three special cases, and that decision is not easy because relative comparison of the magnitudes of m , k , and C are not enough to provide the right answer. In order to help us with an answer for this, we will introduce a new quantity here. It is called “activity.” Activity is a term used to indicate energy associated with each of the components that make up the system. By measuring the activity associated with each component in the model, we can determine how much of the total energy in the system goes into each component in the system. The relative activity of each system will in turn tell us the relative importance of each component in the system. In other modeling approaches, it could be hard to keep track of the energy, but in the bond graph method, that is very easy since the product of effort and flow is the power and the time integral of the absolute value of power can be tracked as the activity associated with each component. To calculate the activity in a model a very simple statement or two of code is necessary as shown next.

Variables

```
real power;
real activity;
```

Equations

```
state = int(p.e);
p.f = state / i;
power = p.e*p.f;
activity = int (abs(power)); // integral of the absolute
                             value of power
```

As these few lines of code that can be used for the I element illustrate, power in each element is easily calculated from the product of effort and flow and is integral to activity.

To explore how this concept works, we can consider the bond graph in Figure 8.66 (same as the bond graph for the spring-mass-damper system seen before with a few integral elements to calculate the displacements). A derivative box is added to calculate the acceleration.

The I , C , and R elements represent the mass, compliance (inverse of stiffness), and the damping coefficients, respectively. All three of these elements have been modified to calculate the activity. The input to the Msf is a cosine function. The properties used for the initial analysis are shown in Figure 8.67.

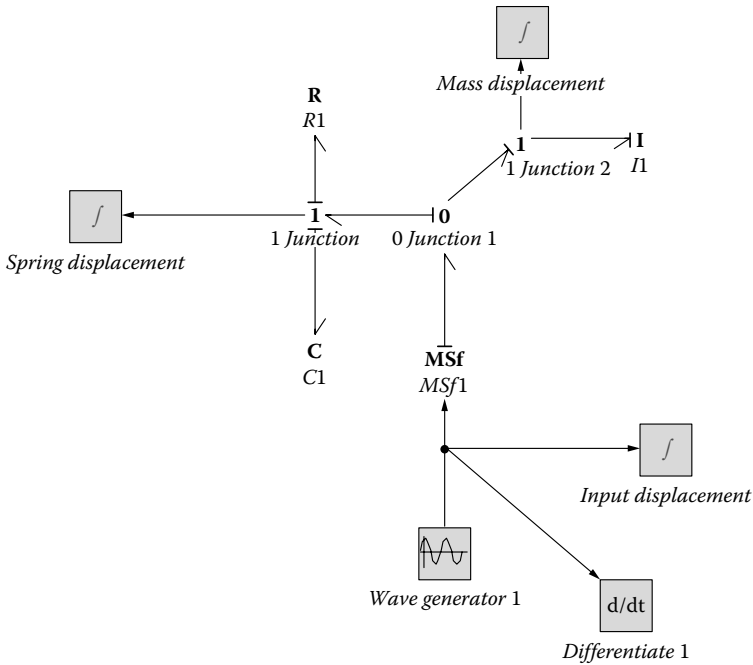


FIGURE 8.66
Modified bond graph to calculate the activities.

Parameters Initial Values Constants				
Name	Value	Quantity	Unit	Arithmetic
I1\i	0.5 (kg)	Mass	kilogram	Real
R1\i	10 (mN.s/m)	Friction	newton second per ...	Real
C1\c	700 (mm/N)	Compliance	meter per newton	Real
WaveGenerator1\amplitude	1	Magnitude	none	Real
WaveGenerator1\omega	1 (rad/s)	Angular Velocity	radian per second	Real

FIGURE 8.67
Parameters used.

For this set of parameters, the activity plots for the three components are as shown in Figure 8.68. As the plot shows, the damping effect is negligible, but the spring and mass activities are comparable.

To see the relative importance of parameters now, the mass is changed to 50 kg and the plot changes as shown in Figure 8.69. Clearly, now the activity in the spring is far more than the other two components. Under these

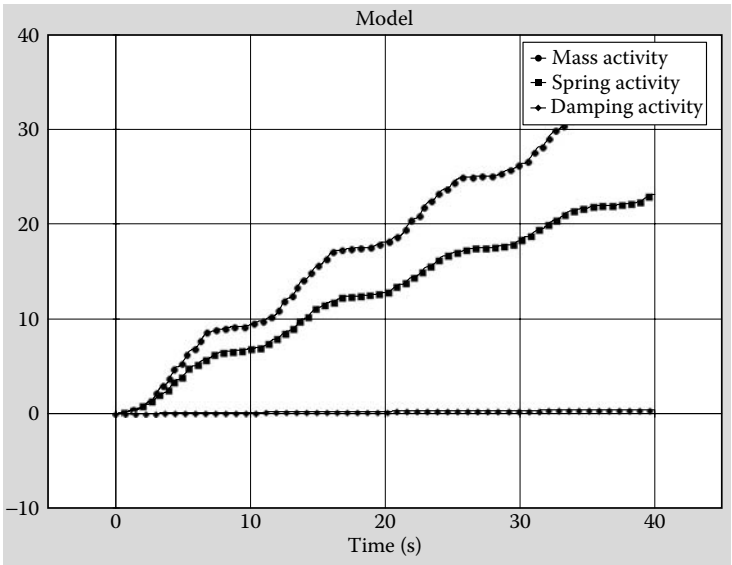


FIGURE 8.68
Relative activity values for the three components.

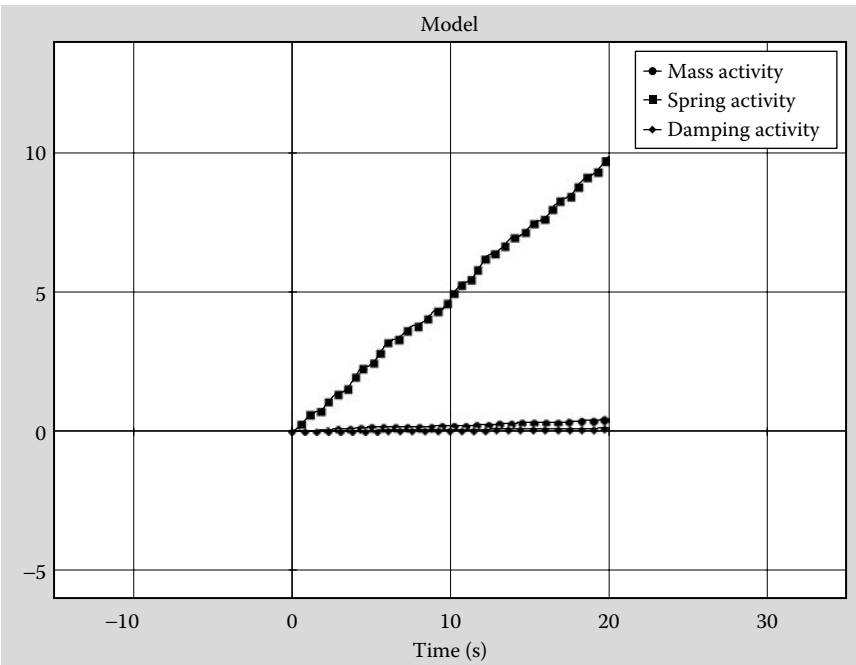


FIGURE 8.69
Activity values with mass = 50 kg.

conditions, the sensor is going to work as an accelerometer (as discussed before). The next plot (Figure 8.70) shows the acceleration associated with the input and the displacement for the spring element, and we can see that one is clearly a negative of the other, so a measurement of the spring displacement will show how much the acceleration is, just as the equations before indicated.

If we change the input parameters such that the mass is back to 0.005 kg and the compliance is 70 mm/N (inverse of stiffness) and plot the activity plots, we get Figure 8.71. This shows that the mass-activity is significantly higher than the activity in the spring and the damper. In this case, the displacement associated with the mass should be indicative of the overall displacement. The next plot (Figure 8.72) shows that, indeed, it is true. Now the sensor works as a seismometer.

If we alter the parameter values so that mass is 50 kg, damping coefficient is 1 Ns/m and compliance is 700 m/N. The activity plot is shown in Figure 8.73.

Clearly, in this case, the activity in the damper is far higher than in the mass and the spring. So this sensor should be dominated by the damper and will work as a velocimeter. Figure 8.74 compares the input velocity and the damper displacement (same as mass displacement). The plot shows the two quantities to be essentially the same with only a small phase shift. So this arrangement can be used to measure velocity.

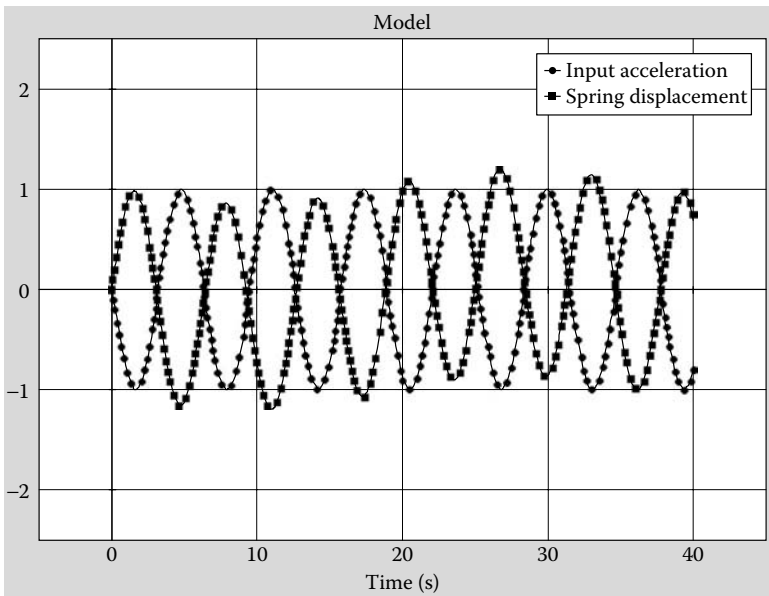


FIGURE 8.70

System response when activity for the spring is dominant.

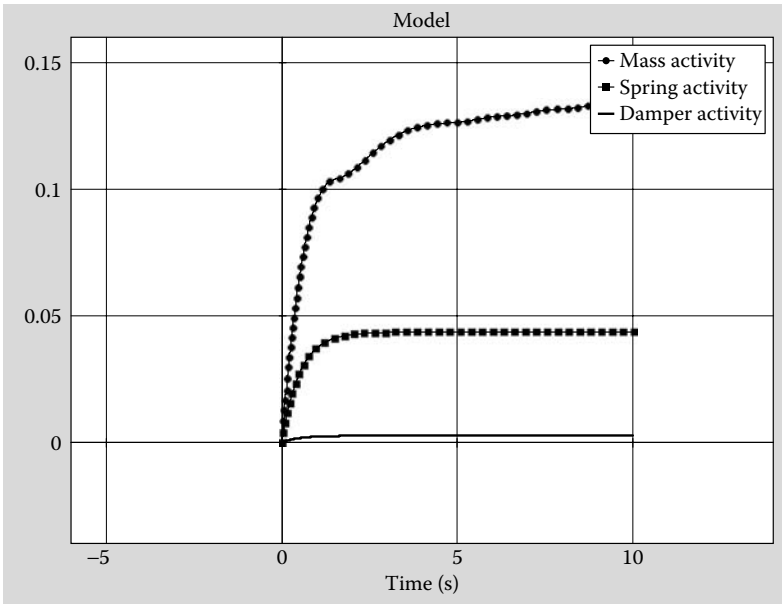


FIGURE 8.71
Relative activity with dominant mass activity.

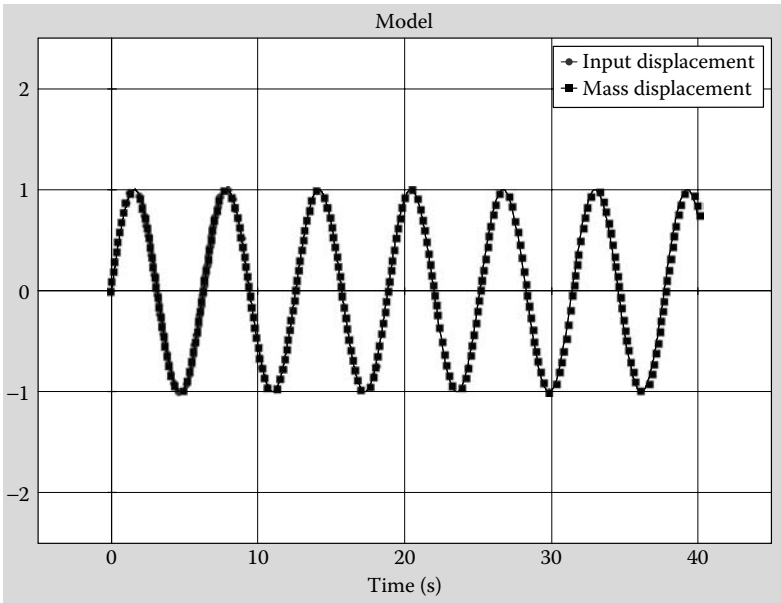


FIGURE 8.72
System response when activity of the mass dominates.

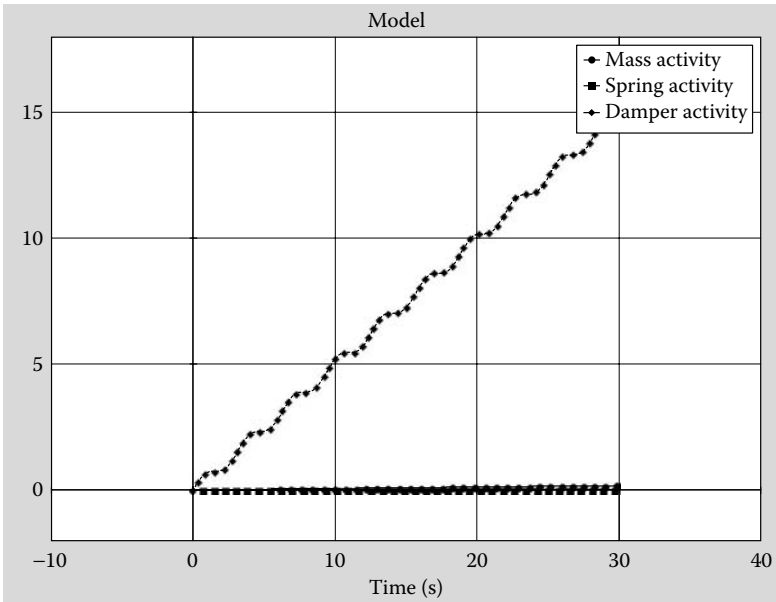


FIGURE 8.73
Relative activity values when damper activity dominates.

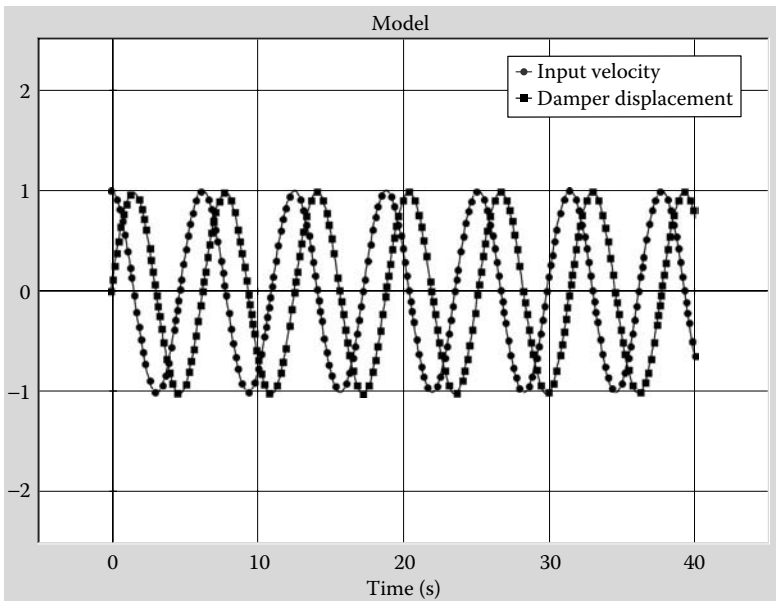


FIGURE 8.74
System response when activity of the damper dominates.

8.8 Signal Conditioning

Signal conditioning is a necessary, vital step in the use of sensors in any mechatronic application. The raw signals received from a sensor may have different problems, such as the magnitude may be very small, noisy, or may contain unwanted frequency content, and so forth. Thus, cleaning up signals so that the final output to be received by the user is a good clean signal is a very important step in the use of sensors. This cleanup process may contain steps such as amplification, filtering, addition, integration, and so forth. These tasks are performed by signal conditioning circuits and devices through which the data signals are fed. The outputs of these devices are the good clean signals that the user desires. In this section, we will consider a few of the signal conditioning circuits, develop their models, and demonstrate how the signal conditioning function works in one case. The others will be left as exercises for the reader. A more detailed discussion of such circuits can be found in texts on electronic circuits and signals. Our goal here is to demonstrate how bond graph modeling may be used to develop models of signal conditioning devices.

Figure 8.75 shows the standard circuit for a low-pass filter that is supposed to allow low frequencies to pass through and block high frequencies. The bond graph model of the low-pass filter is shown in Figure 8.76. The basic representation of the operational amplifier is the same as that discussed in an earlier chapter. The capacitor is added, as shown in the figure. The source of effort “inputvoltage2” represents the ground and supplies 0 volts. Similarly, the 0 flow source added at the output is used

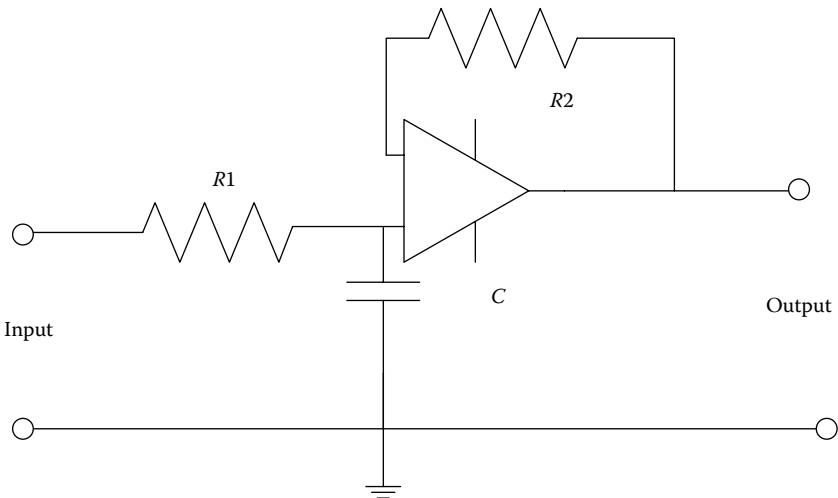


FIGURE 8.75

Circuit for a low-pass filter.

wave form. It is clear that the low frequency is passed through by the filter and the high frequency is blocked. In the exercise section, circuits of several signal conditioning devices are given. Modeling and simulating the behavior of these devices are left for the readers to carry out.

8.9 Summary

In this chapter we have discussed the first part of modeling transducers by concentrating on modeling different types of sensors. The sensors were separated according to the physical phenomena used in the sensor design. This is the logical way to discuss sensors, especially in the context of modeling them. We have touched on different types of sensors and established the methodology for modeling each one of them. One of the important components in the modeling of sensors is the use of field elements in bond graphs, especially C-field elements. Also, we have discussed the concept of activity and its use in designing sensors by choosing sensor parameters such that they behave in a desired fashion. This is a powerful technique similar to sensitivity analysis. The beauty of this technique in the context of bond graph modeling is that no new calculations need to be done in order to calculate this quantity, because both flow and effort quantities are already being calculated as part of the bond graph methodology.

Problems

- 8.1. Figure P8.1 shows a schematic representation of a capacitive sensor that is made of two parallel plates with a dielectric material of known ϵ_r inbetween the plates. The sensor is used to measure motion of a moving object that is linked to the dielectric material. So, when the dielectric core material moves, it results in a dynamic change in capacitance. This is registered as a voltage change in the recording circuit and the actual motion (i.e., displacement or speed) can be determined from the changing voltage signal. Using the approach shown in class, derive the constitutive equations for this C-field element and develop a simple bond graph model of this sensor along with a recording circuit as an instrument to record movement. If needed, you may use the plate areas to be 0.002 sq. m , the distance between the plates as 0.01 m , ϵ_0 (dielectric constant for air) $= 8.854 \times 10^{-12} \text{ F/m}$ and ϵ_r (relative dielectric constant for the material) $= 2000$. Therefore, the ϵ for the medium

is written as $\epsilon_0 \epsilon_r$. And the ϵ for air is equal to ϵ_0 . L can be taken as 0.1 m.

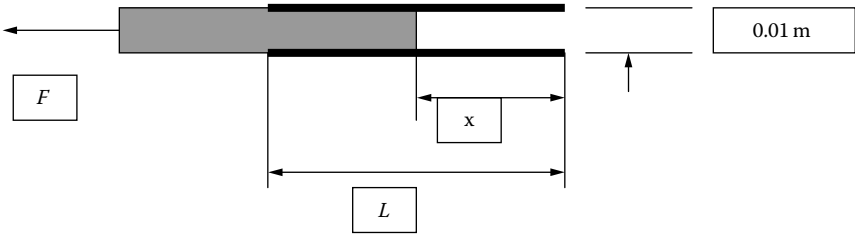


FIGURE P8.1

Figure for Problem 8.1, schematic representation of a capacitive sensor.

The total capacitance C in a dynamic situation is $C_1 + C_2$ where C_1 is the capacitance of the portion with the dielectric, and C_2 is the capacitance of the portion with air as dielectric. Report the derivation of the constitutive equations for the C-field element and the bond graph model of the sensor and associated recording circuit.

- 8.2. Consider a cylindrical capacitive sensor that is made of an outer shell of radius R_o and an inner core of radius R_i (Figure P8.2). For this type of capacitors, the capacitance is given by:

$$C = \frac{2\pi\epsilon L}{\ln \frac{R_o}{R_i}}$$

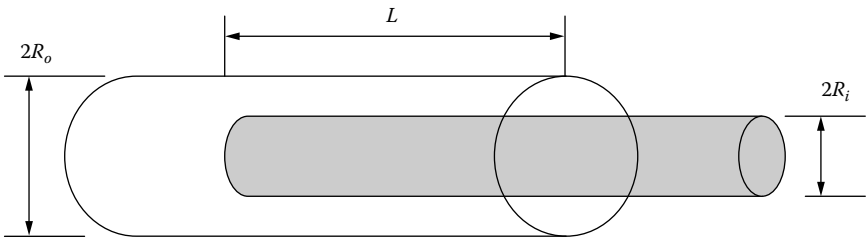


FIGURE P8.2

Figure for Problem 8.2, cylindrical capacitive sensor.

where L is the length of the overlapping section as shown in the figure. If this capacitive sensor is to be used to measure horizontal movement, derive the constitutive equations for this sensor and draw the bond graph representation of the circuit that will be used to implement the sensing activity.

8.3. Figure P8.3 shows the circuit of a voltage amplifier. Using the bond graph method, model this device and simulate its behavior.

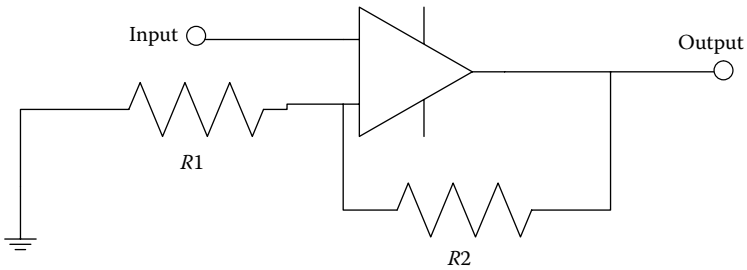


FIGURE P8.3

Figure for Problem 8.3, circuit of a voltage amplifier.

8.4. Figure P8.4 shows the circuit of a current amplifier. Using the bond graph method, model this device and simulate its behavior.

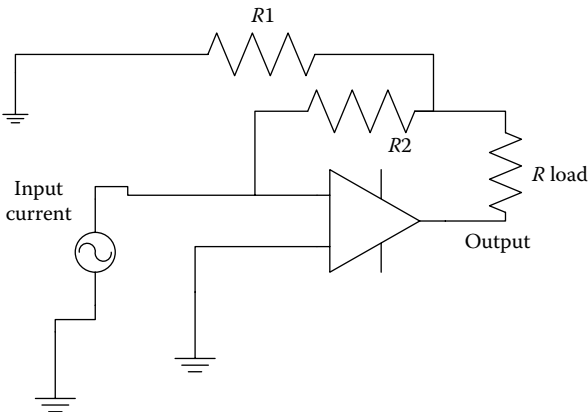


FIGURE P8.4

Figure for Problem 8.4, circuit of a current amplifier.

8.5. Figure P8.5 shows the circuit of a differential amplifier where the output is the amplification of the voltage difference between V_1 and V_2 inputs. Using the bond graph method, model this device and simulate its behavior.

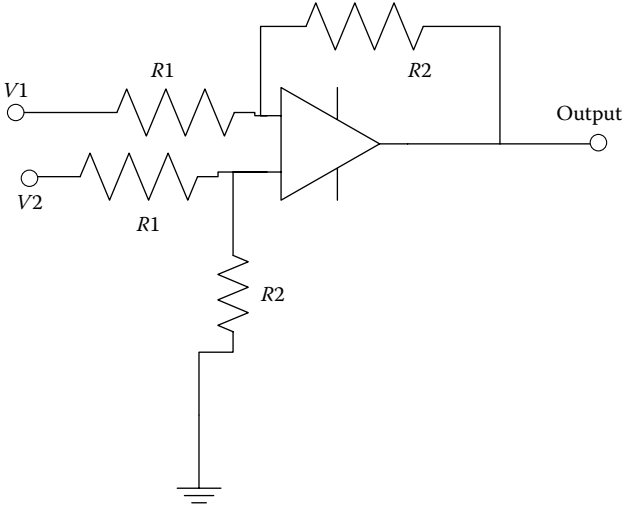


FIGURE P8.5

Figure for Problem 8.5, circuit of a differential amplifier.

8.6. Figure P8.6 shows the circuit of a high-pass filter. Using the bond graph method, model this device and simulate its behavior.

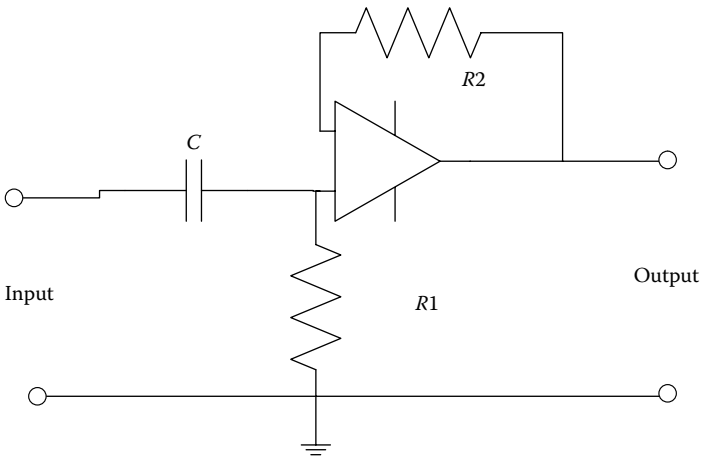


FIGURE P8.6

Figure for Problem 8.6, circuit of a high-pass filter.

- 8.7. Figure P8.7 shows the schematic of a microscopic comb drive where the piece on the left remains fixed and the shaded piece on the right moves in the horizontal direction. Using a variable N as the number of parallel surfaces that work as capacitors and other representative variables, develop the complete bond graph model of this device along with all the constitutive equations.

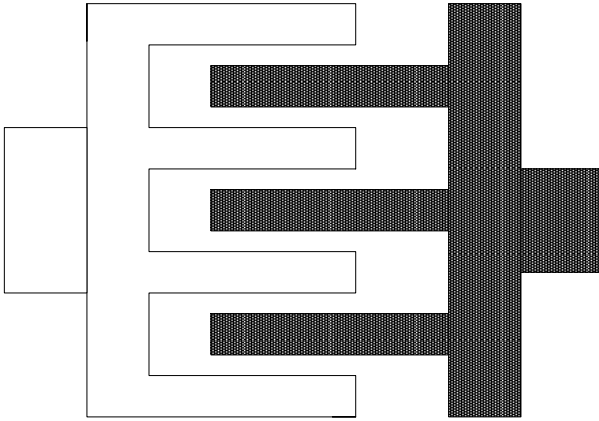


FIGURE P8.7

Figure for Problem 8.7, schematic of a microscopic comb drive.

- 8.8. Figure P8.8 shows a schematic of a seismometer that involves a spring–mass–damper system along with a magnet that moves in an electrical coil as a result of the base motion. Develop a bond graph model of this system, and develop system parameters that will enable us to easily determine the velocity of base motion from the measurement of the voltage induced in the coil. You may use the approach using the activity calculations, as discussed in this chapter.

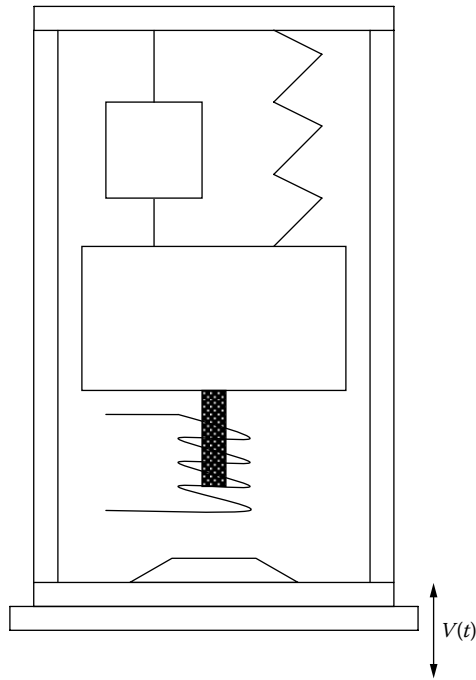
**FIGURE P8.8**

Figure for Problem 8.8, schematic of a seismometer.

- 8.9. In strain gauge applications, the voltage change in the bridge is usually very small in magnitude, and it is necessary that it be amplified. Combine the bridge circuit with an amplifier circuit, and develop the bond graph model of the whole system. Simulate its behavior using typical values for all parameters. Usually strain gauges are 120 ohm nominally and the applied voltage is 12 V.
- 8.10. Figure 8.45 in the text describes a variable reluctance sensor to be used to determine the speed of rotation. Develop a bond graph model of this sensor, simulate its behavior using the information provided in the text, and discuss from the output graphs how speed may be measured using this sensor.

9

Modeling Transducers: Actuators

In Chapter 8 modeling of transducers was introduced, but we confined our discussion primarily to sensors. The second half of that discussion related to actuators is taken up in this chapter. Actuators are an important component in a mechatronic system. They are sometimes called the muscles of the system. The decision taken by the algorithm that drives the system instructs the actuator to take specific action, and the actuator needs to take that action. Actuators may be broadly divided into several categories based on the means of actuation, such as electrical actuators, mechanical actuators, hydraulic actuators, and even chemical and biological actuators. Many of the actuators that were once macro-actuators (i.e., larger sized ones) are now available as micro-actuators or MEMS actuators. As in the chapter on sensors, we will categorize and discuss actuators by the means of actuation (rather than by application) for our study here. Thus, we will study the modeling approaches used for electrical actuators, electromagnetic actuators, hydraulic actuators, and so forth.

The overall objectives of this chapter are to

- Understand how different phenomena can be used to actuate a mechatronic system.
- Learn how actuator models can be developed using bond graph elements.
- Model actuators such that causes and effects can be related to each other accurately through the model.
- Understand how transducers can be designed using system models.

9.1 Electromagnetic Actuators

9.1.1 Linear

Figure 9.1 shows a magnetic circuit that is energized by electric current. The electromagnet then attracts the moveable piece until it moves and gets stuck to the electromagnet. Hrovat (2000) and others have reported on this example. The movable piece is attached to a spring and a damper

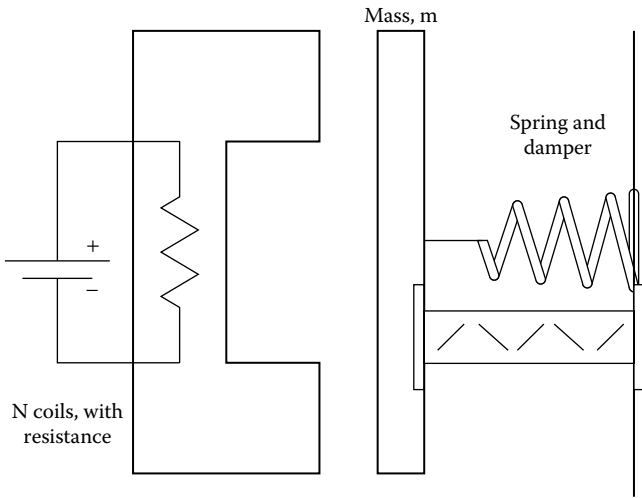


FIGURE 9.1
Schematic of a linear electromagnetic actuator.

that helps in controlling the motion. Before the bond graph is drawn, let us consider the magnetic circuit with the air gap that changes as the circuit is energized. A magnetic circuit, we know, can be represented by a set of capacitive elements. The electromagnet is modeled as a GY element. The details of this process were discussed in the previous chapter. Here, one capacitive element represents the iron core section, and the other represents the air gap. Since the air gap changes with time, the capacitance changes with motion. So, to represent the air gap portion of the capacitive element, we need to use a capacitive field element. The left side of the C-field element is the magnetic side, and the right side is the mechanical side. On the mechanical side, there are two C elements, an R and an I element. The I element represents the mass of the moving piece, the R element is used to model the damper, and one of the C elements models the spring. The second C element is used to model the mechanical stop when the moveable piece comes into contact with the electromagnet. Figure 9.2 shows the bond graph representation of this system.

The C-field equations need to be derived in the same fashion as before (in Chapter 8).

One expression of energy in a magnetic C-field is $= \frac{\Phi^2}{2}$. Reluctance

Inside C-Field

$\dot{\phi}, \dot{x}$ are received

Integration of $\dot{\phi}$ to get ϕ , $\phi = \text{int}(\dot{\phi})$

Integration of $\dot{\phi}, \dot{x}$ to get x , $x = \text{int}(\dot{\phi}, \dot{x})$

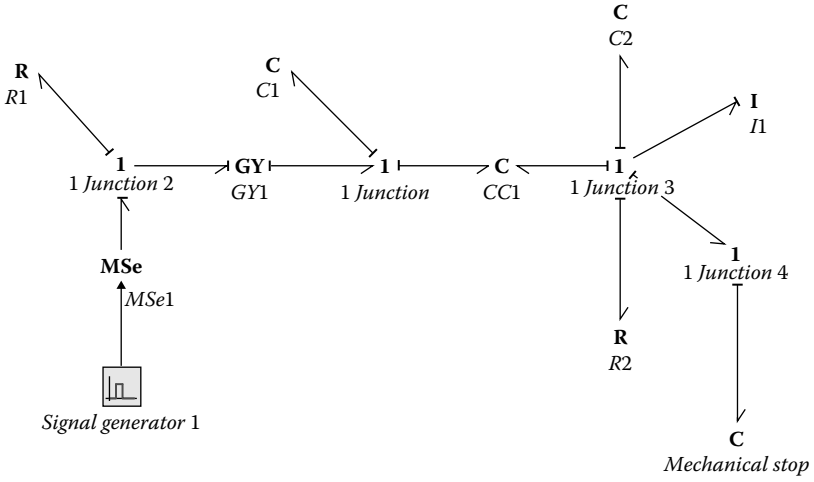


FIGURE 9.2
Bond graph model of the linear electromagnetic actuator.

Differentiate energy w.r.t time:

$$\frac{d}{dt}(\text{Energy}) = \text{Power} \quad (9.1)$$

$$\frac{d}{dt}(\text{Energy}) = \frac{\partial}{\partial \phi} \left(\frac{\phi^2 \cdot R}{2} \right) \cdot \frac{d\phi}{dt} + \frac{\partial}{\partial x} \left(\frac{\phi^2 \cdot R}{2} \right) \cdot \frac{dx}{dt} \quad (9.2)$$

Power on magnetic side:

$$= \frac{\partial}{\partial \phi} \left(\frac{\phi^2 \cdot R}{2} \right) \cdot \frac{d\phi}{dt} = \text{effort} \cdot \text{flow} \quad (9.3)$$

Effort on the magnetic side:

$$\begin{aligned} &= \frac{\partial}{\partial \phi} \left(\frac{\phi^2 \cdot R}{2} \right) \\ &= \frac{2\phi R}{2} \\ &= \phi \cdot R \end{aligned} \quad (9.4)$$

Power on mechanical side:

$$= \frac{\partial}{\partial x} \left(\frac{\phi^2 \cdot R}{2} \right) \cdot \frac{dx}{dt} \quad (9.5)$$

Effort on the magnetic side:

$$\begin{aligned}
 &= \frac{\partial}{\partial x} \left(\frac{\varphi^2 \cdot R}{2} \right) \\
 &= \frac{\partial}{\partial x} \left(\frac{\varphi^2 \cdot x}{2\mu A} \right) \\
 &= \frac{\partial}{\partial x} \left(\frac{\varphi^2 \cdot x}{2\mu A} \right) \\
 &= \frac{\varphi^2}{2\mu A}
 \end{aligned} \tag{9.6}$$

The constitutive equation for the C-field is

$$\text{Effort}_{\text{left}} = \varphi \cdot R = \frac{\varphi \cdot x}{\mu \cdot A} \quad \dots x \text{ is the air gap} \tag{9.7}$$

$$\text{Effort}_{\text{right}} = \frac{\varphi^2}{2\mu A} \tag{9.8}$$

The model of the C-field element as programmed is

```
// this model represents a 2-port C element: p.e =
(1/C)*p.f written here as p.e = A*p.f
// A = [a11, a12; a21, a22]
```

Parameters

```
real a11 = 1.0;/μ
real a12 = 0.0;
real a21 = 1.0;
real a22 = 2.0;/Area
```

Equations

```
// You can change these equations into any (nonlinear)
version by adding your own functions.
// Use f(x) button at the left of the window to see all
available functions.
state1 = int (p1.f);
state2 = int (p2.f);
p1.e = state1*state2/(a11*a22);
p2.e = state1*state1/(2*a22*a11);
```

The parameters used in the simulation are shown in Figure 9.3.

As mentioned before, in the model, the capacitive element C3 is used as a mechanical stop to simulate the behavior of the system when the

Parameters			
Initial Values			
Constants			
Name	Value	Quantity	Unit
◆ C1\c	2		
◆ GY1\r	10		
◆ CC1\%a11	1		
◆ CC1\%a12	0		
◆ CC1\%a21	1		
◆ CC1\%a22	2		
◆ I1\i	0.025		
◆ R1\r	50		
◆ C2\c	0.025		
◆ R2\r	0.001		
◆ C3\c	1e-005		
◆ SignalGenerator1\start_time	0 {s}	Time	second
◆ SignalGenerator1\stop_time	8 {s}	Time	second
◆ SignalGenerator1\amplitude	12	Magnitude	none

FIGURE 9.3
Simulation parameters for the linear electromagnetic actuator.

moving iron piece eventually comes into contact with the electromagnet and comes to a stop. In this case, that situation is modeled by a C element that is a mechanical spring with a spring constant that is close to 0 as long as the gap is not filled up and is very high (i.e., close to infinite, a perfectly rigid surface) when the two surfaces eventually come in contact. This behavior is modeled through the following spring model:

Variables

real u;

Equations

```
state = int(p.f);
if (state >- 0.1) then
  u = 0.0000000001; // this means that as long as the gap
  not filled up the u value //(u = 1/k) is insignificant
else
  u = 350000; //when the gap is filled the u value goes to a
  very high number.
end;
p.e = state*u;
```

The simulation results obtained from the analysis are shown in Figure 9.4. This figure shows how the mass that is attracted by the electromagnet moves toward the magnet when the electromagnet is energized, its movement is

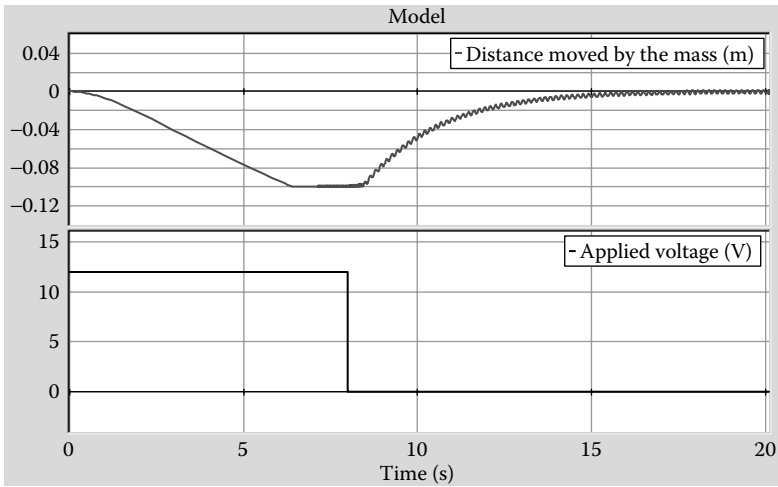


FIGURE 9.4
Simulation results for the linear magnetic actuator.

stopped when it comes into contact with the magnet, and then moves back to its initial position when the magnet is de-energized. The figure also shows how the voltage applied to the electromagnet varies with time.

EXAMPLE 9.1: SOLENOID

Solenoids are a group of linear actuators that are used in many applications. Solenoids work in the following manner: with a current passing through a coil, a magnetic field is created around the core of the solenoid. By design, air gaps are left in the magnetic path. The plunger, which is made of a ferromagnetic material, is able to move such that the air gap (and, thus, the reluctance of the path) is minimized. This movement in the plunger can be used to open or close hydraulic valves used for control applications or perhaps hit a surface to work as a doorbell, and so forth. The plunger is mounted with a return spring so that when the coils are de-energized, the plunger can move back to its initial position, thus maintaining the designed gap in the magnetic path. Usually, solenoid valves are quite fast acting, but the stroke lengths are short. Figure 9.5 shows a schematic of a solenoid cross-section. The coils around the inner core, the plunger, and the magnetic path are shown in the picture. Figures 9.6 and 9.7 show two possible magnetic circuits for modeling the solenoid. One or the other can be used based on the solenoid construction.

Let us consider a device such as a doorbell that uses a solenoid as an actuator and the configuration in Figure 9.6 as the possible design. The moving plunger hits the chime to make the doorbell ring. The bond graph in Figure 9.8 shows how the system needs to be modeled. The critical component of the system is the modeling of the solenoid and plunger movement. The other parts of the model include the mechanical stop and damping, the mass of the solenoid

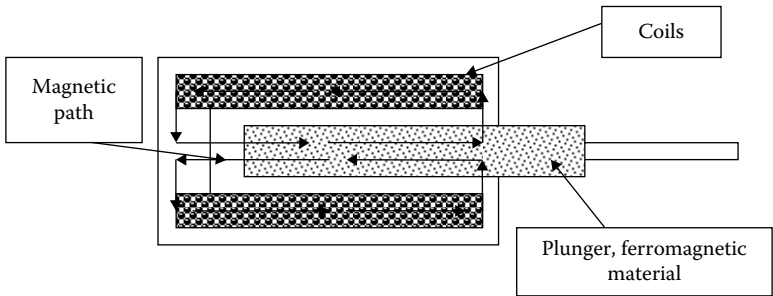


FIGURE 9.5
Schematic of the solenoid cross-section.

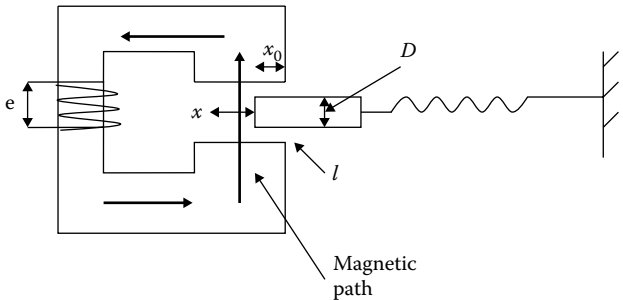


FIGURE 9.6
One possible magnetic circuit for the solenoid.

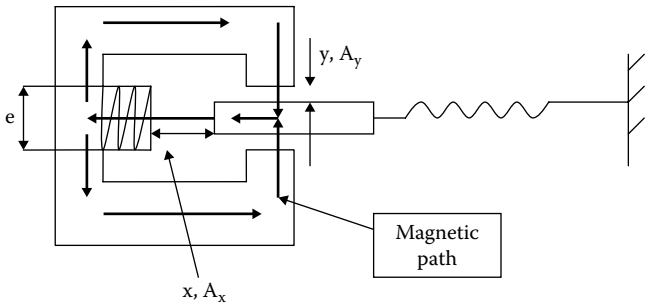
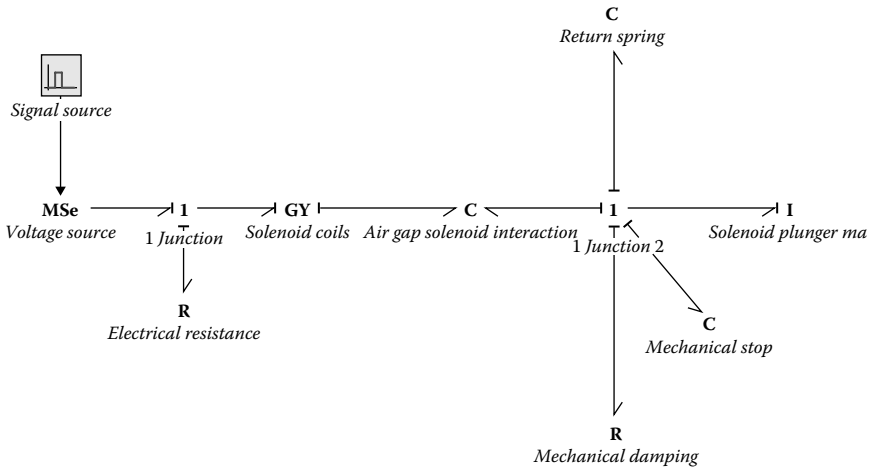


FIGURE 9.7
A second possible magnetic circuit for the solenoid.

plunger, and the return spring. The action of the solenoid is a result of the tendency of the plunger to move to an orientation of minimum reluctance. To begin with (before energizing the solenoid), the plunger is at a position that is not the equilibrium position. When the solenoid is energized, the plunger tends to move to the equilibrium position.

The electromagnetic circuit and the mechanical movement of the solenoid are being modeled as in Figure 9.6. In the figure, D represents the diameter of

**FIGURE 9.8**

Bond graph model of the solenoid doorbell.

the plunger, x is the movement of the plunger, x_0 is the initial overlap of the plunger with the outer casing, and l is the air gap between the plunger and the outer bobbin where the windings are mounted. The GY factor in this case is N , the number of windings there are on the solenoid coil. The C-field equations need to be derived in the same fashion as before:

The expression of energy in a magnetic C-field is $= \frac{\Phi^2}{2}$. Reluctance

Inside C-Field

$\dot{\Phi}, \dot{x}$ are received

Integration of $\dot{\Phi}$ to get Φ , $\Phi = \text{int}(\dot{\Phi})$

Integration of $\dot{\Phi}, \dot{x}$ to get x , $x = \text{int}(\dot{\Phi}, \dot{x})$

Differentiate energy w.r.t time:

$$\frac{d}{dt}(\text{Energy}) = \text{Power} \quad (9.9)$$

$$\frac{d}{dt}(\text{Energy}) = \frac{\partial}{\partial \Phi} \left(\frac{\Phi^2 \cdot R}{2} \right) \cdot \frac{d\Phi}{dt} + \frac{\partial}{\partial x} \left(\frac{\Phi^2 \cdot R}{2} \right) \cdot \frac{dx}{dt} \quad (9.10)$$

Power on magnetic side:

$$= \frac{\partial}{\partial \Phi} \left(\frac{\Phi^2 \cdot R}{2} \right) \cdot \frac{d\Phi}{dt} = \text{effort} \cdot \text{flow} \quad (9.11)$$

Effort on the magnetic side:

$$\begin{aligned} &= \frac{\partial}{\partial \Phi} \left(\frac{\Phi^2 \cdot R}{2} \right) \\ &= \frac{2\Phi R}{2} \\ &= \Phi \cdot R \end{aligned} \quad (9.12)$$

Power on mechanical side:

$$= \frac{\partial}{\partial x} \left(\frac{\varphi^2 \cdot R}{2} \right) \cdot \frac{dx}{dt} \quad (9.13)$$

Effort on the mechanical side:

$$\begin{aligned} &= \frac{\partial}{\partial x} \left(\frac{\varphi^2 \cdot R}{2} \right) \\ &= \frac{\partial}{\partial x} \left(\frac{\varphi^2 \cdot l}{2\mu\pi Dx} \right) \\ &= \frac{\partial}{\partial x} \left(\frac{\varphi^2 \cdot l}{2\mu\pi Dx} \right) \\ &= -\frac{\varphi^2 l}{2\mu\pi Dx^2} \end{aligned} \quad (9.14)$$

The constitutive equation for the C-field is

$$\text{Effort}_{\text{left}} = \varphi \cdot R = \frac{\varphi \cdot l}{\mu \cdot \pi Dx} \dots x \text{ is the movement of the plunger} \quad (9.15)$$

$$\text{Effort}_{\text{right}} = -\frac{\varphi^2 l}{2\mu\pi Dx^2} \quad (9.16)$$

When the flow on the mechanical side is integrated, we get the displacement x of the mechanical side. We need to be careful that there is an initial position of x , that is, x_0 .

The C-field model can be shown as follows:

Parameters

```
real D = 0.01;
real mu = 1e-7;
real l = 0.001;
```

Equations

```
// You can change these equations into any (nonlinear)
// version by adding your own functions.
// Use f(x) button at the left of the window to see all
// available functions.
state1 = int (p1.f);
state2 = int (p2.f);
p1.e = state1*l/(mu*3.14159*D*state2);
p2.e = - state1*state1*l/(2*mu*3.14159*D*state2*state2);
```

The parameters used for the simulation are shown in Figure 9.9, and the simulation results, that is, the movement of the plunger are shown in Figure 9.10. The results show that while the solenoid circuit is energized, the plunger

Parameters			
Initial Values		Constants	
Name	Value	Quantity	Unit
Electrical_resistance\r	5 {ohm}	Electric Resistance	ohm
Return_Spring\c	100 {um/N}	Compliance	meter per newton
Solenoid_plunger_mass\i	0.001		
Mechanical_Damping\r	0.02		
Mechanical_stop\c	1		
Signal_source\start_time	1 {s}	Time	second
Signal_source\stop_time	1.5 {s}	Time	second
Signal_source\amplitude	20	Magnitude	none
Solenoid_Coils\r	1300		
Airgap_solenoid_interaction\D	0.01		
Airgap_solenoid_interaction\mu	1e-007		
Airgap_solenoid_interaction\l	0.001		

FIGURE 9.9
Parameters used in the simulation.

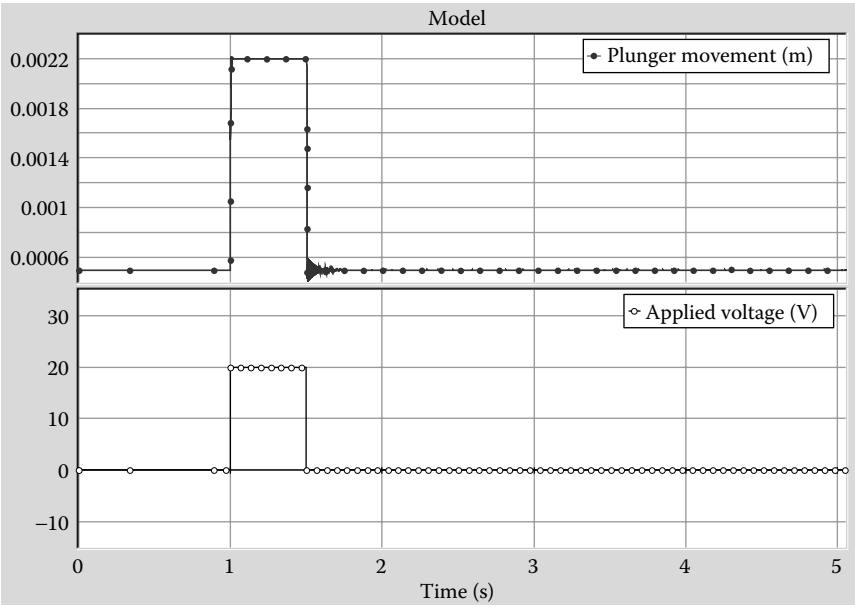


FIGURE 9.10
Plunger movement and applied voltage.

moves until it hits the mechanical stop and then moves back to its original position when the voltage is cut off.

A more realistic solenoid schematic is shown in Figure 9.7. These are extensively used in controlling flow of hydraulic fluid through a valve that is controlled by the movement of the plunger. The components that make up such an

arrangement are the windings around a nonferromagnetic material, a housing, an end stop, the plunger, and the return spring that is attached to the plunger so that the plunger can move back to its original position when the electric current is turned off. In the figure, the flux path is also shown. The flux in the circuit is essentially controlled by the two air gaps, the constant gap in the y direction and the variable gap in the x direction.

The governing equations may be derived in the following fashion as:

Inside C-Field

$\dot{\phi}, \dot{x}$ are received

Integration of $\dot{\phi}$ to get ϕ , $\phi = \text{int}(\dot{\phi})$

Integration of \dot{x} to get x , $x = \text{int}(\dot{x})$

Differentiate energy w.r.t time:

$$\frac{d}{dt}(\text{Energy}) = \text{Power} \quad (9.17)$$

$$\frac{d}{dt}(\text{Energy}) = \frac{\partial}{\partial \phi} \left(\frac{\phi^2 \cdot R}{2} \right) \cdot \frac{d\phi}{dt} + \frac{\partial}{\partial x} \left(\frac{\phi^2 \cdot R}{2} \right) \cdot \frac{dx}{dt} \quad (9.18)$$

Power on magnetic side:

$$= \frac{\partial}{\partial \phi} \left(\frac{\phi^2 \cdot R}{2} \right) \cdot \frac{d\phi}{dt} = \text{effort} \cdot \text{flow} \quad (9.19)$$

Effort on the magnetic side:

$$\begin{aligned} &= \frac{\partial}{\partial \phi} \left(\frac{\phi^2 \cdot R}{2} \right) \\ &= \frac{2\phi R}{2} \\ &= \phi \cdot R \end{aligned} \quad (9.20)$$

Power on mechanical side:

$$= \frac{\partial}{\partial x} \left(\frac{\phi^2 \cdot R}{2} \right) \cdot \frac{dx}{dt} \quad (9.21)$$

Effort on the mechanical side:

$$\begin{aligned} &= \frac{\partial}{\partial x} \left(\frac{\phi^2 \cdot R}{2} \right) \\ &= \frac{\partial}{\partial x} \left(\frac{\phi^2 \cdot \left(\frac{x}{A_x} + \frac{y}{2A_y} \right)}{2\mu_0} \right) \\ &= -\frac{\phi^2}{2\mu_0 A_x} \end{aligned} \quad (9.22)$$

The constitutive equation for the C-field is

$$\text{Effort}_{\text{left}} = \Phi \cdot R = \frac{\Phi \cdot l}{\mu_0} \left(\frac{x}{A_x} + \frac{y}{2A_y} \right) \dots x \text{ is the movement of the plunger} \quad (9.23)$$

$$\text{Effort}_{\text{right}} = -\frac{\Phi^2}{2\mu_0 A_x} \quad (9.24)$$

We have not included the simulation of this variation of the design here since it would be quite similar.

9.1.2 Rotational Actuators: Motors

The most common type of electrical rotational actuator is the electrical motor. Figure 9.11 is an incomplete diagram summarizing the different types of motors that have been used in practice. The broad division is between AC and DC motors. Within each type, there are many subtypes. A more complete view of this can be found in the text by Alciantore and Histan (2005). Obviously, we will not be able to discuss all of these in detail, but we will look at a few that are relevant to mechatronic applications.

The output of all motors is torque and rotation. Torque is produced by an electric motor through the interaction of either stator and armature currents (by conduction), as in DC motors and synchronous motors, or through interaction between stator fields and armature fields (by induction), as in induction motors. The by-conduction method is based on Lorentz's law and applying the right-hand rule. The by-induction method is based on like field poles repelling and unlike poles attracting.

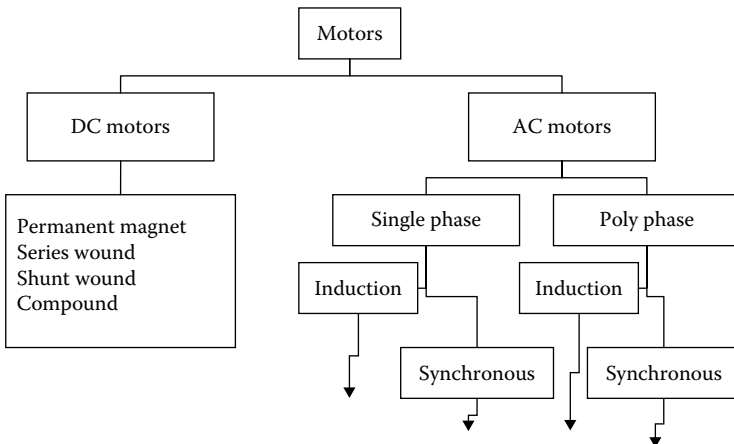


FIGURE 9.11
Motor types.

DC motors are more commonly used in many mechatronic applications because torque speed characteristics can be controlled smoothly and due to the high ratio of torque to rotor inertia (i.e., the higher torque generated per unit rotor weight), which responds quickly. In our discussion here, we will only discuss the DC motors.

The operation of DC motors is based on two principles. The first one is called the Lorentz effect. It states that a current carrying conductor in magnetic field experiences a force. The second principle is based on Faraday's/ Lenz's law. It states that a conductor moved in a magnetic field generates a (back) emf that opposes the change that produces it. This back emf is proportional to the rate of change of flux. The current due to back emf in closed circuit will create a flux opposite the magnetic flux.

Figure 9.12 shows a schematic that can be used to explain the motor action. The three directions B , I , and F , show the directions of the magnetic C-field, current direction, and the resulting direction of the force. If you consider sketch (a), the direction of the current in section A and B are opposite to each other. Hence, the forces in the conductors are in opposite directions resulting in a net torque or turning moment. However, during the next half of the cycle, when A and B have moved and switched positions (as shown in sketch [b]), the current directions in A and B need to switch. If they don't, the force direction will switch and the coil will tend to oscillate and move in one direction. To ensure that the direction of the current is switched, the coil is attached to the voltage source through a split ring called a commutator. This ensures that as the coil rotates, the contact of its arms with the voltage terminals switch as well. Following are some of the characteristics of a DC motor.

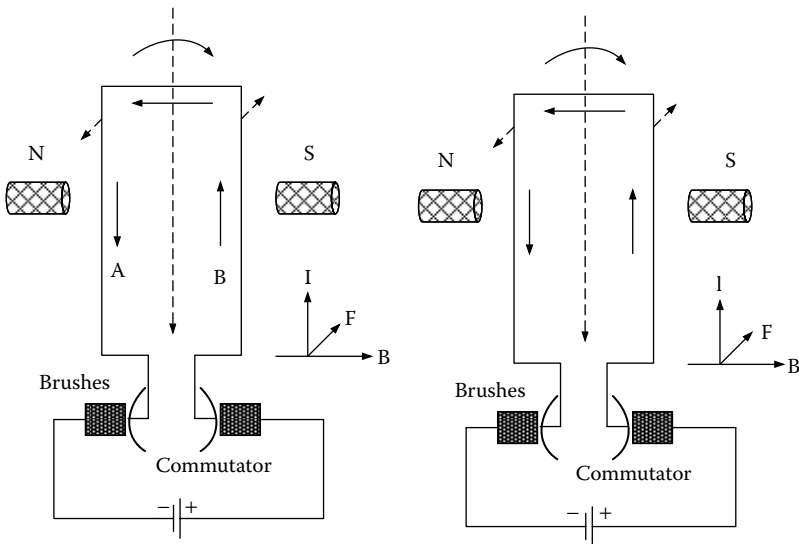


FIGURE 9.12
Schematic for motor action.

- Armature coil is free to rotate in the magnetic C-field.
- Loop of wire is connected through the commutator to the brushes (brushes stationary, commutator rotates).
- Current flows when power is supplied to brushes; opposite forces on opposite sides generates a torque.
- Commutator changes current direction when the plane of wire is vertical.
- Torque direction remains unchanged.
- Multiple wires are wound in a distributed fashion over cylindrical rotor of ferromagnetic material.
- Multiple loops increases and also evens out the torque.
- Motor direction is reversed by reversing the polarity of voltage.

Construction of an electric motor consists of the following components:

Stator: The outer housing supports radial magnetized poles (either permanent magnet or field coils that provide the magnetic C-field).

Rotor: Rotating shaft supported by bearings, conducting coils (armature), and an iron core.

Air gap: Between the stator and the rotor where the two magnetic C-fields interact.

Commutator: In DC motors only, to control direction of current through armature windings.

Brushes: For motors with commutators. Provide stationary electrical contact to the moving commutators conducting segments.

Figures 9.13 through 9.16 illustrate some of these components in a motor.

9.1.2.1 Permanent Magnet DC Motor

This is the simplest DC motor where the magnetic field is created by a set of permanent magnets that act as the stator, and the armature windings are the rotor. A permanent magnet provides a constant value of flux density. For an armature conductor of length L and carrying a current I , the force resulting from a magnetic flux density B at right angles to the conductor is $B I L$. With N conductors, the force is $F = N B I L$. The forces result in a torque of Fc about the coil axis, if c is the width of the coil. So the torque may be written as $T = (NBLc)I$. Torque is thus written as $T = K_T I$; I = armature current, K_T is a constant based on motor construction. Since the armature coil is rotating in a magnetic field, electromagnetic induction will occur, and a back emf will be induced. The back emf E is related to the rate at which the flux linked by the coil changes. For a constant magnetic field, this is proportional to the angular velocity of rotation. Hence, back emf is related to flux and angular rotation (in rpm) $E = K_E \omega$; where ω = motor speed in rpm.

K_T and K_E depend on motor construction, and they are of the same magnitude (but of different units). Armature current, at steady state (because the armature inductance behaves like a connecting wire at steady state) $I = (V - E)/R$. R is the armature resistance and E is back emf. The torque,



FIGURE 9.13
Armature.

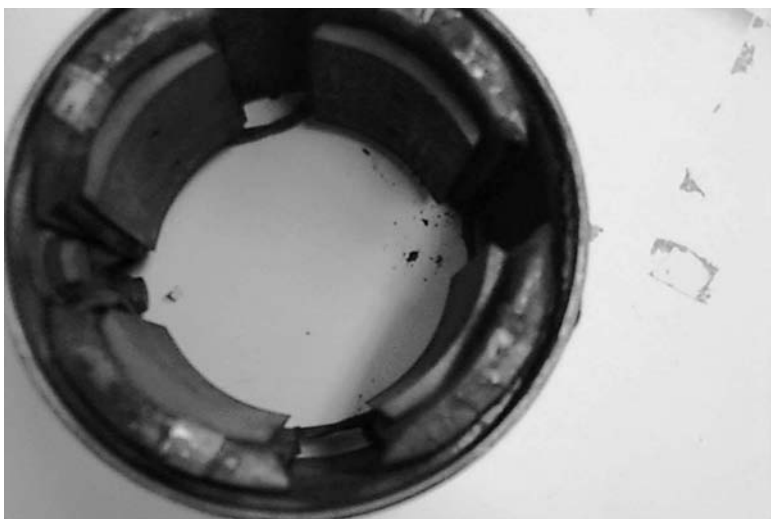


FIGURE 9.14
Field coils.



FIGURE 9.15
Brushes.

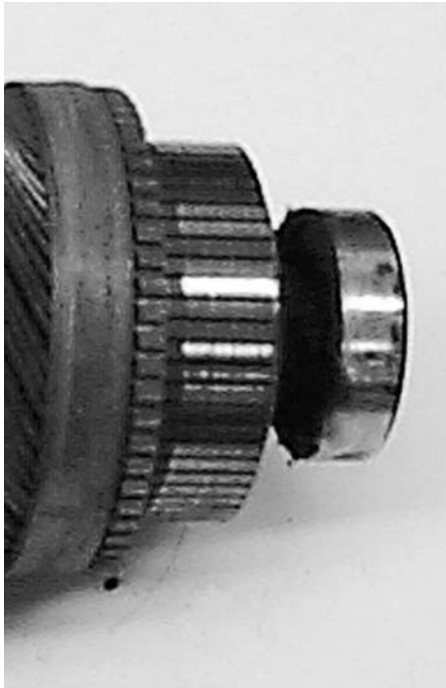


FIGURE 9.16
Commutator.

therefore, is $T = T = K_T I = K_T (V - E)/R = K_T (V - K_E \omega)/R$. At start-up, back emf is minimum, therefore, I is maximum and torque is maximum. The faster it runs, the smaller the current and, hence, the torque. The motor circuit is shown in Figure 9.17. The current in the circuit is $I = (V - E)/R$ at steady state.

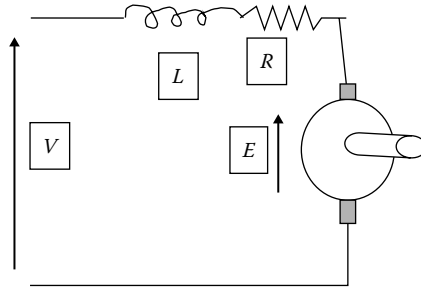


FIGURE 9.17

A circuit representing the PM DC motor.

When one considers the unsteady state situation, the rate of change of current at the initial state needs to be considered (due to the presence of the inductor). This results in a system of two coupled first order equations (one each for the storage element on the electrical and mechanical side). All the motor equations together are

$$\begin{aligned}\frac{dI}{dt} &= \frac{1}{L}(V - E - IR) \\ \frac{d\omega}{dt} &= \frac{1}{J}(T - T_L - B\omega) \\ E &= K_E \omega \\ T &= K_T I\end{aligned}\tag{9.25}$$

The first two equations are the governing differential equations, and the next two are the gyrator relationships. The system parameters are: L , J , R , B , and $K_T = K_E$.

The bond graph representation of the permanent magnet DC motor can therefore be represented as in Figure 9.18.

The GY element models the relationship between the rotation and back emf (mechanical flow and electrical effort) and the current and torque (electrical flow and mechanical effort). The GY factor is the same as the K_T and K_E .

The bond graph representation has two sides. The electrical side consists of the applied voltage, armature resistance, and armature inductance.

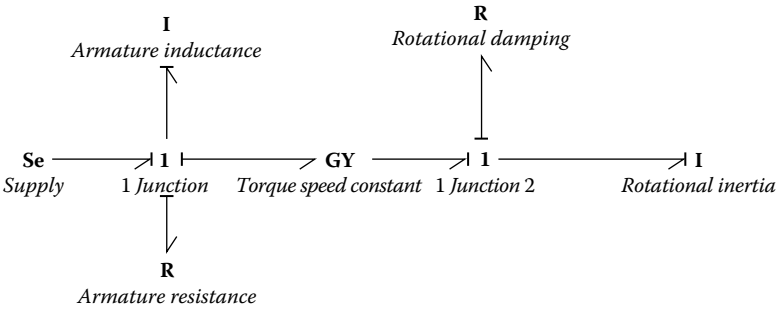


FIGURE 9.18
Bond graph representation of a permanent magnet DC motor.

The GY element works as the link between the electrical side and the mechanical side. On the mechanical side, the loads are the rotor inertia and the rotational damping, if any. This model does not have any external load mounted on it. The table in Figure 9.19 shows the parameter values used in simulating the system and subsequent plots (Figures 9.20, 9.21, and 9.22) show how the system responds.

Figure 9.20 shows how the armature current and the output torque change with time and eventually reach a steady state value. Figure 9.21 shows the variation of rotational speed and the back emf induced.

Figure 9.22 shows three curves: the total output torque, the portion of torque used to drive the inertia load, and the portion needed to overcome

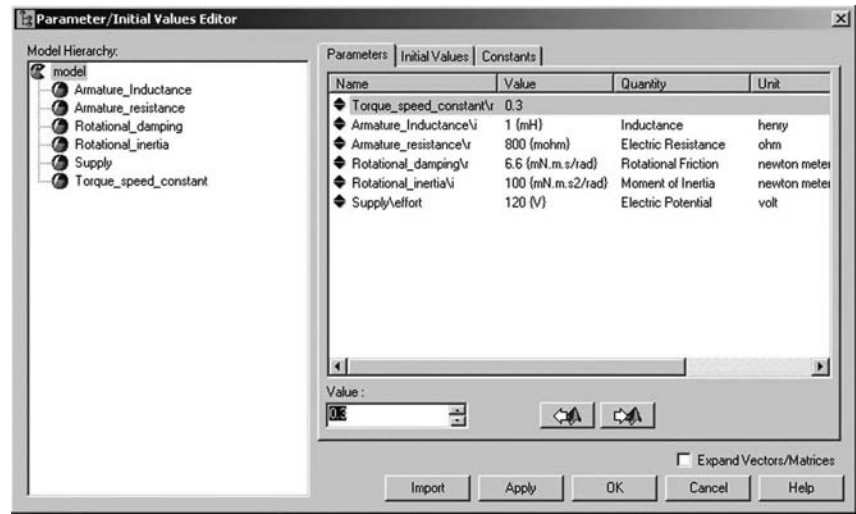


FIGURE 9.19
Parameters used for simulation.

damping. It is clear from the plots that, initially, almost all the torque is needed to accelerate the inertia, but once it reaches the steady speed, the torque necessary is only the portion that is overcoming friction/damping.

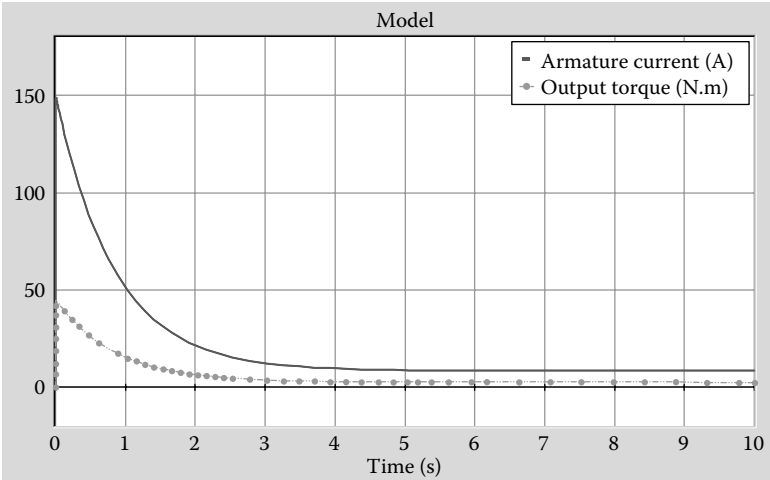


FIGURE 9.20
Armature current and output torque versus time.

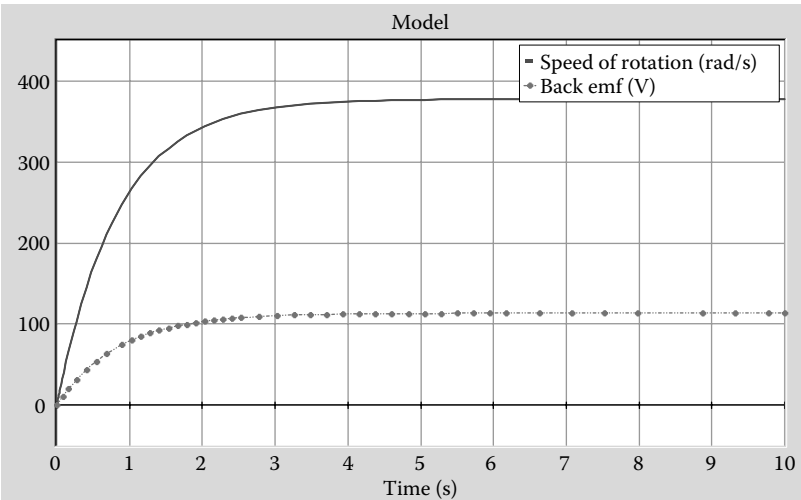
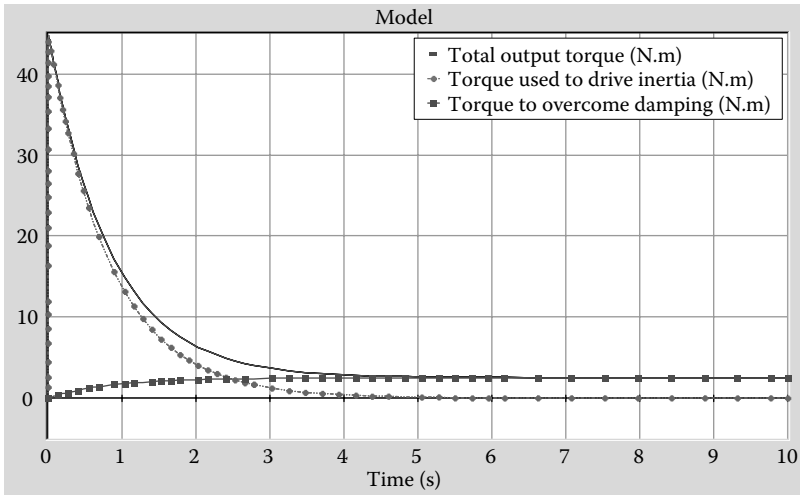


FIGURE 9.21
Back emf and rotational speed versus time.

**FIGURE 9.22**

Distribution of the total torque among the inertia and the damping elements.

9.1.2.2 Motor Load

There are usually two types of torque loads that are commonly observed in practice. They are

1. Constant load torque—Mostly generated from a constant amount of friction to drive a system.
Example—Conveyor.
2. Torque (T)—Directly proportional to the square of velocity (ω^2).
Example—Centrifugal pumps, fans, and so forth.

There are several ways to model a load parameter in a bond graph model. One way is using a source of effort with a negative magnitude (then it acts as a sink or load rather than source). This can work as a constant load on the system. The other way to handle this would be to use a resistance element and modify the constitutive equation for the resistance. By default, the constitutive equation for the resistance is programmed as follows:

Equations

$p.e = r \cdot p.f$; Here the effort is proportional to the flow.

This can be modified in the following way:

Equations

$p.e = r \cdot p.f \cdot p.f$; Now the effort becomes a function of the square of the flow, that is, the velocity.

This way most common types of motor loads may be easily modeled for simulation studies.

9.1.2.3 Parallel Wound Motor (Shunt)

The schematic shown in Figure 9.23 shows the electrical circuit for a motor that is shunt wound or parallel wound. The same supply voltage is applied on two parallel paths, one for the field coils that generate the electro-magnetic field and the other for the armature coil that will rotate in this field. Both these coils will have inductances and resistances, as shown in the schematic. The mechanical power output of the motor is in the form of a torque and angular rotation. When no external load is applied, the torque generated still needs to rotate the rotor inertia, and there may be some frictional losses at the bearings. If there is an external load, most of the output power is used to drive this external load.

The corresponding bond graph model for this motor is shown in Figure 9.24. In this case, a modulated gyrator is used to represent the motor action since the magnetic field is not constant but is dependent on the field current. The following analysis discusses the behavior of a shunt

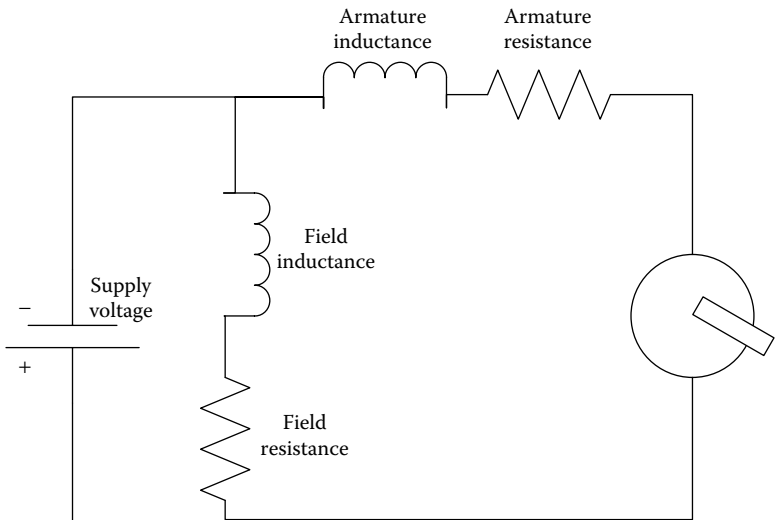
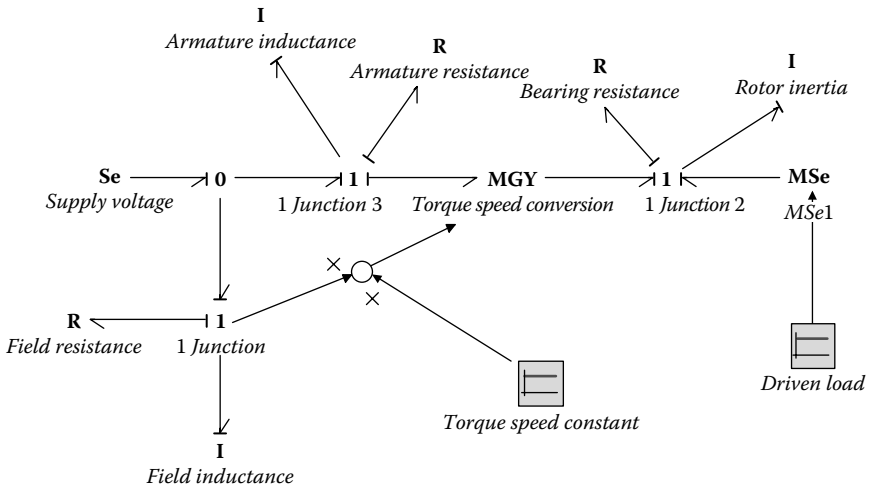


FIGURE 9.23
Schematic for a shunt wound DC motor.

**FIGURE 9.24**

Bond graph model of a shunt wound DC motor.

wound motor at steady state, that is, by treating the inductances as connecting wires, and, thus, the currents have become steady.

ω is the angular speed

k is a motor constant

Φ is the magnetic flux

E_b is the back emf

T is the torque

R_a and i_a are the armature resistance and armature current respectively.

$$\begin{aligned}\omega &= \frac{E_b}{k\Phi} \\ \omega &= \frac{V - R_a i_a}{k\Phi} \\ \omega &= \frac{V - R_a \left(\frac{T}{k\Phi}\right)}{k\Phi} \quad \therefore \omega = \frac{E_b}{k\Phi} \\ &\quad \therefore T = k\Phi i_a\end{aligned}\tag{9.26}$$

$$\omega = \frac{V}{k\Phi} - \frac{R_a T}{(k\Phi)^2}\tag{9.27}$$

To obtain the torque speed characteristics of a shunt motor, consider Equation 9.27. ω is the angular speed is practically independent of load

torque since the denominator of the torque term is so much larger than the denominator of the first term. Speed can be kept constant over a large range of load. Φ is the magnetic flux and is directly proportional to field current i_f . Therefore:

$$\begin{aligned} k\Phi &= k_s i_f \\ \omega &= \frac{V}{k_s i_f} - \frac{R_a T}{(k_s i_f)^2} \end{aligned} \quad (9.28)$$

The bond graph model for the whole system is shown in Figure 9.24. The MGY element is the element that transforms electrical to mechanical power. The flow from the electrical side determines the effort on the mechanical side. And the flow on the mechanical side determines the effort on the electrical side.

$$\begin{aligned} \therefore E_b &= k\Phi\omega = k_s i_f \omega \\ \therefore T &= k\Phi i_a = k_s i_f i_a \end{aligned} \quad (9.29)$$

In the bond graph, the factor for MGY is computed by taking the product of torque speed constant (k_s from the above formula) and the flow information from the field coil (i_f in the above formula).

The parameter values shown in the Figure 9.25 are the system parameters used to simulate the system. Figures 9.26, 9.27, and 9.28 show the

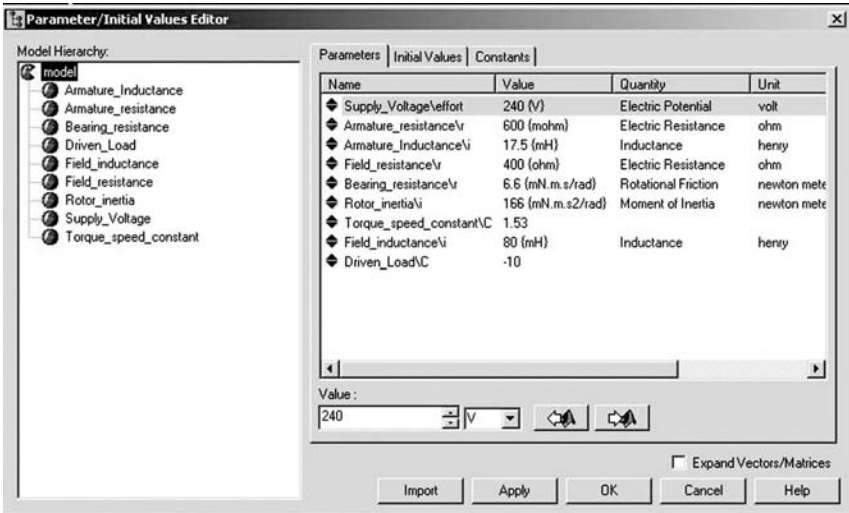


FIGURE 9.25

Parameter values used in simulation.

system response. The first one (Figure 9.26) shows how the current in the circuit varies. The plot shows the total current, the current through the armature circuit, and the field current. The field current is small because the field resistance is high.

Figure 9.27 shows the variation of torque output with time. Total torque output is used to drive the load, rotate the rotor inertia, and overcome the

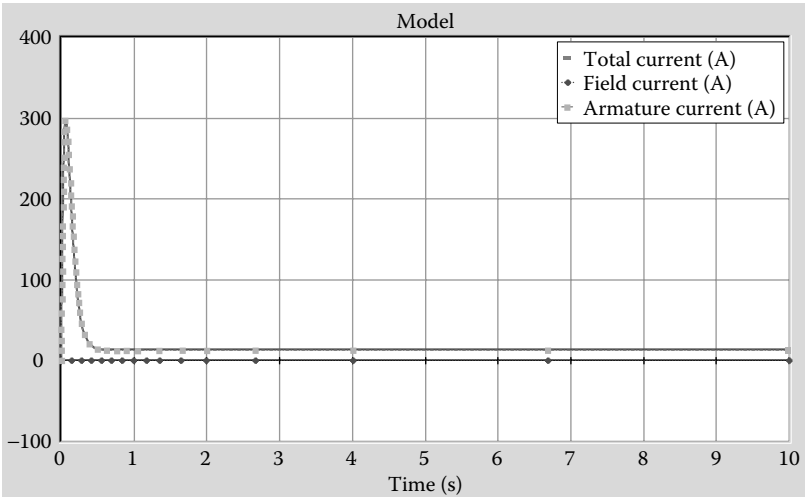


FIGURE 9.26
Field, armature, and total currents.

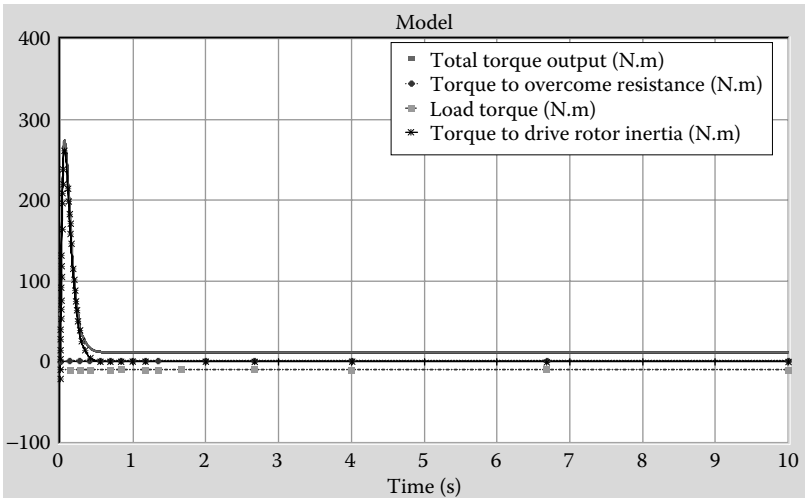


FIGURE 9.27
Distribution of the total torque output.

bearing resistance. Figure 9.28 compares the output torque and the speed of rotation as a function of time.

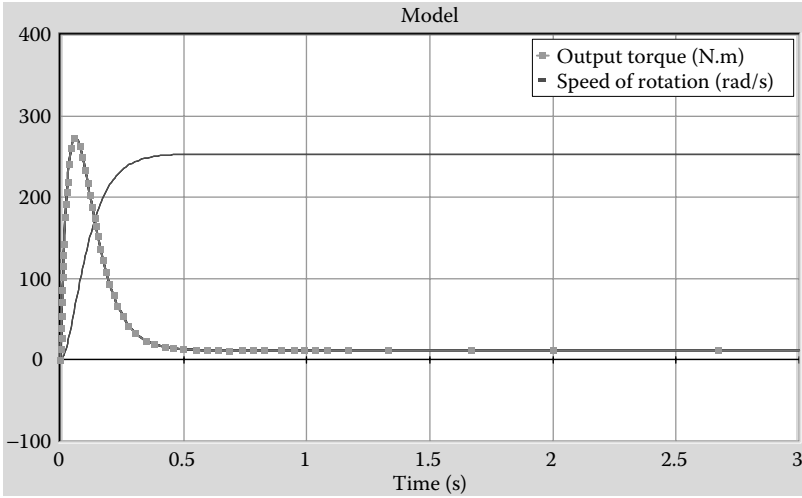


FIGURE 9.28
Output torque and rotation speed versus time.

Shunt motors are sometimes referred to as the constant speed motor, since at steady state the motor speed remains practically constant for a large range of motor load. Some of the applications of this motor are centrifugal pump, machine tools, blowers, fans, reciprocating pumps, and so forth.

9.1.2.4 Series Wound Motor

Figure 9.29 shows the schematic for a series wound motor. In a series wound motor, the armature and field currents are the same.

$$i_a = i_f \quad (9.30)$$

At steady state, the inductors work as connecting wires. So if the relationships at steady state are written, the equations look like the following:

ω is the angular speed

k is a motor constant

Φ is the magnetic flux

E_b is the back emf

T is the torque

R_a and i_a are the armature resistance and armature current, respectively,

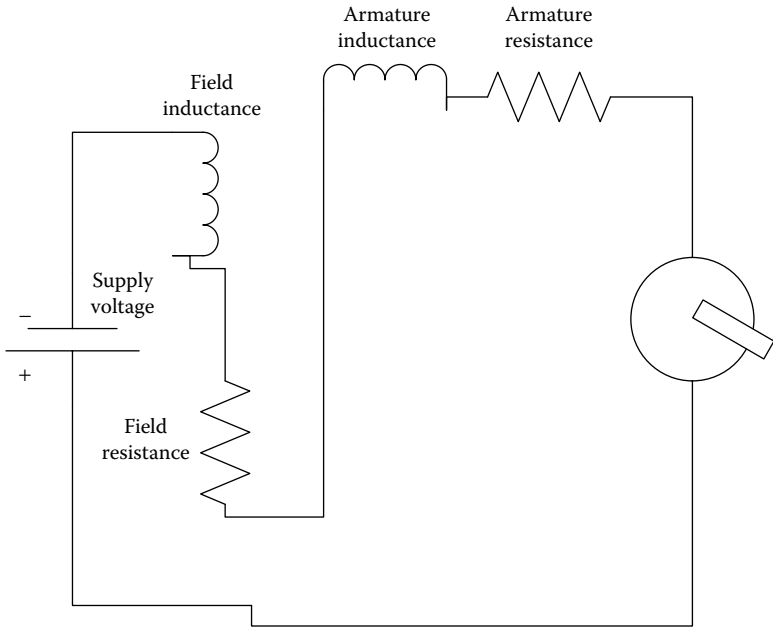


FIGURE 9.29
Circuit for series wound motors.

$$\begin{aligned}
 k\Phi &= k_s i_a \\
 V &= E_b + (R_a + R_f) i_a \\
 E_b &= V - (R_a + R_f) i_a \\
 \therefore k\Phi &= k_s i_a
 \end{aligned} \tag{9.31}$$

$$\begin{aligned}
 E_b &= k\Phi\omega \\
 \omega &= \frac{E_b}{k\Phi} = \frac{E_b}{k_s i_a}
 \end{aligned}$$

$$\begin{aligned}
 T &= k\Phi i_a \\
 T &= k_s i_a \cdot i_a \\
 T &= k_s i_a^2
 \end{aligned} \tag{9.32}$$

$$i_a = \sqrt{\frac{T}{k_s}} \tag{9.33}$$

$$\begin{aligned}
 \omega \cdot k_s i_a &= V - (R_a + R_f) i_a \\
 \omega &= \frac{V}{k_s \sqrt{\frac{T}{k_s}}} - \frac{(R_a + R_f) i_a}{k_s i_a} \\
 \omega &= \frac{V}{\sqrt{k_s \cdot T}} - \frac{(R_a + R_f)}{k_s}
 \end{aligned} \tag{9.34}$$

The bond graph model for the whole system is shown in Figure 9.30. The MGY element is the element that transforms electrical to mechanical power. The flow from the electrical side determines the effort on the mechanical side. And the flow on the mechanical side determines the effort on the electrical side.

$$\begin{aligned}
 \because k\Phi &= k_s i_a \\
 E_b &= k\Phi\omega \\
 \omega &= \frac{E_b}{k\Phi} = \frac{E_b}{k_s i_a}
 \end{aligned} \tag{9.35}$$

$$\begin{aligned}
 T &= k\Phi i_a \\
 T &= k_s i_a \cdot i_a \\
 T &= k_s i_a^2
 \end{aligned} \tag{9.36}$$

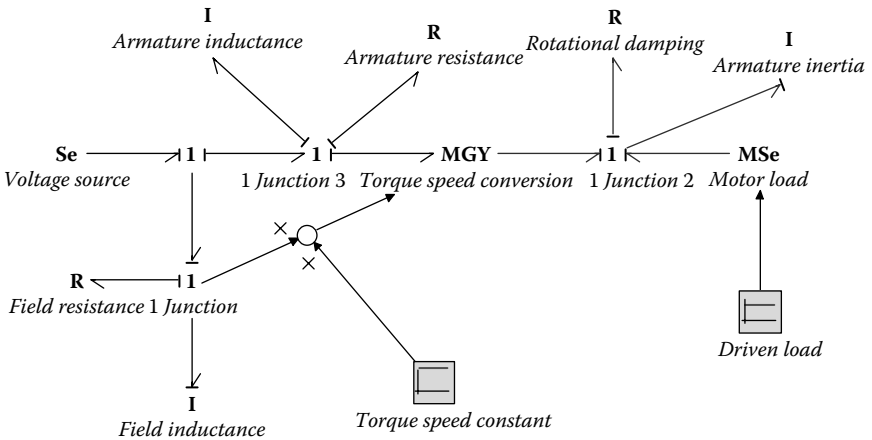


FIGURE 9.30

Bond graph model for a series wound motor.

The bond graph model is simulated using the parameters shown in Figure 9.31. The graphs shown in Figures 9.32, 9.33, and 9.34 show the response of the system as obtained by simulating using the parameters.

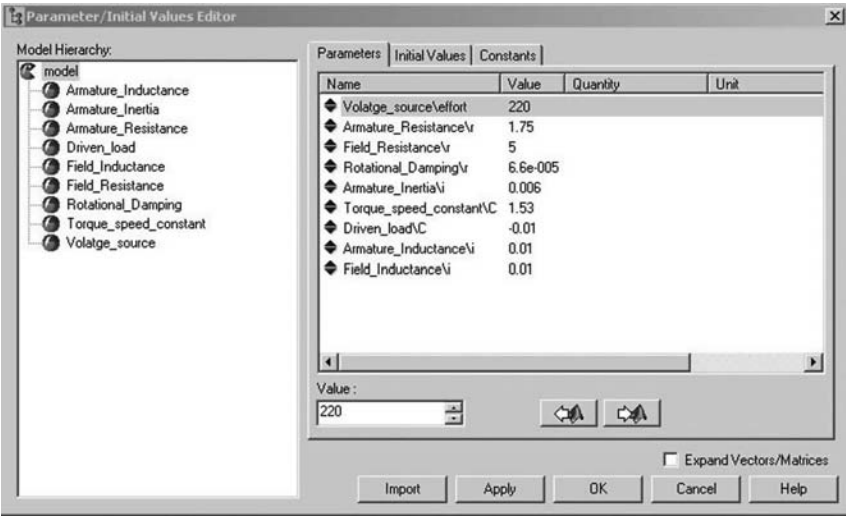


FIGURE 9.31
Parameters used in the simulation of the series wound motor.

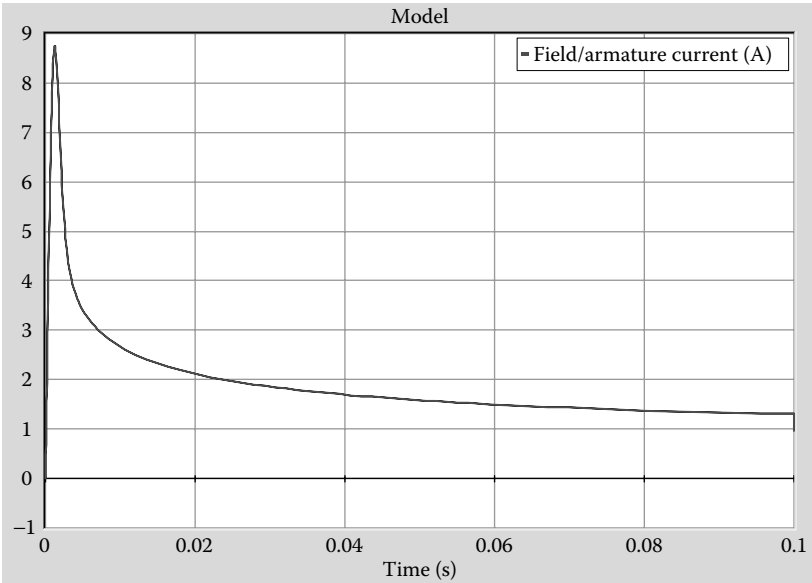


FIGURE 9.32
Armature and field current versus time.

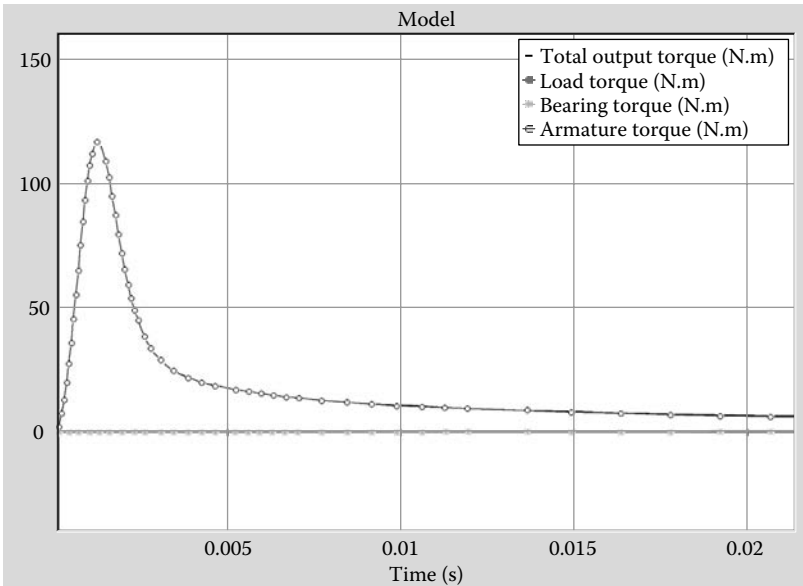


FIGURE 9.33
Different torque components versus time.

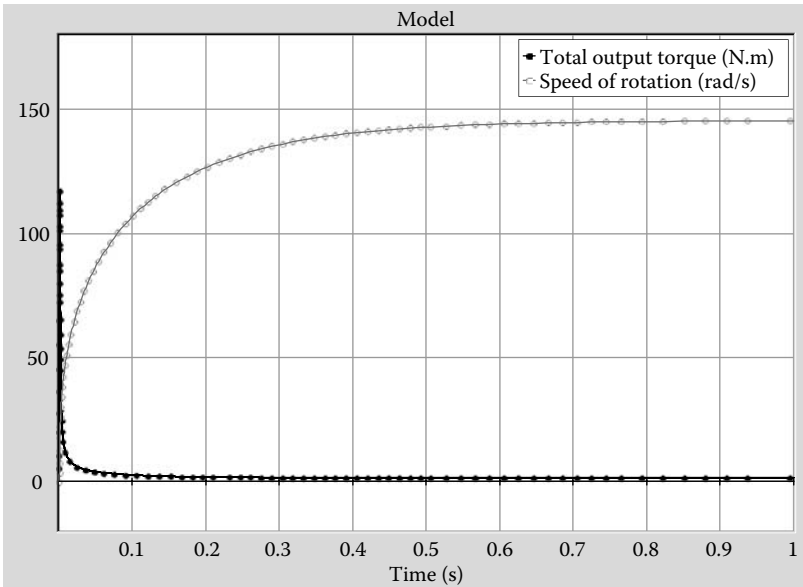


FIGURE 9.34
Total torque output and speed of rotation versus time.

Some of the typical characteristics of the series wound motors are that they change speed drastically as the load condition changes. Also, the starting torque is very high. Typical applications of these types of motors are hoists, electric trains, conveyers, elevators, electric cars, and so forth. Series wound motors should not be started with no load on them since the speed could get very high.

There are compound motors that are also used in some applications. For compound motors, the field circuit is made of two parts: a series and a shunt part. The model for such a motor would be a simple extension of the concepts discussed here. The compound motors typically have a high starting torque, and the no load speed is more controllable than the series motors.

9.1.2.5 Separately Excited DC Motors

Separately excited DC motors have a field winding circuit that is separate from the armature circuit. The model for the separately excited DC motor is shown in Figure 9.35. It is not discussed in any detail, and it is left to the reader to go through this as an exercise.

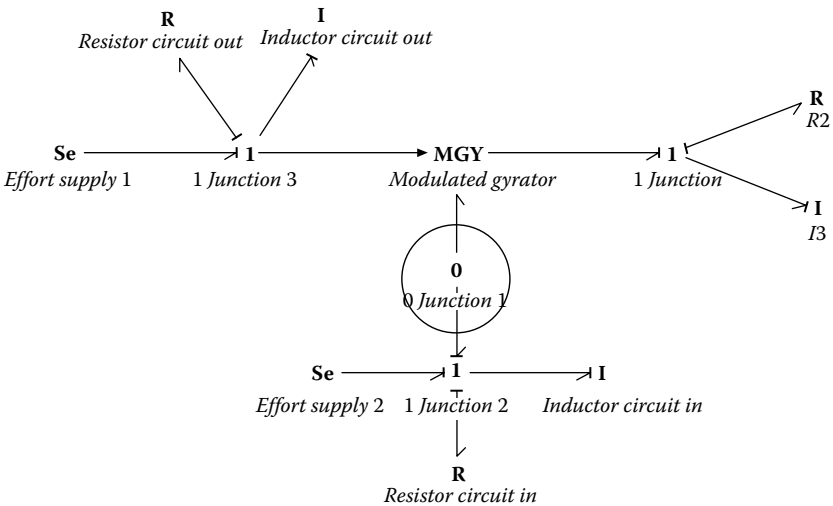


FIGURE 9.35

Separately excited DC motor.

9.1.3 Example of a Motor That Is Driving a Load

Here is an example of a permanent magnet DC motor that is driving a load. As Figure 9.36 shows, it consists of a PM DC motor, the output of

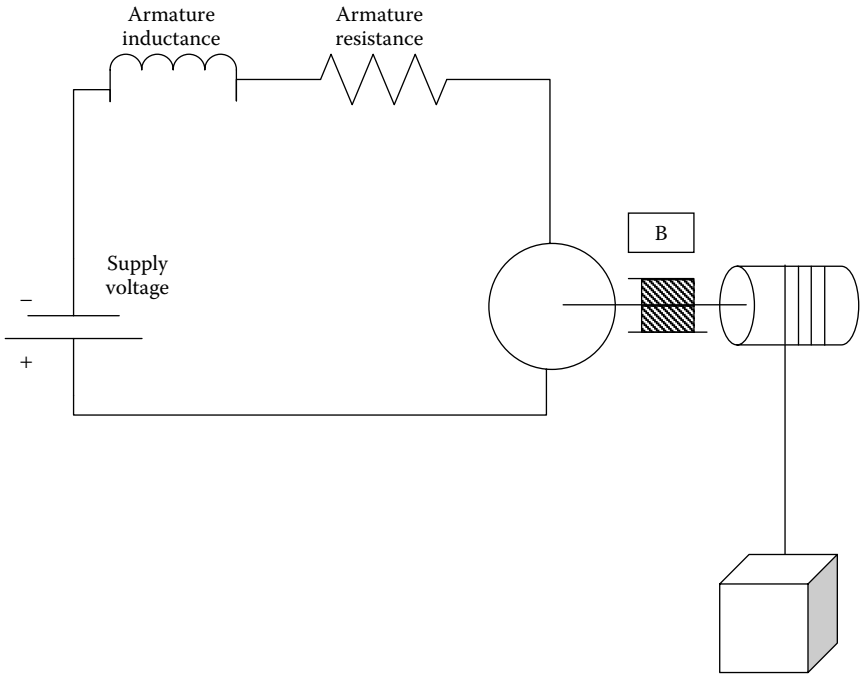


FIGURE 9.36
Schematic of a system where a motor is driving a load.

which is a shaft's rotation. There is drum that rotates on the shaft and a cable that is hoisting a load on that drum. There are three regions of this system. The first region is the electrical circuit for the motor. The second region is the mechanical rotation, and the third region is the translation motion of the cable and the mass that is being hoisted.

The system has three distinct regions: electrical, rotational, and translation. The GY element is the link between the electrical domain and the rotational domain. And the TF element is the link between the rotational domain and the translation domain. The bond graph model of the system is shown in Figure 9.37.

This system was simulated using the parameters shown in Figure 9.38. The system response in terms of the mass velocity and force on the mass are shown in Figure 9.39. A close-up of the initial stages of the response is shown in Figure 9.40. Careful review of the plots indicates a few interesting aspects. At the initial stages, the force on the mass oscillates since the torque at the start is high until the back emf builds up. Subsequently, the force reduces as the velocity increases and reaches a steady state. When the velocity is finally steady, the net force on the mass becomes 0, and it moves at a steady rate.

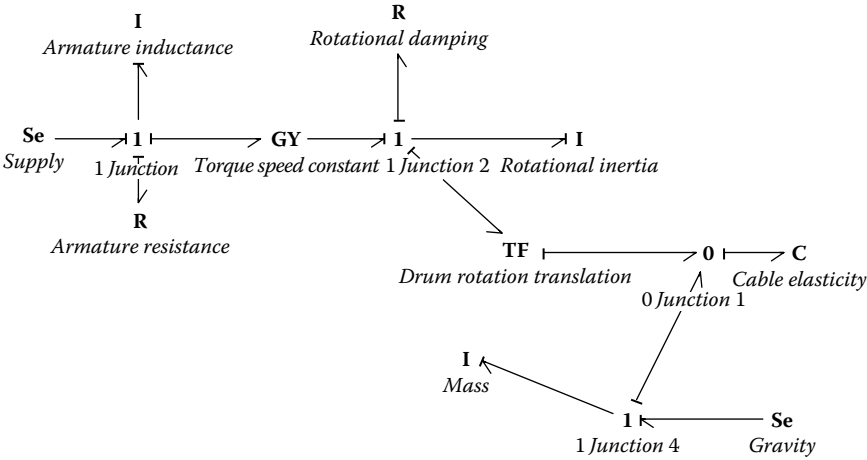


FIGURE 9.37
Bond graph model of a motor hoist system.

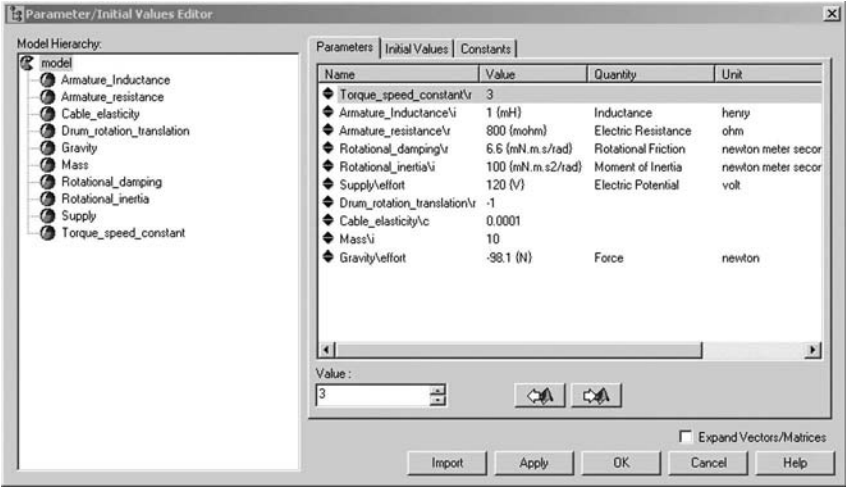


FIGURE 9.38
Parameters used in the simulation.

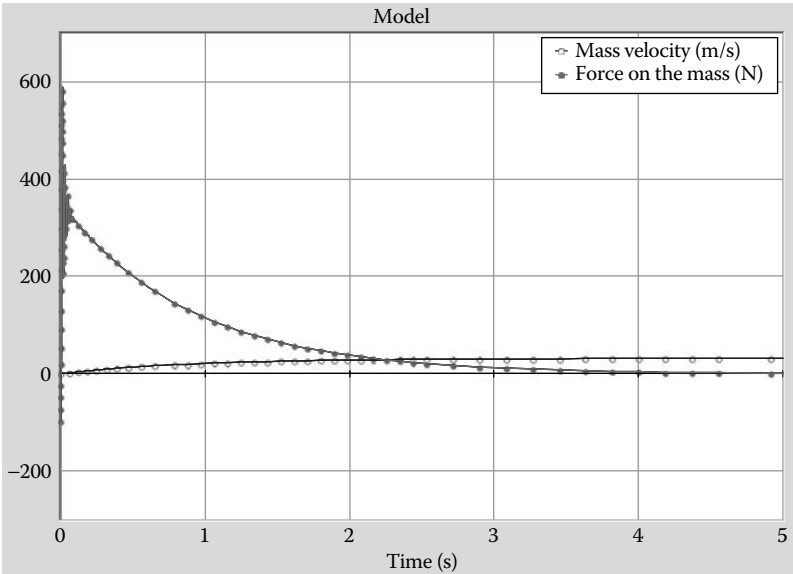


FIGURE 9.39
System response in terms of force on mass and mass velocity.

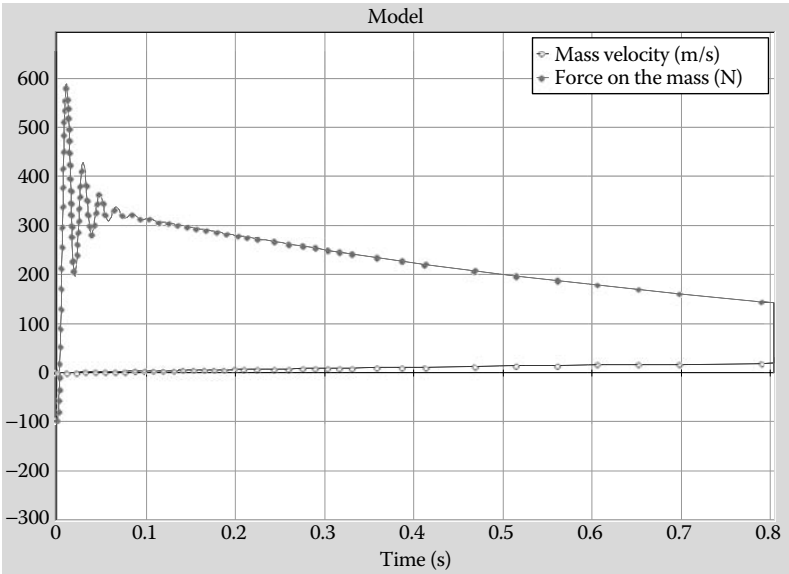


FIGURE 9.40
A close-up of the initial stages of the response.

9.2 Hydraulic Actuators

In Chapter 4, we discussed the basic components in a hydraulic system, their constitutive relationships, and how they are modeled using bond graph methodology. In this section, we will build on some of the concepts described earlier to specifically discuss the modeling of hydraulic actuators. As in the other domains discussed here, hydraulic actuators can be in many different forms. Hydraulic cylinders are well known as linear actuators and have a large variety of applications. Various types of pumps fall under the category of hydraulic actuators as well. There is a large class of components called valves that play a significant role in hydraulic actuation by controlling the direction and magnitude of flow in a hydraulic circuit. No discussion of hydraulic actuators will be complete without a discussion of some of the valve models.

9.2.1 Hydraulic Cylinders

Hydraulic cylinders, or power cylinders, are used to transform the power from the hydraulic domain to the mechanical domain, that is, pressure*flow rate to force*velocity. So at the core of the model for the hydraulic cylinder, one needs to include a transformer. On the hydraulic side, the capacitive effect of the compressible hydraulic fluid may be included. On the mechanical side, the friction in the piston and the inertia of the ram are two components that can be part of the model.

Figure 9.41 shows a schematic of the hydraulic cylinder and the corresponding bond graph model. The bond graph model shows a representa-

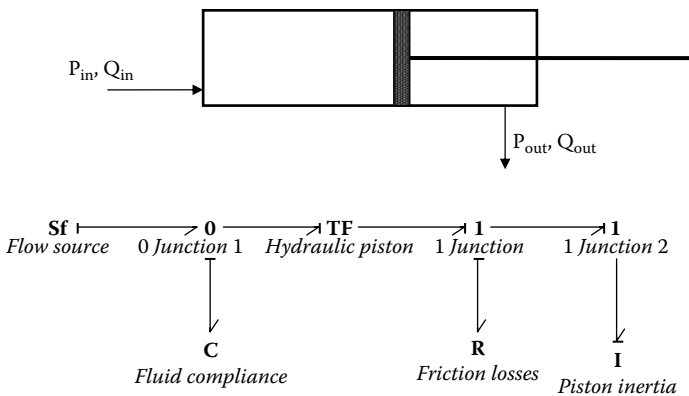


FIGURE 9.41
Hydraulic cylinder and its bond graph model.

tion of the hydraulic ram. The S_f (flow source) used in the model could be replaced by an appropriate source of power in a given situation. This model can be simplified by ignoring the friction losses and piston inertia if their effects are negligible. The capacitive (compliant) effect of the hydraulic fluid is captured through the C element in the model. Bulk modulus of the hydraulic fluid is the property that determines the compliance of fluids. The most commonly used hydraulic fluid is mineral oil with bulk modulus of the order of 1750 Mpa. The compliance characteristic of the fluid can be determined by the equation:

$$\Delta P = -\frac{\beta}{V} \Delta V \quad (9.37)$$

where, β is the bulk modulus, V is the initial volume of the fluid, and ΔV is the change in the volume. From this it can be seen that the capacitance will be V/β . In a linear actuator, the volume V is not a constant but changes linearly with the movement of the piston. Volume at any time can be expressed as:

$$V = V_{\text{initial}} + XA \quad (9.38)$$

where X is the linear movement of the piston and A is the effective piston area.

9.2.2 Pumps

A pump can be treated as simple source of flow if it is continuously running and the purpose of the model is to explore the dynamic behavior of the system that is driven by the pump. For fixed displacement pumps, pump inertia and internal friction can be neglected and the pump can be treated as a transformer that receives rotational input and provides hydraulic flow as the output. If hydraulic leakage losses are included, the bond graph representation looks like the one shown in Figure 9.42.

The rotational power source supplies power that is transformed into hydraulic power. Note that the outlet is a volume flow rate. The pressure at the outlet will be determined by the pump load that is being driven. For variable TF, a MTF element may also be used, and if the inertia of the rotational components and frictional losses are to be included, they may be added on the mechanical side as shown in Figure 9.42. If the pump inertia is included in the model, the input to the pump will not be a constant flow input but will have to be a constant effort input. The pump inertia will determine the rotational speed.

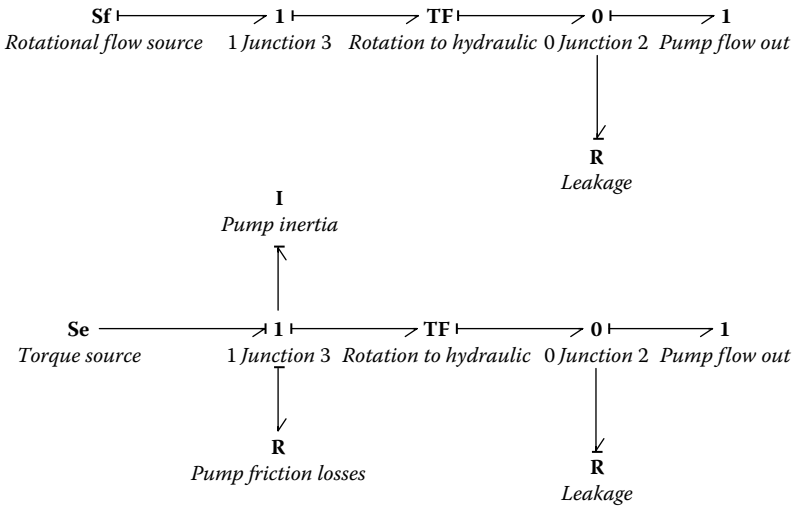


FIGURE 9.42

Bond graph representation of a pump (without and with additional components).

9.2.3 Hydraulic Valves

Hydraulic valves are a very important part of hydraulic systems. They play an important role in controlling both the direction as well as the quantity of flow. Careful modeling of control valves is necessary in order to successfully model any hydraulic system. Valves and their behavior play an important role in the dynamic behavior of the system that is controlled by the valves.

Figure 9.43 shows the schematic of a control valve that is well known as a four-way control valve. The spool can be actuated to move left or right and can open up or cover one or two of the control lines Y and Z. The supply is provided through the supply port, and the exhaust ports lead to

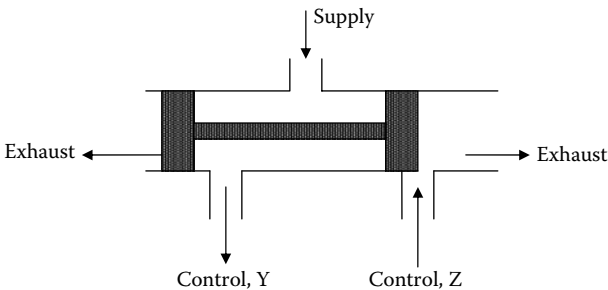


FIGURE 9.43

Schematic for a four-way control valve.

storage tank. When the spool is in the position shown in the Figure 9.43, the high pressure supply is provided to feed through the control line Y and fluid flows through the valve into the exhaust from the control line Z. When the spool moves toward the right, the opposite happens; that is, the supply is passed through the control line Z, and the control line Y is directly linked to the exhaust.

The flow through a control valve is determined by the flow through orifices that are opened or closed to different degrees. The orifice equation may be written as in Equation 9.39:

$$Q = C_d A \sqrt{\frac{2\Delta P}{\rho}} \quad (9.39)$$

where Q is the volume flow rate through the valve, C_d is the orifice flow coefficient (most of the time this is taken to be ~ 0.6 but a variable value could be used as well), A is the flow area and is directly proportional to the linear movement of the spool, ρ is the density of the fluid, and ΔP is the pressure difference. For the sake of convenience, this equation may be rewritten as:

$$Q = CX\sqrt{\Delta P} \quad (9.40)$$

where X is the movement of the spool and C is a constant that captures all other terms in Equation 9.39.

The flow through an orifice can be modeled as a flow through a resistor (i.e., the orifice needs to be modeled as a resistive element). However, the governing equation for this resistor is nonlinear. If we write the orifice equation in a form that is standard for a resistance element, the equation will be written as:

$$\begin{aligned} \Delta P &= RQ \\ Q &= \frac{1}{R} \Delta P \end{aligned} \quad (9.41)$$

where

$$R = \frac{\sqrt{\Delta P}}{CX} \quad (9.42)$$

This representation for R clearly shows that R is not a constant. It is also nonlinear because it is proportional to the square root of the pressure difference and also because it is dependent on the spool movement X . Although the above equations are representations for the flow rate through the orifice, the actual resistance model needs to contain more information about the limits of this representation. More on that will be discussed a little later.

The bond graph model for this valve is shown in Figure 9.44. The fluid input from the supply comes from a source of pressure. The exhaust, or sink, is also linked to a source of effort (with a value of 0) so that the flow to the exhaust/sink can be calculated. The four modulated resistances are the resistances in the four possible flow paths, that is, source to controls Y or Z and controls Y or Z to the exhaust/sink. The 0 and the 1 junctions are used in locations where the flow and the pressures are getting separated, respectively. For example, the 0 junction marked source receives the flow from the source and separates it into two paths, one towards the Y control path and one towards the Z control path.

We will now describe how the modulated resistances are modeled. Figure 9.45 shows the schematic of the valve used to develop the model equations (same view as Figure 9.43).

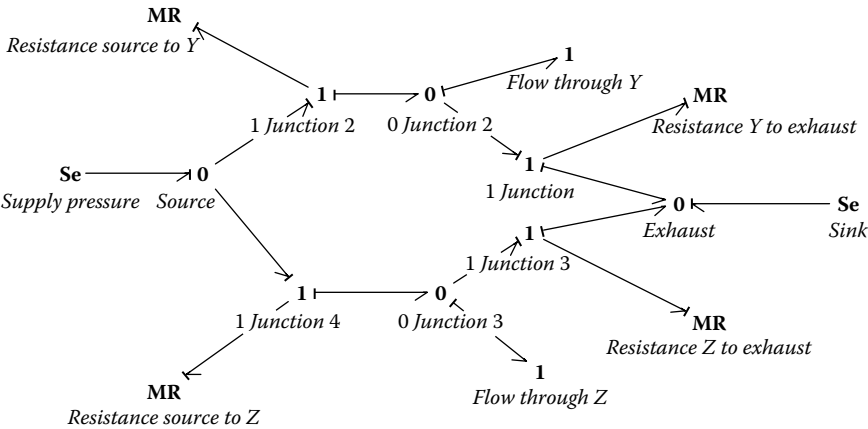


FIGURE 9.44
Bond graph model of the four-way valve.

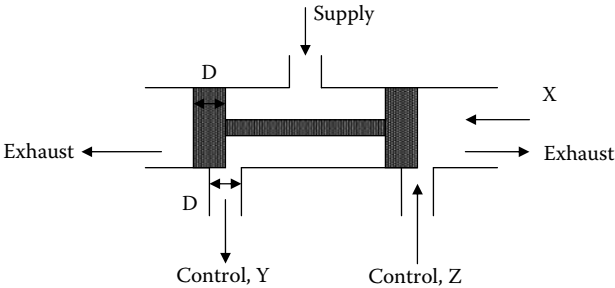


FIGURE 9.45
Schematic used to develop the valve model.

between supply and control Y

$$Q = 0, \text{ if } X \text{ is } 0$$

$$Q = CX\sqrt{\Delta P}, \text{ if } X \text{ is positive and } X \leq D$$

$$Q = CD\sqrt{\Delta P}, \text{ if } X \text{ is positive and } X > D \quad (9.43)$$

$$Q = 0, \text{ if } X \text{ is negative}$$

between supply and control Z

$$Q = 0, \text{ if } X \text{ is } 0$$

$$Q = 0, \text{ if } X \text{ is positive}$$

$$Q = C|X|\sqrt{\Delta P}, \text{ if } X \text{ is negative but } X \leq D \quad (9.44)$$

$$Q = CD\sqrt{\Delta P}, \text{ if } X \text{ is negative and } X > D$$

between control Y and exhaust

$$Q = 0, \text{ if } X \text{ is } 0$$

$$Q = 0, \text{ if } X \text{ is positive}$$

$$Q = C|X|\sqrt{\Delta P}, \text{ if } X \text{ is negative and } X \leq D \quad (9.45)$$

$$Q = CD\sqrt{\Delta P}, \text{ if } X \text{ is negative and } X > D$$

between control Z and exhaust

$$Q = 0, \text{ if } X \text{ is } 0$$

$$Q = CX\sqrt{\Delta P}, \text{ if } X \text{ is positive and } X \leq D$$

$$Q = CD\sqrt{\Delta P}, \text{ if } X \text{ is negative and } X > D \quad (9.46)$$

$$Q = 0, \text{ if } X \text{ is negative}$$

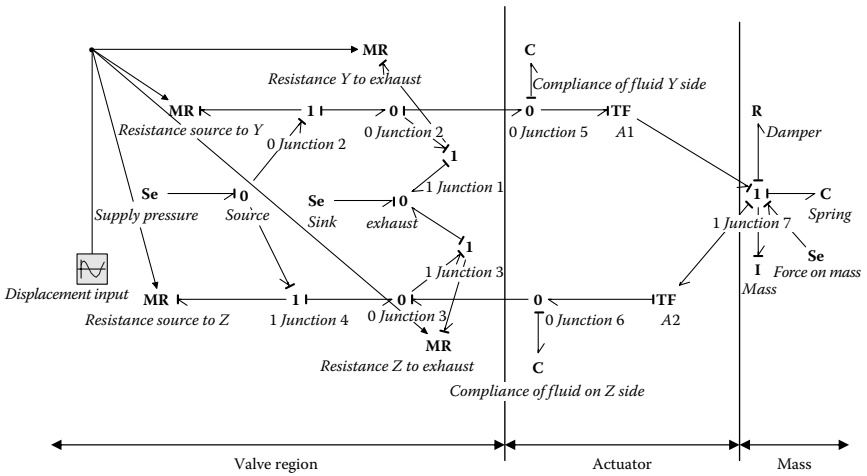


FIGURE 9.47
Bond graph model for system in Figure 9.46.

Constants

```
real D = 1;
```

Equations

```
if (r == 0.0) then
p.f = 0.0;
else
if (r < 0.0) then
p.f = 0.0;
else
if (abs(r) <= D) then
p.f = 0.1*abs(r)*sqrt (abs(p.e));
else
if (abs(r) > D) then
p.f = 0.1*D*sqrt (abs(p.e));
end;
end;
end;
end;
```

The values of different variables used in the model are shown in Figure 9.48. The system inputs are chosen arbitrarily. In an actual system, these have to be chosen as per system properties. The system response for this set of input variables is shown in Figure 9.49. This figure shows the flow through the valve as the displacement changes with time. The flow is shut off on either side as

Parameters			
Initial Values			
Constants			
Name	Value	Quantity	Unit
Sink\effort	0		
Supply_pressure\effort	1000		
Spring\c	0.001		
Mass\i	1		
Damper\r	10		
A2\r	1.2		
A1\r	1		
Compliance_of_fluid_on_Z_side\c	1		
Compliance_of_fluid_Y_side\c	1		
Force_on_mass\effort	0		
Displacement_input\amplitude	5		
Displacement_input\omega	1 (rad/s)	Angular Velocity	radian per second
Displacement_input\phase	0 (rad)	Plane Angle	radian

FIGURE 9.48
Parameters used in the simulation of the model.

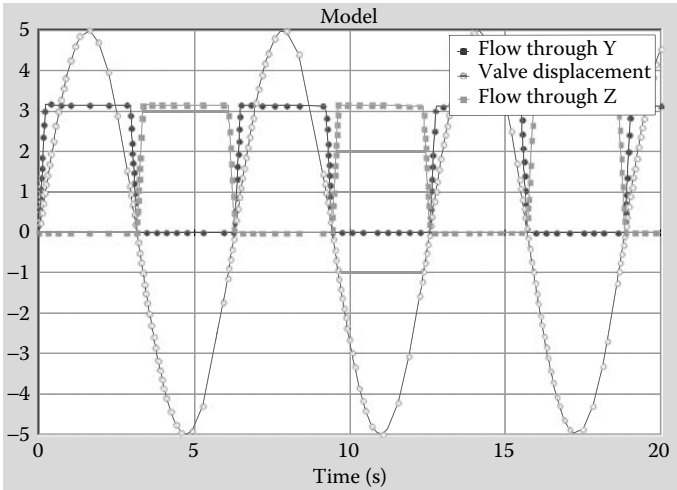


FIGURE 9.49
System response of the model.

the displacement changes from positive to negative. Also, the maximum flow is determined by the orifice size and will not be altered beyond a certain amount of displacement input.

9.3 Summary

There are many types of actuators used in practice. In this chapter we have touched on the two most common types of actuators, specifically, electromagnetic actuators and hydraulic actuators. Within the electromagnetic actuators, we have discussed linear actuators and different types of DC motors. These are commonly used actuators for mechatronic applications. There are some other motors, such as stepper motors and AC motors, that we have not touched on for now. Within the hydraulic actuators, we have paid most attention to the modeling of the behavior of hydraulic valves that are the most critical components in any hydraulic actuator circuit. The behavior of the valves is the most challenging component in the modeling of such devices.

Problems

- 9.1. Figure P9.1 shows a schematic for a solenoid valve where the opening and closing of a hydraulic circuit is controlled by the movement of the plunger of a solenoid. Using the concepts covered in this chapter, develop a bond graph model of such a valve and list all the important valve parameters necessary to model the behavior of this valve.

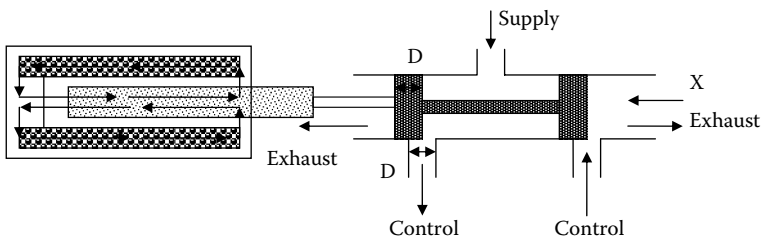


FIGURE P9.1

Figure for Problem 9.1, schematic for a solenoid valve.

- 9.2. Figure P9.2 shows the schematic of a PM DC motor driven tape winding device. The different parameters for this system are as follows: $J_1 = 5E-5 \text{ kgm}^2$, $B_1 = 1E-2 \text{ Nms}$, $r_1 = r_2 = 0.002 \text{ m}$, K_t (motor torque constant) = $3E-2 \text{ Nm/A}$, $K = 2E4 \text{ N/m}$, $B = 20 \text{ Ns/m}$, $B_2 = 2E-2 \text{ Nms}$, $F = 10 \text{ N}$. Develop a bond graph model of this system, and simulate its behavior for the given system parameters. What is the steady state rotational speed of the pulleys? Do you get any oscillation in the rotation of the pulleys?

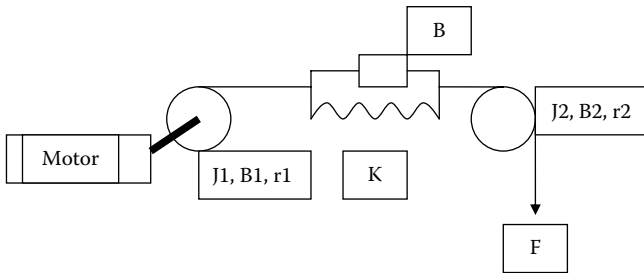


FIGURE P9.2

Figure for Problem 9.2, schematic of a PM DC motor driven tape winding device.

- 9.3. Figures P9.1 and P9.2 show a system and its bond graph model respectively. Derive the governing equations for the system shown in these figures.
- 9.4. Figure P9.3 shows the schematic of a system where the hydraulic valve is used to control the force on the roller and thus control the thickness of a rolled sheet. Using the schematic shown, develop a bond graph model of this system and simulate it with suitable system parameters.

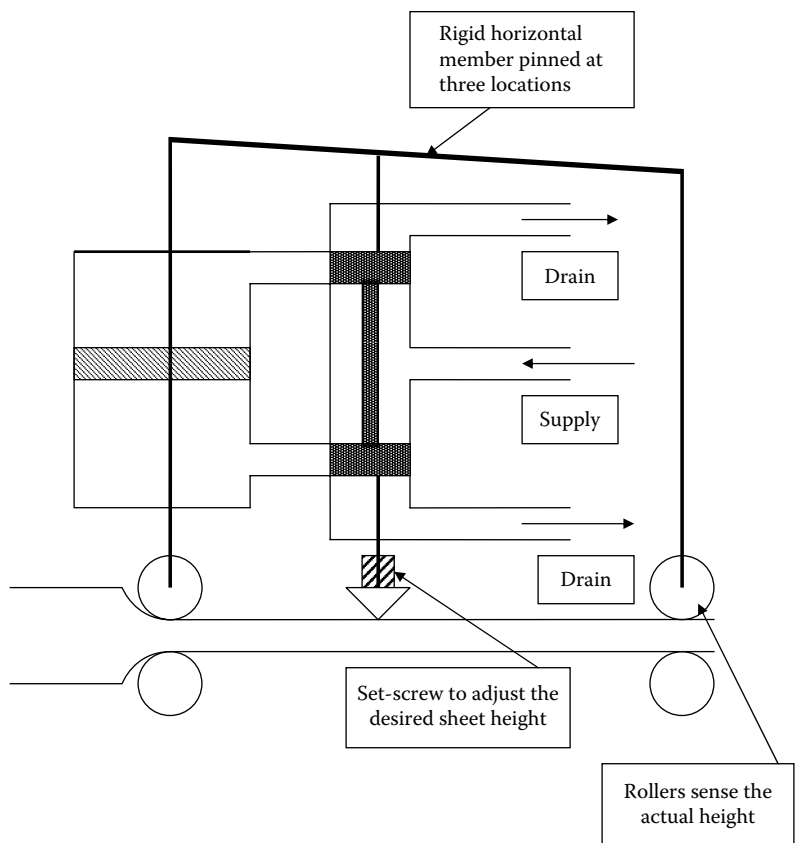


FIGURE P9.3
Figure for Problem 9.4, system involving hydraulic valve to control the thickness of a rolled plate.

9.5. Figure P9.4 shows the schematic of a solenoid switch. Develop the bond graph model of this at demonstrate its working through simulation.

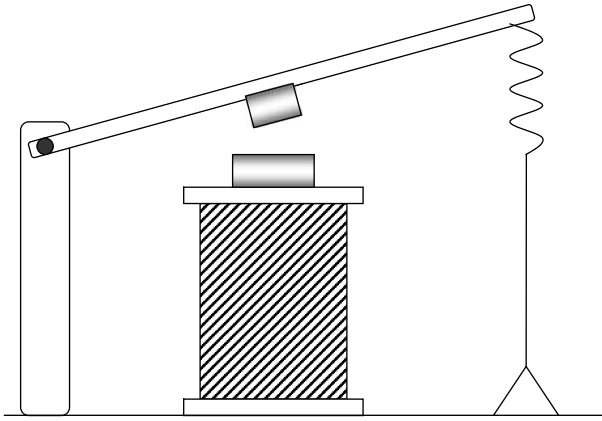


FIGURE P9.4

Figure for Problem 9.5, schematic for a solenoid switch.

- 9.6. Figure P9.5 shows how the load to be driven by a motor varies with time. Use the PM DC motor and the shunt wound DC motor models to simulate their behavior for this load. How does the motor speed vary as the load is applied as per this function?

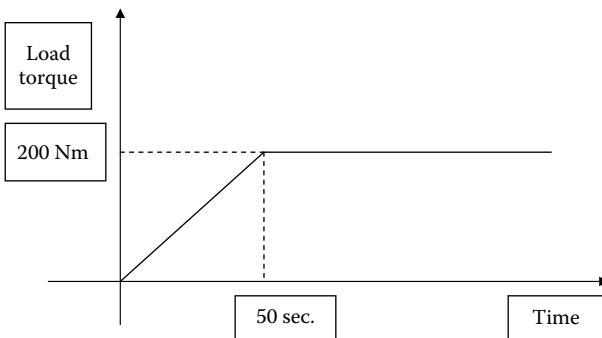


FIGURE P9.5

Figure for Problem 9.6, motor load profile.

- 9.7. A series wound DC motor is used to rotate an inertial load. The speed of rotation is to be measured with a Hall effect sensor for the purpose of motor speed control. Using the Hall effect sensor model from the previous chapter as well as the relevant motor model in this chapter, develop the complete bond graph model to measure the speed of rotation of the inertial load. What is the speed profile if a series wound motor is used to drive this load?

9.8. Here are some typical values for shunt motor parameters. Supply voltage = 120 V, Armature Resistance = 0.6 Ohms, Field Resistance = 400 Ohms, Armature inductance = 0.0175 H, Field Inductance = 0.175 H, Mechanical friction (in rotating shaft) = 0.000066 Ns/m Rotational moment of inertia = 0.08 kg m², torque constant = 1.53 (in consistent units). For the exercise below, you should use these values. Develop a bond graph representation of a motor where the field winding is parallel to the armature winding (also called shunt wound motors). For the shunt motors, the field resistance is usually made very high so that a small current is drawn by it. Use the bond graph model to develop simulations of the behavior of this motor.

- To model a constant torque load, use a *MSe* element attached to a constant negative input. Change the value of this constant torque load from -1 to -5 to -10. Plot the speed of rotation versus time, armature current versus time, and power output of the motor versus time for the *above three conditions*. Modify the equations of MGY so that you can generate power data at the gyrator output.
- To model a load where the torque is proportional to the square of the speed of rotation, modify the equation for the mechanical friction element to model effort as a function of the square of the velocity. Remove the *MSe* that you were using in the previous case to simulate the constant torque load. Change the R factor from 0.000066 to 0.00066 and then to 0.0066. Plot the speed of rotation versus time, armature current versus time, and power output of the motor versus time for the above three conditions.

This page intentionally left blank

10

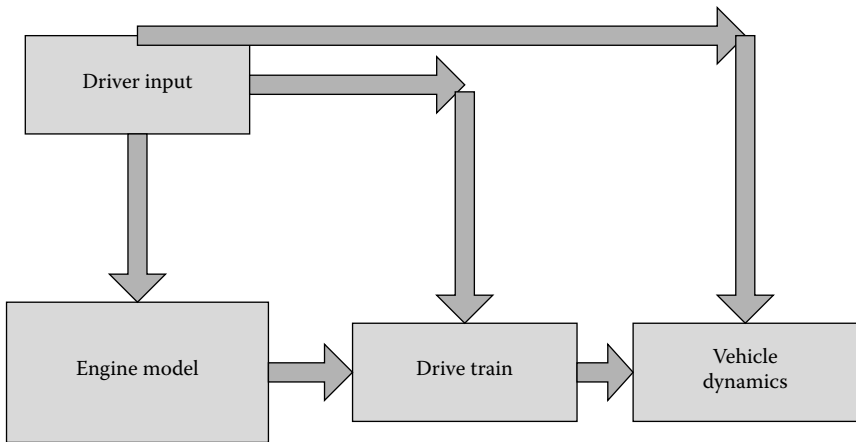
Modeling Vehicle Systems

Automobiles have evolved a lot over the last century. While the first cars made were modeled after horse-drawn carriages and were purely mechanical devices, the modern-day automobile is a marvel of complex interdisciplinary engineering. As customers have demanded more from vehicles, designers have used newer and newer technology to meet the needs in the most efficient manner possible. As a result, many systems and subsystems in today's car are mechatronic in nature. While the core of the automobile is still a mechanical device consisting of a power source connected to a drive train that helps take the vehicle down the road, most controls and so-called "smart" features are achieved through the use of microcontrollers, smart algorithms, and sensors and actuators. The number of sensors used in a modern vehicles has increased exponentially over the last 20 years. Many of the subsystems, such as steering, braking, and so forth, are being replaced by "by-wire" systems. Even the power source, the traditional internal combustion engine, is being replaced by hybrid architectures consisting of a combination of electric motors, fuel cells, and engines. Power sharing among these sources is dynamically controlled for optimal performance through highly refined algorithms residing on microchips that are implanted on subsystems within the automobile. The automobile of today is a quickly evolving system, but its evolution is clearly moving from a purely mechanical device to an intricate mechatronic device.

Mechatronic or multidomain systems and subsystems in an automobile are too numerous to be tackled in a single chapter within this book. Our goal in this chapter is, therefore, to touch on only some of them. More modeling examples can be found in a variety of other publications, some of which are mentioned here. Researchers and modelers have used the bond graph methodology to model the automobile at a variety of different levels. There are full vehicle models, such as the ones discussed by Horovat et al. (2000), and component or subsystem models, such as the ones found in publications by Thoma (2000); Karnopp (1974, 1984); Margolis (1982, 2001); Louca, Stein, and Rideout (2001), and others.

There are three broad areas to consider. These can be shown in a block diagram as: power generation (or engine), power transmission (or power train), and vehicle dynamics (Figure 10.1).

Figure 10.1 only shows a high-level description of a vehicle, but there are many details; and to model features in detail, a lot more needs to be

**FIGURE 10.1**

Major areas of a vehicle to be considered.

considered. In this chapter we will not attempt to model all aspects in detail but will make an attempt to model some of the systems and subsystems in a vehicle. The chapter will be divided into sections that will focus on different aspects of a vehicle, such as overall vehicle model, vehicle dynamics and ride, power train, and vehicle subsystems.

The objective of this discussion is not necessarily to be comprehensive, but rather to provide an exposure to the reader about how the modeling and simulation of vehicle systems and subsystems are achieved.

10.1 Vehicle Systems

In order to put things in perspective, an automobile/ground vehicle system can be broadly represented as in Figure 10.2. The power generated from the engine combustion is supplied to the drive train as a torque profile. The drive train transfers power through the transmission, the power transformation mechanism, to the front and the rear axels, which in turn transfer power to the front and rear wheels. The vehicle dynamic characteristics (dynamic behavior of the vehicle under different driving conditions) dictate vehicle behavior.

Even though this big picture captures the essentials of an automobile, a modern automobile has many other subsystems, such as the braking system, steering system, and so forth. These subsystems are not explicitly addressed in this schematic but are still very vital.

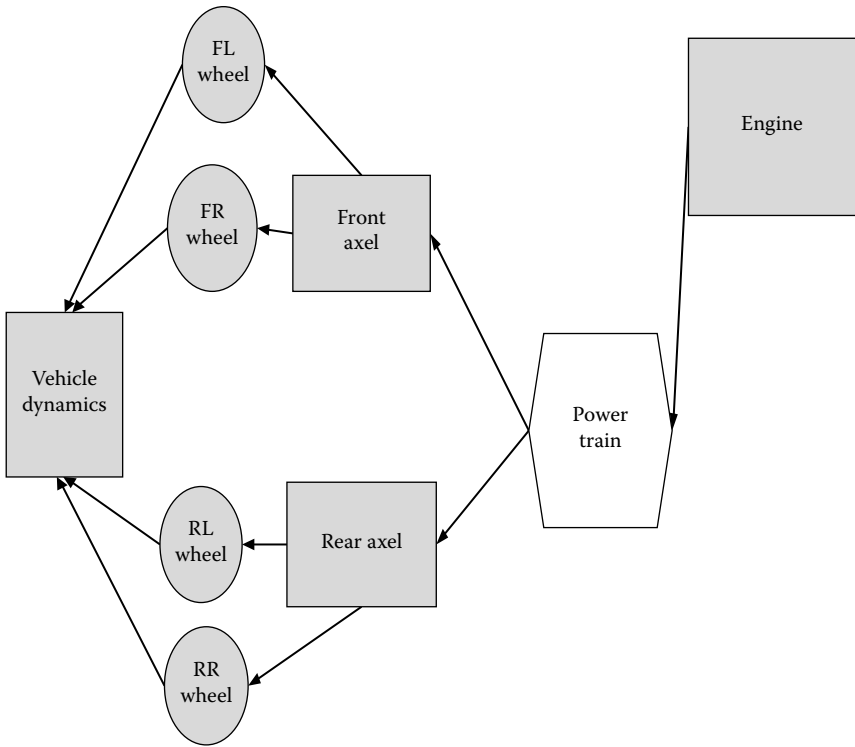


FIGURE 10.2
Schematic of vehicle power flow.

Figure 10.3 shows a representation of Figure 10.2 (vehicle drive line) using subsystems to represent the blocks in Figure 10.2. A bond graph representation of the vehicle drive line schematic is shown in Figure 10.4.

This is one of the simplest bond graph representations of a rear wheel drive vehicle system with gross approximations of most of the subsystems. The source of power is the engine that is represented as a source of effort (or torque). The engine inertia is represented as an I element and the clutch resistance as a variable resistance signifying the approach to model the engaging and disengaging of clutch through a signal to the MR element. The gear box has several inertia elements associated with it, and all of them are represented as a single lumped inertia. The variable gear ratio is represented as the MTF element. The C element represents the compliance of the shaft that transfers power from the gear box to the differential, which is in turn connected to the rear wheels by a TF element. The outlet from the differential is supplied to the two driving wheels through a 0 junction. As a result, the flow on the two sides (left and right) could be different, resulting in different speeds of rotation of the wheels. When

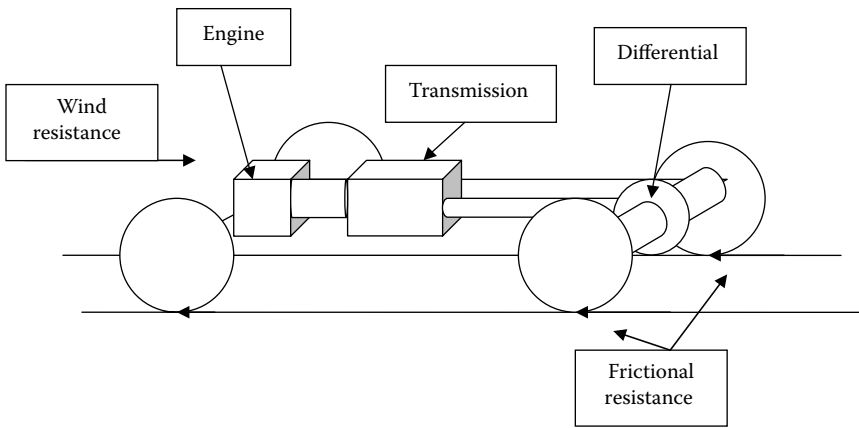


FIGURE 10.3
Subsystems that make up a vehicle drive line.

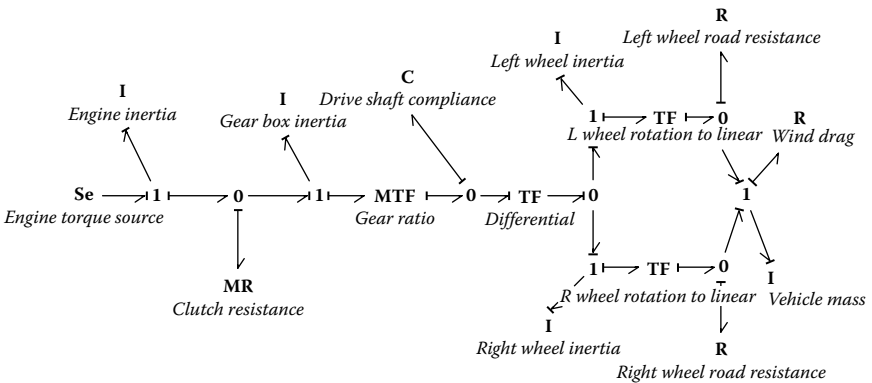


FIGURE 10.4
Bond graph model of vehicle drive line.

the vehicle is moving in a straight line, both wheels will be rotating at the same speed, and the output from the differential to both the wheels will be identical. When taking a turn, the outer wheel needs to turn more than the inner wheel, and, hence, the velocity output from the differential would be different to the two wheels. In the model, this flexibility of the differential is achieved through the use of a 0 junction, which equates the effort in all bonds, but the flows are different. This enables the incoming torque to be equal, but the velocities can be different.

Wheel inertias are included in the model as well as the road resistance in the form of R elements connected through rotation-to-linear motion transformers. Finally, a 1 junction brings the efforts from both wheels together and is connected to an R element to capture the effects of wind resistance, (drag), and an I element that represents the vehicle mass.

Although this model (or variations of this model) is found in many publications as the basic vehicle model, others can be found that account for different complexities in a vehicle. For example, Hrovat et al. (2000) reported on a model that accounted for losses in the engine and gearbox through additional *R* elements. They also accounted for tire elasticity and resistance of tires through *MR* and *C* elements to capture specific tire models. Complex vehicle dynamics, steering input, throttle positions, and so forth, can be added as well by introducing additional complexities in the model.

Using the simple example of the vehicle drive train shown here, we can still obtain very good estimates of many aspects of vehicle behavior. For example, a comparative analysis of fuel use/power requirement can be done at different speed levels for vehicles. It is well known that at low speeds, most of the power spent in driving vehicles is used to overcome friction at the wheels (especially at stop-and-go type of traffic situations). In these situations, the vehicle weight is a key factor in influencing the power requirements. However, at high speed, the effort needed to overcome wind resistance plays the most important role in fuel consumption because the drag on vehicles is proportional to the square of the relative velocity of the wind with respect to the car. The vehicle's projected surface area and the drag factor play a very important part at high vehicle speeds. So, in this model, the wind resistance is modeled such that the resistance value is proportional to the square of the vehicle velocity and the resistance at the wheels is modeled as equivalent representations of rolling resistances that are proportional to vehicle weight that is supported at each wheel. Figure 10.5 shows some representative parameters

Parameters Initial Values Constants				
Name	Value	Quantity	Unit	Arithmetic Type
Engine_Inertia <i>i</i>	1			Real
Right_wheel_inertia <i>i</i>	0.5			Real
Engine_Torque_source\effort	3000			Real
Differential <i>r</i>	10			Real
R_wheel_rotation_to_linear <i>r</i>	0.6			Real
Gear_Box_Inertia <i>i</i>	1			Real
Left_wheel_inertia <i>i</i>	0.5			Real
Wind_Drag <i>r</i>	1.8			Real
Drive_Shaft_Compliance <i>c</i>	1e-007			Real
L_wheel_rotation_to_linear <i>r</i>	0.6			Real
Vehicle_Mass <i>i</i>	500			Real
Left_wheel_road_resistance <i>r</i>	240			Real
Right_wheel_road_resistance <i>r</i>	240			Real
Constant1 <i>C</i>	1			Real
Constant2 <i>C</i>	3			Real

FIGURE 10.5

Vehicle parameters used for the vehicle drive train model.

for different components of the model that is used (in consistent units) in the simulation. Figure 10.6 shows a set of plots that show how the power expended changes at the wheels due to the wind resistance as the velocity of the vehicle increases. At low speeds, the wheel resistances are more important than the wind drag, but as the vehicle speed increases, the wind drag quickly becomes the more important factor. It is, thus, very important to try and keep wind drag effect to as small a value as possible. Wind drag force is equal to the product of the drag coefficient, the projected area, and the square of the vehicle velocity.

$$F_d = C_d A v^2 \quad (10.1)$$

This explains why so much effort is placed on vehicle aerodynamics, which helps in reducing the drag coefficients.

We can use this model to study other aspects of a vehicle. For example, to replicate the process of turning, we can alter the resistance at the left and the right wheels. When the vehicle is being driven along a straight line, the friction forces at the two wheels are identical, and, as a result, the wheel speeds are identical as well. When the vehicle is turning, the ground reaction forces at the inner and outer wheels are different, and, therefore, the

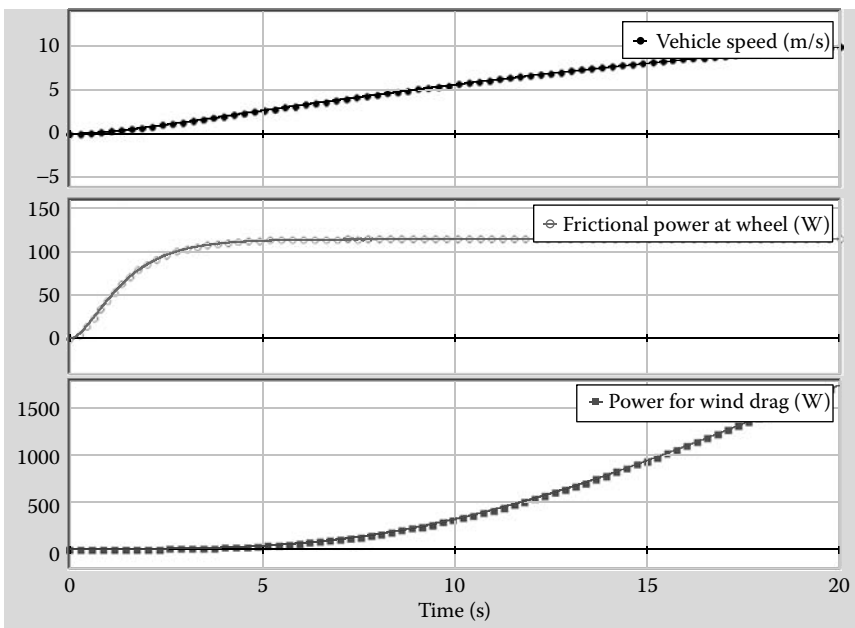


FIGURE 10.6

Simulation results for the vehicle drive train model.

friction forces are different as well. In the model, if the friction forces (or resistances) at the two wheels are altered, the wheel speeds turn out to be different at the two wheels. This indicates a turning situation. Figure 10.7 shows such a plot depicting a turning situation.

Throughout the years, many researchers have used bond graphs to model several aspects of the power train as well as other parts of the vehicle. We will not be able to discuss all of them in any detail here but will mention some of them for the benefit of the reader. Cichy and Konczakowski (2001) developed a model for internal combustion engines. Several significant studies have been done in the modeling of transmissions. Horovat et al. (2000) reported extensively on the model of manual transmissions, Coudert et al. (1993) and Wehrein et al. (2006) have published models of automatic transmissions. A key building block of the transmission model is the model of a planetary gear train. Figure 10.8 shows this “building block” bond graph model. In the area of hybrid electric vehicles, several publications report the use of bond graph as a modeling tool. Of particular note among these are the works of Gao et al. (2007), Filippa et al. (2005), and Hubbard et al. (1997). One of the important aspects of modeling hybrid power trains is modeling of the algorithm that is used to dynamically alter the power consumption from the engine and

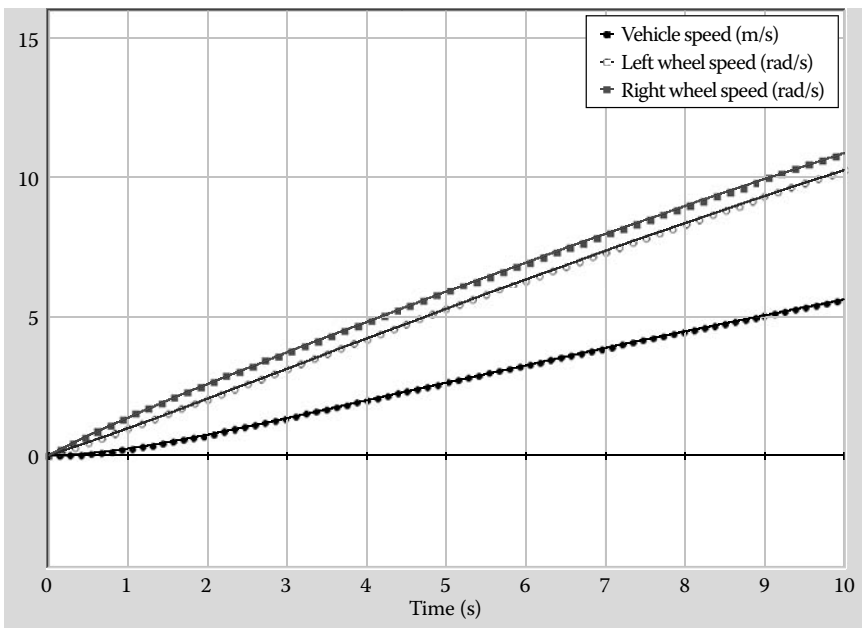


FIGURE 10.7

Comparison of different wheel speeds during turning.

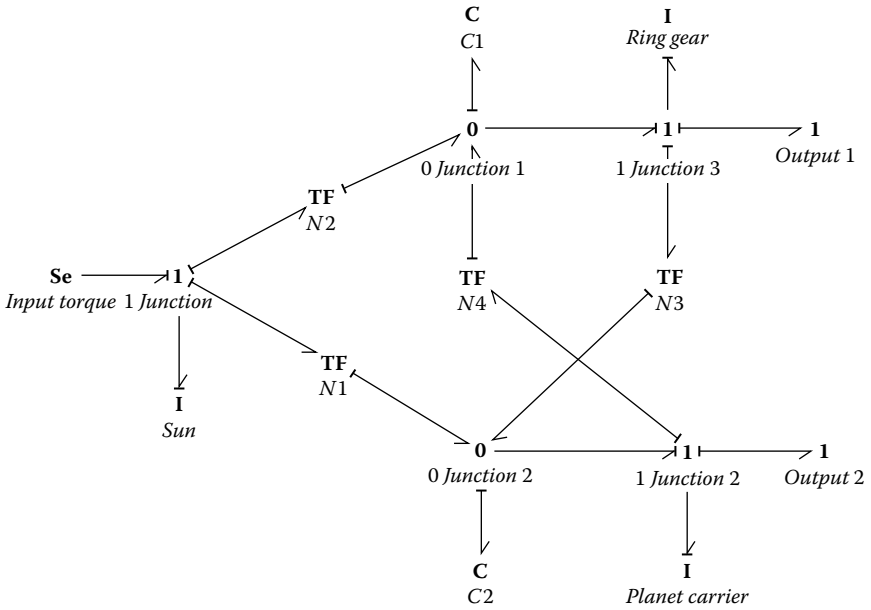


FIGURE 10.8
Bond graph model of a planetary gear train.

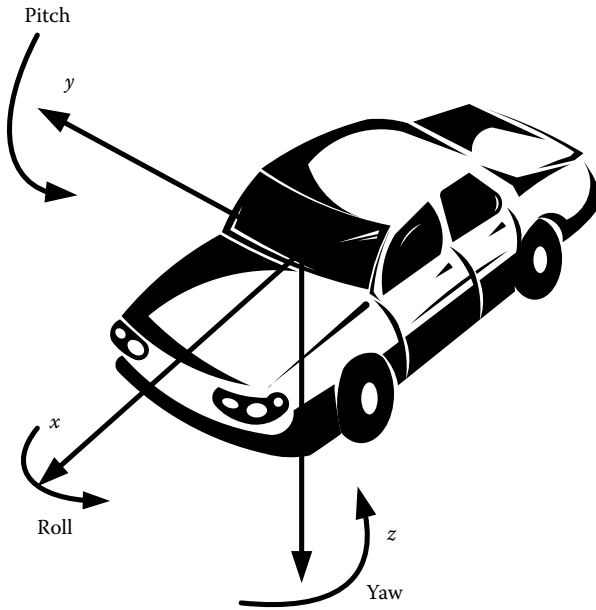
the battery. For optimum performance, this has to be tightly controlled, and bond graph based modeling provides a very good tool to work out the necessary algorithms.

10.2 Vehicle Dynamics

10.2.1 Ride: Heave and Pitch Motion

The study of dynamics of vehicles is a study of the dynamics of a 3-D rigid body. Some of the pioneering works using bond graph methodology in this area were done by Karnopp (1976), Margolis (1982), and Granda et al. (2003). The use of active suspension in the model has been reported by Hrovat et al. (2000), Khemliche et al. (2004), and others.

In a 3-D model, there are six degrees of freedom: translations in three mutually perpendicular directions x , y , z ; and Φ , θ , ψ , the rotations about the three axes. The three rotations are also called pitch, yaw, and roll (Figure 10.9). A complete vehicle dynamics model needs to consider all these motions since they are coupled to each other. Directly trying 3-D modeling with all six degrees of freedom (DOF) intact will be a complicated exercise. So, first we will look at some of the simplified versions

**FIGURE 10.9**

Pitch, yaw, and roll motion directions of a vehicle.

because a lot can still be learned about vehicle behavior from these. Some of the common simplifications are

1-D Model: A single spring–mass–damper model. This model is called the quarter car model. Here the single mass represents the mass of the vehicle, and the spring and the damper represent the vehicle suspension system. The road input can be modeled using a simple source of flow. Using this model, the only thing that can be studied is the vertical motion of the vehicle in response to the road input. Figure 10.10 shows a schematic of the model and the corresponding bond graph.

2-D Model: This model is a little more complex and takes into account not only the mass but also the inertia, and at least one translation and one rotation of the vehicle can be modeled. This model is called the half car model. If the model is for the front and the rear wheel and the view presented is the view of the vehicle from the side, the two motions that can be modeled are the vertical motion (also called heave) and the rotation about the y axis (also known as the pitch). Figures 10.11 through 10.13 show the vehicle schematic and the corresponding bond graph. The level of details to be included in the bond graph model could be determined by the user. The simpler

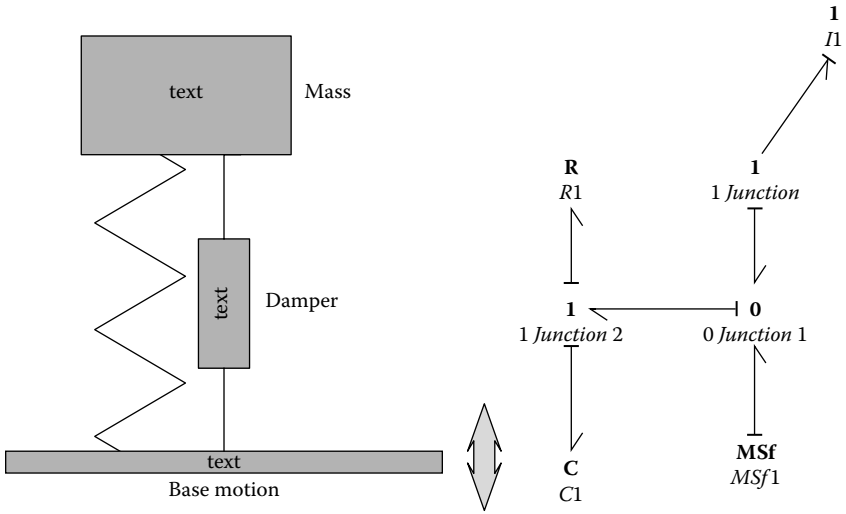


FIGURE 10.10

A quarter car and its bond graph model.

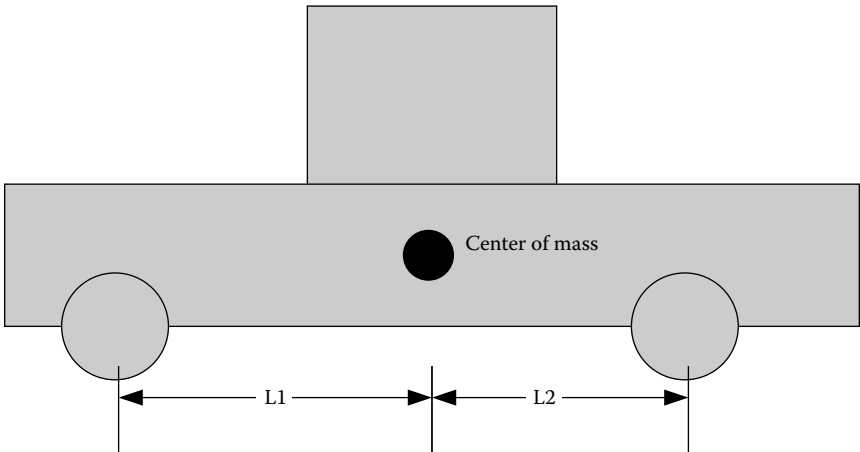


FIGURE 10.11

Schematic for half car model.

approach is to include the vehicle mass along with the suspension at the front and rear represented through a pair of spring and damper elements. If more complexity is desired, the tire masses and the corresponding tire stiffness could be included as well.

There are two DOFs in the 2-D model (see Figure 10.12).

1. Heave
2. Pitch

Bond graph development procedure (refer to Figure 10.13) is

1. There are six velocity points (the two velocity inputs from the road, the two velocity points where the suspension is attached to the vehicle mass, the heave motion of the vehicle center of mass, and the pitch motion of the vehicle center of mass). Each point is represented by a 1 junction on the figure.
2. In the front and back wheels, we have spring and damper systems, which are connected through the 0 junctions.

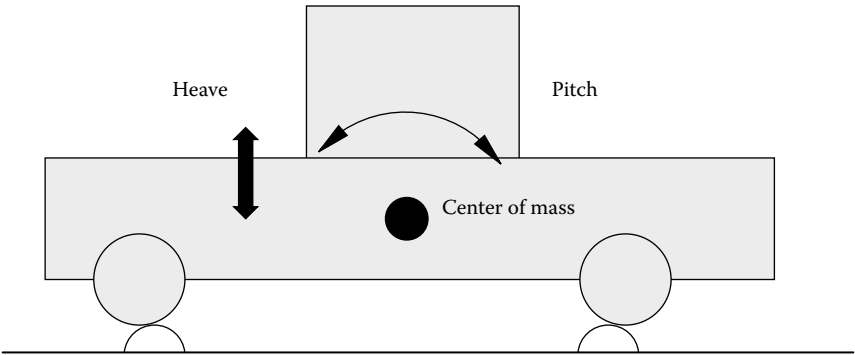


FIGURE 10.12
Half car model showing heave and pitch direction motion.

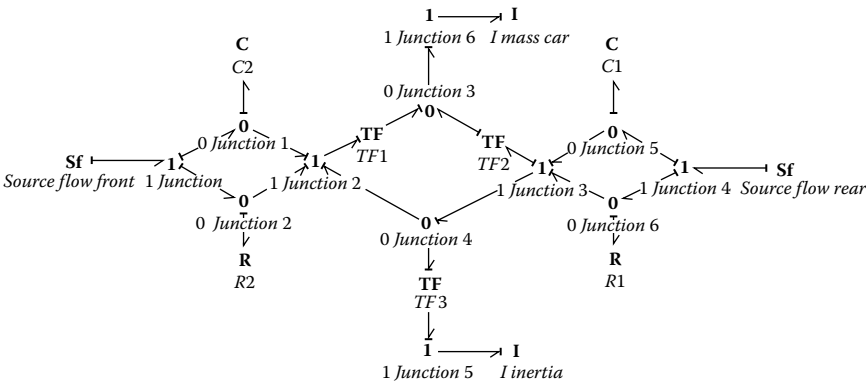


FIGURE 10.13
Bond graph representation of the half car model.

3. The heave and the pitch motions of the vehicle center of mass are related to the velocities at the locations where suspensions are attached through some geometrical parameters. These parameters are accounted through the three transformers in the bond graph representations.

10.2.1.1 Transformer Parameter Calculation

To determine the transformer parameters, the vehicle is approximated as a rectangular piece, and two of its positions, shown in Figure 10.14, illustrate the movement of three different locations of the vehicle, specifically the point of attachment of the front and the rear suspensions and the center of mass.

$L_1 + L_2$ is the total distance between the front and back wheel.

θ is the rotational angle.

y is the vertical displacement of the center of the mass.

$$\begin{aligned}\theta &= \frac{y_2 - y_1}{L_1 + L_2} \\ \dot{\theta} &= \frac{\dot{y}_2}{L_1 + L_2} - \frac{\dot{y}_1}{L_1 + L_2} \\ \dot{\theta} &= \frac{\dot{y}_2 - \dot{y}_1}{L_1 + L_2}\end{aligned}\quad (10.2)$$

Therefore:

$$TF3 = 1/(L_1 + L_2) \quad (10.3)$$

This transformer relates linear velocities to angular velocities.

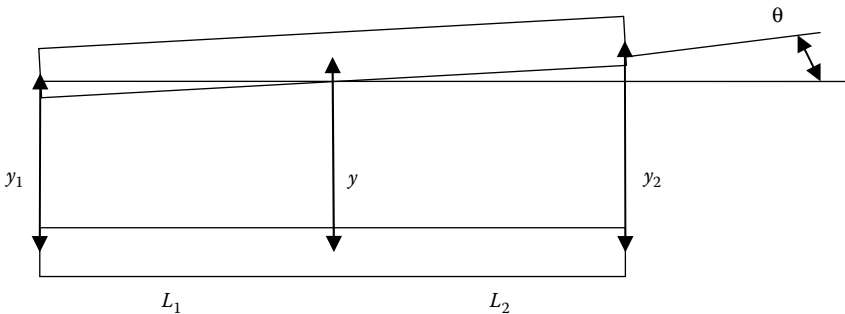


FIGURE 10.14

Transformer parameter calculations.

The vertical displacement of the center of mass can be written as:

$$\begin{aligned}\dot{y} &= \dot{y}_1 + \frac{\dot{y}_2 - \dot{y}_1}{L_1 + L_2} \cdot L_1 \\ \dot{y} &= \frac{\dot{y}_1(L_1 + L_2) + \dot{y}_2 L_1 - \dot{y}_1 L_1}{L_1 + L_2} \\ \dot{y} &= \frac{\dot{y}_1 L_2 + \dot{y}_2 L_1}{L_1 + L_2} \\ \dot{y} &= \dot{y}_1 \left(\frac{L_2}{L_1 + L_2} \right) + \dot{y}_2 \left(\frac{L_1}{L_1 + L_2} \right)\end{aligned}\tag{10.4}$$

Since the two y dots on the right-hand side are the velocities at the two junctions on front and back, the

$$TF1 = L_2 / (L_1 + L_2)\tag{10.5}$$

and

$$TF2 = L_1 / (L_1 + L_2)\tag{10.6}$$

the simplified BG representation would be as shown in Figure 10.15.

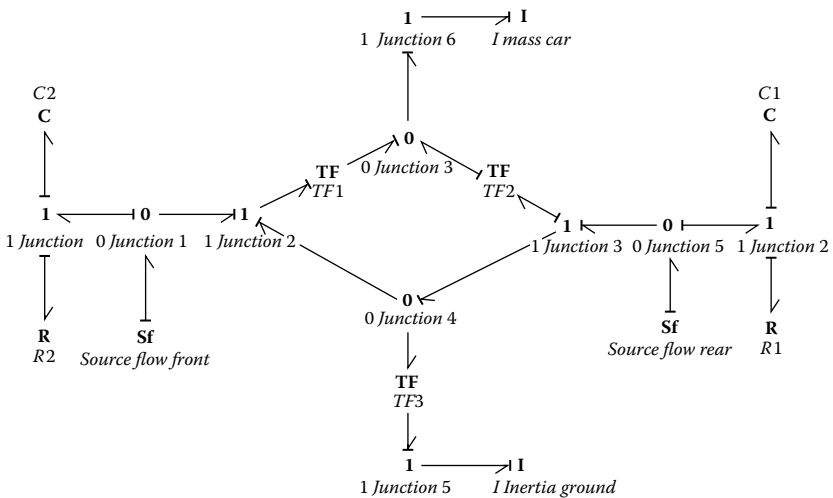


FIGURE 10.15

Bond graph after simplification.

To model additional complexity, such as tire mass and tire elasticity, the above bond graph model may be modified by including an additional I element and a C element for the front and the rear. The bond graph for the (modified) front part would be as shown in Figure 10.16. The elements inside the oval are the new additions. The bond graph for the (modified) rear part would be as in Figure 10.17.

Once again, the elements inside the oval are the new additions. In an actual vehicle, the response of the vehicle mass in terms of the heave motion and the response of its inertia in terms of its pitch motion can be investigated through the use of the Bode plot for the system that has been described here.

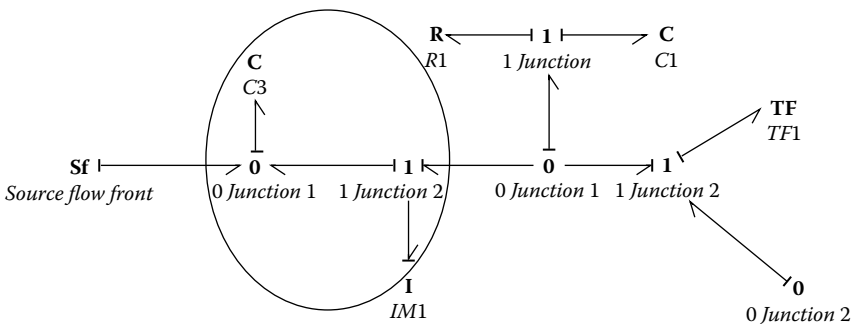


FIGURE 10.16

Modified front part bond graph to incorporate tire stiffness and damping.

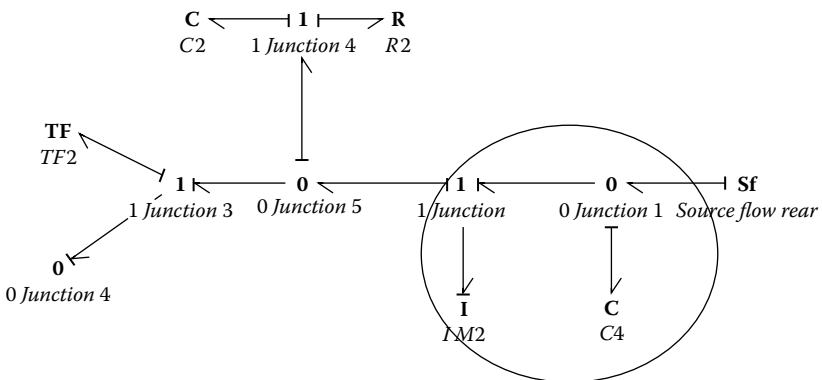


FIGURE 10.17

Bond graph of the modified rear.

Consider the following parameters for a vehicle:

Vehicle mass (sprung mass) = 1500 kg

Moment of inertia about the CG for pitch motion = 2160 kgm²

K1 (suspension, front) = 35,000 N/m

K2 (suspension, rear) = 38,000 N/m

B1 (damping coefficient, Front) = 1000 Ns/m

B2 (damping coefficient, Rear) = 1100 Ns/m

Distance between front axel and center of gravity, $L_1 = 1.4$ m

Distance between rear axel and center of gravity, $L_2 = 1.7$ m

The bond graph representation of the model is shown in Figure 10.18. At both the wheels, a pulse input is used to simulate the behavior of the system running over a bump. The pulse generator on the front wheel has a magnitude of 1 unit at the front wheel and the pulse generator has a magnitude of 0.0 unit at the rear wheel. These inputs are used to develop the frequency response of the system through the use of the Bode plot. Also, for this initial analysis, the damping coefficient at both wheels is is

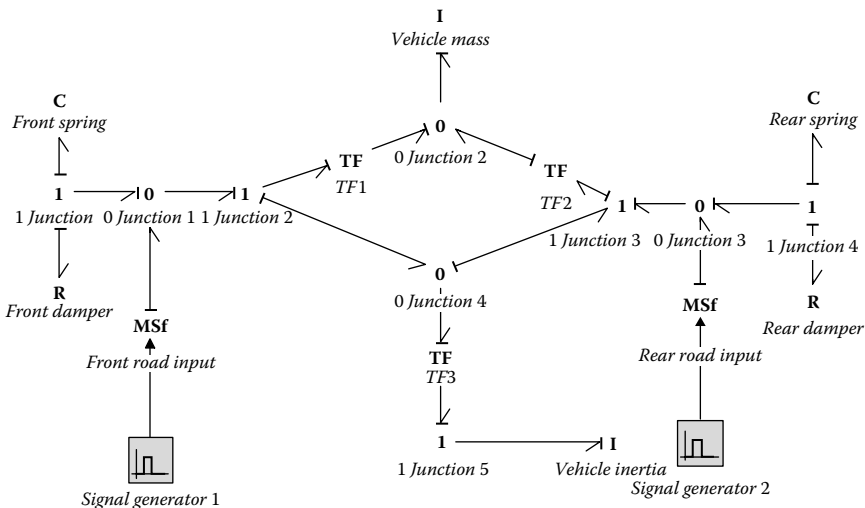


FIGURE 10.18
Bond graph of the half car example.

reduced to a very small value of 1 Ns/m. As a result of this simulation, the pitch and the heave velocity at the vehicle center of mass is shown in Figure 10.19. The transfer function between the heave and pitch velocity with respect to the input disturbance velocity is then plotted in the form of two Bode plots. This first plot is for the heave motion (Figure 10.20), and the next is for the pitch motion (Figure 10.21).

In both these plots, the two peaks of resonance are at the two natural frequencies for the heave and the pitch motion. The system has very little damping, hence, the resonance peaks are very sharp. In order to reduce this high magnification of the motion at resonance, the damping can be set back to the original values. The Bode plots (Figures 10.22 and 10.23) show that at the resonance frequencies, the peaks are reduced. However, while the peaks were reduced at the resonance frequencies, the attenuation at the high frequencies got worse.

For suspension design, the two primary goals are to reduce the gain at resonance frequency and to keep the attenuation as high as possible at high frequencies. This set of Bode plots demonstrates that if passive dampers are used in automotive suspensions, when their magnitudes are adjusted to get the desired response at resonance frequencies, the attenuation at high frequencies gets worse and vice versa. Suspension designers have to fine tune the suspension parameters for optimized ride or optimized handling or some acceptable (not optimized) performance level for both aspects.

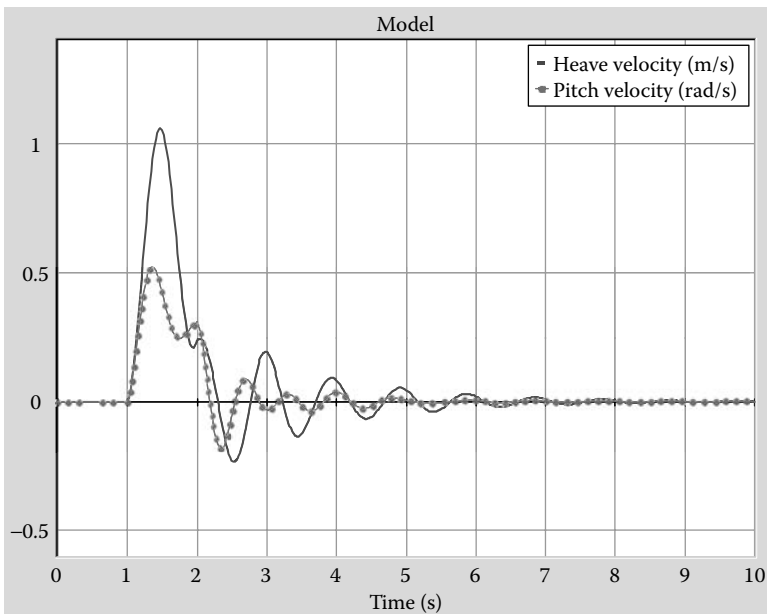


FIGURE 10.19

Heave and pitch velocity from simulation.

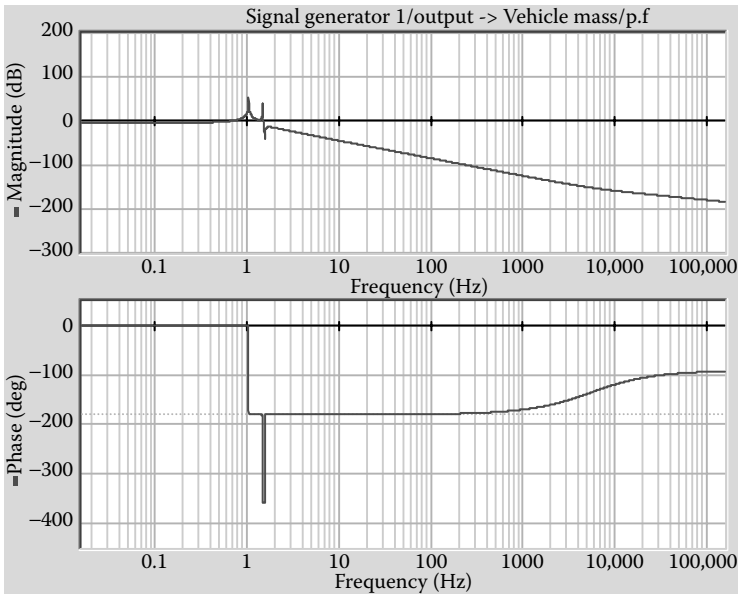


FIGURE 10.20
Transfer function (Bode plot) of heave motion w.r.t. input velocity.

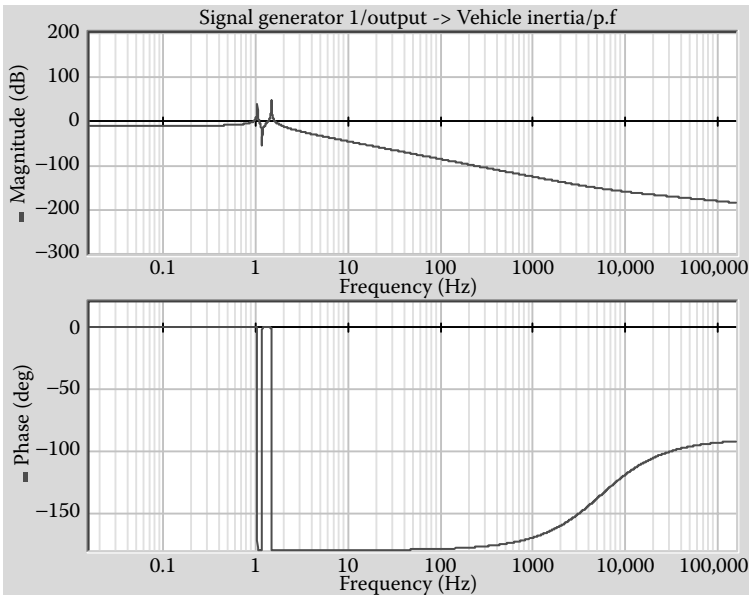


FIGURE 10.21
Transfer function (Bode plot) of pitch motion w.r.t. input velocity.

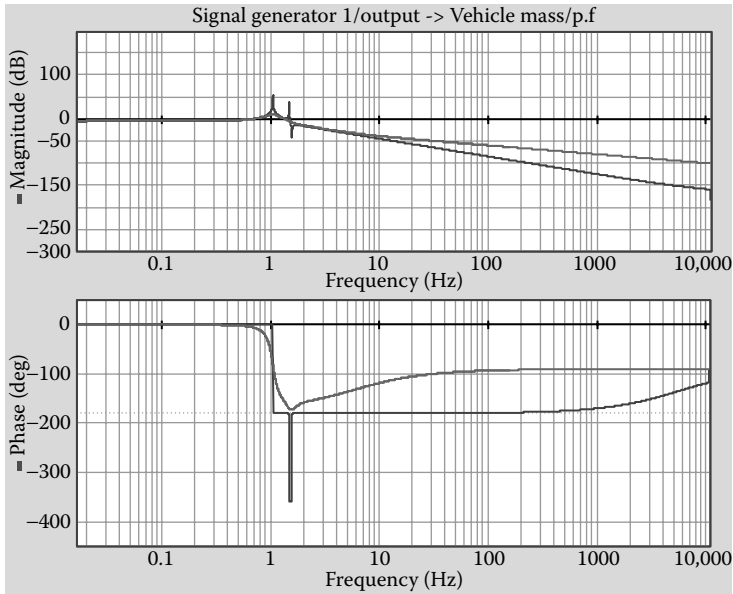


FIGURE 10.22

Transfer function (Bode plot) of heave motion w.r.t. input velocity and with increased damping (superposed on Figure 10.20).

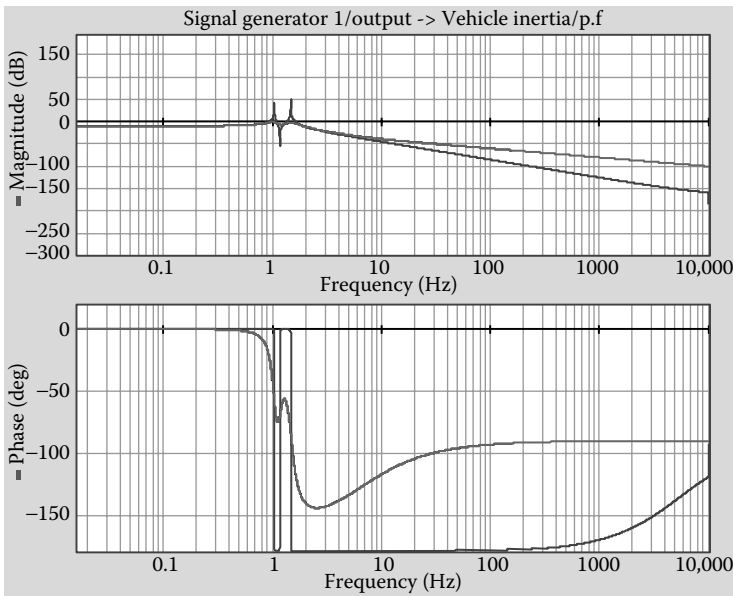


FIGURE 10.23

Transfer function (Bode plot) of pitch motion w.r.t. input velocity and with increased damping (superposed on Figure 10.21).

10.2.1.2 Active Dampers

Dampers that are designed to address the problems encountered by passive dampers. These are semi-active dampers or active dampers. Many of these active dampers use the concept called “skyhook damping,” passive dampers use is proportional to the difference in the velocity of the two end points to which the damper is attached (i.e., to the relative velocity). In active dampers, such as the skyhook dampers, the damping force is proportional to the absolute velocity of the mass that is being damped.

$$\text{Damping force in passive damper} = R * (\text{mass velocity} - \text{road velocity})$$

$$\text{Damping force in active damper} = -R * \text{mass velocity}$$

The force in an actively damped system needs to be a negative value so that it works as intended, that is, as a dissipater of forces.

To implement active damping in vehicles, the absolute velocity of the point where the damper would be attached is used to generate a source of effort, and it is fed back at the same location. Hence, the bond graph model looks like Figure 10.24.

For this analysis the constant value that multiplies the absolute velocity is made equal to -1000 on both sides, the passive resistor value is reduced to a bare minimum of 1 unit, and the system is reanalyzed. The Bode plots for both heave and pitch motion are shown in Figures 10.25 and 10.26. It is now clear from the plot that by using these active dampers, not only is the response at resonance frequency controlled but also the attenuation at high frequencies is very good.

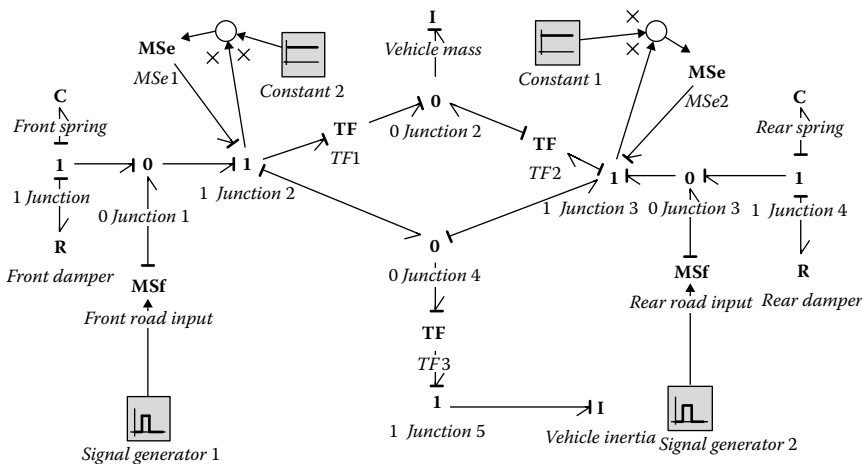


FIGURE 10.24
Modified bond graph with active damping.

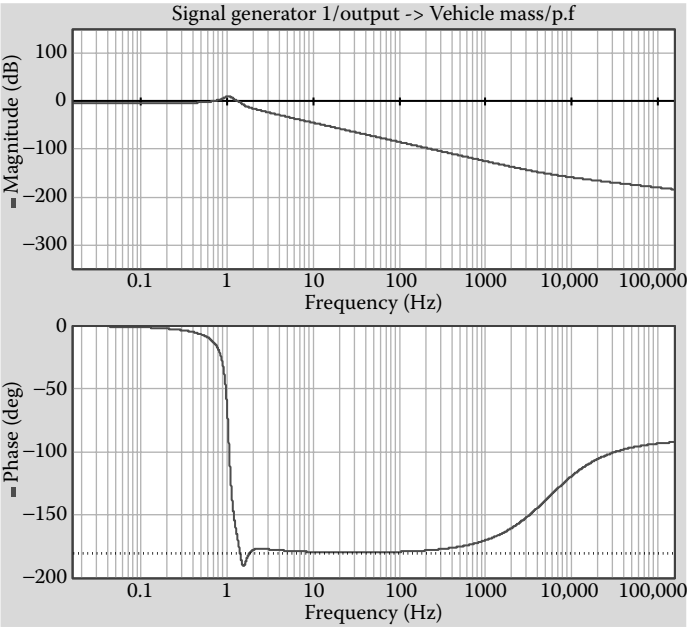


FIGURE 10.25
Transfer function (Bode plot) of heave motion w.r.t. input velocity with active damping.

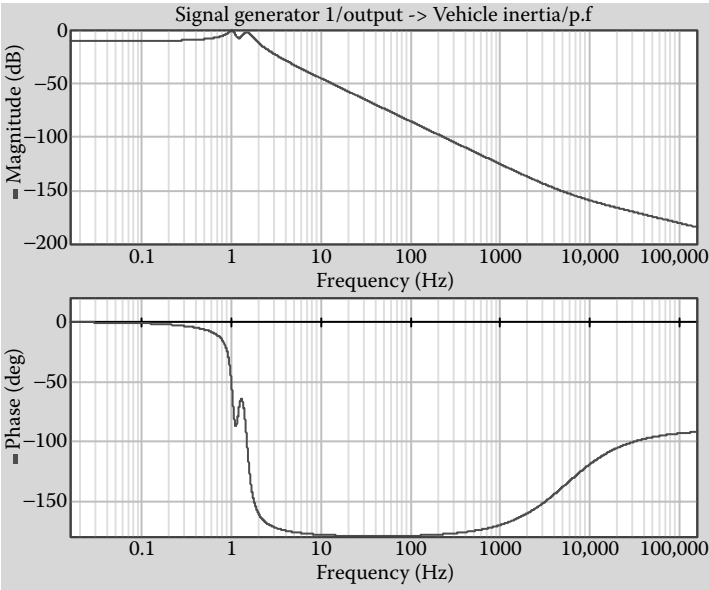


FIGURE 10.26
Transfer function (Bode plot) of pitch motion w.r.t. input velocity with active damping.

10.2.2 Handling: Bicycle Model

The cornering behavior of a motor vehicle is an important performance measure that relates to handling. Steady state handling performance is concerned with the directional behavior of a vehicle during a turn under non-time varying conditions. An example of a steady state turn is a vehicle negotiating a curve with constant radius at a constant forward speed. It is important to note that in the analysis of steady state behavior, the inertia properties of the vehicle are not involved.

A 2 DOF bicycle model is useful for handling dynamics studies. The model can be used to study the lateral/yaw dynamics of vehicles subject to front steering inputs. When a vehicle is negotiating a turn at moderate or high speeds, the effect of the centrifugal force acting at the center of gravity cannot be neglected (Gillespie, 1992).

Typically on a broad area, cornering can be classified into two classes.

1. Low speed cornering
2. High speed cornering

At low speed (e.g., parking lot maneuvers), the tires need not develop lateral forces. Thus, they roll with no slip angle (Gillespie, 1992) and the analysis of the vehicle behavior is quite simple. We will not consider the low speed behavior here anymore.

At high speed, the turning equations differ because lateral acceleration will be present. To counteract the lateral acceleration, the tires must develop lateral forces, and slip angles will be present at each wheel. Under cornering conditions, in which the tire must develop a lateral force, the tire will also experience a lateral slip as it rolls. The angle between its direction of heading and its direction of travel is known as slip angle, α (Wong, 2001) (Figure 10.27).

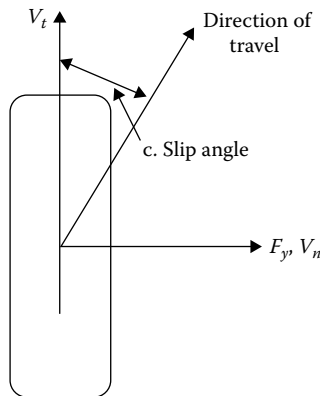


FIGURE 10.27

Tire motion and slip angle.

The lateral force, denoted by F_y , is called the cornering force when the camber angle is 0. At a given tire load, the cornering force grows with the slip angle. At low slip angles (5 degrees or less), the relationship is linear; hence, the cornering force is described by:

$$F_y = C_\alpha \alpha \quad (10.7)$$

The proportionality constant C_α is known as the cornering stiffness and is defined as the slope of the curve for F_y versus α . The cornering stiffness is dependent on many variables, such as tire size and type, number of plies, cord angles, wheel pressure, and so forth. But for a limited range for all practical purposes, cornering stiffness can be assumed constant, especially since it does get affected by speed (Wong, 2001).

At high speeds, the radius of the turn is much larger than the wheel-base of the vehicle. Then small angles can be assumed, and the difference between the steer angles on the outside and the inside front wheels is negligible. Thus, for convenience, the two front wheels can be represented by one wheel at a steer angle δ , with a cornering force equivalent to both wheels. The same assumption is made for the rear wheels. The pictorial representation of the bicycle model is as shown in Figure 10.28.

The velocity relations for the two wheels can be written as:

$$V1_n = (V + \omega a) \cos \delta - U \sin \delta \quad (10.8)$$

$$V1_t = (V + \omega a) \sin \delta + U \cos \delta \approx U \text{ (for small } \delta) \quad (10.9)$$

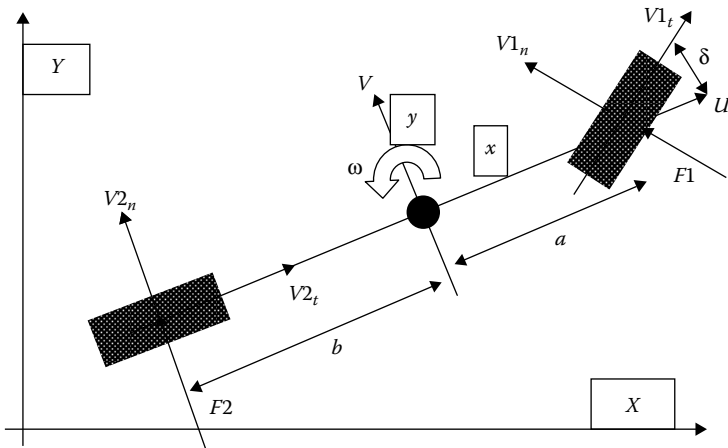


FIGURE 10.28

A schematic of the bicycle model.

$$V2_n = V - \omega b \quad (10.10)$$

$$V2_t = U \quad (10.11)$$

Using the description of the velocities, the cornering force on the front wheel may be written as:

$$F1 = C1\alpha = C1\left(\frac{V1_n}{V1_t}\right) = C1\left(\frac{(V + \omega a)\text{Cos}\delta - U\text{Sin}\delta}{(V + \omega a)\text{Sin}\delta + U\text{Cos}\delta}\right) \quad (10.12)$$

In a similar manner, the $F2$ on the rear wheel may be written as:

$$F2 = C2\alpha = C2\left(\frac{V2_n}{V2_t}\right) = C2\left(\frac{V - \omega b}{U}\right) \quad (10.13)$$

Acceleration of the vehicle in inertial frame of reference can be written as (Mukherjee and Karmakar [2000]):

$$\begin{aligned} \dot{\vec{V}}_{XYZ} &= \dot{\vec{v}}_{xyz} + \omega \times \dot{\vec{v}}_{xyz} \\ m\dot{\vec{u}}_{XYZ} &= m\dot{\vec{u}} - m\omega\vec{v} = F_x \\ m\dot{\vec{v}}_{XYZ} &= m\dot{\vec{v}} + m\omega\vec{u} = F_y \end{aligned} \quad (10.14)$$

$$\begin{aligned} m\dot{\vec{u}} &= m\omega\vec{v} + F_x \\ m\dot{\vec{v}} &= -m\omega\vec{u} + F_y \end{aligned} \quad (10.15)$$

F_x and F_y are the external forces in the axial transverse directions, and the cornering forces are the only external forces. The contributions due to the cross-product term can be modeled using a gyrator element.

The bond graph representation of this system is shown in Figure 10.29. The bond graph demonstrates all the aspects discussed here. This is just a simpler version of the model. The model can become more and more complex as we add on things, such as force at the wheels in the direction of roll, or if we add calculations in displacement in the x and y directions, including the complex tire models available in literature. Some of these complexities have been included in a more detailed model by Kramer (2001). The reader may refer to that paper for more information on this model.

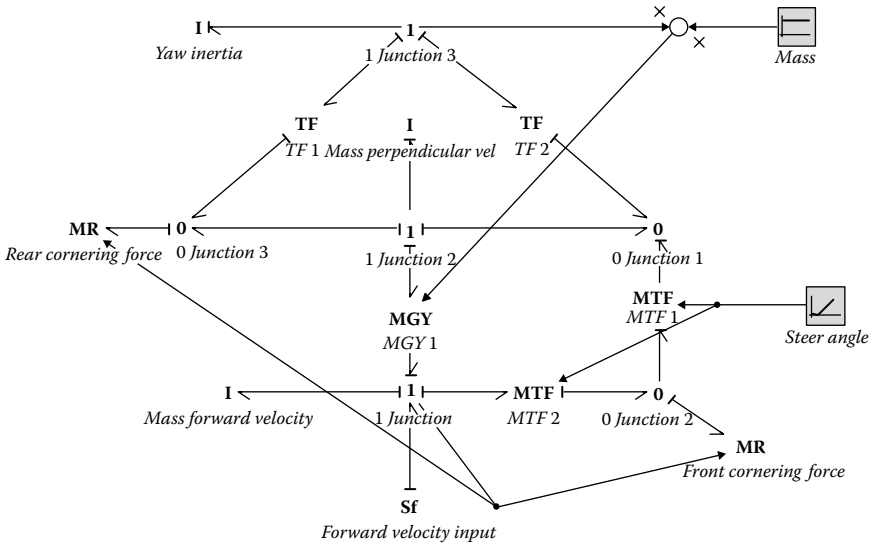


FIGURE 10.29
Bond graph representation of the bicycle vehicle handling model.

10.3 Vehicle Systems

In this section we will discuss some vehicle systems for which the bond graph methodology has been applied for simulating the system behavior. Of the several systems discussed here, there are some that are now available in vehicles as a standard feature, and there are others that are relatively new, such as the type of systems that fall under the category of by-wire systems.

10.3.1 Electric Braking

The first system presented here is an electric braking system. The model of this system is presented in a paper by Margolis and Shim (2001).

Figure 10.30 shows a schematic of the brake system, and Figure 10.31 shows the bond graph representation of this system. The electric motor is modeled using a source of flow (or current). It could have been modeled as source of effort and an inductance element in the circuit (just as a motor was modeled in the actuators chapter). The motor is connected to a transformer element that would transform rotational to linear motion. This could be a ball-and-screw system that is used to apply force on the brake pad. The brake pad–disk contact is modeled as a modulated resistance. The wheel/tire inertia is modeled as well as a transformer element

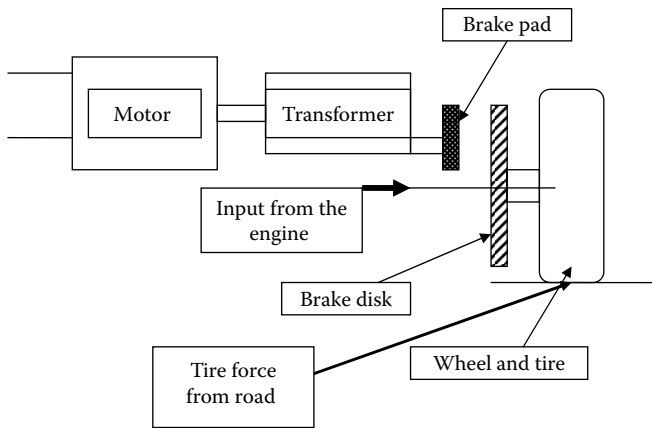


FIGURE 10.30
Schematic for an electric braking system.

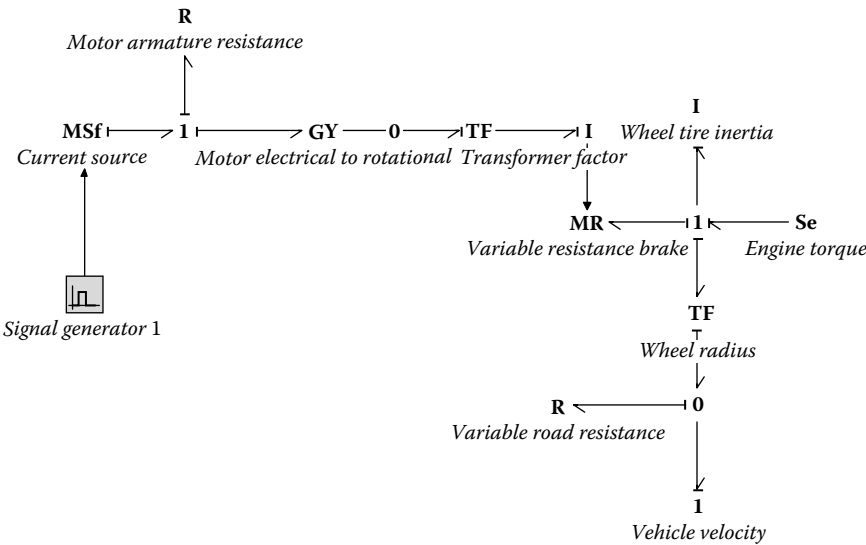


FIGURE 10.31
Bond graph representation of the electric braking system.

to transfer rolling velocity to linear velocity at the wheel/ground interface. For wheels that receive direct power from the engine, an engine input is included in the model as well. The road resistance needs to be modeled using the constitutive behavior of the tire. These models are relatively complex but can be found in literature and can be incorporated in the overall model. The resistance is a function of the relative velocity between the longitudinal velocity of the wheel center and the wheel rolling velocity.

The behavior of the model is demonstrated in Figure 10.32. The plots show the rotational velocity of the tire as motor current comes on and is then turned off. The velocity is brought down to 0 and then rises as the current is removed. The simulation is only a sample representation based on arbitrarily chosen parameters shown in Figure 10.33.

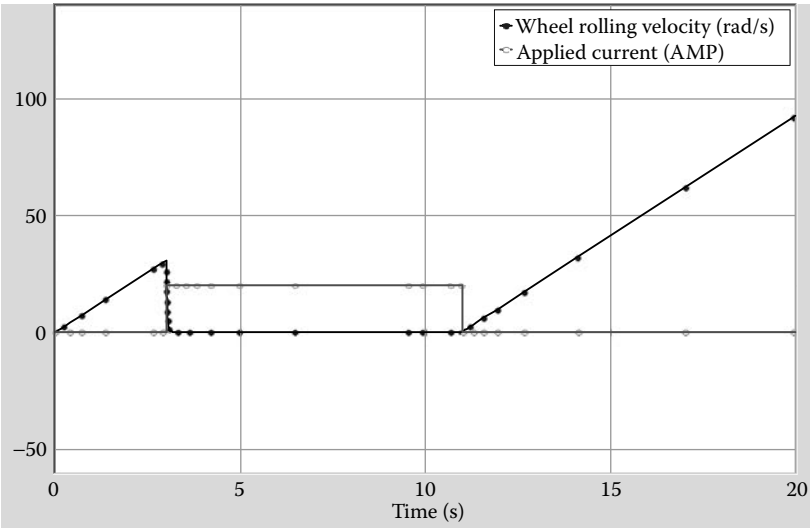


FIGURE 10.32
Electric brake behavior simulation.

Parameters			Initial Values	Constants
Name	Value	Quantity		
Motor_Armature_Resistance\r	1			
Motor_Electrical_to_Rotational\r	10			
Transformer_Factor\r	0.5			
Wheel_Tire_Inertia\i	10			
Engine_Torque\effort	100			
Wheel_Radius\r	0.03			
Variable_Road_Resistance\r	10			
SignalGenerator1\start_time	3 {s}	Time		
SignalGenerator1\stop_time	11 {s}	Time		
SignalGenerator1\amplitude	20	Magnitude		
Sf1\flow	10			

FIGURE 10.33
Parameters used for simulating the electric brake.

The description and discussion of this system is kept at a generic level. This model can be easily modified to model a hydraulic braking system as well, where the force input is provided by hydraulic pressure rather than electric motors.

10.3.2 Power Steering Model

The hydraulic power steering of an automobile consists of interaction of two energy domains. The steering wheel is used to provide the intended input from the driver. The steering mechanism is connected to a hydraulic booster circuit that adds to the effort from the driver and helps in turning the wheel in a fashion desired by the driver. Figure 10.34 shows a schematic of the hydraulic power steering consisting of the steering wheel that is connected to the upper column. The upper column is connected to the lower column through a torsion bar. The torsion bar has a spool valve attached to it. The spool valve is also part of a hydraulic circuit. When the steering wheel is turned in one direction, the rack and pinion arrangement transforms rotary motion into translation so that the wheels can be turned in the same direction as the rotation of the steering wheel. As the steering wheel turns, the spool valve also opens in a way such that the hydraulic pressure helps in augmenting the force necessary to turn

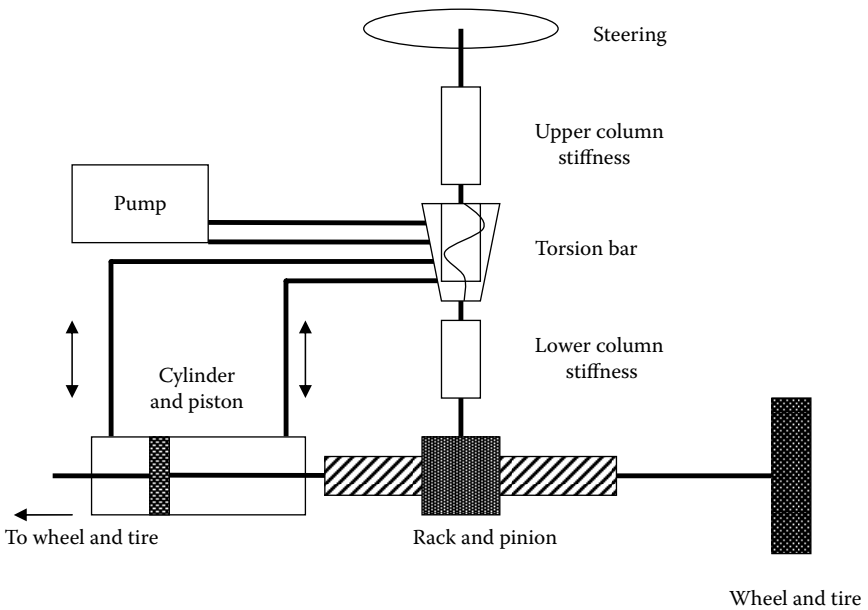


FIGURE 10.34
Power steering system schematic.

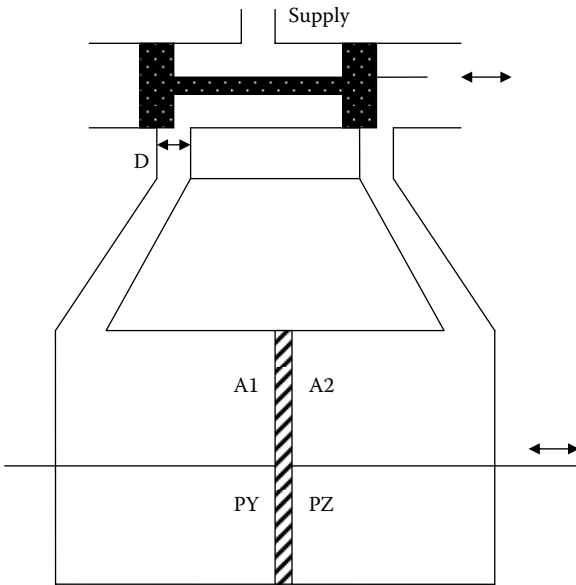


FIGURE 10.36
Schematic of a spool valve and the cylinder.

on one side of the ram is increased, and fluid from the other side of the ram is pushed out to the sink. This enables the hydraulic ram to move in the desired direction, thus augmenting the human effort provided to turn the vehicle wheel. In this bond graph model, the variable resistance for the valve is shown using a single *MR* element. This is not necessarily a complete model, but rather an approximate representation. A better way to model is to use part of the model used in the hydraulic actuator in Chapter 9. The valve model from that example can be used to replace the single *MR* element used here.

Experimental results from the work of Diet et al. (1998) and Bogdan Proca (1998) show that the area of the orifice varies as a function of the angle of rotation. It increases almost linearly with angle of rotation and remains constant when the maximum area is reached. The orifice behaves like a resistive element whose flow is not proportional to the effort but to the square root of effort. This particular behavior was discussed in Chapter 9 during the discussion of orifice valves. This behavior needs to be part of the *MR* model. One of the factors in the equation is the drag coefficient, C_d . The variation of C_d as a function of the angle of rotation is also available in the publication by Birching (1999). Since the data reported by Birching indicate that the C_d value varies between 0.5 and 0.7, a constant value of about 0.6 may also be assumed for C_d .

10.3.3 Steer-by-Wire System (SBW)

The function of a steering system is to steer the front wheel in response to the driver's input. The development of electric power-assisted steering is driven by factors like driver comfort and active safety. The SBW is a part of X by wire technology, in which X stands for safety related applications such as steering, braking, or suspension.

SBW eliminated the mechanical link between steering wheel and front wheel, which is a steering column and a hydraulic system. The driver's command is transferred via control unit and processed to send a signal to a DC motor, which steers the wheel. This reduces the overall cost and weight and provides more safety as the control unit assists the driver. The most meritorious features of SBW are the improvement in the driver's steering feel and better handling of the vehicle.

At present, there are few high-end vehicles using such systems. SBW is more popular in aviation industry because pilots prefer getting the same reaction from the system for large as well as small aircraft. There have been constant discussions about taking control from a driver in case of an emergency, because sometimes the driver's decision might not be the best option. For instance, trying to avoid a huge collision might involve high steering input, which might be tough in case of SBW.

Figure 10.37 shows a simple layout of the steer-by-wire (SBW) system. The SBW can be divided into three major subsystems: a steering wheel subsystem, a controller subsystem, and front wheel subsystem. Figure 10.38 shows a detailed system-level model of SBW. Each subsystem is again

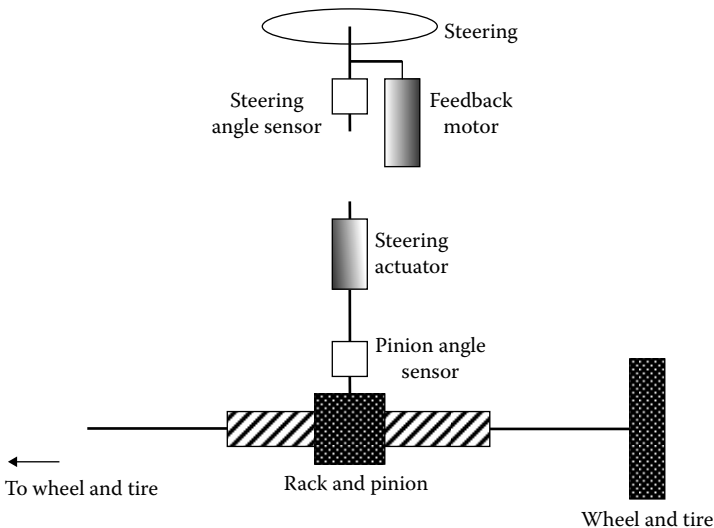


FIGURE 10.37
Schematic for a steer-by-wire (SBW) system.

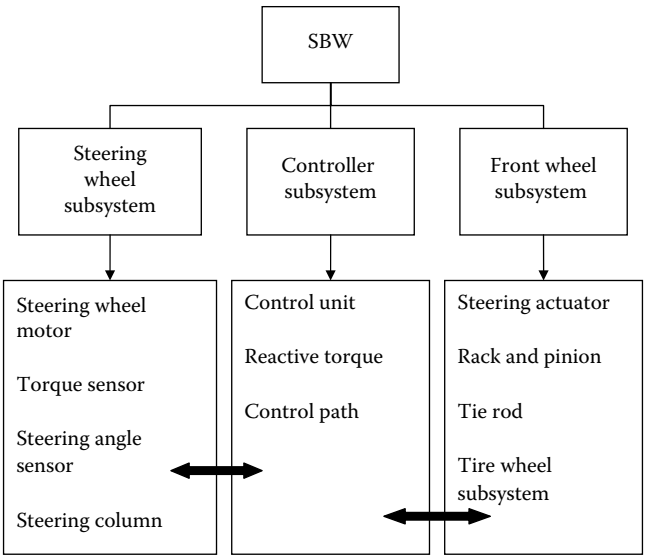


FIGURE 10.38
System level model including components.

broken down into main components. The component-level modeling helps achieve the aim of preparing a bond graph modeling. Each of the subsystems is now explained in detail.

The steering subsystem consists of a steering wheel, torque sensor, angle sensor, and steering motor. A controller subsystem receives a signal from the torque sensor and an angle sensor, along with the vehicle speed sensor. The torque sensor senses driver torque input, and the angle sensor senses steering angle. These sensor inputs are used by the control algorithm to a calculated output that goes to the steering motor. The steering motor acts as a steering column functionally and provides resistance to the driver.

As there is no steering column, the driver wouldn't feel anything back from the road, which is quite misleading and dangerous. To bridge this gap, a steering motor is used and provides feedback torque to the driver. The feedback torque generated from the motor depends on vehicle speed and steering wheel angle. The controller subsystem is discussed in detail under the section of SBW controls.

The controller subsystem is an electronic control unit that takes input data from all the sensors and runs an algorithm to drive the steering motor and front wheel motor (discussed in the next section). Most important feature of the controller subsystem is that it not only imitates the manual steering system, but it also goes a step beyond to make steering more comfortable than manual systems. So, for instance, the torque required in parking lot conditions is quite high for a manual steering

system. Using SBW controls, the reaction torque generated is much less as compared to manual steering. Also, controllers help improving handling characteristics and maneuverability by accounting for understeer gradient (Oh, 2003).

The main components of the front wheel subsystem are a steering actuator, rack/pinion gear, tie rod, position sensor, steering arm, and tires Qiang and Ren (2005).

The steering actuator is a permanent magnet (PM) DC motor that receives a signal from the electronic control unit (ECU). The motor transmits power to the steering wheel via rack/pinion and tie rod. The steering arm is responsible for converting the linear movement of the tie rod into angular movement, which rotates the tires to steer the vehicle.

The position sensor is used to track the steering angle of wheel and provides data to the ECU.

In order to make a bond graph model of SBW, each component is assumed to be a combination of lumped parameters of resistance, capacitance, and inertial elements. The DC motor is broken down into electrical and mechanical domains, as shown in Figure 10.39.

The electrical part consists of armature resistance, armature inductance, and an input voltage. The mechanical part is the shaft with motor inertia, rotational resistance, and motor shaft compliance. The energy transformation from electrical to mechanical domain is represented by a gyrator element with a gyrator ratio of the motor constant.

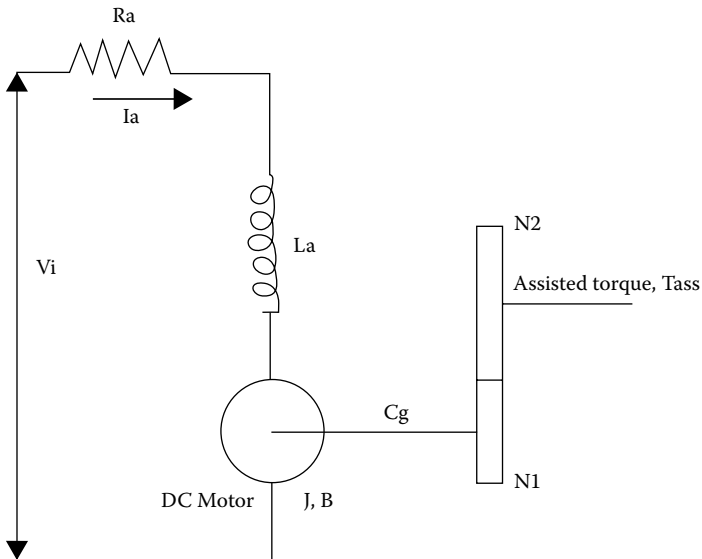


FIGURE 10.39
Layout of DC motor.

is transmitted to the pinion with a set of gears represented by transformer ratio.

- The steering wheel is represented by the wheel moment of inertia. The driver torque is represented through signal generator fed to the steering wheel (at 1 junction) via modulated source of effort.
- The steering column bearing provides resistance and shaft compliance.
- The rack and pinion assembly is represented by gear ratio (transformer) and mass of rack (inertia element).
- The tie rod is lumped into compliance of rod and bearing resistance.
- The translation motion of tie rod is transformed into angular motion by the steering arm. This is represented by a transformer. The steering arm's mass has been neglected here.
- The tires are represented by moment of inertia.
- When a lateral force acts on tires, the tires generate self-aligning torque. This is represented by the resistance element because this torque opposes the steering torque.

Figure 10.40 shows a bond graph model with all lumped parameters, though this particular model doesn't use any feedback or control mechanism. Figure 10.41 shows the values used for all the parameters.

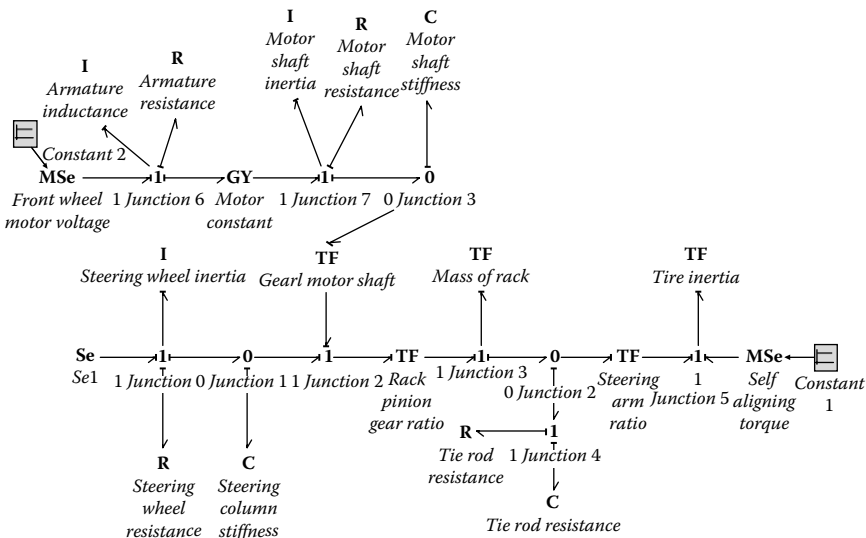


FIGURE 10.40
Bond graph model of the steer-by-wire system.

Name	Value	Quantity	Unit	Arithmetic Type
SteeringWheelInertia <i>i</i>	30 {mN.m.s ² /rad}	Moment of Inertia	newton meter secon...	Real
SteeringWheelResistance <i>r</i>	100 {mN.m.s/rad}	Rotational Friction	newton meter secon...	Real
SteeringColumnStiffness <i>c</i>	152 {urad/N.m}	Rotational Compliance	radian per newton m...	Real
RackPinionGearRatio <i>r</i>	0.04			Real
MassofRack <i>i</i>	0.04 {kg}	Mass	kilogram	Real
TieRodStiffness <i>c</i>	53.3 {mN/m}	Stiffness	newton per meter	Real
TieRodResistance <i>r</i>	100 {mN.s/m}	Friction	newton second per ...	Real
SteeringArmRatio <i>r</i>	1			Real
TireInertia <i>i</i>	1.8 {N.m.s ² /rad}	Moment of Inertia	newton meter secon...	Real
ArmatureInductance <i>i</i>	269 {uH}	Inductance	henry	Real
ArmatureResistance <i>r</i>	168.5 {mohm}	Electric Resistance	ohm	Real
MotorConstant <i>r</i>	0.045			Real
MotorShaftInertia <i>i</i>	480 {uN.m.s ² /rad}	Moment of Inertia	newton meter secon...	Real
MotorShaftResistance <i>r</i>	3.4 {mN.m.s/rad}	Rotational Friction	newton meter secon...	Real
MotorShaftStiffness <i>c</i>	1.59 {mN.m/rad}	Rotational Stiffness	newton meter per ra...	Real
GearMotorShaft <i>r</i>	0.49			Real
Constant1 <i>V</i>	800			Real
Constant2 <i>V</i>	20			Real
Set <i>V</i> effort	2 {N.m}	Torque	newton meter	Real

FIGURE 10.41

Data used for the steer-by-wire model in Figure 10.40.

The design of the controller has not been attempted here since it is an advanced control exercise. However, with a good understanding of the algorithm for control as outlined in the work of Oh (2003), it can be modeled with some decent effort on the part of the bond graph modeler. The bond graph model was simulated using 20-Sim. Some results are shown in Figure 10.42.

Figure 10.42 shows the plot of steering wheel angle and front wheel angle against time. The driver torque used was 2 Nm. The plot shows that there is a small lag in the system (~0.05 seconds). But the system response is very steady and linear otherwise.

Figure 10.43 shows the plot from a publication by Qiang and Ren (2005). The plot shows the front wheel angle at a different torque input. The simulation data gives similar characteristic as in the above plot used for validation. Hence, the simulated data is quite close to validation data.

Figure 10.44 shows the plot of the front wheel angle versus the steering wheel angle. The plot suggests a linear relation that is quite obvious and, hence, proves the validity of the results. Also, the steering gear ratio comes out to be approximately 22, which seem close to real world data.

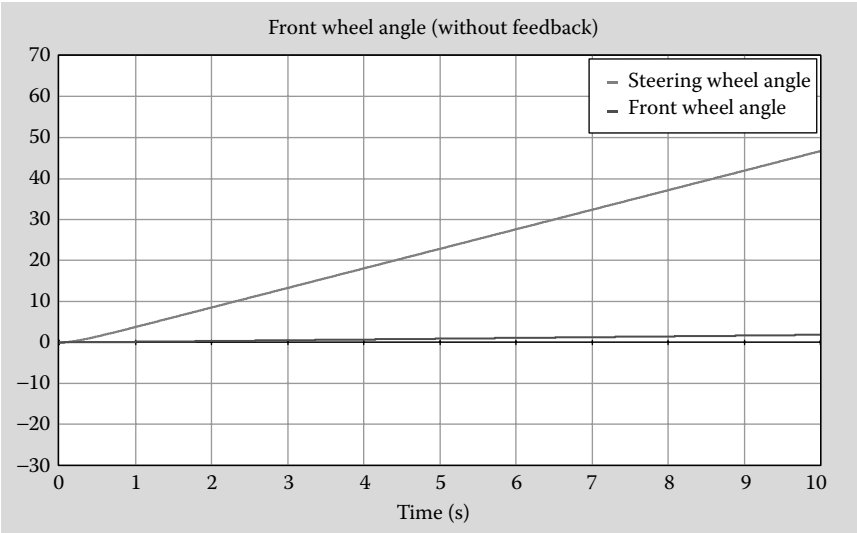


FIGURE 10.42
Steering wheel angle and front wheel angle plots versus time.

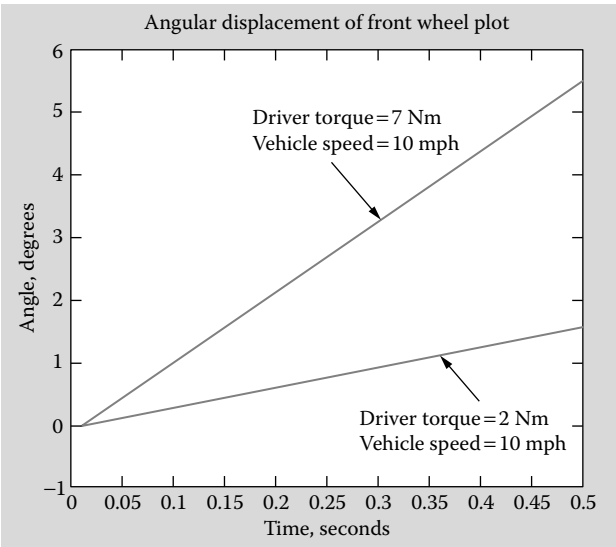


FIGURE 10.43
Validation data.

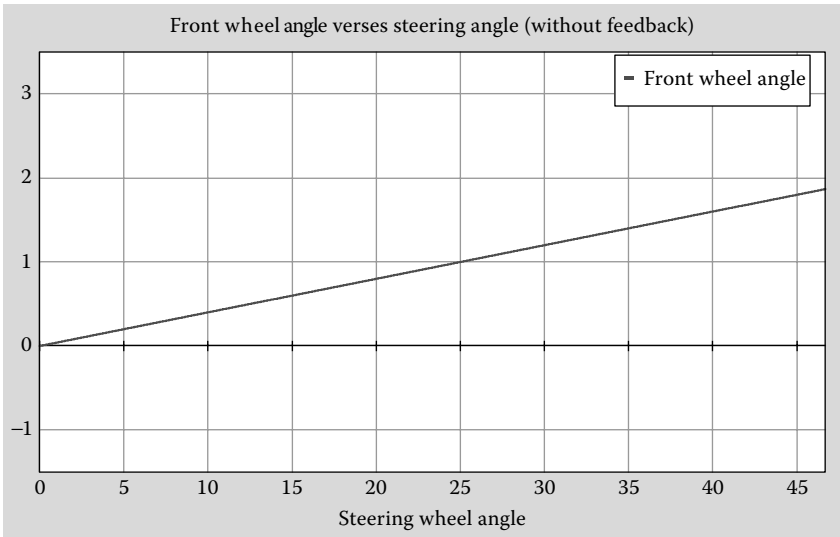


FIGURE 10.44
Front wheel angle versus steering wheel angle (in degrees).

10.4 Energy Regeneration in Vehicles

With the advent of hybrid technology and significant efforts in improving energy efficiency of vehicles, effort has been under way to make sure that energy can be recovered and used from different aspects of vehicle motion. It is quite well known that only a small percentage of the energy generated by the internal combustion engine is used productively. A large portion of the energy is lost as heat. Also, during braking, all the kinetic energy that was generated from the combustion is lost as heat as well.

In hybrid vehicles using the general approach of “regeneration,” part of the braking energy is used to drive a motor/generator in a reverse direction to generate electrical energy that is then used to charge the battery. Another similar approach has been tried to recover energy from the damping effects of a suspension. Whenever an automobile in motion hits a bump on the road, undesirable vertical motions are introduced in the system. Conventional shock absorbers in vehicles dampen this motion, and energy is thus dissipated to the surroundings. The possibility of generating electrical power from the above-mentioned energy has been explored experimentally by researchers (Goldner et al., 2001). The electric power can then be used to recharge the battery of an electric car.

One of the two experiments in Goldner’s (2001) work was the electrical generator experiment. Figure 10.45 shows a schematic of the setup. It was

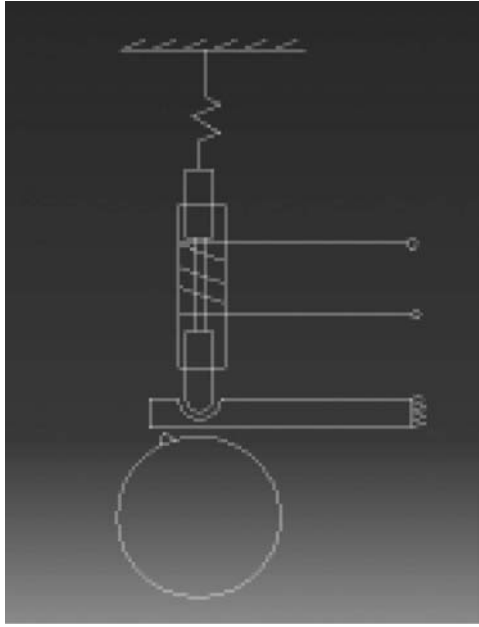


FIGURE 10.45

Schematic of the electric generator experiment.

used to simulate a periodic road bump. This was in the form of a grinder that had one of its grinding wheels replaced by an aluminum disk that had a rounded, adjustable height, bump. This is clear from Figure 10.45, which is a schematic of the test stand. A neodymium(Nd)–iron(Fe)–boron(B) magnet was concentric with a Teflon tube with a copper wire coil wound on it. Also contained in the copper tube were two Teflon push rods—one above and one below the magnet—as well as a stiff spring at the top of the piston, and the spring was restrained from moving above a restrainer. The bottom Teflon push rod was rounded at its lower end, and the rounded nose loosely fit into a concave cutout in a flexible $\frac{1}{8}$ -inch thick Teflon plate that was cantilevered at one end. This allowed the plate, and therefore the piston, to be pushed up by a rotating bump and pushed down by the upper constrained spring. The output voltage from the coil was measured with an oscilloscope.

The magnetic flux density of the magnet was 0.23 Tesla and the length of the coil was 5.2 m. The bump height was chosen to be 2 mm. The rotational frequency of the disk was 20 Hz and the disk radius was 80 mm. Using these magnitudes of the various elements of the system, the output voltage that was generated was 1.3 volts.

The schematic diagram in Figure 10.45 helps us in preparing a bond graph of the experiment. Figure 10.46 shows the bond graph model. The input signal to the modulated source of flow has not been shown in this figure. It will be discussed later in detail. The gyrator element was chosen for the conversion of the mechanical disturbances due to the vertical motions induced by the road bump into electric power. The gyrator factor (1.196) was calculated by multiplying the magnetic flux density (0.23T) with the length of the coil (5.2m), that is, Bl . The road bump signal consists of two square wave generators, a delay element, and a $+/-$ element. The equation of one square wave generator was modified, and the delay element was connected to it to obtain a wave output, as shown in Figure 10.47.

It should be noted that this waveform and magnitude of the signal was generated with a magnitude of 2 mm, frequency of 125 rad/sec, and a delay of 50 milliseconds. The parameters used in the simulation are shown in Figure 10.48. Two square wave generators were used along with an offset to generate the effective pulse that is created from the small bump on the rotating wheel. The equations of the two generators are shown in Sections 10.4.1 and 10.4.2.

10.4.1 First Square Wave Generator

Variables

```
real hidden s, half;
boolean hidden change;
```

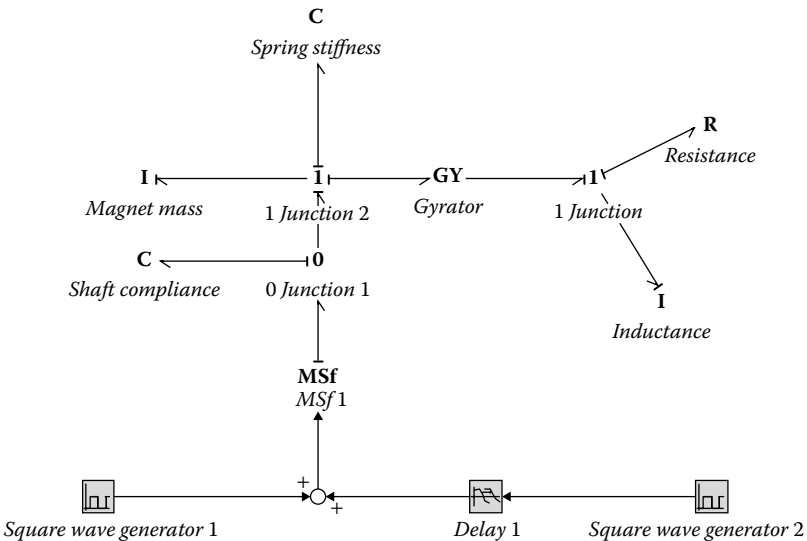


FIGURE 10.46

Bond graph model of the electric generation experiment.

Equations

```
"calculate at least 2 points per period  
(just after the change in sign)"  
half = pi/omega;  
change = frequencyevent (half, 1e-15);
```

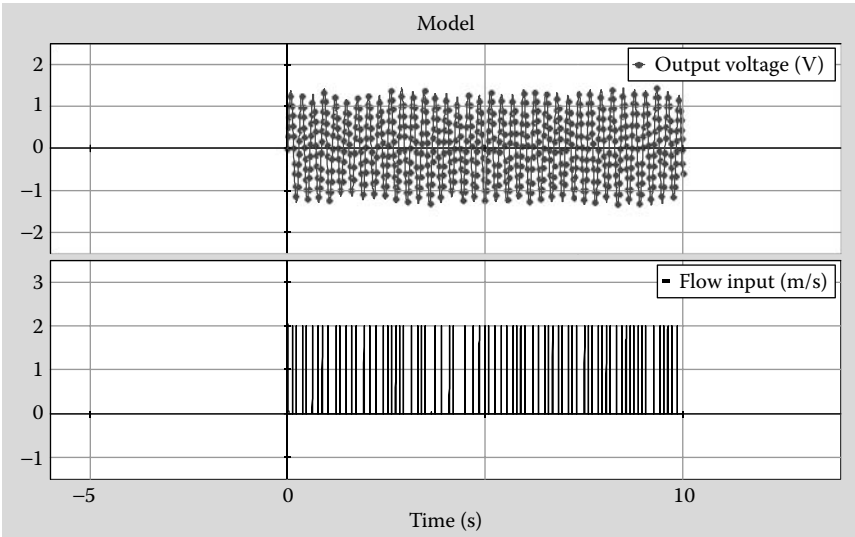


FIGURE 10.47
Output voltage and input velocities.

Name	Value	Quantity	Unit
◆ GYRATOR\i	1.196		
◆ SHAFT_COMPLIANCE\c	100 {mN/m}	Stiffness	newton per meter
◆ MAGNET_MASS\i	0.02 {kg}	Mass	kilogram
◆ INDUCTANCE\i	3 {mH}	Inductance	henry
◆ RESISTANCE\i	99.999 {kohm}	Electric Resistance	ohm
◆ SPRING_STIFFNESS\c	100 {N/m}	Stiffness	newton per meter
◆ SQUARE_WAVE_GENERATOR_1\amplitude	2 {m}	Length	meter
◆ SQUARE_WAVE_GENERATOR_1\omega	125 {rad/s}	Angular Velocity	radian per second
◆ SQUARE_WAVE_GENERATOR_2\amplitude	2 {m}	Length	meter
◆ SQUARE_WAVE_GENERATOR_2\omega	125 {rad/s}	Angular Velocity	radian per second
◆ Delay_1\initial	50 {ms}	Time	second
◆ Delay_1\delay	0.05		

FIGURE 10.48
Parameters used for the experiment.

```

"calculate the square wave"
s = sign (sin (omega * time));
output = if( s == 0 ) then
amplitude
else
(amplitude/2)*(s + 1)
end;

```

10.4.2 Second Square Wave Generator

Variables

```

-real hidden s, half;
-boolean hidden change;

```

Equations

```

"calculate at least 2 points per period
(just after the change in sign)"
half = pi/omega;
change = frequencyevent (half, 1e-15);
"calculate the square wave"
s = sign (sin (omega * time));
output = if( s == 0 ) then
-amplitude
else
-(amplitude/2)*(s + 1)
end;

```

In order to validate the results of the simulation, it is required to prove that a voltage of 1.3 volts maximum output can be obtained in the electrical part of the system. The voltage measured across the resistor is shown in the figure as output voltage, and the maximum value is 1.3 V. In the experimental results, a single wave of output from the oscilloscope was reported and the maximum value obtained was 1.3 V [Goldner (2001)].

10.5 Planar Rigid Body Motion

We would like to discuss possible ways to model the transfer of power that is generated in the engine chambers to the crank shaft via the connecting rod. This involves modeling the movement of rigid bodies in a plane. In order to explore the motion of planar rigid bodies, we need to consider a generic body that is capable of moving in a plane, that is, it has three degrees of freedom, movement in the horizontal and vertical directions

and rotation about an axis perpendicular to the plane. These degrees of freedom may also be referred as freedom to move in the x or y directions and ability to rotate about the z axis. For planar bodies, it is easier if we use global coordinate systems (rather than body fitted coordinate systems) for analysis. Figure 10.49 shows an arbitrary body in a two-dimensional plane with its center of mass shown in the figure. The horizontal and the vertical axes shown at the CG are fixed to the body and at the current instant of time they happen to be inline with horizontal and vertical directions. The three degrees of freedom of the center of mass are also shown in the figure in the form of linear velocities about the x and y directions and angular velocities about the axis perpendicular to the plane. The directions shown in the figure are the accepted positive directions of the above quantities. Inertia quantity mass, m , is associated with the motion of the center of mass in the x and y directions. Inertia quantity moment of inertia about the z axis, J , is associated with the rotational motion about the z axis (axis perpendicular to the plane shown).

The figure also shows two points that are located away from the center of mass on opposite sides at distances $R1$ and $R2$, respectively from the center of mass. The $R1$ and $R2$ vectors make an angle of θ and $(180 + \theta)$, respectively, to the positive x direction. For this arrangement, the x and y velocities of these points are shown on the figure as $V1_x$ and $V1_y$ and $V2_x$ and $V2_y$ for the second point. Therefore, from the geometry of the system it can be shown that:

$$\begin{aligned} V1_x &= V_x - \omega R1 \sin \theta \\ V1_y &= V_y + \omega R1 \cos \theta \end{aligned} \quad (10.16)$$

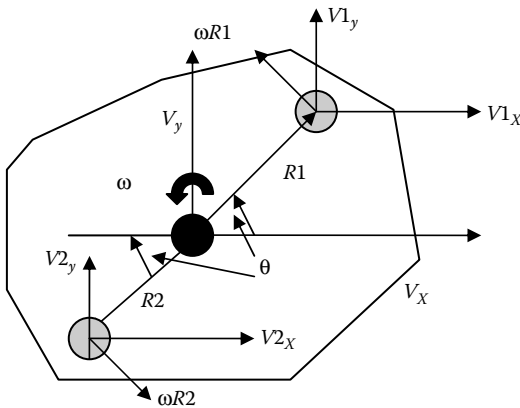


FIGURE 10.49

Movement of an arbitrary rigid body in a plane.

and

$$\begin{aligned} V_{2x} &= V_x + \omega R \sin \theta \\ V_{2y} &= V_y - \omega R \cos \theta \end{aligned} \quad (10.17)$$

Although θ is shown in the figure as a particular angle, it changes with time as the body rotates. So θ can be obtained by integrating ω .

In order to model any rigid body motion, it is important to understand the bond graph model of this basic rigid body representation. The velocities at three points (the center of mass and the other two points) can be related to each other through the above equations.

The bond graph representation of the movement of this generic rigid body is shown in Figure 10.50.

In the bond graph model, there are seven 1 junctions, which represent the seven velocity points that we are discussing. Three are associated with the three velocities at the CG, and the other four are associated with the x and y velocities at the two points that are chosen on the rigid body. Inertia elements associated with the three 1 junctions representing the center of gravity are mass $X = \text{Mass}$, $Y = \text{mass of rigid body}$, and $J = \text{rotational inertia}$. The transformer elements are used to multiply the radius and angular velocity to get the two components in the x and y directions at the two non-CG point. Since the coordinates are fixed to the ground and gravity acts vertically downwards, a source of effort is included with the Y component of

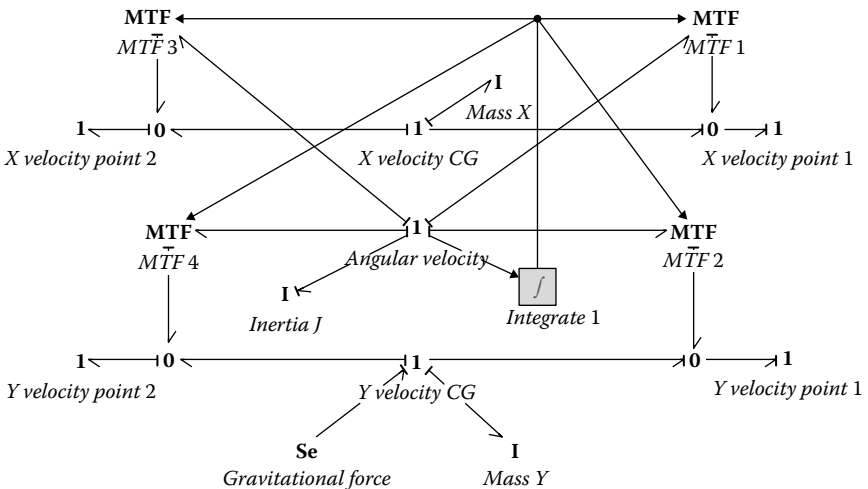


FIGURE 10.50

Bond graph of a generic rigid body motion in a plane.

the center of gravity. This source of effort represents the gravitational force. The model for one of the MTF element is shown below. The others are similar to this one with slight variations of the actual expressions.

Parameters

```
real R1 = 0.25;
```

Equations

```
p1.e = -R1*sin(r)*p2.e;  
p2.f = -R1*sin(r)*p1.f;
```

On the right and the left-hand sides of the model, the two 0 junctions add the velocity components as shown in the earlier equations. The bond directions for the two 0 junctions representing the x and y velocities of the point are chosen such that the two velocity equations shown earlier are modeled correctly (i.e., addition and subtraction are properly taken care of). The x and y velocity components of points 1 and 2 are represented by 0 junctions. Now that the basic structure of a rigid body is developed, we will explore some of its applications. Figure 10.51 shows a rigid rectangular pendulum that oscillates in a plane.

The point of attachment of the pendulum is at the top, and its center of gravity around the midpoint is also shown. The two ground-fitted axes at the point where the pendulum is hinged are shown in the figure as well. The bond graph representation of this system (Figure 10.52) is built

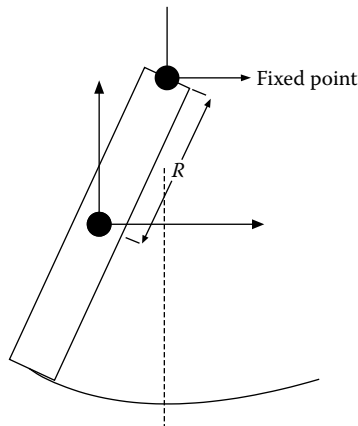


FIGURE 10.51

Rigid pendulum swinging in a plane.

based on the earlier general model of a rigid body with the addition of two sources of flow added to the 1 junctions representing point 1. The flow sources provide 0 flow at this point, and this approach is taken to model the pinned joint at point 1. Once the pendulum end is pinned, the number of degrees of freedom of the pendulum is reduced to 1. This is reflected in the causal structure of the three *I* elements. Two of the *I* elements, the ones representing the two mass elements, have differential causality. The *I* element representing the inertia has integral causality indicating that it behaves as an independent energy storage device.

The arbitrarily chosen property values are shown in Figure 10.53. Along with this, the initial value of the angle is chosen to be 0.2 radians

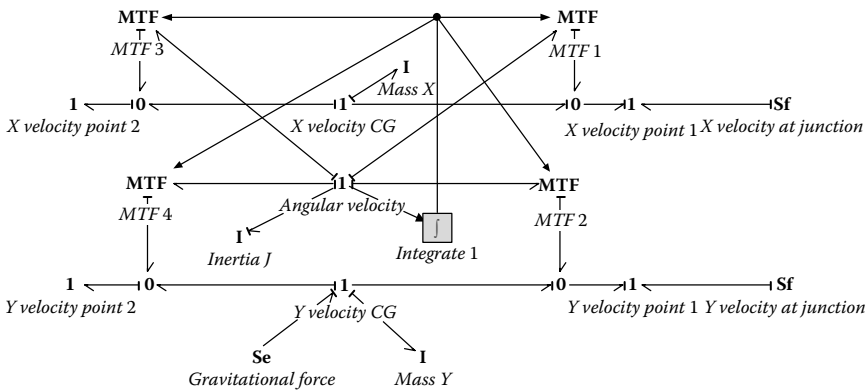


FIGURE 10.52
Bond graph representation of the pendulum.

Parameters Initial Values Constants			
Name	Val...	Quantity	Unit
Mass_X\i	1		
Mass_Y\i	1		
Inertia_J\i	0.1		
Y_velocity_at_junction\flow	0		
X_velocity_at_junction\flow	0		
Gravitational_force\effort	-9.81		
MTF1\R1	0.25		
MTF2\R1	0.25		
MTF3\R2	0.5		
MTF4\R2	0.5		

FIGURE 10.53
Parameters used for the pendulum.

for the integrator. Without the non-0 initial conditions, there will not be any movement. The resulting system behavior is shown in the plot of the angular velocity of the pendulum with respect to time (Figure 10.54). As expected, it is sinusoidal in nature. Other parameters calculated in the simulation may be similarly obtained. Figure 10.55 shows how the x and y components of forces vary at the point where the pendulum is attached by

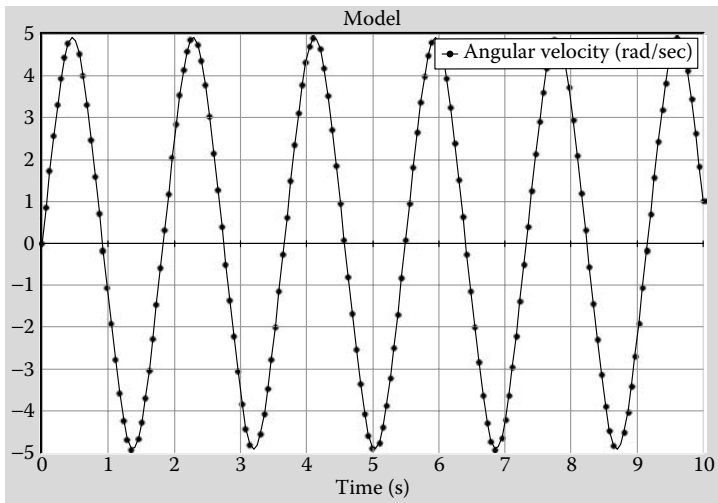


FIGURE 10.54
Angular velocity of the pendulum.

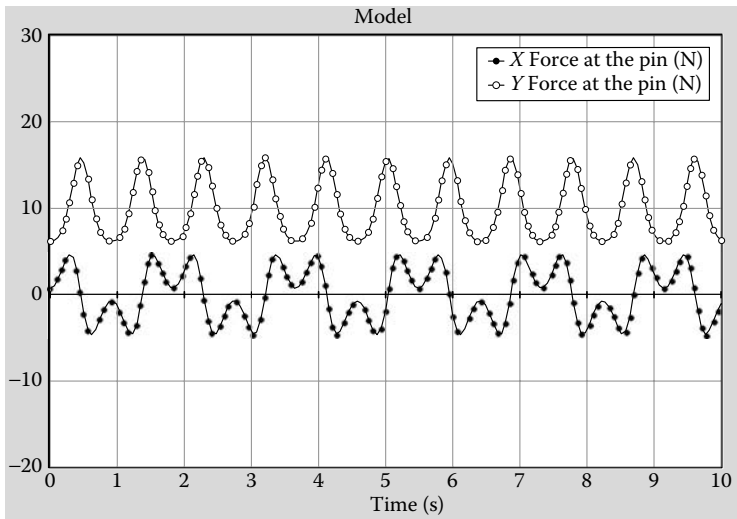


FIGURE 10.55
Forces at the pin.

a pin joint. Note that the y direction force oscillates around the weight of the component and the x direction force oscillates about 0. This also confirms expected behavior.

We will use the concept developed about the movement of rigid bodies to develop a model for the slider–crank mechanism that is the basis of an internal combustion engine.

Figure 10.56 shows a schematic of the slider–crank mechanism. The bond graph model of this is built by using two of the basic models for the rigid links. The joint 1–2 is the location where the two links are joined. At the ground, x and y velocities are 0 at all times. This is achieved by adding

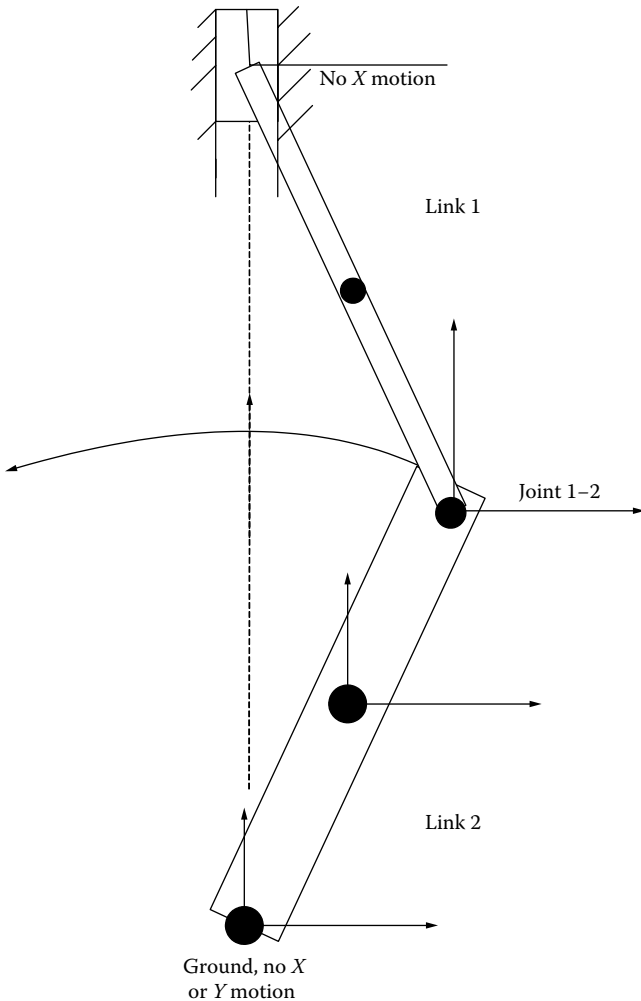


FIGURE 10.56
Schematic for the slider–crank mechanism.

two flow sources to this element with 0 flow. At the location where link one is attached to the piston, no flow is allowed in the x direction, and a source of effort is added to the y direction to indicate the force as a result of the pressure from combustion. The bond graph representation of this model is shown in Figure 10.57.

The slider–crank mechanism is also a single degree of freedom mechanism. Thus, when the bond graph model is created, four of the six I elements have differential causality. Of the two I s that represent the inertia of the two links, one should have a differential causality. However, when that was created in 20Sim, the simulation software reported difficulty in inverting the constitutive equations for the I elements. The model is slightly modified by adding an R element with a very small value so that the causal structure of the system is consistent and the simulation works. The kinetic behavior of this model is rather complex and nonlinear because

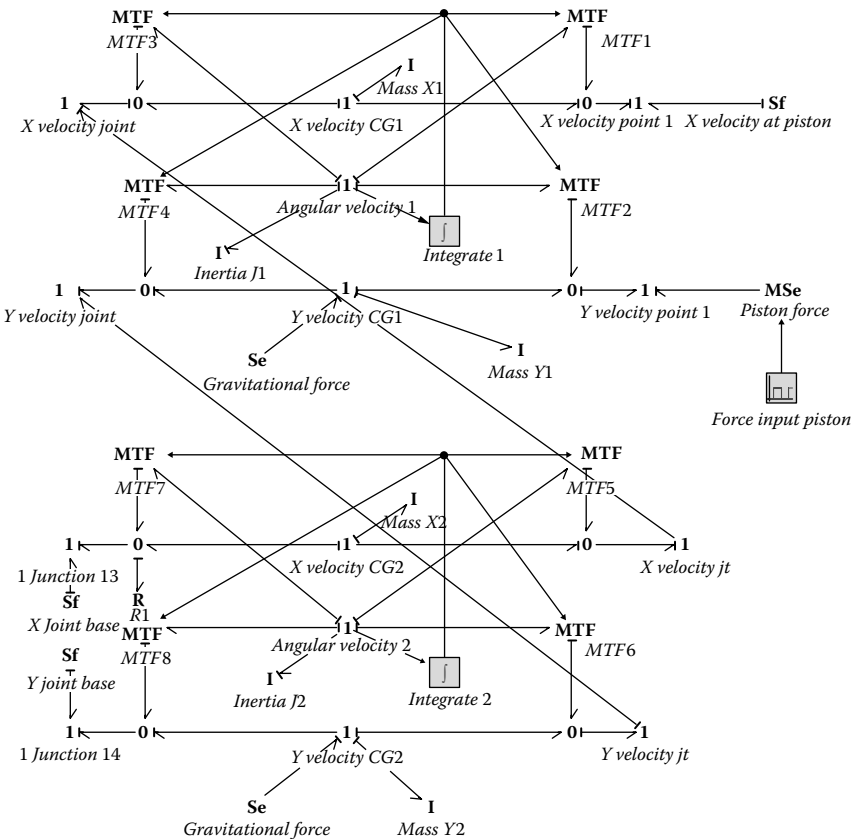


FIGURE 10.57
Bond graph of the slider–crank mechanism.

the behavior is dependent on the sine and cosines of angles, which are nonlinear functions of the angles.

Figure 10.58 shows the plots from a simulation using this model. The data used in this simulation are shown in Figure 10.59. The actual results

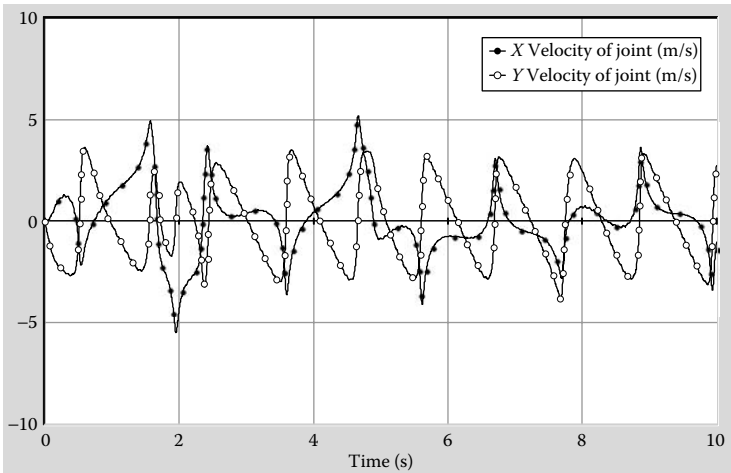


FIGURE 10.58
Response of the slider-crank system.

Name	Value	Quantity	Unit
Mass_X1\i	1		
Mass_Y1\i	1		
Inertia_J1\i	0.1		
X_velocity_at_piston\flow	0		
Gravitational_force\effort	-9.81		
MTF1\R1	0.5		
MTF2\R1	0.5		
MTF3\R2	0.5		
MTF4\R2	0.5		
Mass_X2\i	1		
Mass_Y2\i	1		
Inertia_J2\i	0.1		
Y_joint_base\flow	0		
X_joint_base\flow	0		
Gravitational_Force\effort	-9.81		
MTF5\R1	0.5		
MTF6\R1	0.5		
MTF7\R2	0.5		
MTF8\R2	0.5		
Force_Input_Piston\amplitude	10		
Force_Input_Piston\omega	100 {rad/s}	Angular Velocity	radian per second
R1\i	1e-006		

FIGURE 10.59
Parameters used.

will vary both in nature and magnitude as the relative dimensions of the links change, the frequency of the forcing function changes, and other factors in the model change. This plot is included here just as a sample of some of the results one could expect from this simulation.

10.6 Simple Engine Model: A Different Approach

For this simulation exercise, a six-cylinder internal combustion engine was chosen. The objective was to use real-life cylinder pressure data as an input to a power cylinder model (all six), and then observe the torque generated. Figure 10.60 is a generic power cylinder.

Dynamometer test data for a 4.0L V6 commercial engine was obtained. The data was broken up by cylinder and converted from crank angle per cylinder to overall engine crank angle. This data was converted to an input versus time so that the data can be used to apply to each cylinder as a source of effort. Since the data was steady state at 3000 rpm, this was relatively easy. A .txt file for each of the six cylinders was created containing the time and cylinder pressure data.

The foundation of a successful simulation is obviously a sound and accurate bond graph. As mentioned above, the cylinder pressure data feed into the *MSe* using a file input element linked to the appropriate .txt file. The *MSe* element feeds the first TF, which converts the cylinder pressure data in psi to force in lbf. This was done by multiplying the cylinder pressure by the piston area (12.54 in^2). The force data then feeds into the MTF, where it is converted from translational force to torque. Six of these lines of elements feed into a single 1 junction, which simulates the crankshaft. This 1 junction does feed back the crank angle to each cylinder thru six feed back lines. Each line takes the angular velocity from the 1 junction, integrates it, then feeds the crank angle back into the MTF

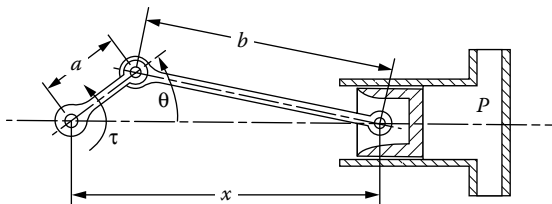


FIGURE 10.60

Schematic showing a generic cylinder.

(depending on the cylinder number, an initial value was added to get the proper firing phase). The formula in each MTF uses the translational force and the angle to calculate the previously mentioned torque using the below formula:

$$T = F[-a\sin\theta - (b^2 - a^2\sin^2\theta)^{-1/2} a^2\sin\theta\cos\theta] \quad (10.18)$$

where a = stroke length and b = connecting rod length.

Also connected to the 1 junction is an R element. This serves as a both a lump sum loss and also a means to draw out the total torque for the system. See Figure 10.61 for the model of the setup. It is important to note that the data file input is correctly phased and the integrators are properly phased.

As can be seen in the graphs (Figures 10.62 and 10.63), both the input cylinder pressure (psi) and translational force (lbf) look reasonable. Using an R value of 1.55 in-lb-s/radian, reasonable torque values were obtained. The graph in Figure 10.64 is in in-lb. (3000 in-lb is roughly 250 ft-lb). Max torque (obtained experimentally) for this engine was 243 ft-lb @ 3000 rpm.

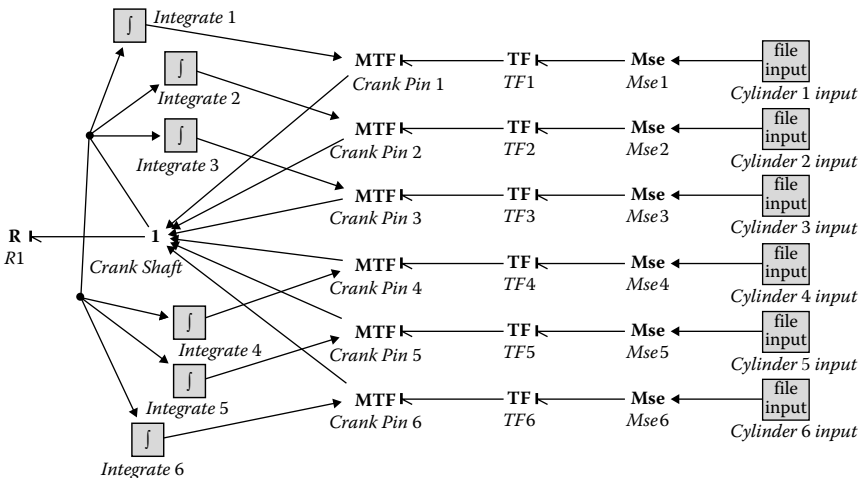


FIGURE 10.61
Bond graph model of the engine.

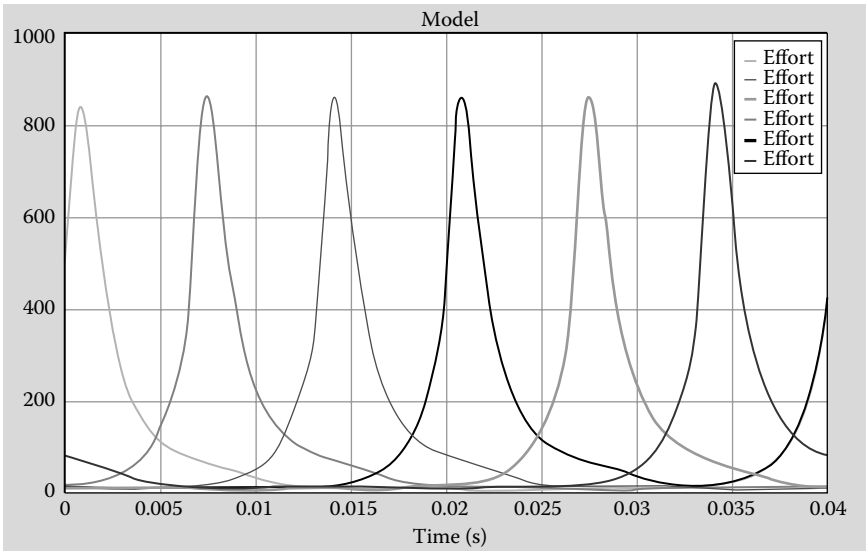


FIGURE 10.62
The pressure (psi) input at the six cylinders.

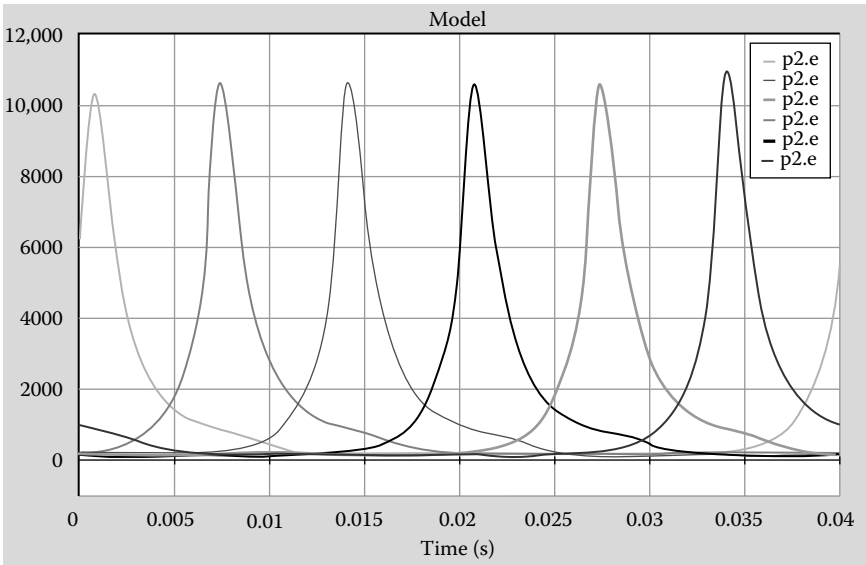
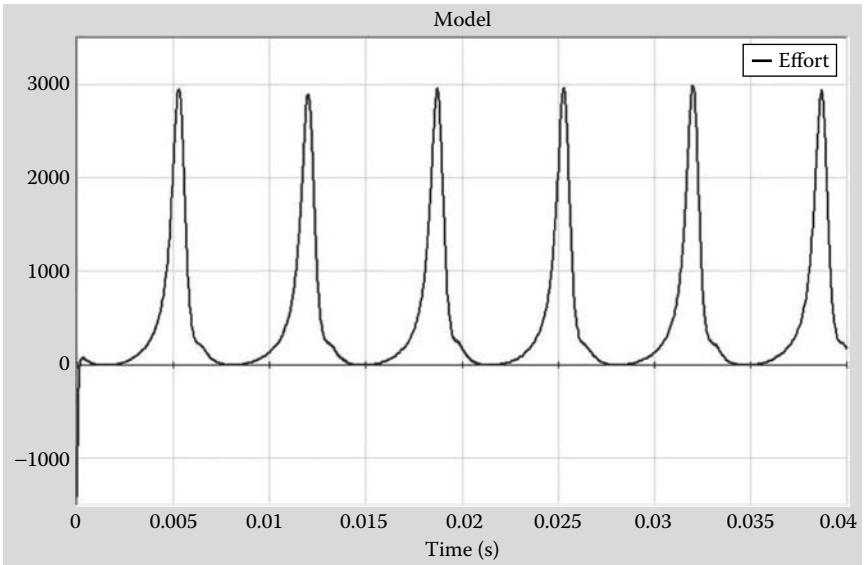


FIGURE 10.63
The force (lbf) at the six cylinders.

**FIGURE 10.64**

Torque output at the crank shaft (in-lb).

10.7 Summary

In this chapter we have discussed different aspects of modeling systems that are related to the automobile. We feel that even with this discussion, we have just scratched the surface and have just introduced the topic. For about 30 years, many researchers have been working on modeling automotive systems using the bond graphs. One of the aspects of modeling automotive systems is that on many occasions, to avoid complexities in the model, one has to rely on experimental data. For example, in modeling the drive train, one can opt to model the exact thermodynamics of the engine or use experimental data to represent the engine effort generated. These are the types of decisions that need to be taken and are aspects new modelers need to learn about, through practice. One needs to focus on getting solutions the best way rather than getting every little aspect of the situation modeled from first principles.

Problems

- 10.1. The power steering model described in this chapter is a simplified one. One gross simplification is the use of a single MR element to denote the hydraulic valve behavior. Using the bond graph model given in the text as a starting point and using the hydraulic valve model from the previous chapter, modify the power steering model so that the complete behavior of the valve can be incorporated. Once the full model is developed, make a list of all the parameter values necessary to simulate the behavior of this device. Simulate the behavior of the model using representative parameter values.
- 10.2. Figure P10.1 shows a schematic of a hydraulic braking system. Develop the bond graph model of this system, and demonstrate its behavior through simulation.

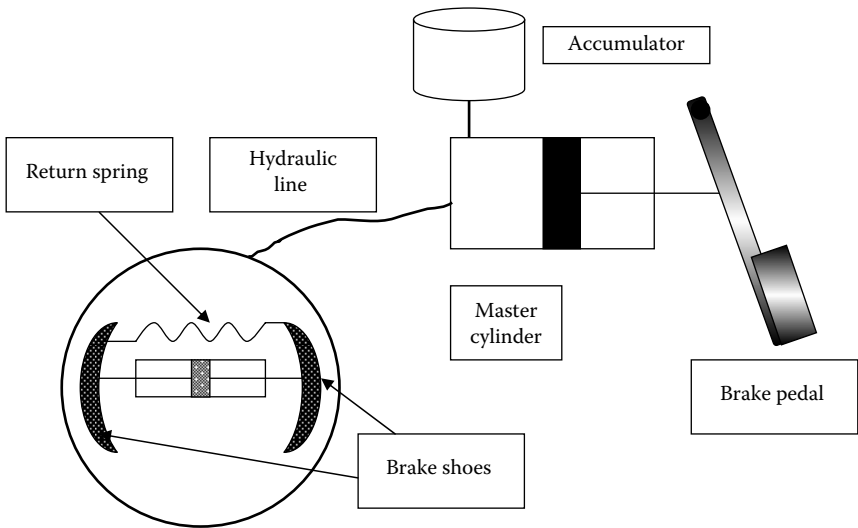


FIGURE P10.1

Figure for Problem 10.2, schematic of a hydraulic braking system.

- 10.3. Develop a quarter car model with a sprung and an unsprung mass (sprung mass representing the quarter car model vehicle body and unsprung mass representing the tire). Include the suspension and also the tire stiffness. Develop the bond graph model and the transfer function for both the force on the vehicle body and the

tire deflection. The force on the vehicle (in turn the acceleration) is a measure of ride quality, and the tire deflection is a measure of the handling. Alter the suspension stiffness, suspension damping and tire stiffness (only one at a time) by orders of magnitude, and develop a chart to summarize your findings at low, resonant, and high frequencies. What conclusions can you draw from this activity?

- 10.4. Figure P10.2 shows a schematic of a bicycle model along with a trailer that is attached using a ball joint at the trailer hitch. On the side of the figure is shown the picture of the joint with the velocities of both the points parked. The velocity relationships at the joint are:

$$U_2 = U_1 \cos \phi - V_1 \sin \phi$$

$$V_2 = U_1 \sin \phi + V_1 \cos \phi$$

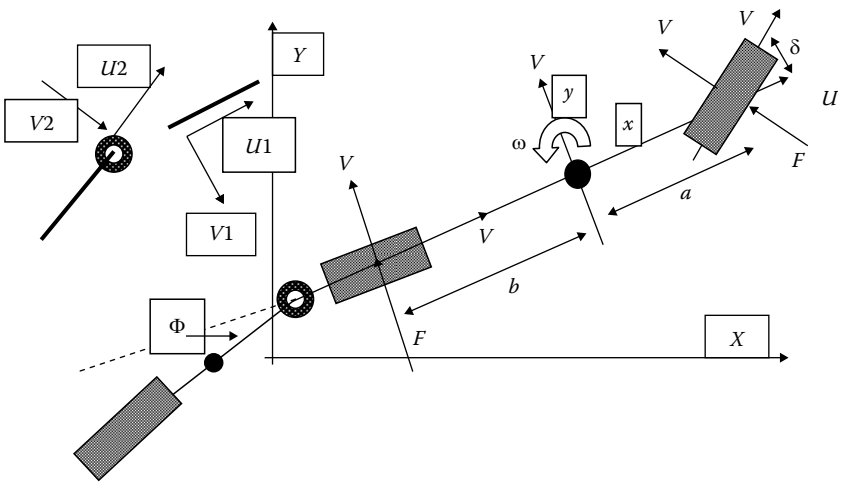


FIGURE P10.2

Figure for Problem 10.4, bicycle model for a car–trailer combination.

Using these relationships and the similar set of variables for the trailer as the main vehicle develop the bond graph representation for this system.

11

Control System Modeling

Controlling system behavior is an important necessity for practical systems. No matter how well a system is designed, its response (or system output) is not always exactly what was desired or expected. Also, external disturbances can affect the system; and its behavior, as a result, may change from what was desired. Hence, it is necessary to have a control system that will adjust system behavior by altering the input so that the desired output is achieved. There are some simple control techniques, such as a “bang-bang” (on/off) control, which are of limited use. The most well-known and useful technique is feedback control, where the response of the system is monitored and compared with the expected response, and the error in the response is used to alter the input dynamically to achieve the desired result. The block diagram in Figure 11.1 shows a schematic of the feedback control system. The system’s (or plant’s) response is subtracted from the set point to obtain the error. The error signal is used in a control algorithm to determine the system input that is fed into the system, and the response is adjusted, as a result, to achieve the desired output.

Similar in concept to the feedback control, there is also a control technique known as feed-forward control. This technique is used (many times in combination with feedback techniques) to account for disturbances in the system that are not measurable in the form of an output. These types of disturbances are usually unanticipated inputs to the system, and in the feed-forward methodology, the disturbance inputs are themselves

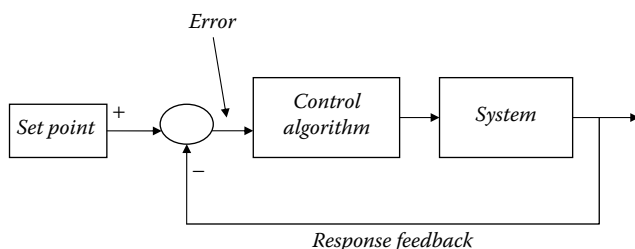


FIGURE 11.1
Schematic showing a feedback control loop.

measured and a signal is added to the controller to account for the effects of these disturbances.

Figure 11.2 shows a schematic of the feedback and feed-forward control system. Control system designers use several different measures of system performance. These measures include:

Stability: Initial condition disturbances should die off quickly.

Speed: The system needs to react quickly.

Sensitivity: System sensitivity to noise should be low and to control inputs should be high.

Accuracy: Error should be low.

Dynamic coupling: Reduced coupling among system variables.

When designing control systems, one has to judge effectiveness using some of these criteria.

In this chapter we have discussed some of the very basic and most commonly used concepts related to control algorithm. Our discussion is by no means exhaustive. We have focused on controls within the context of modeling mechatronic systems. Thus, in the next few sections, we will discuss ways to model some of the common control algorithms and how they are implemented in bond graph models. For more discussion on controls, the reader should refer to some of the texts on control systems.

The objectives of this discussion, therefore, are to

- Understand how to implement proportional, integral, and derivative controls.
- Understand how to tune control systems to design control parameters.
- Apply control algorithms to linear systems and nonlinear systems.

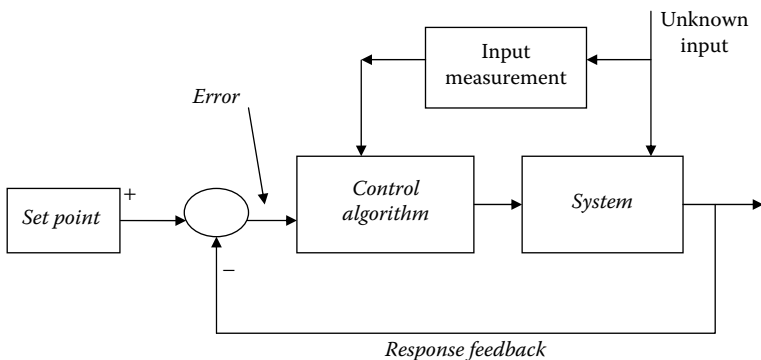


FIGURE 11.2
Feedback and feed-forward control.

11.1 PID Control

In all feedback control algorithms, the actual output is fed back into the control system so that an error measure (the difference between expected and actual output) is computed, and the error measure is used to set the change in the input needed to minimize the error. More than 90% of all control strategies revolve around the use of PID controls in some form. PID stands for proportional, integral, and derivative control. PID control is made of three different control strategies that are a function of the error, the rate at which this error changes (derivative), and the accumulation of error (integral).

11.1.1 Proportional Control

This is a control strategy where the control signal is proportional to the error.

We could write the control signal as:

$$\text{Control Signal} = K_p(\text{error}) \tag{11.1}$$

where error = (expected output – actual output)

The parameter that needs to be adjusted in this case is the multiplier parameter K_p . As an example, consider a permanent magnet DC motor whose speed needs to be controlled. If we use a proportional controller, the bond graph can be modified as shown in Figure 11.3.

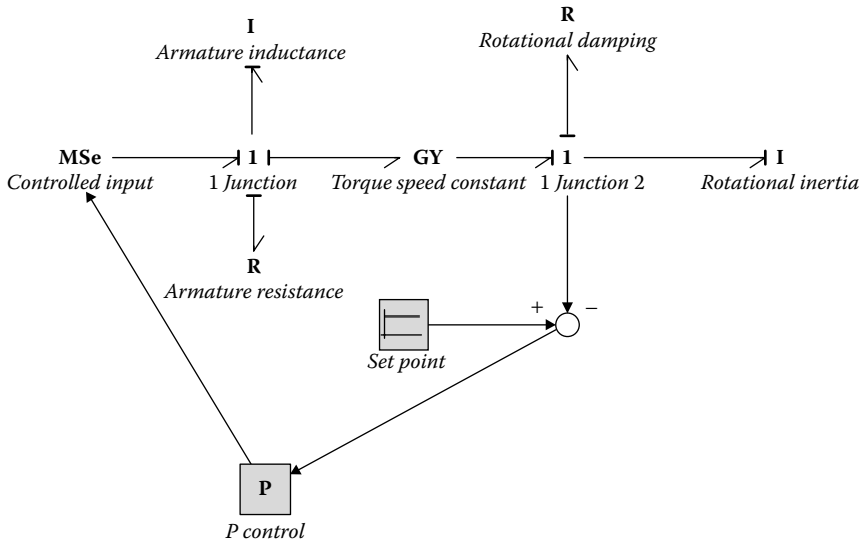


FIGURE 11.3
Motor bond graph with proportional control.

The P control module shown in the figure receives the error information (the difference between set point output and actual output). The model for the P control module is expressed through the following statements:

Equations

`output = kp*error;`

So, the difference between the expected speed and the actual speed is multiplied by the K_p factor to determine the source of effort that will be used for the system. The proportional control method is simple and works relatively fast. However, it has poor stability characteristics and may end up giving offset errors. Through this example, we will demonstrate these characteristic behaviors.

Figure 11.4 shows the initial parameters used in this exercise. The set point (i.e., the expected velocity) is fixed at 10 and the K_p value is set to 1 (because we do not know any better). The plot in Figure 11.5 shows the response of the system.

The plots show one of the difficulties of using a proportional control. There is a steady state or offset error that remains. We can try increasing the K_p factor. If we increase K_p to 10, the response changes as shown in Figure 11.6.

The response is significantly better, but a smaller offset error between the set point and the actual output still persists. We can try and correct this by increasing K_p even more, say to 100. The plot we get this time is shown in Figure 11.7. As can be seen, the error has been reduced even more, but the system response has now become oscillatory.

This example illustrates some of the important behavioral characteristics of a proportionally controlled system, specifically, a steady state error usually persists; its magnitude can be reduced by increasing the K_p value, but beyond a certain limit, the higher K_p will make the system behavior oscillatory or less stable. If K_p is made 1000, the plot looks like the one shown in Figure 11.8, with an even more oscillatory behavior.

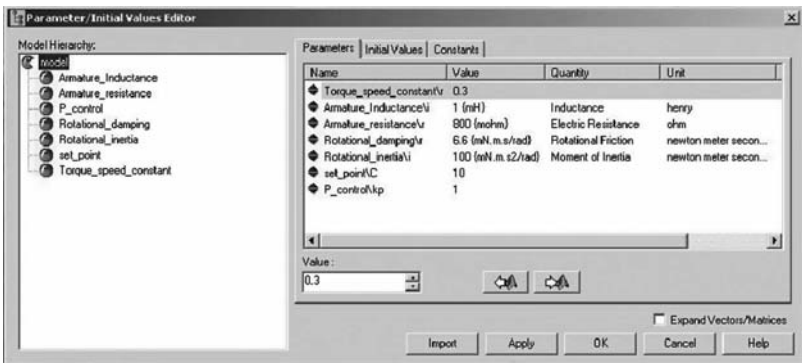


FIGURE 11.4

Initial parameters used for the proportional motor speed control.

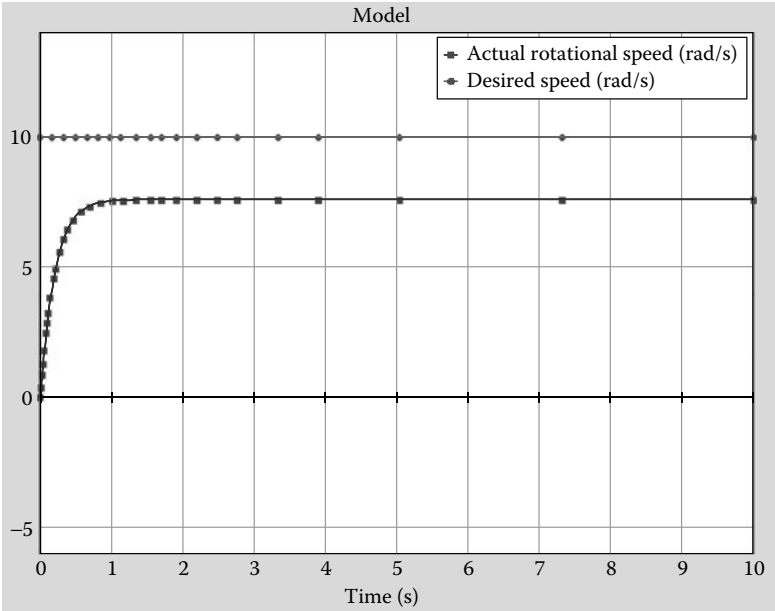


FIGURE 11.5
P controlled speed with initial parameters.

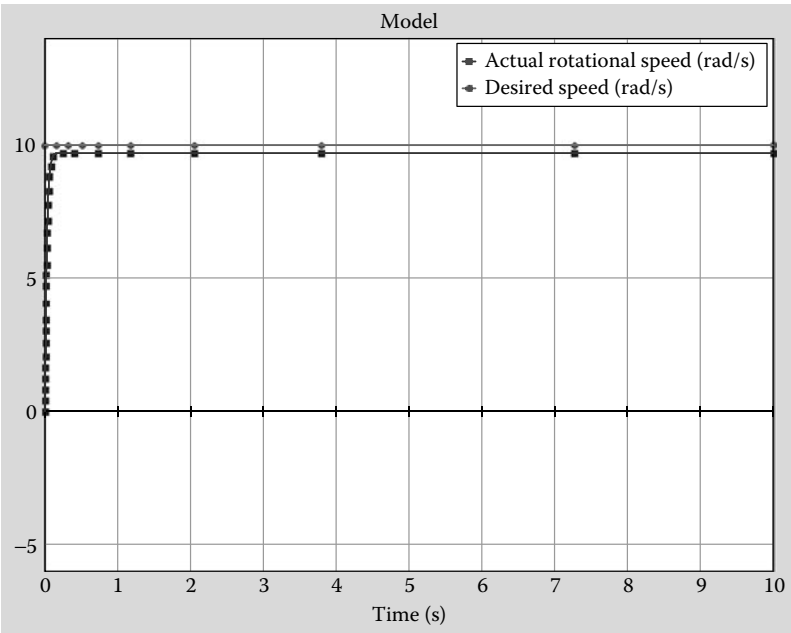


FIGURE 11.6
New response with $K_p = 10$.

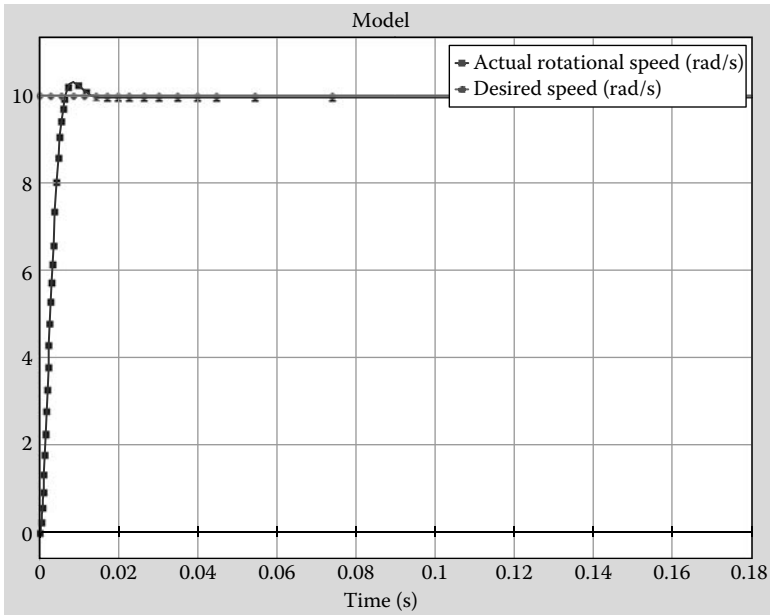


FIGURE 11.7
New response with $K_p = 100$.

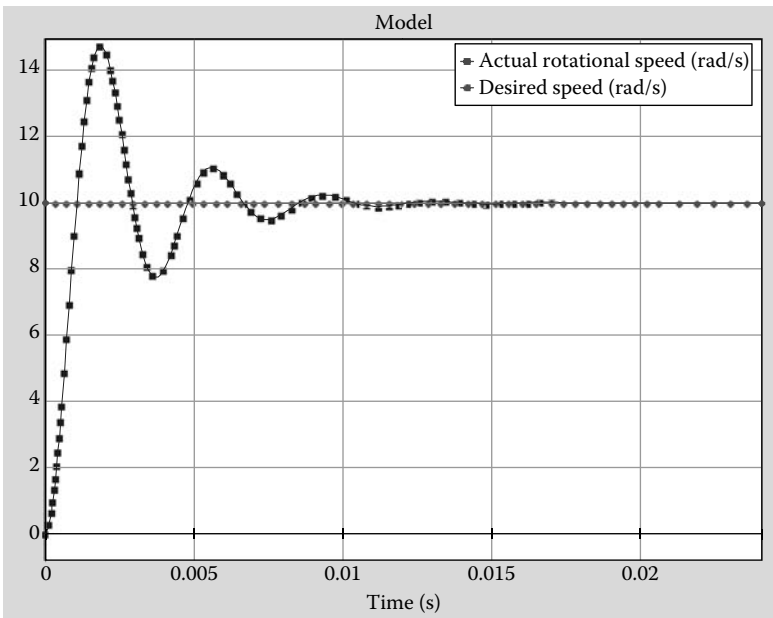


FIGURE 11.8
Modified response with $K_p = 1000$.

11.1.2 Proportional Integral Control

PI control stands for proportional integral control where the control signal can be written as:

$$\text{Control Signal} = K_p(\text{error} + \frac{1}{T_i} \int (\text{error}) dt) \quad (11.2)$$

This means that the control signal is dependent not only on the actual error but also on how much error is accumulating over time (i.e., the integral of error). Two parameters in this control algorithm are to be adjusted in order to tune the control signal: the K_p factor and the T_i factor. While K_p factor is the same error multiplier as before, T_i is the integral time constant of the error, and its reciprocal is sometimes referred as integral rate. The special characteristics of the integral controller are that it is good at eliminating offset errors and reducing noise. However, response is slow and may have stability issues. But in general, it complements the P controller very well and is often used in conjunction with the P controller.

We use the same example as before to demonstrate the behavior of this control algorithm. Consider the same permanent magnet DC motor as before. Its speed is to be controlled again, but we are using a PI controller this time. The bond graph model is shown in Figure 11.9.

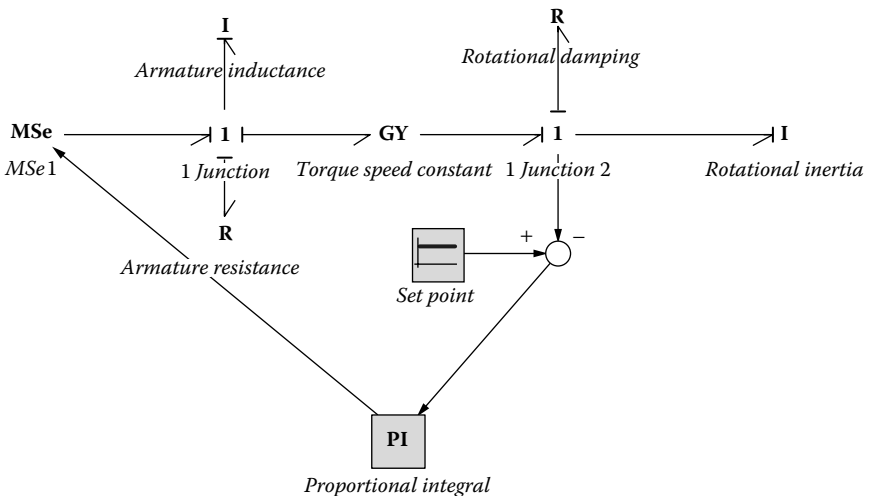


FIGURE 11.9

Bond graph model with PI controller.

The PI model code looks like the following:

Variables

```
real uP, uI;
```

Equations

```
uP = kp*error;
uI = (kp / tauI)*int (error);
output = uP + uI; // the output is the control signal.
```

The parameters used for the initial simulation are shown in Figure 11.10. The simulation results are shown in Figure 11.11. A close observation

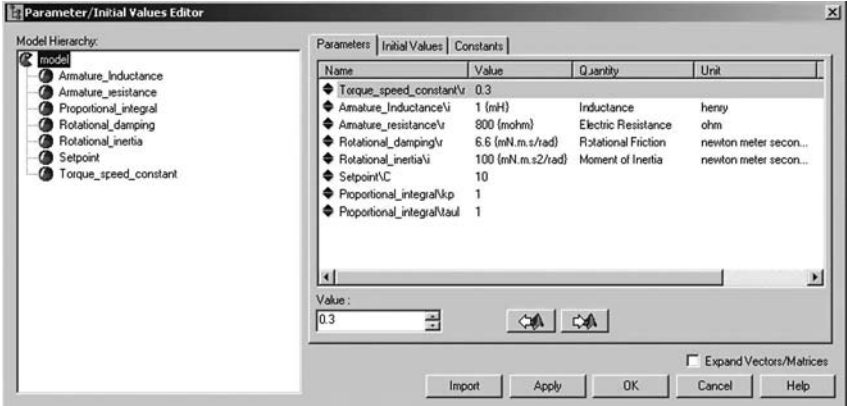


FIGURE 11.10
Initial parameters used for the PI controller.

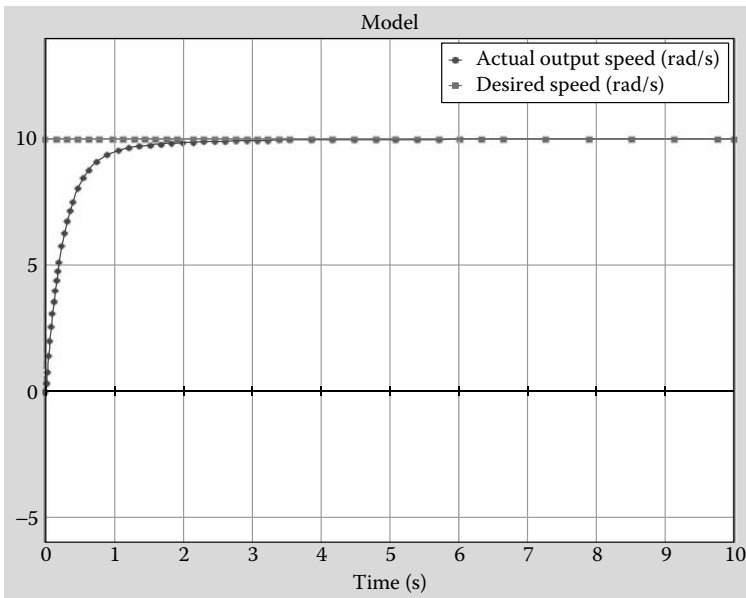


FIGURE 11.11
Simulation result with $K_p = 1$.

indicates that this behaves much better than just the proportional controller. If the K_p factor is now increased to 10, we observe that the system behavior rises more sharply to reach the set point value, as shown in Figure 11.12.

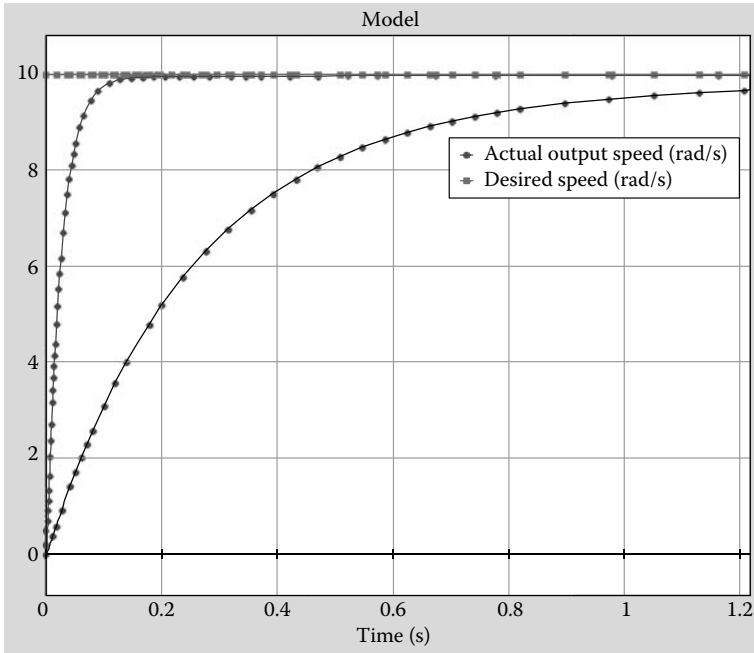


FIGURE 11.12

New results with $K_p = 10$ versus $K_p = 1$.

11.1.3 Proportional Derivative Control

There is another mode of feedback control that is called the PD control. PD stands for proportional and derivative control. In this case, the control signal or control input may be written as:

$$\text{Control Signal} = K_p(\text{error} + T_d \frac{d(\text{error})}{dt}); \quad (11.3)$$

We can see that for the PD control, the control signal is a function of both the error itself as well as the derivative of the error or the rate at which the error is changing. The two user-defined factors that control the behavior of this algorithm are K_p and T_d . The parameter T_d is known as the

derivative time constant. The response of a derivative controller is very fast and this generally improves stability of the controller. But this controller also tends to amplify noise.

The bond graph model that can be used to implement this is shown in Figure 11.13. The model equations are:

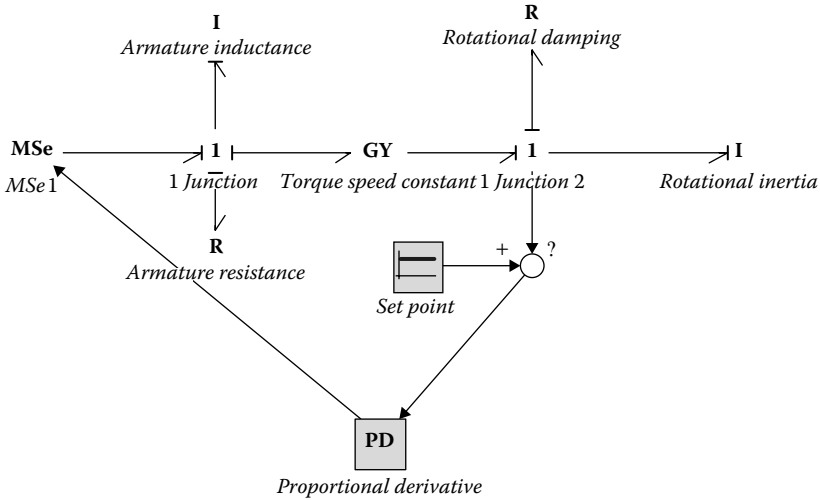


FIGURE 11.13

Bond graph model with PD controller.

Variables

real state, rate;

Equations

```
rate = ddt (error);
output = kp*(error + (tauD*rate));
```

The model for the PD control is essentially a code to include the PD equations in the model. The parameters used initially for the simulation are shown in Figure 11.14. With these initial values, the response of the system is shown in Figure 11.15. By increasing K_p to 10 and then 100 we significantly speed up the process. The plots in Figure 11.16 show the effect on increasing the K_p from 1 to 10 to 100. The offset error can be reduced, and the speed of the controller is improved without it becoming oscillatory.

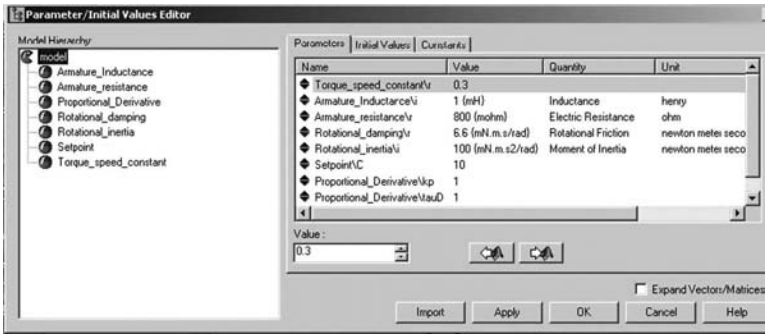


FIGURE 11.14
Parameters used for initial PD control.

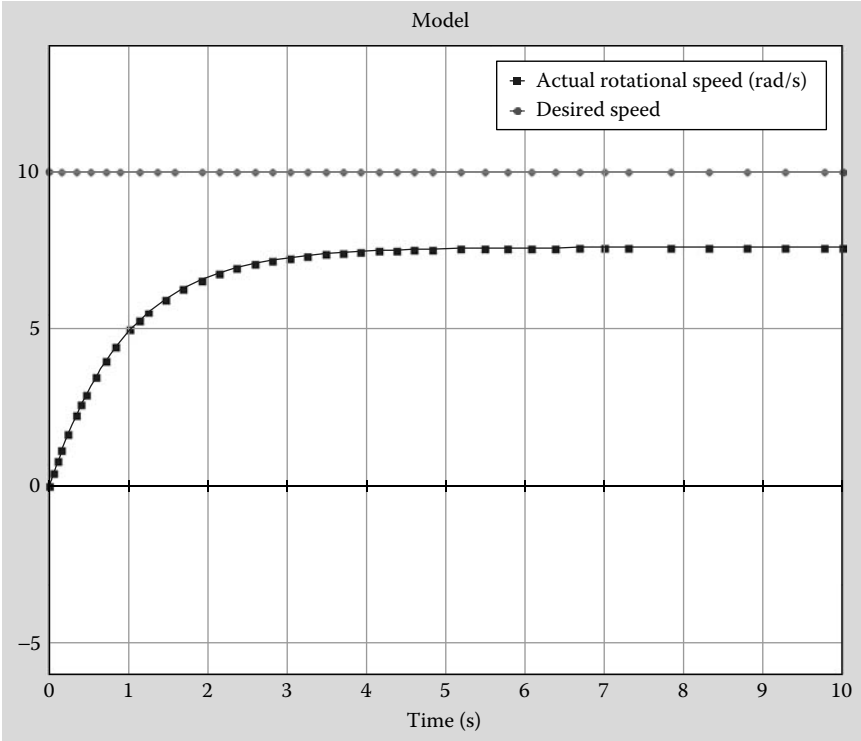
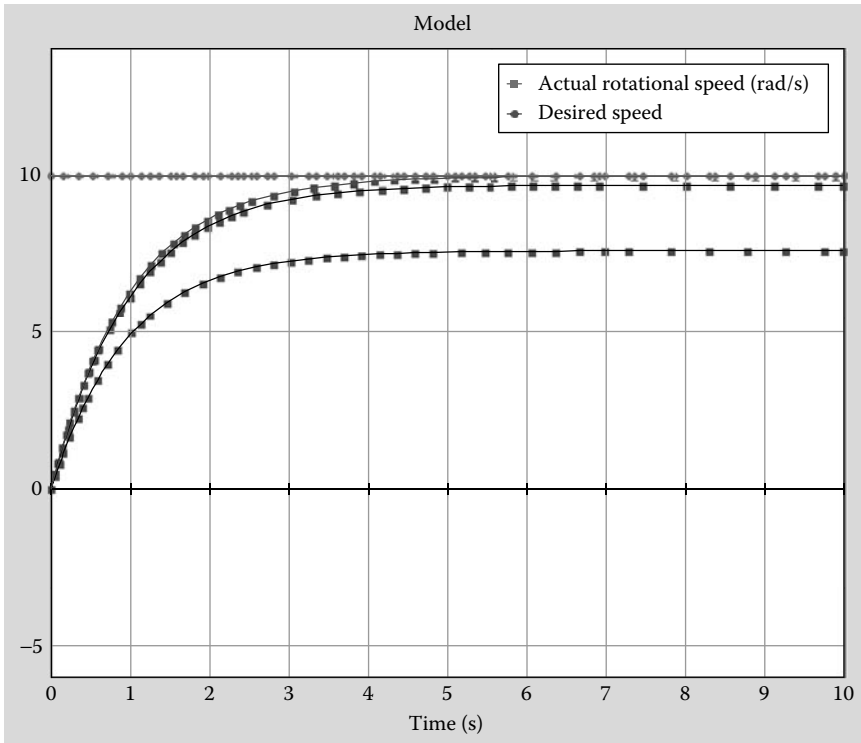


FIGURE 11.15
System response with initial values.

**FIGURE 11.16**

System responses with K_p values of 1, 10 and 100 (solution approaching the desired speed as the factor increases).

11.1.4 Proportional Integral Derivative Control

The last and most frequently used control algorithm is the PID control, which stands for proportional, derivative, and integral control all together. Obviously, all three control algorithms that make up the PID control have some advantages and some disadvantages. With this approach of combining all three, the control system designers attempt to maximize the advantages and minimize the disadvantages. This process is carried out in reality by adjusting the three parameters in the PID controller, namely K_p , T_i , and T_d . The process of adjusting these parameters is also known as tuning.

The control signal in this case can be written as a sum of three components, the proportional, integral, and the derivative. The control signal in this case is represented as:

$$\text{Control Signal} = K_p(\text{error}) + \frac{1}{T_i} \int (\text{error}) dt + T_d \frac{d(\text{error})}{dt} \quad (11.4)$$

The bond graph model for this situation is shown in Figure 11.17.

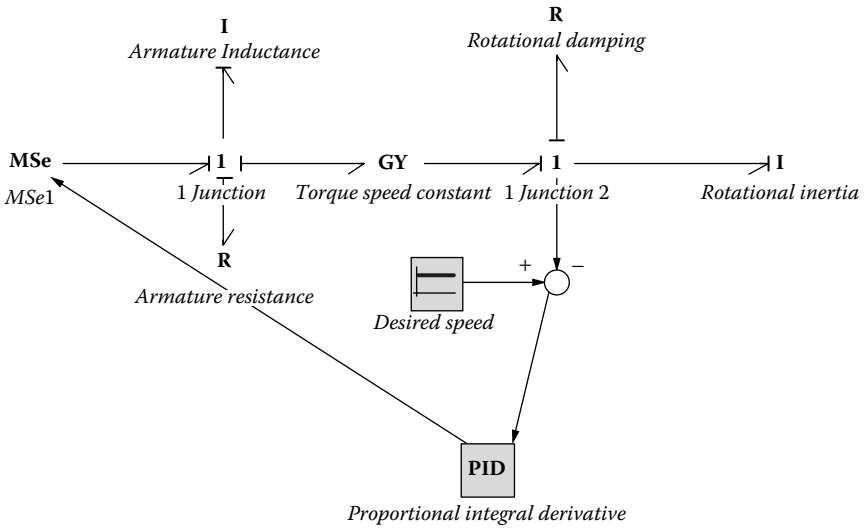


FIGURE 11.17

Bond graph model with the PID controller.

The PID algorithm is implemented in the following way:

Variables

```
real pdout, pdrate, pdstate;
real pirate, pistate;
```

Equations

```
pdrate = ddt (error);
pirate = int(error);
output = kp*(error + pirate/tauI + tauD*pdrate);
```

The different parameter values used in the simulation are shown in Figure 11.18. The response we get by simulating the system using these parameters is shown in Figure 11.19. Just by increasing K_p to 10 the plot changes to look like the one shown in Figure 11.20. This is not the desired output. The output can be modified by suitably adjusting all the control variables. For $K_p = 10$, $T_i = 1$, and $T_d = 0.001$, the response we get is shown in Figure 11.21.

The simulation model changes slightly if the parameter to be controlled is the displacement of the rotor and not the velocity. We change

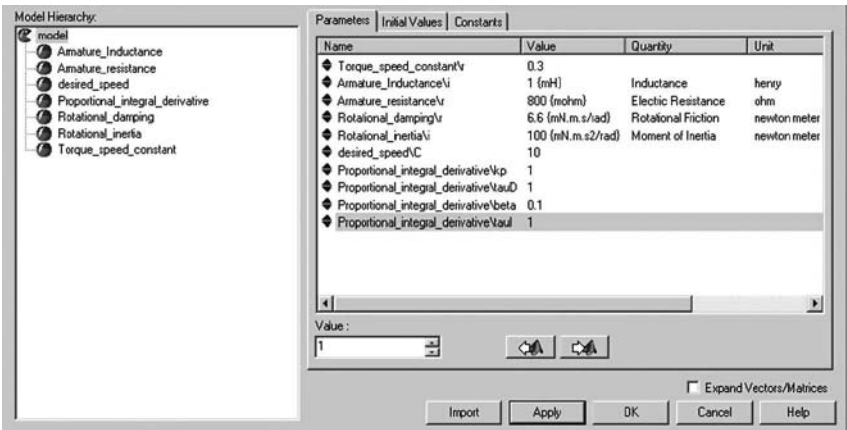


FIGURE 11.18

Initial parameter values used in the PID controller.

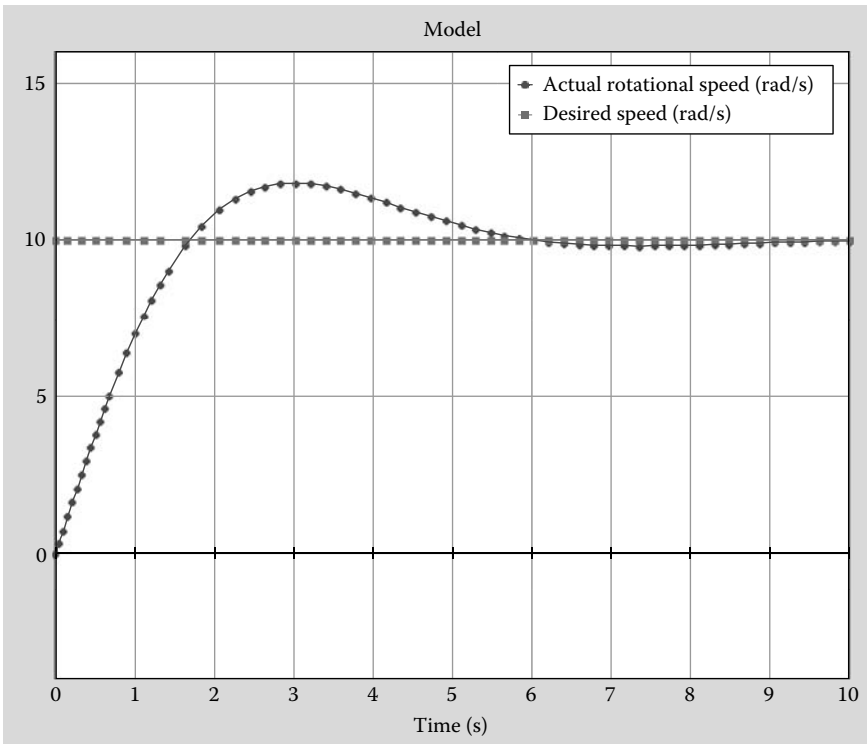


FIGURE 11.19

System response with the initially chosen control parameters.

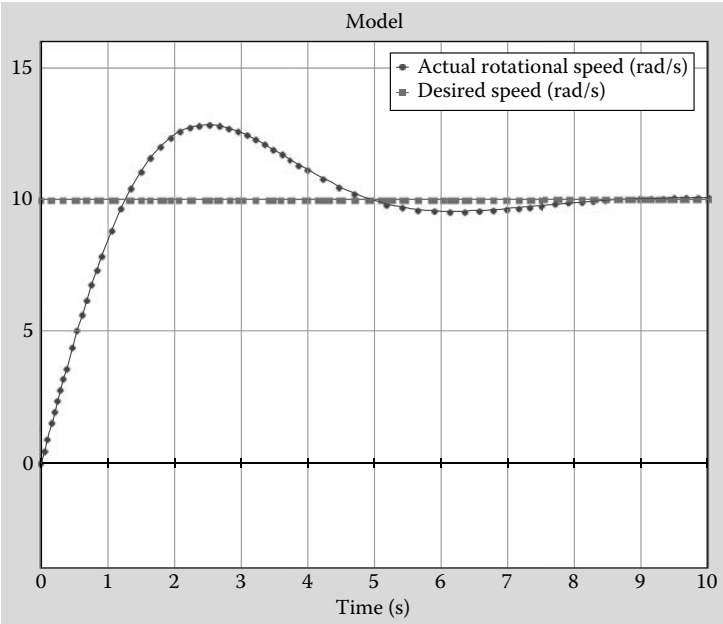


FIGURE 11.20
System response when $K_p = 10$ is used.

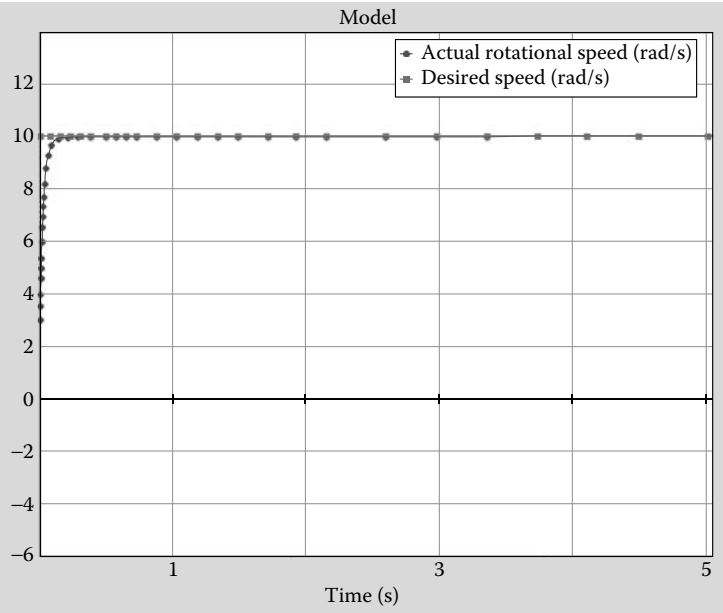


FIGURE 11.21
System response obtained with all the parameters tuned.

the model slightly so that we are now monitoring the integral of the velocity, displacement, and comparing that with the desired displacement. Also, the desired displacement is altered and made into something a little more complex than a steady state output. The bond graph is shown in Figure 11.22.

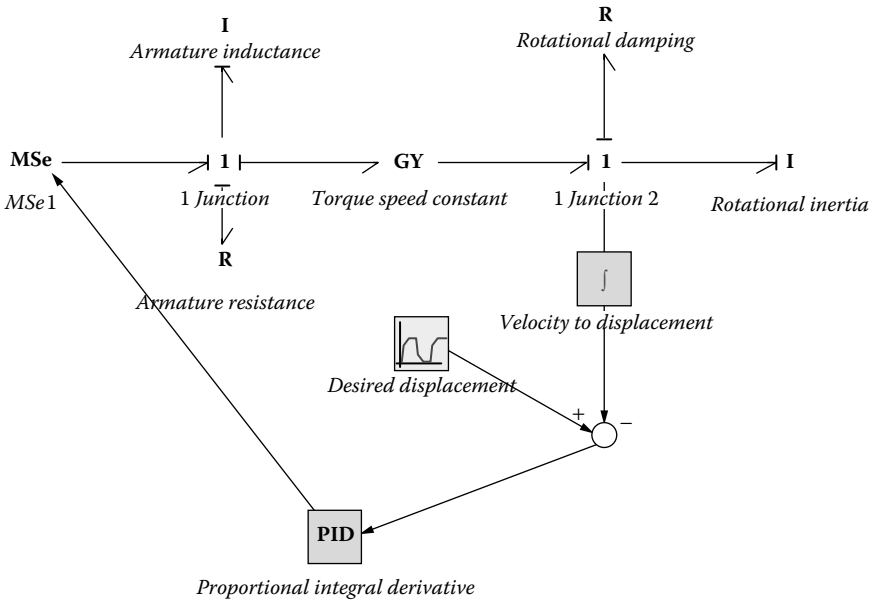


FIGURE 11.22

Bond graph model with PID control of displacement.

The system is simulated with the following PID parameters: $K_p = 10$, $T_i = 1$, and $T_d = 0.1$. The results are shown in Figure 11.23. There is some oscillation seen in the results. The values are further modified as for $K_p = 10$, $T_i = 1$, and $T_d = 1$. The results obtained are shown in Figure 11.24. And we can easily see how the system response improves as the parameters are adjusted.

This shows that the control algorithm works very well once the adjustable parameters are properly set. In this case, the parameters were obtained by trial and error. It is believed that obtaining the right control parameters requires some experience and practice working with the particular system. Control experts have come up with different algorithms of tuning these control parameters. The most well known among these is the Ziegler–Nichols criteria for PID control.

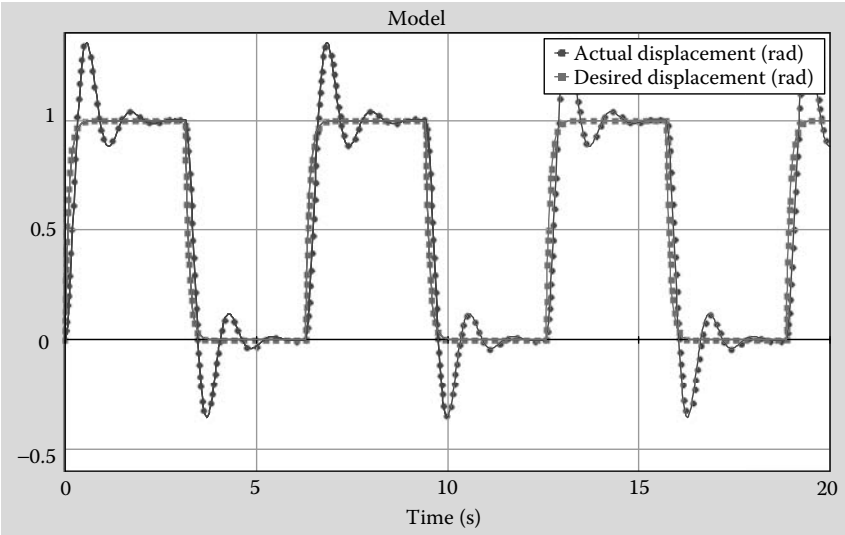


FIGURE 11.23
Displacement control with $K_p = 10$, $T_i = 1$, and $T_d = 0.1$.

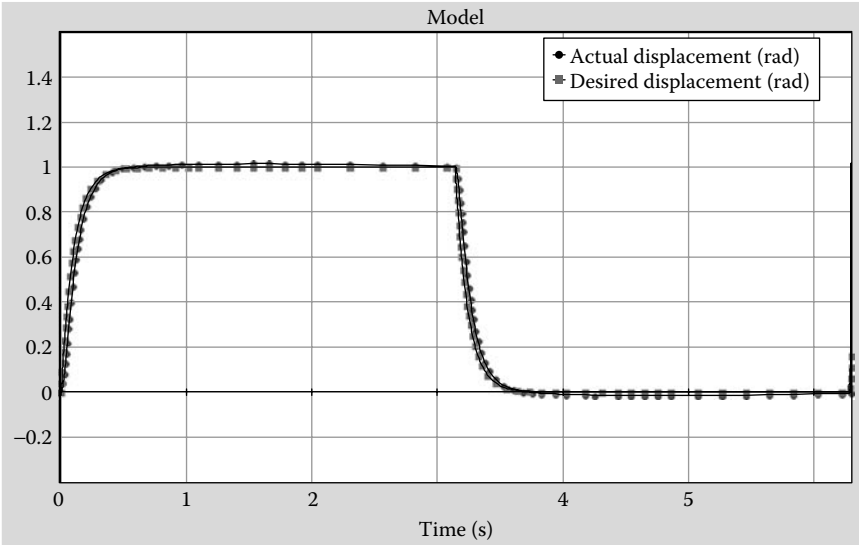


FIGURE 11.24
Displacement control with $K_p = 10$, $T_i = 1$, and $T_d = 1$.

11.1.5 Ziegler–Nichols Closed Loop Method

This technique provides a systematic approach to tuning the three parameters for the PID control. First, the controller is set to proportional mode. Next, the gain of the controller (K_p) is set to a small value. The load or set point is changed a little, and the response of the controlled variable is tracked. If K_p is low, the response will be quite slow. Now K_p is increased by a factor of 2 and the set point or the load is changed a little. At every trial, K_p is increased by a factor of 2 until the response becomes oscillatory. Finally, K_p is adjusted until the response is completely oscillatory. This particular value of K_p is called the ultimate gain (K_u). For this value of K_p , the period of oscillation is also recorded as T_u . The control law settings are then obtained in terms of K_u and T_u and are listed in Table 11.1.

TABLE 11.1

Parameters for Tuning the PID Controller

	K_p	T_i	T_D
P	$K_u/2$		
PI	$K_u/2.2$	$T_u/1.2$	
PID	$K_u/1.7$	$T_u/2$	$T_u/8$

It is unwise to force the system into a situation where there are continuous oscillations because this represents the limit at which the feedback system is stable. Generally, it is a good idea to stop at the point where some oscillation has been obtained. It is then possible to approximate the period (T_u), and if the gain at this point is taken as the ultimate gain (K_u), it will provide a more conservative tuning regime.

11.2 Control Examples

It is possible to add a large variety of examples with control systems in action. We will not repeat the same types, but will add one or two to illustrate a few issues. The first example is speed control of a motor using varying current rather than varying voltage. The bond graph model of this setup is shown in Figure 11.25. The variable current is achieved by varying the armature resistance, MR. The parameters used for this simulation are shown in Figure 11.26. And the simulation results are shown in Figure 11.27. The parameters used for the PID controller are the same as those used in the previous example and they are quite optimum in this case as well. Figure 11.28 shows the control parameter and the armature current as the system starts up and stabilizes.

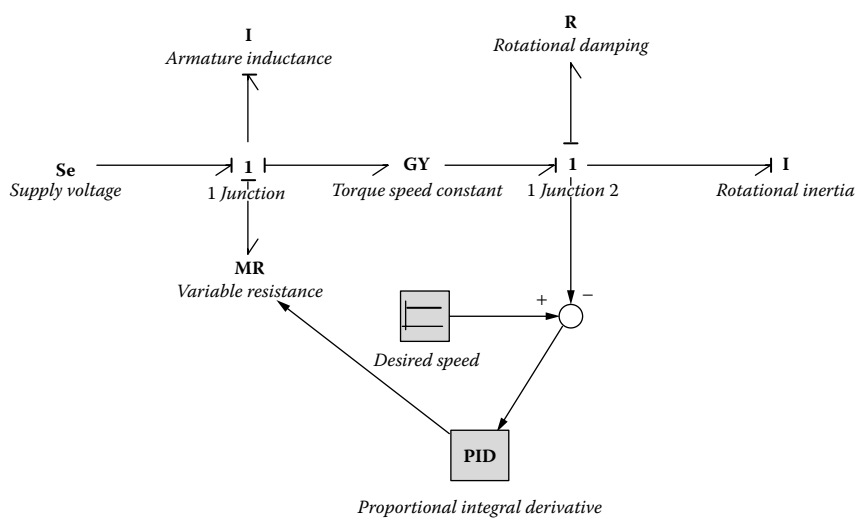


FIGURE 11.25
Motor speed control by varying armature current.

Name	Value	Quantity	Unit
Torque_speed_constant\tr	0.3		
Armature_Inductance\i	1 {mH}	Inductance	henry
Rotational_damping\tr	6.6 {mN.m.s/rad}	Rotational Friction	newton meter secon...
Rotational_inertia\i	100 {mN.m.s2/rad}	Moment of Inertia	newton meter secon...
desired_speed\VC	10		
Proportional_integral_derivative\kP	10		
Proportional_integral_derivative\tauD	0.001		
Proportional_integral_derivative\tauI	1		
Supply_voltage\effort	12		

FIGURE 11.26
Parameters used for speed control by current control.

The next example is a simple-looking control problem (shown in Figure 11.29) where the speed of mass M2 has to be controlled by controlling the force that is applied on mass M1. The control results will show this problem is inherently very difficult to control since the problem becomes unstable.

The bond graph model, along with the control loop, is shown in Figure 11.30, and the properties used for the simulation (in consistent units) are shown in Figure 11.31. The spring constant is 1E5 so the C (1/k) is written as 1E-5. The plots in Figure 11.32 show how the speed of the

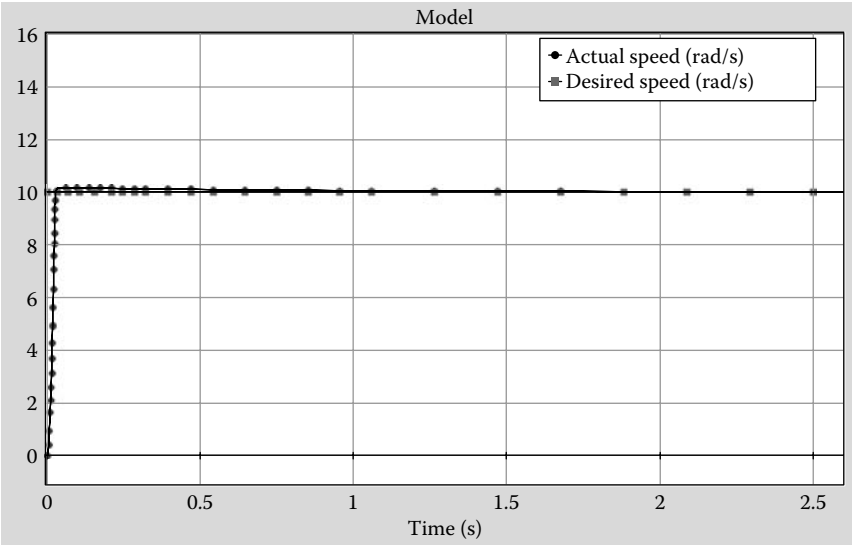


FIGURE 11.27
System response for speed control by varying armature current.

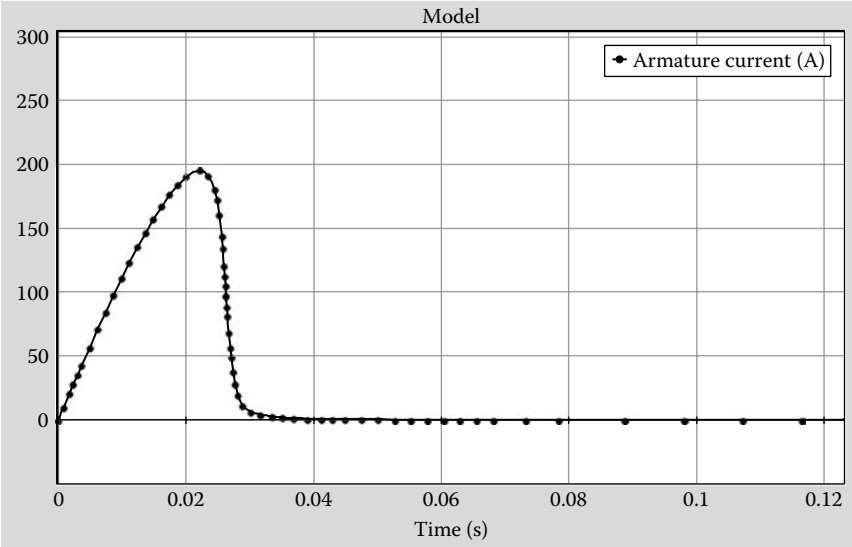


FIGURE 11.28
Variation of armature current during the control process.

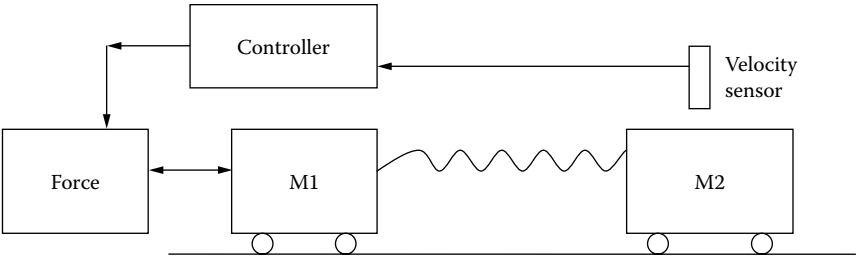


FIGURE 11.29
Speed control of M2.

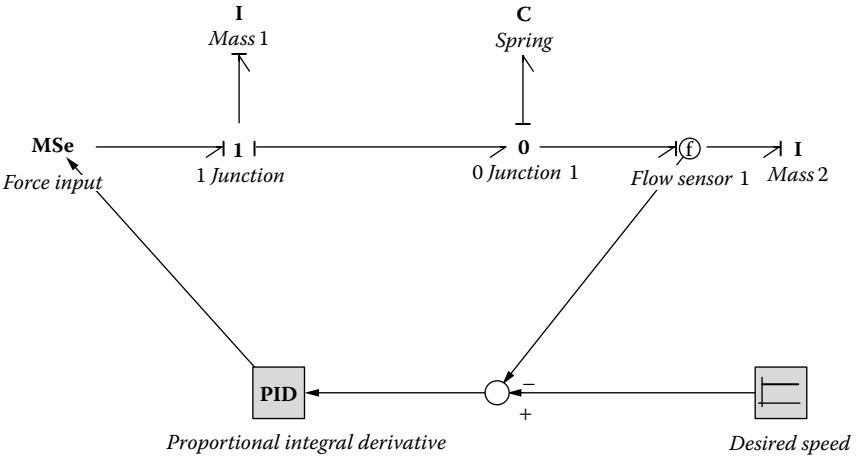


FIGURE 11.30
Bond graph of the system in Figure 11.29.

Name	Value	Quantity	Unit
desired_speed\C	10		
Proportional_integral_derivative\kp	10		
Proportional_integral_derivative\tauD	0.001		
Proportional_integral_derivative\taul	1		
Mass1\i	1		
Spring\c	1e-005		
Mass2\i	1		

FIGURE 11.31
Parameters used for simulation.

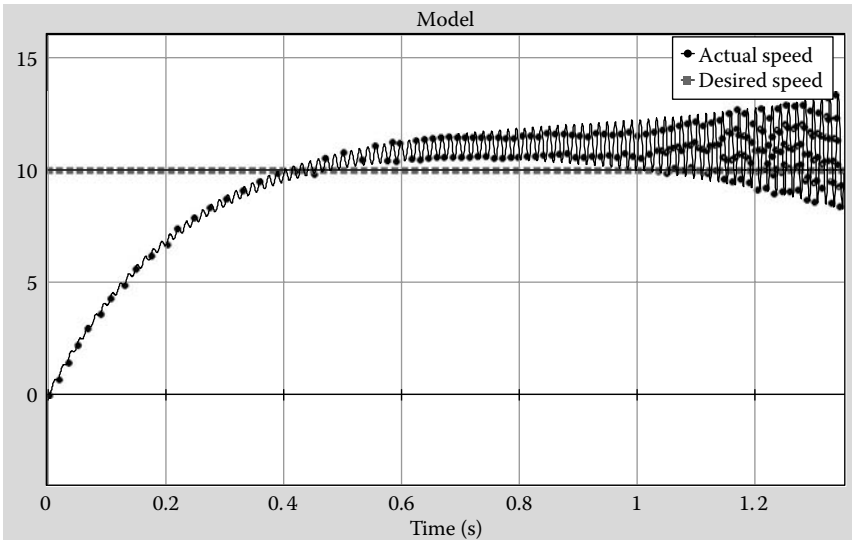


FIGURE 11.32
System response, speed of mass M2.

second mass becomes unstable. In this particular instance, no matter how the control parameters are adjusted, this system cannot be stabilized. This system needs to have a damping along with the spring to make it stable and controllable. When a damper (with a value of 3 units) is added along with the spring inbetween the two masses, the bond graph representation changes (Figure 11.33) and system response (Figure 11.34) shows how the system has stabilized.

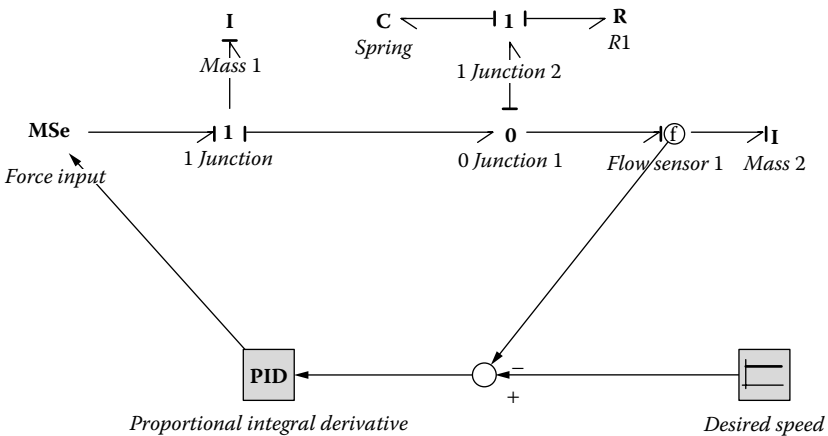


FIGURE 11.33
Modified bond graph with added damping.

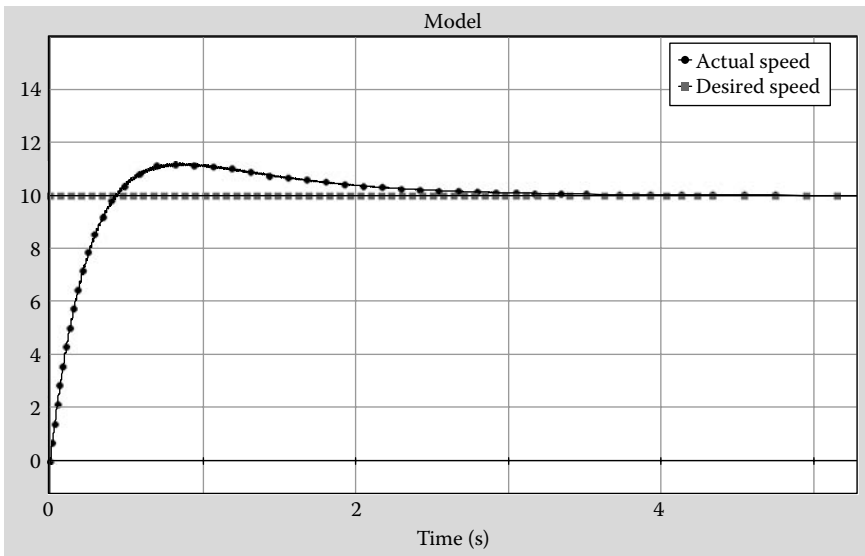


FIGURE 11.34
System response with modified model.

11.3 Nonlinear Control Examples

This next example is a well-known nonlinear control problem of the inverted pendulum.

An inverted pendulum consists of a thin rod attached at its bottom to a moving cart. The cart is capable of moving on a horizontal rail (or some other surface) by the use of motors to control the wheel. The system has to maintain the rod in a vertical position as the cart moves. A simple demonstration of this system can be carried out by trying to balance a long stick (e.g., a ruler) on one's palm. One can then easily see that the palm needs to move horizontally, back and forth, to keep the ruler balanced.

The dynamics of an inverted pendulum are used in many technologies. This concept is used to stabilize the behavior of a rocket during launch. One new technology which has these dynamics and is becoming popular in airports and tourist areas is a Segway (Figure 11.35). A Segway is a self-balancing personal transportation device. It uses a LeanSteer technology, which is basically controlling the 2-wheel device in

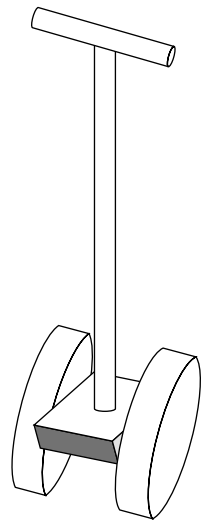


FIGURE 11.35
Segway scooter schematic.

response to the body's natural inclination to lean in the direction the user wants to travel. Microcontrollers and motors in the base keep the Segway upright at all times. Users lean forward to go forward, backward to move backwards, and turn by leaning left and right.

The overall model of an inverted pendulum setup consists of three main components/systems, as shown in Figure 11.36. The first component is the actual cart with the pendulum. The second is a DC motor to control the wheel of the cart. And the third is a controller to maintain the rod in a vertical position by controlling the speed of the cart.

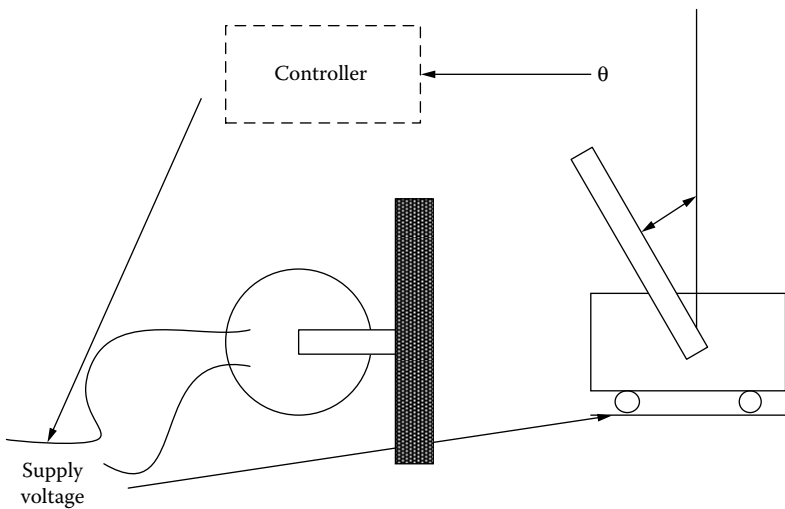


FIGURE 11.36

Inverted pendulum with motor and controls.

11.3.1 Inverted Pendulum

Figure 11.37 is a diagram of the inverted pendulum that will aid in the explanation of the system and its model derivation. The figure shows two important locations of interest, the pendulum's center of mass and the point where the pendulum is attached to the cart. Their coordinates are shown on the figure as well, measured from a ground-fixed Cartesian system.

The relationship between the velocities at different points in the system can be used to develop the bond graph representation of the system. Let us first consider the movement of the cart. The cart moves horizontally within the plane and is driven by input from the motor. Hence, the cart only has a velocity in the horizontal direction. As a result, the point of attachment between the cart and the vertical bar has the same horizontal

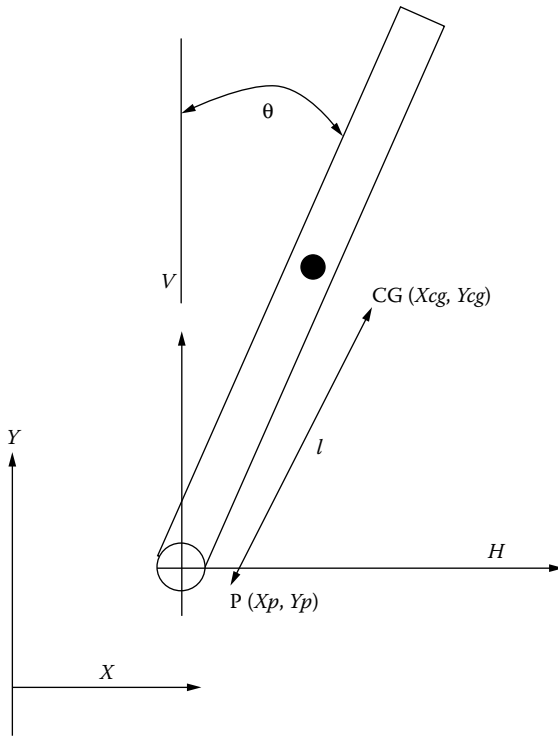


FIGURE 11.37
Equation of motion diagram.

velocity as the cart. But the vertical rod (the pendulum) will have an angular motion about the point where it is pinned to the cart. Therefore, the center of gravity of the pendulum has both a horizontal and vertical velocity. The horizontal component is a sum of the horizontal velocity at the pinned end as well as a trigonometric function of the angular rotation. The vertical component is a function of only the angular rotation. Equation 11.5 shows these relationships.

$$\begin{aligned}\dot{Y}_{cg} &= -l\dot{\theta} \sin \theta \\ \dot{X}_{cg} &= \dot{X}_p + l\dot{\theta} \cos \theta\end{aligned}\quad (11.5)$$

According to these equations of motion and analyzing the inverted pendulum, the bond graph of the system is produced as shown in Figure 11.38. Following the approach taken by Gawthrop and Balance (web document), the bond graph for the inverted pendulum is developed. The different velocity parameters associated with each bond are shown on the bond graph.

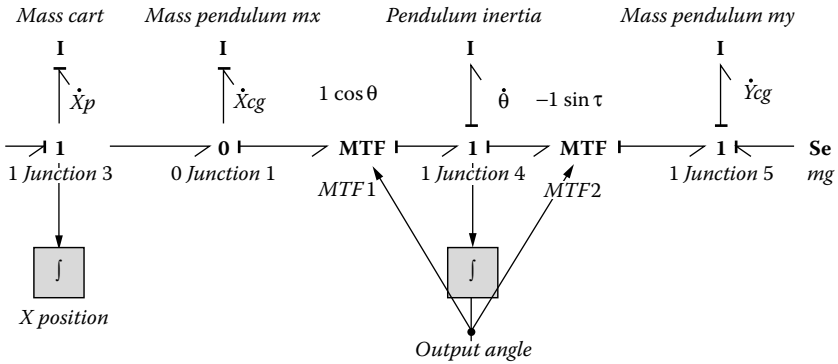


FIGURE 11.38

Bond graph, inverted pendulum only.

The integral of the output from the first 1 junction produces X , which is the cart position. The mass of the pendulum is included twice, once for the horizontal direction motion and once for the vertical direction motion. The SE shown in the graph is gravity, and it is represented as a negative number in the parameter. The equations of the modulated transformers were modified as:

MTF1

$$\begin{aligned} p1.e &= l * \cos(r) * p2.e; \\ p2.f &= l * \cos(r) * p1.f; \end{aligned} \quad (11.6)$$

MTF2

$$\begin{aligned} p1.e &= -l * \sin(r) * p2.e; \\ p2.f &= -l * \sin(r) * p1.f; \end{aligned} \quad (11.7)$$

Therefore, with all these combinations, the integral of the output of the second 1 junction comes out to be the angle of the rod. Note that 0° represents the rod at exactly a vertical position, while 90° (or 1.57 radians) represents the rod exactly in the horizontal position.

The relevant equations for this dynamic problem are discussed as follows. The variables and parameters in the system are

X_{cg} = X coordinate of center of gravity

\dot{X}_{cg} = First derivative of X_{cg}

\ddot{X}_{cg} = Second derivative of X_{cg}

Y_{cg} = Y coordinates of center of gravity

\dot{Y}_{cg} = First derivative of Y_{cg}

\ddot{Y}_{cg} = Second derivative of Y_{cg}

X_p = X coordinate of pivot point

\dot{X}_p = First derivative of X_p

\ddot{X}_p = Second derivative of X_p

Y_p = Y coordinates of pivot point

\dot{Y}_p = First derivative of Y_p

\ddot{Y}_p = Second derivative of Y_p

H = Force in Horizontal direction

V = Force in Vertical direction

l = 1/2 length of pendulum

Summing the forces in the free body diagram of the cart in the horizontal (x direction), and neglecting any friction, Equation 11.8 is retrieved. Note that the friction of the cart is neglected.

$$M\ddot{X} + H = F \quad (11.8)$$

Summing of the pendulum in the horizontal (x direction), Equation 11.9 is derived (Carnegie Mellon site, Deley site).

$$H = m\ddot{X}_p + ml\ddot{\theta}\cos\theta - ml\dot{\theta}^2\sin\theta \quad (11.9)$$

Summing the forces in the vertical (y direction), Equation 11.10 is derived.

$$V = -ml\ddot{\theta}\sin\theta - ml\dot{\theta}^2\cos\theta + mg \quad (11.10)$$

Note that the equations of motion could also be derived using the Lagrangian method, where the classical mechanics is taken to be the difference between the kinetic energy and the potential energy. The following equation is derived:

$$L = \frac{1}{2}(M+m)\dot{x}^2 + ml\dot{x}\dot{\theta}\cos\theta + \frac{1}{2}ml^2\dot{\theta}^2 - mgl\cos\theta \quad (11.11)$$

The equations of motions are

$$\begin{aligned} \frac{d}{dt} \frac{\partial L}{\partial \dot{x}} - \frac{\partial L}{\partial x} &= F \\ \frac{d}{dt} \frac{\partial L}{\partial \dot{\theta}} - \frac{\partial L}{\partial \theta} &= 0 \end{aligned} \quad (11.12)$$

In either case, the two equations of motion for the inverted pendulum are as follows:

$$(M+m)\ddot{X}_p + ml\ddot{\theta}\cos\theta - ml\dot{\theta}^2\sin\theta = F \quad (11.13)$$

$$(I + ml^2)\ddot{\theta} - mgl\sin\theta = -ml\ddot{X}_p\cos\theta \quad (11.14)$$

These equations of motion are nonlinear. In the simulation, we will use a PID controller to control the system, making the angle be around 0° .

11.3.2 Motor

A DC motor is simulated to control the wheels of the cart. Figure 11.39 shows a motor circuit, which consists of armature inductance and resistance connected to a motor powered by a voltage source (as discussed in the chapter on actuators). The motor output is connected to a rotational

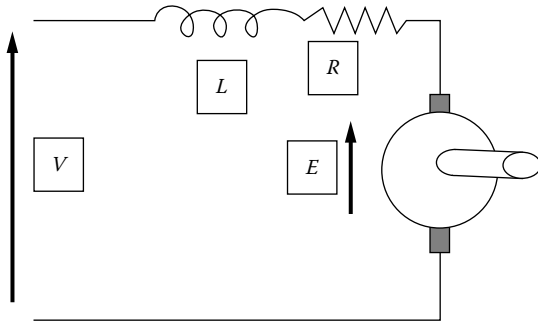


FIGURE 11.39
DC motor circuit.

moment of inertia and may have a rotational bearing resistance. The bond graph is shown in Figure 11.40.

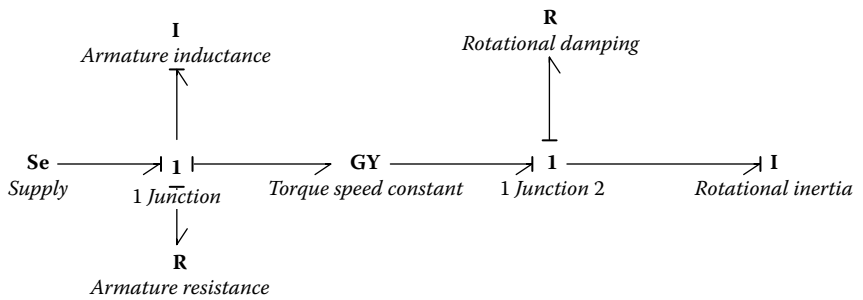


FIGURE 11.40
DC motor bond graph.

11.3.3 Controller

The type of controller used for controlling the inverted pendulum is a PID controller.

The control equation as discussed earlier is

$$\text{Control Signal} = K_p (\text{error} + \frac{1}{T_i} \int (\text{error})dt + T_d \frac{d(\text{error})}{dt}); \quad (11.15)$$

In the current simulation exercise after some initial trials and tuning, the parameters for the PID controller are

K_p	Proportional	100,000
T_i	Integral	100
T_d	Derivative	0.001

Following are some of the parameters used for the simulation:

M	mass of the cart	0.5 kg
m	Mass of the pendulum	0.2 kg
l	length to pendulum	0.3 m
i	Inertia	0.006 kg*m ²
mg	Source of gravity	-9.8 *0.2 = -1.96

The parameters chosen for the DC Motor are

V	Voltage Source	modulated
Ra	Armature Resistance	0.8 Ω
Ia	Armature Inductance	0.001 H
B	Rotational Damping	0.0066 N.m.s
J	Rotational Inertia	0.01 kg*m ²
T	Torque Constant	0.3

Figure 11.41 illustrates the open loop bond graph, which consists of the DC motor and the inverted pendulum. The source of effort here is not modulated; a value of 120v was chosen. Note there are two transformers that were not discussed earlier and that represent the gear ratio and the driven wheel, respectively. These values were assumed.

TF1	Gear ratio	N1/N2	0.5
TF	Driven Wheel	1/r	10

As shown from the results of the open loop system simulating the output angle of the pendulum in Figure 11.42, the system is not balanced, so the pendulum drops 90°, which is shown in the plot in radians.

Figure 11.43 illustrates the model of the system, which includes the PID controller. The controller consists of a desired angle input (0° for this case) subtracted from the actual output angle. The difference of the two is fed into a PID controller, which is fed back to the input of the system as a modulated source.

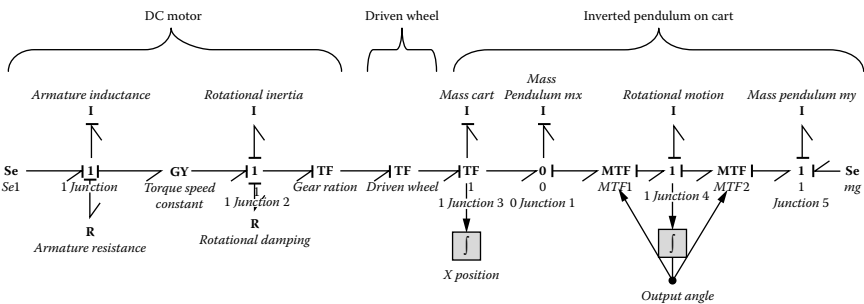


FIGURE 11.41
Open loop system.

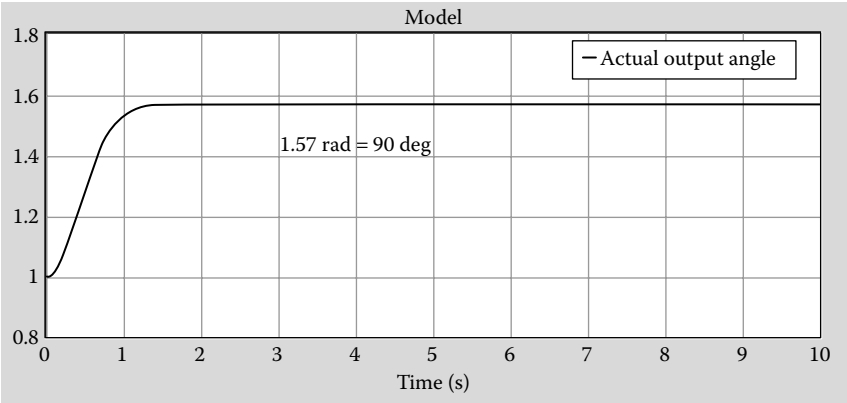


FIGURE 11.42
Simulation of the open loop system.

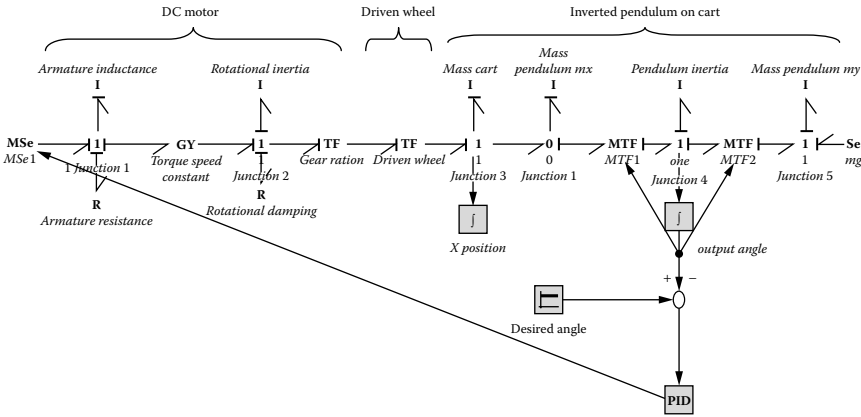


FIGURE 11.43
Closed loop system.

Initially, following values for the control parameters were chosen:

K_p	10,000
T_i	100
T_d	0.001

Figure 11.44 shows the results of the output angle compared to the desired angle according to different values for K_p . The pendulum starts

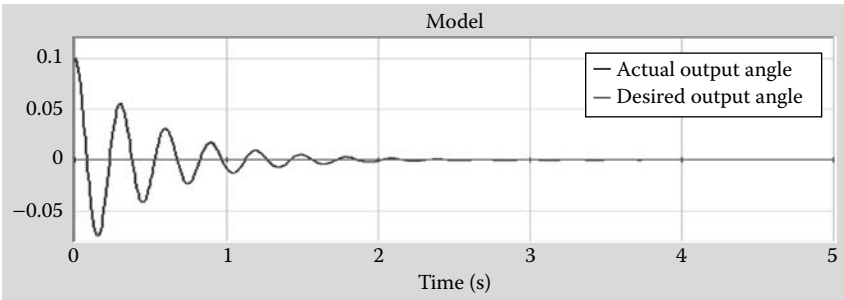


FIGURE 11.44

Closed loop output angle, $K_p = 10,000$.

unstable and eventually stabilizes in about 3sec, which is too long for the angle to stabilize. With K_p increased to 100,000, the angle reaches 0 in less than 0.4sec (Figure 11.45). This is good; however, it can get better.

Increasing K_p to 1,000,000, the angle reaches 0 in less than 0.05sec (Figure 11.46). This is an even better result. As you can see, the angle does not even fluctuate much. Now that we have looked at the output angle, let's look at the cart position. It is expected that the cart position maintains stability when the desired angle is reached.

Looking at the results of Figures 11.47 and 11.48, after the angle becomes stable at around 0, the cart still has a small velocity, and, therefore, the x distance keeps slowly changing around 0.33 m.

As shown in Figures 11.49 and 11.50, velocity increases and then decreases until the final position is reached. The higher the K_p , the less fluctuation in velocity. The time at which velocity reaches 0 is exactly the time when the position is stabilized. Note that the initial disturbance in the output angle is done by inputting initial value to the parameter. Initially, the disturbance, which was being simulated, was 0.1 rad = 5.7° (Figure 11.51).

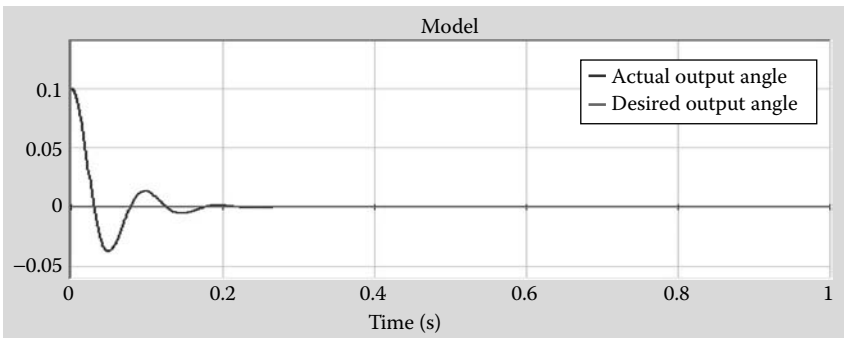


FIGURE 11.45

Closed loop output angle, $K_p = 100,000$.

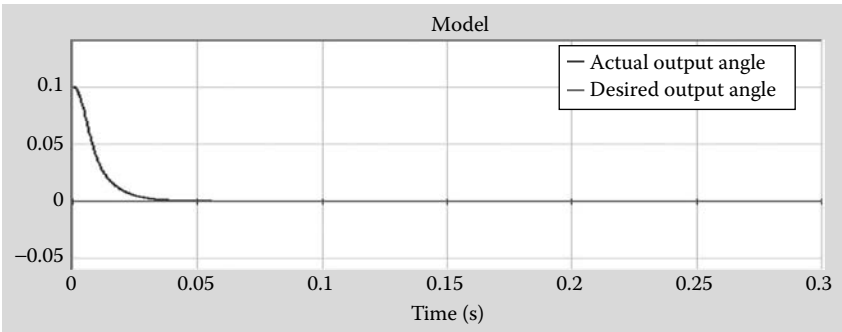


FIGURE 11.46
Closed loop output angle, $K_p = 1,000,000$.

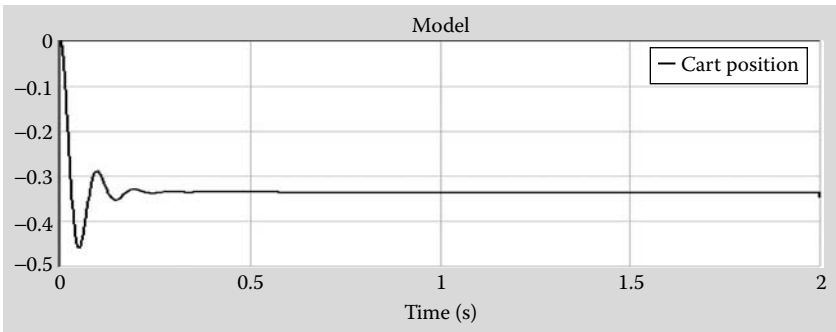


FIGURE 11.47
Closed loop cart position, $K_p = 100,000$.

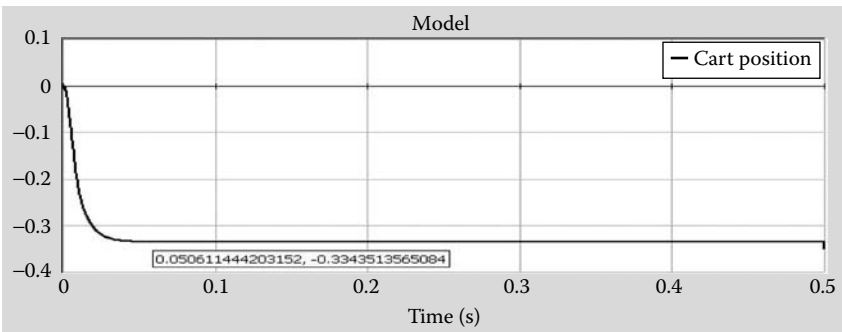


FIGURE 11.48
Closed loop cart position, $K_p = 1,000,000$.

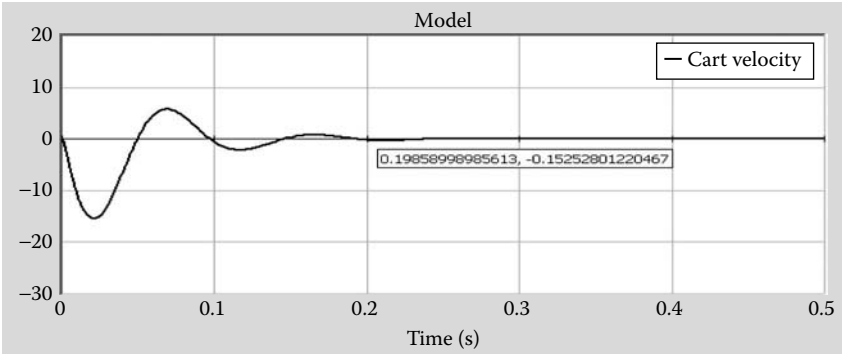


FIGURE 11.49
Closed loop cart velocity, $K_p = 100,000$.

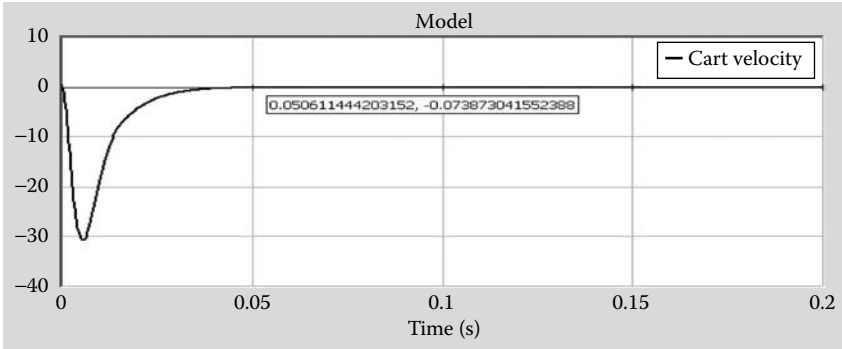


FIGURE 11.50
Closed loop cart velocity, $K_p = 1,000,000$.

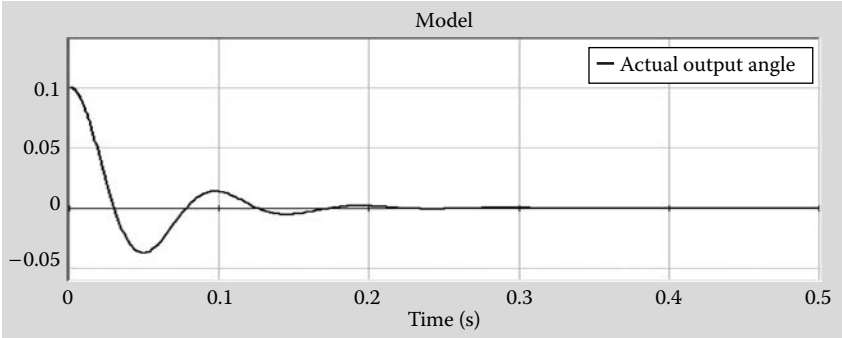


FIGURE 11.51
Closed loop angle output, angle = 5.7° .

As this initial value was increased got closer to 90° , it appears the system became harder to stabilize and took longer to stabilize, as shown in Figure 11.52, where the initial disturbance was $1.57 \text{ rad} = 89.95^\circ$. Obviously, as expected, once this angle crosses 90° , the system no longer works, as proven in Figure 11.53.

Those who are familiar with the inverted pendulum problem know that vertical balancing of the pendulum becomes harder and harder as the length of the pendulum decreases. (One can try this out easily by balancing a long versus a short stick on the palm.) To demonstrate this, the simulation exercise was carried out again by decreasing the length of the pendulum from 0.3 units to 0.01 units, and Figures 11.54 and 11.55 show how the system responds. In both, the cases compare the magnitudes of time, velocity, and distance traveled by the cart with previous results shown to realize the effect of reduction in length on system performance.

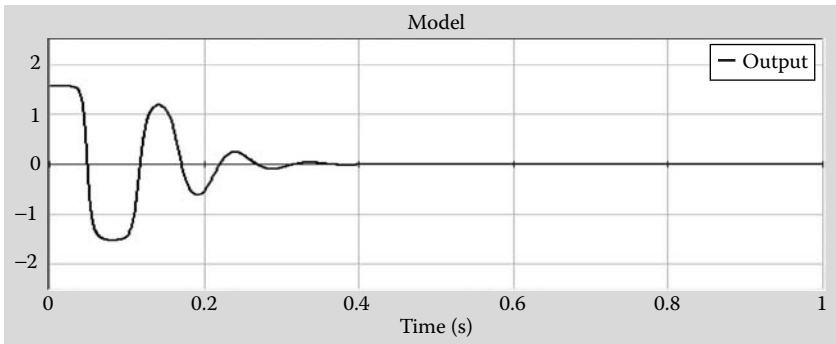


FIGURE 11.52
Closed loop angle output, angle = 89.95° .

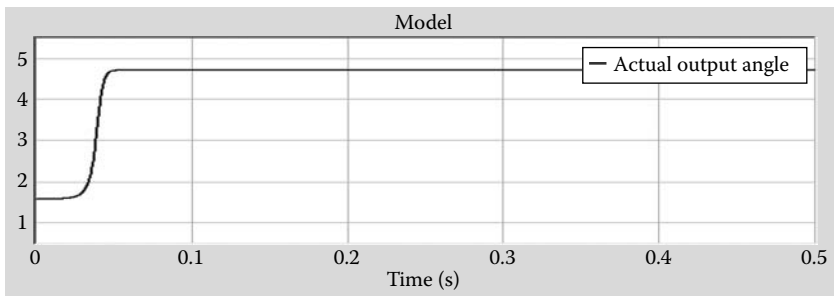


FIGURE 11.53
Closed loop angle output, angle = 90.52° .

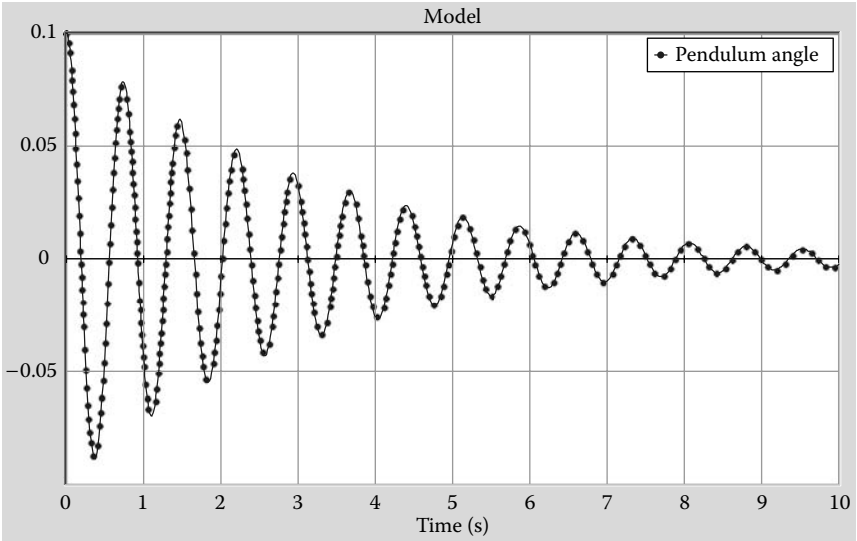


FIGURE 11.54
Balancing the pendulum angle with shortened height.

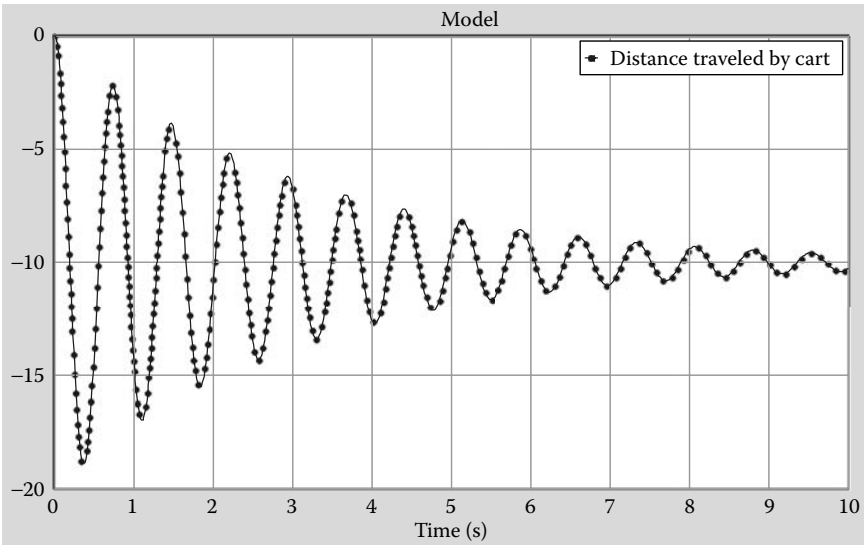


FIGURE 11.55
Distance traveled by cart for shorter pendulum.

11.4 Summary

In this chapter we have discussed the modeling of control loops and control algorithms, along with bond graph models to simulate the behavior of controlled systems. As far as the discussion of control theory is concerned, we have only discussed the basics. Our goal was to introduce the PID control, the control algorithm used 95% of the time, in the context of bond graph based system modeling. Along with linear system control, we have also introduced nonlinear control through the example of balancing an inverted pendulum.

Problems

- 11.1 Figure 10.51 in Chapter 10 shows a rigid pendulum swinging in a plane. Its bond graph model was discussed in that chapter. Consider this to be a representation of a robot arm that is to be moved by a motor. Using the motor input as the source of effort to drive this device, develop a control model for this system so that the angle of rotation can be controlled. Use a PID controller, and tune the parameters to the best performance possible.
- 11.2 Figure P11.1 shows a simple setup to control the height in a tank. Develop a bond graph model for this system.

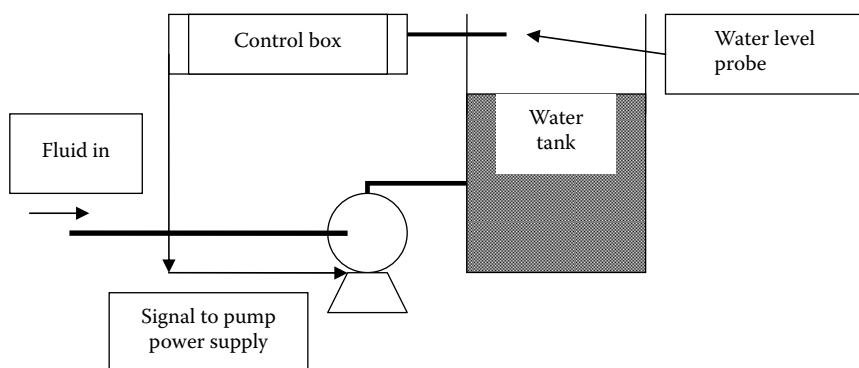


FIGURE P11.1

Figure for Problem 11.2, setup to control the height in a tank.

- 11.3 Figure P11.2 shows a mechanism to lift a weight using the hydraulic plunger. Develop a bond graph model of this system,

along with a control loop that will control the distance the weight moves (model the plunger as a component).

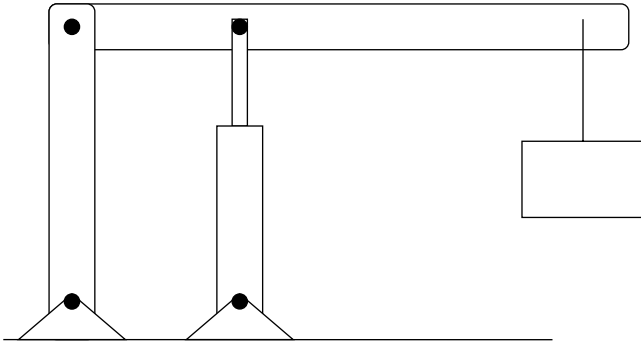


FIGURE P11.2

Figure for Problem 11.3, mechanism to lift a weight.

- 11.4 Figure P11.3 is a schematic that shows a very basic representation of an elevator. Using the bond graph representation of the system (which was discussed in a prior chapter), develop a control system model for this system as an elevator. Remember how the elevator has to work: it will travel between floors rather fast, but it will slow down as it approaches a floor and will not overshoot the floor so that the passengers can get off comfortably. Use simulation results to demonstrate how all of these requirements could be achieved.

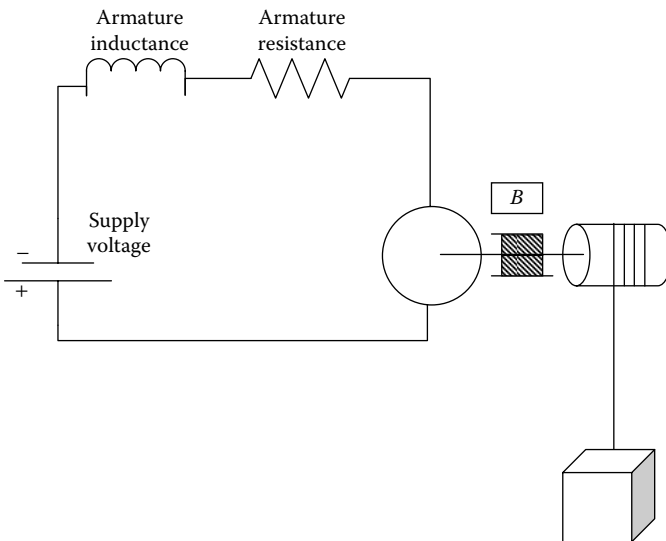


FIGURE P11.3

Figure for Problem 11.4, schematic of an elevator.

12

Other Applications

In the previous chapters we touched on many aspects of bond graph modeling as it applies to the modeling of mechatronic systems. The capability and use of this technique reaches far beyond the topics we have discussed so far. It is not possible to cover everything in one volume, and we did not even dare to do so. Not only has this technique been used in domains that we have not talked about, but it has been combined with other techniques to solve difficult problems. In this chapter we will briefly touch on some of the material that we have not been able to address in any of the earlier discussions. Mostly what we will do is refer to work that is underway in research groups across the world and is being presented in conferences and published in journals. Also, we will discuss a couple of case studies that this author has worked on.

Since the early days of bond graph modeling, researchers have found use of the technique in the domain of thermodynamics and heat transfer. The works of Thoma (1974, 2000), Schnakenberg (1981), Thoma and Bouamam (1999), and Thoma and Mocellin (2006) are of note in this particular area. Anyone seeking to apply this technique in the thermal sciences domain should start with one of these texts.

In more recent times, bond graph based modeling has found a lot of applications in biological sciences, including biomechanics and biofluidics. Pop et al. (2003), Wojcik (2003), Mukherjee et al. (2003), and others have used the technique successfully and modeled the walking motion and musculoskeletal interactions in humans and have also extended that technique to the modeling of walking robots. Modeling of walking is a nontrivial problem involving inverse dynamics. The concepts of inverse dynamics have been studied by many researchers both in the context of human gait or otherwise, and the bond graph methodology in inverse dynamics has been used by Gawthrop (2000) and others.

Bond graph methodology has found applications in the modeling of hand prosthesis (Vaz and Shinichi, 2004, 2007) and outer hair cell active force generation (Wangcharoenrung and Longoria, 1999). Fakri et al. (2005) used it in the modeling of the behavior of cardiac muscles. A search of relevant publications will reveal many more applications of the bond graph methodology in the field of biological sciences and bioengineering.

Other areas in which bond graph based modeling has been applied (along with other techniques, such as genetic algorithm-based optimization) are system identification, fault diagnosis in engineering systems,

and optimal design and layout of systems. A quick search will reveal a large number of recent publications in this area. There is a large group at Michigan State University working in this area under the leadership of professors Rosenberg and Goodman (Fan et al., 2003, 2007), some French research groups (Samantaray et al., 2008), and others (Mukherjee et al., 2006, Lo et al., 2004). These are truly cutting-edge applications of the technique of bond graph modeling, and a separate volume will be necessary to accommodate some detailed discussion of these topics.

In the next few pages, we have discussed two cases that comprise the use of bond graph methodology to solve specific system modeling problems. These discussions may give the reader some idea of how this technique may be adapted for problems of practical importance.

12.1 Case Study 1: Modeling CNC Feed-Drive System

The feed-drive system (Abdul-Baqi et al., 2005) of a CNC machine is a combination of various electrical and mechanical units. These units can be modeled by dividing them into subunits consisting of a spring (C element), damper (R element), source of effort (Se/MSe element), and source of flow (Sf/MSf element) connected through appropriate bonds. Schematic diagrams of open and closed loop feed-drive systems of a CNC are shown in Figures 12.1 and 12.2.

All the essential components of this system are listed below.

ω_L = angular velocity of the lead screw

ω_m = angular velocity of the motor shaft

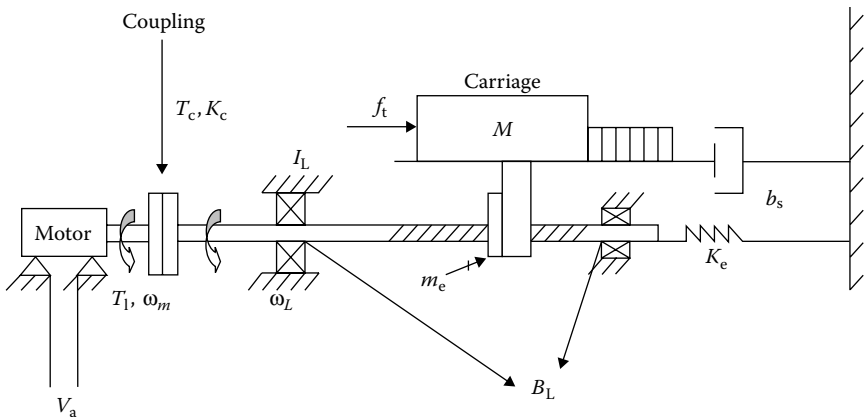
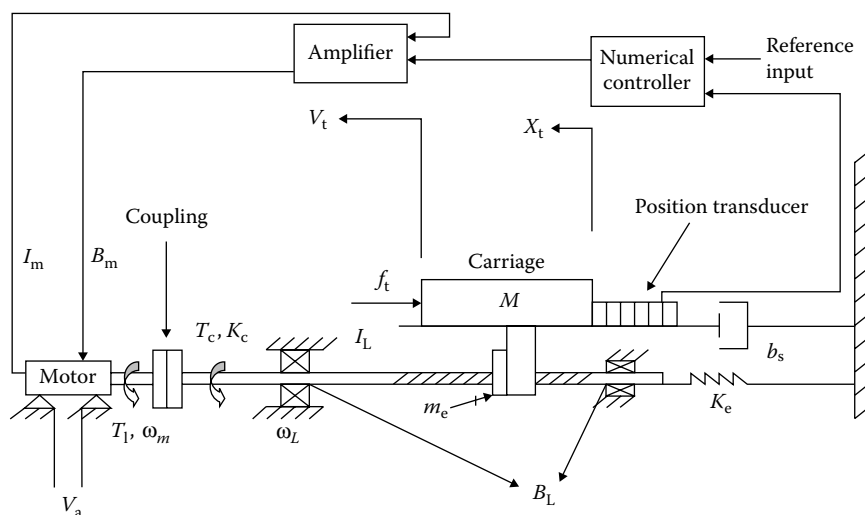


FIGURE 12.1

Schematic diagram of open loop feed drive.

- A_p = cross-section area of the lead screw
 B_L = coefficient of viscous friction of the lead screw
 b_s = coefficient of viscous damping of the slide ways
 T_c = torque of the couple
 K_e = lead screw stiffness
 F_L = axial force of the lead screw
 E_p = modulus of elasticity of the lead screw
 $f(t)$ = axial component of cutting force
 h = lead of the lead screw
 I_L = moment of inertia of a lead screw
 I_m = moment of inertia of a motor
 i_m = armature current
 K_E = gain of position transducer
 K_c = coupling stiffness
 K_p = position loop gain
 K_v = velocity loop gain
 K_m = voltage constant of motor
 L = inductance of the motor armature
 L_i = length of the portion of lead screw between the support and the tool table
 M = mass of the table
 m_e = equivalent mass of the lead screw
 m_p = total mass of the lead screw
 R = resistance of the motor armature
 E_m = back emf

**FIGURE 12.2**

Schematic diagram of closed loop feed drive.

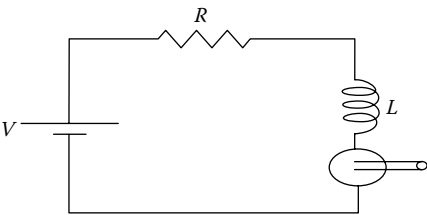


FIGURE 12.4
Electric circuit of a motor.

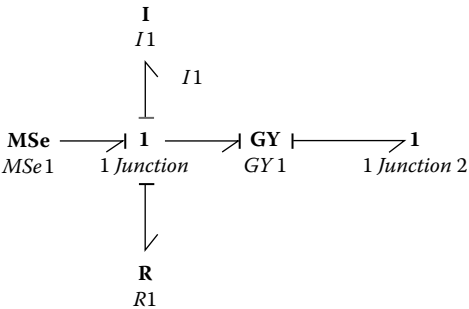


FIGURE 12.5
Bond graph model of electric motor.

Shaft, coupling, and lead screw (Figure 12.6) are connected to the motor to transfer the motion to the work table and can be modeled as shown in Figure 12.7.

Here I_2 is the moment of inertia of motor; R_2 and R_6 are used to model coefficient of viscous friction of lead screws, R_5 is the coefficient of viscous friction of the motor, I_4 is the moment of inertia of the lead screw, and C_2 is used to model the torsional dynamics of the lead screw. In this study

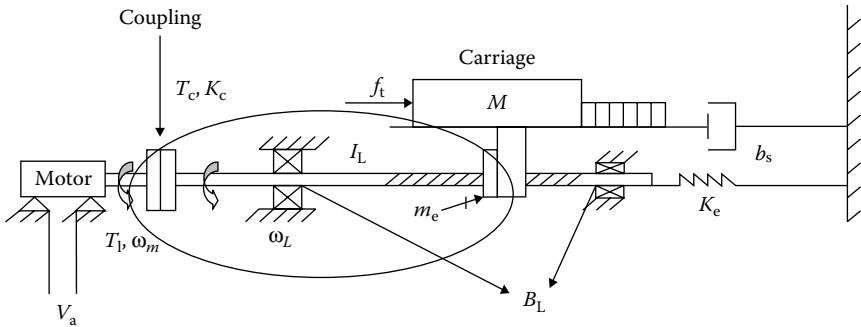


FIGURE 12.6
CNC system schematic; shaft, coupling, and lead screw circled.

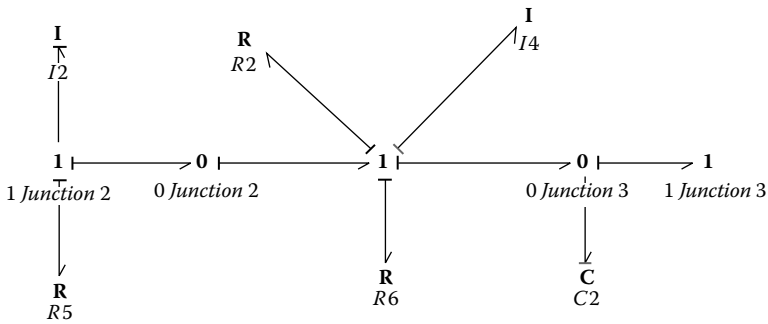


FIGURE 12.7

Bond graph model for shaft, coupling, and lead screw.

(as in many previous ones), torsional dynamics (C2) has been neglected due to its small effect.

The next step is to model the transformation of the rotational motion in the lead screw to the linear motion of the work table (Figure 12.8).

Figure 12.9 shows the bond graph model. Here C2 represents the lead screw stiffness, R4 is coefficient of viscous damping of the slide ways, whereas I3 and I5 are the mass of the table and the equivalent mass of the lead screw, respectively. TF1 and TF2 are transformer factors to transform the rotational motion of the lead screw into linear motion of the table and bearings, respectively.

The first three steps just described in modeling a CNC are same in both open and closed loop systems. The control system in close loop consists of an amplifier, a numerical controller, and position and velocity transducers (Figure 12.10), which can be modeled as shown in Figure 12.11.

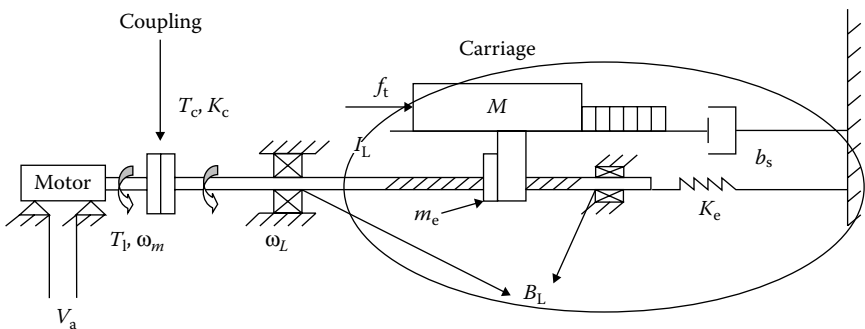


FIGURE 12.8

CNC system schematic; screw, table encircled.

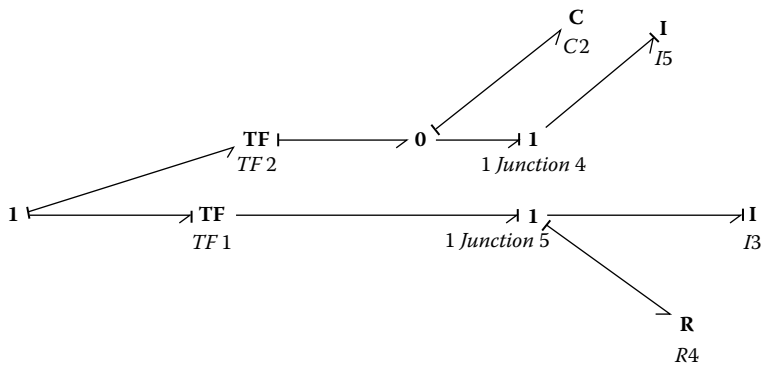


FIGURE 12.9
Bond graph representation of transformation of rotational motion into linear motion.

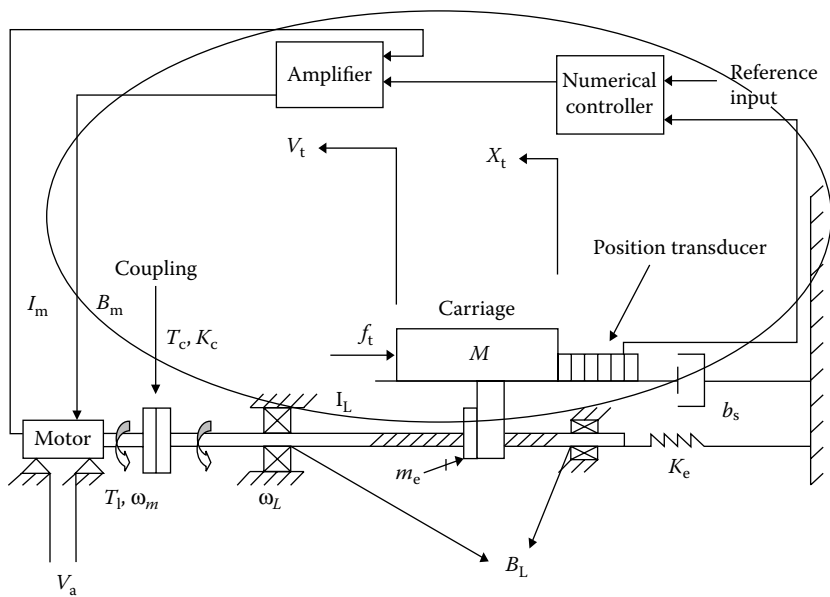


FIGURE 12.10
CNC system schematic; feedback loop encircled.

In Figure 12.11, the position transducer and velocity transducer are modeled as controllers 1 and 2, respectively. The integral function is used to integrate the flow/velocity of table w.r.t. time to obtain the actual displacement of the table. Constant 1 denotes the desired value for position, whereas constant 2 denotes the desired value of the velocity of the table.

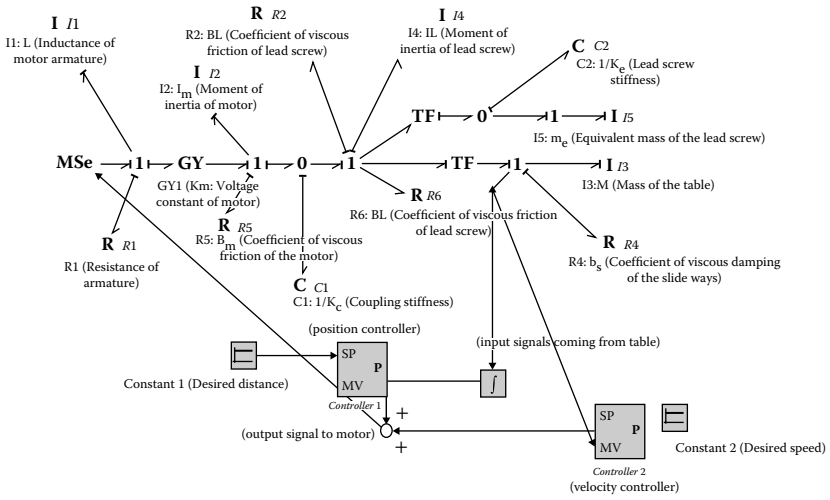


FIGURE 12.13
Bond graph of closed loop system.

12.1.2 Backlash, Stick-Slip, and Cutting Force

12.1.2.1 Backlash

Backlash (Younkin, 1991) plays an important role in the accuracy of the part machined. It can be described as the amount of lost motion due to clearance or slackness when movement is reversed and contact is reestablished. Backlash can be modeled in open and closed loop systems by adding an extra C element connected to the 0 junction between the transformer factor and the slide way. The backlash is modeled in such a way that, during the backlash period, the lead screw stiffness will behave as a very soft spring, and, as soon as this distance is overcome, the stiffness will behave as a hard spring. This behavior of the lead screw is incorporated in the model by writing the appropriate code for the state space equation of the C3 element (extra element added to both bond graphs to model backlash). The backlash behavior is illustrated in Figure 12.14. The extra part added for backlash in the bond graph model is illustrated in Figure 12.15.

Here, the extra C element, that is, C3, is connected to the 0 junction to model backlash between the transformer factor and the lead screw. The expected behavior of backlash in the machine is incorporated through the following lines of codes shown in the following 20Sim model.

```
// 0.001 is backlash distance//
// c1= 1/k1: k1 is soft spring constant & similarly c2 = 1/
// k2: k2 is hard spring constant//
```

Parameters

```
real c1;  
real c2;
```

Equations

```
state = int (p.f);  
if (abs (state) <= 0.001) then  
p.e = state / c1;  
else  
p.e = state/c2;  
end;
```

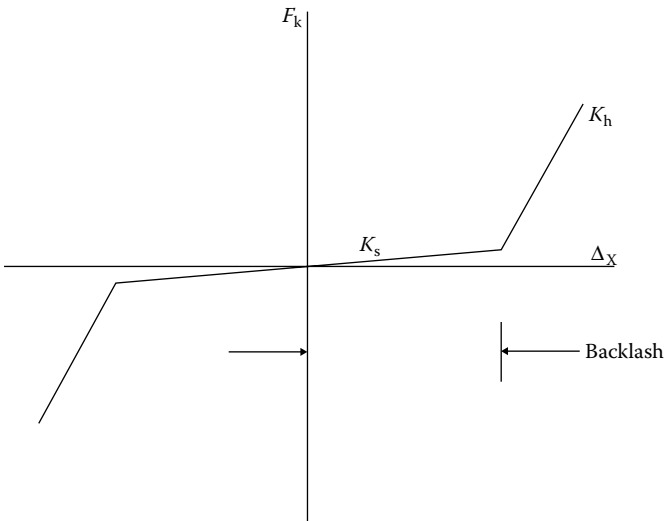


FIGURE 12.14

Behavior of velocity due to backlash.

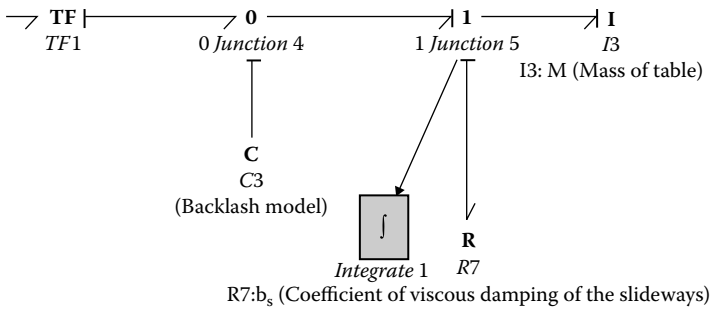


FIGURE 12.15

Backlash model.

12.1.2.2 Stick-Slip Friction

When a machine tool slide is moving, its motion will be jerky and intermittent as the objects slow down during shear and start accelerating after that. The process will continue throughout the operation. When the machine tool slide is not moving, the friction is static friction F_s . As soon as tool slide starts to move, the friction is coulomb friction F_c . These friction forces are not dependent on velocity but are sign dependent (Figure 12.16) on the direction of motion (Karnopp, 1984). The stick-slip friction effect can be modeled in the bond graph by adding an extra damping element, that is, R with the table. The stick-slip friction models for CNC are shown in Figure 12.17.

In Figure 12.17, the $R4$ element is added to model the stick-slip friction between the slide ways and the table. Stick-slip effect can be modeled through the following lines of code:

Parameters

```
real fact; // coulomb frictional force
real r; // ratio of static to coulomb
```

Equations

```
if (abs (p.f) <= 0.01) then
p.e = fact*r*sign (p.f); // equations for static friction
else
p.e = fact*sign (p.f); // equations for coulomb friction
end;
```

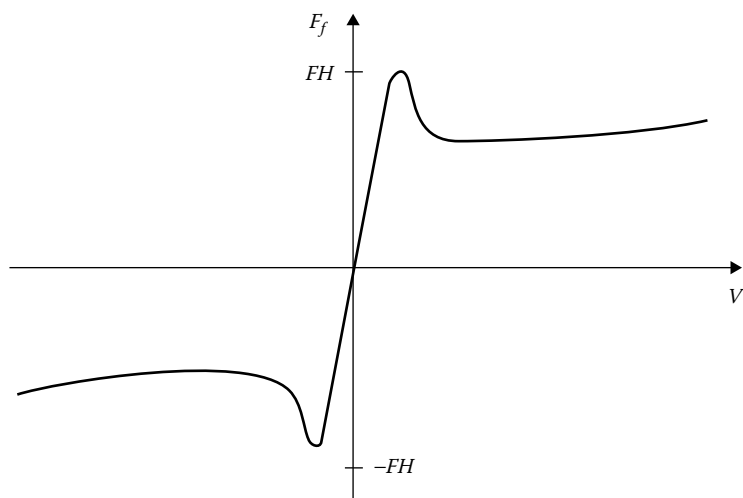


FIGURE 12.16

Behavior of velocity due to stick-slip effect.

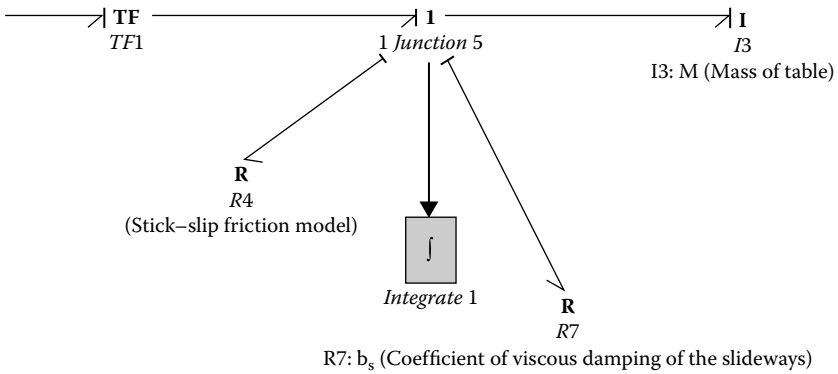


FIGURE 12.17
Stick-slip friction model.

12.1.2.3 Cutting Force Model

Cutting force is an important factor when machining a part. It is generated when material flows against the cutting tool. It applies an extra load or source of effort to the servo system and also contributes unwanted oscillations to the CNC machine. The cutting force can be modeled as a sinusoidal (Ebrahimi et al., 2000) sawtooth wave (Erkorkmaz et al., 2001), and so forth. The cutting force can be added, as shown in Figure 12.18.

According to results in published literature (Erkorkmaz et al., 2001), cutting force signal is a sawtooth wave. A real-time sawtooth signal is generated for cutting force to simulate the feed drive to know the exact behavior of the system. An example of a sawtooth wave is demonstrated in (Erkorkmaz et al., 2001). A sawtooth signal is generated by multiplication of a square wave signal and a saw wave signal, then adding a square wave signal to the result of the multiplication knot at \pm knot to form a sawtooth signal.

In this work, the cutting force signal is fed into the bond graph as an extra source of effort MSe directly to the work table. Cutting force, or Mse , can feed into the model through a 0 junction to which the work table can be connected. This way of modeling will ensure that the cutting force is directly acting on the work table. But, according to the rules of bond graph modeling, this 0 junction can be collapsed into 1 junction because effort will remain the same on both sides of the junction. Hence, the final bond graph model for cutting force is shown in Figure 12.19, and the cutting tool signal is shown in Figure 12.20. Bond graph models of the closed loop feed-drive system with all nonlinear models are shown in Figure 12.21. The model with the feedback control loop was simulated using the feed-drive parameters shown in Figure 12.22. The controller has two parts and controls the speed and distance traveled by the work table. For the sake of simplicity, we used only a P controller. The results from the simulation

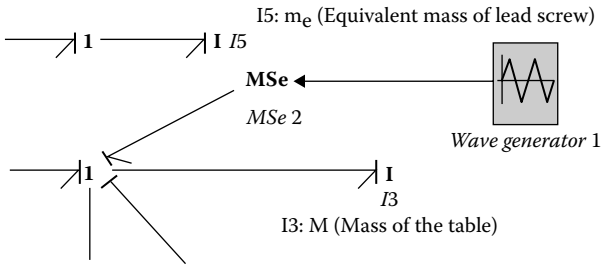


FIGURE 12.18
Cutting force model.

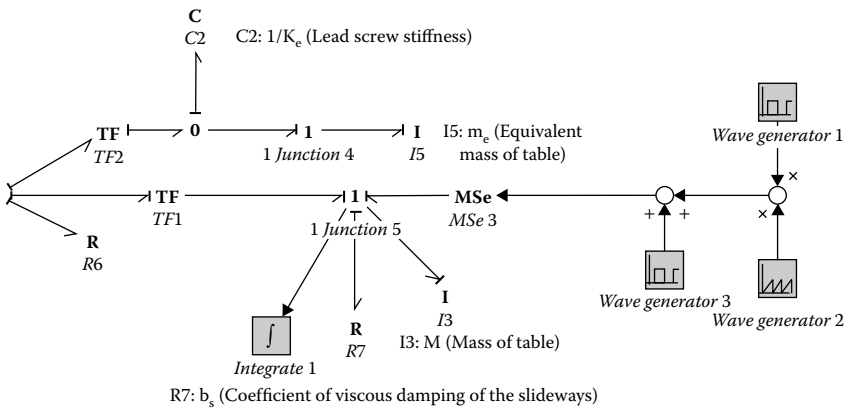


FIGURE 12.19
Bond graph model of sawtooth cutting force in the main bond graph model.

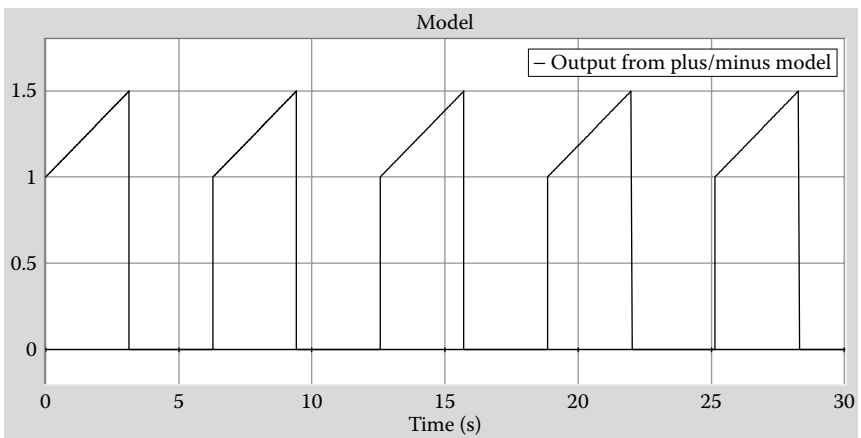
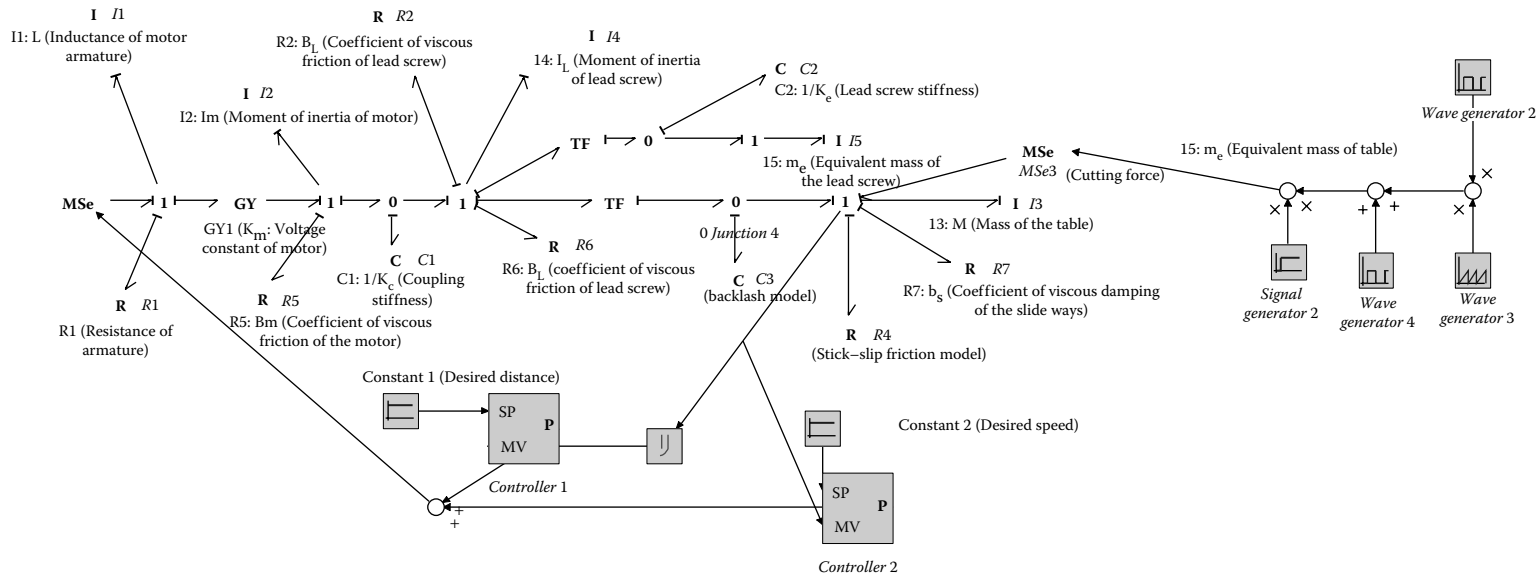


FIGURE 12.20
Sawtooth signal generated in 20Sim.

**FIGURE 12.21**

Complete model including all nonlinearities.

Symbol	Parameter	Unit	Value	Symbol	Parameter	Unit	Value
$C1=1/K_c$	K_c	N/m	2700	I3	M	Kg	77
$C2=1/K_e$	K_e	N/m	1.59×10^8	I4	I_L	$\text{Kg}\cdot\text{m}^2$	7.791×10^{-4}
C3 (backlash)	c1: soft sprin	N/m	10,000	I5	m_e	Kg	5.45
	c2: hard spr		$(1/K_e)$				
R1	R	Ohms	1.09	Controller 1	K_p	(Rad/s)/m	32900
R2	B_L	N.m.s/rad	0.03	Controller 2	K_v	V/(Rad/s)	20
R4 (stick-slip)	r fact	N	$\frac{1}{6.77}$		h	M	6.4×10^{-3}
R5	B_m	N.m.s/rad	2×10^{-5}		TF1	(h/2r)	0.001019108
R6	B_L	N.m.s/rad	0.03		TF2	(h/2r)	0.001019108
R7	s	N.s/m	1×10^4	Kp1	Distance controller factor		32900
I1	L	Henry	0.0252	Kp2	Velocity controller factor		800
I2	I_m	$\text{Kg}\cdot\text{m}^2$	0.0022				

FIGURE 12.22
Parameters used for feed-drive system.

are shown in Figures 12.23 and 12.24. The velocity of the table is supposed to go down to 0 when it has moved by a distance of 0.1 m, and the two plots show that this desired outcome is achieved quite easily. Some jagged changes in velocity are due to the effect of cutting forces. Also, both

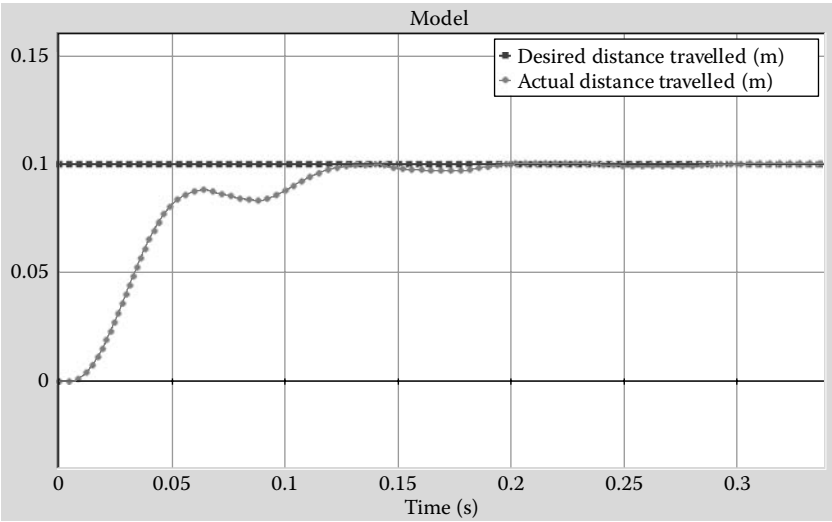
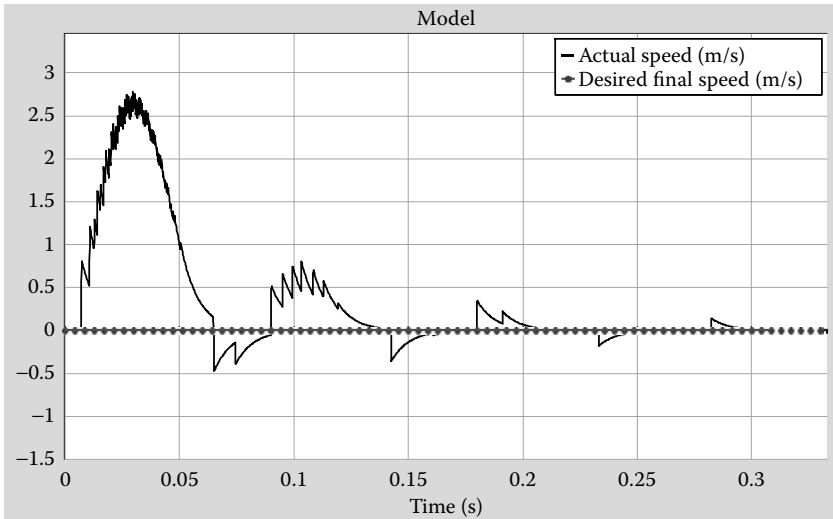


FIGURE 12.23
Comparison of actual distance traveled and desired distance traveled.

**FIGURE 12.24**

Comparison of actual speed and desired speed.

the velocity and distance traveled take some time to change from 0 initial value because of the backlash in the system. With the use of a PID controller, the oscillation of the velocity plot may be better controlled.

12.2 Case Study 2: Developing a System Model for a MEMS Electrothermal Actuator

The most common modes of actuation in MEMS devices are electrostatic, magnetostatic, piezo-electric, and thermal expansion. But the forces produced by electrostatic and magnetostatic tend to be small, and, to achieve large displacements, it is necessary to either apply a large voltage or operate the devices in a resonant mode. On the other hand, piezo-electric and thermal expansion actuators can be configured to produce large forces and large displacements. Unfortunately, piezo-electric materials are not routinely supported in the fabrication processes offered by commercial MEMS foundries. As a result, these limitations many have focused attention on thermally actuated devices for generating large forces and displacements.

Electro-thermo-mechanical (ETM) actuators play an important role in the rapidly growing MEMS area, particularly as a part of more complex MEMS assemblies. An electrothermal MEMS actuator device consists of a

hot arm and a cold arm. The hot arm is narrower than the cold arm, and, thus, the electrical resistance of the hot arm is greater. When the electrical current passes through the device (both hot and cold arms), the hot arm is heated to a higher temperature than the cold arm. This temperature differential causes the hot arm to expand along its length, thus forcing the tip of the device to rotate about the flexure. In this case study, a simple thermal actuator was modeled using 20Sim such that when voltage is given as input, we get deflection as the output. The gyrator factor that is necessary to achieve this is determined through finite element based simulation of a single actuator. Then the same procedure was followed to model a 3×2 actuator array. The voltage input was varied and the deflection output was plotted for varying voltage. The 20Sim results were validated with the results published in the reference papers.

This case study focuses on the deflection on the tip of the actuator with varying voltage input. As depicted in Figure 12.25, the conventional MEMS polysilicon electrothermal microactuator uses resistive (Joule) heating to generate thermal expansion and movement. When current is passed through the actuator from anchor-to-anchor, the larger current density in the narrower hot arm causes it to heat and expand along its length more than the cold arm. Since both arms are joined at their free (released) ends, the difference in length of the two arms causes the microactuator

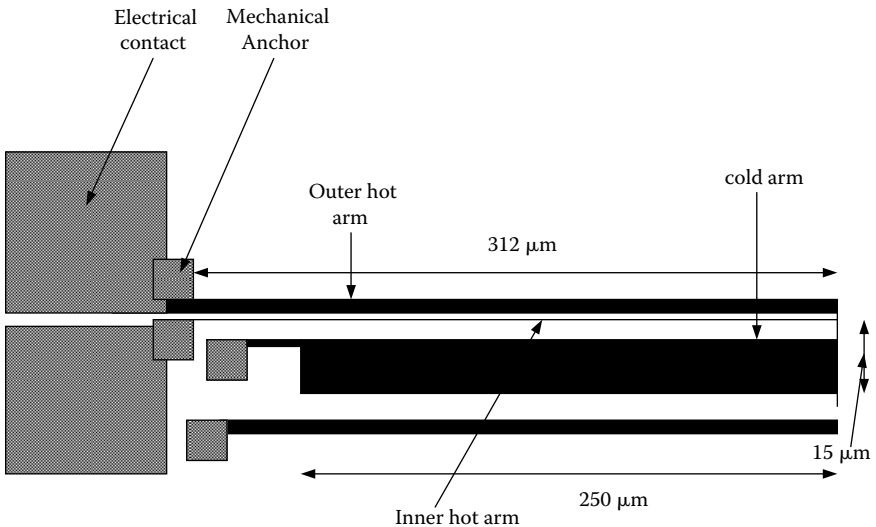


FIGURE 12.25

Double 'hot' arm polysilicon electrothermal microactuator design with an adjacent simple cantilever used to measure deflection force. (Based on Kolesar et al. 2003. *Thin Solid Films* 447/448: 481–488.)

tip to move in an arc-like pattern about the flexure element incorporated at the anchor end of the cold arm. Removing the current from the devices allows it to return it to its equilibrium state.

12.2.1 FEA Analysis

A finite element analysis was done using Abaqus 6.4. The FEA analysis was planned to obtain the exact thermomechanical behavior of the micro-actuator so that the data from the FEA analysis can be used to build a lumped model using bond graphs. The data used in the FEA analysis for designing and analyzing the actuator is given in Tables 12.1 and 12.2.

Using the geometry and material data, the MEMS actuator was designed and meshed as shown in Figure 12.26.

12.2.1.1 Steps Involved in the FEA Analysis

1. The actuator is designed and properties of the material are given as input.
2. A coupled thermoelectric analysis is first done on the model to get the electric potential and nodal temperature output.
3. After the thermoelectric analysis is done, the output data acquired from this analysis is used to run another analysis, specifically the heat transfer analysis.
4. The temperature output in the previous analysis is put in as an input data during the heat transfer analysis.

TABLE 12.1

Geometrical Dimensions of the Double Hot Arm Thermal Actuator

Geometrical Data	Double Hot Arm Actuator (μm)
Length of outer hot arm	321
Width of outer hot arm	2.0
Length of inner hot arm	306
Width of inner hot arm	2.0
Length of the cold arm	241
Width of the cold arm	15
Length of the flexure	62.6
Width of flexure	1.2
Length of gap	2
Thickness of polysilicon	2
Thickness of air	2
Thickness of nitride	0.6

Source: Based on Borovic et al. 2004. In *Ninth Intersociety Conference on Thermal and Thermomechanical Phenomena in Electronic Systems*, Vol. 2, 541–548. New York: IEEE.

TABLE 12.2
Properties for Used Materials at Room Temperature

Material Properties	Value	Unit
Polysilicon Material Properties		
Young’s modulus	160E3	MPa
Poisson’s ratio	0.22	
Thermal expansion coefficient	2.9E-6	K ⁻¹
Thermal conductivity	150E6	Wμm ⁻¹ K ⁻¹
Resistivity	1.21E-11	TΩμm
Nitride Material Properties		
Young’s modulus	300E3	MPa
Poisson’s ratio	0.27	
Thermal expansion coefficient	1.6E-6	K ⁻¹
Thermal conductivity	15E6	Wμm ⁻¹ K ⁻¹

Source: Based on Borovic et al. 2004. In *Ninth Intersociety Conference on Thermal and Thermomechanical Phenomena in Electronic Systems*, Vol. 2, 541–548. New York: IEEE.

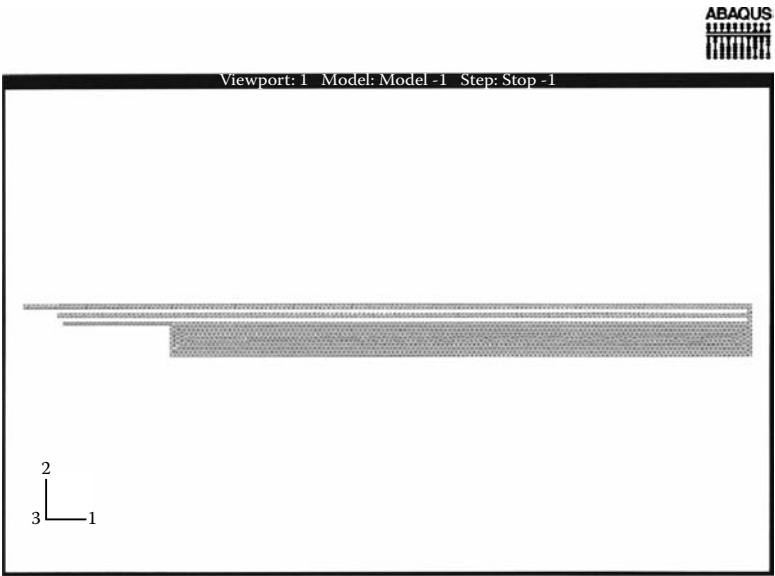


FIGURE 12.26
Abaqus model of a double hot arm ETM MEMS actuator.

- 5. The electrical voltage is the input, and the temperature data is used to get the deflection or deviation of the tip of the actuator as the output.
- 6. This is repeated for every change in voltage and different deflection outputs.

These deflection outputs are used in the 20Sim model to develop lumped parameters of the model.

12.2.2 Simulation of ETM Actuator Using 20Sim

The simulation of the electro–thermo–mechanical MEMS actuator in 20Sim is the core of the project. First, a simple actuator (single ETM actuator) was modeled (using bond graphs) in 20Sim. The results were obtained and then a 3×2 actuator array was modeled. The graphs were plotted for every change in voltage.

A single actuator was modeled using bond graphs in 20Sim as shown in Figure 12.27, and a test run was done to obtain a standard gyrator modulus r by varying the stiffness C and damping R . After the required standard results were obtained, simulation test runs were done for different varying input voltages.

The various elements and the data used in the bond graph are

- A constant wave generator for the voltage input sends the constant data to the modulated source of effort. Voltage varies from 0 to 9 volts.
- MSe, the modulated source of effort, is set to the constant input signal source.
- GY, gyrator to transform the effort coming in (voltage) into flow going out.
- r , gyrator modulus (or the multiplying factor to get the deflection)
 $r = 0.275 \times 10^6$.
- R , damping $= 0.0018 \frac{Ns}{m}$.

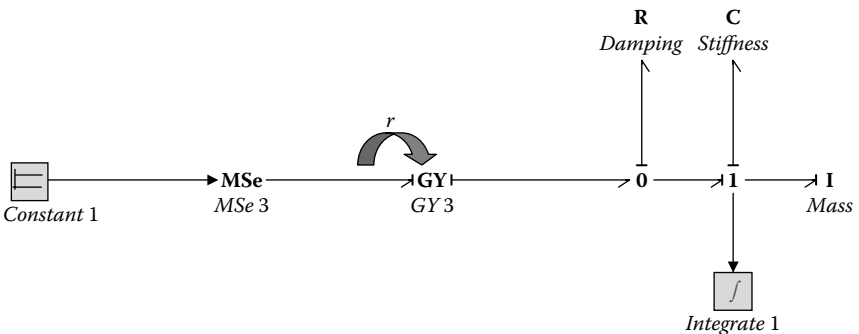


FIGURE 12.27

Bond graph model of a single ETM MEMS actuator modeled in 20Sim.

- C , stiffness = $1.176 \frac{N}{m}$ (for a single actuator).
- I , Moving mass of the element = $1.50 \times 10^{-12} kg$ (single actuator).
- Integrator to get the deflection output in μm .

These parameters were adjusted based on fitting the bond graph result with the FEA results.

Simulation tests were run on the bond graph model shown in Figure 12.27, and the results were obtained. The graphs were plotted for deflection on the y axis with respect to time on x axis. The deflection value at each voltage was noted from the plot, which is the point where the value becomes constant.

The plots obtained from the bond graph model of a single ETM actuator are as shown in Figures 12.28, 12.29, and 12.30 for three different voltage conditions.

Then the same process was repeated for the bond graph model of an array of actuators, which is a combination of a number of actuators arranged in different patterns. An array of actuators representing the 3×2 array is shown in Figure 12.31.

The actuator array in Figure 12.31 is modeled in 20Sim similar to the procedure followed for the single actuator. The array is modeled by adding MSe and GY to the existing model for the single actuator bond graph model. The bond graph model of the 3×2 actuator array is shown in Figure 12.32.

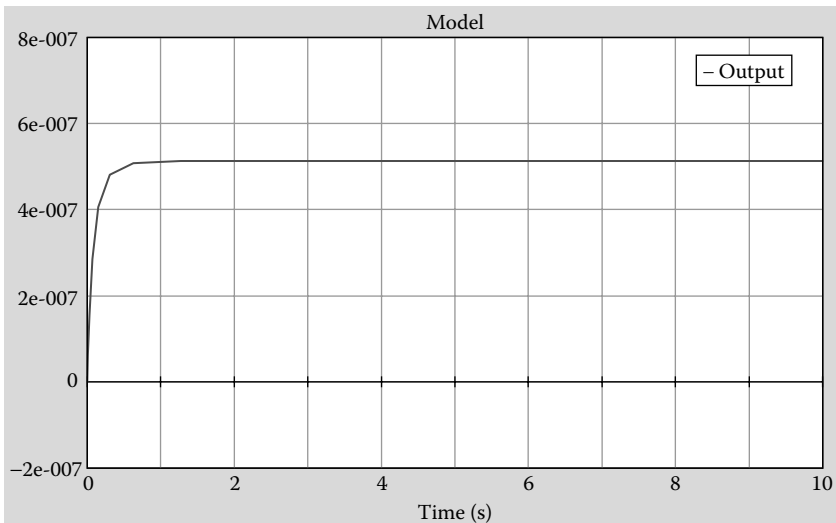


FIGURE 12.28

For input of 2v, deflection is $0.5605 \mu m$.

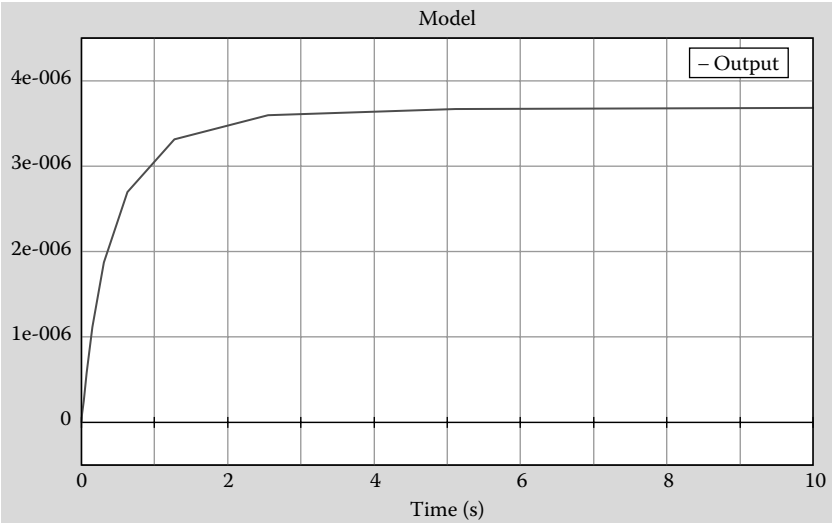


FIGURE 12.29
For input of 6v, deflection is 3.66 μm .

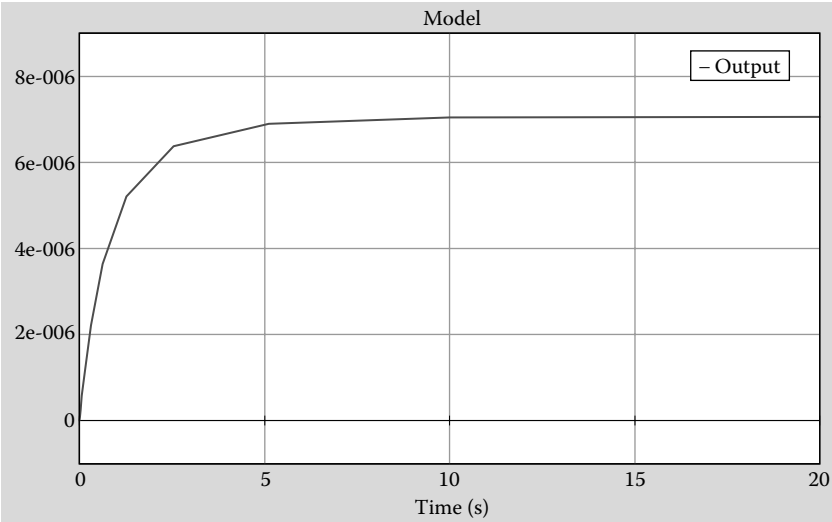


FIGURE 12.30
For input of 8v, deflection is 7.03 μm .

Sample results from simulation of the actuator array are shown in Figures 12.33 and 12.34, and all the results are shown in Table 12.3. It can be observed from the above tabulated results that the values obtained from the 20Sim are in good agreement with the results obtained from the

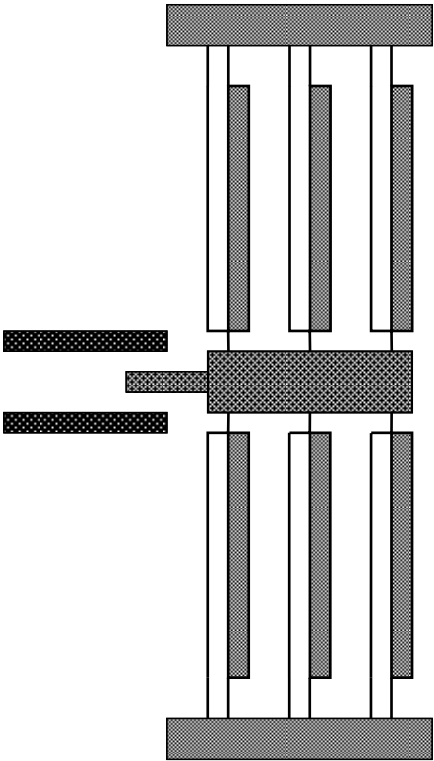


FIGURE 12.31
An integrated ETM device with 3×2 array. (Based on Mankane, N. and Ananthasuresh, G.K. 2000. In *Technical Proceedings of the 2000 International Conference on Modeling and Simulation of Microsystems*. Danville, CA: Nano Science and Technology Institute.)

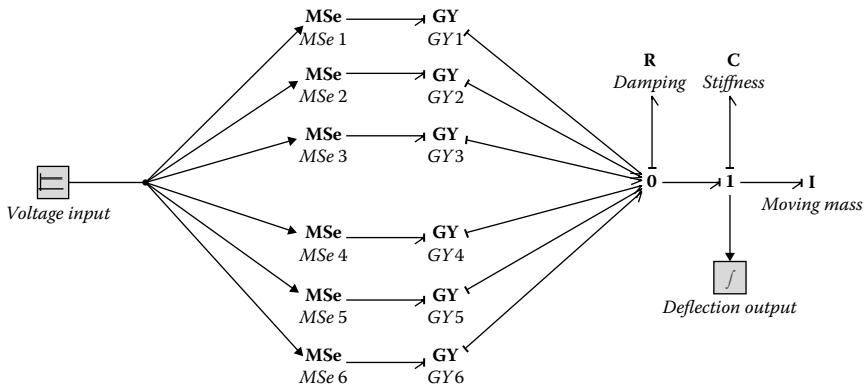


FIGURE 12.32
Bond graph model of a integrated 3×2 ETM actuator array modeled in 20Sim.

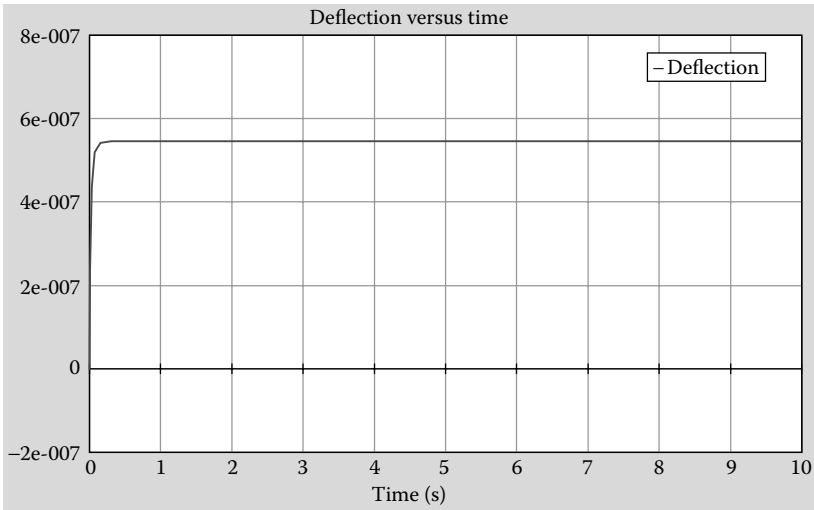


FIGURE 12.33

For input of 2v, deflection is 0.5537 μm .

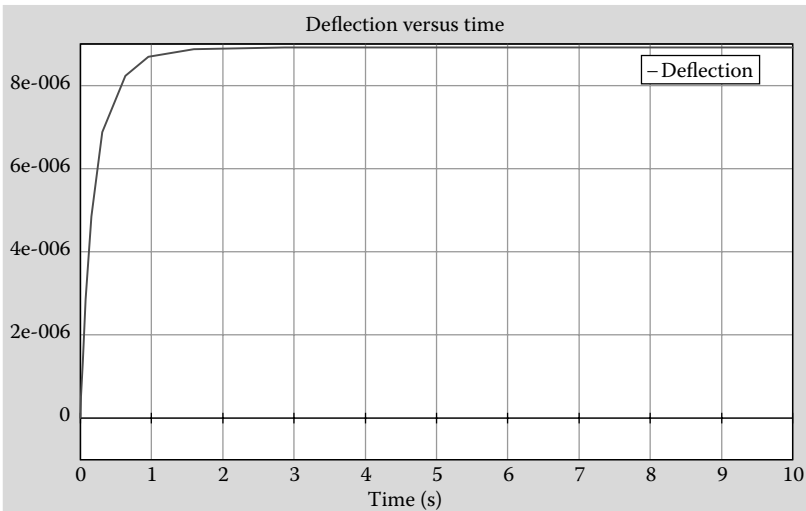


FIGURE 12.34

For input of 9v, deflection is 8.9619 μm .

published work. To understand the validation even better, the numbers from Table 12.3 are plotted in Figure 12.35.

The procedure of modeling and extracting the deflection value by conducting simulation test of the ETM actuator in 20Sim was presented. The procedure has been illustrated by first modeling the actuator separately

TABLE 12.3
Validation of Simulated Data and Experimental Data

Voltage Input (in Volts)	20Sim Results (in μm)	Experimental Results (in μm)
0	0	0
1	0.2338	–
2	0.5537	0.55
3	1.0401	1.1
4	1.7345	1.76
5	2.5079	2.53
6	3.7476	3.74
7	5.1355	5.17
8	7.033	6.93
9	8.9619	8.8

Source: Based on Mankane, N. and Ananthasuresh, G.K. 2000. In *Technical Proceedings of the 2000 International Conference on Modeling and Simulation of Microsystems*. Danville, CA: Nano Science and Technology Institute.

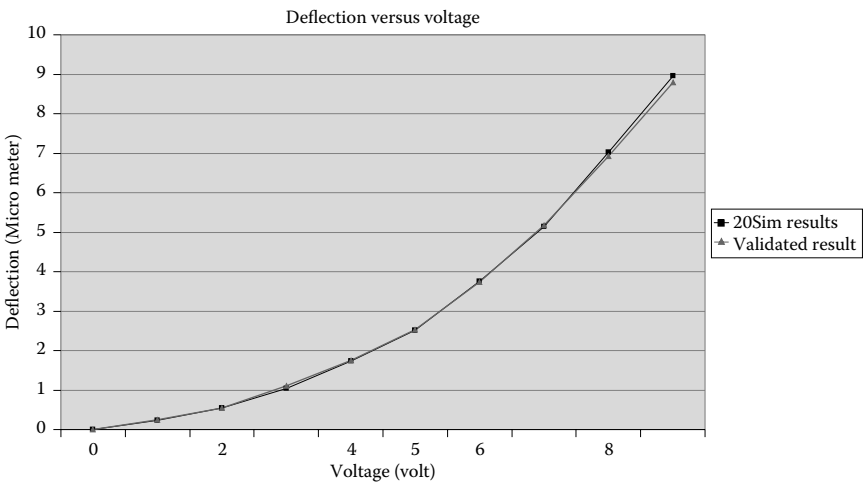


FIGURE 12.35
Deflection at different voltages, simulation, and experiment.

and conducting to obtain the deflection results and then modeling it for a array in a 3×2 pattern. From the validation results, we can conclude that the bond graph model produces good results that were similar to the results published and were used for validation.

This page intentionally left blank

References

- 20Sim, <http://www.20sim.com> (accessed December 13, 2008).
- Abdul-Baqui, O.J., Mehrabi, M., and Yost, S.A. 2005. "Application of Sensitivity Theory to Performance Analysis of Feeddrive System of CNC Machines." In *Transactions of the North American Manufacturing Research Institute of SME*, Vol. 33, Dearborn, MI: Society of Manufacturing Engineers, 297–304.
- Alciatore, D. and Hstand, H.B. 2005. *Mechatronics*. Boston: McGraw-Hill.
- Ashley, S. 1997. Getting a hold on mechatronics. *Mechanical Engineering Magazine (ASME)*, May 1997, 60–63.
- Birching Joel, E. 1999. Two dimensional modeling of a rotary power steering valve (1999-01-0396). Paper presented at the SAE International Congress and Exposition 1999, Detroit, MI, March 1999.
- Bogdan Proca, A. and Keyhani, A. 1998. Identification of power steering system dynamic models. *Mechatronics* 8(3):255–270.
- Borovic, B., Lewis, F.L., Hossain, M. M., Agonafer, D., and Kolesar, E.S. 2004. "Experimentally Verified Procedure for Determining Dynamical Model of the ETM MEMS Structures." In *Ninth Intersociety Conference on Thermal and Thermomechanical Phenomena in Electronic Systems*, Vol. 2, 541–548. New York: IEEE.
- Brown, F.T. 2001. *Engineering System Dynamics: A Unified Graph Centered Approach*. New York: Marcel Dekker.
- Bolton, W. 2004. *Mechatronics: Electronic Control Systems in Mechanical and Electrical Engineering*. Harlow: Longman.
- Busch Vishniac, I.J. 1999. *Electromechanical Sensors and Actuators*. New York: Springer.
- Carnegie Mellon Control Tutorials for MATLAB, <http://www.engin.umich.edu/group/ctm/examples/pend/invpen.html>.
- Cetinkunt, S. 2007. *Mechatronics*. Hoboken, NJ: Wiley.
- Cichy, M. and Konczakowski, M. 2001. Bond graph model of the IC engine as an element of energetic systems. *Mechanism and Machine Theory* 36:683–687.
- Coudert, N., Dauphin-Tanguy, G., and Rault, A. 1993. "Mechatronic Design of an Automatic Gear Box Using Bond Graphs." In *1993 IEEE Systems, Man and Cybernetics Conference Proceedings, Systems Engineering in the Service of Humans*, 2: 216–221. New York: IEEE.
- Cui, Y., Gao, R.X., and Kazmer, D.O. 2005. "Energy Efficiency Analysis of a Self-Powered Pressure Sensor Using Bond Graphs." In *Smart Structures and Materials 2005: Sensors and Smart Structures Technologies for Civil, Mechanical, and Aerospace Systems*, ed. Tomizuka, M. Proceedings of the SPIE 5765: 167–175. Bellingham, WA: SPIE.
- De Silva, C.W. 2005. *Mechatronics: An Integrated Approach*. Boca Raton, FL: CRC Press.
- Deley, D., personal Web site, <http://members.cox.net/srice1/pendulum/page0.htm> (accessed December 13, 2008).

- Diet, J.N., Moszkowicz, P., Sorrentino, D., Bogdan Proca, A., and Keyhani, A. 1998. Identification of power steering system dynamic models. *Mechatronics* 8(3):255–270.
- Dransfield, P. 1981. *Hydraulic Control Systems-Design and Analysis of Their Dynamics*. Berlin: Springer.
- Ebrahimi, M. and Whalley, R. Analysis, modeling and simulation of stiffness in machine tool drives. 2000. *Computers and Industrial Engineering* 38:93–105.
- Erkorkmaz, K. and Altintas Y. 2001. High speed CNC system design. Part II: Modeling and identification of feed drives. *International Journal for Machine Tools and Manufacturing* 41:1487–1509.
- Fan, Z., Seo, K., Hu, J., Rosenberg, R.C., and Goodman, E.D. 2003. “System-Level Synthesis of MEMS via Genetic Programming and Bond Graphs.” In *GECCO 2003*, 2058–2071. Berlin: Springer.
- Fan, Z., Wang, J., Wen M., Goodman, E.D., and Rosenberg, R.C. 2007. “An Evolutionary Approach for Robust Layout Synthesis of MEMS.” In *Studies in Computational Intelligence*, Vol. 51, *Evolutionary Computation in Dynamic and Uncertain Environments*, ed. Yang, S., Ong, Y.-S., and Jin, Y., 519–542. Berlin: Springer.
- Fakri, A. and Rocaries, F. 2005. “Study of Cardiac Muscle Dynamics Utilising Bond Graph Modeling.” In *Proceedings of the 2005 International Conference on Bond Graph Modeling*. San Diego, CA: Society of Modeling and Simulation.
- Felez, R.C.J. and Vera, C. 2000. Deriving simulation models from bond graphs with algebraic loops: The extension to multibond graph systems. *Journal of the Franklin Institute* 337(5):579–600.
- Filippa, M., Mi, C., Shen J., and Stevenson, R. 2005. Modeling of a hybrid electric test cell using bond graphs. *IEEE Transactions of Vehicle Technology* 54(3):837–845.
- Gao, D.W., Mi, C., and Emadi, A. 2007. Modeling and simulation of electric and hybrid vehicles. *Proceedings of the IEEE* 95(4):729–745.
- Gawthrop, P. and Balance, D.J, Virtual actuator control of mechanical systems. <http://www.gawthrop.net/Papers/Publications/csc2005/GawBal05.pdf>.
- Gawthrop, P. and Smith L. 1996. *Metamodelling: Bond Graphs and Dynamic Systems*. Englewood Cliffs, NJ: Prentice-Hall.
- Gawthrop, P. 2000. Physical interpretation of inverse dynamics using bicausal bond graphs. *Journal of the Franklin Institute* 337:743–769.
- Gillespie, T. 1992. *Fundamentals of Vehicle Dynamics*. Warrendale, PA: SAE Publications.
- Granda, J. 1984. “Bond Graph Modeling Solutions of Algebraic Loops and Differential Causality in Mechanical and Electrical Systems.” In *Proceedings IASTED Applied Simulation and Modeling Conference*. San Francisco: ASM.
- Granda, J. and Montgomery, R.C. 2003. “Automated Modeling and Simulation Using the Bond Graph Method for the Aerospace Industry (AIAA 2003-5527).” In *AIAA Modeling and Simulation Technologies Conference and Exhibition*. Reston, VA: AIAA.
- Goldner, R.B., Zerigian, P., and Hull, J.R. 2001. A preliminary study of energy recovery in vehicles by using regenerative magnetic shock absorbers (SAE Paper 2001-01-2071). Paper presented at the government/industry meeting, Washington, DC, May 14–16, 2001.

- Hrovat, D., Asgari, J., and Fodor, M. 2000. Automotive Mechatronic Systems. In *Mechatronic Systems Techniques and Applications*, Vol. 2, *Transportation and Vehicular Systems*. Boca Raton, FL: CRC Press.
- Hsu, T.R. 2001. *MEMS and Microsystems: Design and Manufacture*. Boston: McGraw-Hill.
- Huber, P. and Mills, M. 2005. The End of the M.E.? *Mechanical Engineering Magazine* (ASME), May 2005, 26–29.
- Hubbard, G.A. and Youcef-Toumi, K. 1997. “Modeling and Simulation of a Hybrid-Electric Vehicle Drivetrain.” In *Proceedings of 1997 American Control Conference*, Vol. 1, 636–640. Piscataway, NJ: IEEE.
- Karnopp, D.C. 1983. Alternative bond graph causal patterns and equation formulation for dynamic systems. *Transactions of the ASME Journal of Dynamic Systems, Measurement and Control* 105:58–63.
- Karnopp, D.C. 1976. Bond graphs for vehicle dynamics. *Vehicle Systems Dynamics* 5:171–184.
- Karnopp, D.C. 1984. Computer simulation of stick-slip friction in mechanical dynamic systems. *Journal of Dynamic Systems, Measurement, and Control* 107(1):1083–1138.
- Karnopp, D.C., Margolis, D.L., and Rosenberg, R.C. 2006. *System Dynamics: Modeling and Simulation of Mechatronic Systems*. Hoboken, NJ: Wiley.
- Khemliche, M., Dif, I., Latrache, S., and Ould Bouamama, B. 2004. “Modeling and Analysis of an Active Suspension 1/4 of Vehicle with Bond Graph.” In *First International Symposium of Controls, Communications and Signals*, 811–814. Piscataway, NJ: IEEE.
- Kim, S. and Chun, K. 2002. A gyroscope array with capacitive detection. *Journal of Korean Physical Society* 40(4):595–600.
- Kolesar, E.S., Odom, W.E., Jayachandran, J.A., Ruff, M.D., Ko, S.Y., Howard, J.T., Allen, P.B., Wilken, J.M., Boydston, N.C., Bosch, J.E., Wilks, R.J., and McAllister, J.B. 2003. Design and performance of an electrothermal MEMS microengine capable of bi-directional motion. *Thin Solid Films* 447/448: 481–488.
- Kramer, U. The application of bond-graphs to real-time simulation modelling of vehicle dynamics. Paper presented at the 7th International Conference on Automatic Control and Computer Science, Iasi, Romania, October 26–27, 2001.
- Lo, C.H., Wong, Y.K., and Chow, K.M. 2004. Fusion of qualitative bond graph and genetic algorithms: A fault diagnosis application. *ISA Transactions* 41(4):445–456.
- Louca, L.S., Stein, J.L., and Rideout, D.G. 2001. “Integrated Proper Vehicle Modeling and Simulation Using a Bond Graph Formulation.” In *Proceedings of the 2001 International Conference on Bond Graph Modeling*, Vol. 33. San Diego, CA: Society for Computer Simulation.
- Lobontiu, N. and Garcia, E. 2005. *Mechanics of Microelectromechanical Systems*. New York: Kluwer.
- Margolis, D. 1982. Semi-active heave and pitch control for ground vehicles. *Vehicle System Dynamics* 11:31–42.
- Margolis, D. and Shim T. 2001. A bond graph model incorporating sensors, actuators, and vehicle dynamics for developing controllers for vehicle safety. *Journal of the Franklin Institute* 338:21–34.

- Mankane, N. and Ananthasuresh, G.K. 2000. "Effect of Thermal Boundary Condition and Scaling on Electro-Thermal Compliant Micro Devices." In *Technical Proceedings of the 2000 International Conference on Modeling and Simulation of Microsystems*. Danville, CA: Nano Science and Technology Institute.
- Mukherjee, A. and Karmakar, R. 2000. *Modeling and Simulation of Engineering Systems through Bond Graphs*. New Delhi, India: Narosa International Publishing House.
- Mukherjee, A., Karmakar, R., and Samantaray, A. 2006. *Bond Graph in Modeling, Simulation and Fault Identification*. New Delhi, India: Narosa International Publishing House.
- Mukherjee, A., Pathak, P.M., and Dasgupta, A. 2003. "Self-Balancing Two Legged Walking Robot." In *International Conference on Bond Graph Modeling and Simulation*. San Diego, CA: Society for Modeling and Simulation International.
- Oh, S.W. 2003. The development of an advanced control method for the steer-by-wire system to improve the vehicle maneuverability and stability (2003-01-0578). Paper presented at the SAE 2003 World Congress and Exhibition, Detroit, MI, March 2003.
- Piyabongkarn, D. and Rajamani R. 2002. The development of MEMS gyroscopes for absolute angle measurement. Paper presented at the Proceedings of the American Control Conference, Anchorage, AK, May 8–10, 2002.
- Pelesko, J.A. and Bernstein, D.H. 2003. *Modeling MEMS and NEMS*. Boca Raton, FL: CRC Press.
- Press, W.H., Flanner, B.P., Teukolsky, S.A., and Vetterling W.T. 1992. *Numerical Recipes: The Art of Scientific Computing*. Cambridge, U.K.: Cambridge University Press.
- Pop, C., A. Khajepour, Huisson, J.P., and Patla, A.E. 2003. Experimental/analytical analysis of human locomotion using bondgraphs. *Transactions of ASME* 125:490–498.
- Qiang, L. and Ren, H. 2005. "Modeling and Simulation Study of the Steer by Wire System Using Bond Graphs." In *Conference on Vehicular Electronics and Safety*, 7–11. Piscataway, NJ: IEEE.
- Rizzoni, G. 2004. *Principles and Applications of Electrical Engineering*. Boston, MA: McGraw-Hill.
- Samantaray, A.K. and Ould Bouamama, B. 2008. *Model-Based Process Supervision: A Bond Graph Approach*. Berlin: Springer.
- Schnakenberg, J. 1981. *Thermodynamics Network Analysis of Biological Systems*, 2nd ed. Berlin: Universitext.
- Shetty, D. and Kolk, R. 1997. *Mechatronics System Design*. Boston, MA: PWS Publishing.
- Thoma, J. 2000. *Modeling and Simulation in Thermal and Chemical Engineering: A Bond Graph Approach*. Berlin: Springer.
- Thoma, J. and Mocellin, G. 2006. *Simulation with Entropy in Engineering Thermodynamics*. Berlin: Springer.
- Thoma, J.U. 1974. "Models, Bond Graph and Entropy." In *Physical Structure in Systems Theory*. eds. van Dixhoorn, J.J. and Evans, F.J. New York: Academic Press.
- Thoma, J. and Ould Bouamama, B. 1999. *Modeling and Simulation in Thermal and Chemical Engineering: A Bond Graph Approach*. Berlin: Springer.

- Vaz, A. and Shinichi, H. 2007. A bond graph approach to the analysis of prosthesis for a partially impaired hand. *Journal of Dynamic System, Measurement and Control* 129:105–113.
- Vaz, A. and Shinichi, H. 2004. “Application of Vector Bond Graphs to the Modeling of a Class of Hand Prostheses.” In *7th Biennial ASME Conference on Engineering Systems Design and Analysis*, 19–22. New York: ASME.
- Wangcharoenrungs, C. and Longoria, R.G. 1999. A bond graph model of outer hair cell active force generation. *Simulation Series* 35(2):257–268.
- Wehreim, D. and Misrelates, Z.P. 2006. Reliability based design optimization of dynamic vehicle performance using bond graphs and time dependent models (2006-01-0109). Paper presented at the 2006 SAE World Congress and Exhibition, Detroit, MI, March 2006.
- Wojcik, L. 2003. Modeling of musculoskeletal structure and function using a modular bond graph approach. *Journal of the Franklin Institute* 340(1):63–76.
- Wong, J.Y. 2001. *Theory of Ground Vehicles*. Hoboken, NJ: Wiley.
- Younkin, G.W. 1991. Modeling machine tool feed servo drives using simulation techniques to predict performance. *IEEE Transactions on Industry Applications* 27(2):268–274.

This page intentionally left blank

Bibliography

- AMESIM, <http://www.lmsintl.com/imagine-amesim-platform>.
- Artus, S., Hayat, S., Staroswiecki, M., and Cocquempot, V. 2003. "A Brake Disc's Temperature Estimation Module." In *Proceedings of the Summer Computer Simulation Conference 2003, Montreal, Canada*, ed. Bruzzone, A.G., 608–613. San Diego, CA: Society for Computer Simulation.
- Breedveld, P.C. and Dauphin-Tanguy, G. 1992. *Bond Graphs for Engineers*. Amsterdam: Elsevier.
- CAMP-G Bond Graph Modeling and Simulation Software for MATLAB, <http://www.bondgraph.com> (accessed December 13, 2008).
- High Tech Consultants, Symbols2000, <http://www.htcinfo.com> (accessed December 13, 2008).
- Karnopp, D.C. and Rosenberg, R.C. 1970. Application of bond graph techniques to vehicle drive line dynamics. *Transactions of the ASME Journal of Dynamic Systems, Measurement and Control* 92(2):355–362.
- Karnopp, D.C. and Margolis, D.L. 1984. Adaptive suspension concepts for road vehicles. *Vehicle System Dynamics* 13(3):145–160.
- Louca, L.S. and Stein, J.L. 1999. Energy-based model reduction of linear systems. In *Proceedings of the 1999 International Conference on Bond Graph Modeling and Simulation*. San Francisco: Society of Computer Simulation International.
- The MathWorks, SIMULINK Simulation and Model-Based Design, <http://www.mathworks.com/products/simulink> (accessed December 13, 2008).
- Mera, J.M., Vera, C., Felez, J., and Espirella, J.J. 2003. "Influence of the Roll Axis Consideration in Vehicle Dynamics: Bond Graph Models." In *Proceedings of the International Conference on Bond Graph Modeling and Simulation*. Danville, CA: Nano Science and Technology Institute.
- Ogata, K. 2003. *System Dynamics*. Englewood Cliffs, NJ: Prentice-Hall.
- Parallax, Inc. Basic Stamp II, <http://www.parallax.com>.
- Redfield, R. 2003. "Extreme Mountain Biking Dynamics: Development of a Bond Graph Model." In *Proceedings of the IASTED International Conference Modeling and Simulation*. Alberta, Canada: International Association for Science and Technology for Development.
- Rowell, D. and Wormley, D.N. 1997. *System Dynamics: An Introduction*. Upper Saddle River, NJ: Prentice-Hall.
- Vijaykumar, S. 2003. Analysis of an electric power assisted steering system (2003-01-0586). Paper presented at the 2003 SAE World Congress and Exhibition, Detroit, MI, March 2003.
- Vijaykumar, S. 2002. Application of bond graph technique to the design of passenger car steering system (2002-01-0617). Paper presented at the 2002 SAE World Congress and Exhibition, Detroit, MI, March 2002.
- Yallapragada, N. and Alperin, N. 2003. "Patient's Specific Modeling of the Spinal Canal Hydrodynamics Using Bond Graph Techniques and Magnetic Resonance Imaging." In *Medical Imaging 2003: Physiology and Function: Methods, Systems, and Applications*. eds. Clough, A.V. and Amini, A.A. Proceedings of SPIE, Vol. 5031. Bellingham, WA: SPIE.

This page intentionally left blank

Index

1-port components, 26, 33–35
 1-port capacitor, 28–30
 1-port inductor/inertia, 30–33
 1-port resistor, 27–28
2-port components
 gyrator element, 39–41
 transformer element, 35–39
3-port components, 41
 0 junction, 42–43
 1 junction, 43–45
20Sim model, 10, 211, 451, 462–467

A

Abaqus model, *see* Electro-thermo-mechanical (ETM) actuators
Active dampers, 369–371
Actuators
 categories of, 303
 electrical rotational, 314
 electromagnetic, 303–334
 electro-thermo-mechanical, 458–467
 hydraulic, 336–345
 linear, 336
 linear electromagnetic, *see* Linear electromagnetic actuator
 MEMS, 278
 rotational, 314–332
Adaptive methods, 220–221
Algebraic loops, 162–165
AMESIM, 10
Ampere's law, 243

B

Backlash
 modeling of, 451
 velocity behavior due to, 452
Backward Euler's method, 215–217
Basic Stamp II, 2
Bernoulli's equation, 116, 119
B-H relationship, 245
Bicycle model, 371–374

Black boxes, 223
Bode plot, 199–205, 365–366
 bond graph for, 200
 parameters for, 200
Bond graph, 23–26
 closed loop, 435
 differential causality in,
 159–162
 elements in, 85–105
 full-arrow, 24
 half-arrow, 24
 open loop, 434
 power directions, 46–47
 simplification rules for, 56–62
Bulk modulus, 115
By-conduction method, 314
By-induction method, 315

C

CAMP-G, 10
Capacitance, 233–234
Capacitive (C) elements, 89–90, 117
 differential causality for, 90
 examples of, 31
 integral causality for, 90
Capacitive field elements, 234,
 304, 306
 bond graph of, 235
 with differential causality, 236
 with integral causality, 236
 LVDT used for deriving, 256
 with mixed causality, 236–237
 multiport storage fields, 235
Capacitive field model, 311
Capacitive sensors, 233–242
 bond graph of, 239
 examples, 237–242
 parameter used in
 simulation, 240
 simulation results, 241
Causality, 83–106
 algorithm for assigning, 92–99

differential, *see* Differential causality
 integral, *see* Integral causality
 Causal stroke, 65, 85, 90, 104
 Center of mass
 pitch and heave velocity at, 366
 vertical displacement of, 363
 Closed loop system, 422, 435, 446–451, 454
 CNC feed-drive system, 444–446
 closed loop, 444
 open loop, 445
 parameters used for, 457
 Comb drives, 281
 Common effort junction, 42
 Common flow junction, 43
 Commutator, 315
 Constant load torque, 322
 Controller subsystem, 381
 Control systems
 in close loop, 448
 examples, 422–427
 feedback, 405–406
 feed-forward, 405–406
 Coriolis forces, 282
 Cutting force model, 454–458
 Cylinder pressure data, 399

D

Damping coefficient, 365
 Damping force in active and passive damper, 369
 DC motors, 382; *see also* Motors
 bond graph of, 433
 circuit, 432
 parameters for, 434
 separately excited, 332
 Degrees of freedom (DOF), 358, 361
 Differential causality, 89, 105–106
 in bond graph system, 159–162
 for C element, 90
 for I element, 89
 vs. integral causality, 100–105
 Diodes
 applications of, 134–135
 current profile in, 133
 DOF, *see* Degrees of freedom

Doorbell solenoid, 308, 310
 Double hot arm thermal actuator, 460
 Dynamic pressure, 116

E

Effort junction, 43
 Electrical rotational actuator, 314
 Electrical systems, drawing bond graphs for, 62–69
 Electrical transformer, 37
 Electric braking, 374–377
 bond graph of, 375
 parameters used for simulation, 376
 simulation of, 376
 Electric generator
 experiment, 387–388
 Electric motor
 bond graph model of, 447
 electric circuit of, 447
 Electromagnetic actuators, 303–334
 Electromagnetic circuits, 246
 Electromotive force, 243
 Electronic components, 113, 128
 Electronic control unit (ECU), 382
 Electronic systems, 127
 diodes, 133–135
 operational amplifiers, 128–132
 Electrostriction, 272
 Electro-thermo-mechanical (ETM) actuators
 Abaqus model of double hot arm, 461
 bond graph model of single, 465
 simulation using 20Sim, 462–467
 system model for, 458–467
 Energy dissipating device, 1-port resistor, 27–28
 Energy storage device
 1-port capacitor, 28–30
 1-port inductor/inertia, 30–33
 Energy variables, 20–21
 Engineering systems, 14–15
 components in, 26–46
 subsystems of, 15
 ETM actuators, *see* Electro-thermo-mechanical actuators
 Euler's method, 212
 backward, 215–217

comparison of analytical results
with, 213–214
implicit, 215–217

F

Faraday's law, 243, 315
Ferromagnetic materials, 244
Field elements, *see* Capacitive field elements
Finite element analysis (FEA), 460
First-order differential equation, 178–180
First order systems, 176–180
bond graph of, 177
example, 176
Flow junction, 42
Flow sources, 121
Fluid compliance, 117–118
Fluid inertia, 118
Fluid resistance, 119
Fluids
behavior, 113
bulk modulus, 115
energy conservation, 116
force, pressure, and head, 115
mass conservation, 115
mass density, 114
properties and concepts, 114
Flux density, 268
bond graph of, 269
parameters for simulation, 270
Flux linkage, 21
Formal method
for electrical systems, 65–69
for mechanical systems, 72–73
Four-way control valve, 338, 340
Frequency response, 197, 199
Front wheel subsystem, 380, 382

G

Gauss's law, 243–245
Gear ring, 268
Generalized variables, 20–22
Gravitational forces, 73
Gyrator coefficient, 268
Gyrator elements, 122, 319–320, 446
bond graph of, 39

causal structure of, 246
examples of, 40–41
in hydraulic circuits, 122
in magnetic circuits, 86
Gyrator factors, 40, 256, 261
Gyrator model, 270
Gyroscope, 40
Gyroscopic sensors, MEMS, 281–286
bond graph model of, 284
parameters used for, 284

H

Half car model, 360
bond graph representation of, 361
heave and pitch direction
motion, 361
Hall, Edwin, 266
Hall effect sensors, 266–271
Homogenous equation, 182, 189
Hydraulic actuators, 336–345
Hydraulic circuits, 114
gyrator elements in, 122
transformer elements in, 121
Hydraulic cylinders, 336–337
Hydraulic power steering, 377–378
Hydraulic systems, 45, 342–345
bond graph model of, 117, 122, 343
examples, 123–127
fluid compliance, 117–118
Hydraulic valves, 338–342

I

Inductor (*I*) element, 118
causal structure for, 88
differential causality for, 89
examples of, 33
Integral causality, 88, 105–106
for *C* element, 90
for *I* element, 89
vs. differential causality, 100–105
Integrated ETM actuator array
bond graph model of, 463, 465
simulation of, 464
Inverted pendulum, 427–432
bond graph, 430
controller, 433–440
Inverting amplifier, 131–132

J

- Junction power directions, 147
- Junction structure, simplification rules for, 56–62

K

- Kirchoff's law, 62

L

- Linear actuators, 336
- Linear electromagnetic actuator, 303–314
 - bond graph model of, 305
 - parameters for, 307
- Linear variable differential transformers (LVDTs), 255
 - bond graph of, 256
 - C-field, 256–258
 - circuit for, 255
 - parameter used in simulation, 259
- Lorentz's law, 315
- Low-pass filter
 - bond graph model of, 296
 - circuit for, 295
- LVDTs, *see* Linear variable differential transformers

M

- Magnetic bond graph elements, 249
- Magnetic circuit, 242–247
 - with air gap, 247–249
 - bond graph of, 247–249
 - circuit equations for, 248
 - gyrator elements in, 86
 - with permanent magnet, 249–250
- Magnetic fluxes, 244
- Magnetic sensors
 - magnetic circuits and fields, 242–245
 - with permanent magnet, 260–263
 - simple magnetic circuit, 245–247
- Magnetomotive force, 243, 245, 249
- Mass conservation, 115–116
- Mass density, 114
- Mass elements, 88–89

- Mathematical modeling techniques, 7–10
- MATLAB®, 211
- Mechatronic system
 - autonomous vehicle, 2–3
 - field of, 2
 - flow of information within, 2
- MEMS devices, 227, 277–286
 - actuators, 278
 - comb drives, 281
 - gyroscopic sensors, 281–286
 - microcantilever-based capacitive sensors, 279–281
 - sensors, 277–278
- Microactuation, 278
- Microcantilever-based capacitive sensors, 279–281
- Micro-electro-mechanical system devices, *see* MEMS devices
- Microsuspension, 278
- Modulated source of effort (MSe), 446, 454
- Motor driven system, 18–19
- Motor hoist system, 334
- Motor load, 322–323
- Motors, 314–332
 - parallel wound motor, 323–327
 - permanent magnet DC motor, 316–322
 - separately excited DC motors, 332
 - series wound motor, 327–332
 - shunt wound motor, 323–327
- Motor speed control, 423
- Multipoint systems, 16

N

- Natural frequency, 199
- Nonlinear control examples, 427–440

O

- Ohm's law, 15
- One junction, 43–44
- Open loop bond graph system, 434, 446–451
- Operational amplifiers (op-amps), 128–132

Ordinary differential equations,
techniques for solving,
211–212

P

Parallel junction, 42
Parallel plate capacitor, 233–234
Parallel wound motor, 323–327
Passive dampers, 369
Permanent magnet (PM), 249–250,
260–263, 382
Permanent magnet DC motor, 8, 157,
316–322
 bond graph of, 320
 example of, 332–335
Permeability, 244
Permittivity, 234
PID control, 407, 416–421, 433
Piezo-electric coefficient, 273
Piezo-electric crystals, 272–273
Piezo-electric materials, 271
Piezo-electric sensors, 271–277
Planar rigid body motion, 390, 392
Polysilicon electrothermal
 microactuator, 459
Ports
 1-port system, 16
 2-port system, 16
 in subsystems, 17–18
Position transducer, 449
Positive displacement pumps, 121
Potentiometric sensor, 229
 bond graph of, 229
 parameter used in
 simulation, 230
Power bonds, 24
Power cylinders, 336–337
Power steering model, 377
Power variables, 20
Proportional, integral, and derivative
 control, *see* PID control
Proportional control, 407–410
Proportional derivative (PD) control,
 413–416
Proportional integral (PI) control,
 411–413
Proportional motor speed control, 408
Pumps, 337–338

Q

Quarter car model, 359

R

Real-time sawtooth signal, 454
Resistive (R) elements, 29, 91–92, 119
Resistive sensors, 228–233
Reynold's number, 119
RLC circuit, 24, 62–64, 93–94, 150
Rotational actuators, 314–332
Rotational motion, examples of
 systems in, 79–83
Rotational variable differential
 transformers (RVDTs), 255
Runge–Kutta–Fehlberg method,
 221–222
Runge–Kutta (R–K) methods, 217–219
 fourth order, 218–221, 223
 second order, 218
RVDTs, *see* Rotational variable
 differential transformers

S

SBW, *see* Steer-by-wire system
Second order system, 180
 and bond graph model, 182
 generic homogenous, 186
 response to sinusoidal inputs,
 191–194
 response to step input, 189–191
 using state–space representation,
 194–196
Segway scooter, 427
Seismic sensor, 260
 bond graph of, 261
 parameters used in
 simulation, 262
 simulation results, 263
Seismometer, 288
Sensors
 capacitive, 233–242
 Hall effect, 266–271
 magnetic, 242–247, 260–263
 MEMS gyroscopic, 281–286
 microcantilever-based capacitive,
 279–281

- potentiometric, 229–230
 - resistive, 228–233
 - seismic, 260–263
 - variable reluctance, 250–254, 263–266
 - Series junction, 43
 - Series wound motor, 327–332
 - Shunt wound motor, 323–327
 - Signal bond, 24
 - Signal conditioning, 295–297
 - Simplification rules for bond graphs, 56–62
 - SIMULINK, 8
 - Single spring–mass–damper model, *see* Quarter car model
 - Skyhook damping, 369
 - Slider–crank mechanism, 396
 - bond graph representation, 397
 - response, 398
 - Solenoids, 308, 310
 - Source of effort, 34
 - Source of flow, 34–35
 - Speed control
 - bond graph of, 425
 - parameters used for, 423
 - Spring elements, *see* Capacitive (C) elements
 - Spring–mass–damper equation, 153
 - Spring–mass–damper system, 24, 73, 76–77, 93, 283, 359–360
 - Square wave generator, 388–390
 - Stagnation pressure, 116
 - State–space equations, 7, 9, 181–182, 198
 - Static pressure, 116
 - Steady state handling
 - performance, 371
 - Steer-by-wire system (SBW), 380
 - bond graph model of, 382–383
 - controller subsystem, 381
 - features, 380
 - front wheel subsystem, 382
 - system-level model of, 380–381
 - Steering subsystem, 381
 - Steering wheel, 377
 - Stick–slip friction
 - behavior of velocity due to, 453
 - modeling, 453–454
 - Storage elements, 87–90
 - Strain gauge, 231–232
 - Strong bond, 86–87
 - Subsystems, 15, 17
 - Surface tension, 278
 - Symbols2000, 10
 - Synergy, 2
 - System boundary, 5
 - System equations, derivation of, 146–158
 - System models, 5–7
 - Systems viewpoint, 5
 - System variables, 145
- T**
- Tetrahedron of state, 21–22, 33
 - Thermoelectric analysis, 460
 - Time constant, 180
 - Torque (T), 314–316
 - Torque loads, 322
 - Transduction mechanisms, 266
 - Transfer function, 197
 - with active damping, 370
 - heave motion with respect to input velocity, 366–368, 370
 - with increased damping, 368
 - pitch motion with respect to input velocity, 367–368, 370
 - Transformer compliance, 104
 - Transformer elements, 35–39, 85–86, 121
 - bond graph, 35
 - within different domains, 36
 - examples of, 36
 - in hydraulic circuits, 121
 - Transformer factor, 122
 - Transformer parameter calculation, 362–368
 - Trapezoidal method, 215–217
- V**
- Variable differential transformers, *see* Linear variable differential transformers; Rotational variable differential transformers
 - Variable reluctance sensor, 250–254
 - bond graph of, 251–252
 - parameters used in simulation, 254

- rotational motion, 263–266
 - simulation results from, 254
- Vehicle drive line
 - bond graph representation of, 353
 - simulation results for, 356
 - vehicle parameters used for, 355
- Vehicle dynamics, 358–374
 - 1-D model, 359
 - 2-D model, 359–362
 - 3-D model, 358
- Vehicles, energy regeneration in,
 - 386–390
- Vehicle systems
 - modeling of, 352–358
 - power flow of, 352–353
- Velocity transducer, 449
- Vode–Adams method, 221–222

W

- Wave generator, 46
- Wheatstone bridge, 67, 231
 - bond graph for, 68–69, 232
 - simplified model for, 68
 - simulation results, 233
- Wind resistance, 355–356
- Word bond graphs, 23–26; *see also*
 - Bond graph

Z

- Zero junction, 42
- Zeroth order system, 173–176
- Ziegler–Nichols closed loop
 - method, 422